

GDANSK UNIVERSITY OF TECHNOLOGY  
FACULTY OF OCEAN ENGINEERING AND SHIP TECHNOLOGY  
SECTION OF TRANSPORT TECHNICAL MEANS  
OF TRANSPORT COMMITTEE OF POLISH ACADEMY OF SCIENCES  
UTILITY FOUNDATIONS SECTION  
OF MECHANICAL ENGINEERING COMMITTEE OF POLISH ACADEMY OF SCIENCE

**ISSN 1231 – 3998**  
**ISBN 83 – 900666 – 2 – 9**

# **Journal of**

# **POLISH CIMAC**

## **DIAGNOSIS, RELIABILITY AND SAFETY**

**Vol. 4**

**No. 2**

Gdansk, 2009

**Science publication of Editorial Advisory Board of POLISH CIMAC**



### Editorial Advisory Board

**J. Girtler** (President) - *Gdansk University of Technology*  
**L. Piaseczny** (Vice President) - *Naval Academy of Gdynia*  
**A. Adamkiewicz** - *Maritime Academy of Szczecin*  
**J. Adamczyk** - *University of Mining and Metallurgy of Krakow*  
**J. Blachnio** - *Air Force Institute of Technology*  
**L. Będkowski** - *WAT Military University of Technology*  
**C. Behrendt** - *Maritime Academy of Szczecin*  
**P. Bielawski** - *Maritime Academy of Szczecin*  
**J. Borgoń** - *Warsaw University of Technology*  
**T. Chmielniak** - *Silesian Technical University*  
**R. Cwilewicz** - *Maritime Academy of Gdynia*  
**T. Dąbrowski** - *WAT Military University of Technology*  
**Z. Domachowski** - *Gdansk University of Technology*  
**C. Dymarski** - *Gdansk University of Technology*  
**M. Dzida** - *Gdansk University of Technology*  
**J. Gronowicz** - *Maritime University of Szczecin*  
**V. Hlavna** - *University of Žilina, Slovak Republic*  
**M. Idzior** - *Poznan University of Technology*  
**A. Iskra** - *Poznan University of Technology*  
**A. Jankowski** - *President of KONES*  
**J. Jaźwiński** - *Air Force Institute of Technology*  
**R. Jedliński** - *Bydgoszcz University of Technology and Agriculture*  
**J. Kiciński** - *President of SEF MEC PAS, member of MEC*  
**O. Klyus** - *Maritime Academy of Szczecin*  
**Z. Korczewski** - *Naval Academy of Gdynia*  
**K. Kosowski** - *Gdansk University of Technology*  
**L. Ignatiewicz Kowalczyk** - *Baltic State Maritime Academy in Kaliningrad*  
**J. Lewitowicz** - *Air Force Institute of Technology*  
**K. Lejda** - *Rzeszow University of Technology*

**J. Macek** - *Czech Technical University in Prague*  
**Z. Matuszak** - *Maritime Academy of Szczecin*  
**J. Merksiz** - *Poznan University of Technology*  
**R. Michalski** - *Olsztyn Warmia-Mazurian University*  
**A. Niewczas** - *Lublin University of Technology*  
**Y. Ohta** - *Nagoya Institute of Technology*  
**M. Orkisz** - *Rzeszow University of Technology*  
**S. Radkowski** - *President of the Board of PTDT*  
**Y. Sato** - *National Traffic Safety and Environment Laboratory, Japan*  
**M. Sobieszczkański** - *Bielsko-Biala Technology-Humanistic Academy*  
**A. Soudarev** - *Russian Academy of Engineering Sciences*  
**Z. Stelmasiak** - *Bielsko-Biala Technology-Humanistic Academy*  
**M. Ślęzak** - *Ministry of Scientific Research and Information Technology*  
**W. Tarelko** - *Maritime Academy of Gdynia*  
**W. Wasilewicz Szczagin** - *Kaliningrad State Technology Institute*  
**F. Tomaszewski** - *Poznan University of Technology*  
**J. Wajand** - *Lodz University of Technology*  
**W. Wawrzyński** - *Warsaw University of Technology*  
**E. Wiederuh** - *Fachhochschule Giessen Friedberg*  
**B. Wojciechowicz** - *Honorary President of SEF MEC PAS*  
**M. Wyszynski** - *The University of Birmingham, United Kingdom*  
**M. Zablocki** - *Vice President of KONES*  
**S. Żmudski** - *Szczecin University of Technology*  
**B. Żółtowski** - *Bydgoszcz University of Technology and Life Sciences*  
**J. Żurek** - *Air Force Institute of Technology*

### Editorial Office:

GDANSK UNIVERSITY OF TECHNOLOGY  
Faculty of Ocean Engineering and Ship Technology  
Department of Ship Power Plants  
G. Narutowicza 11/12 80-233 GDANSK POLAND  
tel. +48 58 347 29 73, e – mail: sek4oce@pg.gda.pl

[www.polishcimac.pl](http://www.polishcimac.pl)

This journal is devoted to designing of diesel engines, gas turbines and ships' power transmission systems containing these engines and also machines and other appliances necessary to keep these engines in movement with special regard to their energetic and pro-ecological properties and also their durability, reliability, diagnostics and safety of their work and operation of diesel engines, gas turbines and also machines and other appliances necessary to keep these engines in movement with special regard to their energetic and pro-ecological properties, their durability, reliability, diagnostics and safety of their work, and, above all, rational (and optimal) control of the processes of their operation and specially rational service works (including control and diagnosing systems), analysing of properties and treatment of liquid fuels and lubricating oils, etc.

All papers have been reviewed

@Copyright by Faculty of Ocean Engineering and Ship Technology Gdansk University of Technology

All rights reserved

ISSN 1231 – 3998

ISBN 83 – 900666 – 2 – 9

Printed in Poland



K.F. Abramek: ANALYSIS OF POSSIBILITIES IN USING CRANKSHAFT CASING PRESSURE MEASUREMENTS FOR DIAGNOSING TECHNICAL CONDITION OF THE PRC SYSTEM .....	7
M. Babiak, M. Ciałkowski, M. Giersig, A. Iskra, J. Kałużny: SELECTED POSSIBLE APPLICATIONS OF NANOMATERIALS IN AUTOMOTIVE INDUSTRY .....	15
J. Borgoń, J. Sarnecki, J. Zieliński: PROPOSITION OF METHODOLOGY FOR ENGINE LUBRICANTS RHEOLOGICAL PROPERTIES ESTIMATION .....	21
P. Bzura: PROBLEMS OF THE USE OF PIEZOELECTRIC GAUGES FOR LUBRICITY TESTING WITH THE T-02 FOUR-BALL TESTER .....	27
C. Dymarski, M. Narewski: ANALYSIS OF SHIP SHAFT LINE COUPLING BOLTS FAILURE .....	33
W. Dziegielewski: THE LIMITATION OF USE OF BIOCOMPONENTS IN THE FORM OF FATTY ACID METHYL ESTERS BASED ON ANALYSIS OF ELECTED TURBINE FUEL PROPERTIES .....	41
A. Erd: ELEMENTS OF THE UML MODEL OF THE RAIL VEHICLE MAINTENANCE SYSTEM .....	49
J. Girtler, W. Darski, J. Sikora, W. Majewski, I. Baran, M. Nowak: THE USE OF ACOUSTIC EMISSION TO IDENTIFICATION DAMAGES BEARINGS THE MAIN AND CRANK ENGINES ABOUT THE AUTOMATIC IGNITION .....	57
M. Idzior: NOWADAYS ASPECTS OF THE SELECTION OF THE PARAMETRS OF THE INJECTION OF THE FUEL IN DIESEL ENGINES ...	71
A. Janicka, W. Szczepaniak, W. Walkowiak: THE EFFECT OF PLATINUM-RHODIUM INNER CATALYST APPLICATION IN A SELF-IGNITION ENGINE ON TOXICITY EQUIVALENT FACTOR (TEF) OF VOLATILE ORGANIC COMPOUNDS (VOC'S) IN EXHAUSTS .....	77
A. Janicka, W. Szczepaniak, W. Walkowiak: THE IMPACT OF PLATINUM-RHODIUM ACTIVE COATING INSIDE A SELF-IGNITION ENGINE ON VOLATILE ORGANIC COMPOUNDS (VOC's) EMISSION .....	85
G. Karp: EFFECT OF FATTY ACID METHYL ESTERS (FAME) ON PHYSICAL AND CHEMICAL PROPERTIES OF AVIATION TURBINE FUELS .....	91
O. Klyus, A. Krainyuk: ORGANIZATION PRINCIPLES OF THE OPERATING PROCESS OF THE CASCADE COMPRESSION UNITS AND SOME DIRECTIONS OF THEIR APPLICATION .....	103
Z. Korczewski: ENDOSKOPIC EXAMINATIONS OF MARINE DIESEL ENGINES' TURBOCHARGING SYSTEMS .....	111

P. Kowalak: THE ANGLE MEASUREMENT UNCERTAINTY EVALUATION BY MEANS OF INCREMENTAL ENCODER .....	121
P. Krasowski: PRESSURE IN SLIDE JOURNAL PLANE BEARING LUBRICATED OIL WITH MICROPOLAR STRUCTURE .....	129
P. Krasowski: CAPACITY FORCES IN SLIDE JOURNAL BEARING LUBRICATED OIL WITH MICROPOLAR STRUCTURE .....	137
B. Krupicz: EROSION PROBLEMS IN PNEUMATIC TRANSPORT INSTALLATIONS .....	145
A. Kułaszka, M. Chalimoniuk, J. Błachnio: TYPES OF DAMAGE TO TURBINES OF AIRCRAFT TURBINE ENGINES AND POSSIBILITY OF THEIR DIAGNOSING .....	153
B. Landowski: SEMI-MARKOV MODEL OF MAINTENANCE OF URBAN TRANSPORT BUSE .....	161
K. Lejda, A. Ustrzycki: EFFECT OF SUPPLY VOLTAGE ON THE DOSAGE FUEL IN INJECTION SYSTEM THE COMMON RAIL TYPE .....	169
J. Lewitowicz, O. Wieczorek, A. Żyluk: GAS TURBINE ENGINES – THROUGH IMPROVED MAINTAINABILITY TO IMPROVED OPERATIONAL READINESS IN NAVY HELICOPTERS .....	177
J. Lewitowicz, O. Wieczorek, A. Żyluk: DAMAGES TO STRUCTURAL COMPONENTS AND UNITSO F A GAS TURBINE ENGINE .....	183
R. Liberacki: DRAWING CONCLUSIONS ABOUT RELIABILITY OF POWER SYSTEMS FROM SMALL NUMBER OF STATISTICAL DATA .....	191
Z. Łosiewicz: ANALYSIS OF THE ACTUAL M.E. DIAGNOSTIC PROCESSES ON VESSELS – USEFULNESS OF SELECTED SYSTEMS DIAGNOSING THE SHIP ENGINES AND OF THE OPERATING PROCEDURES ON EXAMPLE OF THE ACTUAL OPERATING EVENTS .....	199
Z. Matuszak. G. Nicewicz: ASSESSMENT OF FAILURE DISTRIBUTIONS OF MARINE POWER PLANTS FUEL OIL SYSTEMS GROUP .....	207
J. Merkisz, J. Pielecha, J. Gis: HEAVY DUTY DIESEL EMISSION ROAD TESTS	217
M. Narewski: HISMAR - UNDERWATER HULL INSPECTION AND CLEANING SYSTEM AS A TOOL FOR SHIP PROPULSION SYSTEM PERFORMANCE INCREASE .....	227
M. Pawlak, L. Piaseczny: A MODEL OF MARINE VESSELS MOVEMENT TO ESTIMATE HARMFUL COMPOUNDS IN THE VESSELS EXHAUSTS	235
L. Piaseczny, T. Kniaziewicz: MODELLING EXHAUST EMISSION FROM VESSELS IN THE GULF OF GDAŃSK AREA .....	245

D. Pielka, Z. Łosiewicz: APPLICATION OF ARTIFICIAL INTELLIGENCE FOR DIAGNOSTIC TESTING OF SHIP COMBUSTION ENGINE – MAPS OF DIAGNOSTIC PARAMETERS .....	253
W. Serdecki, P. Krzymień: MODEL TESTS OF PISTON RING-CYLINDER LINER COLLABORATION ON HIGH POWER ENGINES .....	259
Z. Smalko: SELECTED PROBLEMS TO LOSS AND MAINTAIN THE PROPRIETES OF TECHNICAL OBJECTS .....	267
M. Styp-Rekowski: RANDOMNESS OF ROLLING BEARINGS' ELEMENTS GEOMETRY AS PROBABILISTIC FACTOR OF BEARINGS FATIGUE LIFE .....	271
L. Tomczak: APPLICATION OF MARINE ENGINE ROOM SIMULATORS WITH 3D VISUALIZATION IN THE TRAINING PROCESS OF EMERGENCY OPERATING PROCEDURES .....	279
H. Tylicki: THE RULES OF INFERENCE IN MACHINE STATE RECOGNITION .....	289
M. Walkowski: SELECTED ISSUES OF MODELING THE ACCUMULATOR INJECTION SYSTEMS IN NAVAL COMBUSTION ENGINES .....	299
P. Wirkowski: INFLUENCE OF AXIAL COMPRESSOR FLOW PASSAGE GEOMETRY CHANGES ON GAS TURBINE ENGINE WORK PARAMETERS .....	307
R. Zadrag: THE MULTI-EQUATIONAL MODELS IN THE ANALYSIS OF RESULTS OF MARINE DIESEL ENGINES RESEARCH .....	315
J. Zimniak: CONSTITUTION OF USEFUL PROPERTY OF COMPOSITE MATERIALS .....	325
J. Ziółkowski: METHODS OF ESTIMATING THE AVAILABILITY OF VEHICLES .....	331
B. Żółtowski: DIAGNOSTIC SYSTEM OF EXPLOITATION MACHINES .....	341
B. Żółtowski: PROCEDURE OF CONSTRUCTING AND EVALUATING LINEAR DIAGNOSTIC MODELS OF COMPLEX OBJECTS .....	349







## ANALYSIS OF POSSIBILITIES IN USING CRANKSHAFT CASING PRESSURE MEASUREMENTS FOR DIAGNOSING TECHNICAL CONDITION OF THE PRC SYSTEM

**Karol Franciszek Abramek**

*West Pomeranian University of Technology in Szczecin*  
*al. Piastów 19, 70-310 Szczecin, Poland*  
*tel.: +48 91 4494811, fax.: +48 91 4494820*  
*e-mail: karol.abramek@ps.pl*

### **Summary**

*In the paper is presented statistical analysis of the effect of compression-ignition engine working time on the phenomenon of exhaust gas pressure increase in crankcase and cylinder liner, pistons and rings wear. Characteristics of the crankcase pressure variations were made for the start-up speed and for selected rotational speeds of the 359 compression-ignition engine crankshaft as well as micrometric measurements of the cylinder liner and pistons and rings wear. The engine was operated under normal traction conditions while pressure analyses and cylinder liner micrometric measurements were made, respectively, after an operational run of: 5378 km, 100128 km, and 204864 km. Crankcase exhaust gas pressure measurements were made both with air vent open and closed for a cold (lubricating oil temperature of 285 K) and a warm engine (333 K). Basing on the analysis of obtained examination results, it was showed that crankcase exhaust gas pressure measurement (also during the start-up) may be used for determination of engine run and life.*

**Keywords:** scavenging, wear, piston, rings, cylinder, crankcase

### **1. Introduction**

Construction of the piston-cylinder system, into which such elements as piston, piston rings and cylinder liner (PRC) can be included, should ensure a slide fit under variable conditions of mechanical and thermal loads as well as preserve as large leak-tightness as possible [4]. Penetration of exhaust gases into crankcase in the form of scavenging between a piston, piston rings and a cylinder liner results in development of a specific pressure in crankcase. Moreover, a growth in scavenging intensity brings about increase of crankcase pressure, drop of engine power, increase of fuel and lubricating oil consumption, difficulties in engine start-up, in particular at low ambient temperatures, and excessive environmental pollution with combustion products. Too high excess pressure developing in crankcase is unfavourable for turbo-compressor lubrication system [7]. Every turbo-compressor has dynamic seals of the labyrinth type which are very sensitive to an increased level of excess pressure in crankcase. At that time, a free outflow of the oil lubricating turbo-compressor's bearings into oil sump is much hampered or even obstructed. Therefore, evaluation of the technical condition of the PRC system is very important, which can be a measurement of exhaust gas pressure in crankcase. This is because a pressure increase occurs together with a rise in wear.

## 2. Evaluation criteria for measurement method

When estimating the usefulness of crankcase exhaust gas pressure measurements for evaluation of cylinder liner wear degree, two criteria were adopted. First of all, results of crankcase exhaust gas pressure examination should be considerably correlated with cylinder liner wear and secondly, dynamics of determined signal change should be as large as possible. It results from literature [2, 3] that considerably correlated variables should be characterised by the correlation coefficient  $r \geq 0.51$ . It is known from experience that in case of statistical diagnostic analyses it is rather difficult to obtain such a considerable value of correlation coefficient and it requires large repeatability of measurement conditions. In this case, growth of exhaust gas pressure in crankcase induced by a rise in exhaust gas scavenging intensity in result of the increase of wear in the PRC group, in particular of cylinder liner wear, is regarded as a determined signal change. The following value was adopted as a dynamics index  $d_p$ :

$$d_p = \frac{X_m - X_o}{X_o}, \quad (1)$$

where:

$X_m$  - is a boundary value of signal indicating the necessity of performing a repair or taking an object out of service,

$X_o$  - is an initial value of signal characterising a new object after termination of the running-in period.

## 3. Formulation of research problem

The wear processes in the PRC assembly are unavoidable. Nevertheless, the most intensive is wear induced by friction phenomena and processes, which is reflected in cylinder liner wear. Material losses in co-operating parts bring about development of greater and greater clearances between PRC elements [5]. This favours increase in the intensity of exhaust gas scavenging into crankcase, destruction of oil film layer, development of more intensive erosion processes and increase of oil pressure in crankcase [6]. Therefore, pressure increase in crankcase [crankshaft casing] pressure can be used for forecasting the degree of engine wear, in particular that of cylinder liner.

Diameter measurements were taken with an inside micrometer calliper in horizontal plane being distant cylinder liner end face by 20 mm, which corresponds to the piston position in the upper dead centre (UDC). It is well-known that cylinder circularity becomes deteriorated in result of wear and resembles an oval. Its larger diameter (defined as  $D_B$ ) corresponds to a plane perpendicular to the axis of engine crankshaft (it results from the dynamics of crankshaft-pistons-connecting rods system), while a smaller one (defined as  $D_A$ ) occurs in a plane parallel to the axis of engine crankshaft. A clearance that develops then between a piston with rings and a cylinder is the main reason of both scavenging and pressure increase in crankcase. The character of clearance was determined by the following measures:

- circularity deviation measure:

$$\Delta D'_A = D_A - D_{avg} [\mu m] \quad (2)$$

where:

$$D_{avg} = \frac{D_A + D_B}{2} \quad (3)$$

$$\Delta D'_A = -\Delta D'_B \quad (4)$$

- cylinder liner deformation measure after insertion into engine body; it was assumed here that free cylinder liner diameters did not depart significantly from a  $\phi$  size of  $110^{+0.011}$  mm since

production process in the aspect of precision is set out to that value; the character of clearance was expressed by a ratio of oval diameter deviations ( $\frac{\Delta D_A}{\Delta D_B}$ ) from a cylinder nominal diameter (D) equal to 110.011 mm ( $\Delta D_A = D_A - D$  and  $\Delta D_B = D_B - D$ ).

#### 4. Test results

Figure 1 presents a dependence of crankcase exhaust gas pressure in the function of rotational speed for the 359 engine respectively after a run of: 5378 km, 100128 km, and 204864 km. It can be seen that pressure in crankcase grows together with increase of operational run. For the rotational speed of crankshaft of  $1500 \text{ min}^{-1}$  and that of  $2200 \text{ min}^{-1}$ , local pressure extremes occur. This is caused by the phenomenon of packing ring movements reported in literature [1]. Therefore, these speeds should be avoided when diagnosing technical condition of the PRC assembly. They affect a measurement error connected with the phenomenon of ring movement. However, it is evident that increase of operational run clearly affects pressure increase in crankcase.

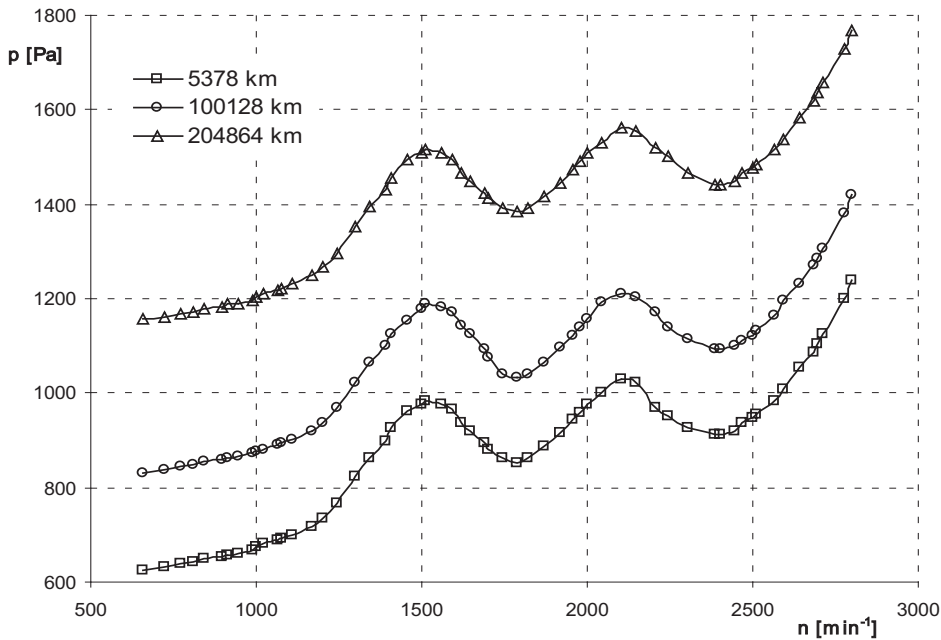


Fig. 1. Dependence of the course of exhaust gas pressure in crankcase of the 359 engine in the function of rotational speed for different operational runs

Figure 2 presents a dependence of crankcase exhaust gas pressure increase for a warm 359 engine (lubricating oil temperature of 333K) in the function of operational run expressed in kilometres. It can be seen that exhaust gas pressure in crankcase grows with increase of run.

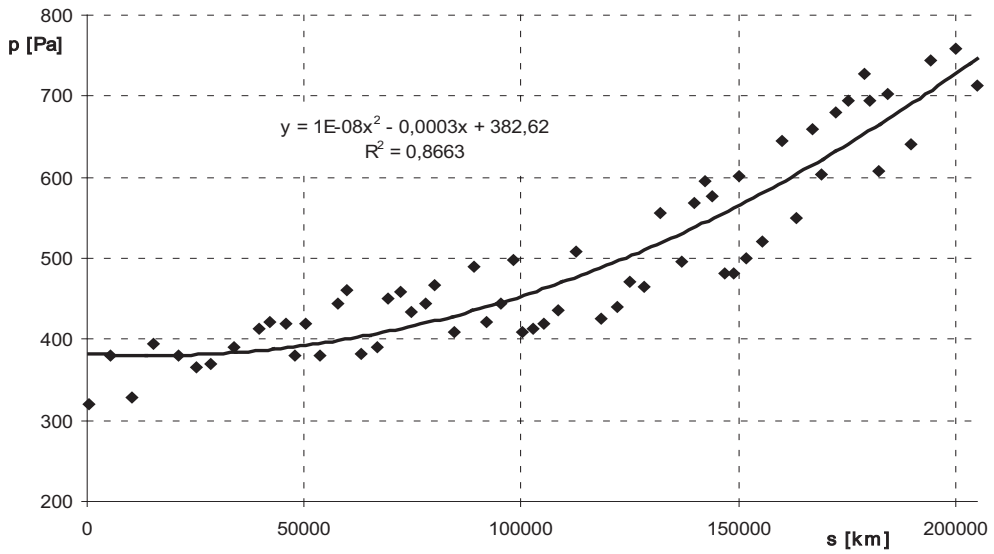


Fig. 2. Increase of exhaust gas pressure in crankcase for a warm 359 engine in the function of operational run

Figure 3 presents a dependence of exhaust gas pressure variations in crankcase in the function of 359 engine run for lubricating oil temperature of 285K.

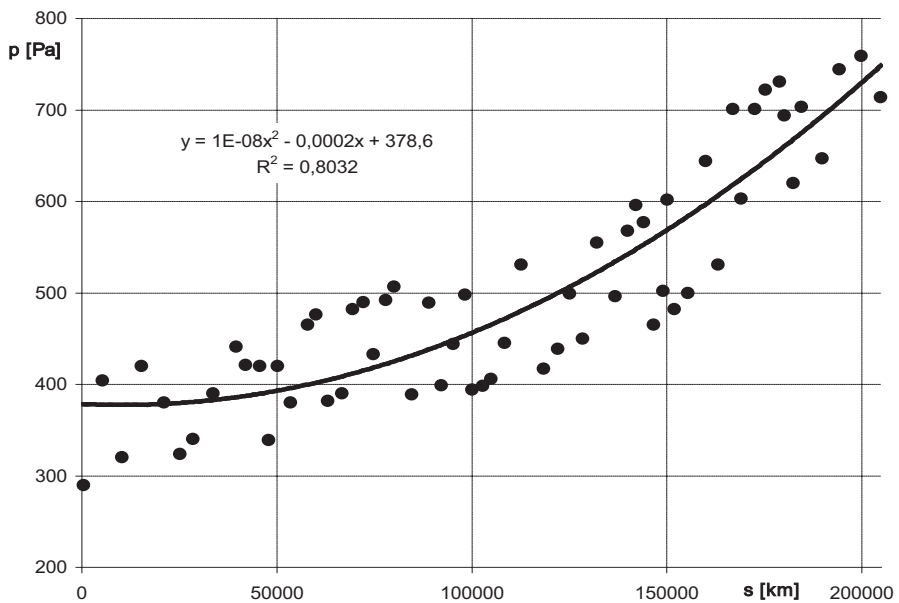


Fig. 3. Increase of exhaust gas pressure in crankcase for a cold 359 engine in the function of operational run

For a closed crankcase air vent, an increase of exhaust gas pressure presented in Fig. 4 was obtained.

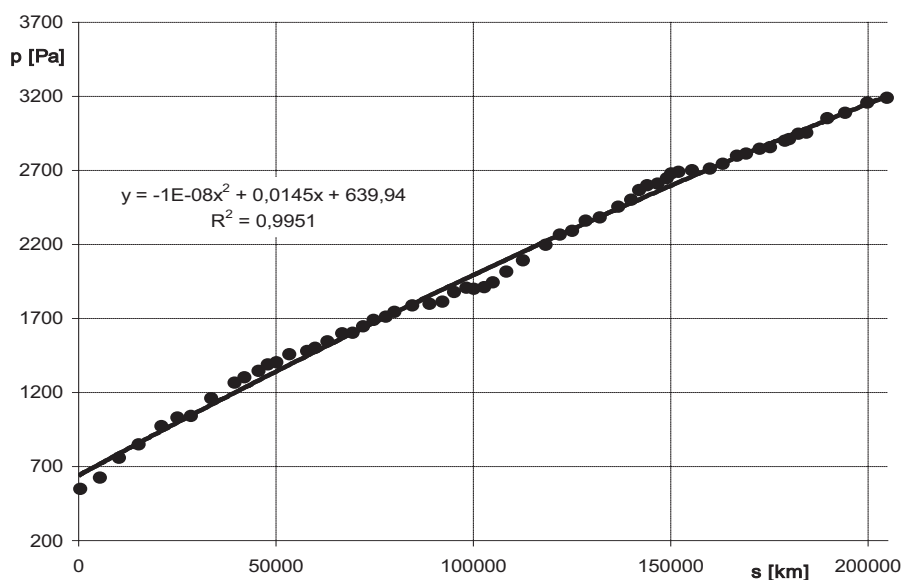


Fig. 4. Increase of exhaust gas pressure in crankcase of the 369 engine for closed air vent in the function of operational run

On the other hand, average tear values for respective cylinders of the 359 engine after a run of 204864 km amounted to:

- for first cylinder – 0,032 mm,
  - for second cylinder – 0,041 mm,
  - for third cylinder – 0,066 mm,
  - for fourth cylinder – 0,081 mm,
  - for fifth cylinder – 0,074 mm,
  - for sixth cylinder – 0,065 mm,
- whereas maximum wear values were as follows:
- for first cylinder – 0,120 mm,
  - for second cylinder – 0,105 mm,
  - for third cylinder – 0,118 mm,
  - for fourth cylinder – 0,124 mm,
  - for fifth cylinder – 0,122 mm,
  - for sixth cylinder – 0,129 mm.

In order to determine a maximum oval, largest differences were calculated in planes A-A and B-B as well as C-C and D-D at one level  $l_1 = 20$  mm from the top edge. The oval sizes were as follows:

- first cylinder	maximum 0.122 mm	minimum 0.012 mm
- second cylinder	maximum 0.140 mm	minimum 0.024 mm
- third cylinder	maximum 0.131 mm	minimum 0.016 mm
- fourth cylinder	maximum 0.099 mm	minimum 0.018 mm
- fifth cylinder	maximum 0.108 mm	minimum 0.014 mm

- sixth cylinder                      maximum 0.127 mm                      minimum 0.022 mm

In order to analyse the conicity, differences in dimensions were calculated in respective planes, i.e. A-A, B-B, C-C and D-D at levels  $l_1 = 20$  mm and  $l_7 = 245$  mm. The results point to negative taper (taper towards a lower part of cylinder should be considered to be a negative one). The conicity values were on average as follows:

- for first cylinder	0.028 mm	negative
- for second cylinder	0.025 mm	negative
- for third cylinder	0.028 mm	negative
- for fourth cylinder	0.023 mm	negative
- for fifth cylinder	0.021 mm	negative
- for sixth cylinder	0.019 mm	negative

Maximum piston wear values in the plane perpendicular to piston pin axis were as follows:

- for first cylinder	0.12 mm
- for second cylinder	0.13 mm
- for third cylinder	0.09 mm
- for fourth cylinder	0.11 mm
- for fifth cylinder	0.12 mm
- for sixth cylinder	0.11 mm

Mean wear values for the height of respective rings were as follows:

- for first packing rings – 0.019 mm,
- for second packing rings – 0.012 mm, and
- for third packing rings – 0.009 mm.

Mean values from maximum wear values for the breadth of respective rings were as follows:

- for first packing rings – 0.189 mm,
- for second packing rings – 0.144 mm, and
- for third packing rings – 0.112 mm.

Mean wear values for the breadth of respective rings were as follows:

- for first packing rings – 0.151 mm,
- for second packing rings – 0.113 mm, and
- for third packing rings – 0.098 mm.

The size of piston-ring joint clearance in all packing rings after their insertion into a cylinder hole was larger than that of entrance clearances by:

- 1.44 mm for first packing rings,
- 1.06 mm for second packing rings, and
- 0.93 mm for third packing rings.

In order to analyse a decrease in ring elasticity, crank pin effort values were measured at ring closure to piston-ring joint sizes measured after insertion into cylinder liner and comparison with initial values. The elasticity decrease was on average as follows:

- for first packing rings – 7.1 N,
- for second packing rings – 5.2 N, and
- for third packing rings – 2.3 N.

## 5. Conclusions

When choosing a regression model, the following criterion was taken into consideration:

$$\begin{aligned} r^2 &\rightarrow 1 & (5) \\ F_{cr} &\leq F \rightarrow \text{maximum} & (6) \end{aligned}$$

where  $F$  is a Snedecor's statistics testing significance of regression. The critical value  $F_{cr}$  read from tables for a confidence interval  $\beta = 0.95$  and a number of degrees of freedom  $n_2 = 12$  and  $n_1 = k - 1 = 1$  ( $k$  is a number of parameters of the regression equation) amounts to  $F_{cr} = 4,75$ . Correlation coefficient for the increase of pressure in crankcase in the function of operational run for a warm 359 engine amounts to  $r^2 = 0,86$ , whereas that for a cold engine is  $r^2 = 0,80$ . On the other hand, the best diagnostic measurement (in relation to pressure measurements) determining the engine run in kilometres is crankcase pressure measurement for closed air vent. Correlation coefficient in that case is  $r^2 = 0,99$ .

The determined signal change amounted for a warm engine to  $d_p = (750-380)/380 = 0,97$ , while for a cold engine it was  $d_p = (740-370)/370 = 1,00$  at open air vent. On the other hand, the dynamics index  $d_p$  at closed air vent amounted to  $(3200-600)/600 = 4,33$  and was the largest. When evaluating the usefulness of maximum crankcase pressure measurement, it should be concluded that measurements ought to be made for closed air vent (largest correlation coefficients and largest signal dynamics change were obtained) and it is possible to clearly state that measurement of exhaust gas pressure in crankcase is closely correlated with operational wear in the PRC group.

## References

- [1] Abramek, K. F., *Effect of phenomenon of piston sealing rings vibrations on tightness of PRC unit*, Journal of Polish CIMAC, Vol. 2, No 1. pp. 9-13, 2007.
- [2] Bobrowski, D., Maćkowiak-Łybacka K., *Wybrane metody wnioskowania statystycznego*, Wyd. Politechniki Poznańskiej, Poznań 1988.
- [3] Bobrowski, D., *Probabilistyka w zastosowaniach technicznych*, Wyd. Naukowo-Techniczne, Warszawa 1980.
- [4] Iskra A., *Studium konstrukcji i funkcjonalności pierścieni w grupie tłokowo-cylindrowej*, Wydawnictwo Politechniki Poznańskiej, Poznań 1996.
- [5] Niewczas A., *Trwałość zespołu tłok-pierścieni-cylinder silnika spalinowego*, Wyd. Naukowo-Techniczne, Warszawa 1998.
- [6] Niewczas A., Koszałka G., *Niezawodność silników spalinowych – wybrane zagadnienia*, Wyd. Politechniki Lubelskiej, Lublin 2003.
- [7] Serdecki W., *Wpływ pierścieni uszczelniających na kształtowanie filmu olejowego na gładzi tulei cylindrowej silnika spalinowego*, Wyd. Politechniki Poznańskiej, Poznań 1990.







## SELECTED POSSIBLE APPLICATIONS OF NANOMATERIALS IN AUTOMOTIVE INDUSTRY

**Michał Ciałkowski, Michał Giersig, Antoni Iskra, Jarosław Kałużny, Maciej Babiak**

*Poznan University of Technology*  
ul. Piotrowo 3, 60-965 Poznan, Poland  
tel.: +48 61 6652705, fax: +48 61 6652204  
e-mail: jaroslaw.kaluzny@put.poznan.pl

### **Abstract**

*The nanotubes and nanotechnologies are relatively new areas of science and engineering practice. This article should be concerned as a review of the selected nanotechnology applications in the automotive industry. The applications were divided into groups in respect of implementation advance level. Special attention was devoted to innovative nanomaterials application in areas where taking advantage of their unique features is possible. Authors presented the catalytic converter for combustion engine exhaust system application in which the nanotubes were used in order to increase the contact area of exhaust gases with catalytic layer. In the paper preliminary results of proposed catalytic reactor conversion ratio were presented and future directions of development were discussed.*

### **1. Introduction**

The automotive industry has its own specificity due to which it can be distinguished on the background of other branches of industry. The cars are characterized by a fact that for more than one hundred years a process of their improvement takes place on a way of evolution and during this period the detailed design solutions are developed while their general design characteristics and functionality are kept unchanged. In fact a modern car is not so different from its prototype as, for instance, modern TV or telephone sets in comparison with their prototypes developed a few dozen years ago. In case of domestic appliances their design improvement process causes that though their original functions are maintained the construction and the way of operation of the former and current versions in some cases are different. However, paradoxically, basing on the above it should not be concluded that the motor industry is characterized by a certain conservatism which provides an artificial barrier for modern technologies and solutions. Though such a barrier really exists, however, it results from the specification of a final product – which due to that improvement process lasting for more than one hundred years – is difficult to be improved in a simple way, and due to large serial production where each modification must be well ransomed by a large investment. At the same time it is worth notifying that large serial production of cars does not only create a certain barrier for the application of new materials, but it is also a driving force which gives bonuses to more effective solutions which are cheaper than the previous ones being used so far.

Nanomaterials are characterized by some especially advantageous mechanical properties unattainable for conventional materials, however, their scale of applications in the motor industry

is limited by their high prices, availability in industrial amounts and instability of properties of the individual lots of products.

## **2. The selected examples of well proved applications of nanomaterials in the motor industry**

The motor industry applies the profitable features of the polymer-nanomaterial composites to a relatively large extent. Such plastics are already in current production on an industrial scale, and their advantages are as follows:

- increased rigidity free of loss in impact strength;
- dimensional stability;
- barrier effect improvement;
- increased thermal stability and fire resistance;
- good optical properties (filler particles with a diameter size smaller than visible light wave length make no barrier for them);
- limitations of the surface defects of products,
- increased crystallization ratio in relation to the original polymer [4].

The dashboards and body panels made of polymer composite materials have a higher resistance for scratching and surface damaging. A possibility of using the barrier properties of the nano-composites for building the fuel tanks is especially profitable. The nano-composites on a PA base are used as an inner layer in the multilayer blowing of fuel tanks while their outer layers are made of PE-HD.

Montmorylonit (MMT), which ensures good barrier properties, is used in another form for improving the characteristics of varnish coating being used for cars especially in order to increase their mechanical resistance [4].

The next group of nanomaterial applications, especially interesting one, has been found in the tribology field, in main nodes of friction of the piston engine. The Schaeffler Company developed a new technological line making possible the use of nanomaterial top layers in cylinder bearings and highly loaded elements of the driving gear systems. [9]

In the project presented in [10] a top layer of the engine cylinder surface, deposited by plasma spraying, in the AL-cylinder block engine was used. The obtained nanomaterial cylinder bearing surface gives a profitable alternative for a standard solution with a cast iron sleeve insert and makes reduction in friction losses and mass of the engine possible. Some examples of tribologic applications of the thermoplastics strengthened by nanomaterials are presented in [1].

Only the most significant domains of applications of nanomaterials in the motor industry with regards to the production scale were presented above. In a wider context those domains could be divided in a following way:

- bodies and elements of the load carrying structure if vehicles;
- engines and power transmission systems;
- varnish coating and other;
- chassis mechanism and brakes;
- tyres;
- lubricants and operation media;
- electric and electronic equipment elements;
- engine exhaust system and exhaust gas cleaning systems [8].

## **3. Possible domains of the new applications of nanomaterials in motor industry**

Nanotechnology is commonly considered as a one of the key technologies of the 21st century and its special role results from some exceptional – mechanical, electric, thermal, and optical

properties of nanomaterials – completely different from the properties of the conventional construction materials. Carbon nanomaterials form crystal lattices with an extremely limited concentration of defects. The crystal structure give them very high hardness and mechanical strength values which are at least by one order of magnitude higher than those in case of steel, at very high elasticity values. Such materials conduct electricity very well, they become superconductors in low temperature and they are resistant to high temperatures and due to their dimensions smaller than the light wave length forming the transparent surfaces is possible. The organized crystal structure created by carbon atoms arranged in a plane forming a side cylinder surface is a form of fullerenes called a nanotube. Organized crystalline structure made by carbon atoms at surface forming graphene is show on fig. 1.

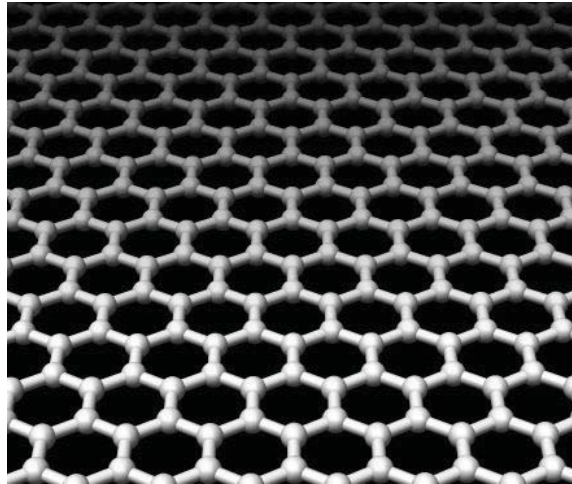


*Fig. 1. Schematic structure of graphene*

Nanotubes present a piezoelectric effect even after applying a relatively low voltage and the observed elongation is several times higher than in case of the quartz crystal pile supplied with a high voltage. Such a characteristic is especially desirable in case of building an actuator for controlling the nozzle needle. Moreover, nanotubes placed in vacuum can act as actuators (Young's modulus 1800 GPa) even under the conditions of very high temperature ranging up to 2800 °C [2, 6, 7]. The peculiar optical properties of nanotubes cause that their use in the car windscreen production, where they could play a role of the electric heating and windscreen deeming depending on the intensity of light, enters the car manufacturers' field of interests.

Some interesting examples of application of nanotubes for building the catalyst converters making the conversion of gases possible can be found in the bibliography [3]. The authors of this paper think that it is advisable to test the usefulness of carbon nanotubes applied as a catalytic converter carrier in the engine exhaust systems. Ratio of solid area to solid volume increases as the solid size decreases. A nanotube considered as a cylinder with a diameter measured in nanometers is characterized by an especially advantageous solid area to solid volume ratio value and by the same it can be considered as a very attractive carrier of the catalytic layer of the converter by increasing its area of contact with the exhaust gases.

#### **4. Carbon nanotubes in the catalytic converter applications**

A standard design of the catalytic converter for clearing the exhaust gas from a car engine uses a ceramic carrier coated with an intermediate layer increasing its roughness and contacting with

exhaust gas area. In case of the oxidation converter used in Diesel engines platinum is deposited on the intermediate layer which is the proper catalyst in a chemical meaning. The authors have built a test converter which is based on a standard ceramic carrier, on which nanotubes functioning as an intermediate layer are deposited and finally pointwisely platinum coated. Due to a limited diameter of 84 mm of the test converter, its carrier length of 20 mm and the density of ducts of 400 cpsi, only a fragment of exhaust gas stream is directed into the test converter. The nanotube test catalytic converter is developed by the Chair of Thermal Engineering of the Poznan University of Technology (PUT) within the international co-operation with Boston College in the United States of America and the Hahn-Meitner-Institut in Berlin in Germany. The typical view of our catalytic converter prototype is shown on fig. 2. The accurate information about carbon tubes growing process can be found in the K. Kempa's publication [5].

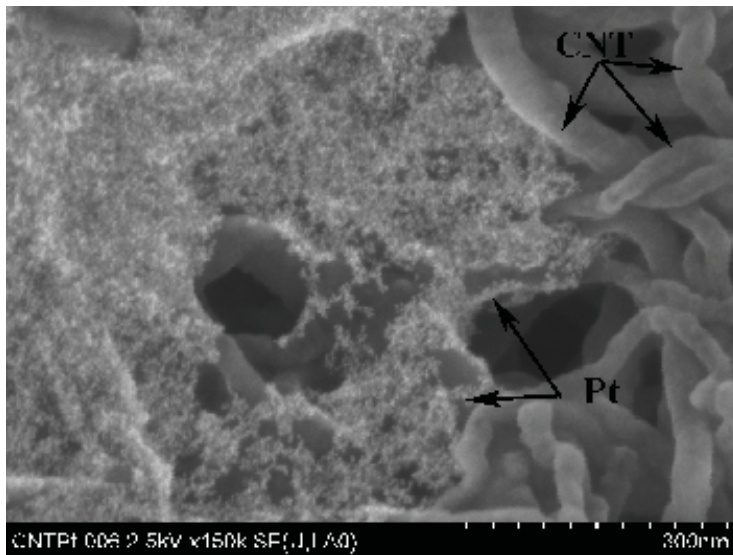


*Fig. 2. Picture of carbon tubes (CNT) on the ceramic face and platinum nanoparticles placed on its surface taken with scanning microscope*

Examinations of the conversion rate for selected toxic exhaust elements were carried out at the laboratory of the Institute of Combustion Engines and Transport of PUT. Volkswagen TDI engine of AXE code was used during the tests. It is a modern 5-cylinder, supercharged Diesel engine being currently mounted in Volkswagen Tranporter and Touareg cars, its swept volume is 2,5 dm<sup>3</sup>, maximum output power is 96 KW and it fulfils the requirements of the Euro 4 exhaust emission standard.

The analysis of the exhaust gas components was carried out by the TESTO 360 exhaust-gas analyser. The concentration of toxic exhaust gas elements is measured by the NDIR method and electrochemical cells, and exhaust gas is delivered to the device via a heated gas line. The engine test stand with the Volkswagen TDI engine, TESTO exhaust – gas analyzer and test converter is showed on fig 3.

Obviously the developed test catalytic converter with the intermediate nanotube layer is not allowed to be considered as a completely functional device with characteristics which could enable it to be mounted in its present form in cars being currently produced. The exhaust gas conversion ratio and resistance of flow would have unacceptable values even if taking into consideration the limited dimensions of the carrier. However, it was the authors intention to find out whether the converter developed by them can work and to obtain the first conclusions.

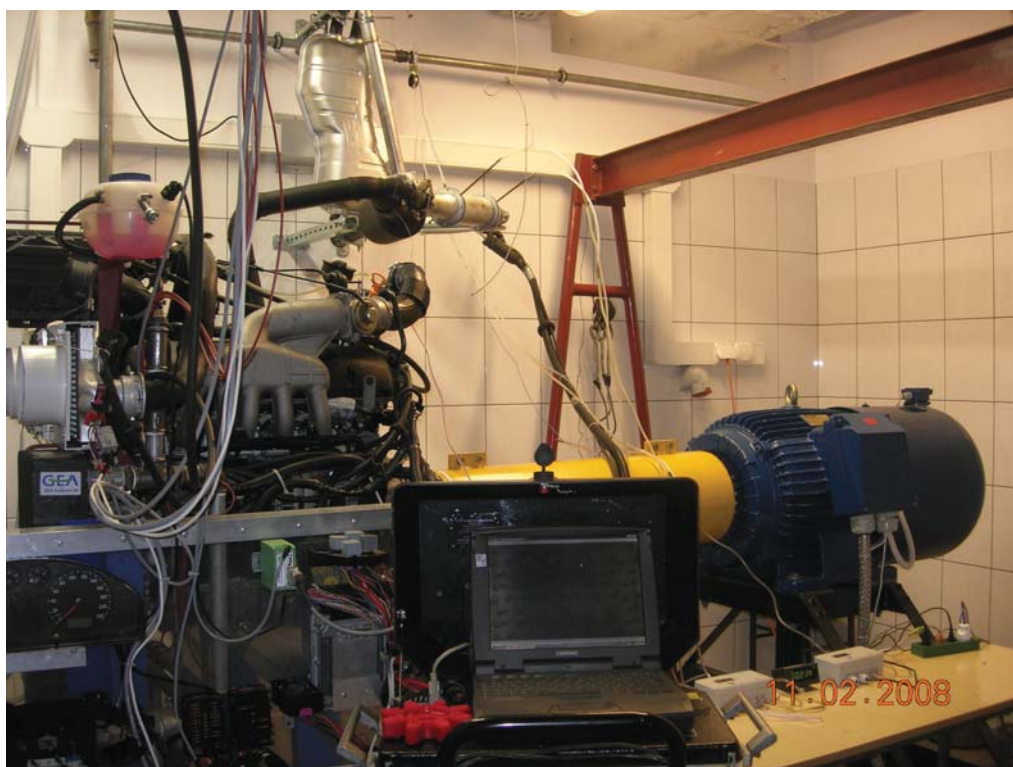


*Fig. 3. The engine test stand for examinations of the catalytic converter conversion ratio*

The preliminary tests, the results of which are presented in Table 1, were performed for several engine operating points in the range of loads most often experienced in real operation. According to the assumed concept of examinations the exhaust gas stream after leaving the engine was separated into the fragments flowing through the test converter and the standard oxidation converter used by the engine manufacturer. The exhaust gas emission measurements concerning the CO and HC concentrations were taken before converters and at the same time behind the test converter and the standard one.

*Tab. 1. Results of the preliminary engine tests*

Engine operating point P	Engine rotational speed	Fuel dose	Exhaust gas temperature after turbine	CO before converter	CO after test/standard converter	HC before converter	HC after test/standard converter
-	[rev/min]	[mg/cycle]	[°C]	[ppm]	[ppm]	[%]	[%]
1	1800	25	467	135	56/7	0,053	0,040/0,041
2	2500	15	387	160	51/7	0,072	0,057/0,038
3	2500	10	282	333	183/6	0,102	0,081/0,039

## 5. Summary and conclusions

The unique properties of nanomaterials suggest that these materials are, at last potentially, able to revolutionize the technical solutions being in use so far, the motorization field including. It can be assumed that at the moment we are at the beginning of the process of the implementation of



nanomaterials in the industrial automotive applications. In the aspect of the automotive design solutions nanotubes possess especially advantageous properties, and one of their possible application is an intermediate layer of the catalytic converter in the engine exhaust system. This paper presents some results of the preliminary measurements of the conversion ratio of the oxidation converter which was obtained by coating a ceramic standard carrier with a layer of nanotubes on which platinum particles with diameters ranging from 2.5 to 5  $\mu\text{m}$  were pointwisely deposited. Thereby some characteristic of nanotubes was used, namely, their especially advantageous area/volume ratio allowing to enlarge an area of the contact of the catalyst, which is platinum, with exhaust gas. According to the authors' opinion the obtained results theoretically confirm the possible profits resulting from the described nanomaterial application and they present the first stage in the optimization process. The industrial use of the nanomaterial converter with the proposed construction solution is conditioned by a cost-and-profit calculation in comparison with costs of the conventional converters. However, in the presence of the observed intensive process of the reduction in nanomaterial production costs it is worth continuing studies on new fields of their applications.

## References

- [1] Gebhard, A., Knör, N., Hauptert, F., Schlarb, A., *Nanopartikelverstärkte Hochleistungsthermoplaste für extreme tribologische Belastungen im Automobilbau*, Tribologie und Schmierungstechnik 4/2008
- [2] Haque M.H., *Application of the month: Carbon Nanotubes Sensors*, NanoSprint Carbon Nanotubes 6/2006, Grenoble 2006.
- [3] Jing Li, Cinke, M., Wignarajah, K., Fisher, J., Partridge, H., *Impregnation of Catalytic Metals in Single-Walled Carbon Nanotubes for Toxic Gas Conversion in Life Support System*, SAE, 2004-01-2492
- [4] Jurkowski, B., *Nanotechnologia i Nanomateriały*, www.put.poznan.pl.
- [5] Kempa, K., *Photonic crystals based on periodic arrays of aligned carbon nanotubes*, NANO LETTERS 3 1, pp. 13-18, 2003
- [6] Kolaric, I., Nemec, D., Weis, D.G., *Kohlenstoffnanoröhrchen für Scheibenheizung und Karosserie*, ATZ 8/2008
- [7] Mazurkiewicz, A., *Nanonauki i nanotechnologie stan i perspektywy rozwoju*, Wydawnictwo instytutu Technologii Eksploatacji – PIB w Radomiu, Radom 2007.
- [8] Multi-author Work, *Analysis Concerning the Use of Nanomaterials in the Automotive Sector*, 6<sup>th</sup> Frame Programme of the EU; SWOT, [http://www.nanoroad.net/download/swot\\_ai.pdf](http://www.nanoroad.net/download/swot_ai.pdf).
- [9] Reichenbach, M., : ATZ Nachrichten 26.04.2007; [www.atzonline.de](http://www.atzonline.de).
- [10] Verpoort, C., Schlaefel, T., *Thermal Spraying of Nano-Crystalline Coatings for Al-Cylinder Bores*; SAE 2008-01-1050.



## PROPOSITION OF METHODOLOGY FOR ENGINE LUBRICANTS RHEOLOGICAL PROPERTIES ESTIMATION

Jan Borgoń, Jarosław Sarnecki, Jerzy Zieliński

*Instytut Techniczny Wojsk Lotniczych, Zakład Materiałów Pędnych i Smarów  
ul. Kolska 13, 01-045 Warszawa  
tel. +48 22 6851714, fax. +48 6852088  
e-mail: jerzy.zielinski@itwl.pl*

### Abstract

*The paper presents methodology of engine lubricants' rheological properties estimation, that is extended in comparison with SAE J 300 specification. Modifications implemented in proposed method allow for better assessment of depressants and viscosity improvers added to engine lubrication oils. This methodology can be applied both at the stage of new formulations as in case of extended assessment of engine lubricants offered on commercial market.*

**Key words:** engines, engine oils, lubricants, rheological properties, laboratory tests

### 1. Introduction

Tribological properties of engine lubricants have been defined, both in the scope of test methods and requirements, in SAE J 300 viscosity classification [1].

Table. 1. SAE J 300 engine oils viscosity classification

SAE Visco- sity grade	Low temperature viscosity (starting), mPas, in temperature, °C  max.	Low temperature viscosity (pumping), mPas, in temperature, °C  min.	Kinematic viscosity in temperature 100°C, mm <sup>2</sup> /s		HT/HS viscosity in 150°C temperature, mPas  min.
			min.	max.	
0W	6200 w -35	60000 w -40	3.8	-	-
5W	6600 w -30	60000 w -35	3.8	-	-
10W	7000 w -25	60000 w -30	4.1	-	-
15W	7000 w -20	60000 w -25	5.6	-	-
20W	9500 w -15	60000 w -20	5.6	-	-
25W	13000 w -10	60000 w -15	9.3	-	-
20	-	-	5.6	<9.3	2.6

SAE Viscosity grade	Low temperature viscosity (starting), mPas, in temperature, °C max.	Low temperature viscosity (pumping), mPas, in temperature, °C min.	Kinematic viscosity in temperature 100°C, mm <sup>2</sup> /s		HT/HS viscosity in 150°C temperature, mPas min.
			min.	max.	
30	-	-	9.3	<12.5	2.9
40	-	-	12.5	<16.3	2.9 (for 0W-40, 5W-40 and 10W-40)
40	-	-	12.5	<16.3	3.7 (dla 15W-40, 20W-40, 25W-40 and 40)
50	-	-	16.3	<21.9	3.7
60	-	-	21.9	<26.1	3.7

## 2. Interpretation of SAE J 300 viscosity classification

Rheological properties test methods differ from one another in the scope of:

- test temperature,
- shear stress,
- cooling or heating time,
- viscosimeters construction.

Table 2. Selected parameters in test methods of engine oils rheological properties

Parameter	Test method	Shear stress	Temperature of testing	Cooling/heating time	Viscosity measurement
Low temperature viscosity (starting)	ASTM D 5293	high	-10, -15, -20, -25, -30 and -35°C	240 s	pointwise
Low temperature viscosity (pumping)	ASTM D 4684	low	-15, -20, -25, -30, -35 and -40°C	from 45 to 51 h	pointwise
Kinematic viscosity	ASTM D 445	low	100°C	900 s	pointwise
HT/HS viscosity	ASTM D 4741 ASTM D 4683	high	150°C	120 s	pointwise

The main advantage of SAE J 300 viscosity classification is that it reflects the operating conditions of lubricant in an engine:



- During start-up,
- Immediately after start-up, during lubricant pumping into tribological system,
- In connecting-rod bearings.

The main advantages of SAE J 300 viscosity classification are:

- Pointwise measurements of viscosity,
- Not reflecting the process of engine lubricant mechanical degradation during normal operation.

The attempt has been made to implement to SAE J 300 viscosity classification a low temperature method, that to complete measurements of dynamic viscosity (pumping), based on continuous measurement of lubricant dynamic viscosity during long-term cooling. It is a Brookfield scanning test performed according to ASTM D 5133 standard.

In the scope of taking into consideration the process of lubricant viscosity decrease due to mechanical degradation of viscosity improvers, no requirements have been implemented. The only test method is testing the decrease of viscosity after 30 shear cycles in „pump-injector” rig, which was implemented in different specifications for engine oils.

### 3. Proposition of a method for estimation of engine lubricants rheological properties

Some percentage of engine lubricants offered on the market do not conform to requirements of SAE J 300 viscosity classification in the scope of rheological properties.

*Table 3. Results of rheological properties tests of SAE 15W-40 engine lubricants (according to ASE J 300) offered on Polish market [2]*

Parameter, unit of measurement	Requirement according to SAE J 300	Results of tests				
		Oil no. 1	Oil no. 2	Oil no. 3	Oil no. 4	Oil no. 5
Kinematic viscosity in 100 <sup>0</sup> C, mm <sup>2</sup> /s	12,5-16,3	13.33	<b>11.96</b>	14.87	<b>16.54</b>	14.39
Kinematic viscosity in 40 <sup>0</sup> C, mm <sup>2</sup> /s	-	97.23	89.34	104.5	154.5	118.7
CCS viscosity in -20 <sup>0</sup> C, mPa·s	max. 7000	6700	6500	6200	<b>9700</b>	<b>7200</b>
MRV viscosity in -25 <sup>0</sup> C, mPa·s	max. 60000	23800	22600	19400	56900	35600
HTHS viscosity in 150 <sup>0</sup> C, mPa·s	min. 3.7	3.7	<b>3.3</b>	4.1	4.7	3.7

Next problem is that engine lubricants, even conforming to requirements of SAE J 300 classification In scope of rheological properties, sometimes are a reason of engines failures.

So the authors of this paper propose the wider consideration of engine lubricants reological properties testing.

Proposed methodology of rheological properties testing extends requirements of SAE J 300 viscosity classification by the following elements:

- Drawing a trapezoid of viscosity decrease with talking into consideration decrease of engine lubricant dynamic viscosity decrease after 150 shear cycles In „pump-injector” rig for tests with both low and high shear stress (testing the resistance against mechanical degradation). This testing enables determination of hysteresis of lubricant viscosity change caused by mechanical degradation [3] [4] (trapezoid area),

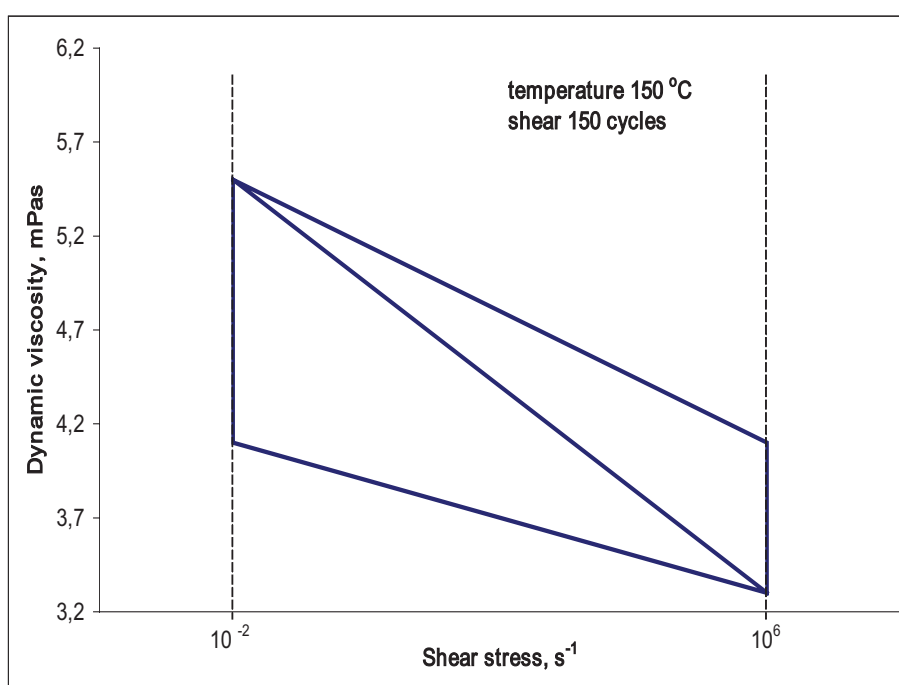


Fig. 1. Viscosity change trapezoid for SAE 20W-50 engine lubricant (low resistance against mechanical degradation)

- Drawing the curves of dynamic viscosity (pumping) change and dynamic viscosity (starting) for a few measurements performed for different testing temperatures, which enables determination of viscosity change during cooling (still not continuous but also not a pointwise) both for low and high shear stress,
- testing dynamic viscosity with Brookfield scanning viscosimeter (dynamic viscosity continous measurements during long-term cooling with low shear stress).

In the future, the next element of this methodology should be testing the influence of time on viscosity change (in this case its progressive increase) after mechanical degradation, due to polymer chains reconstruction in viscosity improvers.

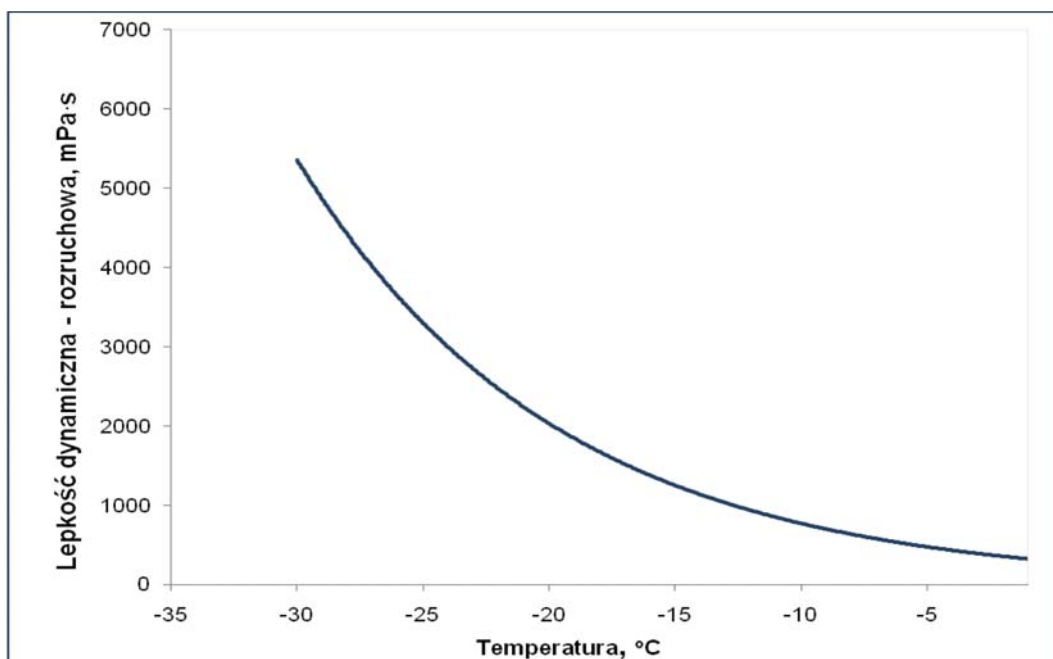


Fig. 2. Change of dynamic viscosity— starting for SAE 5W-40 lubricant

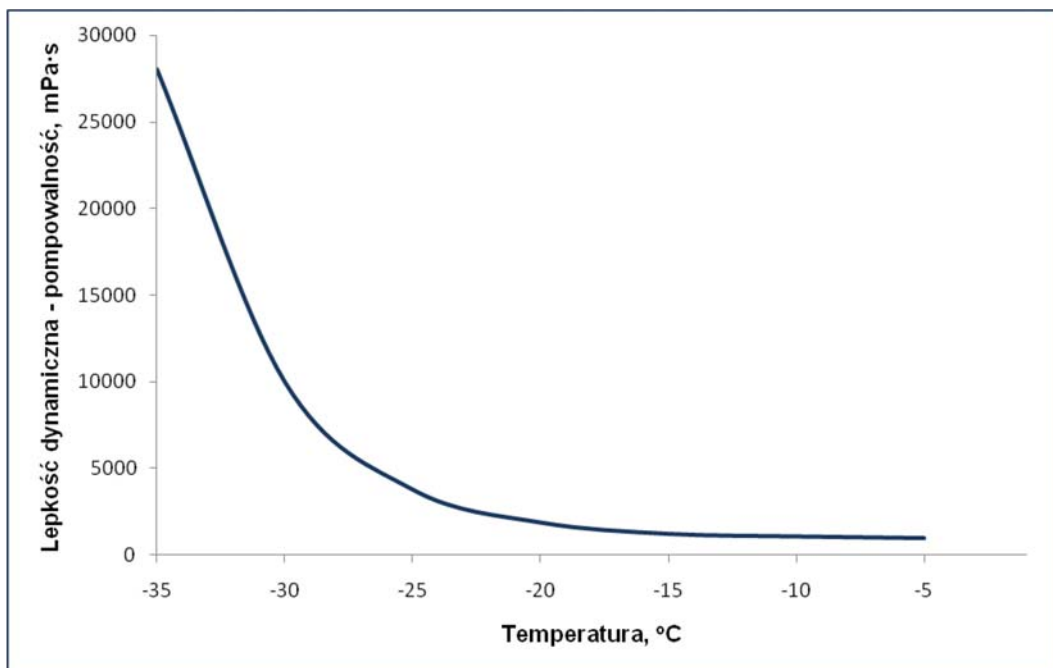


Fig. 3. Change of dynamic viscosity— pumping for SAE 5W-40 lubricant

#### 4. Summary

Proposed methodology of engine lubricants rheological properties testing may be applied in:

- testing of engine lubricants offered commercially on the market i.e. to assess the reason of engine failure,
- creating new technologies for engine lubricants production (viscosity and depressants quality assesment).

This may influence the quality improvement of commercially available engine lubricants in the future.

#### Literature

[1] *SAE Fuels & Lubricants Standard Manual*, HS-23 Edition 2004

[2] Zieliński J., Gołębiowski T., *Badania właściwości reologicznych olejów do silników samochodowych środków transportu – stan aktualny i nowe propozycje*, Materiały międzynarodowej konferencji „Systemy logistyczne – teoria i praktyka”, Spała 2008

[3] Briant J., Denis J, Parc G., *Rheological Properties of Lubricants* - Institut Francais du Petrole, Edition Technip 1989

[4] Fidos H., *Sposoby przeprowadzania badań reometrycznych mediów o parametrach reologicznych zmiennych w czasie*, Materiały konferencji „Reologia – teoria i praktyka”, Łódź 2008



## THE USE OF ACOUSTIC EMISSION FOR ASSESSMENT OF THE OIL LUBRICITY IN A FOUR-BALL TESTER

Piotr Bzura

Gdansk University of Technology  
ul. Narutowicza 11/12, 80-952 Gdansk, Poland  
tel. +48583472573

### Abstract

*In view of the increased dynamic and temperature load in the compression-ignition engine tribological systems, particular attention is drawn to the problem of such lubrication of the friction nodes that after breaking the boundary layer it could be restored without any wear occurring. Therefore, an idea has been devised of introducing to friction nodes, with the lubrication oils, of new substances (operational preparations) modifying the surface layer of friction elements, creating the so called servo-films as an effect of selective transfer at the extreme loads.*

*The paper presents a method of evaluation, by means of the acoustic emission (AE) symptom, of a lubricating oil, without operational preparations, through creation of the servo-film.*

**Keywords:** *acoustic emission, servo-film, friction node*

### 1. Introduction

An ideal situation in the compression-ignition engine operation would be if tribological systems could work in wear-free friction conditions in the extreme working states.

The lubricating oils used today, in spite of their indispensable advantages (e.g. heat abstraction, friction coefficient reduction etc.), still do not solve the problems of under-lubrication in the extreme load conditions. Therefore, research work is being carried out on the operational preparations [6] facilitating the servo-layer creation in the under-lubricated tribological systems.

The paper draws attention to the fact that compounds with similar properties as the operational preparations are spontaneously created in the lubricating oil during normal work and they can be identified by the acoustic emission parameters. Therefore, an analysis and evaluation of the boundary layer "reconstruction" (i.e. servo-film creation) process was performed based on measurements of the T-02 four-ball tester friction node with piezoelectric gauges connected to it.

### 2. The selective transfer phenomenon

In the development of knowledge on tribological phenomena, worthy of attention is the selective transfer effect creating on the friction faces a thin plastic non-oxidizable film of a specific structure. The selective transfer phenomenon consists in using the electric charge generated in the lubricating oil by friction of displacing surfaces for transporting the particles torn out of those surfaces.

The literature studies [4, 6, 7, 8] indicate two dominating hypotheses explaining the selective transfer mechanism:

1. Mechanism based on microadhesive joining the soft metal particles with the hard metal friction face. In the first stage the created protective film is composed of the soft metal particles. That composition can change when conditions favourable to the selective transfer process occur.
2. Mechanism based on the electro-chemical process of protective film creation. The film contains only one metal added to the lubricating oil in the form of a metallizing admixture. In the case of copper alloys - copper is transferred.

The selective transfer effect in a friction node requires the use of lubricating materials allowing to generate oxide films on the friction faces and also capable of electro-chemical copper decomposition. The copper release and transfer process is an outcome of the reaction of lubricating agent with the friction node surface. The copper and iron ions are then generated "reconstructing" the friction node boundary layer.

The ionic bond is a non-directional bond where electrostatic attraction occurs between ions generated in the total transfer of valence electrons from a less electronegative atom to a more electronegative atom. In effect of the electron transfer, the first atom becomes a positive ion (cation) and the second one a negative ion (anion). The ion generating is connected with the ionization energy, i.e. the energy needed for abstraction of the most loosely bound electron from a single atom. The ionization energy is usually expressed in electron volts ( $1 \text{ eV} = 1.60210 \cdot 10^{-19} \text{ J}$ ) [1].

The boundary layer "reconstructing" servo-film is created when a sufficient number of copper ions is generated for the selective transfer process to be started. Therefore, the time needed for generating the sufficient number of copper ions is also a meaningful parameter of the servo-film creation process. Creation process of the servo-film in a friction node may be identified [5] with slide bearing operation and expressed in joule-seconds [J·s].

### 3. Research methodology

The investigations with T-02 four-ball tester were carried out in three variants with the Marinol RG1240 lubricating oil and 8S20UD-H.Cegielski-Sulzer engine, namely:

- fresh oil (not used for lubrication before),
- used oil,
- used oil with 5% content of MDO fuel the engine is fed with.

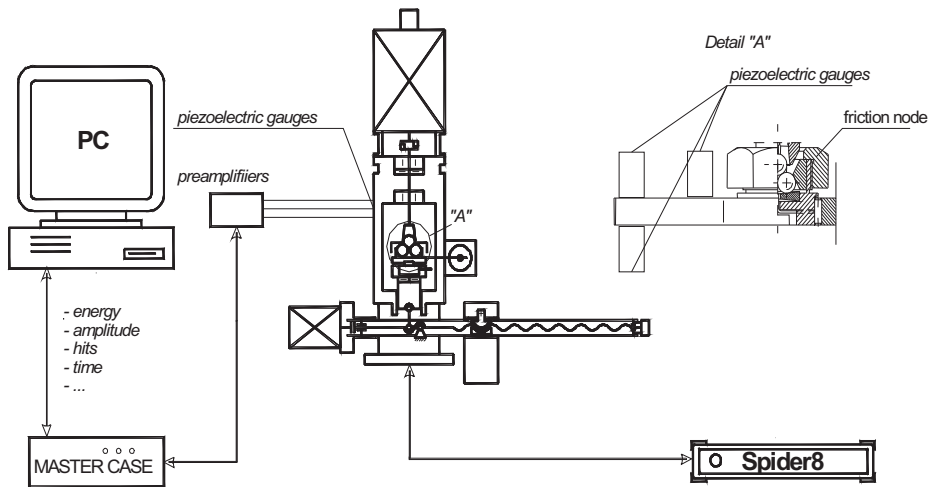
The investigation parameters were the following:

- spindle rotational speed: 1000 rpm
- load increase rate: 409 N/s
- initial load: 0 N
- maximum load: 7400 N

The friction node consisted of bearing balls, 12.7 mm diameter, made from the ŁH15 steel (ferrous alloy with average content of 1% C, 0.02% S, 0.3% Ni, 0.3% Cu), in the accuracy class 16 according to the PN-83/M-86452 standard, submerged in the lubricating oil tested.

Each test in the T-02 four-ball tester was additionally analysed by the acoustic emission gauges of a Vallen AMSY-5 apparatus set (Fig. 1 and 2) [2].

The increased content of copper in the investigated lubricating oil sample of the friction node was measured with a Philips X-Met 920 spectrometer [3].



Schematic diagram of the Vallen-Systeme GmbH

Schematic diagram of the T-02 four-ball tester

Fig.1. Test stand diagram [2]

The acoustic emission phenomenon demonstrates itself by generation and propagation of elastic waves originated in the T-02 four-ball tester friction node during the dynamic processes proceeding in it. The propagating elastic wave is recorded by piezoelectric gauges mounted on the friction node as an acoustic signal (pulse), as shown in the Fig. 2 diagram.

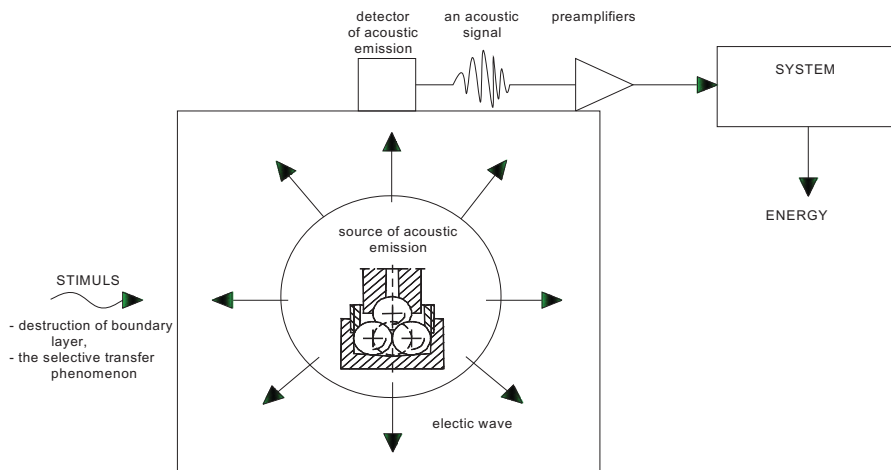


Fig.2. Acoustic emission phenomenon on T-02 four-ball tester friction node

The investigations performed with the T-02 four-ball tester connected with piezoelectric gauges, where the friction node consisted of a set of four steel balls submerged in the tested oil, are aimed at monitoring the boundary layer "reconstruction" process (Fig.3).

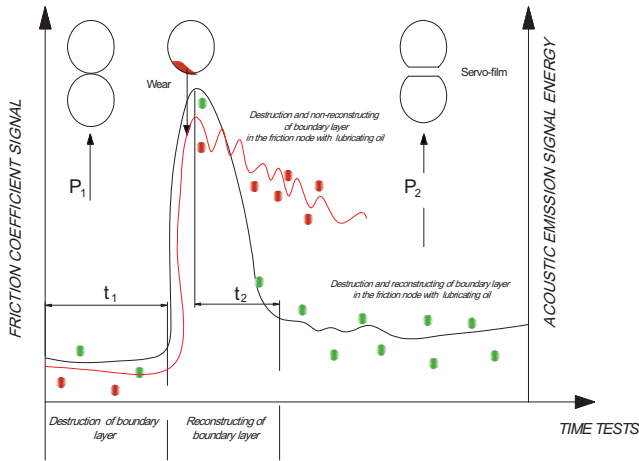


Fig. 3. Destruction and possible reconstruction of boundary layer

where:

- - destruction and non-reconstructing of boundary layer (friction coefficient signal),
- • • - destruction and non-reconstructing of boundary layer (acoustic emission signal energy),
- - destruction and reconstructing of boundary layer (friction coefficient signal),
- • • - destruction and reconstructing of boundary layer (acoustic emission signal energy).

#### 4. Analysis of test results

Results of the investigations of physical and chemical properties during the boundary layer "reconstruction" are presented in graphical figures 4 to 7 and in Table 1.

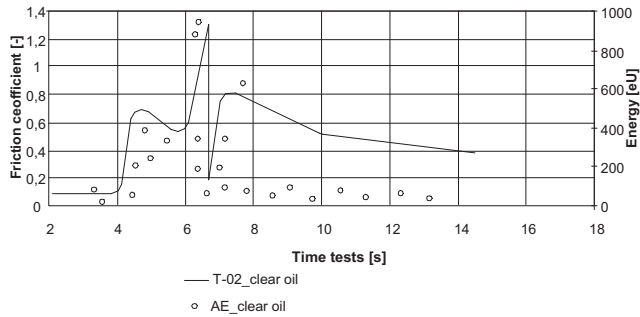


Fig. 4. Destruction and non-reconstructing of boundary layer in the friction node with fresh Marinol RG1240 lubricating oil

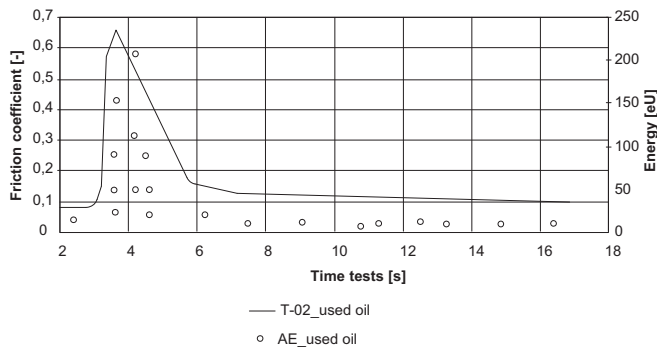


Fig. 5. Destruction and reconstruction of boundary layer in the friction node with used Marinol RG1240 lubricating oil



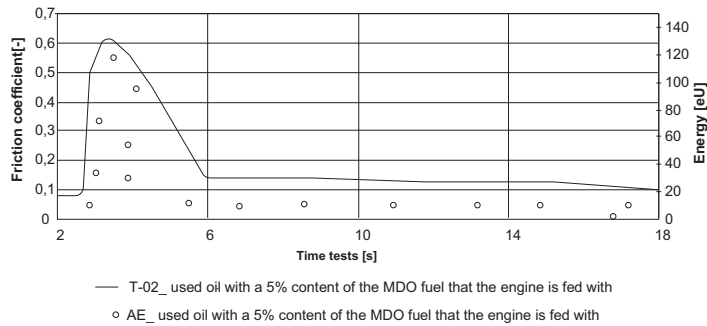


Fig. 5. Destruction and reconstruction of boundary layer in the friction node with used Marinol RG1240 lubricating oil with 5% MDO

Table 1. Results of the investigations of physical and chemical properties during the boundary layer "reconstruction"

Marinol RG1240 lubricating oil	$E_1$ [eU]	$E_2$ [eU]	$E$ [%]	$Cu_1$ [ppm]	$Cu_2$ [ppm]	$\Delta Cu$ [ppm]
clear oil	900	450	50	112,44±1,23	121,06±1,237	8,62
used oil	200	12	94	122,44±1,297	143,11±1,27	20,67
used oil with 5% MDO	120	12	90	122,44±1,297	133,00±1,252	10,56

where:

$E_1$  – acoustic emission signal energy for the boundary layer destruction,

$E_2$  – acoustic emission signal energy for the boundary layer "reconstruction",

$$E = \frac{E_1 - E_2}{E_1} \cdot 100 - \text{loss of the acoustic emission signal as a fitness for use measure,}$$

$Cu_1$  – copper content in an oil sample before the friction node test,

$Cu_2$  – copper content in an oil sample taken after the friction node test.

Small acoustic emission signal loss ( $E = 50\%$ ) shows "non-reconstructing" of the friction node boundary layer, i.e. selective transfer did not occur. Therefore, this acoustic emission signal may be considered a symptom of not full friction node fitness with respect to the extreme loads.

## 5. Acoustic emission as a diagnostic signal

Lubricating oil is a significant element of the compression-ignition engine tribological systems as it contains necessary information for determining diagnostic relations of such systems. Those relations are needed for building a tribological system diagnostic model. Development of such model, useful in practical engine operation, requires reliability of the diagnostics.

The measurement results are a signal, in the form of acoustic emission, containing the status information. It has been demonstrated that there is a possibility of increasing the reliability of diagnostics by using the acoustic emission parameters for determining the servo-film effect.

In the proposed procedure, the servo-film effect is understood as transfer of ionization energy, in the form of work, coming from an extreme load of the friction node in a specified time  $t$  and causing "reconstruction" of the boundary layer.

The servo-film effect in the proposed version may be investigated by carrying out precise measurements and then expressed in the form of a number with joule-second as the measurement unit.

## 6. Final remarks and conclusions

The main objective of the work was to present the possibilities of using the acoustic emission

as a diagnostic parameter in the friction node condition determining laboratory test. Generating the copper ions is worthy of attention. Investigating of samples with the X-Met920 spectrometer allowed to conclude that the increase of copper content in the used Marinol RG1240 oil had a positive impact on the servo-film effect. In the copper ion generating process ionization energy is emitted - a component of the acoustic emission energy defining the servo-film effect.

Additionally it was found that during operation some compounds were spontaneously created in the Marinol RG1240 lubricating oil improving its physical and chemical properties. However, the performed measurements did not provide quantitative conclusions on the friction node effects of that phenomenon (equivalent to introducing operational preparations) as no comparative tests were carried out.

## References

- [1] Astachow A.W., Szirow Ju.M.: *Quantum physics*. (in Polish) Wydawnictwo Naukowo-Techniczne, Warszawa 1990
- [2] Bugłacki H., Bzura P., Eichert P.: *Analysis and evaluation of wear changes in T-02 apparatus friction node revealed by acoustic parameters*, (in Polish) Project financed by the Ministry of Science and Higher Education, No. 08/08 PB
- [3] Bzura P.: *The use of spectrometric diagnostics in identification of the Technical condition of tribological systems*. Journal of Polish CIMAC (vol.3, No.2), Gdańsk 2008
- [4] Garkunov D.N.: *Effect der Verschleiblosigkeit – eine neue Etapie bei der Verbesserung des Verschleiblosigkeit von Maschinenelement*. Schmierungstechnik, nr 3/87
- [5] Girtler J.: *Concept for interpretation and assessment of slide bearing operation in diesel engines in probabilistic approach*. Journal of KONES , Warszawa 2007
- [6] Laber St.: *Investigation of the operational and lubricating properties of a metal refining agent*. (in Polish) Uniwersytet Zielonogórski - 2003
- [7] Marczak R., Burakowski T.: *Operational top layer and its testing*. (in Polish) Zagadnienia Eksploatacyjne Maszyn, z.3 (103) 1995;
- [8] Marczak R.: *Progress in the Perkunov effect investigations*. (in Polish) *Materiały konferencji "Problemu bezzużyciowego tarcia w maszynach"*. Wydaw. WSI Radom, Maj 1993



## ANALYSIS OF SHIP SHAFT LINE COUPLING BOLTS FAILURE

**Czesław Dymarski**

Gdansk University of Technology  
Ul. Narutowicza 11/12, 80-952 Gdansk, Poland  
tel.: +48 58 34716 08, fax: +48 58 3414712  
e-mail: [cpdymars@pg.gda.pl](mailto:cpdymars@pg.gda.pl)

**Mgr inż. Marek Narewski**

Polski Rejestr Statków SA  
Al. gen. J. Hallera 126, 80-416 Gdańsk, Poland  
tel.: +48 58 3461700, fax : +48 58 3460392  
e-mail: [m.narewski@prs.pl](mailto:m.narewski@prs.pl)

### *Abstract*

*The ship propulsion shaft line is one of the most critical ship components having big influence on a ship safety. Because of that, there is well known need for proper shaft line survey either by ship crew, ship owner technical services as well as by classification society surveyors. One of the most dangerous and frequent kind of shaft line failures, especially on old ships, is a fatigue break of the collar coupling bolts. It usually causes the loss of the possibility to use the main propulsion system. In case of the bad weather and severe sea conditions it can lead even to the ship loss. The paper presents some data on failure statistics that was observed to shaft lines and propulsion system machinery. Furthermore, analyses of causes and generation mechanism of the mentioned fatigue breaks of the collar coupling bolts is presented.*

**Keywords :** ship propulsion system, shaft line, alignment, failure

## 1. INTRODUCTION

Ship machinery equipment failures and in particular propulsion systems are quite frequent cases during ship operation. Failures in shafting are also important figure in all machinery failures. An example of specific failure is breaking of coupling bolts in main propulsion shaft collars.

However, that type of machinery damage is not very frequent, the failure itself is potentially very dangerous as it could lead to the loss of control over propulsion and manoeuvrability of the ship. That situation could result further in severe losses like the ship and cargo and possibly environmental disaster. A severe sea conditions can multiply potential damages and turn them from local to global scale that could finally be very costly and ship operator or owner could be taken to court.

The risk of ship failures is much higher in worse sea conditions due to dynamic nature of propulsion system with diesel engine as it operates with shaft overloading by torque and bending moments and resultant load pulsation.

Underneath, there are given some examples of the above mentioned failures and related discussion of damages in the analysed shaft joints for the two specific types of propulsion systems.

a)

Failure statistics in shipping for years 1996-2000 [1] according to insurance companies							
Failure reason	Heavy weather	Contact	Collision	Grounding	Machinery	Fire/Explosion	Other
	3%	9%	21%	20%	31%	6%	10%

b)

Machinery claims by cost in period 1998-2004 [1] according to insurance companies						
Failure place	Main engine	Steering gear	Aux. engine	Boilers	Propulsion	Other
	43%	10%	20%	31 %	23%	2%

Fig. 1 Failure statistics in shipping according to data collected by insurance companies:  
a) Failure Statistics for 1996-200, b) (Machinery claims by cost 1998-2004) [1].

Type of ship	Number of shaft alignment failures
Bulk carrier	3
Chemical carrier	1
Container carrier	1
General cargo carrier	3
Offshore supply vessel	43
Oil carrier	7
Passenger vessel	1
Special purpose vessel	15
Tug	32
Yacht	7
Source: ABS	

Fig. 2 Alignment related failure statistics [2].

## 2. The main types of loading in shaft-line joints

In a typical ship propulsion system, there are the following types of load that are generated during the propulsion system operation:

- Torque moment;
- Bending moment
- Axial thrust force
- transverse loads that consists of gravity force of the shaft line system components and inertial and centrifugal forces.

The influence of the listed above loads on the strength and durability of the shaft line joints depends on the type of the main propulsion diesel engine and the shaft line construction. We analyse two the most popular types of the ship propulsion systems.

### 2.1. Conventional propulsion system with low speed reversible diesel engine and fixed pitch propeller

In the conventional propulsion system the dominating load is torque moment. Due to the shaft connection of the diesel engine with shafts and propeller without highly elastic couplings and due to the low engine diesel speed (even for steady sailing conditions – ahead) there are pulsations of the load. The reason for this is a limited number of propeller blades as well as the number of engine heads. The amplitude of pulsation values depends mainly on actual sea conditions and changes of ship hull resistance and propeller submersion that results from action of waves. It must be pointed out, that maximal load due to torque occurs in case of the requirement to stop ship instantly. The change of the engine rotation direction, which takes relatively short time, leads to substantial increase of the nominal torque (could be even doubled) during the procedure of the engine reverse manoeuvre. It could be clearly observed in the Fig 3 presenting characteristic curves of the propulsion system during this maneuver.

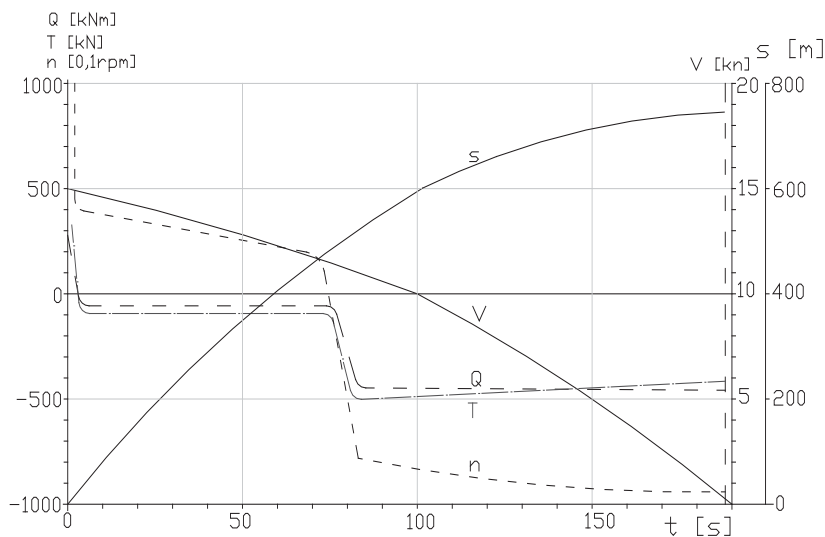


Fig. 3 Characteristic curves of major parameters of a propulsion system composed of diesel engine – constant pitch propeller during “crash stop” of the sea ferry at speed  $V=15$  knots (7,7 m/s).

Legend:  $n$  – propeller rpm;  $s$  – breaking distance;  $Q$  – torque moment at propeller shaft;  $T$  – thrust;  $V$  – vessel speed;  $t$  – time. [3]

The change of rotation direction of the shaft is accompanied not only by torque moment overloading and moment direction change but also by change of the thrust force direction.

As a consequence, the force that pressed shaft collars by means of coupling bolts is decreasing. The frictional moment that takes vital part of maximal torque moment decreases accordingly.

Other important issue is the increase of possibility of mutual displacement of the shaft collar joints. The same risk could appear during main engine reverse on shallow water or in the area of floating ice when the propeller blade could hit bottom or other obstacle. The probability of the discussed displacement of collars and the relative sag and gap are dependant on the initial tension force of coupling bolts and the fit force of the bolts

In case there will appear displacement of the shaft collars under load than the new position of collars will have no advantages for normal working conditions and sailing with “ahead speed”. The reason is the decrease or even disappearance of participation of the cylindrical surfaces of fitted bolts in bearing of the torque moment. Appearance of overloading by torque or presence of bending moment could lead to additional movement of coupled collars in the direction of original position. Taking into consideration of the dynamics of that displacement and resulting micro-deformations and wearing of contacting surfaces we can assume that new position is not to be exactly the same.

Having in mind longer operational time, we can observe repeating action as previously described.

It is for sure, that with each displacement of shafts collars the probability of next displacements grows and grows also the value of movements and wearing rate of the contacting surfaces.

The presented wearing process that exists where micro displacements of adjacent surfaces are known as fretting. As a result of fretting the creation of micro notches that further could develop into fatigue cracking. With the increase of wearing area and value of collars displacements, the bolts linking the collars are subjected more to bending, that also accelerates fatigue up to final breaking. The breaking of one bolt, leads to the increase of loading of the remaining bolts and further breaks of collar bolts up to total lost of the shaft integrity. The view of shaft collar where fitted bolts were broken is presented in Fig 4.



*Fig.4. An example of failure of the shaft collars and fitted bolt holes in the propulsion shaft [4].*

The case of coupling bolts, failure in the propulsion shaft line has been described in paper [1]. It took place on the small tanker during engine reversing and ship moving astern. The all, eight bolts coupling bolts linking collars of intermediate and propeller shaft were broken and consequently it resulted in the lost of ship propulsion and manoeuvring abilities. Fig. 5a and b presents more details of that case with indication of the bolts cross-sections and their position in the shaft collar.

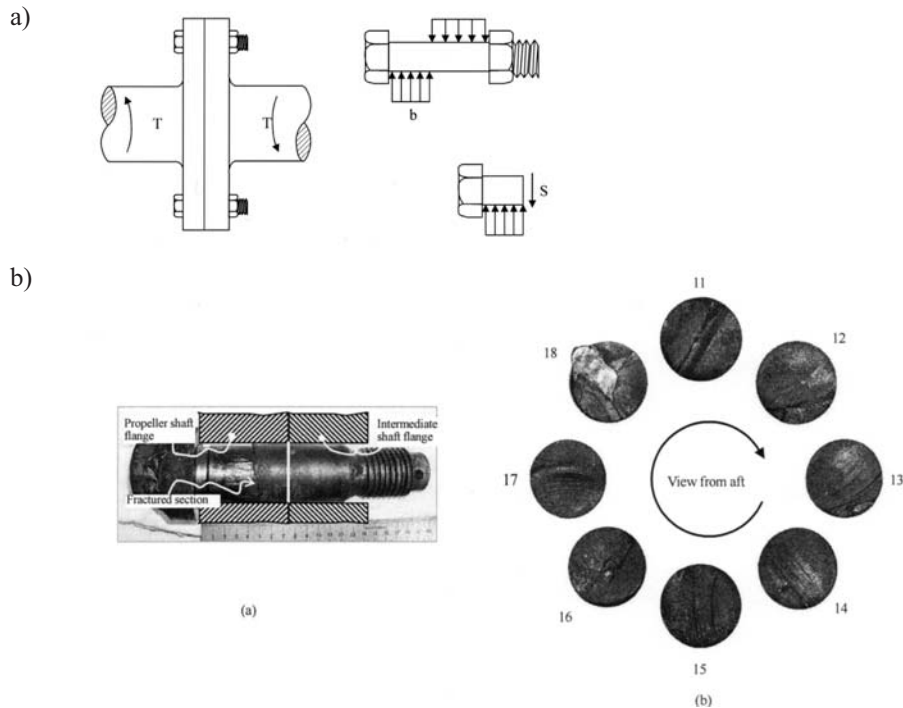


Fig. 5. a) Bolted connection of the shaft collars and collar with broken bolt, b) View of the fatigue cross-section with original position of the broken bolts in the shaft collar [5].

The specific feature of the presented cross sections is direction of failure growth, that according to the authors of the reference [5] is angled  $35^\circ$  to  $60^\circ$  from the action line of the shear force. The publication do not contain the explanation of the phenomena.

We must point out the one more important issue of the discussed failure - the plane of fracture is not lying in the shear plane of the bolt but is located in the fitted area of shaft collar holes. It means that creation of fatigue fracture is result of variable bending stresses in coupling bolts. The hypothesis was further proofed by experimental research and calculation with using of numerical methods as is presented in Fig 6.

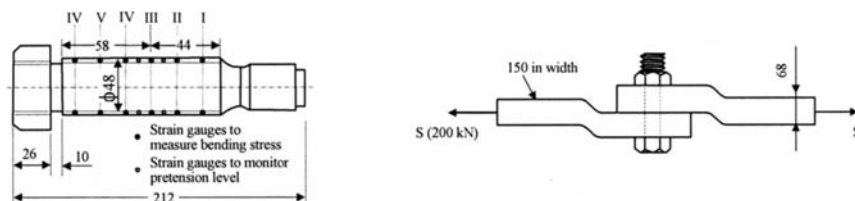


Fig. 6. The view of the bolt used for experimental testing and position of the strain gauges in the tested bolt [5]



The experiment included the measurement of stresses in the fitted area of the bolt using strain gauges technique. Strain gauges were placed in two shallow grooves cut along the bolt and located at 180 arc in the plane of the load action. The gauges were fitted in pairs – one opposite another in six cross-sectional planes as it is presented in the Fig. 6. The final testing was carried out for five different values of pretension ranging from 0 to 0,55  $R_e$  of the bolt material and for three different clearance values of the bolt: 0,16 mm clearance, 0,007 interference and 0,013 interference. Tensioning force has been varied in the range of 150 – 250 kN.

The results of the research, showed that highest bending stress exists in the long fitted area of the bolt outside of the shear plane. The lowest value that stress was found to be in case of highest bolt tensioning and tight interference. On the other hand, there is no evidence that the experiments has not been carried out to initiate fatigue breaking of the bolts. Lack of that testing did not allow to check, whether direction of the fatigue fracture growth rate is in agreement with the shear load acting on the bolt.

It could be stated, that the directional deflection of the fracture growth direction and shear load direction is also result of the bending moment of the shaft. The reason for that is that described failure took place in the joint of propeller and intermediate shaft, where bending moment are taking highest values, even in a correctly assemblies and aligned shaft line. The explanation is in a fact of substantial loading of the shaft line tail by dynamically rotating ship propeller and typical plain bearing solutions.

Due to the necessary radial clearance, plain bearings do not protect the shaft against deflection and deviation from the theoretical shaft line axis. It means, that bolts joining and fixing shaft collars will be loaded additionally by axial force, variable in value. The variation of that force results not only from loading by the propeller mass but also from non uniform hydrodynamic pressure field that is passed by the propeller blades during every rotation. Moreover, in case of big ships or hulls having low stiffness, substantial shaft line bending load may appear as a result of ship hull deformation on waves, particularly important in high sea states, when displacement of the bearing axis takes place, as it is presented in Fig. 7.

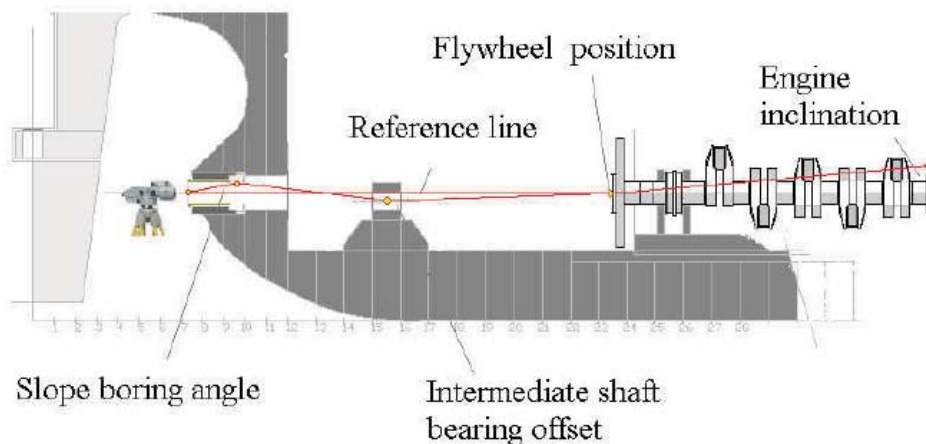


Fig.7. Positioning the Bearings to Actual Design Values [2].

It can be assumed, that the listed above factors were reasons for the change of the resultant bearing load plane acting on the bolts in the shaft coupling and the observed deflection of the fatigue fracture growth up direction.



## 2.2. Propulsion system with low speed diesel engine and controllable pitch propeller (CPP)

Propulsion systems with CPP experience much better conditions of loading of the collar coupling bolts by torque. The torque keeps constant direction and overloads (if exist) are lower and are not so frequent, practically only during instant stopping manoeuvre or in case the propeller blade hits an obstacle. On the other hand, the loading of the shafts and their joints by the bending moment grows up. There are two reasons for that. First, the mass of the propeller is higher comparing fixed pitch propeller. Secondly, the intermediate shaft coupled with the propeller shaft named camshaft do not have bearing in the hull but is hanging on the propeller shaft and a intermediate shaft. Moreover, it is loaded additionally by oil distribution box, which is used to introduce oil from the fixed hydraulic supply unit to the servo-motor located usually inside the propeller hub. Consequently, the mass of shaft assembly and hydraulic components for pitch control are also additional source of the bending moments. It must be pointed out, that the loads in such case are relatively simple for numerical calculations and propulsion system designers are able to provide suitable strength to the shaft line.

The worse situation exists with accidental and non predictable loads that originates during ship operation. Some possible sources that we can list are: deflections of ship hull due to action of waves, bending of the shaft or loss of bearings alignment that possibly could be result of repair, maintenance services done for machinery or machinery equipment replacement that could took place on every ship.

As an example, the shaft bending or bearing that is not aligned correctly with the shaft line axis could generate shaft bending loads leading to the permanent change of shaft geometry and in a consequence it will result in variable loading of the coupling bolts in shaft line collars. In the worse case, the coupling bolts could be broken by the fatigue. A characteristic feature of that type of failure is that it could have place during normal sailing conditions and quite probably not all the bolts could fail at once. Most frequent situation will be the case where the highest loaded bolt could break first or failure will happen to two neighbouring bolts. Consequently, the stiffness of the shafts joint will be decreased and bending stresses in other bolts will be lowered due to bending. An example of bolts destruction due to that type of failure a partly presented in the Fig 8. The contact area of the collars as well as fitted bolts and their holes were worn substantially. It is non disputable in that case, that failure was accompanied by mutual displacements of mating parts as well as by fretting.



*Fig. 8. The view intermediate shaft collar with broken bolts and fractures cross-section of the failed bolts with nuts. [4]*

### 3. Conclusion

The problem of fitted bolts failure in coupling collars of the main propulsion shaft line originates in a complex stress condition during the real ship drive system operation. The possible failure of that type is more probable in case of older ships, that are in operation for more than 15-20 years. Breaking of the fitted bolts in the shaft line collars is potentially very dangerous event and its avoidance is possible due to proper control over propulsion system in ship operation. Suitable control of the shaft line alignment using the proper tools should be used as obligatory diagnostic procedure in case of detection certain abnormal behavior of shaft line i.e. excessive wearing of intermediate bearings, accelerated stern bearing clearance growth, bearings foundation structure or its weld cracks or shaft vibrations that were not observed during earlier ship operation. The cost of potential failure of that type could be very high and resultant repair could take several weeks.

Due to the fact, that providing the continuity of survey over ship machinery requires repeatable observations and follow on analysis of the observed events during the propulsion system operation. It is very important to note and record all that events as they may have possible influence on abnormal behavior of the shaft line. The biggest number of observations can be done by the machinery crew, providing they have suitable training and basic knowledge regarding shaft line problems during operation. The instrumentation for propulsion system or shaft monitoring is almost not available for majority of ships that are currently in operation. Due to financial reasons it will be probably very rarely used in case of older ships. The availability of the dedicated propulsion monitoring systems in future may be much wider and we can expect that there will be more data collected regarding the shafting behavior or failures and the data collected could be suitable for propulsion shaft line failure analysis, if such will be required.

In case of shaft line failure of the similar type as the cases described above, we recommend to gather sufficient details (including broken bolts and nuts) and also all other evidence immediately after failure as that could be very helpful for determination of the optimal repair technology and for taking corrective measures for ship safety due to elimination of the failure source.

### References

- [1]. Lars A. Malm, Mechanical Failure – the facts, Marine Claims Conference, 2007
- [2]. Chris Leontopoulos, Shaft alignment and powertrain vibration, ABS
- [3]. Brownlie K.: *Controllable Pitch Propellers*. The Institute of Marine Engineers. London, 1998.
- [4]. Materiały Polskiego Rejestru Statków
- [5]. V.Song, H.Shiihara, d.Shiraki, Y.Nagayama, Failure Analysis of propulsion shafting coupling bolts, Class NK, World Maritime Technology Conference, London 6-10 March 2006



## THE LIMITATION OF USE OF BIOCOMPONENTS IN THE FORM OF FATTY ACID METHYL ESTERS BASED ON ANALYSIS OF SELECTED TURBINE FUEL PROPERTIES

Wojciech Dzięgielewski

*The Technology Institute of Air Force  
Petroleum Oils and Lubricants Division  
13 Kolska str., 01-045 Warsaw, Poland  
tel./fax: +48 22 6852088  
e-mail: wojciech.dziedzielewski@itwl.pl*

### Abstract

*This paper describes part of results of research work consisting in testing the possibility to use biocomponents in fuels for turbine engines. Because of some similarity and availability as well as that this is the first stage of work, the fatty acid methyl esters (FAME) (from rapeseed oils) were used as the basis biocomponent. Up till now, this ester was used as component of fuel for compression engines. There is no proved information on other use of FAME. The aim of research work is to show possibilities or rather restrictions and risk in case of new application. Some behaviour of biofuels or biocomponents are known. The common virtue is perfect lubricity, and the flaw is chemical and thermal stability. But, these are not only parameters we should notice analysing the applicability. This paper also tries to show other properties, that could restrict the use. It presents biofuels laboratory test results and points the expected problems in case of practical use of such mixtures. The results would be base to engine bench testing.*

**Keywords:** transport, turbine engines, fuel, biocomponents, properties

### 1. Introduction

There is no need to prove anybody that in recent times one of the most important, and publicized definitely thing is emission of various contaminants created during majority of fuels combustion process. Traditional source of energy necessary to power engines, to heat generation etc. are fossil fuels, mostly coal, crude oil and natural gas. Crude oil particularly is very troublesome raw material. Beside future problems regarding deposits mining and continuous rise of extracting cost, harmful effect of crude oil-based combustion products on environment is the second, very important aspect. Though more and more modern engine designs with better efficiency and restricted emissions, the range of engines use is so huge that they are one of the primary causes of environment pollution. The intensive work on developing and extense use of so called alternate fuels from other than crude oil sources has been undertaken. Currently, the biofuels and biocomponents are of most interest. There is some diversity resulting mostly from requirements set by various appliances - engines. In case of spark engines the biocomponents with low boiling points, mostly alcohols and their

derivatives - ethers are in use. In case of compression ignition (CI) engines mostly fatty acid esters are employed. It is also possible to power CI engines with specially modified ethyl alcohol-based fuel. Also there is one more very large group of engines - the turbine ones. They use very large quantities of fuel, so they have much more emissions in relation to piston engines. Moreover, it's more difficult to employ equipment for exhaust gases purifying or emissions restricting. It is important to replace oil-based fuel with alternate one that is less harmful to environment, even in the smallest extent. Of course there are also limitations, probably even more important than in case of fuels for piston engine. The primary limitation is engine purpose. The purpose determines engine operation conditions which in turn determine requirements regarding fuel characteristics. Though the rule of operation is similar, requirements regarding aviation engine fuels and fuels used in engines used at less severe conditions are quite different.

This paper covers fragment of the work regarding the possible use of fatty acid methyl esters (FAME) as component of hydrocarbon fuel. Selection of such biocomponent was conditioned by big similarity to base fuel (in the extent of essential physical and chemical properties) as well as availability. There is extended research work on various biocomponents in recent years however, FAME is the best recognized one so far. Besides, there are many manufacturers producing high quality products. This is very important since low quality would cause distortion of the results. Biocomponent was introduced into aviation kerosene (trade name Jet A-1). Intention of such selection was to check the application in as most severe as possible conditions. In such case every other application could be easier to fulfill requirements.

## **2. Description of selected physical and chemical properties**

There are some stereotypes used as base to evaluate biocomponents usefulness. Main reason for their use is lubricity. This parameter is the best known and the most frequently mentioned as biocomponents advantage. Actually, presence of even small FAME amount results in significant decrease of wear of mating elements. But, it should be noted that lubricity is not everything. The second parameter "improving" fuel properties is flash point. After introducing biocomponent of lower volatility into kerosene, the flash point of such biofuel increases resulting in better safety of fuel use. Unfortunately, besides these two advantages we can yet add only one - less harmful effect on environment. Rest of properties doesn't change with biocomponent content or become worse. It is not tantamount to elimination components of vegetable origin. It's important to not to allow to worsen parameters that influence on later use. Parameters that can change after biocomponent introduction are the following:

- + lubricity improvement,
- + flash point increase,
- + lower emission of most of toxic and undesirable exhaust components,
- density change,
- kinematic viscosity increase, and greater vulnerability to temperature lowering,
- freezing point increase,
- possible acid number increase (particularly in case of poor FAME quality or ageing process starting),
- thermal stability worsening,
- boiling range increase (influence on distillation),
- existent gum content increase,
- sudden decrease of water separation index and water reaction index,

- possible corrosivity increase,
- net heat of combustion decrease,
- possible water content increase,
- better conditions for microbial contamination.

Above mentioned are only some - the most important - changes caused by biocomponent presence in hydrocarbon fuel. As mentioned earlier, not all the changes can disqualify biofuel from use. Moreover, not all the mentioned changes can appear together at the same moment. This relates such properties that depend practically on manufacturing process parameters as water content, acid number, corrosivity, sulphur content etc. When components quality is appropriate, the quality and properties of finished biofuel (in above mentioned extent) don't change.

The characteristics of selected parameters regarding potential influence on fuel use in turbine engine are presented below.

### 3. Thermal stability

Thermal stability is recognized as fundamental reason for biofuels use restriction, especially in turbine engines. Performed tests confirm such thesis not entirely. Modern biocomponents are more often manufactured using technologies that allow to obtain stable product resistant to elevated temperatures. Antioxidants inserting is additional advantage.

Thermal stability testing in dynamic conditions (JFTOT) was performed according to modified technique consisting in repeated testing without change of fuel, test tube, and filter, until total disqualification of fuel. The results are presented on Fig. 1. From plots of upstream and downstream pressure it can be read that though cycle multiple repetitions there was no pressure increase showing building up of deposits - thermal decomposition products.

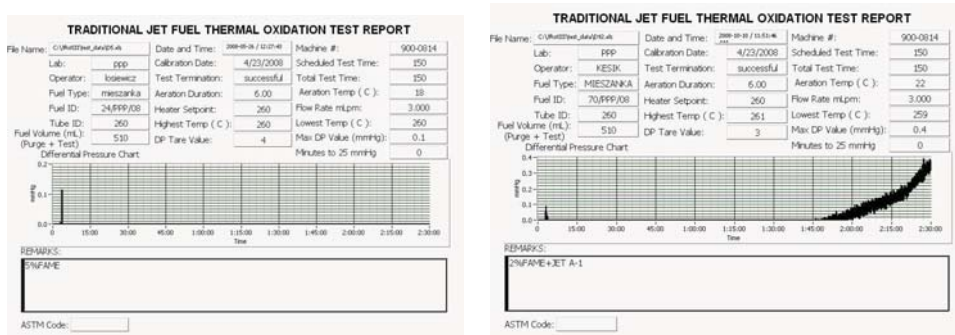
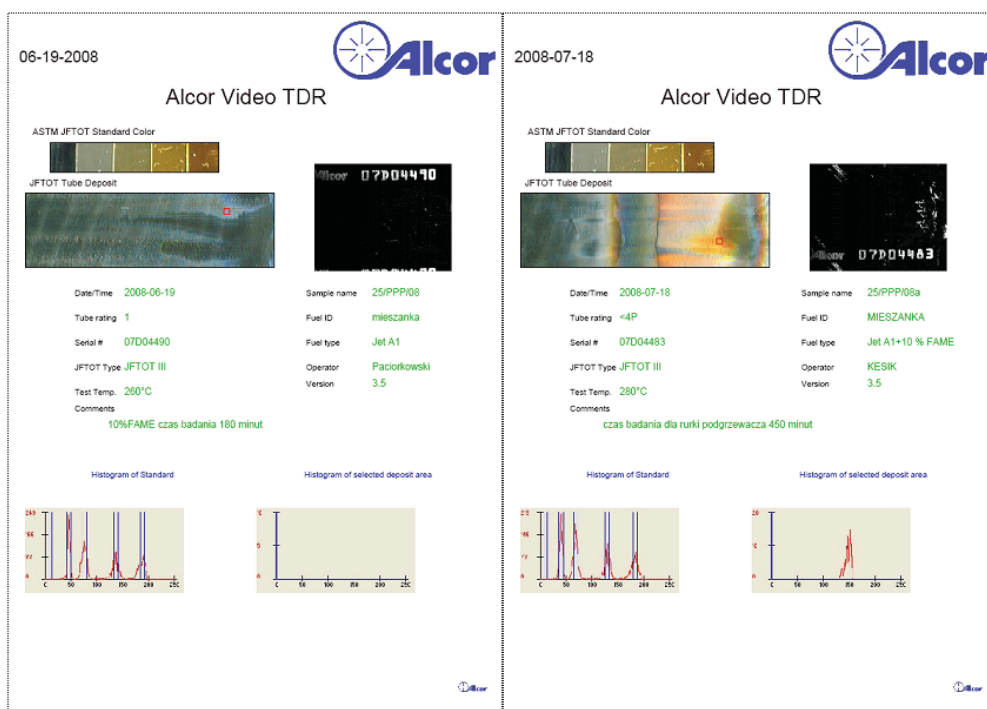


Figure 1. Example reports of thermal stability testing cycle course (cycle I and VI)

Spectra of tube deposits are displayed on fig. 2. It can be seen that coloured deposits were created after every 150-min cycles. Presence of such deposits formally disqualifies the fuel as usable. Test results of fuel with 10 % (V/V) biocomponent content showed that it behaves not worse than neat aviation fuel, so it's impossible to explicitly assess fuel applicability basing on this parameter.



Rys. 2. Example spectrum of tube deposit rating after thermal stability testing cycle course (cycle I and VI)

#### 4. Rheological and low temperature properties

Flaw of biofuels is restricted use connected with effect of low temperatures having much stronger influence on biofuels rheological properties than on hydrocarbon ones. The most evident symptom is internal friction resistance. It has decisive influence on resistance to fuel flow in fuel lines, and on quality of fuel spraying. Preparation of fuel-air mixture has an effect on ignition and combustion process.

Too low viscosity causes at particular injection pressure that fuel atomisation is not complete. Such conditions create small droplets that slow down quickly in thickened air, so the combustion process takes place in the vicinity of injectors. This causes local fuel excess resulting in incomplete combustion.

Too high viscosity also disrupts air-fuel mixture preparation process. It's because of too large fuel droplets that evaporate to slow causing incomplete combustion as well. Unburned fuel can build up on injectors causing injection characteristics change, and on other components of combustion chamber causing change of thermal properties of structural components. Moreover, range of the droplets is prolate causing combustion zone shifting. It can lead to shift flame front to inlet guide zone. This can cause excessive thermal effect on such components of engine. Moreover, too large droplets (coarse mixture) can have bigger range, so they can fall on vanes of inlet guide and on I-stage turbine causing mechanical degradation of their surface. Such phenomenon can, in the long range, lead to impairing external coating strength, and fatigue-based mechanical damages.



Too high viscosity also means pressure increase inside fuel system. This causes excessive forces generation in fuel system, especially in appliances generating high pressures leading to damages and leaking.

Introduction of FAME into traditional aviation turbine fuel means kinematic viscosity raise. So it is possible to meet problems caused by appearance of bigger particles and elevated pressures in supply system. According this we can assume that this parameter can restrict use of biocomponents.

There is another problem regarding kinematic viscosity. Viscosity depends on temperature and pressure, so environment conditions change influence on rheological parameters. Since the changes nature and course depend on substance construction, it is possible that course of viscosity changes can change according to particular mixture components. In case of aviation engine fuels such changes are very important (fig. 3).

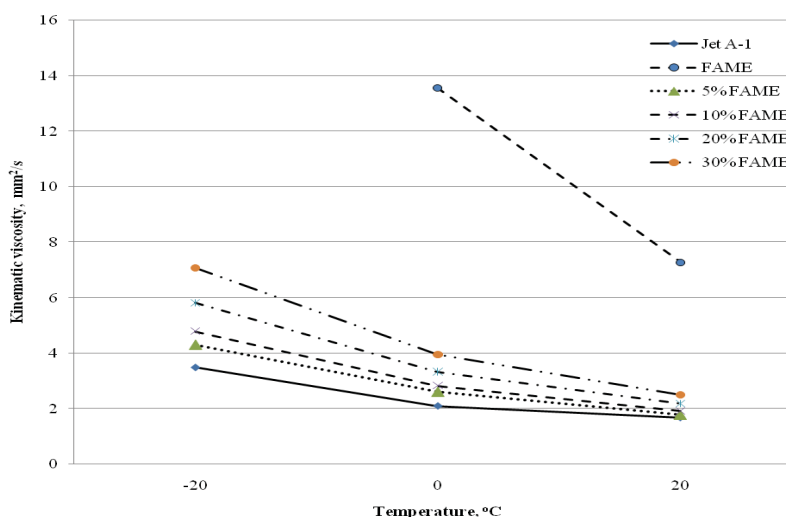


Figure 3. Viscosity change vs. temperature of aviation fuel, FAME and their mixtures

Decreasing ambient temperature causes product temperature lowering. At the beginning it causes mostly viscosity and density change, but beyond limit characteristics, the phase transition starts for every substance. The crystallisation starts. Since crystallisation temperature of individual components is different, there is no exact freezing point of the mixture.

Crystals start to appear in liquid phase. Their amount, or rather volume rise with temperature decrease. The fuel becomes cloudy though is still fluid that means it can be used safely. Further temperature decrease, however, leads to fluidity loss. Such situation is unacceptable, because it leads to fuel feeding continuity disturbance at the beginning (mostly due to filter sticking by crystals), and total breaking of fuel flow through the supply system.

In case of use of biocomponent that is vulnerable to low temperatures, there is serious threat and restriction regarding its use. First phase transitions of aviation fuels take place only under temperature of -50 °C, while in case of FAME first signs of crystallisation process beginning are visible at temperature under 0 °C a bit. So the discrepancy is huge. This can significantly restrict use of biocomponent in fuel.

## 5. Water separation tendency during filtration process

Hindered filtration at low temperatures due to filtration materials sticking can be intensified by water presence. In case of traditional turbine fuels, water presence is restricted using coalescence-separation filters during fuelling. Basic property used during use of these appliances is surface tension. Since the surface tension of fuel and water is different, the fuel passes through the filter gauze covered with surface-active material (i.e. polytetrafluoroethylene - PTFE), and small water droplets are trapped on filter gauze, and then they combine together, and flow to sediment trap as bigger drops. The FAME disturbs coalescence process, so the water removal is not sufficient. Such phenomenon is not connected with surface tension since its values for petroleum fuel and FAME are similar (accordingly 25.36 and 28.27). In comparison to surface tension for water (72.75) it shouldn't be a problem. The reason is different. At this stage of testing it can be supposed that FAME particles stick to coalescer surface and block its operation. Such hypothesis needs to be confirmed.

As a consequence of dewatering lack during fuel cooling down, water separation from fuel will take place at first (due to water solubility in fuel reducing with temperature decrease), and then the water can crystallize and can disturb engine fuelling process.

*Tab. 1. Effect of biocomponent on properties connected with ability to fuel dewatering at coalescers*

Pos.	Property	Biocomponent (FAME) content in aviation fuel % (V/V)				
		2	5	10	15	20
1	Water reaction: interface rating	2	3	>3	>3	-
2	Water reaction: interface separation rating	3	4	4	>4	-
3	Water reaction: water phase volume change, cm <sup>3</sup>	1	1	1	-	-
4	Water separation index	39	0	0	0	0

## 6. Tendency to microbial contamination

In some cases, especially at positive temperatures, presence of small water content doesn't constitute problem for combustion process. In case of non aviation engines, water contained in fuel has, among others, even positive effect on harmful exhaust gases emission. However, it cannot be recognised that fuel dewatering is unnecessary. Every fuel is exposed to microbial contamination in presence of separated water. Due to perfect biodegradability, and hygroscopicity, biocomponents are very prone to microbial growth. Because it's impossible to maintain anhydrous fuel, the only way to prevent such infection is biocides use. However, it should be noted that biocides are mostly chemicals of relatively high aggressiveness, so they can have harmful effect on distribution and storage facilities, and on construction materials of involved engine components as well.



## **7. Summary**

Basing on above test results and preliminary conclusions it can be found that there are some restrictions regarding use of biocomponents as ingredients of aviation turbine fuels. Obviously, such restrictions are more extensive in case of use in aviation, and less extensive for marine and land transport applications. According to performed testing, problems appear not only where they are obviously expected. The issues not fully recognized theoretically yet, and yet less utility experience can be the reason for that. Moreover, it's possible that because of chemical diversity of petroleum fuels and biocomponents, analytic methods developed for the first ones, in some cases are unsuitable for the latter ones. As a consequence some test results distortion is possible, and in turn, false interpretation.

Results obtained by laboratory test methods should be verified by engine bench testing. This is the subject of the next stage of the research work.





## ELEMENTS OF THE UML MODEL OF THE RAIL VEHICLE MAINTENANCE SYSTEM

Andrzej Erd

Politechnika Radomska  
Ul. Malczewskiego 29, 26-600 Radom, Poland  
Tel. 483617723  
e-mail: andrzej.erd@gmail.com

### Abstract

*The paper accounts for the construction of the rail vehicle maintenance model. It points to selected, possible to use, software tools applied for modelling in the Unified Modelling Language. Commonly accepted solutions are presented aiming to represent the maintenance system in UML. Such a model can be an input datum for the application generator in order to generate a code automatically. A more general application of this model is to create a design pattern to construct other maintenance assistance system of, e.g. ships or power station equipment.*

**Keywords:** system modelling, Unified Modelling Language, design pattern, maintenance, diagnostics systems, Maintenance systems

### 1. Introduction – purpose of system modelling

Looking at the development of computer systems from the historical perspective one can notice a significantly delayed development of software in comparison to hardware. Hardware development was often accomplished abruptly. New series of microprocessors were introduced, new computer architectures appeared which led to significantly improved results. New memory types were constructed expanding the data storage capacity and decreasing the time of access to them.

Simultaneously, the progress of less spectacular nature, within the framework of existing technology, occurred. The path width within integrated circuits was reduced, which allowed for more data packing. The rotational speed of hard discs was increased, the transfer speed within network interfaces was accelerated.

Looking in the same way at the development of software it is much more difficult to see such breakthroughs. Undoubtedly the subsequent steps which affected the way in which software was created were the stages in the development of methodology, first – structural one and then – object-oriented one. Although the foundations of the latter were presented in the 1980s, object-oriented programming is still the dominating way of presenting reality in the information systems. The reason for such a state of affairs is the immense complexity of systems [2].

The sources of system complexity are rooted in:

*The problem domain* – a great number of interdependent factors occurring in the real world.

*Design technologies* – necessity to reproduce the real world in the virtual world

*Design team* - a group of people of limited abilities of perception, information transfer and information throughput.

*Programming technologies* – a vast number of standards to be observed, a wide range of required skills

*Users* – necessity of transition from the virtual world to the real world and interpretation problems related to this. Limited abilities and limited knowledge of the system.

The ways to limit the problems of complexity are as follows:

1. Wider usage of computers in system design and creation.
2. Development of new methodologies of analysis and development.
3. Data and system modelling.
4. Creating new generations of programming languages
5. Construction of tools automatically generating the object code on the basis of the model.
6. Creating model patterns.

This paper is a contribution to points 3 and 6, i.e. with the help of modelling tools an attempt was undertaken to reproduce the maintenance system elements of the rail track vehicles, especially those with the combustion engine. Similar problems appear in the maintenance of other complex objects, such as ships or power stations.

## **2. Applied tools**

In the simplest case it is enough to have paper and a pencil to create a concept of the system model. However, relatively early the programming tools were developed to enable simplification of editing activities by means of objects inserted into text editors. A particularly convenient and popular tool is provided by the universal VISIO package (Microsoft) which in its menu has the *Software* option and within it, among other techniques of data representation, the sub-option *UML system*. It contains symbols typical for the most important types of diagrams, i.e.:

UML Static Structure

UML Collaboration

UML Deployment

UML Statechart

UML Sequence

UML Use case

Some programmes for system modelling allow for automatic generation of the software code. One can mention here Visual Paradigm UML (Visual Paradigm). A possibility of importing diagrams coming from VISIO is its interesting feature. Contrary to VISIO, this system can check automatically the object code integrity and generation on the basis of created diagrams.

This system is a transitory product for a typical CASE (Computer Aided Software Engineering) software, i.e. sets of tools for analysis, design, modelling and programming.

Such packages are most often paid and the best known among them include:

*IBM Rational Rose* is one of the oldest CASE solutions taken over by IBM. Apart from the tools for visual modelling, it contains the functions of code generation in languages such as Ada, ANSI C++, C++, CORBA, Java/J2EE, Visual C++ and Visual Basic.

*Enterprise Architect* – a tool running under the control of Windows and Linux systems.

*Sybase Power Designer* – a solution of the leading manufacturer of the systems of database management

*Visual Paradigm SDE* – an UML modelling tool and which later transfers the model into a code in the C# or Java languages to the Eclipse platform.

Apart from paid tools there is also a great number of programmes based on the GNU licence:

*Argo UML* – enables generation of the code based on the Eclipse platform.

*Atlas Transformation Language* – allows for a transformation of the UML model to Java code

*ESS-Mode* – a tool for reverse engineering of the UML model from Delphi or Java code

*Star UML* – a simple UML diagram editor (at the moment one must pay for it, but there is a possibility of obtaining of a full value, time restricted trial version after registration on the producer's home page).

### 3. System modelling

The system construction consists of the determination of:

- information elements allowing for a full description, also static one (database construction)
- outcome information expected by the user (User's interface)
- the way of input data processing into output data (application logic)

Thus the problems are naturally divided into 3 layers, i.e. data access, logic and presentation.

It is reflected in the latest design trends as the so called three-layer architecture. The essence of layer structure consists in such a construction of applications as to make the functions of individual layers independent from one another and to prevent the changes within each of them from affecting the remaining ones.

*Tab. 1: Layers of system architecture*

Layer of	Function
Presentation (User's interface)	Receiving user's commands, Entering data, deriving outcomes
Logic	Correct application logic
Data access	Maintaining source data, communication with external bases, reception of external communiqués

Principally, the basic element of a model are classes representing its components. The class possesses attributes (parameter values) and methods, which operate on these attributes. An example of attributes of the class of locomotive data is shown in Table 2..

*Tab. 2. Attributes of the Locomotive Class*

Class _ Locomotive Data	
Series	: SeriesType;
LocomotiveNumber	: LocomotiveTypeNumber;
LocomotiveAcceptanceDate	: word;
AcceptanceOrderNumber	: string20;
AcceptanceOrderDate	: word;
ConstructionYear	: word;
IntroInServiceDate	: word; Warranty : Word;
LastPeriodicRepairSymbol	: string3; ZNTKCode : Word;
LastRepairCourse	: longint; CurrentState : string[3];
LastInspectionSymbol	: string3; SBData : word;
LastInspectionDate	: word; SBChange : word
LastInspectionCourse	: longint;

Component assemblies are described in a similar way although in their case there are more attributes used to describe the measured values. The assemblies are aggregated and belong to the locomotive, which is illustrated in Figure 1.

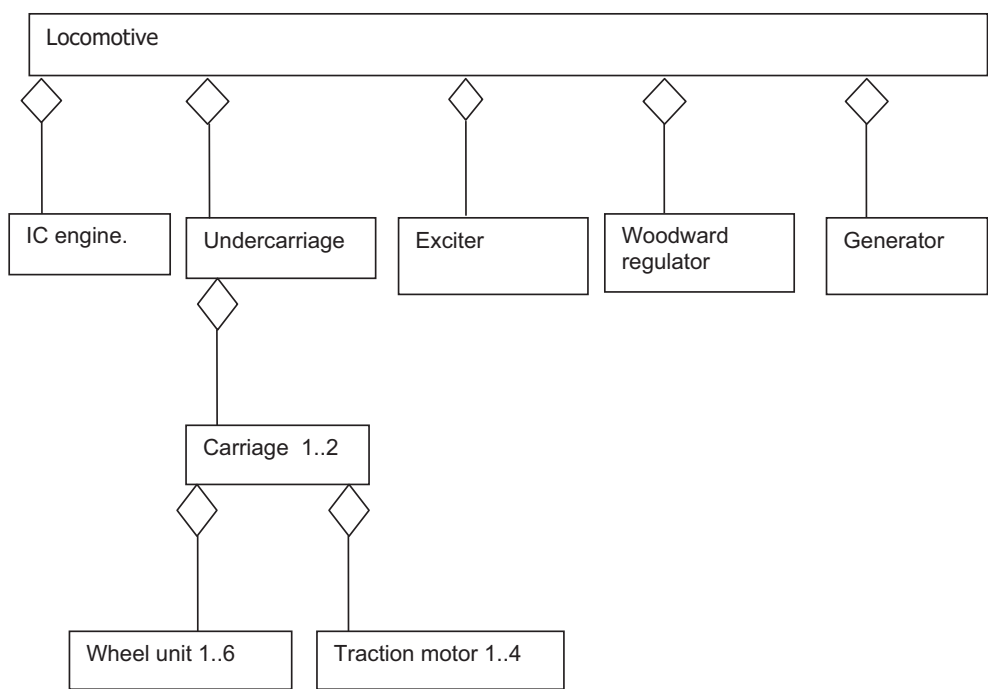


Fig. 1. Aggregation of component classes into the Locomotive class

Classes can describe physical elements but also can constitute a description of measurement results, e.g. the class of oil-water analyses presented in Table 3 below.

Tab.3 Attributes of the Oil-Water Analyses Class

Class_ OilWaterAnalysesData
Series : SeriesType; LocomotiveNumber : LocomotiveNumberType; InspectionRepairDate : word; InspectionRepairType : string3; OilContamination : real; OilViscosity : real; WaterContent : real; AlkalineReserve : real; OilAssessment : char; OilContent : real; OilToWaterRatio : real; OilType : string10; WaterAssessment : char; IntroCode : word; Comment : string20; NotifyingPerson : string20

The range of data indispensable to describe the system is very broad and Table 4 below presents only examples of further elements of this type without a detailed description of attributes.

*Table 4: Range of static data of the diagnostic system and vehicle maintenance(examples)*

<b>Constant data</b>	
	Data of the railway rolling stock dispatching unit
	Data of the repair plants (address , repair plant Number)
	Number of a vehicles in stock
	Configuration data of the vehicle series ( assembly types and their numbers)
	Configuration data of vehicles (what types of assemblies are components)
	Configuration data of assembly types (description of parameters – name, number, unit)
	Configuration data of analysis ( what is included in analysis – parameter, scope)
	Model characteristics of engine and power transmission system measured at the test stand

<b>Measurement data</b>	
	Measured characteristic of the power transmission systems
	Measurement results of oil consumption
	Measurement values of wheel sets
	Measurement values of traction motors
	Measurement values of the main generator
	Analyses results

*Table 4: Range of static data of the diagnostic system and vehicle maintenance(cont.)*

<b>Variables</b>	
	Register of vehicles within the railway rolling stock in the plant
	Composition of a vehicle unit – configuration of elements – actual specimens identified by registration numbers

Principally, these data can be divided into 3 groups:

- Non-changeable (constant) data – dictionary-wise, they are characterised by stability or the changes are very rare.
- Measurement data – results of diagnostic inspections; their registration and analysis is the basis of making decisions about replacements and qualifying vehicles for repair. Individual results can be in the form of single numbers but they can also be records of more complexity, e.g. sets of data from the measurements of wheel sets or characteristics of a power transmission system measured at the test stand.
- Changeable data (variables) – illustrating the turnover of vehicles in the register and also, which is even more intense, the turnover of assemblies within vehicles (replacements)

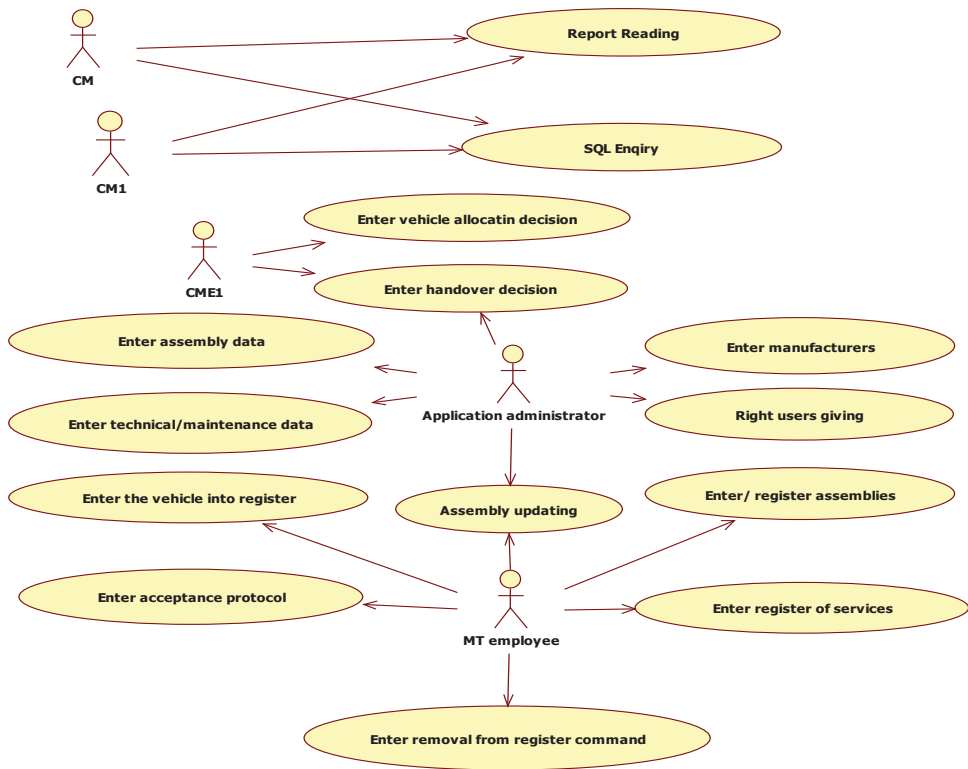


Fig. 2 Use case diagram (limited)  
 CM- Directors. CME- Departament of Traction and rolling railway stock maintenance;  
 MT- Railway Rolling Stock Plant (used StarUML)

The scope and degree of data processing depends on the information recipient and its intended use. In order to facilitate a further analysis of the real system, the diagrams of use cases are created. A fragment of such a diagram is shown in Figure 2. The use case diagrams are particularly useful when it comes to specifications of the system element behaviour as seen from outside. Owing to them the sub-systems and classes become easier to understand. They allow to grasp who the information producers and recipients are and which thematic ranges of the information take part in individual actions. They facilitate testing of a ready system in the start-up phase.

A subsequent stage of system modelling is representation by means of change diagrams in the course of the individual actions implementation. While creating them, a lot of attention is given to the place and manner of data taking and the algorithm for data processing. Thus, it can be assumed that these charts are included in the second layer of application, i.e. the layer of logic.



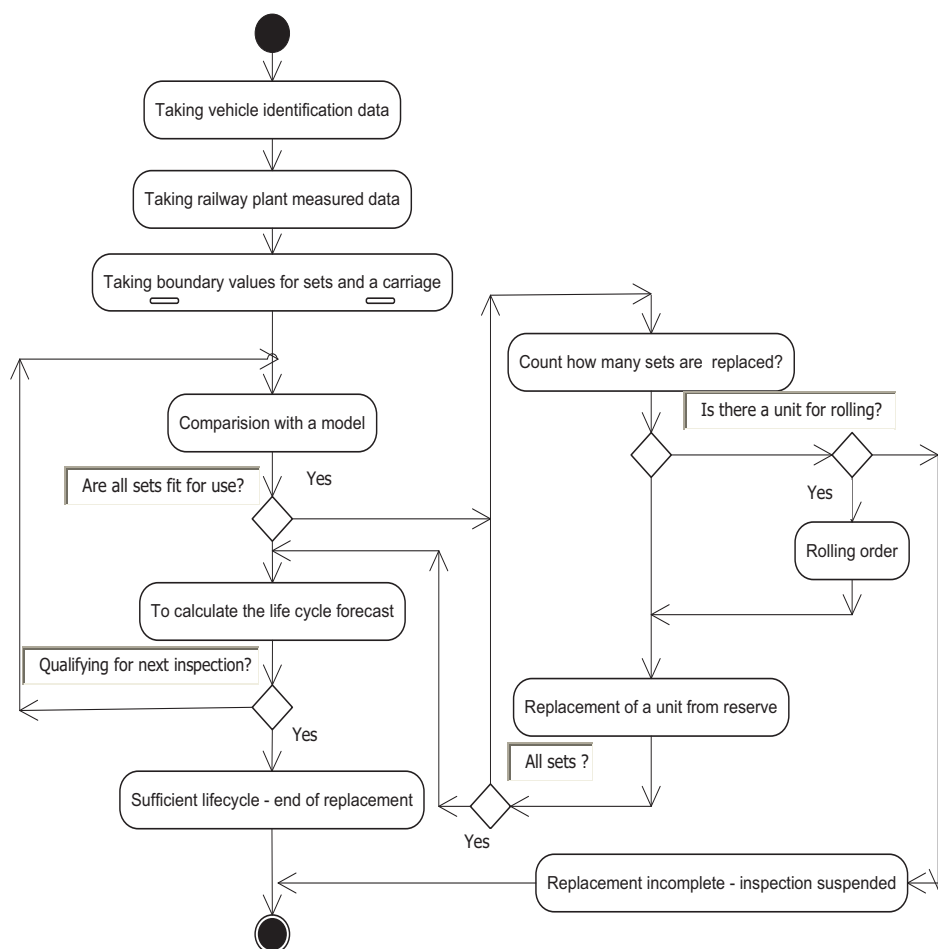


Fig. 3 Change diagram for replacement of wheel sets – parts of use case – Updating of sub-assemblies.

Basically, the state chart (change diagram) is so detailed that by following it, one can create the processing procedures implementing specific tasks. If manual coding is forecast, individual SA blocks are usually implemented in the language of the third generation. In the case of automatic generation it is necessary to write out further algorithm blocks up to the level of single variables.

## 4. Effects

The model developed is the starting point for creating a model design of the maintenance assistance system. Having it will allow for significant shortening of the period of creating computer systems meant for diagnosis and maintenance.

The essence of a design pattern (model) is the existence of an application skeleton which could be used in a possibly broad range of applications. The role of analysts, designers and programmers is to adjust the model to user's needs. The UML model is a tool to show the interdependencies between the system elements (static part) and its operations (dynamics). In the traditional approach

the „manual coding” of the entire designed system is necessary. It is then followed by mundane testing. A tremendous amount of work from programmers is required to re-build the existing solution, if there is one. Technology of the 4th-generation languages, which is supposed to reduce the coding process, may turn out to be extremely useful provided one has suitable models. In general, the human work outlays are shifted from coding to a better reproduction of reality.

## References

- [1] Boch Grady, Rumbaugh James, Jacobson Ivar, UML przewodnik użytkownika. WNT Warszawa 2002
- [2] Subieta Kazimierz. Obiektość w projektowaniu systemów bazach danych. Akademicka Oficyna Wydawnicza PLJ. Warszawa 1998
- [3] IBM developerWorks Live – IBM materials. Warszawa. 2004.
- [4] IBM Software Evaluation Kit – IBM electronic materials Warszawa 2004.
- [5] Rational Software Atlantic Launch IBM materials, Warszawa 2006.



## THE USE OF ACOUSTIC EMISSION TO IDENTIFICATION DAMAGES BEARINGS THE MAIN AND CRANK ENGINES ABOUT THE AUTOMATIC IGNITION

**Jerzy Girtler, Wojciech Darski**, Gdansk University of Technology,  
**Artur Olszewski**, Gdansk University of Technology, *Faculty of Mechanical Engineering*,  
**Ireneusz Baran, Marek Nowak**, Cracov University of Technology, *Department of  
Mechanical, Institute M6*

*Gdansk University of Technology  
Faculty of Ocean Engineering & Ship Technology  
Department of Ship Power Plants  
Ph. (=48 58) 347 – 24 – 30  
FAX (+48 58) 347 – 19 – 81  
e-mail: [jgirtl@pg.gda.pl](mailto:jgirtl@pg.gda.pl)*

### **Abstract**

*The article describes the laboratory tests, which make the first stage of the study concerning the use of the AE method to determine the technical state of the slide bearings in engines with self-ignition. The aim of the present tests was to compare the recorded signals in relation to the technical state of the material of the bearing bush and to check the possibility of using the AE method in determining the transition moment from the fluid friction into the semi-dry friction in the bearing and signaling the first micro-defects of the material of the bearing bush. The experiment has not solved the problem, but they are of a development character and will be continued in the nearest future.*

**Keywords:** *Frequency analysis, slide bearing, friction factor, bearing bush.*

### **1. INTRODUCTION**

Their bearings frequent damages undergo in the exploitation of engines about the automatic ignition [13, 15]. Prevention the damages of these bearings requires the uses of the diagnostics [9, 12, 15]. In the diagnostics of the bearings of combustion engines, especially shipping, the credibility of the diagnosis essential is. He from introduced in publications [5, 7, 8, 9] conditions of functioning every system diagnosing (*SDG*) of the any engine about the automatic ignition results, that the credibility of the diagnosis depends from:

- the condition technical *SDG*, and now from the possibility of his damage,
- possibility of appearing the conditions of the engine about the automatic ignition as the system diagnosed (*SDN*) not considered in the diagnostic task (*ZD*),
- the possibility of changes (especially random) the vector of the power supply (*Z*) and the vector of steering (*E*) and the property of random disturbances (*N*), as a result of what remembers *Z*, *E*, *N* can be known while diagnosing the condition *SDN*,
- the sensibility *SDG* on the change *Z* and *E* and the existence *N*.

The credibility of the diagnosis about the state has the technical or energetic engines about the ignition automatic principal influence on the undertaking rational decisions, and the same on the efficient working of this kind of engines who the assurance makes possible of the desirable course of the process then the exploitation. This results from this that the diagnosis makes up the basic component of any working, not only exploitative, but also projects (in this constructional), technological etc. [6, 7]. The study of the credible diagnosis marks unambiguous identifying the condition of the given engine of the combustion system diagnosed (SDN), and the same recognition potential his property. Because of this, that the guilds SDN are changing random, so the identification of the condition of this system is only approximate which means that diagnosis about this will stand up he is credible, but in the definite degree.

You should now, as the attribute of the diagnosis, estimate this degree of credibility and aim to enlargement of her value near this [3, 4, 8]. The selection of diagnostic parameters is one of the possibilities of enlarging the diagnosis about the condition of these engines to credibility about the possibly largest diagnostic usefulness. You should doubtless seek such parameters among parameters acoustic vibration and the parameters of the acoustic emission. He marks these parameters as the carriers of information about the technical condition of combustion engines, in the comparison with different diagnostic parameters, about many larger informative capacity and the speed of passing on the information about this state. Preliminary investigations showed that the acoustic emission was however more useful, because he discloses the changes of the condition of the structure of the materials of which the elements of remembered engines are made. This results from this that the acoustic emission (EA) is the result of appearing the springy wave of generated by sudden liberation accumulation energy in the material of the elements of engines. They cause such liberation of energy, e.g.:

- micro slips setting on the border of grains being in micro domain about large tensions reaching the border of the plasticity of the given material,
- the movement of vacancies and dislocation, especially joining oneself and the moving the dislocation,
- formation of micro slots and their propagation in the materials of the elements of engines.

This last cause is the strong source generating EA particularly. He results from this that use in the diagnostics of engines about the automatic ignition of the acoustic emission as the diagnostic signal is necessary. In essential relationship with this become investigations aiming to identification and the opinion of the usefulness of the parameters of acoustic emission in the diagnostics of engines about the automatic ignition. This problem was undertaken in article this in the reference to the main and connecting-rods bearings of this kind of engines.

## **2. THE CONCEPTION OF THE INVESTIGATION USEFULNESS OF DIAGNOSTIC PARAMETERS EMISSION OF THE ACOUSTIC**

In the diagnostics top layer of elements bush of the bearings of sliding engines about the automatic ignition, he can be applied the method of analysis and the opinion of their technical state, in the result of the use of acoustic emission (AE) as diagnostic signal according to pattern introduced on fig. 1.

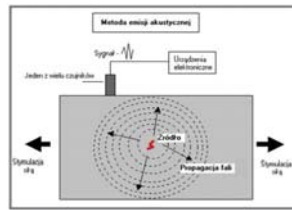


Fig.1. The pattern of spreading springy waves in the solid body [16]

Method this consists in the registration of the course of springy waves (rys.1), being the effect of the liberation of internal springy energy accumulations in material and suitable statistical processing the measured values of the parameters of these waves [1, 2, 10, 15, 17].

The acoustic emission (AE) comes into being in the bearings of combustion engines both in the result of existence micro processes (micro cracks, slides on borders, the movement of vacancies and dislocation) how and in as a result of macro phenomenon (macro cracks, considerable slackness), the connected with the superficial and volumetric waste elements (bearing bush and shaft neck) of these bearings.

The advantage of the method of AE in the use to the diagnostics this first of all the possibility of the registration of signals low energy - consuming coming into being beyond the transducer, what he first of all allows to detect the infringement of the cohesion of the layers of top materials, from which the elements of the bearings of combustion engines are made.

The possibility the registration parameters AE generates by he depends sliding bearings remembered engines on tenderness, resolution and the capacity of the measuring apparatus. You should also have this on the attention that the method of EA requires the not only suitable apparatus, but and applications can process and analyses the huge quantity of data got during the registration of signals [2, 14]. The temporary difference of the attainment of the signal from the source AE to individual sensors makes possible situating this source. In the analysis AE as the change of amplitude and energy in the course among individual sensors the diagnostic signal essential is [10, 15].

They infringement of the cohesion of the top layer of the elements of bearings in the scale micro are detected on long before extensive infringement of this cohesion (damage, in this destruction). Should affirm near this, that deforms (deforming) and they are the cracking the material be sure basic sources AE, but also the processes of corrosion, erosion, frictions and different, causing waste (both superficial as and volumetric) they the elements of sliding bearings also give the perceptible and characteristic growth of this kind of signals [1, 11, 15].

The comparison of recorded signals AE was the aim of the investigations whose results are put in this article dependent on the condition of the technical bearing alloy and proof the method AE of to usefulness to:

- the qualification of the moment he in the bearing crosses in the mixed friction in whose smooth friction,
- disclosing the (signaling) of appearing first micro of the damages of the materials of the elements of the bearing.

The position whose pattern was introduced on fig. 2 was applied to the achievement of remembered investigative aims. Position this made possible [14]:

- the change of the value of the rotary speed,
- measurement and the registration of the value of the moment of appearing the mixed friction in the bearing,
- the measurement of the temperature of bearing studied and lubricate oil,
- the obtainment of the repeatability led tests through the use of automatic steering and the acquisition of results,

- the change of the value of the burden transverse strength according to the plan of the experiment.

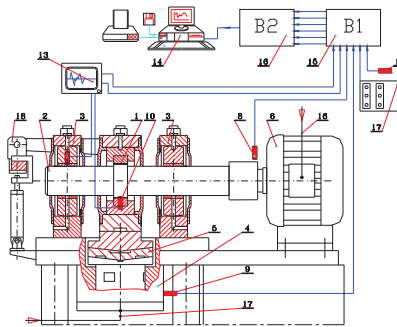


*Fig. 2 The investigative position - PG2-1L the suitable parameters of smearing the bearing studied the position were equipped [14]*

In the aim of the assurance in independent external current arrangement of smearing with possibility of heating up oil (fig. 3). The ultra thermostat of the type U15C was applied in the arrangement about the capacity 15 l and power 1.75 kW [14, 15]. Heated up to the set temperature oil was pressed to the bearing studied the decentralizing pump plunged in the reservoir ultra thermostat. Oil this flowed down to the reservoir gravitations. Contact thermometer installed in the arrangement of power supply heaters assured the maintenance set value of the temperature of oil.



*Fig. 3 The view of the external arrangement of smearing the bearing studied [14]*

The investigations AE were led with the use of the system Vallen AMSY-5 (the firm Vallen - Systeme GmbH), and various types of sensors AE (table 1), assuring the registration of signals in the wide strand frequencies [1, 14]. The system Vallen made possible the registration of parameters AE (the moment of appearing the mixed friction, rotary speed, strength burdening bearing, the temperature of oil) simultaneously and the correlation of registered values of remembered parameters. Such sensors AE were applied in investigations how: PAC, PAC + wave-guide, VS 30-V, VS 75-V, VS 150-RIC, VS 150-RIC + wave-guide, VS 375-RIC, SE 45-H. These sensors were fixed on the measuring head of the investigative position and the side surfaces of hydrostatical bearings.

The measurement of the acoustic background was first stage of investigations and the disturbances of generated by the work devices on the investigative position. The schedule of the strands of the frequency of signals registered during these investigations was introduced on fig. 4.

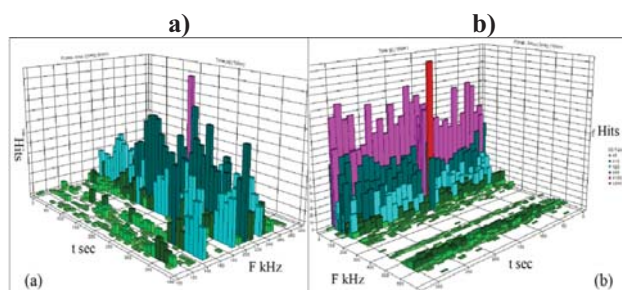


Fig. 4 The schedule of the strands of the frequency of signals registered for broad – gauge sensors: a) the range 100 – 300 kHz, b) the range 20-850 kHz [14]

The conducted frequencies analysis of registered signals AE allowed to the qualification the main strands of disturbances and choice of the frequency of filters the *high pass* and the *low pass* to next measurements in the aim of elimination of disturbances coming from the work of the position of investigative and inside and outside the laboratory [14].

The results of the investigations of bearings with the new pans of the type MB10 (two-ply, overflow 212 -CuPb22Sn) and MB35 (four layers, overflow 331- PbSn10Cu2), with use of the filters of the frequency, near the received conditions of the burden and the rotary speed becomes them left, according to next tests, put in the table 1. The solid rotary speed of the rampart was accepted as exit sizes 1700 rot. /min. the faces and two sizes of the burden of the transverse bearing -1 kN and 2 kN. The settled parameters of acquisition for these conditions of the work of the new bearing made up later the base for the comparison in remaining tests.

In the aim of the comparison of signals AE recorded near the investigation of the new bearing with signals coming from the bearing with simulated damage, measurements of three sliding bearings of the type MB10 were conducted [1, 14]:

- the new bearing bush,
- bearing with openings simulating the local damages of the material bearings bush e.g.: superficial crack or the plucked out particles of the bearing alloy causing disorders of the flow of oil smearing (fig.5),
- the bearing with cut longitudinal and district grooves, simulating the damage of the surface bearings bush in result of transfusion of strange bodies among pan and suppository (fig. 6 and 7).

On the fig.5 was introduced the fatigues damage of the bearing alloy (a) and simulated damage (b). On the fig.6 was introduced in the turn the damage of the surface of the bearing in the result of the transfusion of strange bodies among pan and suppository, and on fig. 7 executed simulated damage similarly as on fig. 5.

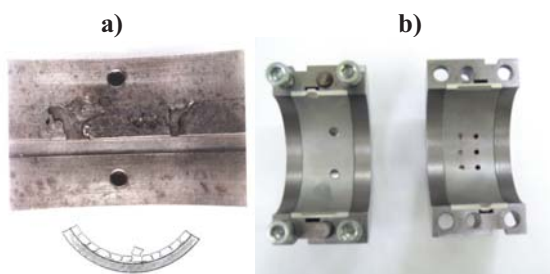


Fig. 5 View bush with the fatigues damages of the bearing alloy: a) the propagation of the cracks of hard basis and crumbling up the particles of the bearing alloy, b) simulated damages in the figure 6-ciu the openings about the diameter  $\varnothing = 4$  mm, what  $15^\circ$  [14]

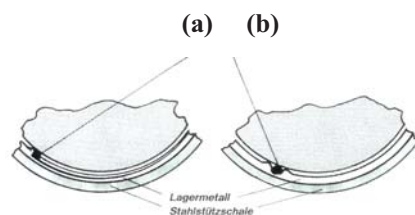


Fig. 6 The pattern of the damages of the sliding surface bearings caused through strange bodies: (a) pumps through grains and the rifling of the sliding surface, (b) polishing shaft neck through grains fixed in the sliding layer [14]



Fig. 7 The view realization of the damages of the surface bearings which can come into being in the result of the transfusion after them of strange bodies [14]

The reports were established in investigations between damages bearings bush of the bearings bush of sliding engines about the automatic ignition, introduced on fig. 5 ÷ 7, and the measures parameters of the acoustic emission (AE).

### 3. THE RESULTS OF MEASUREMENTS PARAMETERS EMISSION OF ACOUSTIC

During investigations were recorded:

- the counting the events (hits) - the basic parameter of the activity of the source AE,
- quantity exceeds of the level of discrimination (counts),
- the value of the energy of the signal,
- the amplitude of signals,
- RMS - the average square intensity of the signals of the continuous emission - parameter to defining the value of the continuous emission below the threshold of detect ability,
- the burden,
- the moment of the rise of the mixed friction,
- the rotary speed,
- the temperature of bearing and lubricate oil.

Exchanged parameters AE were used to monitoring the technical condition of sliding bearings [11, 15, 16].

Results of registration of value RMS for new bearing and bearings with simulated damages (fig. 5, 6, 7) were introduced on fig. 8, 9 and 10.



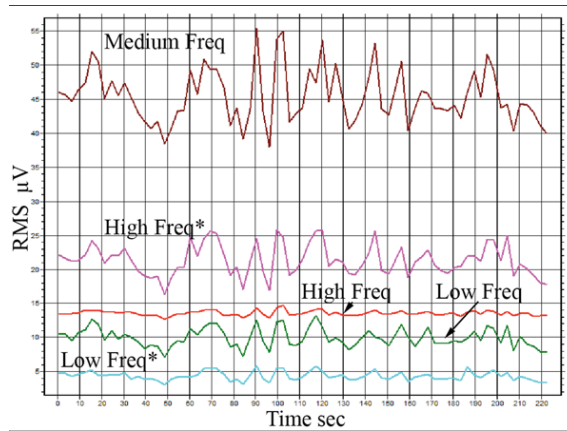


Fig. 8 RMS for the various compartments of the filters of the frequency - the sliding bearing new [14]

The stability of the value (fig.8) steps out for RMS about the high frequency (orange line). You can see the growth of the value RMS AE in all channels for the except of the frequency low from the analysis of the data generally low\* and high\*. The value of measurements puts in the table 1 got in channels from low, the central (medium) and high the frequency answering state (generic) the damages of the bearing was introduced on fig. 9 and 10.

Tab.1. RMS in the function of time for the various strands of the frequency [14]

Condition of the bearing	Low [μV]	Low* [μV]	Medium [μV]	High [μV]	High* [μV]
New	10	4	46	13	27
Holes	27	3	67	27	23
Grooves	34	8	105	0	47

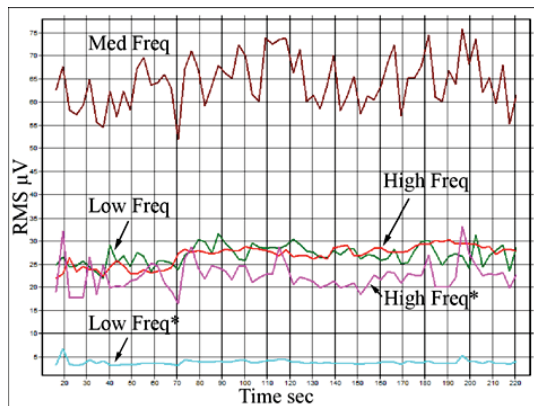


Fig. 9 RMS for the various compartments of the filters of the frequency - the damage of the type of the fatigues bearing alloy [14]

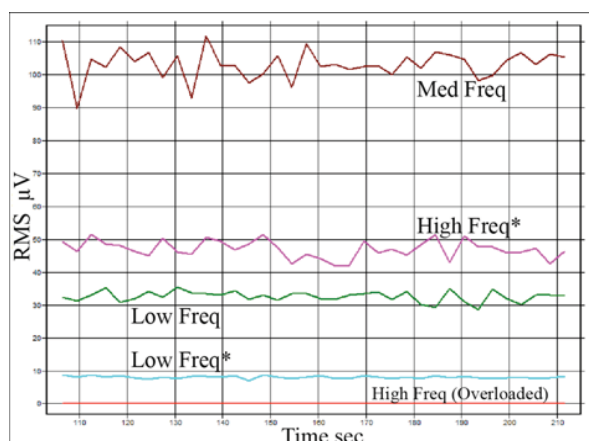


Fig. 10 RMS for the various compartments of the filters of the frequency - damage in the figure furrows of the bearing alloy [14] was introduced

On the fig.11 was introduced the activity of the emission for new bearing and bearing simulating wrench of the particles of the alloy near these alone parameters of the acquisition, near the use of resonance sensors VS75-V and VS150-RIC and frequency filters on measuring channels.

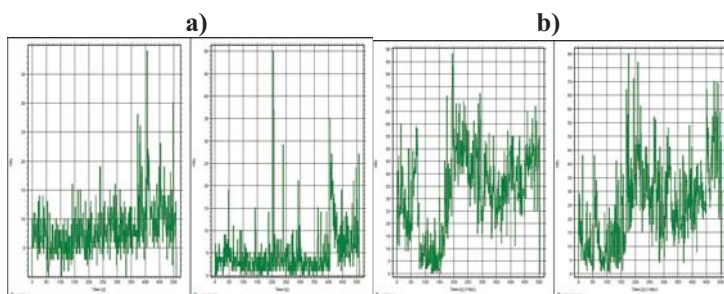


Fig. 11 The parameters AE the activity of the acoustic emission in dependence from the time for the bearing: a) new, b) with opening simulating wrench of the particles of the alloy were recorded [14]

After the serial changes of the rotary speed during the work of the bearing near the solid settled rotary speed 1700 rot./min. the faces and settled burden 2 kN. The example of the single temporary range signals AE were recorded in which, was introduced on fig. 12.

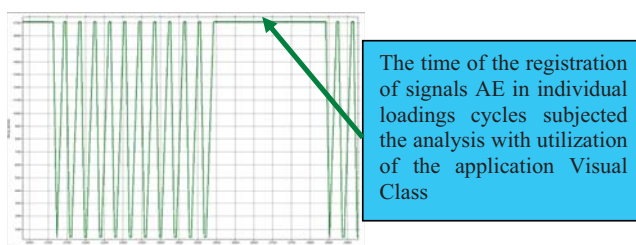


Fig. 12 The example single loading cycle of bearing with the marked range of the time of the registration of signals AE subjected the more far analysis [14] was introduced

On the fig. 13 the sum of registered signals during the work settled. The visible change of the activity of recorded signals on the sensor VS150-RIC, she signaled the change in the work of the bearing. First traces were the cause of the sudden growth of the activity AE (hits) the waste oneself the bearing layer of the bearing.

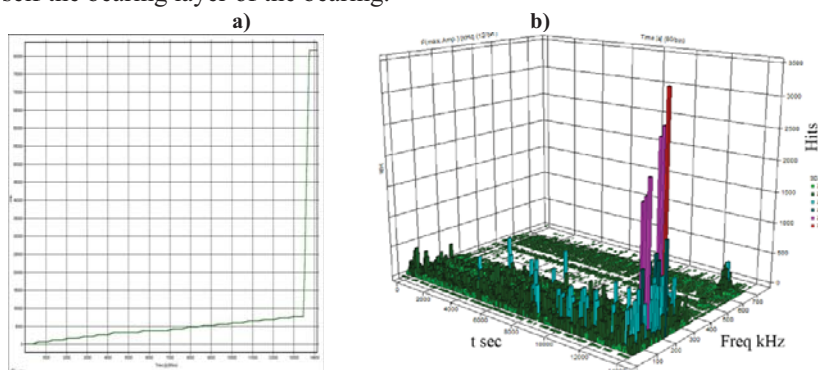


Fig. 13 The results of investigations: a) - the sum of registered events (hits) in the time of the settled work of the bearing, b) - the sum of the schedule of events (hits) in the strands of the frequency [14]

For the example on fig. 14 the condition of the surface of the sliding layer of pans after investigations was introduced



Fig. 14 The view split bearing bushings of the type MB10 and MB35 after investigations □ visible first traces the waste of the sliding layer [14]

The measurement AE was one of the essential aims of investigations while the disappearance of smooth friction and passage in the mixed friction, that is in the moment of the appearing first contact micro roughness shaft neck from the micro roughness of the pans of the bearing. The methodology of investigations enabling decrease of the coefficient of the friction was worked out in this aim as much as to appearing the contact metallic shaft neck with pans. The value of the rotary speed was reduced during the test near the behaviors of the solid value of pressures gradually. Reducing the value of the rotary speed results in decrease of the thickness of the oil film, what he leads fall of moment of friction generated in bearing (fig. 15, 16) in the consequence. The moreover decrease of the rotary speed results in appearing the contact metallic shaft neck from bearing bush. He appears then the mixed friction, which causes enlargement the value of the moment of the friction in the bearing. The minimum value of the moment of the take measurements friction in the bearing studied answers the moment in which first contact turning shaft neck appears from motionless bearing bush bearing bush and cutting first tops of unevenness in the face of this exactly. The value of this moment grows since this moment.

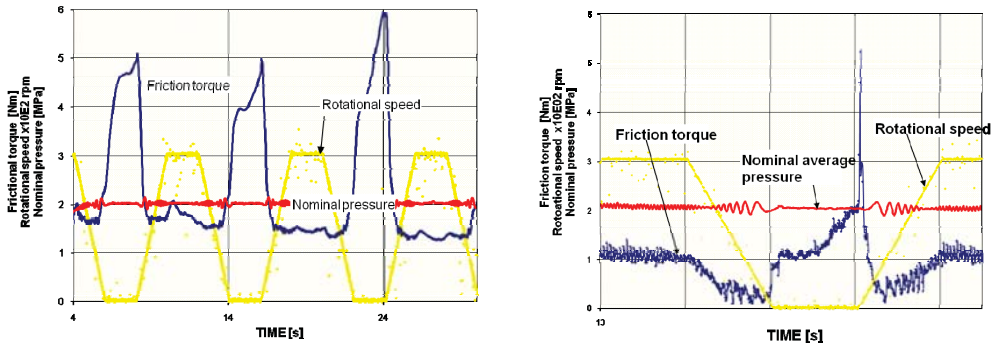


Fig. 15 Result of test in the conditions of the interruption of the smooth friction. Solid nominal pressures [14]

After stopping shaft neck in the bearing the moment of the friction in the bearing bush. Together with from the growth the district speed  $u$  the hydrokinetic pressure begins gradually to appear raise the suppository and reducing the number of cut uneven nesses. The coefficient of the friction  $\mu$  achieving the minimum value in the moment of the achievement of the smooth friction he undergoes the decrease. More far enlarging the rotary speed results in enlargement of the speed of the flow of oil in the crack and enlarging the coefficient of the friction.

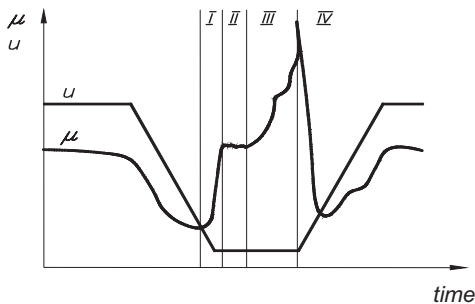


Fig. 16 The graphs  $\mu = f_u(t)$  and  $u = f_u(t)$  and the dealt out areas of the coefficient frictions observed during the movement [13]:  $\mu$  – the coefficient of the static friction,  $u$  – the speed district shaft neck of the bearing

Analyzing the shape of the course of the value of the coefficient of the friction  $\mu$  one can distinguish four characteristic areas as the function of the time (fig.17):

- the area I, II and III in which the growth of the value of the coefficient of friction in the consequence of the worsening conditions of smearing as a result of diminishing the rotary speed follows as much as to the stop of the suppository of the bearing
- area IV, in which in the consequence of the starting and the fall of the value of the coefficient of the friction called out the improvement of the conditions of smearing gradual enlarging the rotary speed follows.

The coefficient of the friction begins his value to grow up together with the growth of the speed rotary shaft neck after the crossing the minimum value. The dependence of the coefficient of the friction represents the profile of the sliding bearing from value forced (rotary speed, nominal pressures) and the stickiness of lubricate oil. Recorded in this time activity AE introduced on rys.17, she signaled getting smaller the coefficient of the friction through the atrophy of the activity of signals AE. Meanwhile the increase coefficient of the

friction between the surface shaft neck and pans, the sudden growth of the value of the parameters of signals AE accompanied.

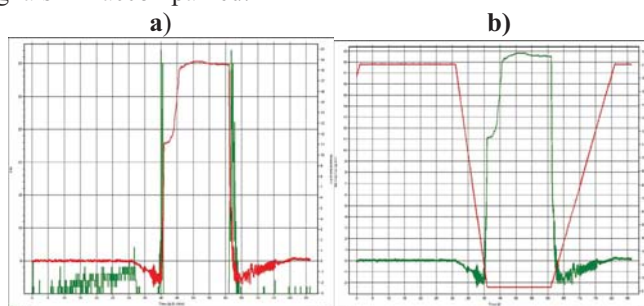


Fig. 17 Turns and the moment of the friction and the activity of signals AE during the change of the kind of the friction in the bearing [1]

On fig.18 the course of parameters as: were introduced additionally the course of the changes of the activity AE - the quantity of events (hits) for the various strands of the frequency. The value of the rotary speed of the rampart is even to null, when the friction achieves the largest value. The activity AE was not recorded in the period, until the rotary speed of the rampart did not reach the value  $\sim 700$  rot./min. faces (fig. 18b).

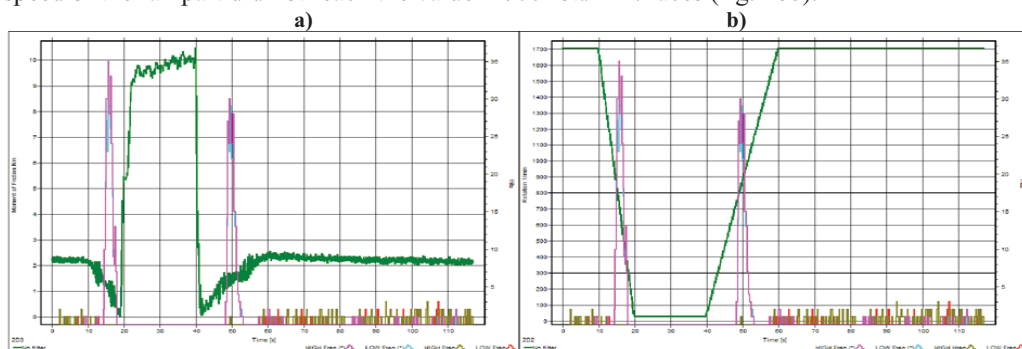


Fig. 18 The change of parameters and activity AE as: a) - the moment of the friction (from the left side) and RPM (from right), b) - RPM (from the left side) and the quantity of events (hits) (from right), during the change of the kind of the friction in the bearing [1]

For the classic hydrokinetic bearing transverse, dependence this illustrates the graph Hersey'a. Example graph such was introduced on fig.19.

Three areas distinguish themselves on graph this:

- the area I - of the smooth friction, area laid on the right from the minimum value of the coefficient of the friction  $\eta_{as}$  appointed by  $\lambda a$ . Area this answers range full smearing of hydrokinetic, in which surfaces sliding shaft neck and bearings bush are separated the comparatively fat layer of grease. Accident from pressures in this layer balances the burden external bearings,
- the area II - on trick from the minimum of the friction ( $\eta_e \eta_{as}$ ;  $\lambda a$ ) he answers the range mixed friction. The value of the coefficient of the friction together with the diminishing value of the number Hersey'a  $\lambda$  grows in the result of the growing of the friction border part in area this and the diminishing part of the smooth friction in the bearing,

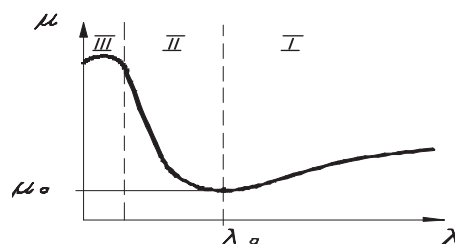


Fig.19 The graph Hersey'a [13]

- the area III – he answers the range border friction, placed on graphs Stribeck-Hersey'a, he is in experimental investigations very difficult to the achievement. Such state to appear can in the bearing, in the whole area of the friction the very thin lubricate film would have to step out about the thickness of line a dozen or so to tens molecules of grease

## ATTENTIONS AND CONCLUSIONS

From conducted research. The qualification of disturbances necessary is during the work of the tested combustion engine in more far investigations. Introduced examples from investigations illustrate that the use of the acoustic emission (AE) possible is to the qualification of the technical condition (damage) of sliding bearings. The tenderness of the method AE allows to record in the conditions of laboratory signals AE testifying about the passage from the smooth friction in mixed.

The study should be the next stage of investigations and the construction of the classifiers with utilization of the application Visual Class, being based on the spacious library of measuring data got during executed investigations on the investigative position of the type PG2-1Ł. The classifiers will make possible the identification the signals AE come from damages near the analysis of the phantom of signals AE, received during the investigations of the engine about the automatic ignition in laboratory conditions.

He was notified at the Office Patent Polish Republics in the result of conducted investigations, by the authors of the article, invention pt. *Way and position to construction of the classifiers to the identification of the accident condition of bearings, especially engines about automatic ignition near the use of the acoustic emission as the diagnostic signal.*

## REFERENCES

1. Baran I., Nowak M., Darski W.: *Application of acoustic emission in monitoring of failure in slide bearings*. Proceedings of the International Conference on Acoustic Emission. Advances in Acoustic Emission – 2007. The Sixth International Conference on Acoustic Emission ICAE-6, Nevada. U S A, October, pp.155-160.
2. Gill J.D., Rauben R.L., Scaife M., Bron E.R., Steel J.A.: *Detection of Diesel Engine Faults using Acoustic Emission.*, Proc. 2 Conference. Planned Maintenances, Reliability and Quality, 2-3 April, Oxford 1998, pp. 57-61.
3. Girtler J.: *Statistic and probabilistic measures of diagnosis likelihood on the state of self-ignition combustion engines*, Journal of Polish CIMAC. Vol. 2, No 2(2007), pp.57-63.
4. Girtler J.: *Probability measures of likelihood of diagnosis of the technical state of main combustion engines of sea-going ships*. Journal of KONES. Vol. 16, No 2(2009), pp.125-132.



5. Girtler J., Kuszmidar S., Plewiński L.: Wybrane zagadnienia eksploatacji statków morskich w aspekcie bezpieczeństwa żeglugi. Monografia. Wyższa Szkoła Morska w Szczecinie, Szczecin 2003.
6. Girtler J.: Zastosowanie bayesowskiej statystycznej teorii decyzji do sterowania procesem eksploatacji urządzeń. Materiały XXII Zimowej Szkoły Niezawodności nt. Wartościowanie niezawodnościowe w procesach realizacji zadań technologicznych w ujęciu logistycznym. SPE KBM PAN, Szczyrk 1994, s.55–62.
7. Girtler J.: *Wiarygodność diagnozy a podejmowanie decyzji eksploatacyjnych*. Materiały Kongresu Diagnostyki Technicznej KDT'96 TII. Zespół Diagnostyki SPE KBM PAN, PTDT, IMP PAN w Gdańsku, Politechnika Śląska w Gliwicach, Politechnika Poznańska, Gdańsk 1996, s.271–276.
8. Girtler J.: *Probabilistic measures of a diagnosis' likelihood about the technical state of transport means*. Archives of Transport, vol. 11, iss. 3-4. Polish Academy of Sciences. Committee of Transport, pp.33–42.
9. Girtler J.: Diagnostyka jako warunek sterowania eksploatacją okrętowych silników spalinowych. Monografia, Studia Nr 28. Wyższa Szkoła Morska w Szczecinie, Szczecin 1997.
10. Malecki I., Ranachowski J.: *Emisja akustyczna, źródła, metody, zastosowanie*. KBN, Warszawa 1994.
11. Ono K.: *Fundamentals of acoustic Emission*. University of California, Los Angeles 1976.
12. Włodarski J. K., Makowski L.: *Sposób i układ do sygnalizacji stanów zagrożenia awaryjnego łożysk silników spalinowych*. Patent nr 112916, 1982.
13. Włodarski J. K.: *Uszkodzenia łożysk okrętowych silników spalinowych*. Wydawnictwo Akademii Morskiej w Gdyni, Gdynia 2003.
14. Darski W., Girtler J.: *Pomiary parametrów emisji akustycznej generowanej przez zmęczeniowe uszkodzenia panwi łożysk MB50, MB02 na stanowisku badawczym SMOK Część VIII (wykonanie pomiarów na stanowisku, opracowanie wyników, wnioski z badań)*". Sprawozdanie z wykonania badań w ramach realizacji projektu badawczego Ministerstwa Nauki i Informatyzacji (nr. 3480/TO2/2006/31) pt.: „Identyfikacja stanu technicznego układów korbowo-tłokowych silników o zapłonie samoczynnym ze szczególnym uwzględnieniem emisji akustycznej jako sygnału diagnostycznego”. Prace badawcze Wydziału Oceanotechniki i Okrętownictwa Politechniki Gdańskiej nr 05/2009/PB, Gdańsk 2008.
15. Girtler J.: Sprawozdanie z realizacji projektu badawczego własnego, Grant Nr N504 043 31/3480 pt. „Identyfikacja stanu technicznego układów korbowo tłokowych silników o zapłonie samoczynnym ze szczególnym uwzględnieniem emisji akustycznej jako sygnału diagnostycznego”, kierownik projektu: prof. Jerzy Girtler.
16. ASME, Acceptance Test Procedure for Lass II Vessels, Article RT – 6, Section X, Boiler and Pressure Vessel Code (December 1988 Addendum and latter editions).
17. Instrukcja: Course Handbook for SNT-TC-1A Qualification/Certification Course for Acoustic Emission Personal, Level II, Physical Acoustic Corporation 1991.







## **NOWDAYS ASPECTS OF THE SELECTION OF THE PARAMETRS OF THE INJECTION OF THE FUEL IN DIESEL ENGINES**

**Marek Idzior**

*Poznań University of Technology  
ul. Piotrowo 3, 60-965 Poznań, Poland,  
tel. +48 61 6652350, fax . (+48 61) 6652402  
e-mail: Marek.Idzior@put.poznan.pl*

### **Abstract**

*In the article one introduced the problems of the selection of diesel engines injector nozzles parameters and limitations of the pressure of the fuel injection. One talked over conditioning being with the stimulator of their systematical height. The methods of the selection guilty so to embrace, except the selection of constructional parameters , also the selection taking into account concurrent occurrences , for example the pressure and the speed of injected fuel or the stress distribution. One executed analyses of restrictive factors of the endeavour to the further lifting of maximum values of the pressure of the fuel injection. In the recapitulation one underlined important of the problem and his participation on the future development diesel engines.*

**Key words:** diesel engine, development, new technologies, fuel equipment

### **1. The introduction**

Is difficulty univocally to give methods of principle of the selection of parameters of injector nozzles, considering additionally their influence on impurities of combustion gases of the diesel engine. The methods of the selection, taking into account the environment protection, cannot assemble exclusively on parameters of the part executive, is what just the injector nozzle. It should make allowance for also the construction and parameters of co-operative parley and reasons and consequences of concurrent occurrences to the injection and the atomization of the fuel in the cylinder of the diesel engine.

The methods of the selection guilty so to embrace, except the selection of constructional parameters , also the selection taking into account concurrent occurrences , for example the pressure and the speed of injected fuel or the stress distribution.

Considering placings requirements and occurrences happening {reaching} in the correctly working nozzle, methods of the selection of parameters of constructional injector nozzles one can divide on two core groups:

a) methods of the selection:

- methods optimization, leaning on the theory of the optimization of the construction,

- methods simulatory, leaning on findings with the use of specialized computer programmes (for example the stress distribution and thermal charges);
- b) empirical methods of the selection:
  - methods visualization leaning on the investigation (for example by means the instrument AVL Engine Video System) of the construction {the build} and the shape sprayed fuel,
  - motor leaning methods on the practical investigation of sets of injector nozzles about accepted parameters with the regard of measurement of concerning issues of toxic relationships.

## **2. The selection of parameters of injector nozzles by means mathematical optimization methods**

These methods consist in finding of best solution (in relation to the settled criterion) from the set of possibly (admissible) solutions. The conduct relies so on the research of the value of parameters for which is the realizing condition determining recorded mathematically the criterion of the examined occurrence, at the realization of recorded mathematically limitations.

The course of optimization problem one can divide on three stages:

- the acceptance of the criterion function and suitable groups of independent variables,
- the elaboration of the set of limitations,
- solution of optimization problem.

As the criterion function one can accept one from parameters of the work of the engine, for example the effective power  $N_e$  or the moment torque  $M_o$ . Answering to them independent variables will be each parameters of injector nozzles.

These parameters are treated independently, in the reality however the influence on the issue of impurities of combustion gases and the power or the moment generated by the engine have all combinations of occurrent sizes in at present the investigated injector. The only individual approach to every size gives the full possibility of the use of worked out technics and optimization algorithms.

The most of performance characteristics of the diesel engine can be approximated with the polynomial quadratic. Solution of the assignment must contain himself in the set of solutions admissible, appointed in our chance by admissible values of the issue of toxic relationships in combustion gases. This postulate assure only restrictive non-linear conditions, irregularity, for example  $HC_{tot}(\text{parameters of the nozzle}) \leq HC_{totDOP}$ .

Solution of optimization problem consists in the effective research the minimum of the criterion function in the admissible area traced by limitations - for example on the delimitation of the direction research of the point the minimum and on his qualification.

This type the approach to the theme of the selection of parameters of injector nozzles is, thanks to the quick development of computers and their possibilities counting, more and more often practical, from the regard even if on low costs of working out of optimum- solutions.

One cannot here however forget that is this typical theoretical approach and not always finding of best theoretical solution ties in with his immediate use in effect, because the progress in the development of computational methods considerably outdistances possibilities of their utilization in real model solutions.

Heaps of times on the hindrance to these best mathematical solutions stand up technological limitations or rememberings strength of materials limitations.

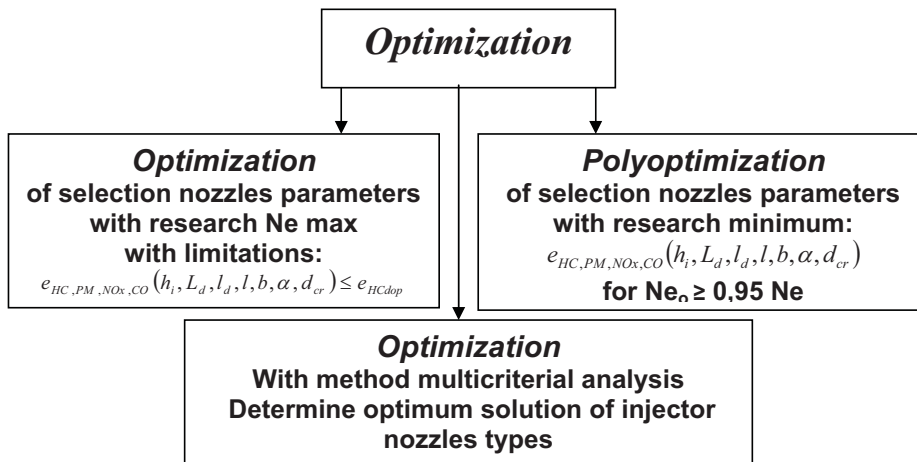


Fig. 1. Methods of the optimization of the selection of parameters of injector nozzles [2]

### 3. The selection of parameters of injector nozzles with the regard of the shape and the construction of the stream

The spray pattern of the fuel, his construction, the quality of spraying - the drop diameter and their schedule chiefly decide about the degree of the entire and complete combustion in the cylinder of the diesel engine, and what himself with this binds and emissivities of this engine.

For the purpose of the graphic performance of the quality of spraying one prepares the characterization of the proportional participation drops of the fuel in the dependence from their diameter. These characterizations are often called in the literature unjustly a phantom of spraying; in reality are a thickness of the probability of drop diameters and can be prepared for different of their decisive sizes about spraying.

In at present produced engines self-igniting more and more are more often practical injectors with two spring which make possible the realization of the two-grade injection. How show research, the use of the two-grade injection and injector nozzles VCO lowers the issue of nitrous oxides and hydrocarbons in combustion gases [1].

Simultaneously research showed that such fuel injection conjointly with injector nozzles VCO unfavourably bore on the smokiness of combustion gases. Enlarging smokiness is especially visible at low engine loads.

### 4. The selection of parameters of injector nozzles with the regard of limitations of the height of the pressure of the injection

Introduced to production engines are already provided into container parley Common Rail of the second generation, with enlarged pressure of the injection (160-180 MPa), in nearest years one foresees the enlargement of the pressure even to 220 MPa.

Nascent tensions at pressures 200 MPa are already too large for the persistence of some elements, first of all talked over injector nozzles. In spite that trunks of injector nozzles are executed steel

chromic-nickel-tungstenic, about the large endurance on the extension, this however due tensions with high pressures of the injection can reach the border of the plasticity of given material. Such state of the load can as result of of the fatigue of material bring to the damage of the sprayer.

Calculations of the nozzle with eight holes [2] whose the section one showed on the fig. 2, laden with the pressure 200 MPa and with the pressure 300 MPa, so such, what appears at the destruction of the sprayer in some parley of the power supply, showed that greatest tensions came into being on the passage of the nest of the cone-shaped trunk into the well. They carry out for the first chance 710 MPa, while for second 1065 MPa. Large tensions come into being also at edges of intake- injection's openings and carry out properly 510 MPa and about 947 MPa. Itself bottom of the well is not strongly laden, because prevalent there tensions in the dependence from the pressure of the fuel hesitate from 80 to 125 MPa. From these calculations it results that the pressure of the injection carrying out 300 MPa seems greatest, possibly to the usage for the fuel injection in the diesel engine for the endurance and the persistence of injector nozzles. So high pressures demand usages of materials about greater than till now endurances on the extension, what doubtless increases costs of the realization of injector nozzles. Practical until quite lately universally to this end chromic-nickel-aluminium steels, chromic-nickel- tungstenic and similar, are taken place steels about the greater endurance, for example steels nickel- and other modern materials. Such are carbide-steels in which the participation of carbides, mostly TiC, carries out to 50%. Constantly these, after the heat-treatment, attain the hardness about 70 HRC, even in elevated operating temperatures and the large resistance on the erosion and cavitation, are however difficult in the tooling and expensive.

On injector nozzles of greater engines it begins to comply stellites. This are very hard alloys (What - 65%, Cr - 25%, In - 5%, C - 2% and V, Fe and other) about the very small linear expansion, what causes the very good dimension- stability in elevated temperatures, the high abrasion resistance and the resistance on aggressive fuels, the corrosion and the oxygenation.

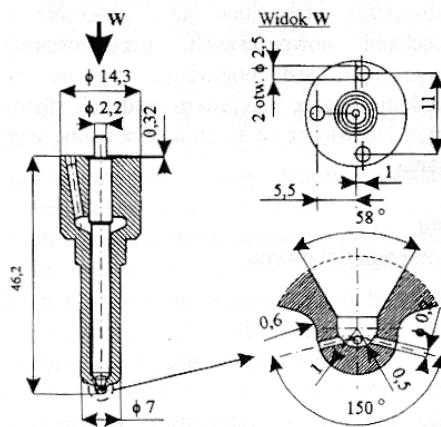


Fig.2. Injector nozzle with eight holes [2]

Stellites have the high price, but are not as usual permanent and make possible the diminution of the mass of the nozzle, what for greater injector nozzles begins to be profitable economically.

The height of the pressure of the injection can be also limited by the compressibility and the stickiness of the fuel, and also rectifier valves master with the flow of the fuel which will have to quickly and unfailingly to work conditioned of enlarged loads.

The diesel fuel under the pressure 300 MPa diminishes her own volume about 15-20%. Such his wring at small doses of injected fuel can cause disturbances of the injection. Higher pressures cause also the height of the stickiness of oil, what favours to the formation large, badly burning up drops of the fuel.

## **5. Conclusion**

Introduced problems of the selection of parameters of injector nozzles show as not as usual difficult is optimum- synchronizing of all parameters, so that they realize requirements placed to the present diesel engine, inclusive of with more and more sharper ecological requirements.

Perfecting of the injection's apparatus in today's engines of this type, with taking into account of norms of concerning issues of impurities, is one from most important criteria of the choice of best solutions of these decisive engines about the success of chosen constructions.

## **References**

- [1] Idzior M.: Nowe metody rozwiązywania problemów współczesnych silników o zapłonie samoczynnym. Zeszyty Naukowe Instytutu Pojazdów Politechniki Warszawskiej nr 3(66)/2007
- [2] Idzior M.: Studium optymalizacji doboru parametrów rozpylaczy wtryskiwaczy silników o zapłonie samoczynnym w aspekcie właściwości użytkowych silnika. Wydawnictwo Politechniki Poznańskiej, Poznań 2004.
- [3] Meyer S., Krause A., Krome D., Merker G.: Flexible Piezo Common-Rail-System with 3. Direct Needle Control. Motortechnische Zeitschrift nr 2, 2002.
- [4] Zbierski K.: Układy wtryskowe Common Rail. Łódź 2001.
- [5] Materiały firm: BMW, Honda, Mercedes, Toyota, Volkswagen





## **THE IMPACT OF PLATINUM-RHODIUM ACTIVE COATING INSIDE A COMPRESSION IGNITION ENGINE ON VOLATILE ORGANIC COMPOUNDS EMISSION**

**Anna Janicka, Wojciech Walkowiak, Włodzimierz Szczepaniak**

*Wroclaw University of Technology  
Wyb. Wyspiańskiego 27  
50-370 Wrocław  
tel./fax. +48 71 3477918  
e-mail: anna.janicka@pwr.wroc.pl*

### **Abstract**

*This paper presents the results of the researches on platinum-rhodium inner catalyst application in self-ignition engine (SB 3.1). A main aim of this study was volatile organic compounds (VOC's) marking in exhaust gases. Platinum and rhodium was used as an active coating. The catalyst was put onto the engine valves surface. As a catalyst support a zirconium ceramic was used. The ceramic layer was also used as a local thermal barrier. The results of the experiment was VOC's quantity-quantitative analysis in function of chosen points of the engine work. The results shows that platinum-rhodium active coating inside of the diesel engine caused about tenfold total VOC's concentration decrease. Because of significant toxicity of benzene and formaldehyde, for those compounds separate comparison analysis was done. Decrease of benzene concentration was also observed but catalyst effectiveness was lower than for total VOC's concentration. The results of analysis of the catalyst influence on formaldehyde concentration in exhaust are ambiguous.*

*Keywords: combustion engines, inner catalyst, volatile organic compounds, exhaust toxicity*

### **1. Introduction**

Several anthropogenic activities lead to volatile organic compounds emission into the atmosphere. One of the most important is motorization. VOC's emitted from combustion engines are very often hazardous compounds for human and environment [1, 3-5]. In the atmosphere, VOC's contribute to tropospheric ozone formation, stratospheric ozone layer depletion and to the greenhouse effect [3]. Inside the human body this organic compositions are able to resolve in fat and to cumulate in tissues.

Volatile organic compounds are significant group among 200 identified compounds in diesel engine exhaust (mainly aldehydes but also alcohols, ketons, esters, paraffin and aromatic hydrocarbons). In group of VOC's the most toxic and common in human environment are particularly: benzene, formaldehyde (methanal) and acrolein [5].

### **2. Experiment**

A modified SB3.1. compression ignition engine (diesel engine) was employed as a research engine. An engine modification was application of platinum-rhodium coating on engine valves. Conventional fuel (commercial diesel oil) was used as engine fuel. SB3.1 engine was loaded

with Hennan-Froude engine break. The most characteristic points of functional engine work (rotation speeds and loads) was chosen in experiment: 1200 r.p.m., engine loads: 5 Nm, 10 Nm, 20 Nm, 30 Nm and 1600 r.p.m., engine loads: 10 Nm, 20 Nm, 30 Nm (it was not possible to stabilize engine work for 5 and 30 Nm in initial conditions and 5 Nm when engine working with catalyst on the engine valves).

An engine modification was based on application of platinum-rhodium active coating on surface of the engine valves. Zirconium ceramic was used as a catalyst support.

A scheme of research work stand – engine test house – is presented in the figure 1.

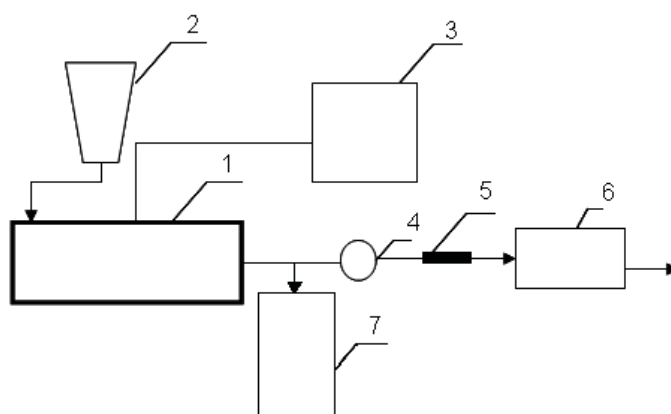


Fig. 1. Research workstand: engine test house. 1 – engine with a break, 2 – fuel reservoir, 3 – NO, CO and smoke level analyzers, 4 – formaldehyde absorber, 5 – tube with active coal, 6 – exhaust gases uptake system, 7 – engine control system

VOC's samples were up-taken by tubes with active coal (ex. prepared). Formaldehyde was up-taken by special absorption bulb with distilled water. The analysis was done according to polish standard: PN – EN ISO 16017-1: 2006. The laboratory analysis contains two analytic methods: colorimethry (formaldehyde marking according to directive PN-71/C-04539) and chromatography. Carbone disulfide (CS<sub>2</sub>) was used for VOC's extraction from active coal. Gas chromatograph Hewlett-Packard 5890 with FID detector and capillary column (HP-5, 30 m, 0,53 mm) was used for quantity and quality analysis. The chromatography conditions were: column temperature (110 °C), dozers (150 °C) and detectors (250 °C).

### 3. Results and discussion

The results of the experiment was VOC's quantity-quantitative analysis in function of chosen points of the engine work.

The VOC's concentration, mg/dm<sup>3</sup>, during engine work without catalytic coating application on engine valves is presented in table 1.

Tab. 1. Volatile Organic Compounds concentration in SB 3.1 engine gases. Initial conditions (engine without catalyst). Benzene and formaldehyde concentration is presented also separately because of its separate analysis in function of chosen points of engine work

Engine speed	1200 , r.p.m.				1600 , r.p.m.	
Engine load, Nm	5	10	20	30	10	20
VOC's groupe name	Concentration , mg/dm <sup>3</sup> *					
Aldehydes	0,042	0,059	0,061	0,061	0,059	0,086



Alcohols	0,0066	0,0064	0,0054	0,0051	0,0066	0,0058
Ketons	n.d.**	n.d.**	0,0075	0,0009	0,015	n.d.**
Aromatic hydrocarbons	0,0027	0,0034	0,0052	0,010	0,0060	0,0064
Praffin hydrocarbons	n.d.**	n.d.**	0,00028	0,0045	0,0049	0,0044
<b>Total VOC's</b>	<b>0,051</b>	<b>0,069</b>	<b>0,080</b>	<b>0,081</b>	<b>0,091</b>	<b>0,10</b>
Benzene	0,0014	0,0022	0,0015	0,0028	0,0012	0,0018
Formaldehyde	0,0032	0,0039	0,0043	0,0044	0,0040	0,010

\* the total method relative error is estimated on 20 % level

\*\* non detected

Total VOC's concentration is presented on figure 2. It is shown that with engine speed and engine load also volatile compounds emission is rising.

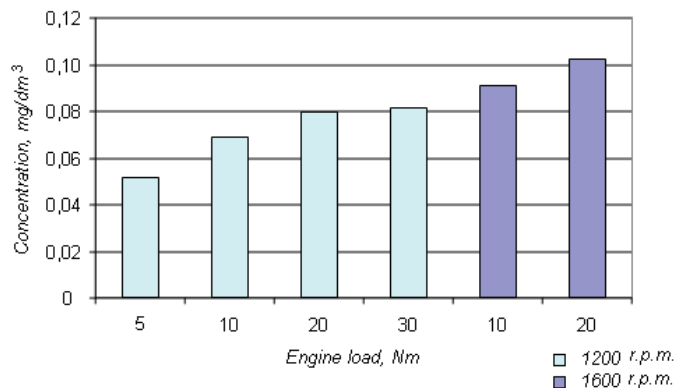


Fig. 2. Total VOC's concentration in SB 3.1 engine gases (initial conditions – engine without catalyst)

On following figures benzene (figure 3) and formaldehyde (figure 4) concentrations in function of engine work is shown.

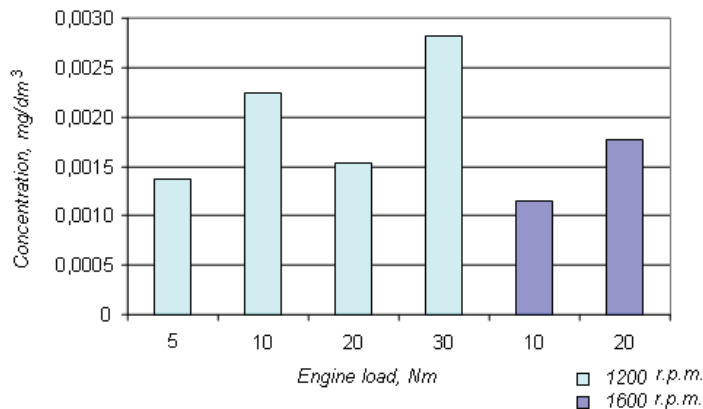


Fig. 3. Benzene concentration in SB 3.1 exhausts (initial conditions – engine without catalyst)

The lowest benzene concentration (0,0016 mg/dm<sup>3</sup>) was observed when engine was working with 10 Nm load and higher rotational speed and the highest concentration (0,0028 mg/dm<sup>3</sup>)

was detected for lower rotational speed and engine load 30 Nm. Benzene emission seems to rise proportional to engine load for both engine speeds but the results are ambiguous.

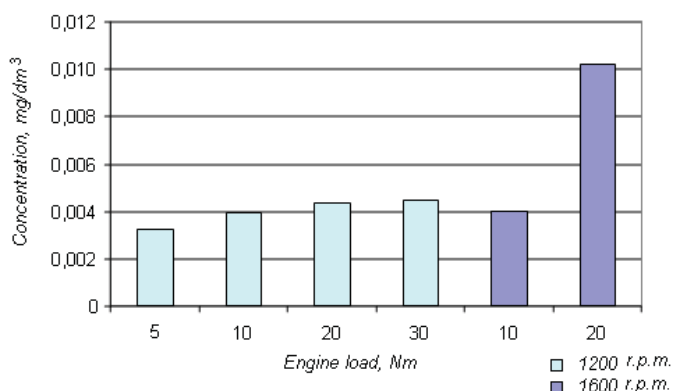


Fig. 4. Formaldehyde concentration in SB 3.1 exhausts (initial conditions – engine without catalyst)

In case of formaldehyde, insignificant concentration increase with engine load was observed when engine was working with lower engine speed. When engine was working with 1600 r.p.m. concentration of this compound rise rapidly (over 250 %) when engine load increase from 10 Nm to 20 Nm.

The results of VOC's analysis for the engine with platinum-rhodium active coating on the engine valves are presented in table 2.

Tab. 2. Volatile Organic Compounds concentration in SB 3.1 engine . Engine without catalyst (Pt/Rh active coating on the engine valves surface). Benzene and formaldehyde concentration is presented also separately because of its separate analysis in function of chosen points of engine work

Engine speed	1200 , r.p.m.				1600 , r.p.m.		
Engine load, Nm	5	10	20	30	10	20	30
VOC's groupe name	Concentration , mg/dm <sup>3</sup> *						
Aldehydes	0,00058	0,00202	0,00535	0,07085	0,00579	0,02904	0,01888
Alcoholes	0,00346	0,00153	0,00175	0,00089	0,00102	0,00142	0,00061
Ketons	n.d.**	0,00086	0,00048	0,00068	n.d.**	n.d.**	n.d.**
Aromatic hydrocarbons	0,00127	0,00292	0,00137	0,00198	0,00208	0,00662	0,00114
Praffin hydrocarbons	0,00028	0,00067	0,00031	0,00079	n.d.**	0,00025	0,00021
<b>Total VOC's</b>	<b>0,006</b>	<b>0,008</b>	<b>0,009</b>	<b>0,075</b>	<b>0,009</b>	<b>0,037</b>	<b>0,021</b>
Benzene	0,00095	0,00208	0,00096	0,00150	0,00085	0,00110	0,00114
Formaldehyde	n.d.**	0,00060	0,00500	0,00934	0,00320	0,02540	0,01660

\* the total method relative error is estimated on 20 % level

\*\* non detected

Total volatile organic compounds concentration in this condition of engine work (figure 5) seems to be on similar level (about 0,007 mg/dm<sup>3</sup>) for first three engine loads (engine speed 1200 r.p.m.). When engine worked with load 30 Nm total VOC's concentration increased tenfold. It is correlated with tenfold increase of aldehydes concentration in exhausts.

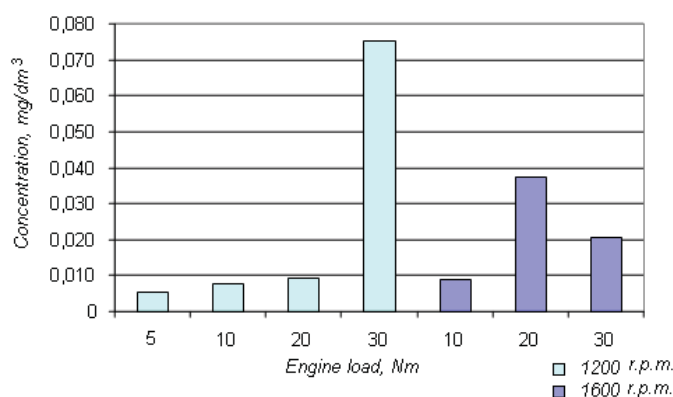


Fig. 5. Total VOC's concentration in SB 3.1 exhaust gases (engine with catalyst)

Benzene concentration in exhausts in engine load function is presented on figure 6.

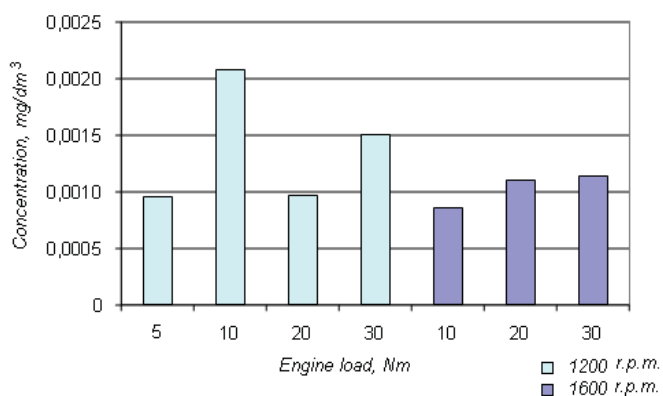


Fig. 6. Benzene concentration in SB 3.1 exhausts (engine with catalyst)

Lower benzene concentration was observed when engine was working with higher engine speed. Despite the fact that benzene concentration for 1600 r.p.m. was lower than for 1200 r.p.m. it was increasing with engine load. When engine was working with 1200 r.p.m. benzene concentration was changing rapidly and without unambiguous trend.

On figure 7 formaldehyde concentration in engine load function is presented.

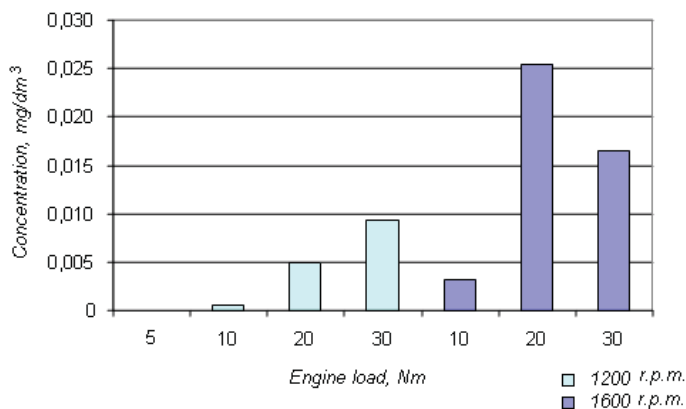


Fig. 7. Formaldehyde concentration in SB 3.1 exhausts (engine with catalyst)

For engine speed 1200 r.p.m. formaldehyde concentration was significant increasing with engine load. When engine was working with higher rotational speed concentration increasing in engine load function was also observed but the highest concentration was detected when engine worked with 20 Nm load.

For effectiveness estimation of active coating application inside diesel engine a comparison total VOC's concentration in engine exhaust gases in both conditions (engine with and without catalyst) was done (figure 8).

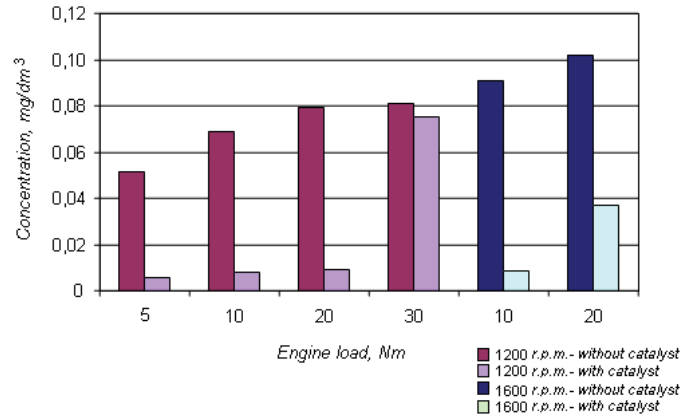


Fig. 8. Comparison of total VOC's concentration in exhausts for both condition: engine with and without catalyst in function of engine work

Platinum-rhodium active coating inside of the diesel engine caused about tenfold total VOC's concentration decrease. Because of significant toxicity of benzene and formaldehyde for those compounds separate comparison analysis was done.

On figure 8 benzene concentration for both conditions of engine work in function of engine work is presented. Decrease of benzene concentration when engine was working with catalyst is observed in every point of engine work but catalyst effectiveness is lower than for total VOC's concentration (figure 9).

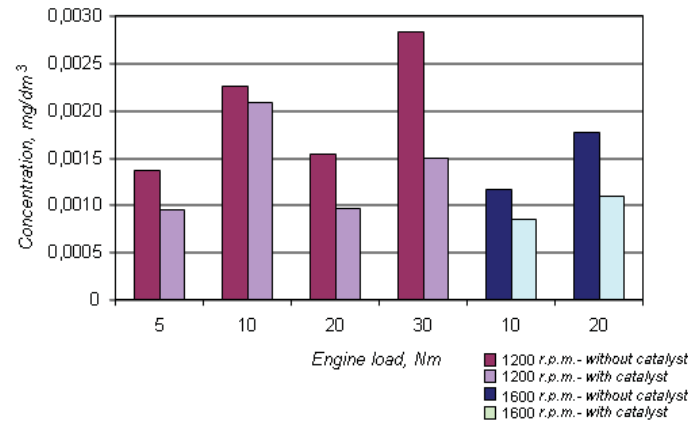


Fig. 9. Comparison of benzene concentration in exhausts for both condition: engine with and without catalyst in function of engine work

For formaldehyde decrease of concentration level when engine was working with catalyst was also observed (except two points of engine work: 1200 r.p.m./30 Nm and 1600 r.p.m./20 Nm) (figure 10).

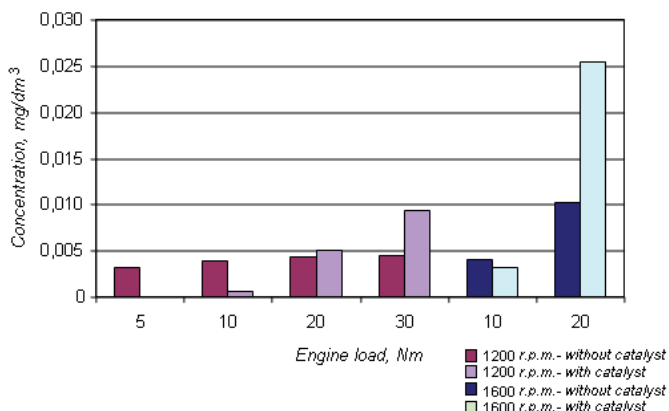


Fig. 10. Comparison of formaldehyde concentration in exhausts for both condition: engine with and without catalyst in function of engine work

Those two points of engine work are maximum engine load in case of both engine speeds. In this points the highest temperature of exhausts was observed. For catalytic process the temperature level is very important (it influence on effectiveness of the process) that's why a complete analysis of VOC's concentration in function of various values in needed.

#### 4. Conclusions:

1. Platinum-rhodium active coating inside of the diesel engine (on the engine valves surface) caused about tenfold total VOC's concentration decrease and significant decrease of the most toxic substances (from VOC's identified in the engine exhaust gases): benzene and formaldehyde.
2. Because of ambiguous results of some stages of the experiment complete analysis of VOC's concentration in function of various values in needed.

#### References:

- [1] Czarny A, Zaczyńska E, Mendyka B., Janicka A., *Influence of biodiesel exhaust on NF- $\kappa$ B activation and TNF- $\alpha$  production in human lung and peripheral blood leukocytes, in vitro*. Materiały Konferencyjne IV Konferencja Naukowo-Szkoleniowa "Immunomodulacja: badania doświadczalne i kliniczne". Jurata, Polska, 25.05.-26.05 2007.
- [2] Fishader G., roder-stolinski C., Wihmann G., Nieber K., Lehmann I., *Release of MCP-1 and IL-8 from lung epithelial cells exposed to volatile organic compounds*. Toxicology in Vitro 22 (2008) 359-366.
- [3] Janicka A., Walkowiak W., Szczepaniak W., *Inert catalyst in compression ignition engine. VOC's emission*, Journal of KONES Powertrain and Transport vol.14, No.5./2007.
- [4] Janicka A., Walkowiak W., *Emisja lotnych związków organicznych i wielopierścieniowych węglowodorów aromatycznych z silnika zasilanego biopaliwem*. Silniki Spalinowe. 2007 R. 46, nr SC3.
- [5] Lebrecht G., Czerczak S., Szymczak W., *Benzen – dokumentacja*. Podstawy i Metody Oceny Środowiska Pracy Numer 1 (35) 2003.





## THE EFFECT OF PLATINUM-RHODIUM INNER CATALYST APPLICATION IN A COMPRESSION IGNITION ENGINE ON TOXICITY EQUIVALENT FACTOR OF VOLATILE ORGANIC COMPOUNDS IN EXHAUST GASES

Anna Janicka, Wojciech Walkowiak, Agnieszka Sobianowska-Turek, Radosław Wróbel

Wroclaw University of Technology  
Wyb. Wyspińskiego 27  
50-370 Wroclaw  
tel./fax. +48 71 3477918  
e-mail: anna.janicka@pwr.wroc.pl

### Abstract

*Emission from mobile sources causes human and environment exposure to hazardous, toxic substances. Because of civilization diseases expansion it is very important to estimate a toxic influence of emitted by combustion engine substances on human health. This paper presents the results of analysis of platinum-rhodium active coating application in diesel engine on toxicity of volatile organic compounds (VOC's) in exhaust gases.. The catalyst was applied on SB.3.1 compression ignition engine valves surface. A special methodology of engine exhaust toxicity was applied: calculation of Toxic Equivalent Factor (TEF). For estimation of volatile organic compounds toxicity in the engine exhaust gases as a indicator benzene was chosen. The calculation of TEFs was base don Recommended Maximum Concentration Limits (RMCL), for one year period, according to polish Minister of Environment Directive (Dz.U.2003 nr 1 poz. 12). Toxicity Equivalent Factor was calculated for total volatile organic compounds identified in every chosen point of SB3.1 engine work and toxic. A comparison analysis of VOC's toxicity in the engine exhausts in both conditions (with and without platinum rhodium active coating on the engine valve surface) was done. The analysis results show that inner catalyst application causes significant toxicity decrease for lower engine loads for both chosen rotational speeds.*

**Keywords:** engine exhaust toxicity, volatile organic compounds, Toxicity Equivalent Factor

### 1. Introduction

The ability of organic chemicals to cause health effects varies greatly from those that are highly toxic, to those with no known health effect. As with other pollutants, the extent and nature of the health effect will depend on many factors including level of exposure and length of time exposed. Eye and respiratory tract irritation, headaches, dizziness, visual disorders, and memory impairment are among the immediate symptoms that some people have experienced soon after exposure to some organics. Many organic compounds are known to cause cancer in animals; some are suspected of causing, or are known to cause, cancer in humans. [4] Volatile organic compounds (VOC's) effects on human health range from odour problems to toxic or carcinogenic effects. As a consequence, more stringent legislation on VOC emission has been implemented worldwide. To comply with this legislation, the use of processes which inherently cause little or no VOC's emission is preferable [4].

A motorization is one of the most important anthropogenic source of VOC's emission. Combustion engines are responsible for benzene, formaldehyde or acrolein emission – those substances belong to VOC's group and there are known from their mutagenic and carcinogenic properties. Because a fact that most of volatile organic compounds are listed as being toxic not only a problem their concentration in exhausts is considered necessary to be solved but also it is very important to monitor their toxic influence on human health. The second problem is very complicated and it strongly depends of the VOC's group composition in emitted exhaust gases. Estimation of toxic influence of particular compounds in VOC's group is also very problematic because not for many substances their toxic properties are unknown. For some substances Recommended Maximum Concentration Limit (RMCL) is settled in governmental directives what constitute a base for VOC's mixture toxicity estimation by using Toxicity Equivalent Factors (TEF) [1-3].

## **2. Experiment**

A modified SB3.1. compression ignition engine (diesel engine) was employed as a research engine. An engine modification was application of platinum-rhodium coating on engine valves. Conventional fuel (commercial diesel oil) was used as engine fuel. SB3.1 engine was loaded with Hennan-Froude engine dyno. The most characteristic points of functional engine work (engine speeds and loads) was chosen in experiment: 1200 r.p.m., engine loads: 5 Nm, 10 Nm, 20 Nm, 30 Nm and 1600 r.p.m., engine loads: 10 Nm, 20 Nm, 30 Nm (it was not possible to stabilize engine work for 5 and 30 Nm in initial conditions and 5 Nm when engine working with catalyst on the engine valves).

An engine modification was based on application of platinum-rhodium active coating on surface of the engine valves. Zirconium ceramic was used as a catalyst support.

A scheme of research work stand – engine test house – is presented in simultaneously printed paper [2].

VOC's samples were up-taken by tubes with active coal (ex. prepared). Formaldehyde was up-taken by special absorption bulb with distilled water. The analysis was done according to polish standard: PN – EN ISO 16017-1: 2006. The laboratory analysis contains two analytic methods: colorimetry (formaldehyde marking according to directive PN-71/C-04539) and chromatography. Carbone disulfide (CS<sub>2</sub>) was used for VOC's extraction from active coal. Gas chromatograph Hewlett-Packard 5890 with FID detector and capillary column (HP-5, 30 m, 0,53 mm) was used for quantity and quality analysis. The chromatography conditions were: column temperature (110 °C), dozers (150 °C) and detectors (250 °C).

## **3. Methodology of VOC's toxicity estimation in engine exhaust**

For estimation of volatile organic compounds toxicity in the engine exhausts as a indicator benzene was chosen because of its well known mutagenic and carcinogenic properties. Benzene is absorbed mainly from respiratory system and alimentary canal. Benzene and its metabolites (i.e. phenol) are able to fixation with liver proteins, bone marrow, kidney, blood, muscles and lien proteins. It cause devastation of nervous system and bone marrow (causes leukemia). Allowable benzene concentration in atmospheric air in Poland amount to 5 µg/m<sup>3</sup>.

For the diesel engine exhaust toxicity estimation Toxicity Equivalent Factors (TEF) related to benzene was applied. Benzene was identified in the engine exhaust in every chosen point of its work. The analysis of VOC's toxicity in exhaust was based on Recommended Maximum Concentration Limits (RMCL), for one year period, according to polish Minister of Environment Directive (Dz.U.2003 nr 1 poz. 12).

TEF for total volatile organic compounds in exhaust was determinate as follow:



- Coefficient R was determinate as a benzene RMCL ratio to RMCL of particulate compound from VOC's group (table 1),
- TEF for single VOC was calculated by multiplication its coefficient R and its concentration in exhausts,
- TEFs determinate for single VOC's detected in exhausts was tot up. The result was TEF for total VOC's.

For some identified in exhaust gases compounds (isovaleric aldehyde, isobutyl aldehyde and ethanol) was not possible to TEF calculated because for those substances RMCL was not determinate. Those substances was not taken into consideration in TEF for total VOC's calculation.

Recommended Maximum Concentration Limit (RMCL),  $\mu\text{g}/\text{m}^3$ , for year period, for VOC's identified in the engine (SB3.1) exhaust and R coefficient are presented in table 1.

Tab. 1. Recommended Maximum Concentration Limit (RMCL),  $\mu\text{g}/\text{m}^3$ , for year period, for VOC's identified in the engine (SB3.1) exhaust

Compound	Chemical formula	RMCL, $\mu\text{g}/\text{m}^3$	R coefficient: $R = \frac{RMCL_{benzene}}{RMCL_x}$
Akrolein	$\text{C}_3\text{H}_4\text{O}$	0,9	5,556
Acetic aldehyde	$\text{C}_2\text{H}_4\text{O}$	2,5	2,00
MIBK (metylisobutylketone)	$\text{C}_6\text{H}_{12}\text{O}$	3,8	1,316
Formaldehyde	$\text{CH}_2\text{O}$	4	1,250
<b>Benzene</b>	<b><math>\text{C}_6\text{H}_6</math></b>	<b>5</b>	<b>1,00</b>
Toluene	$\text{C}_7\text{H}_8$	10	0,500
Xylene	$\text{C}_8\text{H}_{10}$	10	0,500
Butyl alcohol	$\text{C}_4\text{H}_{10}\text{O}$	26	0,192
Acetone	$\text{C}_3\text{H}_6\text{O}$	30	0,167
Ethylbenzene	$\text{C}_8\text{H}_{10}$	38	0,132
Heptane	$\text{C}_7\text{H}_{16}$	1000	0,005
Hexane	$\text{C}_6\text{H}_{14}$	1000	0,005
Octane	$\text{C}_8\text{H}_{18}$	1000	0,005
Nonane	$\text{C}_9\text{H}_{20}$	1000	0,005
Isovaleric aldehyde	$\text{C}_4\text{H}_9\text{O}$	No data	---
Ethanol	$\text{C}_2\text{H}_6\text{O}$	No data	---
Propionate aldehyde	$\text{C}_3\text{H}_6\text{O}$	No data	---
Isobutyl aldehyde	$\text{C}_4\text{H}_8\text{O}$	No data	---

Based of quantity-quantitative analysis [2] Toxicity Equivalent Factor was calculated for total volatile organic compounds identified in every chosen point of SB3.1 engine work. Toxicity Equivalent Factors (TEFs) for total volatile organic compounds emitted by the self-ignition engine are presented in table 2.

Tab 2. Toxicity Equivalent Factors (TEFs) for total volatile organic compounds emitted by the compression ignition engine

Engine work conditions	Engine work phase						
	1200 r.p.m.				1600 r.p.m.		
	5 Nm	10 Nm	20 Nm	30 Nm	10 Nm	20 Nm	30 Nm
	Toxicity Equivalent Factor (TEF)						
Initial conditions (engine without catalyst)	0,00605	0,00775	0,01003	0,01322	0,02434	0,01572	--
Engine with Pt/Rh catalyst	0,00125	0,00627	0,00805	0,01431	0,00546	0,03561	0,02189

A variability of Toxicity Equivalent Factor if function of engine speed and engine load for initial conditions (engine without catalyst) is presented on figure 1.

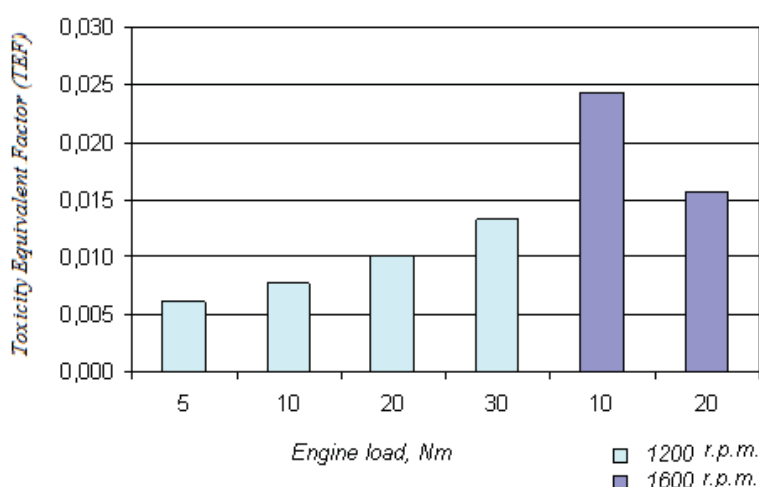


Fig.1. Volatile organic compounds toxicity emitted by SB3.1 diesel engine (initial conditions – engine without catalyst)

When engine was working with lower engine speed (1200 r.p.m.) increase of VOC's toxicity with engine load was observed – this trend was compatible with VOC's concentration and it is also correlated with formaldehyde concentration increase in exhausts [2].

When engine was working with higher engine speed (1600 r.p.m) and inverse trend was observed – the highest TEF characterized VOC's emitted when engine was working with lower load (10 Nm) and for lower load (20 Nm) 30 % TEF reduction was observed.

After platinum-rhodium inner catalyst application similar situation was noticed for engine speed 1200 r.p.m. (figure 2). When engine was working on 1600 r.p.m. engine speed level the highest value of TEF was observed for middle engine load (20 Nm). The tendency of TEF variability is very similar to formaldehyde concentration in this conditions of engine work (engine with catalyst) [2].

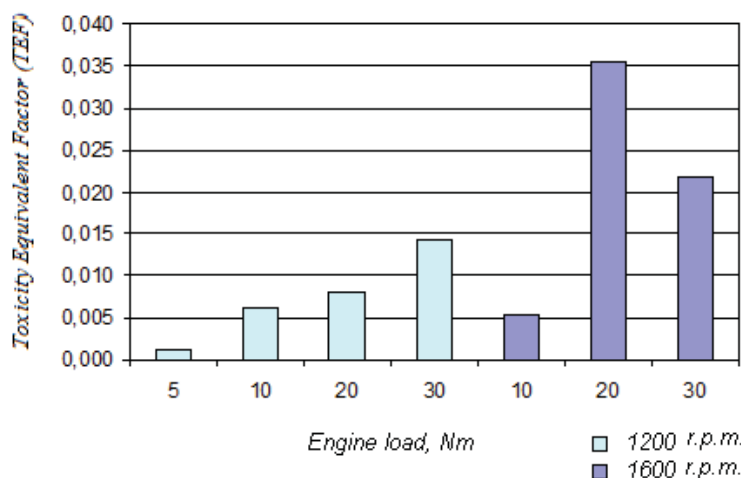


Fig.2. Volatile organic compounds toxicity emitted by SB3.1 diesel engine (initial conditions – engine without catalyst)

A comparison analysis of VOC's toxicity in the engine exhaust gases in both conditions (with and without platinum rhodium active coating on the engine valve surface) was done. The analysis results show that inner catalyst application causes significant toxicity decrease for lower engine loads for both chosen engine speeds (figure 3).

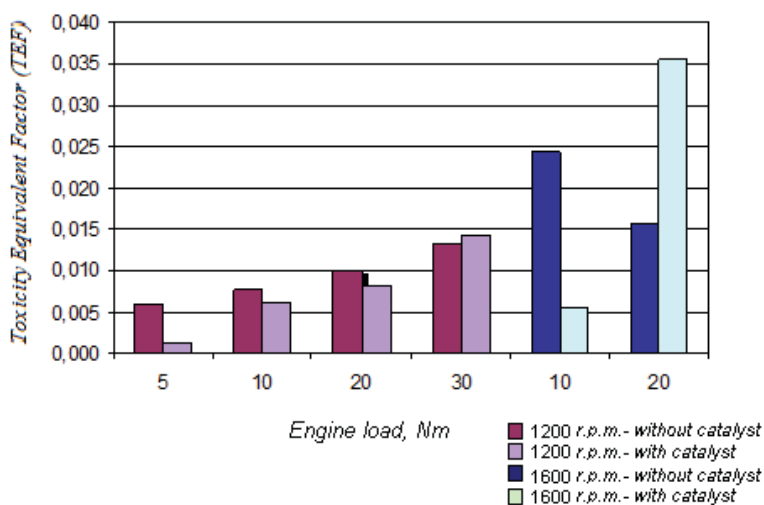


Fig.3. A comparison of VOC's toxicity emitted with SB3.1 diesel engine exhaust

When engine was working whit higher load decrease of catalyst effectiveness was observed. For the highest engine loads (for both engine speeds) catalyst application caused the aggravation of exhaust quantity in their toxicity aspect.

#### 4. Conclusions

1. The platinum-rhodium active coating application causes significant toxicity decrease for lower engine loads, but the catalyst effectiveness was decreasing rapidly with engine load rising.
2. Engine exhausts toxicity strongly depends on exhaust composition (participation of the most toxic compounds).
3. Toxicity Equivalent Factor, because of specific calculation method, is correlated with law regulation (is based on current regulations e.g. Recommended Maximum Concentration Limit), so its value can be changeable.

#### References:

- [1] Fishader G., roder-stolinski C., Wihmann G., Nieber K., Lehmann I., *Release of MCP-1 and IL-8 from lung epithelial cells exposed to volatile organic compounds*. Toxicology in Vitro 22 (2008) 359-366.
- [2] Janicka A, Walkowiak W., Szczepaniak W., *The impact of platinum-rhodium active coating inside a self-ignition engine on Volatile Organic Compounds (VOC's) emission*, paper simultaneously printed.
- [3] Janicka A., Walkowiak W., *Emisja lotnych związków organicznych i wielopierścieniowych węglowodorów aromatycznych z silnika zasilanego biopaliwem*. Silniki Spalinowe. 2007 R. 46, nr SC3.
- [4] United States Environmental Protection Agency (EPA), *Organic Gases (Volatile Organic Compounds – VOC's)*, <http://www.epa.gov/iaq/voc.html#Health%20Effects> (January 15 2008).
- [5] Rozporządzenie Ministra Środowiska z dnia 5 grudnia 2002 r. w sprawie wartości odniesienia dla niektórych substancji w powietrzu (Dz.U.2003 nr 1 poz. 12).



## EFFECT OF FATTY ACID METHYL ESTERS (FAME) ON PHYSICAL AND CHEMICAL PROPERTIES OF AVIATION TURBINE FUELS

Grażyna Karp

*The Technology Institute of Air Force*

*13 Kolska street*

*01-494 Warsaw, Poland*

*phone/fax: +48 22 685 30 84 | e-mail: [grazyna.karp@itwl.pl](mailto:grazyna.karp@itwl.pl)*

### **Abstract**

*In recent years there is tendency to adjust domestic petroleum products to meet world and European standards that establish high requirements regarding environment protection. At the same time, it is tendency to introducing wider spectrum of biocomponents that in turn enables to reduce harmful influence on environment. The work described in this paper, among others, consists in evaluation of effect of various concentration of FAME in aviation turbine fuel on its physical and chemical properties. The research work includes effect of FAME on fuel properties regarding the refinery process (density, distillation, flash point, composition, and the like) but also on properties important in regard to engine operation (kinematic viscosity, acid number, oxidation stability, gum content, freezing point, and the like). The work covers also the effect of selected antioxidants and depressants on FAME containing fuels on turbine engines operation. Considering the environment protection, the work includes evaluation of FAME presence on sulphur content, carbon and ash content. In order to establish stability - resistance to different ambient conditions - such blends undergo cyclic temperature changes. Results will be used to evaluate the possible use of biofuels in turbine engines.*

**Keywords:** *environment protection, biocomponents, biofuels- alternate fuels, greenhouse effect, emission gases*

In recent years there is tendency to adjust domestic petroleum products to meet world and European standards that establish high requirements regarding environment protection. At the same time, it is tendency to introducing wider spectrum of biocomponents that in turn enables to reduce harmful influence on environment [1, 3, 4, 5].

Climate change is one of the biggest challenges that mankind is facing. There is necessity to prepare relevant steps aiming at carbon dioxide emission reduction. Both air and sea transport have similar share in CO<sub>2</sub> emission. This is because the motive technology and employed fuels are not covered by ecological standards. The transport sector has growing share in European and global carbon dioxide emission. One of the ways to reduce this emission is usage of biofuels as components of typical fuels (biofuels of first generation). Growing transportation means emission of harmful exhaust gas components, not only the carbon dioxide and water, but also the nitrogen oxides, particles as well as hydrocarbons. Such emissions cause lowering air quality and contribute to anthropogenic increase of greenhouse effect [2, 4]. So as to the transport would be neutral to environment regarding the emission of greenhouse gases, the work is conducted with aim to use

alternate fuels. In short time we need the fuel that could partially substitute for currently used aviation fuel.

The work described in this paper consists in evaluation of effect of various concentration of FAME in aviation turbine fuel on its physical and chemical properties. The research work includes effect of FAME on fuel properties regarding the refinery process (density, distillation, flash point, composition, and the like), but also on properties important in regard to engine operation (kinematic viscosity, acid number, oxidation stability, gum content, freezing point, and the like). The work covers also the effect of selected antioxidants and depressants on FAME containing fuels on turbine engines operation. Considering the environment protection, the work includes evaluation of FAME presence on sulphur content, carbon and ash content. In order to establish stability - resistance to different ambient conditions - such blends undergo cyclic temperature changes. Results will be used to evaluate possible use of biofuels in turbine engines.

This work covers analysis of change in physical and chemical parameters of aviation fuel Jet A-1 containing various amounts of FAME: 2 %, 5 %, 10 %, 15 %, and 20 %. The Jet A-1 fuel from different plants and FAME from different manufacturers were used in the work. Blends of fuel with FAME were tested in regard to physical and chemical properties. The effect of FAME content on such properties is evaluated basing on plots picturing changes of relevant properties of tested blends.

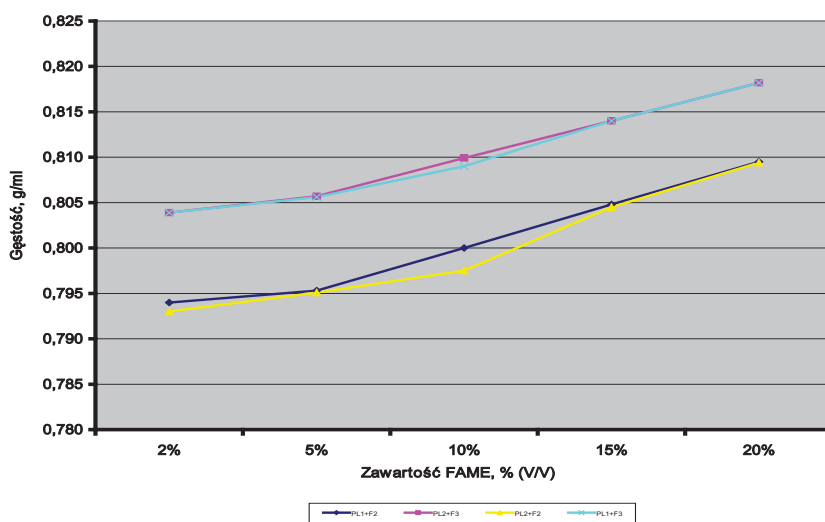


Fig. 1 Density vs. FAME content

More esters content in mixtures means relevant density increase. Blend density mostly depends on FAME density. Densities of blends of two different Jet A-1 fuels with the same FAME, and the same FAME content are very similar. All obtained densities fall into the specification requirements 0.775 - 0.840 g/ml.

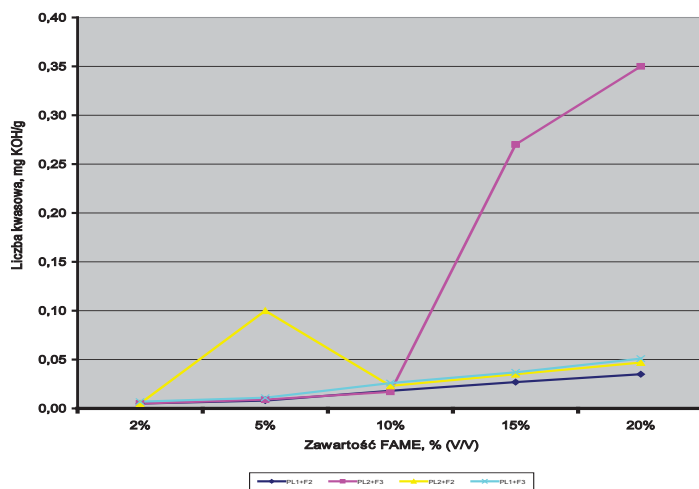


Fig. 2 Acid number vs. FAME content

Despite the used fuel it is difficult to find any dependence on FAME content. Blends of PL1 fuel with esters demonstrated the best behaviour where there was continuous increase of acid number with amount of added FAME. As to PL2+F3 blend, there was sudden increase of acid number for FAME content above 10 % (v/v). As to PL2+F2 blend, after sudden decrease for 5 % (v/v) FAME content, consequent increasing FAME content results in small acid number increase. The acid number value exceeds the specification requirement max. 0.015 mg KOH/g only in case of PL2+F3 blend.

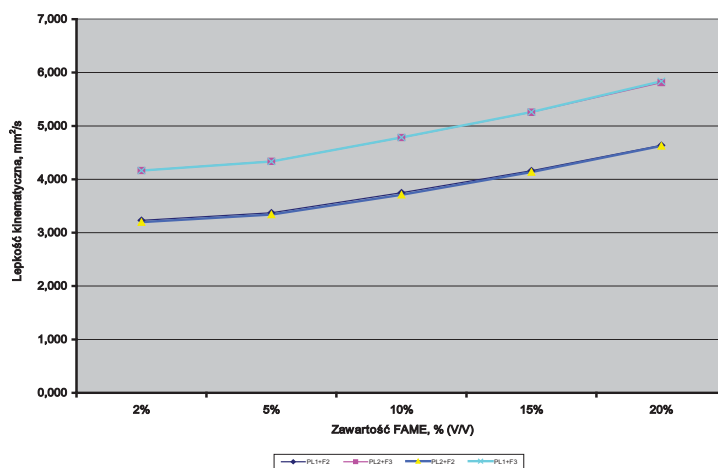


Fig. 3 Kinematic viscosity vs. FAME content

Viscosity of all kind of blends gets higher with ester content increase. For two different Jet A-1 fuels and the same FAME blend viscosity depends mostly on FAME viscosity. Viscosities of blend containing the same amount of FAME are very similar. Viscosities of blend fall into the fuel specification requirement max. 8.0 mm<sup>2</sup>/s for FAME content up to the 20 % (v/v).

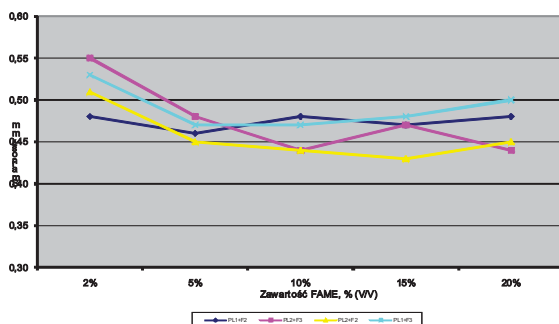


Fig. 4 Lubricity vs. FAME content

It is impossible to explicitly describe the effect of FAME content on BOCLE lubricity. For every mixture lubricity increases with FAME content initially that is indicated by decreasing scar diameter. Then, for different blends, lubricity starts to decrease, but at different FAME content. It should be accepted that such fluctuation are caused by “randomness” which is acceptable by test method precision and at the same time it is possible to eliminate it by performing more repetitions and making statistical evaluation. Blend of PL2 and FAME F2 demonstrated the best lubricity which shows increase up to 15 % (v/v) FAME content.

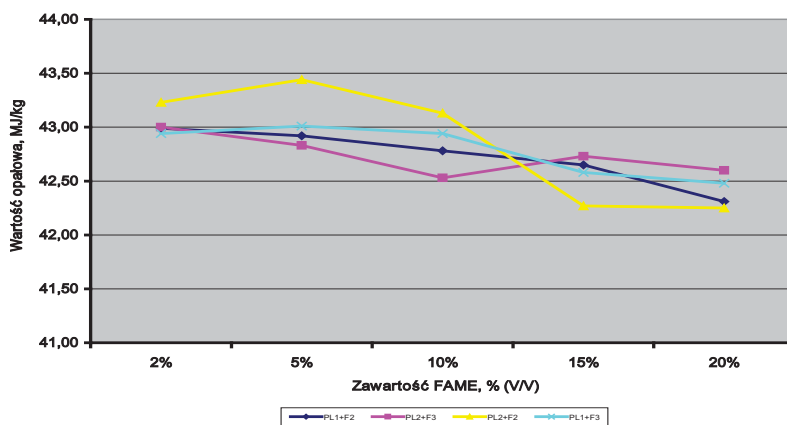


Fig. 5 Net heat of combustion vs. FAME content

Blend containing PL2 fuel and FAME F2 demonstrated the best combustion properties at the initial stage. But the smallest difference in combustion properties was demonstrated by blend of PL2 fuel and FAME F3. Net heat of combustion is stable up to 10 % (v/v) FAME content only for blend of PL1 fuel and FAME F3. As it can be seen at the plot, the change of net heat of combustion of the blend depends greatly on properties of employed FAME.



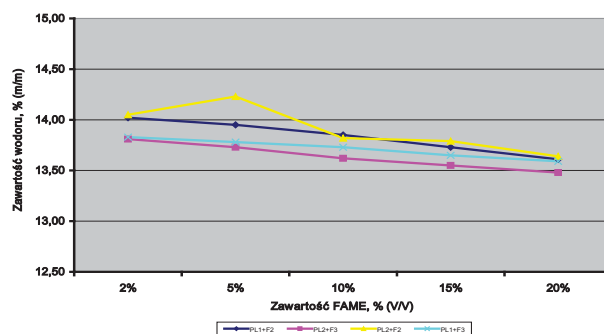


Fig. 6 Hydrogen content vs. FAME content

Generally it can be said that hydrogen content decreases with increase of FAME concentration in fuel. Though, the obtained values comply with minimum requirements for aviation turbine fuels.

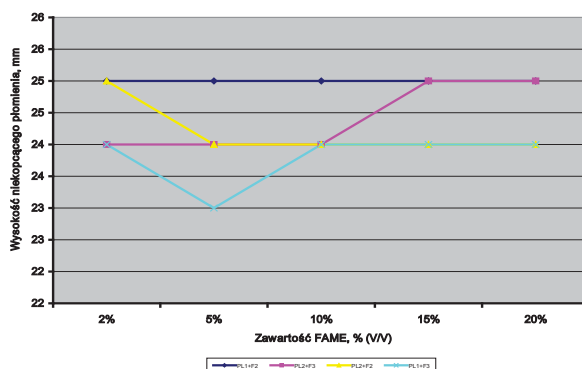


Fig. 7 Smoke point vs. FAME content

It is difficult to explicitly describe obtained values of smoke point and their dependence on FAME content for all samples. The best behaviour was demonstrated by blend of PL1 fuel and esters F2 which achieved minimum requirements for fuel at whole range. So it can be assumed that esters presence have little effect on value of this parameter.

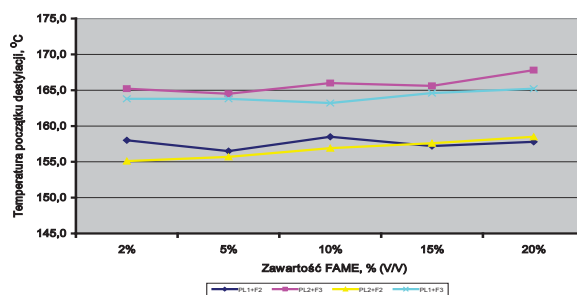


Fig. 8 Initial boiling point vs. FAME content

In case of presented blends the initial boiling point demonstrates slight uptrend. At the same time the used FAME has an effect on initial boiling point. In case of the same ester and different

fuels, temperatures for individual FAME concentrations demonstrate considerable differences. This is because FAME presence doesn't contribute to distillation run these temperature ranges.

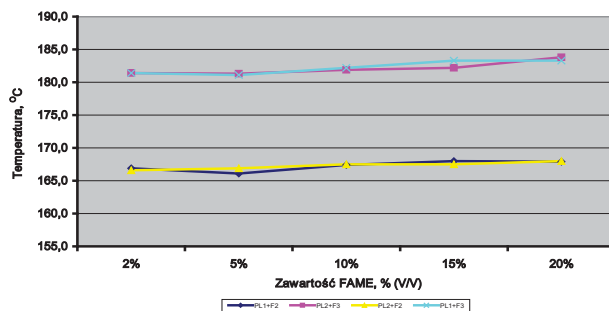


Fig. 9 Temperature of 10 % (v/v) evaporation vs. FAME content

This parameter demonstrates slight uptrend for presented blends. Esters have small effect on this parameter, whereas the properties of aviation fuel have decisive influence on it.

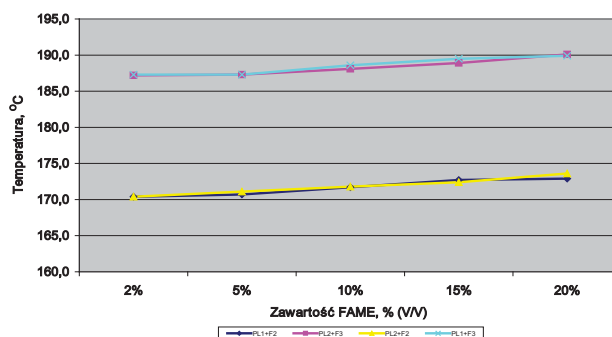


Fig. 10 Temperature of 20 % (v/v) evaporation vs. FAME content

In case of this parameter it also demonstrates slight uptrend. At the same time, effect of used FAME is more noticeable. The temperatures of 20 % evaporation are considerably different at various content of the same FAME in different fuels.

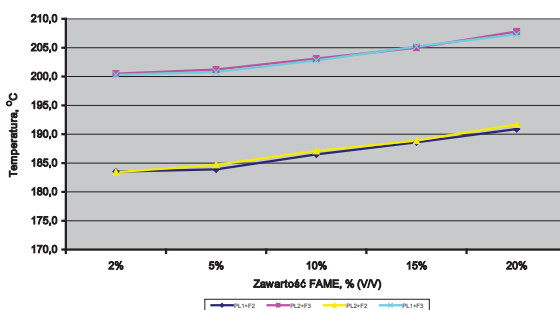


Fig. 11 Temperature of 50 % (v/v) evaporation vs. FAME content

According to tendency shown in fig. 9 and 10 we can see bigger effect of FAME presence on test results, though the petroleum fuel properties are still the most important.

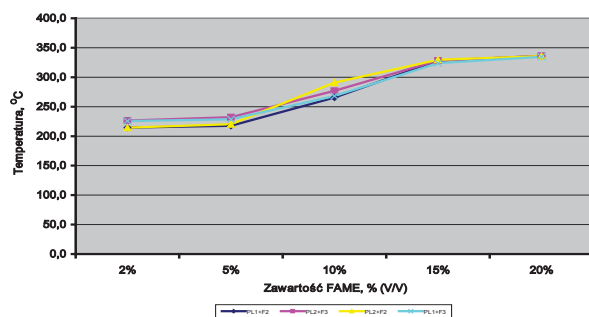


Fig. 12 Temperature of 90 % (v/v) evaporation vs. FAME content

Presented blends demonstrated significant uptrend regarding the 90 % (v/v) evaporation temperature. The FAME effect on blend distillation run at this final fragment of distillation curve is already distinctly visible. It means that more intensive distillation of heavier fractions of biocomponents.

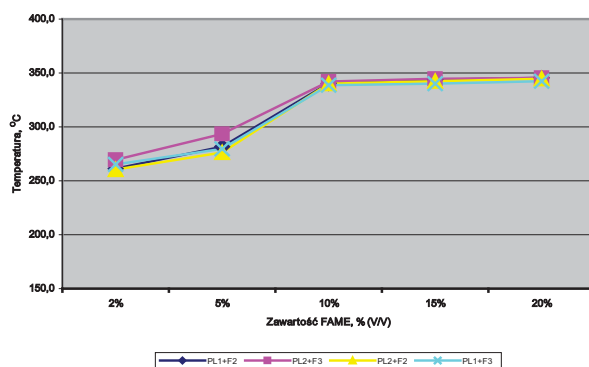


Fig. 13 Final boiling point vs. FAME content

In case of presented blends there is sudden increase of FBP values for FAME content up to 10 % (v/v), and then the increase of FBP is minimal for all blends.

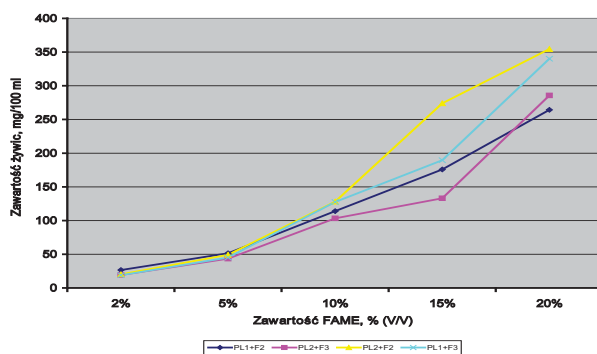


Fig. 14 Existent gum vs. FAME content

There was large uptrend of existent gum for almost every blend. Such trend is not confirmed by thermal stability (JFTOT) results for the blends. Though the existent gum exceeded acceptable

values for aviation turbine fuels it should be noticed that such considerable quality deterioration wasn't observed in case of oxidation stability. Probably, it's because the test method is suited especially to petroleum aviation fuels. This method may be not suitable to biocomponents with quite different chemical structure (for instance, because of too low temperature of evaporating medium - superheated steam).

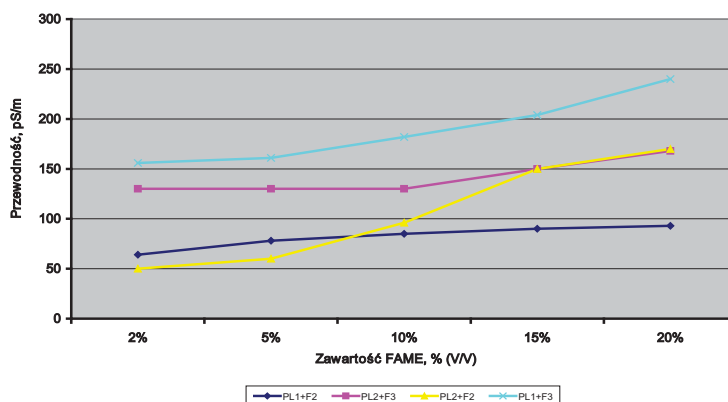


Fig. 15 Conductivity vs. FAME content

Conductivity demonstrates uptrend with FAME content increase in blends. There is no relationship between kind of fuel and FAME. Probably it is because of too large surface tension of esters in relation to petroleum fuels [6].

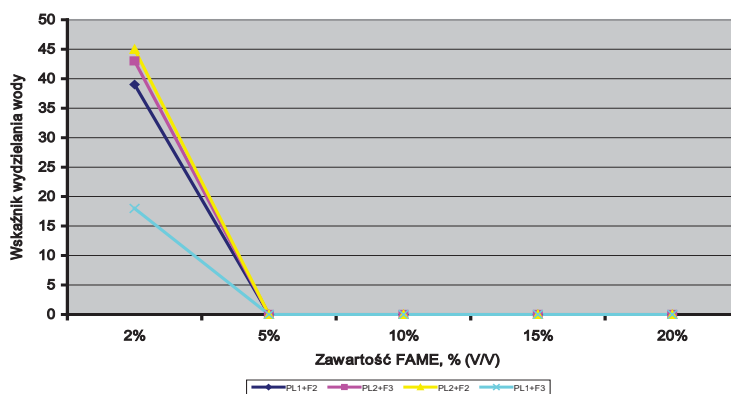


Fig. 16 Water separation index vs. FAME content

The index decreases suddenly after addition of 5 % (v/v) of esters, and reaches zero for every blend. This can disturb operation of coalescing - separating filters. Influence of FAME on water separation index can arise due to high surface tension of esters.

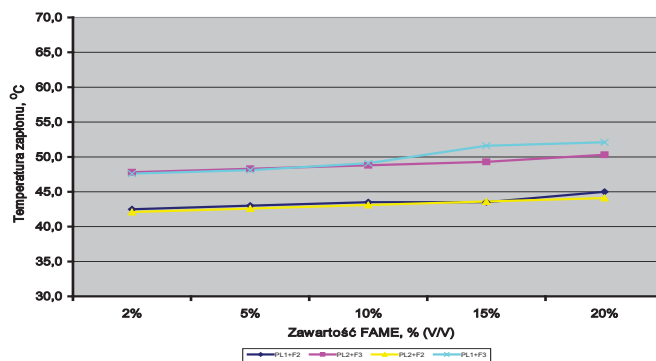


Fig. 17 Flash point vs. FAME content

The flash point increases with FAME content for every blend. Blend's flash point depends mostly on flash point of FAME. In case of two different Jet A-1 fuels and the same FAME, flash points of individual blends with equal FAME content are very similar. The reason is that flash point of FAME is considerably higher than aviation fuel, and has decisive influence on value of this parameter for blends.

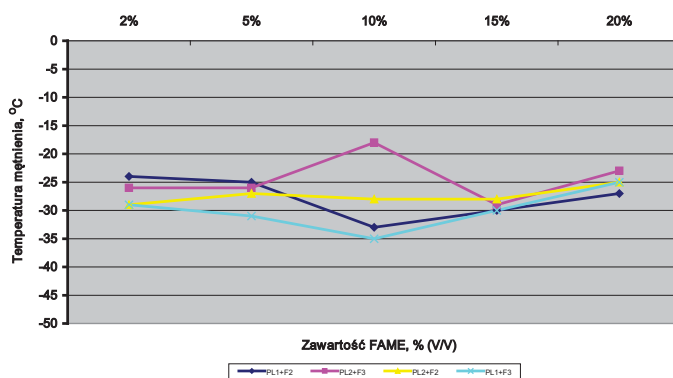


Fig. 18 Cloud point vs. FAME content

It is difficult to evaluate relationship between cloud point and FAME content. Every blend behaves slightly in different way. Different chemical character of both components can be the reason.

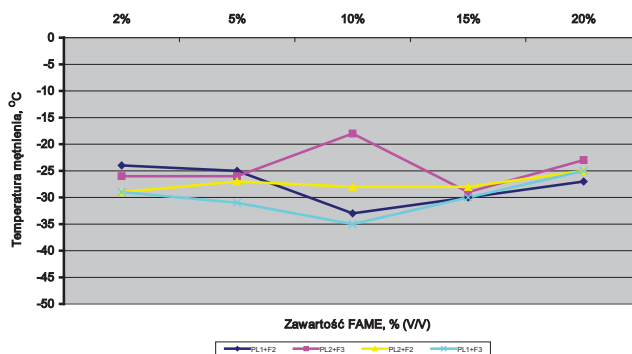


Fig. 19 Pour point vs. FAME content

Pour points are practically unchanged. The differences depend mostly on type of used ester, and not on fuel type.

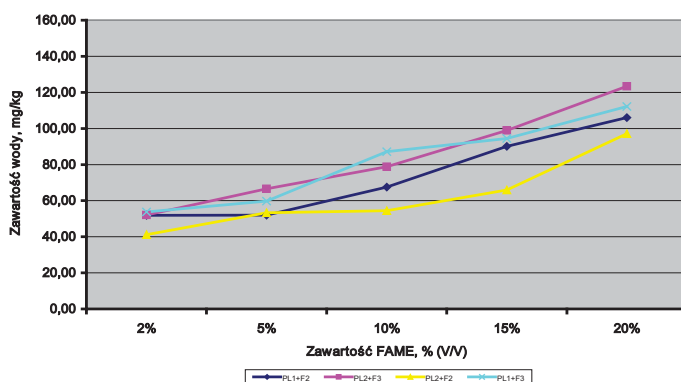


Fig. 20 Water content vs. FAME content

Water content increases with FAME concentration increase. The increase is considerably higher for FAME concentration more than 5 % (v/v). Blends containing the same ester demonstrate similar water content uptrend. It means that ester, as hygroscopic product, contain more water. Furthermore, solubility of water in ester is higher than in petroleum fuel, so ester is the source of water in blend.

## SUMMARY

Basing on presented results it can be assumed that all blends of fuel containing FAME meet requirements of specification NO-91-A258-4 for aviation turbine fuels, excluding such parameters as water separation index and existent gum.

Lowered smoke point may cause slight problem with slight increase of carbon deposits in system, what can cause damage of system components.

Existent gum considerably exceeds aviation turbine fuel specification requirements. This can deteriorate air-fuel mixture combustion and lead to carbon deposits.

Due to different chemical character of FAME, and used test methods suitable for petroleum fuels, above conclusions should be verified by performing engine tests.

Depending employed fuel, fuel blends containing FAME up to 5 % (v/v) demonstrate the lowest tendency to form crystals at low temperatures

According to knowledge basing on the research work, it seems that use of FAME in aviation will be considerably limited. However, it doesn't exclude use some different biocomponents or use biofuels in engines employed for other than airborne purposes.

## References

- [1] Wrota Podlasia – Ekologiczny transport.  
[http://www.wrotapodlasia.pl/pl/wiadomości/z+brukseli/ekologiczny\\_transport.htm](http://www.wrotapodlasia.pl/pl/wiadomości/z+brukseli/ekologiczny_transport.htm).
- [2] T. Stylińska, *Latanie na cenzurowanym*, onet.pl Tygodnik Powszechny, 23.09.2008.

- [3] J. Ostaszewicz, *Środki dla redukcji emisji szkodliwych substancji w transporcie lotniczym*, Start-Biuletyn-Nr 1/2003-Trans. Lotniczy.
- [4] Alternatywne paliwa lotnicze – *Konwencjonalne i alternatywne źródła energii*. <http://www.postcarbon.pl/2008/01/23/alternatywne-paliwa-lotnicze>.
- [5] *Problemy ogólnoresortowe, Strategia ograniczania emisji CO<sub>2</sub> w sektorze transportu*. Główna Biblioteka Komunikacyjna.
- [6] C. Kajdas, T. Wiśniewski, *Wpływ dodatków estrowych na napięcie powierzchniowe oleju napędowego*. PROBLEMY EKSPLOATACJI, nr 1, 2003.







## ORGANIZATION PRINCIPLES OF THE OPERATING PROCESS OF THE CASCADE COMPRESSION UNITS AND SOME DIRECTIONS OF THEIR APPLICATION

**Aleksandr Krainyuk**

*The Vladimir Dal East Ukrainian National University*

*Molodejny 20a, Luhansk, 91034, Ukraine*

*Tel.: +38 642 413 160*

*e-mail: Ljanger@rambler.ru*

**Oleh Klyus**

*Maritime University of Szczecin*

*ul. Waly Chrobrego ½, 70-500 Szczecin, Poland*

*tel.: +48 91 4809425, fax: +48 91 4809575*

*e-mail: olegklus@o2.pl*

### **Abstract**

*In the paper was presented new trend of thermal-power units - operation principle of the cascade thermal compression units of different purposes. In this equipments a working medium compression is carried out owing to supplied heat as a result of internal redistribution of expansion indicator work in the process of cascade mass interchange without the use of mechanical displacers which remove some part of mechanical energy from the power take off shaft. The most important characteristics of cascade thermal-power units was presented.*

**Keywords:** *cascade thermal-power units, cascade pressure interchangers, diesel engine, gas-turbine units, exchange processes*

### **I. Introduction**

A new improvement trend of thermal- power units of wide purpose is connected with creation of cascade compression units of gas- air mediums. The units of cascade- thermal compression (CTC) and cascade pressure interchangers (CPI) are variety of such units.

In CTC units a working medium compression is carried out owing to supplied heat as a result of internal redistribution of expansion indicator work in the process of cascade mass interchange without the use of mechanical displacers which remove some part of mechanical energy from the power take off shaft.

In addition to simplicity and high reliability of the structure, because of absence of mechanical displacers and mobile gas distributed elements discretely controlled, the CTC units are characterized by high efficiency, even while using heat resources with relatively low temperature potential and it stipulates their application attraction as a recovery systems included as components of traditional thermal power plants.

## 2. Principle of the operating process of the cascade compression units

The operation principle and description of the first CTC units are given in the papers [1-3]. At present serviceable samples of CTC compressor are created, and the diagram is shown in fig.1.

In the process of rotor rotation (fig.1 clockwise rotation), each rotor cell is connected in sequence with a stator head interchange channel through which a working medium enters from contiguous cell of the expansion area. De to cascade compression the pressure in the cell steadily increases up to definite value which depends on thermo-dynamical parameters of the working medium in the beginning of the expansion process. While communicating the cells with the windows of high pressure (HPV) of displacing section under the action of centrifugal forces or forced circulation the displacement of preliminarily compressed in the cell of air charge is replaced by heated air or gases (in the case of use of internal combustion chamber). Due to this fact maximum cycle pressure is fixed in the displaced path and in the cells communicated with it. That pressure exceeds the pressure of cascade compression.

Part of compressed air is removed from the displaced path to the consumer through a branch pipe placed in front of heat source.

In the period of further cell communication with head exchange channels part of the working medium is removed to the contiguous cells of the compression section. And it is accompanied by pressure drop in the considered cells. Thus, the expansion work is spent for air charge compression in the process of cascade mass interchange.

Residual pressure at the end of expansion process, as an indicator of working process perfection, depends on the quantity of head interchanged channels towards atmospheric one increasing quantity of channels.

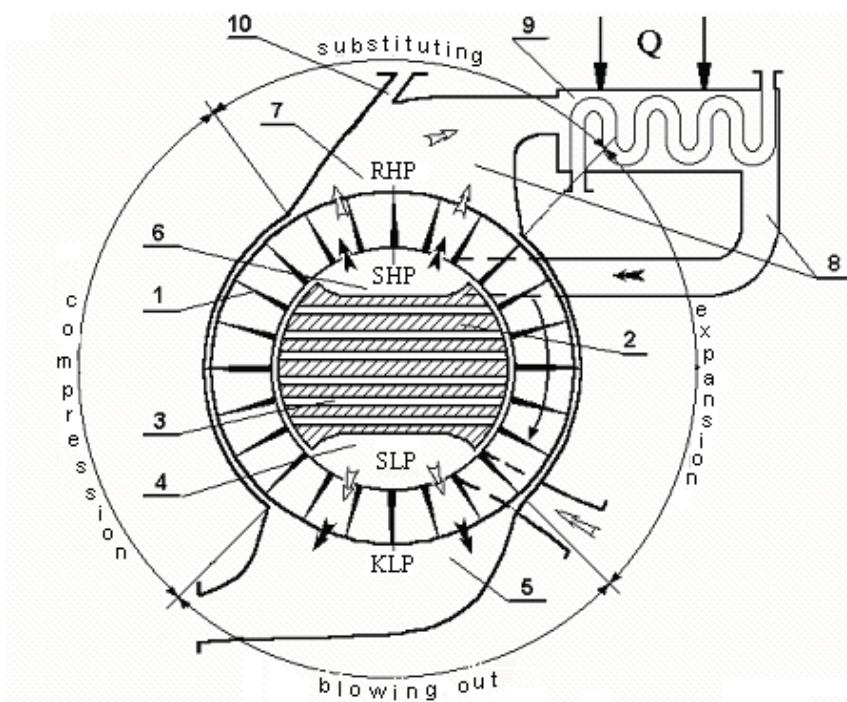


Fig.1. Fundamental diagram of cascade thermal compression compressor. 1 - rotor; 2- stator; 3- head interchange channels; 4, 5- supply window (SLP) and removal low pressure air [KLP]; 6, 7- supply window of high pressure air [SHP] and removal window of high pressure air [RHP]; 8- displaced path; 9- recover heat interchange; 10- branch pipe of compressed air removal to the consumer.

Blow through the cells by means of air charge, which is implemented in the period of cell connection to the windows of low pressure [SLP] and [RLP], closes a working cycle of the cascade thermal compression unit (CTC).

This compressor arrangement is easily transformed into gas or hot air generator by means of branch pipe placement for take off working medium along displacement path near heat source in the direction of gaseous atmosphere motion.

Concerning railway transport, the use of hot air generator in the heating systems of rolling stock is of great interest. The evident advantage of the CTC heater is its independence in maintaining service ability when de-energizing power network. It gives the possibility to apply it with different types of fuel and any heat source. Thanks to hot air blow by means of CTC unit heat-transfer agent transportation into local zones of the heated object is carried out without the use of drive compressor or fan.

Another direction of the cascade compression unit development is connected with development of pressure change used, for example, for supercharging of internal combustion engines.

In cascade pressure changer (CPC) air pressure as well as in the wave pressure changer (WPC) is carried out as a result of close contact with compressing gas but with quite different working process in the cycle.

Cascade pressure exchanger action is easily determined from the diagram 2. which represents the developed views of rotor with longitudinal cells relatively gas distributed windows. General view of the unit is shown in the fig. 3. Compressing gas supplied through the window of high pressure completely compress already compressed air in the cascade process and displace it to the consumer through the high pressure window. The energy of redundant pressure which is left in the cell of compressing gas after disconnections with the high pressure windows is spent for main compression of fresh charge having analogy with considered cycle of cascade thermal compression.

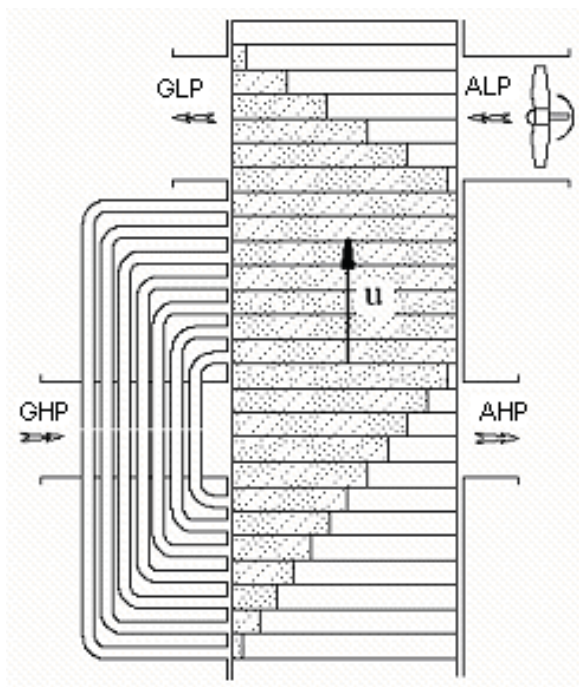
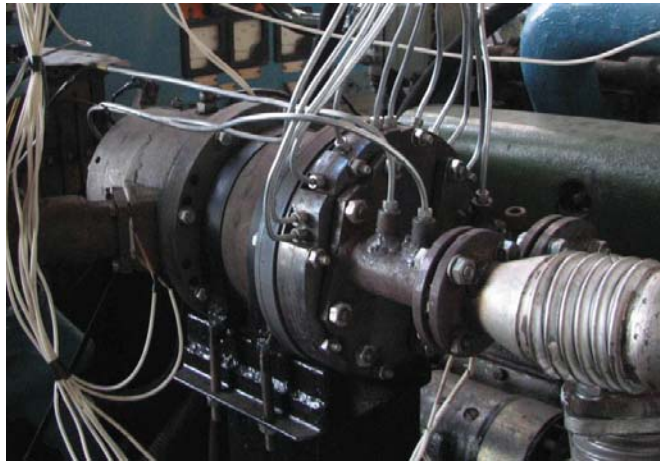


Fig. 2. Unrolling a rotor for windows stator



*Fig. 3. General type of cascade exchanger of pressure*

The advantages of the cascade pressure exchange (CPE) relatively wave pressure exchanger are stipulated by the following.

Wave nature of energy exchange and super- charging of compressed air pre- determines high sensitivity of the working process of wave pressure exchange to the nature of interaction of primary waves with leading edges of gas distributed windows which are easily destroyed when frequency departure of rotor rotation or parameters of compressing gas from calculated values. Impulse charge compression is accompanied by losses which are connected with energy dispersal of formed waves in the result of their interaction and reflection in boundary sections of the cell.

A great influence on wave pressure exchange efficiency is produced by imperfection of displacing compressed air through a window of high pressure. Increase of compressed air which is left in the cell after its separation with high pressure windows causes almost proportional efficiency decrease, which is analogous to negative influence so called “dead” volume in piston compressor.

Taking into consideration the presence of stirring zone of compressing and compressed gases in the cell it is problematic to realize full displacement of compressed air charge, excluding throwing of compressing gas in the low pressure window. These factors are especially displayed when increasing exchange head with frequency change of rotor rotation.

In cascade pressure exchanger in comparison with wave one, air compression is realized in more rational quazi- stationary processes with insignificant amplitude of formed waves.

In this case dissipation phenomena of wave interaction of gas mediums not only do leveling but there considerably reduce negative influence of displacement imperfection of compressed air (“dead” volume) on efficiency action of the changer.

Indeed, compressed air energy left in the cell after separation with air of high pressure window participates in the process of cascade mass changer and together with the energy of compressing gas in the cell is spent for further pressure of fresh charge.

Higher effectiveness of exchange processes of cascade pressure exchange is confirmed by comparison of gas medium rates in the windows of high pressure. As insignificant part of compressing gas is used for complete compressing of preliminarily compressed in the process of mass exchange air in cascade pressure exchange, practical equality of volume costs of pressed and pressing medium takes place. In this case the ratio of mass costs at slight pressure excess of pressing gas  $P_{g1}$ , relatively pressure of supercharged air roughly corresponds to inverse ratio of temperatures of these mediums.

$$\frac{G_k}{G_{gl}} \approx \frac{T_{gl}}{T_k} \quad (1)$$

Pay attention to the fact that wave pressure exchange, which operates in the system of internal combustion engine, realized the balance of mass costs of compressed and compressing mediums ( $G_k=G_{gl}$ ) and in the modes of maximum effectiveness provides some excess of pressure  $P_k$  relatively  $P_{gl}$ . However, the factor of considerably high relative productivity cascade pressure exchange prevails and reflects higher effectiveness of exchange processes. The efficiency of pressure exchanger without the costs for a drive is expressed by the expression

$$\eta_{cpe} = \frac{G_k}{G_{gl}} \cdot \frac{\dot{I}_{gl}}{\dot{I}_k}, \quad (2)$$

where:

$H_k, H_{gl}$ - correspondingly situated heat overfall of the blowed air compressing gas.

For a ideal cascade pressure exchange cycle taking into consideration the equality of volume costs and leakage absence of compressed and compressing mediums and after some simplification we receive:

$$\eta_{cpe}^{id} = \frac{k(k_g - 1) \cdot \left( 1 - \left( \frac{P_k}{B_0} \right)^{\frac{\kappa - 1}{\kappa}} \right) P_k}{k_g(k - 1) \cdot \left( 1 - \left( \frac{P_{gl}}{B_0} \right)^{\frac{\kappa_g - 1}{\kappa_g}} \right) P_{gl}}, \quad (3)$$

where:

$K, K_g$ - indicators of adiabat for air and gas;  $B_0$ - atmospheric pressure.

This expression shows independence of efficiency of the idealized cascade pressure exchange cycle from the temperature of compressing gas  $T_{gl}$ , different from wave pressure exchange cycle where increase  $T_{gl}$  is accompanied by some decrease of use effectiveness of heat difference of compressing gas.

Physical nature of the regularity is connected with the fact that in the working cycle cascade pressure exchange dominating role is given to exchange of potential energy in the processes of cascade mass exchange. Thus the increase of potential energy of compressing gas caused by its temperature is transformed to a great extent into increase of potential energy of the pressing gas pressure.

In the wave pressure exchange considerable part of energy exchange is carried out by transference of the quantity of front motion spreading along the wave cell. Quantity of motion transferred by wave disturbance to compressed air depends on the ratio of densities of interacting mediums. That is why the density decrease of comprising gas while increasing its temperature under other equal conditions is accompanied by wave pressure exchange productivity. Due to this wave pressure exchange is inferior to cascade as for effectiveness of use of heat component of the heat difference  $H_{gl}$ .

Thus from the point of view of recovery of heat release of heat power units and the ability of transformation of heat energy into mechanical working cycle cascade pressure exchange is more perfect.

Fig 4 shows that with ratio increase  $P_k/P_{gl}$  efficiency cascade pressure exchange steadily grows, aiming at unit at  $P_k/P_{gl}=0,9\dots0,85$ . Lower values of effective efficiency cascade pressure exchange, obtained on the basis of experimental data, reflect real leakage of working mediums through incompact of movable matings and also costs of mechanical energy for rotor drive. In

addition to that obtained efficiency values and pressure indicators of samples of cascade pressure exchanges are the best samples of wave pressure exchange [4]. It should be noted that there are no fundamental limitations for ratio increase  $P_k/P_{g1}$  to the values close to the unit. The exception is increase of mass sizes of the exchanger because of decrease of average speed flows in the windows of light pressure.

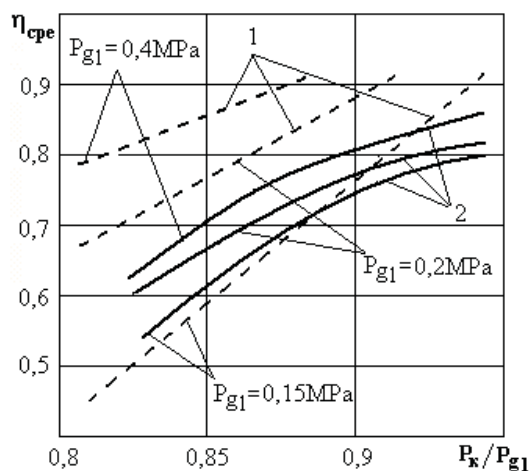


Fig.4. Efficiency dependency cascade pressure exchange on the ratio of pressure  $P_k/P_{g1}$   
 1 – idealized cycle; 2 – test specimen allowing for the costs of power drive.

### 3. Directions of application the cascade compression units

Considerable compressed air discharge permits to use cascade pressure exchange as main unit of the system two-stage supercharging of internal combustion engine with insignificant increase of supercharging in the second stage necessary for realization blow of cylinders of piston part of internal combustion engine. To the opinions of the authors, the use of cascade pressure exchange as heat amplifier of the flow which performs the functions of a multiplier of air discharge is rather perspective

The possibility of cascade pressure exchange as the unit of air compression in gas-turbine units deserves definite attention (fig. 5).



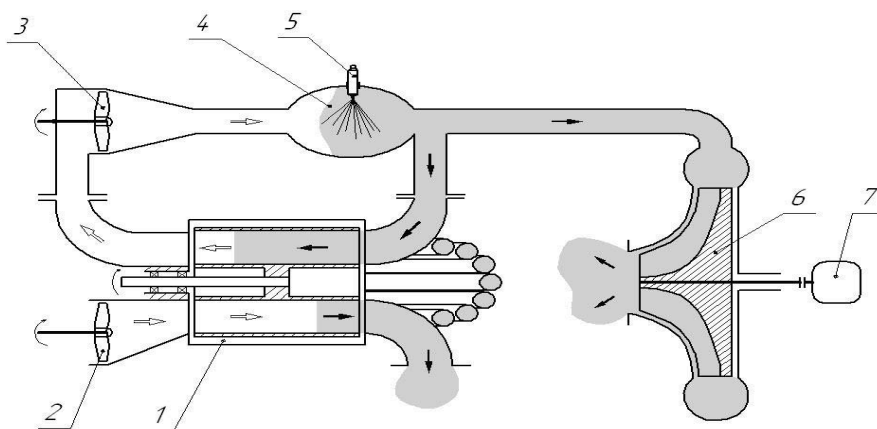


Fig.5. Diagram of gas- turbine unit with cascade pressure exchange  
 1- cascade pressure exchange; 2- scavenger fan; 3 - positive-displacement fan;  
 4 - combustion chamber; 5 - injector; 6 - power turbine; 7 - generator

High thermo-dynamical efficiency of gas- turbine units of cascade pressure exchange is based on higher efficiency of transformation given off in the combustion chamber, heat into the energy of compressed air relatively working process in classical system of gas- turbine units where air compression is carried out in the turbo- compressor which includes vane compressor and part of working steps of turbine.

In gas-turbine units about 50...60% power developed by a turbine for drive of vane compressor is spent. For rotor drive cascade pressure exchange insignificant power of external source is spent – the work of air compression is carried out due to internal energy redistribution of gas flows in running cascade pressure exchange elements. Only part of gas from the combustion chamber is directed into power turbine which has smaller sizes and power. All together at practically non-inertia work cascade pressure exchange the smallest inertia moment turbine stipulates higher quality of transition processes of gas-turbine units.

The above insensibility of the working cycle cascade pressure exchange to non-completeness of compressed air displacement from the rotor at frequency deviation of its rotation or thermo-dynamical parameters of working mediums stipulates satisfactory effective indicators with gas-turbine unit, with cascade pressure exchange.

## References

- [1] Krainyuk, A.I., Storcheus, Yu.V., Danileychenko A.A., *Application of heat compression effect for improvement of power use in heat-power units*. East-Ukrainian National University, № 9, pp. 182-189.2000.
- [2] Krainyuk, A.I., Danileychenko, A.A., Bryantsev M.A., *Working process and perspectives of creation of heat contraction compresso*. Aviation-cosmic technology: Collection of scientific works. Thermal engines and power plants. – Kharkov: state aerocosmik university “CHAI”, pp. 141-145, 2000.
- [3] Krainyuk, A.I., Bogoslovsky, A.E., Storcheus, Yu.V., Danileychenko, A.A., Vasiliev, I.P., Krainyuk, A.A., *Heat compression compressor*, Patent R.F. № 2189497, МПК 7 [0481 19/24/ № 2000106844, Bulletin № 26, 2002.
- [4] Krainyuk, A.I., Storcheus, Yu.V., *Systems of gas dynamical supercharge*, Lugansk: Pub. VUJU, 224 p, 2000.







## ENDOSKOPIC EXAMINATIONS OF MARINE DIESEL ENGINES' TURBOCHARGING SYSTEMS

**Zbigniew Korczewski**

*The Polish Naval Academy*  
Ul. Śmidowicza 69, 81-103 Gdynia, Poland  
Tel.: +48 58 626 23 82  
e-mail: [Z.Korczewski@amw.gdynia.pl](mailto:Z.Korczewski@amw.gdynia.pl)

### **Abstract**

*The paper deals with diagnostic issues concerning endoscopic examinations of marine diesel engines. There will be presented selected information about failures of turbocharging systems and accessible diagnostic method enabling their detection. The author focuses only on the endoscopic research and widely presents the possibilities of this quickly developed diagnostic method. There will be also presented representative results of diagnostic examinations carried out on the main and auxiliary marine diesel engines operated in the Polish Navy.*

**Keywords:** *marine diesel engines, turbocharging systems, diagnostics, endoscopic investigations.*

### **1. Introduction**

Maintenance of marine diesel engine's turbocharging system in a state of full technical ability represents the basic condition for achievement of high efficiency of the working processes worked out in the whole range of possible operation load, especially within the range of dynamic loads of a ship motion system. In such a situation the optimum associating the engine's characteristics (as the flow machine of periodical action) with the turbine and compressor of turbocharging system (which are characterised with a continuity of thermodynamical medium flow) represents the basic energetic problem. Additionally, during unsteady processes, these machines differ essentially with inertia of thermal and flow processes what may cause undesirable thermal and mechanical overloads of the engine's constructional elements when the flow passages' technical state gets worse. There is also possible the compressor's entrance in the area of unstable working and as a consequence - serious damages within the turbocharger's rotor and disturbances in the engine functioning [1].

Accordingly, there is the key operation question: the systematic supervision and reproduction of the technical shape of turbocharging system's flow passages (interblades channels of turbocharger's rotor, guide vanes of a turbine, filter as well as diffuser of a compressor, cooler of supercharging air, the channels of air and exhaust gases), and also technical shape of the engine's fuel fed system, as the activities permanently adapting conditions of gasdynamical coupling of the co-operating flow machines.

## 2. Operational unserviceable states of the turbocharger

During engine operation on a ship, the gas passages of turbocharging system is penetrated with different substances contained, on the one side - in sucking inlet air, on the other - in exhaust gases leaving cylinders of the engine. They create the hard deposable settlings on flow channels' surfaces as well as on surfaces of interblades channels of the turbocharger's rotor. The registered results of endoscopy investigations confirm this phenomenon - fig.1 [2]. The mass of turbocharger's rotor grows up and its rotational speed gets smaller in the result of forming deposits. Moreover, active flow fields of sections in the interblades channels of the compressor and turbine get smaller. The compressor's efficiency, mass flow rate and compression ratio falls as well as a stability margin of the compressor working (particularly during transient processes). Such the compressor's behavior has also negative impact on a quality of the loads exchange process in cylinders as well as the burning process, in this case - incomplete and imperfect.

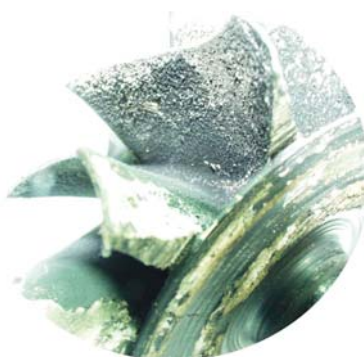


*Fig. 1. Failures of turbochargers; a) surface deposits on a turbine rotor of the turbocharger*



*Fig. 2. Fatigue crack of the turbine rotor blade of the turbocharger*

As an effect, the process of carbon deposit formation on passages' surfaces of the turbine part intensifies. This concerns especially stator blades and rotor blades of the turbine as well as labyrinth seals. It deepens the unfavourable phenomena that concurrent a dirt process of the sucking air channel. Additionally, as a consequence of deposits creation on the turbocharger's rotor the loss of stability of turbocharger mechanical system may occur. It also leads to the vibration resonance phenomenon causing in turn the accelerated waste of shaft bearings, and also fatigue cracks of the rotor blades - fig. 2.

From the operational experiences results, that the thickness of deposits layer on the compressor's blades can reach tens micrometers, meanwhile on the turbines blades - even a few hundred micrometers [2]. It makes the significant influence on the turbocharger's performance and efficiency (and obviously a performance and efficiency of the engine) taking into consideration small mass and size of the turbocharger's rotor working at very large rotational speeds (up to  $100\,000\text{ min}^{-1}$ ).

A different operational factor that has very destructive effect on constructional structure of the

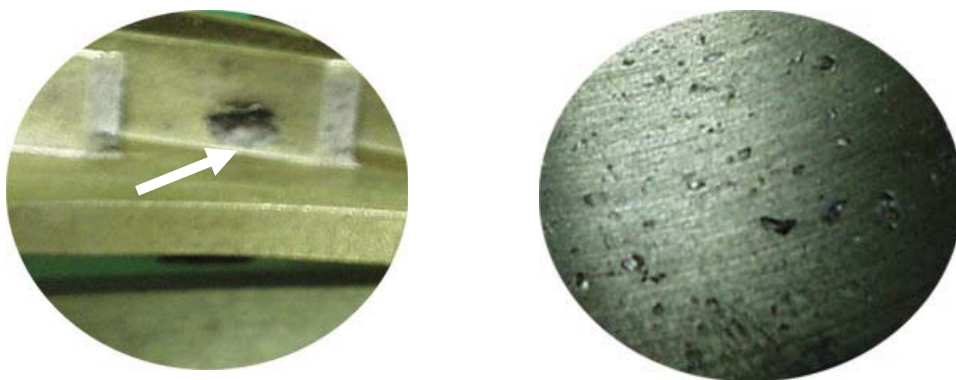


*Fig. 3. Erosion pits on guide vanes of the compressor's diffuser*

turbocharger is the phenomenon of erosion caused by the presence of hard particles of mineral origin in flowed working medium - in case of air, and the carbon deposit and the pitch substances in exhaust gases, as products of incomplete and improper fuel burning in cylinders as well as the remainders of lubricating oil - fig. 3.

Both the unfavourable phenomena might cause the intensive wearing of gas passages surfaces, alterations of the geometry and shape of interblades channels of the compressor and turbine, and also the enlargement (even the several times) of the surface roughness. As the consequence, the hydraulic losses of working medium flowed in the turbocharging system grow up, at the considerable deterioration of dynamic features. Moreover, inertias in mechanical and gasdynamical system grow up, along with all the consequences for the engine's performance [1].

### **3. Endoscopy investigation of the turbocharging system**

The turbocharging system of a standard (serial) marine diesel engine is usually characterized by the low supervision susceptibility, in an aspect of possibilities of an endoscopy application. An access to the interior of air and exhaust flow passages (cooled with water) is limited, and also an access to the rotor unit of the turbocharger. In such a situation there is necessary applying blank technological openings assigned for physical quantities' transducers. The quantities are observed only during an engine running in conditions of factory tests. Thus, a minimum diameter of the optical probe which is to be introduced to the channel's interior, and adjusted to the diameter of technological openings represents an essential limitation of performing endoscopy examinations. Making additional inspection openings on your own, enabling the introducing an endoscopy probe in the most vulnerable parts of gas passages of the turbocharging system stands for a different, commonly applied solution in such limitations. This especially concerns the following parts:

- rotor blade system of the compressor and turbine,
- stator blades of the compressor's diffuser,
- guide vane of the turbine,
- air channels in the vicinity of the inlet valves,
- exhaust channels in the vicinity of outlet valves.

With regard to complexity of a constructional form of turbocharging system as well as a considerable, sometimes, distance among the inspection openings and the observed surface of gas passages there is often necessary to apply a flexible fiberoscope during endoscopic investigations. The elastic fiberoscope possesses the ability of controlling a sector of the deviation of the inspected ending. Because there is often necessary to lead elastic optical parts in horizontal position through the gas passage different inspection leadings of different shape have got very practical utilization – fig. 4. Plastic pipes are perfectly useful to this aim (e.g. the pipes of central heating systems), having the possibility of a plastic deformation and memorization the given

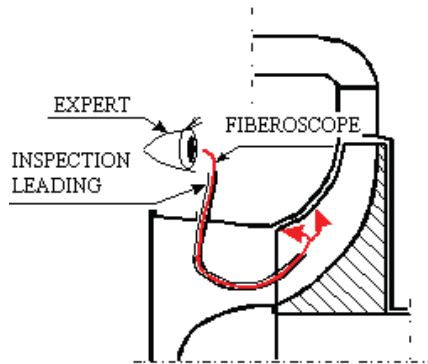


*Fig. 4. The way of the inspection leading's usage for endoscopic examinations of the turbine shape, that is best adapted to the constructional form of observed internal spaces. The way of performing the endoscopic examinations of the marine diesel engines' turbocharging systems by means of the boroscope and fiberscope is presented in fig. 5.*

In which way the access to internal spaces of a turbocharger could be achieved during endoscopic investigations of marine engines Zvezda M401A-1(2) type and Detroit Diesel 16V149TI type is schematically presented in figure 6. Especially elaborated diagnostic methodical guides contain the detailed description of successive procedures of endoscopic examinations, taking into account the specification of diagnostic apparatus as well as the supervisory susceptibility of the engines installed inside the marine power plant [2].

The fiberscope (more seldom the boroscope), after filter's disassembling in the suction channel as well as the blanks' disassembling of technological openings in the air and exhaust channels gives the operator possibility to carry out technical state's evaluation of a blade system of the turbocharger's rotor and also blade-rings of the turbine's guide vanes and the compressor's diffuser (fig. 6). The largest difficulty during endoscopic investigations of a turbocharger's system represent the proper recognition of surface defects in exhaust channels and turbine's rotor which are usually intensively dirtied with the carbon deposits. There is almost impossible to detect erosion and corrosion pits in due time, while they are concealed under a thick layer of the carbon deposit (fig. 8b). The pits appeared on the turbine's rotor might represent an essential threat for the engine's reliability.

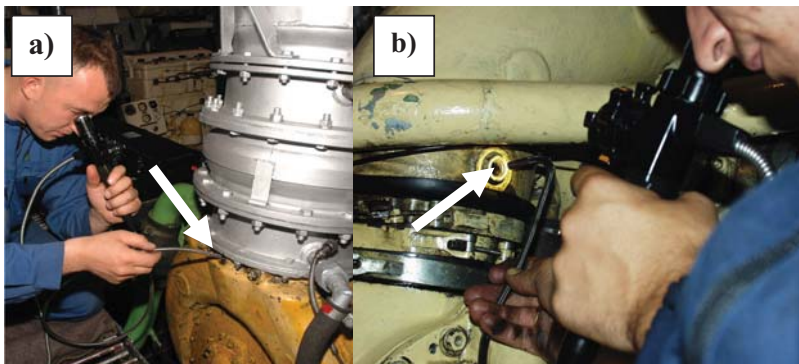


*Fig. 5a,b. The way of introducing the inspection endings of the boroscope and fiberscope into internal spaces of the turbocharger; a) turbine's investigation of the engine of M520 type – through the openings after the removed (dismantled) thermoelement in the exhaust channel, b) turbine's investigation of the engine of M401 type through the openings after the removed (dismantled) blank of measurement connector of the turbine discharge pleasure*

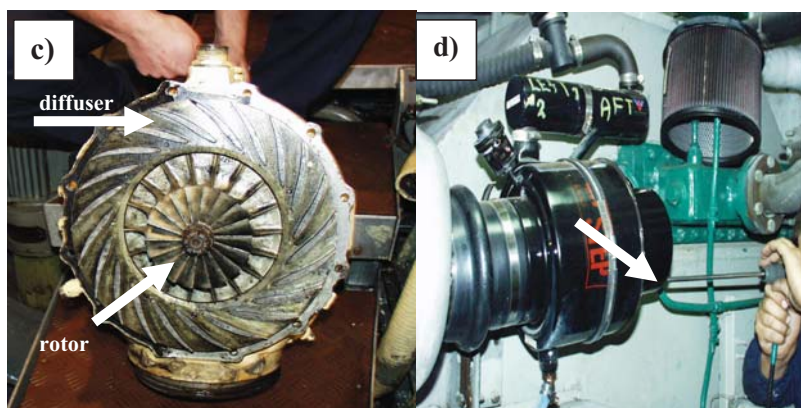


Fig. 5c,d. The way of introducing the inspection endings of the boroscope and fiberoscope into internal spaces of the turbocharger; c) the M401 engine's investigation – the view of the compressor dismantled from the engine, d) the 16V149TI Detroit Diesel engine's investigation – access to the compressor's rotor after the air filter's disassembling.

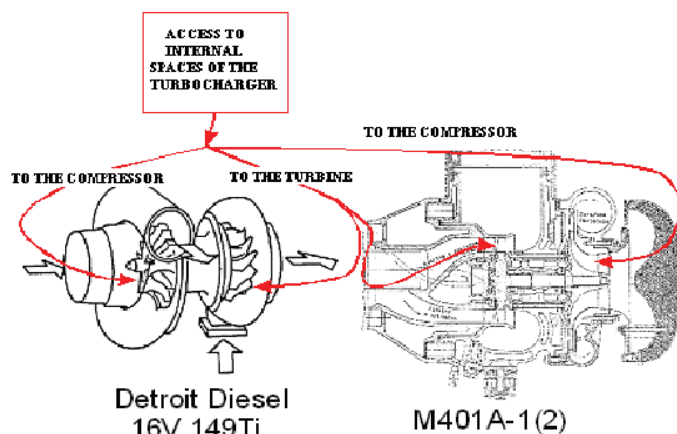


Fig. 6. Endoscopic investigations of Detroit Diesel marine diesel engine 16V149TI type and Zvezda M401A-1(2) type – an access to internal spaces of the turbocharger

As the result of perennial endoscopic investigations of marine diesel engines there have been entered several cases of so intensive dirt of the turbine's rotor that even its manual (hand) turning makes the operator gigantic difficulties. There were cases when there was totally impossible. It meant practically that the engine worked without supercharging. Because it concerned the engines which were not equipped with turbines' washing (cleaning) installation in standard, there was necessary (in every case) to perform the disassembling of the turbocharger from the engine and then, hand removing the carbon deposit from the interblades channels of the rotor.

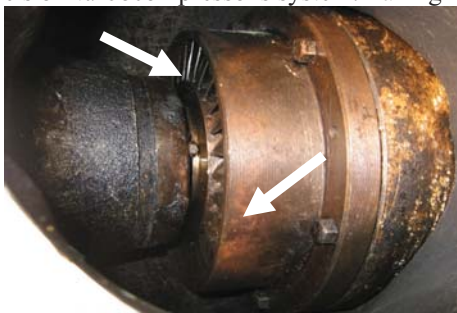
#### 4. Endoscopic images of turbochargers' failures

The chosen failures of turbocharger systems of marine diesel engines identified during operational endoscopic investigations are presented in figures 7, 8 and 9 [1,2]. It is highly surprising, that many dangerously looking defects were not effective with noticeable alterations of values of

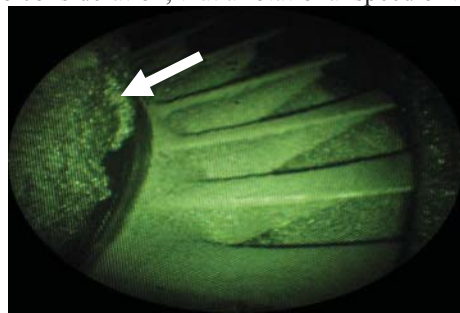


the observed control parameters of the engine. For example, metallic fragment, introduced in fig. 8a, imprisoned in an interblade channel of the turbine's guide vanes was detected during routine diagnostic investigations of the engine in current operation. As a result of optical inspection of the whole system of exhaust gases (the engine at the configuration of a star - 7 blocks of 6 cylinder liners), the extensive damages of the channel off taking gases from cylinder block number 6 were confirmed. The character of detected cracks and decrements of the constructional material showed, that a low-cycle fatigue of the welded joint, which had been working in the chemical active (aggressive) corrosive environment, represented the primary reason of their appearances.

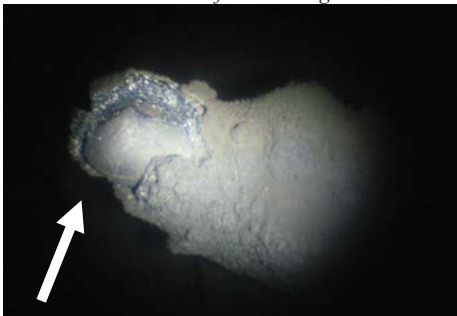
The application of endoscopies allows the user also to detect damages of the compressor's blading that could be dangerous for the engine reliability. Very often there have been found different kind of deformations (fig. 8d , fig. 9d,e), cracks (fig. 7f, fig. 8e,f , fig. 9f) as well as dirt (fig. 7b,c,d,e, fig. 9a,c) of the interblade channels of the compressor's rotor which do not generate the clear diagnostic symptoms that could be identified with the vibration measurements, indicating cylinders or gasdynamical measurements of the working medium in the suction and discharge channels of turbocompressor's system. Taking into consideration, that a rotational speed of the



a) Zvezda M401A-2 type 4-stroke engine – exhaust (discharge) passages of the turbocompressor's turbine after cleaning



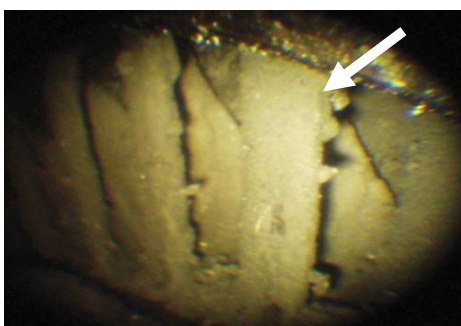
b) Zvezda M401A-2 type 4-stroke engine – intensive carbon deposits on exhaust (discharge) passages of the turbocompressor's turbine



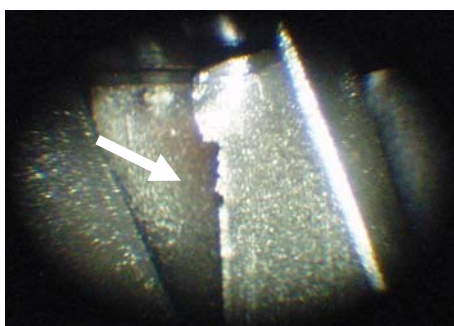
c) Zvezda M401A-1 type 4-stroke engine – intensive carbon deposits on the thermocouple measuring turbine discharge temperature



d) Zvezda M401A-1 type 4-stroke engine – intensive carbon deposits on exhaust (discharge) passages of the turbocompressor's turbine



*e) Zvezda M401A-1 type 4-stroke engine – carbon deposits in interblade channels of the turbine*



*f) Zvezda M503A type 4-stroke engine – material decrements of the turbine's rotor blade*

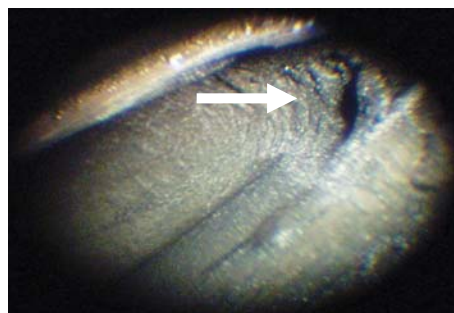
*Fig. 7. Defects of marine diesel engines' turbocompressors detected during endoscopic investigations*

turbocompressor's rotor unit of a medium- or high- speed marine diesel engine achieve tens thousand of rev/min, it is quite clear that the cracks of the compressor's constructional material not detected in time may cause the extensive secondary damages of cylindrical systems, excluding the possibility of the repair execution in shipping conditions.

It is worth pointing out that there is another, very important aspect resulting from the endoscopic examinations of turbocharging systems. Namely, in exhaust channels thermocouples for temperature measurements of exhaust leaving individual cylinders. The measurement likelihood (authenticity) of such parameters decides about the correctness of exploational decisions undertaken during an engine operation. Whether it is possible to confirm an authenticity of the exhaust temperature's measurement worked out by means of the thermocouple in such a technical state as shown in fig. 7c - or not?



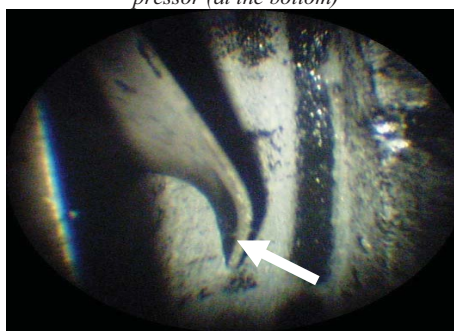
*a) Zvezda M503A type 4-stroke engine – metallic fragment imprisoned in an interblade channel of the turbine's guide vanes*



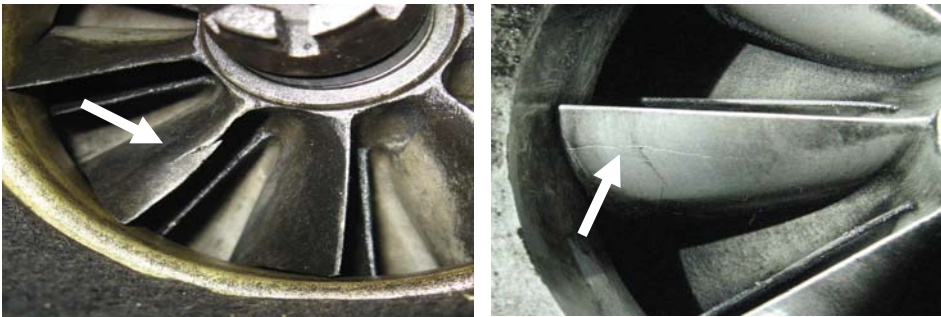
*b) Zvezda M401A-1 type 4-stroke engine – an erosion pit in an interblade channel of the compressor (at the bottom)*



*c) Zvezda M401A-1 type 4-stroke engine – dirt deposits in interblade channels of the compressor*



*d) Detroit Diesel 16V149TI type 2-stroke engine – a curved rotor blade of the compressor on the edge*

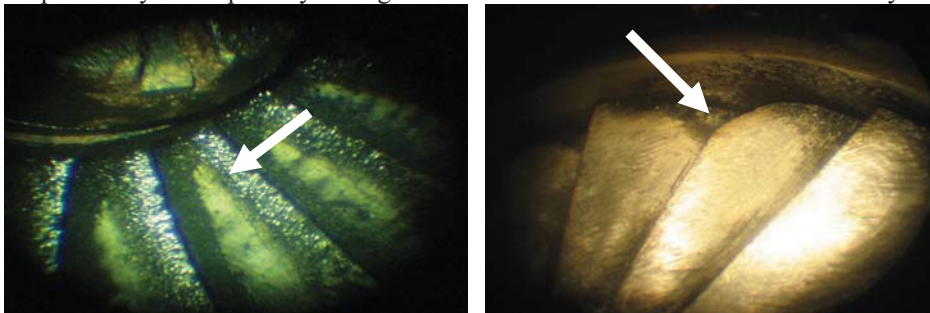


e) Zvezda M401A-2 type 4-stroke engine – an edge crack of the rotor blade of the compressor f) Detroit Diesel 16V149TI type 2-stroke engine – a crack of the compressor rotor blade

Fig. 8. Defects of marine diesel engines' turbocompressors detected during endoscopic investigations

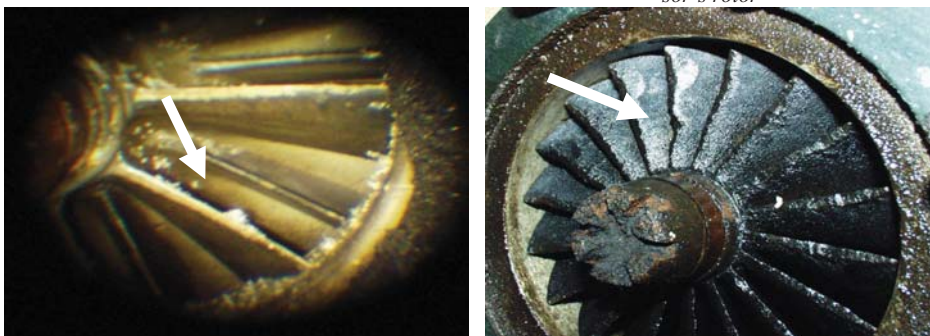
## 5. Conclusion

Endoscopic reviews have been led systematically by the author, on the population of 50 marine engines covered with a diagnostic supervision. Gathered results show that numerous material defects was identified in due time, what means that in case of their father development the engine's reliability would be significantly threatened. In many cases the engines did not generate the observed symptoms of the failures' existence, for example the engine's running with mechanical damages of blading within turbocompressor's rotor (fig. 8 and fig. 9). In author's opinion such circumstances unlock the new investigative perspectives, because the usage of endoscopic methods gives the possibility of the primary damages' detection of constructional elements in early



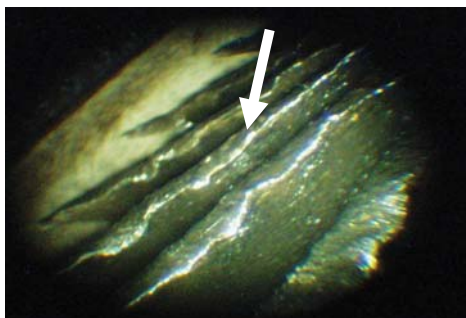
a) Zvezda M401A-1 type 4-stroke engine – oiling up of surfaces of rotor blades of the compressor

b) Zvezda M401A-1 type 4-stroke engine – curvature of the failed edge of attack of the channel's profile on the external diameter of the compressor's rotor





c) Zvezda M401A-2 type 4-stroke engine - dirt deposits in interblade channels of the compressor



d) Zvezda M401A-1 type 4-stroke engine – deformations and mechanical failures of the compressor's rotor



e) Zvezda M401A-1 type 4-stroke engine – deformed profiles of the compressor rotor's blades

f) Zvezda M401A-2 type 4-stroke engine – material decrement on the edge of attack of the compressor rotor's blade

Fig. 9. Defects of marine diesel engines' turbocompressors detected during endoscopic investigations

stages of their development, while measured diagnostic parameters of diagnosing systems are not sufficiently sensitive to the changes in surface layers limiting the engine's working spaces.

## References

- [1] Korczewski Z.: *Endoskopia silników okrętowych*, Wydawnictwo AMW, Gdynia 2008.
- [2] *Sprawozdania z badań diagnostycznych tłokowych silników spalinowych eksploatowanych na okrętach MW RP* – Prace badawcze AMW, Gdynia 2000-2008.





## THE ANGLE MEASUREMENT UNCERTAINTY EVALUATION BY MEANS OF INCREMENTAL ENCODER

Przemysław Kowalak

Maritime University of Szczecin – Department of Engineering  
70-500 Szczecin, Wały Chrobrego 1-2  
tel: +48 91 4809 400, fax: +48 91 4809575  
e-mail: [pkowalak@am.szczecin.pl](mailto:pkowalak@am.szczecin.pl)

### Abstract

*The application of incremental encoders in the marine engines field was briefly described. The problem of the angle measurement uncertainty evaluation by means of an incremental encoder was presented. A theoretical assumption of experiment was discussed and a project of an experimental test allowing statistical evaluation of angle measurement uncertainty was proposed. The uncertainty estimation of a type A as well as the type B according to ISO standards was carried out. The numerical values of the results were presented. The proposition of improvement of test bed for encoders examination was proposed.*

**Keywords:** marine engines, measurements, angle measurements, measurement uncertainty, incremental encoders,

### 1. Introduction

The incremental encoders have a practical application in automation since years. Last years one can meet them in a measurement technology. The modern marine engines manufacturers take advantage of them as a crankshaft angle position transmitter for electronically controlled engines [4,5]. The constructions of a measurement instruments utilizing signals from incremental encoders are in use today as well [2-7].

In the Laboratory of the Marine Engines in Maritime University of Szczecin there are two control and measurement systems utilizing incremental encoders. A problem of an angle measurement precision arose consequently.

No one of the manufacturers of the possessed encoders provided a calibration certificate. No one could specify the precision class of the instrument either. The necessity of an angle measurement uncertainty evaluation by means of an experiment arose subsequently.

In the experiment planning phase a suitable angle measurement standard had to be chosen. The encoders used in the laboratory are of the 3600 and 720 pulses per resolution. The most adequate standard should be of a high precision at a very small nominal value of the angle. Acquiring of such a standard and comparing with every position of the encoder might be as difficult as costly. Finally it was decided to utilize a direct measurement and a statistical work out of the measurement uncertainty. For a recognize experiment the 720 pulses per resolution encoder was chosen. The frequency of generated pulses should be lower and the experiment easier consequently.

At the beginning the assumption was made, that the manufacturer has made every effort to produce the instrument with the highest accuracy. Such an assumption seems to be burden with a

minima uncertainty and is essential for further discussion. It was also assumed that the technology of the encoder production (which is not known to the author) consists in marking of the rotating disk circumference and subsequently filling in with equal marks in a nominal amount. For a tested encoder the nominal amount of marks is 720. Based on those two assumptions it can be assured that the encoder's shaft will rotate exactly  $2\pi$  angle after nominal amount of pulses will be counted. Then the mean value of a measured angle will be equal to:

$$\bar{\alpha} = \frac{2\pi}{n} \quad (1)$$

If the encoder's shaft rotates uniformly with constant angular speed  $\bar{\omega}$ , the angle scale can be transformed into time scale. The advantage of this is that the time scale is much easier to measure than angle scale. In such a case, the angle of the shaft rotation by  $i$  pulses might be expressed as:

$$\alpha_i = T_i \cdot \bar{\omega} \quad (2)$$

Then the mean value of an angle  $\bar{\alpha}$  can be determined by means of equation:

$$\bar{\alpha} = \frac{\bar{\omega}}{n} \cdot \sum_{i=1}^{i=n} T_i = \bar{\omega} \cdot \bar{T} \quad (3)$$

The difference between the value of a singular angle  $\alpha_i$ , and the mean value  $\bar{\alpha}$ , can be recognized as the unknown value of the error:

$$\delta_i = |\alpha_i - \bar{\alpha}| \quad (4)$$

If the set of values  $\alpha_i$  is treated as  $n$  independent observations of the expected value  $\bar{\alpha}$ , the experimental standard deviation of singular measurement can be determined:

$$s(\alpha_i) = \sqrt{\frac{1}{n-1} \cdot \sum_{i=1}^n (\alpha_i - \bar{\alpha})^2} \quad (5)$$

And the experimental standard deviation of a mean value can be expressed as:

$$s(\bar{\alpha}) = \sqrt{\frac{s^2(\alpha_i)}{n}} \quad (6)$$

Those two quantities carry direct information about uncertainty of the angle  $\alpha_i$  measurement.

## 2. The experiment

The incremental encoders, manufactured in TTL standard, generate voltage pulses of 0 and 5VDC alternatively. Those two voltage levels refer to the logic states of 0 and 1 respectively. When the signal, measured at the output of the encoder, is presented on the diagram it forms a square waveform pattern. In the presented experiment the time between the consecutive rising edges of the square waveform was adopted as a period  $T_i$  which reflects the angle  $\alpha_i$ . (Fig. 1).

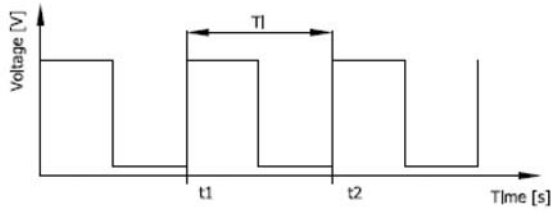


Fig. 1. The priod  $T_i$  determination methodology

The encoder was mounted on a driving assembly which consists of a squirrel-cage motor and a synchronous generator. The motor was supplied from a voltage inverter. The angular speed of the rotating masses is controlled by a variable supply voltage frequency acquired from the inverter (Fig. 2). For the tests a stand for a synchronous generators testing was utilized and the use of the generator is actually not essential for the experiment.

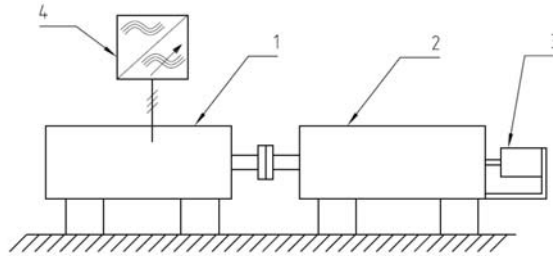


Fig. 2. The diagram of the encoder's drive; 1 – squirrel-cage motor, 2 – synchronous generator, 3 – tested encoder, 4 – inverter

In order to provide suitable accuracy of the period measurement it was necessary to reduce the angle speed of the rotating masses and/or increasing the sampling frequency. In the first case the increased influence of the unbalance of the masses has to be taken into account. The unbalance may cause increased irregularity of the angular speed. In order to determine the critical speed below the influence of the unbalance is essential that experiment was carried out at different speeds. The acquired signals were compared with the timer/counter of 80MHz frequency installed on board acquisition card (Fig. 3). In the table 1 the details of the measuring instruments were presented.

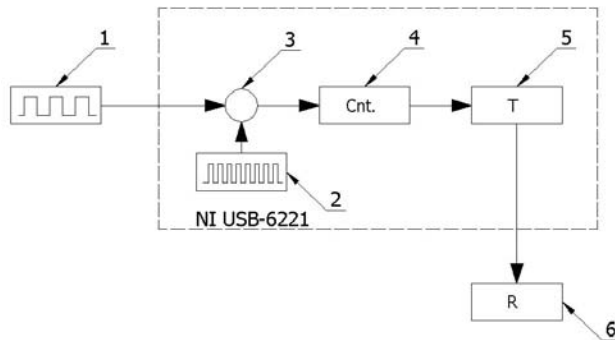


Fig. 3. Measurement diagram; 1 – Encoder's TTL signal filtered by a Schmitt trigger, 2 – on board 80MHz timer/counter, 3 – comparator module, 4 – pulses counter, 5 – period calculation, 6 – recording module (PC).

In the measurement circuit a Schmitt trigger was engaged as a first filtering element. The Schmitt trigger is a semiconductor comparator circuit which generates logical 0 or 1 dependent on the input signal value. The applied Schmitt trigger has a very short latency of 20ns. The shortest recorded period  $T_i$  was 200  $\mu$ s, which is 10000 times longer than the trigger latency. Assuming that the latency is constant, it has no significant influence on the results of experiment.

Tab. 1. Measurement instrumentation data

Instrument	Type
Measurement board	NI USB-6221, National Instruments, with 80MHz counter input gate
Encoder	PFI 60A0720TPT, Intron

### 3. Uncertainty determination

The measurements were conducted for 12 different mean angular speeds of the driving motor. For every mean angular speed at least 5 full revolutions was recorded. The recorded data contains 79 sets of 720 values of the period  $T_i$ . For every set the average was determined:

$$\bar{T} = \frac{1}{n} \sum_{i=1}^{i=n} T_i \quad (7)$$

As well as average angular speed:

$$\bar{\omega} = \frac{2\pi}{n \cdot \bar{T}} \quad (8)$$

Consequently, from equations (2) and (3) the values of the angles  $\alpha_i$  and  $\bar{\alpha}$  could be determined as well as the standard deviation of singular measurement and standard deviation of a mean value from (5) i (6). The calculated values of :  $\bar{T}$ ,  $\bar{\omega}$ ,  $s(\alpha_i)$  and  $s(\bar{\alpha})$ , averaged for every angular speed, are presented in the table 2.

Tab. 2. Determined values averaged for every angular speed

$\bar{\omega}$ [rad/s]	$\bar{\alpha}$ [rad]	$s(\alpha_i)$ [rad]	$s(\bar{\alpha})$ [rad]	n [rpm]
7,82	0,00872665	1246,2E-6	46,6E-6	74,7
11,73		709,0E-6	26,6E-6	112,0
12,54		668,0E-6	25,1E-6	119,8
15,70		153,9E-6	5,76E-6	149,9
19,62		28,7E-6	1,07E-6	187,3
23,54		16,5E-6	0,63E-6	224,8
27,47		17,2E-6	0,65E-6	262,3
28,25		10,4E-6	0,39E-6	269,8
31,39		9,6E-6	0,36E-6	299,8
35,32		13,1E-6	0,49E-6	337,3
39,25		11,9E-6	0,44E-6	374,8
43,17		11,8E-6	0,44E-6	412,3

The above determined values of  $s(\alpha_i)$  and  $s(\bar{\alpha})$  presented in the function of average angular speed are shown on the graphs (fig. 4. and fig. 5.). One can learn that the values of  $s(\alpha_i)$  and  $s(\bar{\alpha})$  rapidly decrease until the speed of about 20 rad/s is reached. Above that speed the variation of the values is not so high. It can be noticed that the influence of the angular speed has no significant

effect. High values of  $s(\alpha_i)$  and  $s(\bar{\alpha})$  at low angular speed are most probably the consequences of the rotary speed irregularities. The irregularities come from the rotating masses unbalance and low power of the driving motor supplied from the inverter at low frequency. Only the values of  $s(\alpha_i)$  and  $s(\bar{\alpha})$  determined for the speeds above the critical 20 rad/s can be considered for evaluation of the encoder's angle measurement uncertainty.

Based on the ISO recommendations [1], the problem of the uncertainty evaluation was identified as a standard uncertainty type A. In such a case, the value of experimental standard deviation of the measurand's average  $s(\bar{\alpha})$  determines directly the uncertainty of the angle  $\bar{\alpha}$ .

Finally the highest value of the standard deviation from the speed range above 20 rad/s was chosen as the value of standard uncertainty type A:

$$s(\alpha_i) = 17,2 \cdot 10^{-6} [rad]$$

$$s(\bar{\alpha}) = 0,65 \cdot 10^{-6} [rad]$$

After the results were rounded off to two significant digits one can express that the tested **encoder** was generating pulses of the rising edge corresponding to the angle of:

$$\bar{\alpha} = 0,00872665 \pm 0,00000065 [rad]$$

$$\alpha_i = 0,008727 \pm 0,000018 [rad]$$

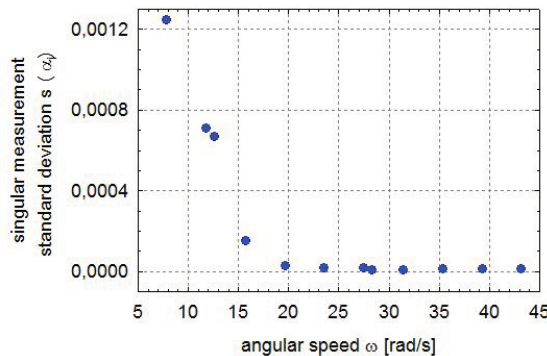


Fig. 4. The standard deviation of singular measurement –mean angular speed characteristic

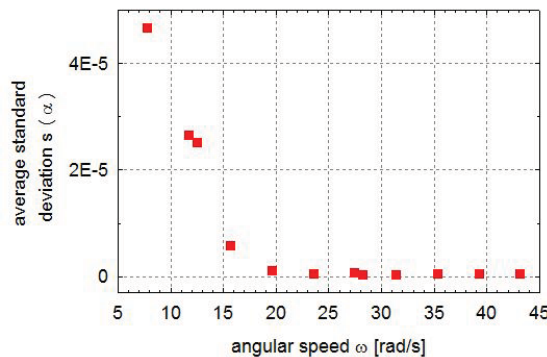


Fig. 5. The standard deviation of average –mean angular speed characteristic

In order to get the full view of the measurement uncertainty, the systematic uncertainty of the measurement should be evaluated. The ISO recommendations regarding determination of uncertainty Type B were applied.

The only physical quantity measured directly was period of singular pulse. That period was compared with the 80 MHz clock/timer. Consequently the scale interval of time measurement was:

$$\Delta T = \frac{1}{8 \cdot 10^7} \text{ s}$$

According to propagation of uncertainty low the same scale interval refers to both, singular value measurement  $T_i$  and to the average  $\bar{T}$ . That enables the equation (3) to be differentiated with respect to  $T_i$  and  $\bar{T}$ :

$$u_\alpha = \sqrt{\left(\frac{\partial \bar{\alpha}}{\partial T_i} \cdot \Delta T\right)^2 + \left(\frac{\partial \bar{\alpha}}{\partial \bar{T}} \cdot \Delta T\right)^2} \quad (9)$$

For every one of 79 sets of  $n$  values of  $T_i$ , the type B uncertainty  $u_\alpha$  was determined (fig 6.). Out of them the highest one was chosen as the value of final uncertainty:

$$u_\alpha = 0,77 \cdot 10^{-6} [\text{rad}]$$

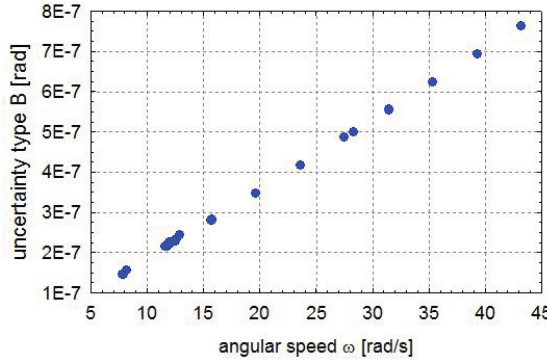


Fig. 6. The type B uncertainty –mean angular speed characteristic

The combined standard uncertainty of average was determined according to the formula:

$$u_{z\bar{\alpha}} = \sqrt{s(\bar{\alpha})^2 + \frac{u_\alpha^2}{3}}$$

$$u_{z\bar{\alpha}} = 0,79 \cdot 10^{-6} [\text{rad}]$$

$$\bar{\alpha} = 0,00872665 \pm 0,00000079 [\text{rad}]$$

$$\bar{\alpha} = 0,00872665 [\text{rad}] \pm 0,01 \%$$

And the combined standard uncertainty of singular measurement was adequately:



$$u_{z\alpha_i} = \sqrt{s(\alpha_i)^2 + \frac{u_\alpha^2}{3}}$$

$$u_{z\alpha_i} = 17,21 \cdot 10^{-6} [rad]$$

$$a_i = 0,008727 \pm 0,000018 [rad]$$

$$a_i = 0,008727 [rad] \pm 0,2 \%$$

The above shown uncertainty is specified for the level of confidence  $p=68\%$ . For level of confidence of  $p=99\%$ , a coverage factor  $k=3$  was set. The expanded uncertainty of average then is equal to:

$$\bar{a}_{p=99\%} = 0,00872665 \pm k \cdot u_{z\alpha} = 0,0087267 \pm 0,0000024 [rad]$$

$$\bar{a}_{p=99\%} = 0,0087267 \pm 0,03 \% [rad]$$

And the expanded uncertainty of singular measurement:

$$a_{i\ p=99\%} = 0,008727 \pm k \cdot u_{z\alpha_i} = 0,008727 \pm 0,000054 [rad]$$

$$a_{i\ p=99\%} = 0,0087267 \pm 0,6 \% [rad]$$

#### 4. Conclusion

It is essential to understand that the above determined uncertainty describes not the encoder alone but the entire measurement chain. In that chain one can distinguish the following elements with the greatest influence on the uncertainty:

- The encoder accuracy itself,
- The unbalance of the rotating masses and the speed irregularity as consequence,
- Frequency of the clock/timer utilized for time domain measurement,
- Possible delays in the electric circuit caused by Schmitt trigger or other element.

Consequently the uncertainty of the angle measurement by an encoder itself can be determined as no lower than presented above. However in the scientific or engineering applications the overall uncertainty of the measurement chain is searched usually. So taking into account the entire measurement chain is justified. In order to limit the problem to the encoder only, the test bed has to be modified and the driving unit with better unbalance should be applied.

The systematic uncertainty of type B (Fig. 6.) depends linearly on the angular speed. This is the result of constant scale interval of time measurement  $\Delta T$  at decreasing period  $T_i$ . During experiments it is important to take into account the systematic uncertainty at the angular speed corresponding to the speed in specific application.

#### Nomenclature

$T_i$  – period of the singular pulse

$\bar{T}$  – average period of pulse  $T_i$  at one revolution

$\bar{\omega}$  – average angular speed of the encoder's shaft

$\alpha_i$  – angle of the shaft rotation during the period  $T_i$

$\bar{\alpha}$  – mean value of a measured angle for one revolution,  
 $n$  – nominal number of encoder pulses per revolution.  
 $s(\alpha_i)$  – experimental standard deviation of  $\alpha_i$  singular measurement  
 $s(\bar{\alpha})$  – experimental standard deviation of a mean value  $\bar{\alpha}$   
 $\delta_i$  – unknown value of the error  
 $\Delta T$  – scale interval of time measurement  
 $u_\alpha$  – uncertainty Type B – systematic uncertainty  
 $u_{z\bar{\alpha}}$  – combined standard uncertainty of average  
 $u_{z\alpha_i}$  – combined standard uncertainty of singular measurement  
 $\bar{\alpha}_{p=99\%}$  - expanded uncertainty of average at level of confidence  $p=99\%$   
 $\alpha_{i\ p=99\%}$  - expanded uncertainty of singular measurement at level of confidence  $p=99\%$

## References

- [1] Główny Urząd Miar, *Wyrażanie Niepewności Pomiaru. Przewodnik*. . Warszawa, 1999.
- [2] GmbH, Maridis, *Complex Diagnostic System Brochure*. [Online] [Cited: 20 June 2007.] [http://www.maridis.de/Products/file\\_store/catalog/CDS\\_brochure.pdf](http://www.maridis.de/Products/file_store/catalog/CDS_brochure.pdf).
- [3] MAN B&W Diesel A/S, *PMI System Pressure Analyser*. [Online] czerwiec 2000. [Cited: 3 July 2007.] <http://www.manbw.com/files/news/files2051/pmi.pdf>.
- [4] MAN B&W Diesel A/S, *50-108 ME Engines. Operation Manual*, Edition 01, January 2006
- [5] Kowalak, Przemysław. *Speed Irregularity Characteristic of Low Speed, Two-Stroke Marine Diesel Engine Applied as Vessel's Main Propulsion. Journal of KONES*. Warsaw 2008, Tom IV, 15.
- [6] Wimmer Andreas, Glaser Josef, *Indykowanie silnika*. Warszawa : Instytut Zastosowań Techniki, 2004. ISBN 83-88691-20-1.
- [7] Wituszyński Krzysztof, *Prędkość kątowna i moment obrotowy, jako nośniki informacji o stanie silnika spalinowego*. Lubelskie Towarzystwo Naukowe, Lublin 1996, ISBN 83-85491-62-7



## CAPACITY FORCES IN SLIDE JOURNAL BEARING LUBRICATED OIL WITH MICROPOLAR STRUCTURE

Paweł Krasowski

Gdynia Maritime University  
ul. Morska 81-87, 81-225 Gdynia, Poland  
tel.: +48 58 6901331, fax: +48 58 6901399  
e-mail: pawkras@am.gdynia.pl

### Abstract

*Present paper shows the results of numerical solution Reynolds equation for laminar, steady oil flow in slide cylindrical bearing gap. Lubrication oil is fluid with micropolar structure. Properties of oil lubrication as of liquid with micropolar structure in comparison with Newtonian liquid, characterized are in respect of dynamic viscosity additionally dynamic couple viscosity and three dynamic rotation viscosity. Under regard of build structural element of liquid characterized is additionally microinertia coefficient. In modeling properties and structures of micropolar liquid one introduced dimensionless parameter with in terminal chance conversion micropolar liquid to Newtonian liquid. The results shown on diagrams of capacity forces in dimensionless form in dependence on coupling number  $N^2$  and characteristic dimensionless length of micropolar fluid  $\Lambda_1$ . Presented calculations are limited to isothermal models of bearing with infinite length.*

**Keywords:** micropolar lubrication, cylindrical journal bearing, capacity force

### 1. Introduction

Presented article take into consideration the laminar, steady flow in the crosswise cylindrical slide bearing gap. Non-Newtonian fluid with the micropolar structure is a lubricating factor. Materials engineering and tribology development helps to introduce oils with the compound structure (together with micropolar structure) as a lubricating factors. Exploitation requirements incline designers to use special oil refining additives, to change viscosity properties. As a experimental studies shows, most of the refining lubricating fluids, can be included as fluids of non-Newtonian properties with microstructure [4,5,7,8]. They belong to a class of fluids with symmetric stress tensor that we shall call polar fluids, and include, as a special case, the well known Navier-Stokes model. Physically, the micropolar fluids may represent fluids consisting rigid randomly orientated spherical particles suspended in a viscous medium, where the deformation of fluid particles is neglected [3,4]. Presented work dynamic viscosity of isotropic micropolar fluid is characterized by five viscosities: shearing viscosity  $\eta$  (known at the Newtonian fluids), micropolar coupling viscosity  $\kappa$  and by three rotational viscosities bounded with rotation around the coordinate axes. This kind of micropolar fluid viscosity characteristic is a result of essential compounds discussed in works [4,5]. Regarding of limited article capacity please read above works. In difference to classical oil with Newtonian properties, micropolar fluid is characterized by microinertia of the fluid part and by microrotation velocity field. This fact

determine the additional system of equation development describing micropolar fluid flow which is described by moment of momentum equation. In result of the above, the conjugation between fluid flow field and the microrotation velocity field. In presented flow, the influence of lubricating fluid inertia force and the external elementary body force field were omit [4,5,6].

## 2. Reynolds equation

Basic equation set defining isotropic micropolar fluid flow are describe following equations [2,4,5,6]: momentum equation, moment of momentum equation, energy equation, equation of flow continuity. Incompressible fluid flow is taken into consideration with constant density skipping the body force. We assume also, that dynamic viscosity coefficients which characterize micropolar fluid are constant. According to above velocity flow field is independent from temperature field and the momentum equation, moment of momentum equation and equation of flow continuity are part of closed system of motion equations. The constant viscosity of micropolar oil, independent from thermal and pressure condition in the bearing. Quantity of viscosity coefficient depend on shearing dynamic viscosity  $\eta$ , which is decisive viscosity in case of Newtonian fluids. Reference pressure  $p_0$  is also described with this viscosity, in order to compare micropolar oils results with Newtonian oil results. In micropolar oils decisive impact has quantity of dynamic coupling viscosity  $\kappa$  [1,3]. In some works concerning bearing lubrication with micropolar oil, it's possible to find the sum of the viscosities as a micropolar dynamic viscosity efficiency. In presented article coupling viscosity was characterized with coupling number  $N^2$ , which is equal to zero for Newtonian oil:

$$N = \sqrt{\frac{\kappa}{\eta + \kappa}} \quad 0 \leq N < 1 \quad (1)$$

Quantity  $N^2$  in case of micropolar fluid, define a dynamic viscosity of coupling share in the oil dynamic viscosity efficiency. From the coupling number  $N^2$  we can determine both dynamic viscosity ratio, which is dimensionless micropolar coupling viscosity:

$$\kappa_1 = \frac{\kappa}{\eta} = \frac{N^2}{1 - N^2} \quad \kappa_1 \geq 0 \quad (2)$$

From the dynamic rotational viscosities at the laminar lubrication, individual viscosities are compared to viscosity  $\gamma$ , which is known as the most important and it ratio to shearing viscosity  $\eta$  is bounded to characteristic flow length  $\Lambda$ , which in case of Newtonian flow assume the zero quantity. Dimensionless quantity of micropolar length  $\Lambda_1$  and micropolar length  $\Lambda$  are defined:

$$\Lambda = \sqrt{\frac{\gamma}{\eta}}; \quad \Lambda \Lambda_1 = \varepsilon \quad (3)$$

Dimensionless micropolar length  $\Lambda_1$  in case of Newtonian oil approach infinity. Momentum equation, moment of momentum equation and equation of flow continuity writing out in cylindrical coordinates  $\varphi$ ;  $r$ ;  $z$  are presented in article [2,3] where individual phases leading to Reynolds equation for laminar, stationary lubricating process in dimensionless form are mentioned. Reynolds equation for stationary flow of laminar micropolar fluid in the crosswise, cylindrical, slide bearing gap can be present [1,2,7] in dimensional form:

$$\frac{\partial}{\partial \varphi} \left( \frac{h^3}{\eta} \Phi(\Lambda, N, h) \frac{\partial p}{\partial \varphi} \right) + \frac{\partial}{\partial z} \left( \frac{h^3}{\eta} \Phi(\Lambda, N, h) \frac{\partial p}{\partial z} \right) = 6 \frac{dh}{d\varphi} \quad (4)$$

where:  $p$  – hydrodynamic pressure,  
 $h$  – gap height of bearing

$\Phi(\Lambda, N, h)$  function in form (5) when in case of the Newtonian fluid it has a value 1 and the Reynolds equation (4) change into a non-Newtonian fluid equation.

$$\Phi(\Lambda, N, h) = 1 + 12 \frac{\Lambda^2}{h^2} - 6 \frac{N\Lambda}{h} \coth\left(\frac{Nh}{2\Lambda}\right) \quad (5)$$

Reynolds equation (4) can be presented in dimensionless form [1,7] using the method of changing into this values:

$$\frac{\partial}{\partial \varphi} \left( \Phi_1(\Lambda_1, N, h_1) \frac{\partial p_1}{\partial \varphi} \right) + \frac{1}{L_1^2} \frac{\partial}{\partial z_1} \left( \Phi_1(\Lambda_1, N, h_1) \frac{\partial p_1}{\partial z_1} \right) = 6 \frac{dh_1}{d\varphi} \quad (6)$$

for  $0 \leq \varphi \leq \varphi_k$ ;  $0 \leq r_1 \leq h_1$ ;  $-1 \leq z_1 \leq 1$

$$\text{where: } \Phi_1 = h_1^3 + 12 \frac{h_1}{\Lambda_1^2} - 6 \frac{Nh_1^2}{\Lambda_1} \coth\left(\frac{h_1 N \Lambda_1}{2}\right) \quad (7)$$

Reference pressure  $p_0$  caused by journal rotation with the angular velocity  $\omega$  was assumed in (8) taking into consideration dynamic viscosity of shearing  $\eta$  and the lubricating gap height  $h_1$  at the wrapping angle  $\varphi$  was taken in relative eccentricity function  $\lambda$  :

$$p_0 = \frac{\omega \eta}{\psi^2} ; \quad h_1(\varphi, \lambda) = 1 + \lambda \cos \varphi ; \quad \psi = \frac{\varepsilon}{R} \quad (8)$$

where:  $\omega$  – angular journal velocity,  
 $\psi$  – dimensionless radial clearance ( $10^{-4} \leq \psi \leq 10^{-3}$ ) ,  
 $\varepsilon$  – radial clearance,  
 $R$  – radius of the journal,  
 $b$  – length of the journal

$$\psi = \frac{\varepsilon}{R} ; \quad L_1 = \frac{b}{R} \quad (9)$$

Dimensionless values in equation (6) : hydrodynamic pressure  $p_1$ , radial coordinate  $r_1$  , length coordinate of the journal  $z_1$ , longitudinal gap height  $h_1$ , bearing length  $L_1$  are in form:

$$p = p_0 p_1 ; \quad r = R(1 + \psi r_1) ;$$

$$z = bz_1 ; \quad h = \varepsilon h_1 ; \quad b = L_1 R \quad (10)$$

$\Phi_1(\Lambda_1, N, h_1)$  function in form (7) when in case of the Newtonian fluid it has a value  $h_1^3$  .

### 3. Hydrodynamic pressure distribution

Below solutions (6) for infinity length bearing is presented. In this solution the Reynolds boundary conditions, applying to zeroing of pressure at the beginning ( $\varphi=0$ ) and at the end ( $\varphi=\varphi_k$ ) of the oil film and zeroing of the pressure derivative on the wrapping angle at the end of the film

where fulfill. The pressure distribution function in case of the micropolar lubrication  $p_1(\varphi)$ , of the Newtonian lubrication  $p_{1N}(\varphi)$  has a form:

$$p_1(\varphi) = 6 \int_0^\varphi \frac{h_1 - h_{1k}}{\Phi_1(\Lambda_1, N, h_1)} d\varphi; \quad p_{1N}(\varphi) = 6 \int_0^\varphi \frac{h_1 - h_{1k}}{h_1^3} d\varphi \quad (11)$$

where:  $h_{1k} = h_1(\varphi_k)$  lubricating gap height at the end of the oil film.

In the boundary case of lubricating Newtonian fluid, pressure distribution function is a pressure  $p_{1N}(\varphi)$ . Example numerical calculation were made for the infinity length bearing with the relative eccentricity  $\lambda=0,6$ .

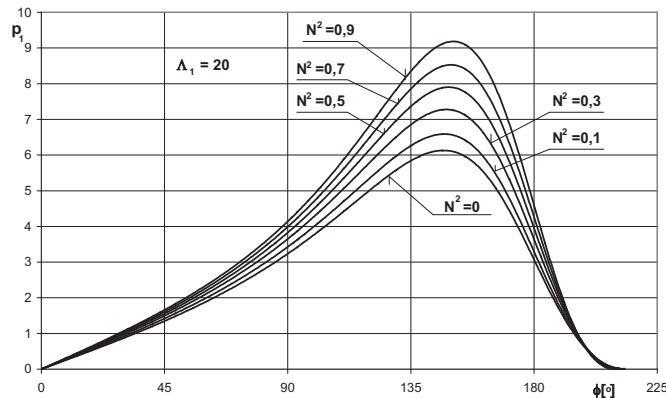


Fig.1 The dimensionless pressure distributions  $p_1$  in direction  $\varphi$  in dependence on coupling number  $N^2$  by micropolar ( $N^2 > 0$ ) and Newtonian ( $N^2 = 0$ ) lubrication for dimensionless eccentricity ratio  $\lambda=0,6$  and characteristic dimensionless length of micropolar fluid  $\Lambda_1=20$

Analyzing the influence of coupling number  $N^2$  and the influence of dimensionless micropolar length  $\Lambda_1$  on hydrodynamic pressure distribution in the bearing liner circuitual direction. At the Fig.1 pressure distribution for individual coupling numbers at constant micropolar length  $\Lambda_1 = 20$ . The pressure increase effect is caused by oil dynamic viscosity efficiency increase as a result of coupling viscosity  $\kappa$ . At  $N^2 = 0,5$ , coupling viscosity is equal to shearing viscosity. Pressure graph in the Fig.1 for micropolar oil lubrication ( $N^2 > 0$ ) find themselves above the pressure graph at the

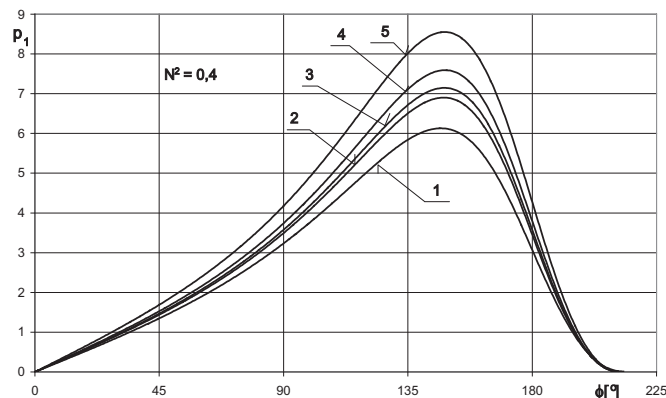


Fig.2 The dimensionless pressure distributions  $p_1$  in direction  $\varphi$  in dependence on characteristic dimensionless length of micropolar fluid  $\Lambda_1$ : 1) Newtonian oil, 2)  $\Lambda_1=40$ , 3)  $\Lambda_1=30$ , 4)  $\Lambda_1=20$ , 5)  $\Lambda_1=10$ , for dimensionless eccentricity ratio  $\lambda=0,6$  and coupling number  $N^2=0,4$

Newtonian oil lubrication ( $N^2=0$ ). Pressure distribution is higher for higher coupling number. It is caused by oil viscosity dynamic efficiency. In the Fig.2 the course of dimensionless pressure  $p_1$  for few micropolar length quantity  $\Lambda_1$  is shown. Decrease of this parameter determine the increase of micropolar oil rotational dynamic viscosity. Pressure distribution are presented at the constant coupling number  $N^2=0,4$ . Rotational viscosity increase determine the pressure distribution increase and is caused, because both the oil flow and microrotation velocities are coupled. Quantities of coupling number  $N^2$  and dimensionless micropolar length where taken from works [1,2,3].

#### 4. Capacity forces

Capacity force  $W$  for cylindrical slide journal bearing has following components  $W_x$  and  $W_y$  to be determined [2,5] in the local co-ordinate systems in Fig. 3.

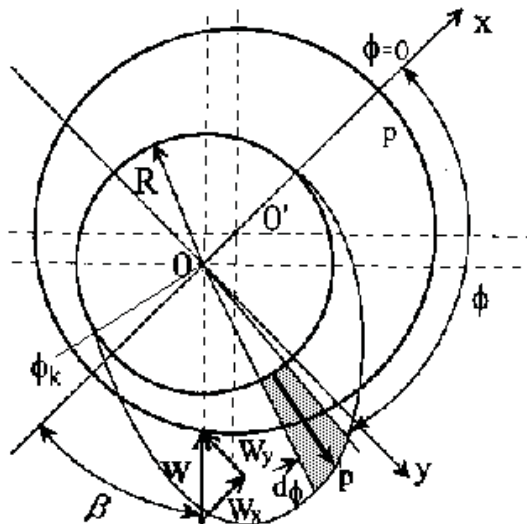


Fig. 3 Capacity force  $W$  and components  $W_x$  and  $W_y$  in the local co-ordinate system

Thus dimensionless components  $W_{1x}$  and  $W_{1y}$  of capacity forces  $W_1$  are as follows [2]:

$$W_{1x} = \frac{W_x}{W_0} = -\int_0^{\varphi_k} p_1 \cos \varphi d\varphi, \quad W_{1y} = \frac{W_y}{W_0} = -\int_0^{\varphi_k} p_1 \sin \varphi d\varphi, \quad (12)$$

$$W_1 \equiv S_0 = \sqrt{W_{1x}^2 + W_{1y}^2} = \frac{W}{W_0}$$

where:  $W_0$  - characteristic value of capacity force  $W_0 \equiv 2Rbp_0$ ,  
 $S_0$  – Sommerfeld Number for slide journal bearing.

Capacity force is situated in the co-ordinate  $\varphi$  angle  $\varphi_{W1}$ :

$$\varphi_w = \pi - \beta = \pi - \arctg \left| \frac{W_{1y}}{W_{1x}} \right| \quad (13)$$

Quantities capacity forces  $W_1$  are presented in the Fig.4 in the coupling Number  $N^2$  function for chosen micropolar length  $\Lambda_1$ . All lines are coming out from the maximal pressure point in case of Newtonian fluid flow. We observe maximal capacity force increase when the coupling number  $N^2$  increases ( coupling viscosity increases  $\kappa$ ) and the micropolar length decreases  $\Lambda_1$  ( rotational viscosity increases  $\gamma$ ) . Full range of coupling number change, that covers the range  $[0;1]$ , apply to coupling viscosity  $\kappa$  change from small to very high quantities. In most of the works, the

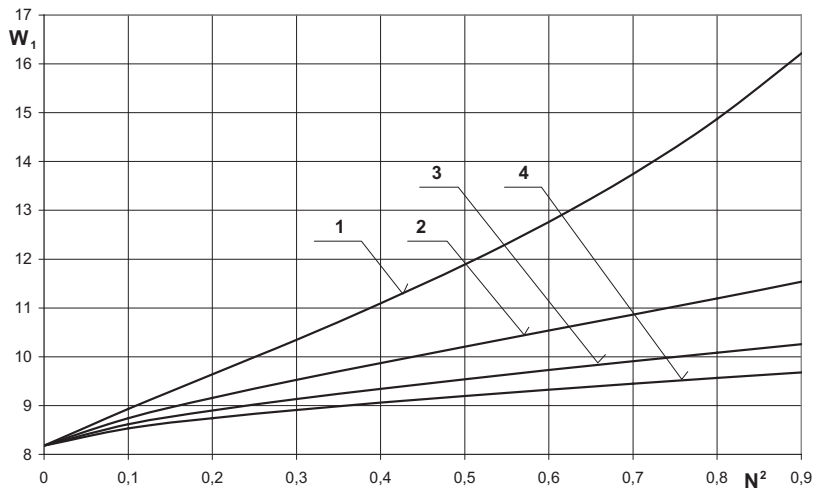


Fig.4 The dimensionless capacity force  $W_1$  in dependence on coupling number  $N^2$  for characteristic dimensionless length of micropolar fluid  $A_1$ : 1)  $A_1=10$ , 2)  $A_1=20$ , 3)  $A_1=30$ , 4)  $A_1=40$

hydrodynamic parameters of the bearing graphs are given in the function, which is Capacity forces courses presented in the Fig.4, can be more suitable for small quantities for parameter  $\kappa_1$ . In the

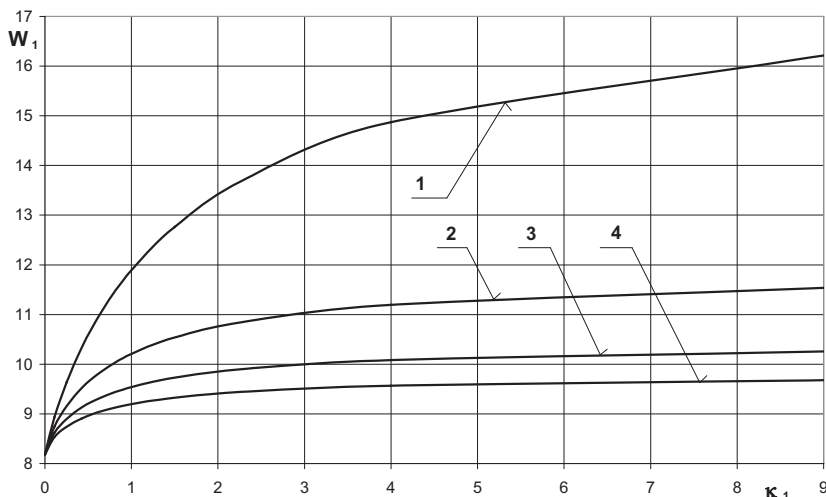


Fig.5 The dimensionless capacity force  $W_1$  in dependence on dimensionless coupling viscosity  $\kappa_1$  for characteristic dimensionless length of micropolar fluid  $A_1$ : 1)  $A_1=10$ , 2)  $A_1=20$ , 3)  $A_1=30$ , 4)  $A_1=40$

Fig.5 presented capacity forces  $W_1$  courses in the dimensionless micropolar length function  $\Lambda_1$  for a few coupling number  $N$  quantities. Broken line show the capacity force in case of Newtonian oil



lubrication. All lines approach asymptotically to the broken line when the micropolar length increases (rotational viscosity decreases  $\gamma$ ). Together with coupling number increase, maximal

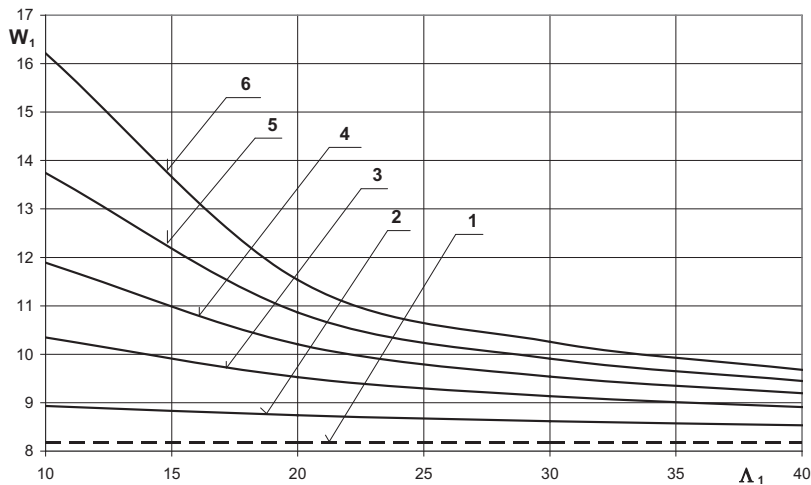


Fig.6 The dimensionless capacity force  $W_1$  in dependence on characteristic dimensionless length of micropolar fluid  $\Lambda_1$  for coupling number  $N^2$  (---- Newtonian oil)

pressure increases (coupling viscosity increases). Angular coordinate  $\phi_{W_1}$  of capacity force position  $W_1$  in the square function of coupling number  $N^2$  for chosen micropolar length  $\Lambda_1$  were shown in the Fig.6. All lines come out from the capacity force position point in case of Newtonian

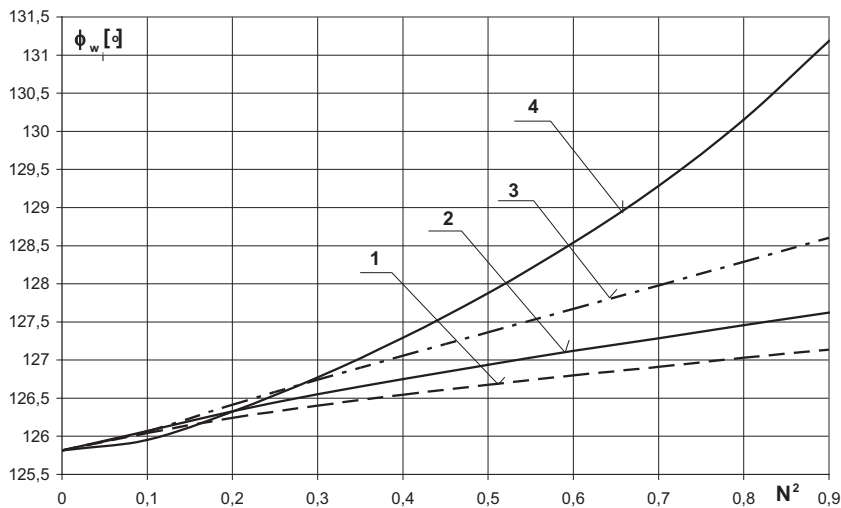


Fig.7 Angle  $\phi_w$  situated capacity force  $W_1$  in dependence on coupling number  $N^2$  for characteristic dimensionless length of micropolar fluid  $\Lambda_1$ : 1)  $\Lambda_1=10$ , 2)  $\Lambda_1=20$ , 3)  $\Lambda_1=30$ , 4)  $\Lambda_1=40$

fluid flow. Increase of capacity force position angle  $\phi_w$  is observed while the coupling number increases  $N^2$  (coupling viscosity increases  $\kappa$ ) and the micropolar length decreases  $\Lambda_1$  (rotational viscosity increases  $\gamma$ ). Graphs in the Fig.6 are described with nonlinear scale of dimensionless coupling viscosity  $\kappa_1$  change.

## 5. Conclusions

Presented example of the Reynolds equation solutions for steady laminar non-Newtonian lubricating oil flow with micropolar structure, enable the hydrodynamic pressure distribution introductory estimation as a basic exploitation parameter of slide bearing. Comparing Newtonian oil to oils with micropolar structure, can be used in order to increase hydrodynamic pressure and also to increase capacity load of bearing friction centre. Micropolar fluid usage has two sources of pressure increase in view of viscosity properties: increase of fluid efficient viscosity (coupling viscosity increase) and the rotational viscosity increase (characteristic length parameter  $\Lambda$ ). Author realize that he made few simplified assumptions in the above bearing centre model and in the constant parameter characterizing oil viscosity properties. Despite this calculation example apply to bearing with infinity length, received results can be usable in estimation of pressure distribution and of capacity force at laminar, steady lubrication of cylindrical slide bearing with infinity length. Presented results can be usable as a comparison quantities in case of numerical model laminar, unsteady flow Non-Newtonian fluids in the lubricating gaps of crosswise cylindrical slide bearings.

## References

- [1] Das S., Guha S.K., Chattopadhyay A.K.- *Linear stability analysis of hydrodynamic journal bearings under micropolar lubrication* - Tribology International 38 (2005), pp.500-507
- [2] Krasowski P. – *Stacjonarny, laminarny przepływ mikropolarnego czynnika smarującego w szczelinie smarnej poprzecznego łożyska ślizgowego* - Zeszyty Naukowe nr 49, pp. 72-90 , Akademia Morska, Gdynia 2003
- [3] Krasowski P. – Pressure in slide journal bearing lubricated oil with micropolar structure – Journal of POLISH CIMAC Vol. 3, No. 2, Gdansk 2008, pp. 99-108
- [4] Łukaszewicz G.– *Micropolar Fluids. Theory and Applications* – Birkhäuser Boston 1999
- [5] Walicka A.– *Reodynamika przepływu płynów nienewtonowskich w kanałach prostych i zakrzywionych* – Uniwersytet Zielonogórski, Zielona Góra 2002
- [6] Walicka A. - *Inertia effects in the flow of a micropolar fluid in a slot between rotating surfaces of revolution* – International Journal of Mechanics and Engineering, 2001,vol.6, No. 3, pp. 731-790
- [7] Wiercholski K.- *Mathematical methods in hydrodynamic theory of lubrication*- Technical University Press, Szczecin 1993.
- [8] Xiao-Li Wang, Ke-Qin Zhu – *A study of the lubricating effectiveness of micropolar fluids in a dynamically loaded journal bearing* – Tribology International 37 (2004), pp.481-490



## PRESSURE IN SLIDE JOURNAL PLANE BEARING LUBRICATED OIL WITH MICROPOLAR STRUCTURE

Paweł Krasowski

Gdynia Maritime University  
ul. Morska 81-87, 81-225 Gdynia, Poland  
tel.: +48 58 6901331, fax: +48 58 6901399  
e-mail: pawkras@am.gdynia.pl

### Abstract

Present paper shows the results of numerical solution Reynolds equation for laminar, steady oil flow in slide plane bearing gap. Lubrication oil is fluid with micropolar structure. Properties of oil lubrication as of liquid with micropolar structure in comparison with Newtonian liquid, characterized are in respect of dynamic viscosity additionally dynamic couple viscosity and three dynamic rotation viscosity. Under regard of build structural element of liquid characterized is additionally microinertia coefficient. In modeling properties and structures of micropolar liquid one introduced dimensionless parameter with in terminal chance conversion micropolar liquid to Newtonian liquid. The results shown on diagrams of hydrodynamic pressure in dimensionless form in dependence on coupling number  $N^2$  and characteristic dimensionless length of micropolar fluid  $\Lambda_1$ . Presented calculations are limited to isothermal models of bearing with infinite breadth.

**Keywords:** micropolar lubrication, journal plane bearing, hydrodynamic pressure

### 1. Introduction

Presented article take into consideration the laminar, steady flow in the crosswise cylindrical slide plane bearing gap. Non-Newtonian fluid with the micropolar structure is a lubricating factor. Materials engineering and tribology development helps to introduce oils with the compound structure (together with micropolar structure) as a lubricating factors. Exploitation requirements incline designers to use special oil refining additives, to change viscosity properties. As a experimental studies shows, most of the refining lubricating fluids, can be included as fluids of non-Newtonian properties with microstructure [4-7]. They belong to a class of fluids with symmetric stress tensor that we shall call polar fluids, and include, as a special case, the well known Navier-Stokes model. Physically, the micropolar fluids may represent fluids consisting rigid randomly orientated spherical particles suspended in a viscous medium, where the deformation of fluid particles is neglected [4]. Presented work dynamic viscosity of isotropic micropolar fluid is characterized by five viscosities: shearing viscosity  $\eta$  (known at the Newtonian fluids), micropolar coupling viscosity  $\kappa$  and by three rotational viscosities bounded with rotation around the coordinate axes. This kind of micropolar fluid viscosity characteristic is a result of essential compounds discussed in works [4-6]. Regarding of limited article capacity please read

above works. In presented flow, the influence of lubricating fluid inertia force and the external elementary body force field were omit [3-6].

## 2. Reynolds equation

Basic equation set defining isotropic micropolar fluid flow are describe following equations [2-6]: momentum equation, moment of momentum equation, energy equation, equation of flow continuity. Incompressible fluid flow is taken into consideration with constant density skipping the body force. We assume also, that dynamic viscosity coefficients which characterize micropolar fluid are constant. According to above velocity flow field is independent from temperature field and the momentum equation, moment of momentum equation and equation of flow continuity are part of closed system of motion equations.

Lubricating gap is characterize by following geometric parameters: maximal gap height  $h_0$ , minimal gap height  $h_e$ , gap length  $L$  and gap breadth  $b$  (Fig. 1) model the following assumption were made: lubricating gap dimensions along it's width of mating surfaces remain

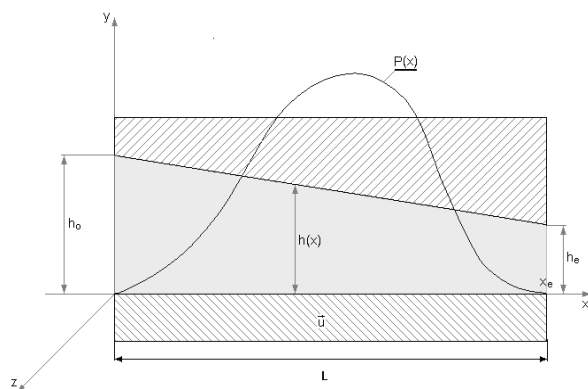


Fig.1. Geometry schema of the slide journal plane bearing gap

identical. Lubricating gap height after gap length was described in cartesian co-ordinate system by the following dimensionless form:

$$h_1(x_1) = \varepsilon - (\varepsilon - 1)x_1 \quad \text{for} \quad 0 \leq x_1 \leq 1 \quad (1)$$

Dimensionless values [2, 3] that characterize lubricating gap are: length coordinate  $x_1$ , gap height coordinate  $h_1$  and gap convergence coefficient  $\varepsilon$ :

$$x_1 = \frac{x}{L}; \quad h_1 = \frac{h}{h_m}; \quad \varepsilon = \frac{h_e}{h_m} \quad (2)$$

The constant viscosity of micropolar oil, independent from thermal and pressure condition in the bearing. Quantity of viscosity coefficient depend on shearing dynamic viscosity  $\eta$ , which is decisive viscosity in case of Newtonian fluids. Reference pressure  $p_0$  is also described with this viscosity, in order to compare micropolar oils results with Newtonian oil results. In micropolar oils decisive impact has quantity of dynamic coupling viscosity  $\kappa$  [1,4]. In some works concerning bearing lubrication with micropolar oil, it's possible to find the sum of the viscosities as a micropolar dynamic viscosity efficiency. In presented article coupling viscosity was characterized with coupling number  $N^2$ , which is equal to zero for Newtonian oil:

$$N = \sqrt{\frac{\kappa}{\eta + \kappa}} \quad 0 \leq N < 1 \quad (3)$$

Quantity  $N^2$  in case of micropolar fluid, define a dynamic viscosity of coupling share in the oil dynamic viscosity efficiency. From the coupling number  $N^2$  we can determine both dynamic viscosity ratio, which is dimensionless micropolar coupling viscosity:

$$\kappa_1 = \frac{\kappa}{\eta} = \frac{N^2}{1 - N^2} \quad \kappa_1 \geq 0 \quad (4)$$

From the dynamic rotational viscosities at the laminar lubrication, individual viscosities are compared to viscosity  $\gamma$ , which is known as the most important and it ratio to shearing viscosity  $\eta$  is bounded to characteristic flow length  $\Lambda$ , which in case of Newtonian flow assume the zero quantity [8]. Dimensionless quantity of micropolar length  $\Lambda_1$  and micropolar length  $\Lambda$  are defined:

$$\Lambda = \sqrt{\frac{\gamma}{\eta}}; \quad \Lambda \Lambda_I = \varepsilon \quad (5)$$

Dimensionless micropolar length  $\Lambda_1$  in case of Newtonian oil approach infinity.

Reynolds equation for stationary flow of laminar micropolar fluid in the lengthwise, plane slide bearing gap can be present [1,2,7,8] in dimensional form:

$$\frac{\partial}{\partial x} \left( \frac{h^3}{\eta} \Phi(\Lambda, N, h) \frac{\partial p}{\partial x} \right) + \frac{\partial}{\partial z} \left( \frac{h^3}{\eta} \Phi(\Lambda, N, h) \frac{\partial p}{\partial z} \right) = 6 \frac{dh}{dx} \quad (6)$$

$\Phi(\Lambda, N, h)$  function in form (7) when in case of the Newtonian fluid it has a value 1 and the Reynolds equation (6) change into a non-Newtonian fluid equation.

$$\Phi(\Lambda, N, h) = 1 + 12 \frac{\Lambda^2}{h^2} - 6 \frac{N\Lambda}{h} \coth \left( \frac{Nh}{2\Lambda} \right) \quad (7)$$

Reynolds equation (6) can be presented in dimensionless form [1,7] using the method of changing into this values:

$$\frac{\partial}{\partial x_1} \left( \Phi_1(\Lambda_1, N, h_1) \frac{\partial p_1}{\partial x_1} \right) + \frac{1}{L_1^2} \frac{\partial}{\partial z_1} \left( \Phi_1(\Lambda_1, N, h_1) \frac{\partial p_1}{\partial z_1} \right) = 6 \frac{dh_1}{dx_1} \quad (8)$$

for  $0 \leq x_1 \leq 1; \quad 0 \leq y_1 \leq h_1; \quad -1 \leq z_1 \leq 1$

$$\text{where:} \quad \Phi_1 = h_1^3 + 12 \frac{h_1}{\Lambda_1^2} - 6 \frac{Nh_1^2}{\Lambda_1} \coth \left( \frac{h_1 N \Lambda_1}{2} \right) \quad (9)$$

The dimensionless values for pressure  $p_1$ , bearing breadth  $L_1$  and remaining coordinates  $y_1$  and  $z_1$  are described as follows:

$$p = p_0 p_1, \quad L_1 = \frac{b}{L}, \quad z = b z_1, \quad y = h_e y_1, \quad (10)$$

Reference pressure  $p_0$  caused by linear velocity  $U$  of slide bearing was assumed in (11) taking into consideration dynamic viscosity of shearing  $\eta$  and the lubricating gap height  $h_e$  in form :

$$p_0 = \frac{U\eta}{\psi L}, \quad \psi = \frac{h_e}{L} \quad (11)$$

where:

$\psi$  – relative clearance ( $10^{-4} \leq \psi \leq 10^{-3}$ )

### 3. Hydrodynamic pressure distribution

Below solutions (8) for infinity breadth bearing is presented. In this solution the Reynolds boundary conditions, applying to zeroing of pressure at the beginning ( $x_1=0$ ) and at the end ( $x_1=1$ ) of the oil film ended. The pressure distribution function in case of the micropolar lubrication has a form:

$$p_1(x_1) = 6 \int_0^{x_1} \frac{h_1 - C_1}{\Phi_1(\Lambda_1, N, h_1)} dx_1 \quad ; \quad C_1 = \frac{\int_0^1 \frac{h_1}{\Phi_1} dx_1}{\int_0^1 \frac{1}{\Phi_1} dx_1} \quad (12)$$

In the boundary case of lubricating Newtonian fluid, pressure distribution function is a pressure  $p_{1N}(x_1)$  and is in form:

$$\lim_{\substack{N \rightarrow 0 \\ \Lambda_1 \rightarrow \infty}} \Phi_1 = h_1^3 \quad \lim_{\substack{N \rightarrow 0 \\ \Lambda_1 \rightarrow \infty}} C_1 = 1 \quad p_{1N}(x_1) = 6 \int_0^{x_1} \frac{h_1 - 1}{h_1^3} dx_1 \quad (13)$$

where:  $p_{1N}(x_1)$  - pressure distribution for Newtonian oil

$$p_{1N} = \frac{6(\varepsilon - 1)(1 - x_1)x_1}{(\varepsilon + 1)(\varepsilon - \varepsilon x_1 + x_1)^2} \quad (14)$$

Example numerical calculation were made for the infinity breadth bearing with convergence coefficient  $\varepsilon$ :  $\varepsilon_{opt} = 1 + \sqrt{2}$  end  $\varepsilon = 1,4$  marked continuous and discontinuous lines.

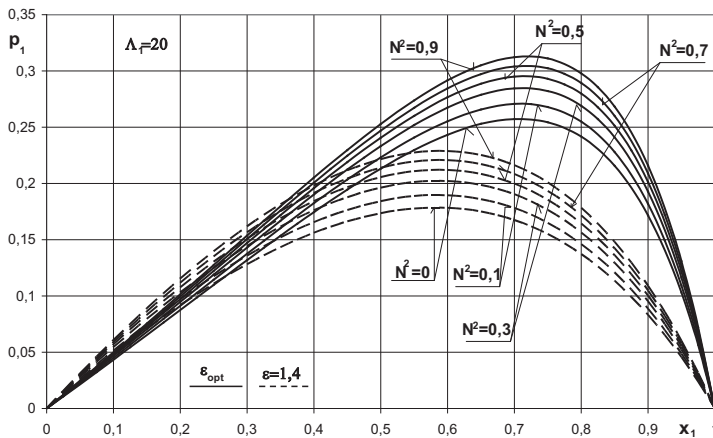


Fig.2 The pressure distributions  $p_1$  in direction  $x_1$  in dependence on coupling number  $N^2$  by micropolar ( $N^2 > 0$ ) and Newtonian ( $N^2 = 0$ ) lubrication for convergence coefficient  $\varepsilon_{opt}$  and  $\varepsilon = 1,4$  from characteristic length of micropolar fluid  $\Lambda_1 = 20$

Analyzing the influence of coupling number  $N^2$  and the influence of dimensionless micropolar length  $\Lambda_1$  on hydrodynamic pressure distribution in the bearing liner circuital direction. At the Fig.2 pressure distribution for individual coupling numbers at constant micropolar length  $\Lambda_1 = 20$ . The pressure increase effect is caused by oil dynamic viscosity efficiency increase as a result of coupling viscosity  $\kappa$ . At  $N^2 = 0,5$ , coupling viscosity is equal to shearing viscosity. Pressure graph in the Fig.2 for micropolar oil lubrication ( $N^2 > 0$ ) find themselves above the pressure graph at the

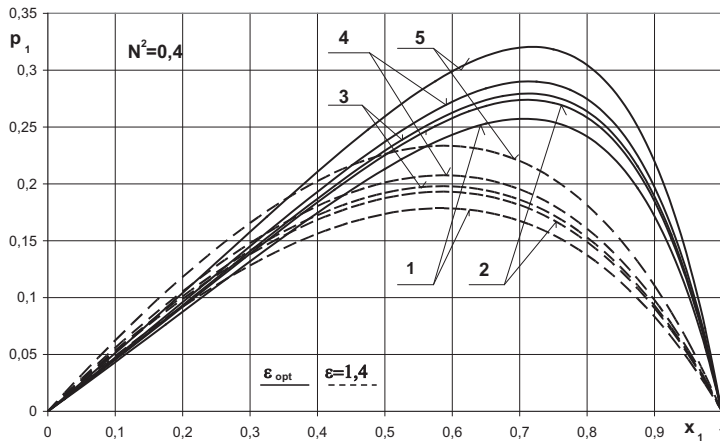


Fig.3 The pressure distributions  $p_1$  in direction  $x_1$  in dependence on characteristic length of micropolar fluid  $\Lambda_1$ : 1) Newtonian oil, 2)  $\Lambda_1=40$ , 3)  $\Lambda_1=30$ , 4)  $\Lambda_1=20$ , 5)  $\Lambda_1=10$ , for convergence coefficient  $\varepsilon_{opt}$  and  $\varepsilon=1,4$  from coupling number  $N^2=0,4$

Newtonian oil lubrication ( $N^2=0$ ). Pressure distribution is higher for higher coupling number. It is caused by oil viscosity dynamic efficiency. In the Fig.3 the course of dimensionless pressure  $p_1$  for few micropolar length quantity  $\Lambda_1$  is shown. Decrease of this parameter determine the increase of micropolar oil rotational dynamic viscosity. Pressure distribution are presented at the constant coupling number  $N^2=0,4$ . Rotational viscosity increase determine the pressure distribution increase and is caused, because both the oil flow and microrotation velocities are coupled. Quantities of coupling number  $N^2$  and dimensionless micropolar length where taken from works [1,2].

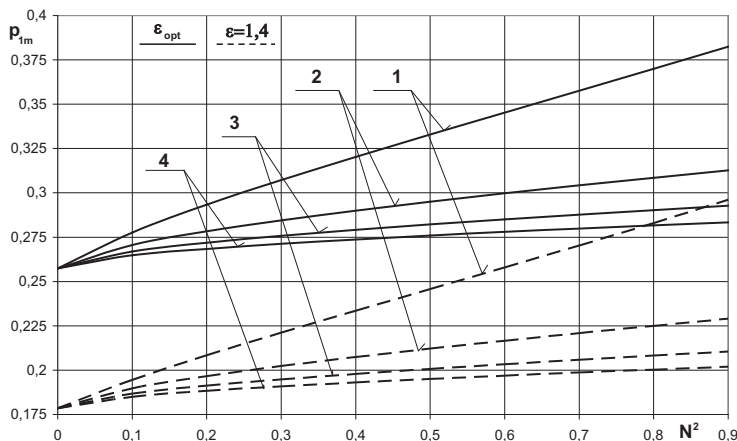


Fig.4 The maximal pressure  $p_{1m}$  in dependence on coupling number  $N^2$  for characteristic length of micropolar fluid  $\Lambda_1$ : 1)  $\Lambda_1=10$ , 2)  $\Lambda_1=20$ , 3)  $\Lambda_1=30$ , 4)  $\Lambda_1=40$  from convergence coefficient  $\varepsilon_{opt}$  and  $\varepsilon=1,4$

Based on given hydrodynamic pressure distribution  $p_1$  on longitudinal of the bearing  $x_1$ , the numerical quantities of maximal pressure  $p_{1m}$  and the lengthwise coordinate  $x_{1pm}$  (at the maximal position) were obtain. Quantities  $p_{1m}$  are presented in the Fig.4 in the coupling Number  $N^2$  function for chosen micropolar length  $\Lambda_1$ . All lines are coming out from the maximal pressure point in case of Newtonian fluid flow. We observe maximal pressure increase when the coupling number  $N^2$  increases ( coupling viscosity increases  $\kappa$ ) and the micropolar length decreases  $\Lambda_1$  (rotational viscosity increases  $\gamma$ ) . Full range of coupling number change, that covers the range  $[0;1)$ , apply to coupling viscosity  $\kappa$  change from small to very high quantities. In most of the works, the hydrodynamic parameters of the bearing graphs are given in the function, which is

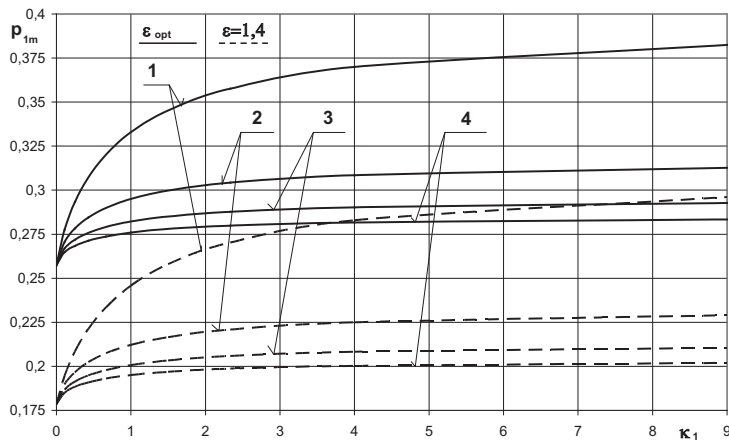


Fig.5 The maximal pressure  $p_{1m}$  in dependence on coupling viscosity  $\kappa_1$  for characteristic length of micropolar fluid  $\Lambda_1$ : 1)  $\Lambda_1=10$ , 2)  $\Lambda_1=20$ , 3)  $\Lambda_1=30$ , 4)  $\Lambda_1=40$  from convergence coefficient  $\epsilon_{opt}$  and  $\epsilon=1,4$

nonlinear scale for coupling viscosity  $\kappa_1$ . In the Fig.5. the same graph is given in the dimensionless viscosity  $\kappa_1$  function. Change range  $N^2$  from the Fig.4 comply to  $\kappa_1$  changes in the Fig.5. Maximal pressure courses presented in the Fig.4, can be more suitable for small quantities for parameter  $\kappa_1$ . In the Fig.6 presented maximal pressure  $p_{1m}$  courses in the dimensionless micropolar length function  $\Lambda_1$  for a few coupling number  $N$  quantities.

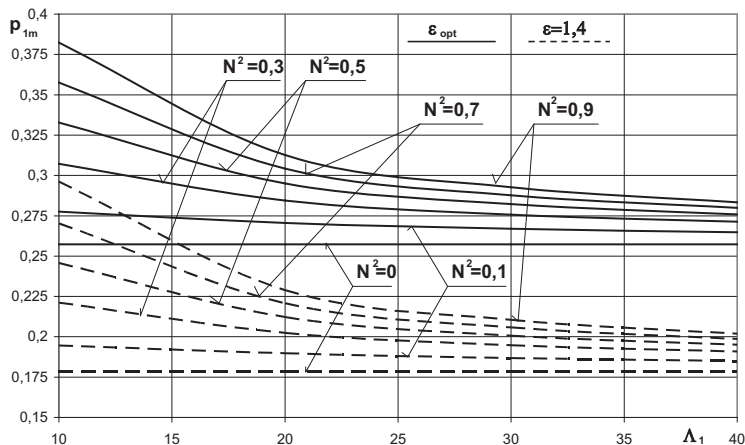


Fig.6 The maximal pressure  $p_{1m}$  in dependence on characteristic length of micropolar fluid  $\Lambda_1$  for coupling number  $N^2$  (---- Newtonian oil) from convergence coefficient  $\epsilon_{opt}$  and  $\epsilon=1,4$



Broken line show the maximal pressure in case of Newtonian oil lubrication. All lines approach asymptotically to the broken line when the micropolar length increases (rotational viscosity decreases  $\gamma$ ). Together with coupling number increase, maximal pressure increases (coupling viscosity increases). Change dimensionless coordinate  $\Delta x_{1p}$  of maximal pressure position  $p_{1m}$  in the square function of coupling number  $N^2$  for chosen micropolar length  $\Lambda_1$  were show in the Fig.7. and calculated in formula:

$$\Delta x_{1p} = x_{1pm} - x_{1pmN} \quad (14)$$

where:

$x_{1pm}$  - dimensionless coordinate  $x_1$  maximal pressure  $p_{1m}$

$x_{1pmN}$  - dimensionless coordinate  $x_1$  maximal pressure  $p_{1m}$  for Newtonian oil flow

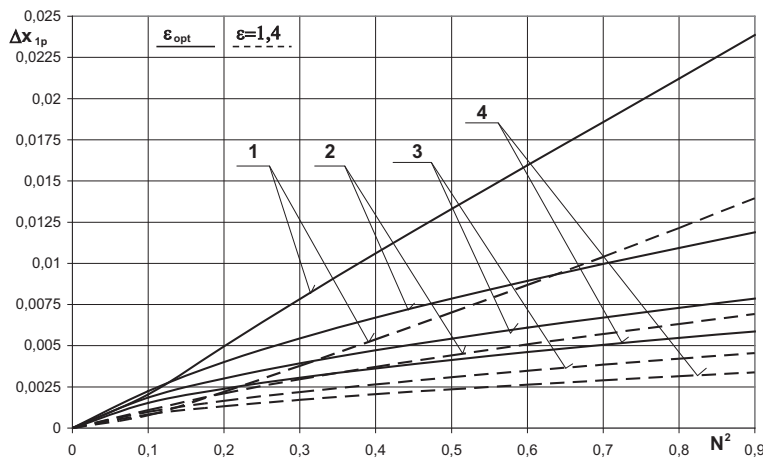


Fig.7 Change coordinate  $\Delta x_{1p}$  situated maximal pressure  $p_{1m}$  in dependence on coupling number  $N^2$  for dimensionless length of micropolar fluid  $\Lambda_1$ : 1)  $\Lambda_1=10$ , 2)  $\Lambda_1=20$ , 3)  $\Lambda_1=30$ , 4)  $\Lambda_1=40$

All lines come out from the maximal pressure position point in case of Newtonian fluid flow. Increase of maximal pressure change dimensionless coordinate position  $\Delta x_{1p}$  is observed while the coupling number increases  $N^2$  (coupling viscosity increases  $\kappa$ ) and the micropolar length decreases  $\Lambda_1$  (rotational viscosity increases  $\gamma$ ). Graphs in the Fig.7 are described with nonlinear scale of dimensionless coupling viscosity  $\kappa_1$  change.

#### 4. Conclusions

Presented example of the Reynolds equation solutions for steady laminar non-Newtonian lubricating oil flow with micropolar structure, enable the hydrodynamic pressure distribution introductory estimation as a basic exploitation parameter of slide plane bearing. Comparing Newtonian oil to oils with micropolar structure, can be used in order to increase hydrodynamic pressure and also to increase capacity load of bearing friction centre. Micropolar fluid usage has two sources of pressure increase in view of viscosity properties: increase of fluid efficient viscosity (coupling viscosity increase) and the rotational viscosity increase (characteristic length parameter  $\Lambda$ ). Author realize that he made few simplified assumptions in the above bearing centre model and in the constant parameter characterizing oil viscosity properties. Despite this calculation example apply to bearing with infinity breadth, received results can be usable in estimation of pressure distribution and of capacity force at laminar, steady lubrication of slide plane bearing with infinity breadth. Presented results can be usable as a comparison quantities in

case of numerical model laminar, unsteady flow Non-Newtonian fluids in the lubricating gaps of lengthwise slide plane bearings.

## References

- [1] Das S., Guha S.K., Chattopadhyay A.K.- *Linear stability analysis of hydrodynamic journal bearings under micropolar lubrication* - Tribology International 38 (2005), pp.500-507
- [2] Krasowski P. – *Stacjonarny, laminarny przepływ mikropolarnego czynnika smarującego w szczelinie smarnej poprzecznego łożyska ślizgowego* - Zeszyty Naukowe nr 49, pp. 72-90 , Akademia Morska, Gdynia 2003
- [3] Krasowski P. – Pressure in slide journal bearing lubricated oil with micropolar structure – Journal of POLISH CIMAC Vol. 3, No. 2, Gdansk 2008, pp. 99-108
- [4] Łukaszewicz G.– *Micropolar Fluids. Theory and Applications* – Birkhäuser Boston 1999
- [5] Walicka A.– *Reodynamika przepływu płynów nienewtonowskich w kanałach prostych i zakrzywionych* – Uniwersytet Zielonogórski, Zielona Góra 2002
- [6] Walicka A. - *Inertia effects in the flow of a micropolar fluid in a slot between rotating surfaces of revolution* – International Journal of Mechanics and Engineering, 2001,vol.6, No. 3, pp. 731-790
- [7] Wierzcholski K.- *Mathematical methods in hydrodynamic theory of lubrication*- Technical University Press, Szczecin 1993.
- [8] Xiao-Li Wang, Ke-Qin Zhu – *A study of the lubricating effectiveness of micropolar fluids in a dynamically loaded journal bearing* – Tribology International 37 (2004), pp.481-490



## Erosion problems in pneumatic transport installations on the example of fan rotor blades

Bazyli Krupicz

Białystok Technical University  
ul. Wiejska 45C, 15-351 Białystok, Poland  
tel.: +48 85 7469305, fax: +48 85 7469210  
e-mail: bazek@pb.edu.pl

### Abstract

*In the paper, the analysis of erosion of a fan blade was conducted. Erosion is recorded into two zones on the blade. In the first zone, erosion occurs at the front of the blade and it is caused by particle's impacts during first contact. This is "impact erosion" zone. Second "friction erosion" zone is formed in the place of the next contact, determined by the angle rotation of the rotor  $\Delta\varphi$  and the path of rebound  $s$ . The impact takes place at the angle  $\alpha$  with participation of friction forces. Dependences of particle's velocities on stress, which cause plastic strains on surface layer, were presented. Coefficient of velocity restitution in the stream  $k_s = \beta k$  was calculated. Restitution coefficient of particle's velocity in a stream always amounts to  $\beta \geq 1$ . Its value can be determined by f.e.: shape of particle's, their diameter, stream velocity. Time  $\tau$  between successive impacts is the function of rotor angular velocity and restitution coefficient  $k$ . Angle of rotation  $\Delta\varphi$  is only depends on coefficient  $k$ . The equation describing dependence of angle rotation  $\Delta\varphi$  on coefficient  $k_s$  is as follows:  $\Delta\varphi(1+k) = \text{tg}(\Delta\varphi)$ . The solution of the equation was presented in a graphical way.*

**Keywords:** stream erosion, restitution coefficient, fan blades

### 1. Introduction

Pneumatic transport of fine-grained materials is the element of many technological processes. It includes: removal of solid fuel combustion products in energy installations, removal of fine-grained waste being the by-product during cutting and grinding, relocation of powder and granulated products. Convection of material solid particles together with the air or gas stream is the basis of the process. Machine and installation elements (fan blades, cyclones, pipe bends) are in a constant contact with the elevating particles and thus they are subject to erosion. Following zones [1] are distinguished (Fig. 1): 1) "impact erosion" zone being the effect of particles' impact, 2) "friction erosion" zone being the effect of sliding of particles on the surface. In the case of fan blades, zone 1) is formed on the edge of the blade from the side of incoming particles, zone 2) is formed at the end of the blade.

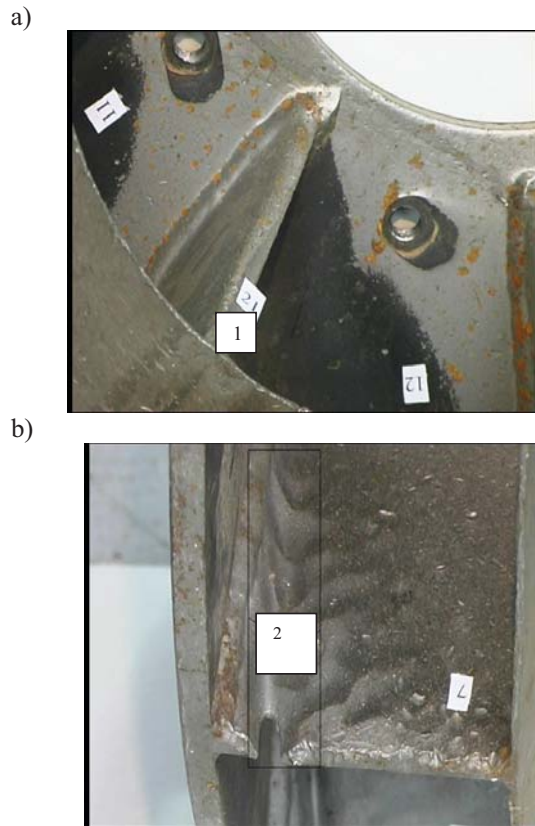


*Fig.1. The view of fan blades exploited in erosion conditions:  
a) impact erosion zone(1), b) friction erosion zone (2)*

Working time of fan blades is mainly determined by the loss of material in the zone (2) (fig. 1b). Working time of rotor mill blade (Fig 2) is determined by zone (1) [2].

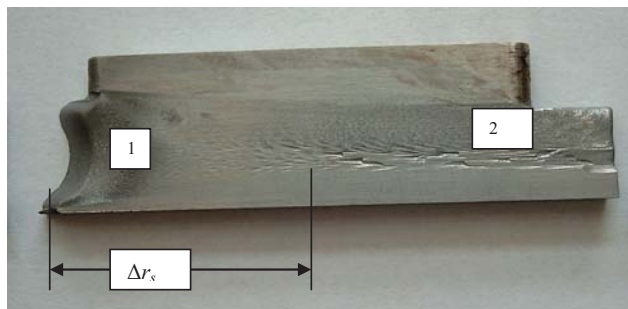


*Fig.2. The view of a rotor mill blade: 1 – impact erosion zone, 2 – friction erosion zone*

In this paper, the analysis will be conducted what is the effect of the contact of the particle with a fan blade and a pipe bend in impact conditions.

## 2. First impact of the particle on a fan blade

It was assumed for analysis, that the impacting particle has spherical shape with half space. In reality, particles in the stream have different shapes [3]. Calculation results are subject to given error, but it does not depreciate recorded phenomena. The velocity of particle's impact amounts to vector sum of particle entry velocity  $V_w$  and peripheral velocity of contact point of a fan blade  $V_l = \omega r$ . As velocity ratio  $V_w / V_l < 0,05$ , it can be assumed that the particle impacts perpendicularly to its surface. In this case, contact stresses can be calculated [4] using following equation:

$$\sigma_H = 0,837 \rho^{1/5} V^{2/5} E^{4/5}, \quad (1)$$

where:  $\frac{1}{E} = \frac{1-\nu_1^2}{E_1} + \frac{1-\nu_2^2}{E_2}$ ,  $\nu_1, \nu_2, E_1, E_2$  – Poisson's ratios, Young's modulus of particle and fan material.

The equation (1) shows that, as far as elastic strains are concerned, contact stresses do not depend on particle's radius, but they are a function of modulus of elasticity of contacting bodies and impact velocity. At the given critical velocity of the particle impacting the material, contact stress reaches dangerous value, which corresponds to resistance or yield point. First plastic strain is formed in the place of maximum shearing stress, i.e. on the depth similar to the radius of circular surface of the contact point (Fig. 3a, point B). At  $\nu = 0,3$ ,  $\tau_{1\max} = 0,31 \sigma_H$  [5]. Material plastic flow appears in this point, when a following condition is fulfilled:

$$\sigma_H = \frac{\sigma_{pl}}{0,62} = 1,61 \sigma_{pl}, \quad (2)$$

which is met at the critical velocity

$$v_1 = \frac{(\sigma_{H_1})^{5/2}}{(0,837)^{5/2} E^2 \rho^{1/2}}. \quad (3)$$

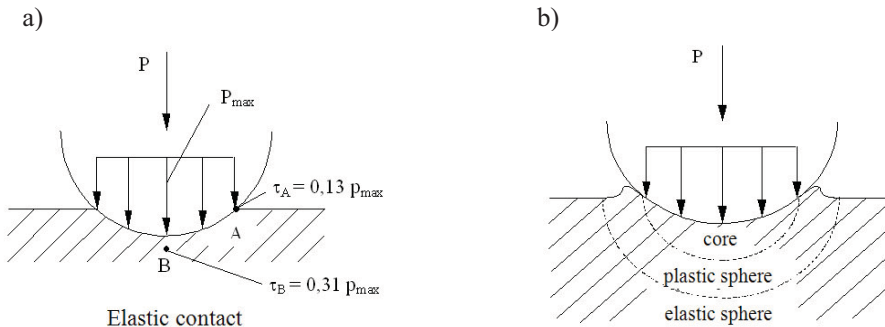


Fig. 3. The scheme of half space strains caused by particle's impact  
a) elastic strain ( $v < v_1$ ) , b) plastic strain ( $v > v_2$ )

When the impact velocity increases, the area of plastified material extends [6] and it reaches the surface (Fig. 3b).

Shearing stresses amount to  $\tau_{2\max} = 0,133 \sigma_H$  at the circular edge of contact area on the blade's surface (fig. 3a, point A) at  $\nu = 0,3$ . In this point, radial stresses  $\sigma_r$  spread out and amount

to circumferential compressive stresses  $\sigma_{\theta}$ . Thus, pure shear amounting to  $\sigma_H(1-2\nu)/3$  occurs along the edge of contact area, where particle's pressure on the blade's surface amount to zero [6]. The output of area of plastic strains on the surface occurs at

$$\sigma_{H2_2} = \frac{\sigma_{pl}}{0.266} = 3,7\sigma_{pl} , \quad (4)$$

caused by particle's velocity during impact.

$$\nu_2 = \frac{(\sigma_{H2})^{5/2}}{(0,837)^{5/2} E^2 \rho^{1/2}} . \quad (5)$$

Further increase in particles' velocity causes extending of the plasticization area by particle's sinking (Fig. 3b) – similar phenomena occurs in Brinell's studies [6]. Surface condition of the blade's impact erosion zone is presented in Fig. 4. Critical velocities  $\nu_1$  i  $\nu_2$  of selected materials from equations (3) i (5) are presented in table 1.

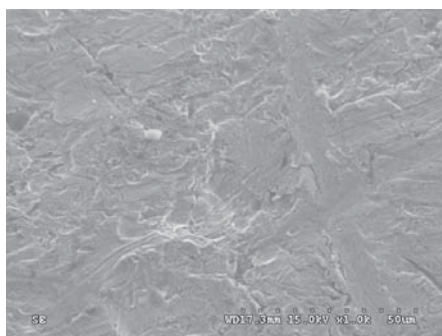


Fig.4. Microphoto of the blade's surface in the area of first impacts of particles.

Table 1. Values of critical velocities for selected materials during dynamic contact of the sphere with half space

Material	Young module $E$ , MPa	Poisson's coefficient $\nu$	Yield point MPa	Tensile strength $R_m$ , MPa	Critical velocity $m/s \times 10^{-2}$	
					$\nu_1$	$\nu_2$
Steel 35	$2 \cdot 10^5$	0,3	270	550	0,9	47,3
Steel 40 H	$2 \cdot 10^5$	0,3	750	900	12,4	162,5
Hatfid's steel	$2 \cdot 10^5$	03	800	1000	14,57	190,95
Polyamide	$1,1 \cdot 10^3$	0,38	43	50	72,1	593,4

Radiuses determining location of the blade (in an industrial fan used in pneumatic transport) amount to: inner radius  $r_w = 1,4$  m and outer radius  $r_z = 1,8$  m. At the angular velocity of the rotor  $\omega = 146,5 \text{ s}^{-1}$ , the velocity of the first impact reaches the value of  $V \approx 205 \text{ m/s}$ . It is the value exceeding (by two grades) values  $\nu_1$  i  $\nu_2$  presented in Table 1. In these conditions, reciprocal

interaction of hard particles with blades is elastic-plastic. During this process part of kinetic energy of particles is used for local plastic strain (Fig. 4) and microcutting.

### 3. Second impact of the particle on a fan blade

After the particle impacts elastic-plastically in the zone (1) it rebounds. [7]. Paper [8] presents how to calculate the point of the next impact basing on the scheme shown in Fig. 5. The first impact takes place in the point  $A_2$  perpendicularly to the blade and the next impacts take place in the point  $A_3$  at the angle  $(\pi/2 - \Delta\varphi)$ . Point  $A_3$  is determined by the angle rotation  $\Delta\varphi$  and the path of rebound  $s$ . The analysis [8] of the particle's motion in the space between the blades brings the following dependence

$$\Delta\varphi(1+k) = \text{tg } \Delta\varphi, \quad (1)$$

where:  $\omega$  – angular velocity of a rotor,  $\tau$  – time of rebound between the first and the second impact. Time  $\tau$  is not depends on the blade's location, but it is the function of the angular velocity  $\omega$  of the rotor and the restitution coefficient  $k$ . Angle rotation  $\Delta\varphi$  is only determined by the restitution coefficient  $k$  [9]. The solution of equation (1) in a graphic-analytical way is presented in Fig. 6.

Coefficient  $k$  is calculated using the method of a free drop of the steel globule – aerodynamic air resistance is not taken into consideration [10]. After the globule impacts elastic-plastically the material, it rebounds with the velocity of  $v''$ , which is lower than the impact velocity  $v'$ , i.e.:

$$v'' = k v'. \quad (2)$$

Authors of the paper [8] proposed that coefficient  $\beta$ , amounting to  $\beta \geq 1$  should be included to calculate the influence of real conditions on velocity restitution. These conditions are as follows: the particle is generally not made of steel, it is not spherical and a free drop does not takes place in a stream. Thus,

$$v'' = \frac{k}{\beta} v' = k_s v'. \quad (3)$$

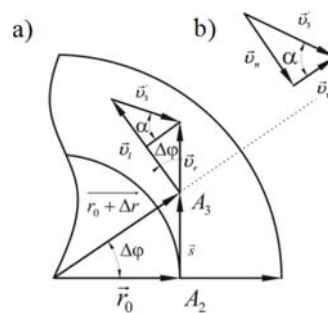


Fig. 5. Calculation diagram for assessing the point and velocity of the second impact of the particle on a fan blade: a) diagram of particle's motion and velocity, b) normal element  $v_n$  and tangent  $v_t$  of the particle's velocity in the point  $A_3$

The value of coefficient  $\beta$  can be calculated by comparing value  $\Delta r$  (Fig. 5), which is calculated by using data in Fig. 6, with value  $\Delta r_s$  determined by the material loss on the blade (Fig. 2). Fig. 3 shows that  $r_0 = (\Delta r + r_0) \cos \Delta \varphi$ . Thus,

$$\Delta r = r_0 \left( \frac{1}{\cos \Delta \varphi} - 1 \right). \quad (4)$$

Angle  $\Delta \varphi$  can be set using the diagram in Fig. 6. It is the coordinate of the point, which is the solution of equation (1) for a given value of coefficient  $k$ . Intersection of straight lines  $f_1 = \Delta \varphi(k+1)$  and curve  $f_2 = \lg \Delta \varphi$  gives the location of the point. In paper [13] it was pointed out that coefficient  $k$  has values 0,35 – 0,45.  $k = 0,4$  was assumed for calculations. At this value, the point of the second impact is determined by the angle  $\Delta \varphi = 1,11$  and  $s/r_0 = 1,99$  (Fig. 6). Radius  $r_0$  amounts to 190 mm in the blade in Fig. 2. Using these values,  $\Delta r$  amounts to 241 mm basing on the equation (4).

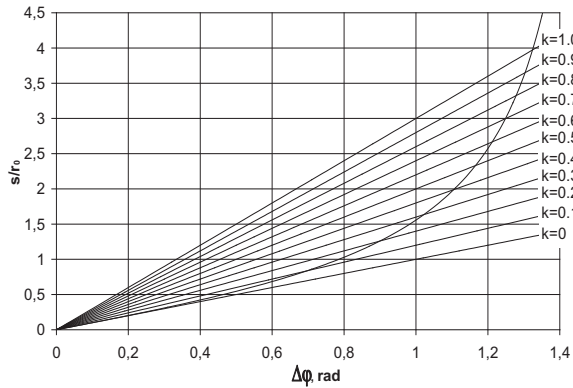


Fig. 6. Diagram of equation's solution (13)

Fig. 2 shows that erosion losses are visible at the middle of the blade's length after rebound in the zone (1), i.e. in a distance  $\Delta r_s \approx 30$  mm (zone.2). This value is possible when  $\Delta \varphi = 0,53$  and  $k_s = 0,05$  (restitution coefficient of the particles in a stream), which is calculated using the equation (1). The value of the coefficient  $\beta$  derives from the following equation (3):

$$\beta = \frac{k}{k_s} = \frac{0,40}{0,05} = 8. \quad (5)$$

The analysis of traces of wear in different blades (Fig. 1b, Fig. 2) shows that coefficient  $\beta$  is included in a given interval, because traces of wear are present on a given length. In the examined case, this is the beginning of wear "path" and  $\beta = 8$ . Kinetic energy of the particles in a stream is diversified, thus coefficient  $\beta$  and the path of rebound  $\Delta r_s$  is characteristic for each diversified group of the particles in a stream.

The question arises, what is the further motion of the particle after the second impact in the zone (2). While the first impact was directed perpendicularly to the blade, the second impact occurred at the angle  $\alpha$ . This angle is set between the velocity of the next impact and the direction tangent to the blade (Fig. 5). The angle can be calculated using following equation:



Table 2. Values of parameters of skew impact of the particle on a fan blade

Parameter	$k_s$									
	0,1	0,2	0,3	0,4	0,5	0,6	0,7	0,8	0,9	1,0
$\Delta\varphi$ , rad	28,66	40,1	47,58	50,4	55,0	58,47	60,76	63,1	64,20	65,92
$1 + \frac{\Delta r}{r_0}$	1,139	1,326	1,498	1,608	1,740	1,910	2,040	2,200	2,340	3,440
$\frac{v_n}{\varpi r_0}$	0,174	0,408	0,621	0,716	0,880	1,070	1,210	1,390	1,510	2,620
$\frac{v_\tau}{\varpi r_0}$	0,528	0,773	0,960	1,080	1,128	1,364	1,480	1,605	1,710	1,826
$\alpha$	18,24	27,83	32,9	33,54	37,96	38,1	39,27	40,89	41,44	55,12

$$\operatorname{tg} \alpha = \frac{v_n}{v_\tau} = \frac{1 + \frac{\Delta r}{r_0} - (1 + k_s) \cos \Delta \varphi}{(1 + k_s) \sin \Delta \varphi} \quad (6)$$

Values  $\alpha, v_n, v_\tau$  i  $v_s$  are presented in Table 2 taking into consideration value of restitution coefficient in a stream. Analysis of values included in Table 2 shows that velocity of the second skew impact depends on  $k_s$  – restitution coefficient in a stream. The higher value  $k_s$  is, the higher impact velocity and the higher erosion losses are, which are located at the end of the blade (Fig. 2). Microphoto of blade's surface in the zone of skew impact (Fig. 7) confirms this type of impact. Traces of plastic lengthwise strains lead to the conclusion that velocity component  $v_\tau$  is dominant,[11,12]. It is possible at the low value of the coefficient  $k_s$ .

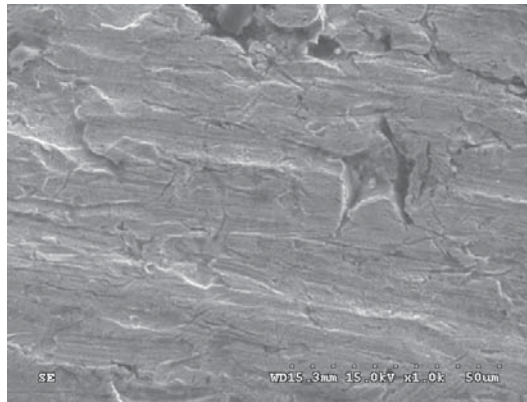


Fig. 7. Microphoto of the surface in the zone of a skew impact

#### 4. Conclusions

Erosion of pneumatic transport installations occurs due to successive impacts of the stream of solid particles. They cause elastic-plastic strain of the surface layer of the element, until the border of plastic strain is reached. Then, the surface layer cracks (Fig. 7).

Coefficient of particle's velocity restitution in a stream  $k_s$  determines the location of next impacts, i.e. the location of erosion in blades.

#### References

- [1] Chmielniak, T., *Erozja pyłowa w maszynach przepływowych. Przegląd zagadnień*. Zag. Eksp. Maszyn, Vol. 76, No. 4, 1988, pp. 339-458.
- [2] Krupicz, B., Liszewski M.: Mechanizmy erozji podczas rozdrabniania w młynie wirnikowym, *Tribologia* t. 37, nr 2, 2007, pp. 123-132.
- [3] Lou, H.Q. , *Erosion of materials by alumina slurry – Part 1*, Wear 134, 1989, pp. 253 –269, *Part 2*, Wear 134, 1989, pp. 271 – 281.
- [4] Bitter, J. G. A., *A study of erosion phenomena* , Wear No. 6, 1962, Part 1, pp. 5-21, Part 2, pp.169-190.
- [5] Timoshenko, S., Goodier, J.N., *Teoria sprężystości*. Wyd. Arkady, Warszawa 1951.
- [6] Мышкин, Н.К., Петроковец, М.И., *Трибология. Принципы и приложения*., ИММС НАНБ,. Гомель 2002..
- [7] Барсуков, В.Г., Крупич, Б., Свириденко, А.И., *Особенности ударного взаимодействия твердых частиц с лопастью вентиляторов*, Трение и износ, vol. 25, nr 1, 2004, pp. 41-47.
- [8] Krupicz, B., *Rola współczynnika restytucji prędkości twardych cząstek w procesie erozyjnym wentylatorów*, Zeszyty Naukowe Nr 10 (82) Akademii Morskiej w Szczecinie, 2006, pp. 299-307.
- [9] Барсуков, В.Г., Крупич, Б., *Трибомеханика дисперсных материалов, Технологические приложения*, GGU, Grodno 2004.
- [10] Крупич, Б., Мухаметвалиев, Р.Ф., Барсуков, В.Г., *Испытания материалов на удар по методу падающего шарика с учетом аэродинамического сопротивления*, Materiały konferencyjne II Symposium Mechaniki Zniszczenia Materiałów i Konstrukcji Augustów 2003, pp. 175-178.
- [11] Fukahori, Y., Yamazaki, H., *Mechanism of rubber abrasion. Part 3: how is friction linked to fracture in rubber abrasion?*, Wear 188, 1995, 19-26.
- [12] Fukahori, Y., Liang, H., Busfield, J.J.C., *Criteria for crack initiation during rubber abrasion*, Wear 265, 2008, 387–395.
- [13] Клейс, Н., Паппель, Т., Хусайнова, И., Щеглов, И., *Исследование процесса ударных взаимодействий частиц*, Трение и износ vol. 18, nr 6, 1997, pp. 730-735.

*Paper was written as a part of the Rector's project W/WM/4/07.*



## TYPES OF DAMAGES TO TURBINES OF AIRCRAFT TURBINE ENGINES; DIAGNOSING CAPABILITIES

Artur Kulaszka, Marek Chalimoniuk, Józef Błachnio

*Air Force Institute of Technology*

ul. Księcia Bolesława 6, 01-494 Warszawa 46, Polska  
tel.: +48 22 6852282, e-mail: artur.kulaszka@itwl.pl

### *Abstract*

*The article presents the analysis of damage to gas turbine blades influencing the reliability of aircraft turbine engines. Characterised are methods of non-destructive testing and capabilities of applying them to the computer-aided objective diagnosing of condition of blades [3]. The computer-aided diagnosing of condition of gas turbine blades will provide some increase in the reliability of the assessment of blade condition, thus will increase the flight safety and reduce cost of the aircraft engine service.*

**Keywords:** gas turbine, blade, damage, diagnostics

### **1. Introduction**

From the moment of development of the first aircraft jet engine by English designer Frank Whittle in the 1930s, as in the case of other machines, we observe persistent technological progress in the field of new designs as well as materials which they are made from. This is the result of increasing efficiency and effectiveness of operation of new designs, and consequently increase in their performance, optimisation of weight, dimensions, etc. The gas turbine being a part of a turbine jet engine is a rotor machine transforming the enthalpy of the working medium (called also the thermodynamic medium) into the mechanical work causing rotation of the rotor. The increase in efficiency of the turbine results in the increase in thrust (power) and reduction in specific fuel consumption, and vice versa. The efficiency of gas turbines in aircraft engines (lying usually 30% - 45%) depends essentially on the temperature of exhaust gas, which has grown in the course of a few recent years by 280 K, what caused the improvement in general efficiency of the turbine and increased the power ratio. The barrier to temperature increase are material problems, i.e. creep resistance, thermal fatigue, high-temperature sulphur corrosion, and erosion. For this reason necessary is application of expensive creep-resistant alloys, complicated geometrical shapes of blades, complicating technological processes of their production and various kinds of treatment, such as the cooling of blades. At present, depending on blade material and cooling intensity, the working temperature of blades lies within the range of 1120-1170 K (without special cooling), 1200-1300 K (with cooling), 1300-1500 K (high-intensity cooling). Unfortunately, operation of turbine blades under complex thermal and mechanical loads (overload and aggressive environment) is only possible at the temperature of blade material lower even by 350 K than the combustion temperature. Therefore, further development and improvement in turbine blade design has been aimed at applying the heat-resistant coatings of good resistance to high-temperature corrosion, low thermal conductivity and high stability of the structure.

## 2. Types of in-service damages

In the process of operation of aircraft turbine engines various types of damages to turbine components occur, especially to their blades. Analysis of current cases suggests that all types of damages can be rated – depending on used classification – in one or a few causal groups, which are often closely related. Thus, we can differentiate damage being the result of production faults, improper repair or operational errors.

Experience gained in the course of implementing and performing prophylactic programs in the Polish Air Force, aimed at securing high safety degree in the military aviation, has proved that in spite of employing huge forces and means it is impossible to completely avoid various kinds of damages while operating so great population of turbine engines. The most frequent damages – except foreign-matter ingestion – are damages to turbines resulting from disadvantageous changes in blade material structure caused by excessive temperature and time over which it affects the blade and aggressiveness of exhaust gas (overheating of material, thermal fatigue of blades). Therefore, it is important to detect and explain as early as possible the symptoms of possible hazards with available diagnostic methods and knowledge.

The structure and the principle of operation of a turbine jet engine is closely related with the high-intensity air flux flowing through its gas path – the intake, compressor, combustion chamber, turbine, exhaust nozzle. The air taken through the intake is not always free from impurities, which penetrate into the engine. This depends on the location of the engine in the airframe (Fig. 1), condition of airfield pavement (Fig. 2), errors made while operating the aircraft.

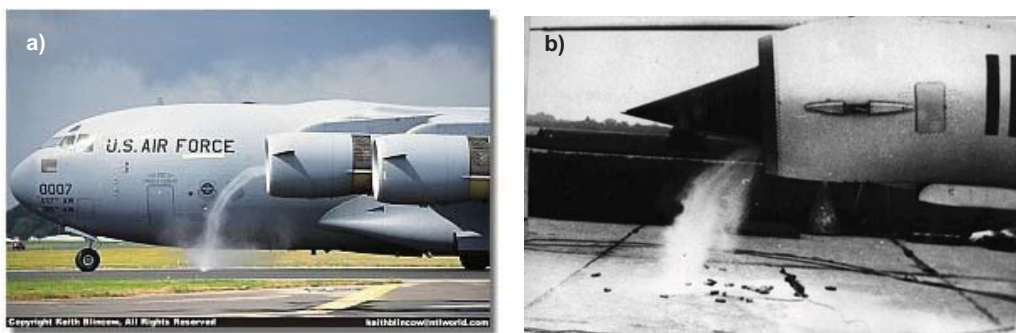


*Fig. 1. Types of vortex at engine intakes [6][7]*

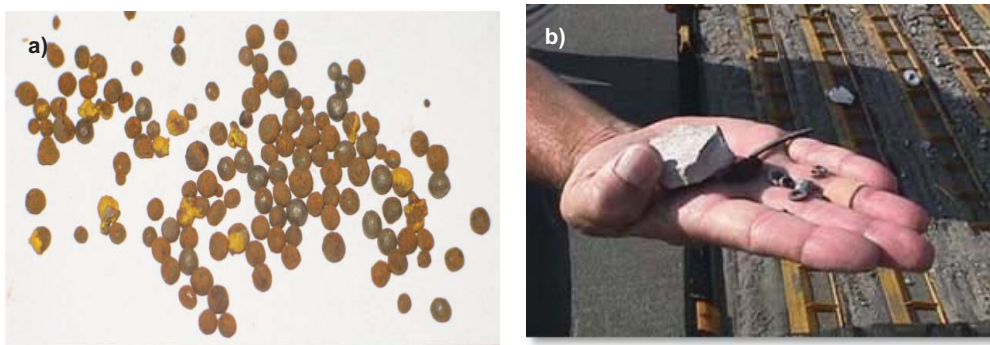


*Fig. 2. Examples of impurities found on a runway: a) steel balls –paint-removing residues [3], b) fragments of concrete, washers, cotter pins [6]*

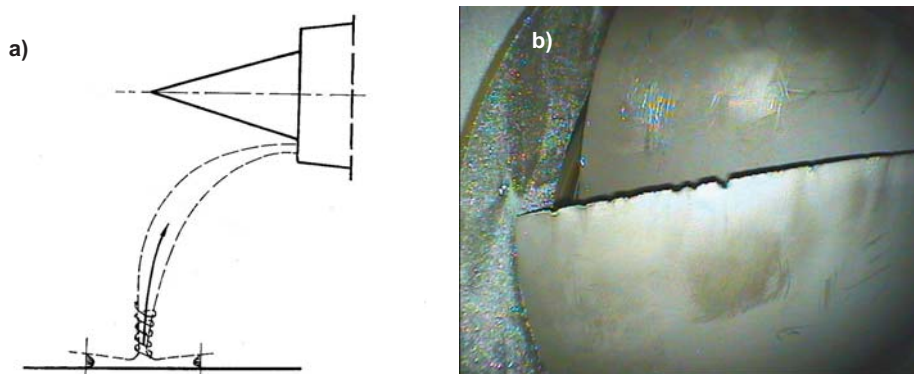


Fig. 3. Schematic diagram of air vortex at engine intake - a) [7], damage to compressor blades caused by impurities ingested by air vortex from the runway - b) [3]

Impurities ingested by air vortex cause mechanical damages to individual components of gas path – in particular, to compressor rotor blades (Fig. 3). The result of such damages is disturbance of engine performance parameters, what has also adverse influence on working temperature of the gas turbine. On account of the complicated nature of thermal and mechanical loads on turbine blades inadmissible are any mechanical and thermal damages to blades, because it may lead to the break-off of a blade, and consequently to the engine damage, and hence, hazard to flight safety. Some types of mechanical damages resulting from the foreign-matter ingestion are detected after finding damages to the compressor's first-stage components during pre- or after-flight maintenance, or in the course of the first borescope examination after the event, carried out during periodical maintenance of the engine (Fig. 4).

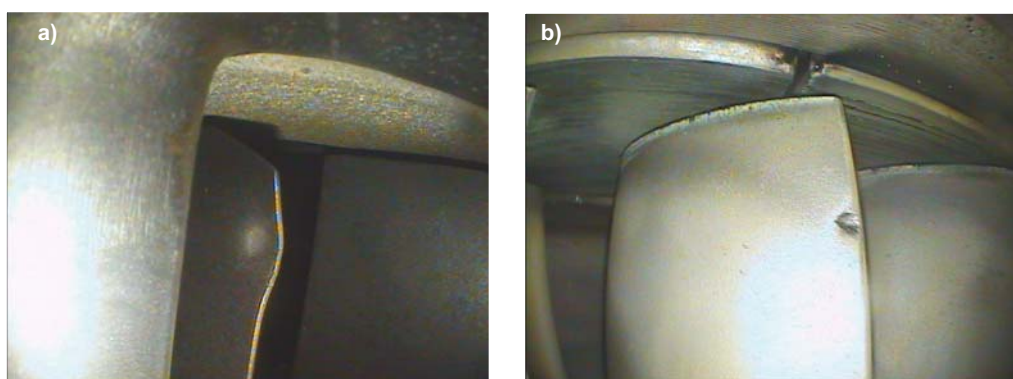


Fig. 4. Examples of damages to: a) compressor blades, b) turbine blades, effected by the ingestion of steel balls from the runway pavement [3]

Small spot damages or small abrasions of blade surface are often invisible during first hours of engine operation after the damage has occurred, and they are not detected by a diagnostician in the course of diagnostic examination. A damage to blade protective coating together with high temperature and exhaust-gas induced aggressive environment may result in the overheating and burnout of the native material of the blade (Fig. 5).





*Fig. 5. Exemplary types of thermal damages to leading edges of turbine rotor blades [3]*

Manufacturing and repair-effected defects are another group of damages detected within the hot section of the engine during preventive diagnostic tests. These are damages beyond the user's reach and can reveal throughout the entire period of engine operation.

The break-off of a turbine rotor blade caused by spreading a new type of a protective coating applied with diffusion method onto the blade material is one of the most interesting and at the same time the most dangerous events. In the course of turbine operation a fragile coating suffered cracking; the crack propagated into the native material of the blade and finally resulted in the break-off of the blade (Fig. 6).

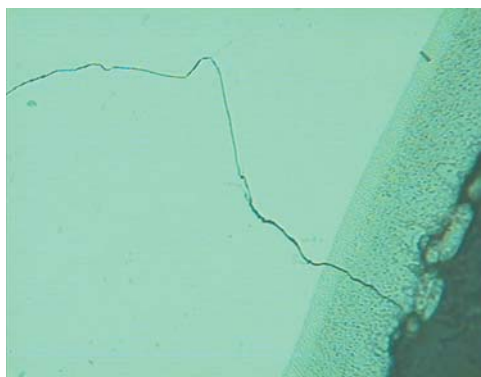


*Fig. 6. Protective-coating cracking; the crack keeps propagating into the blade's native material [3]; magn. x 450*

The hitherto experience gained in the course of research work at the Air Force Institute of Technology shows also that the majority of turbine defects are directly related with incorrect adjustments of the engine and poor quality of aviation fuel.

Incorrect fuel pressure, its physical and chemical properties deteriorated by various kinds of impurities, and misalignment of the flame tube injector prove conducive to the formation of carbon deposit on the injectors (Fig. 7) and other sub-assemblies, what results in faulty fuel spraying. This, in turn, results in disturbance of the combustion-process organisation, and consequently of temperature distribution and cooling of individual components of the hot section of the engine. What results is overheating of material of combustion chamber and turbine blades (Fig. 8).



*Fig. 7. Carbon deposit on fuel injector of a turbojet [3]*



*Fig. 8. Thermal damage to turbine blades [3]*

### **3. Capabilities of diagnosing health of turbine blades**

The process of degradation of components in replaced sub-assemblies is specific to every engine type and is related with its structure, operating conditions, depends also on the repair process engineering. Therefore, the process of preventive diagnostic in-service testing of engines is extremely significant from the user's point of view.

Diagnostic methods can be divided into two groups:

- in-service (non-destructive) methods,
- in the process of repair (not-destructive or/and destructive).

Health of turbine blades while in service is mainly examined during borescope inspections. Detected are defects of the following types: cracks, deformations and erosion from foreign bodies, corrosion, burnout of protective coating or native material of the blade. This is exclusively visual, remote inspection by means of a videoscope. The reliability of such assessment depends mainly on the experience of the diagnostician and quality of available equipment.

The second method of assessing condition of turbine blades is the measurement of oscillation, e.g. measurement of oscillation using microwave sensors. This method makes use of the phenomenon of the reception of a homodyne signal reflected from the turbine blade. On the other hand, while measuring blade vibrations with inductive sensors, use is made of the phenomenon of changes in the magnetic field caused by rotating turbine blades that cross this field. The eddy current inspection is a direct method for checking condition of blade edges built in the airframe.

During any repair we have better access to turbine blades. Thus, more accurate, direct assessment of their health is possible. Among non-destructive methods widely used are:

- visual,
- penetrative,
- ultrasonic, and
- radiographic inspections.

Until now, all these methods do not allow of explicit assessment of changes in the structure of a blade resulting from the material overheating. The diagnostician makes the assessment of the level of the blade overheating with a visual method; his decision is verified with metallographic examination. Conducted are works on the development of a new computer-aided visual method to obtain more objective and reliable results [4].

The assessment of the level of blade-material overheating with a visual method can be verified with eddy-current inspection method. This is a comparative method that makes use of the phenomenon of eddy current generation in the (electrically conductive) material under the alternating magnetic field. Eddy currents generate, in turn, magnetic field opposite to the field that

has initiated them. The eddy-current measuring technique is based on the electromagnetic induction.

In our work we have used the Wirotest 302 with the SNC/04/012 probe, with alternating magnetic field of 1.2 MHz frequency applied. The object under examination were blades made of the EI-867WD alloy with protective coatings made of aluminium alloy. Measurements were taken on a new blade (marked A), a blade withdrawn from service but not overheated (marked B) and an overheated, burnt-out blade (marked C). Results are shown in Tables 1 and 2.

*Table 1. Turbine rotor blades*

Marking	Measured value	Blade description
A	12	New blade
B	35	Used, not overheated blade
C	70	Overheated blade

*Table 2. Turbine nozzle blades*

Marking	Measured value	Blade description
A	1	Used, non-overheated blade
B	30	Used blade with burnouts

Measured values are very much diversified, what is advantageous from the point of view of the method's sensitivity and proves that possible is the assessment of the level of blade overheating with eddy current inspection method. The overheating is caused by excessive temperature of the exhaust gas, time of affecting the material, and aggressiveness of the exhaust gas. The overheating causes some change to the microstructure, which consists – among other things – in modification of strengthening intercrystalline phase  $\text{Ni}_3(\text{Al,Ti})$  called the  $\gamma'$  phase. This phase proves decisive to heat resistance and high-temperature creep resistance of an alloy. In special cases, growth of the  $\gamma'$  phase results in the coagulation of precipitations, and then dissipation thereof in the solid solution. What results is reduction in heat resistance and high-temperature creep resistance of the alloy.

However, it is necessary to emphasise that results obtained with the eddy-current inspection method depend on many factors, i.e. the kind of blade material and protective coating, the eddy-current testing apparatus, the range of pre-set parameters, etc. To get more complete image of capabilities offered by this method it is necessary to carry out tests on much wider population of objects under examination (blades made of different materials). However, preliminary results of initial tests are promising.

#### **4. The use of computer technology for the diagnosing of the gas-turbine blade's condition**

Diagnostic visual inspection being an element of preventive treatment to assure high safety level of operating aeronautical equipment has been from the very beginning closely connected with two elements - technical capabilities of available testing-and-measuring apparatus and the professionalism (knowledge, experience) of the diagnostician who carries out inspection. Introduction of a "human factor" and relying on his subjective assessment of the existing diagnostic reality was and still is the reason for many expensive errors resulting from the decisions taken. It often happens that, due to the application of outdated equipment and/or lack of suitable knowledge, engines are withdrawn from service and transferred for expensive overhaul, although their safe use is still possible. Taking into consideration the above-mentioned fact, the development of diagnostic apparatus has been aimed at the improvement of quality of vision by



application of more perfect visual paths and elimination of the diagnostician from the laborious measuring activities and interpretation of observed images. Videoscopes facilitate measurements of: length, area, depth/height, distance from the straight line with accuracy of 0.01 mm, and at the same time they give the value of error that burdens the resulting measurement, depending on the distance of the measuring probe from the examined object. Special software enables measurements either directly during the inspection or later on, with computers of the PC class. At present, there are a few companies offering instruments/systems of similar capabilities and working parameters; however, differing in the method of calculating certain quantities. The Olympus company uses the stereoscopic method in their videoscopes, GE - the method of "shadow", and KARL STORZ - the most recent laser method. All these methods use mathematical relations between two images obtained with two lenses, properties of the shadow or laser markers thrown on examined object/defect, and hence, provide high-accuracy measurements of the above-mentioned quantities. They also allow to explicitly determine whether there is concavity or convexity of the material.

In [4] presented are methods of measurements of surface defects, which are based on digital recording of the videoscope image with the "Stereo" method ("Stereo Probe") and with the "Shadow" method ("Shadow Probe") - Fig. 9.

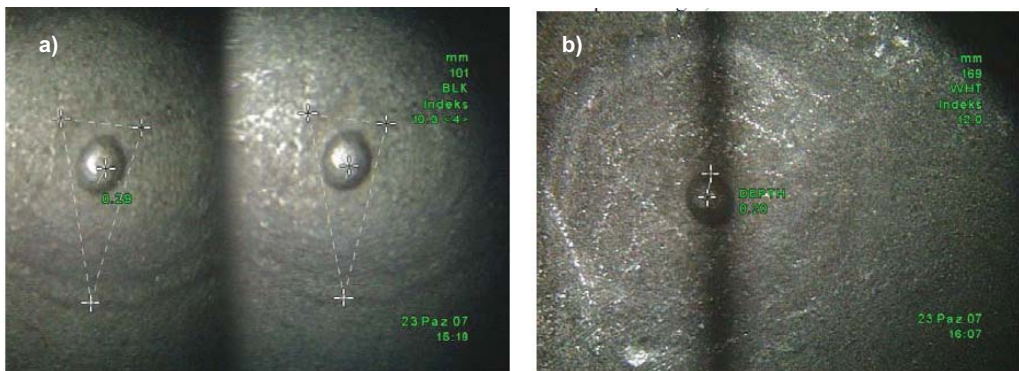


Fig. 9. Measurement of convexity radius with methods [4]: a) „Shadow”, b) „Stereo”

The next method developed as a diagnostic tool is the RGB method. In the RGB model identified are three component colours: **Red**, **Green**, **Blue**. The method employs relations between wave properties of light and physical-and-chemical properties of the examined surfaces, which affect angular relations between the falling and the from the surface reflected light and elimination of individual wave lengths in the spectrum of radiation that lights a given object [5]. Images recorded with the CCD matrix in the course of diagnostic tests are analysed with special computer software using complicated algorithms of image processing and earlier developed patterns that allow qualitative assessment of the condition of the examined surface. The RGB model is a theoretical model, the mapping of which depends on the device, which means that in every instrument/system a particular RGB component can show slightly different spectral characteristics. Therefore, every instrument/system can offer a slightly different range of colours. Thus, it is necessary to develop algorithms for a given type of an instrument/system as well as patterns for every individual type of examined surface, e.g. for turbine blades of particular turbine types.

The method more and more widely used in the technical diagnostics and based on the computer analysis is the recognition of images. Optical methods of image recognition can be classified into correlative and non-correlative. The correlative methods are based on visual comparison between a recognised and a pattern object, and then on the analysis of obtained correlative signal. The non-correlative methods consist in the analysis of characteristic features that describe the object and are applied – among other things - when it is difficult to explicitly determine the target pattern, which

should be compared with the object. Until now, these methods have found their applications in the industry, mainly in the production inspection, for the recognition of face features and fingerprints, land relief, and building development on the basis of air photographs. Continued are also works on the development of methods of image recognition as a commonly used diagnostic tool to be applied in the process of operation/maintenance of aeronautical equipment – including the diagnosing of condition of gas turbine blades.

Implementation of modern computer-based diagnostic tools provides noticeable increase in reliability of the assessment of condition of gas turbine blades. This will also allow to gradually eliminate the adverse effect of the so-called "human factor" on investigation results, and thus to increase flight safety and reduce in-service cost of aircraft turbine engines.

## 5. Conclusions

In the process of operating aircraft turbine engines it may happen that turbine blades heat up to temperature exceeding normal working temperature. The process of the gas turbine blade getting damaged starts with destruction of the protective coating, which in turn results in that the blade native material is directly exposed to aggressive influence of exhaust gas. This causes the overheating of the material, which manifests itself with disadvantageous changes in the microstructure.

The reliable assessment of these changes with non-destructive inspection methods allows in some cases to prolong the period of engine operational use (the so-called controlled service) even after detection of a damage, or withdraw the engine from use before dramatic effects of turbine damage occur. However, any wrong decision of the diagnostician generates huge costs related with hazards to flight safety, or may result in unnecessary engine overhaul, the cost of which may reach even a few million PLZ.

Taking the above-mentioned facts into account it becomes evident that there is a real need to apply – on much wider scale – the non-destructive inspection methods for current assessment of the level of overheating of aircraft turbine engine blades.

## References

- [1] Błażnio, J.: The effect of high temperature on the degradation of heat-resistant and high-temperature alloys. *Solid State Phenomena*, Vols. 147-149, pp. 744-752, 2009.
- [2] Lewitowicz, J., *Basics of use of airships*. T.4, ITWL, Warszawa 2008.
- [3] Kułasza, A., Chalimoniuk, M., *Research reports*. ITWL, Warszawa 2000-2008 (niepublikowane).
- [4] Karczewski Z.: Endoscopic diagnostics of marine engines. *Diagnostyka*, 3(47)/2008, ss. 65-69.
- [5] Błażnio J., Bogdan M.: Diagnostic of condition of used gas turbine blades. *Diagnostyka*. Nr. 1 (45), 2008, pp. 91-96.
- [6] Fotografie - portal FODNews.com
- [7] Szczeciński S., Szczepanik R.: Warunki zasysania zanieczyszczeń mechanicznych do wlotów silników odrzutowych. *Wojskowy Przegląd Techniczny* nr 3/77



## SEMI-MARKOV MODEL OF MAINTENANCE OF URBAN TRANSPORT BUSES

**Bogdan Landowski**

*University of Technology and Life Sciences, Machine Maintenance Department  
al. Kaliskiego 7, 85-789 Bydgoszcz, Poland  
tel.: +48 52 3408495, fax: +48 52 3408495  
email: [lbogdan@atr.bydgoszcz.pl](mailto:lbogdan@atr.bydgoszcz.pl)*

### Abstract

*The object of the investigations is maintenance system of urban transport buses. The subject of the investigations is a determined set of the maintenance states of means of transport and their maintenance processes, as well as the relations occurring between the aforementioned elements, and between them and the maintenance process effectiveness. The paper deals with the selected issues related to modelling, forecasting and controlling the maintenance process of a certain class of technical objects being carried out in a complex maintenance system. Supporting a decision maker in the decisions making process concerning the maintenance system under analysis is to forecast the maintenance system behaviour and evaluate the influence of the selected decision making variants on the course of the maintenance process. The purpose of the work is to present a possibility to use a semi-Markov model of maintenance process of technical objects to preliminarily forecast the state of the maintenance system after changing the values of the model input parameters. Changing the value of the input parameters may simulate an impact of various factors on the system behaviour. The paper presents the assumptions to build a model of the process being performed within the investigation object and the method of analysing it. The values of the model parameters were assessed on the basis of the results of the preliminary test carried out in a real means of transport maintenance system. All the considerations have been illustrated by a computational example. Due to the assumed generalization degree of the description, the method to model and forecast the maintenance process presented herein may be used to other maintenance systems than the urban bus transport system.*

**Keywords:** operation and maintenance, maintenance process, modelling, semi-Markov process, urban public transport

### 1. Introduction

When utilising vehicles, various events occur the results of which affect the courses of their usage and service processes, as well as the economic effect generated by the transport system. The vehicles in the maintenance process may be found in many different maintenance states that create the state space  $S$ .

Evaluating, analysing and forecasting the effectiveness of work, as well as reliability and readiness in the transport systems, are connected with the problems of mathematical modelling maintenance processes of technical objects. Therefore, it is necessary to create a formalised description of the processes performed in the means of transport maintenance system. The most important processes are those of changing the technical states of the objects, and those of using and servicing them. Those processes are random ones and depend on one another. The

mathematical models of those processes, by their very nature, shall be simplified. The practical conclusions resulting from studying those models should be formulated carefully.

The selected maintenance states of vehicles, described in the models of their maintenance processes, may change in various sequences, the order of which depends, to the great extent, on the method of carrying out transportation and the vehicle service processes, type and technical condition of the technical objects (including the means of transport), environmental conditions and the decisions made by the operators and the authorities who manage the system.

Due to analysing the results of the investigations performed in a real vehicle maintenance system, it has been found that there are no grounds to accept a hypothesis about the conformity of empiric distributions of times of duration of the analysed maintenance states with the exponential distribution. Therefore, the random process describing the changes of the maintenance states of the vehicles used in the investigation object is not the Markov process used frequently to model the problems of that type. Thus, the development method and possibilities of using the semi-Markov model of maintenance process of technical objects for preliminary forecasting the state of the maintenance system after changing the values of the model input parameters haven been presented herein.

The values of the model parameters have been assessed on the basis of the results of the preliminary tests carried out in a real means of transport maintenance system.

## 2. Model of maintenance process of a vehicle

The natural model of a bus maintenance process is a random process with a finite space of states  $S$  and a set of the parameters  $R_+$ . This process is denoted with the symbol  $\{X(t) : t \in R_+\}$ . It has been assumed that the semi-Markov process is a model which describes the real process of the maintenance state changes relatively well. In the practical applications it is needed to verify, if there are no grounds to reject the assumptions resulting from the mathematical apparatus applied.

The semi-Markov process  $\{X(t) : t \geq 0\}$  is defined by a homogeneous, two-dimensional Markov chain:

$$\{\xi_n, \vartheta_n : n \in N_0\} \quad \xi_n \in S_k, \vartheta_n \in [0, \infty). \quad (1)$$

such one, that the probabilities of transitions depend on the discrete coordinate:

$$P\{\xi_{n+1} = j, \vartheta_{n+1} \leq t / \xi_n = i, \vartheta_n = t_n\} = P\{\xi_{n+1} = j, \vartheta_{n+1} \leq t / \xi_n = i\} \quad (2)$$

and

$$P\{\xi_0 = i, \vartheta_0 \leq 0\} = P\{\xi_0 = i\}. \quad (3)$$

The two-dimensional Markov chain defined that way is called the Markov renewal process, and the matrix:

$$Q(t) := [Q_{ij}(t) : i, j \in S], \quad t \geq 0 \quad (4)$$

where:

$$Q_{ij}(t) := P\{\xi_{n+1} = j, \vartheta_{n+1} \leq t / \xi_n = i\} \quad (5)$$

is called the renewal kernel.

Let  $\tau_0 = 0, \tau_n := \vartheta_1 + \dots + \vartheta_{n-1}, k \in N$  oraz  $\nu(t) := \max\{n : \tau_n \leq t\}$ . The random process  $\{X_k(t) : t \geq 0\}$  defined by the formula:

$$X(t) = \xi_{\nu(t)} \quad (6)$$

is called the semi-Markov process generated by the renewal kernel  $Q(t)$ .

As it results from this definition, the semi-Markov process takes constant values in the random ranges:

$$X(t) = \xi_n \quad \text{for } t \in [\tau_n, \tau_{n+1}), \quad n \in N_0, \quad (7)$$

Moreover, the sequence of random variables  $\{X_k(\tau_n) = \xi_n : n \in N_0\}$  is a homogeneous chain with the transition probability matrix  $P$ :

$$P=[p_{ij}] = Q_{ij}(\infty) : i, j \in S, \quad (8)$$

which is called the Markov chain embedded in the semi-Markov process.

The symbol  $T_{ij}$  is used to denote the time which is elapsing from the moment of the process entering  $\{X(t) : t \in R_+\}$  the state  $i \in S$  until the first change of that state into the state  $j \in S$ . For the distribution  $F_{ij}$  of the random variable  $T_{ij}$  there are the following relations:

$$F_{ij}(t) = P\{T_{ij} < t\} = P\{\tau_{n+1} - \tau_n \leq t \mid X(\tau_{n+1}) = j, X(\tau_n) = i\} = \frac{Q_{ij}(t)}{p_{ij}} \quad \text{when } p_{ij} > 0. \quad (9)$$

If  $p_{ij} = 0$  it is assumed that:

$$F_{ij}(t) = \begin{cases} 0 & \text{for } t < 1 \\ 1 & \text{for } t \geq 1 \end{cases}. \quad (10)$$

The symbol  $T_i$  is used to denote the time which is elapsing from the moment of entering the state  $i \in S$  until the moment of the first change of that state:

$$G_i(t) = P\{T_i < t\} = P\{\tau_{n+1} - \tau_n \leq t \mid X(\tau_n) = i\} = \sum_{j \in S} Q_{ij}(t). \quad (11)$$

Let  $P_j(t) = P\{X(t) = j\}$ ;  $j \in S$  stands for a one-dimensional distribution of the semi-Markov process. If the analysed process  $\{X(t), i \geq 0\}$  is an ergodic one, then [4]:

$$P_{ij} = \lim_{t \rightarrow \infty} P_{ij}(t) = P_j = \lim_{t \rightarrow \infty} P_j(t) = \frac{g_j m_j}{\sum_{i \in S} g_i m_i}, \quad i, j \in S, \quad (12)$$

where:

$g_i$  - ergodic probabilities of the Markov chain,

and:

$$m_i = \int_0^\infty [1 - G_i(t)] dt \quad (13)$$

is a stationary distribution of the embedded Markov chain  $\{X(\tau_n) : n \in N_0\}$ . The stationary probabilities are the only solutions of the system of equations:

$$\sum_{i \in S} g_i P_{ij} = g_j, \quad j \in S, \quad \sum_{j \in S} g_j = 1. \quad (14)$$

### 3. Essential assumptions for the model of maintenance process of a bus

It has been assumed that the general mathematical model of the bus maintenance process (maintenance state change process) is a stochastic process  $\{X(t), t \geq 0\}$ . The analysed stochastic process  $\{X(t), t \geq 0\}$  has a finite phase space  $S, S = \{S_1, S_2, \dots, S_n\}$ .

As a result of identification of the bus maintenance system in an urban transport system and the maintenance process being performed therein, the following bus maintenance states significant for the analysis of the investigated system operation have been selected:

- the state in which a technical object is used (realization of a transport task),
- the state in which a technical object waits for a corrective service to be performed in the maintenance system environment (waiting for so called technical emergency service units),
- the state in which a service is performed in the maintenance system environment – the state in which a bus is a subject to corrective service processes performed by so called technical emergency service units due to occurrence of a vehicle damage when realizing the transport tasks,
- the state in which a technical object waits for a corrective service to be performed in the maintenance system,
- the state in which a corrective service is performed on a technical object in the maintenance system,

- the state in which a technical object waits for pre-repair diagnosis,
- the state in which pre-repair diagnoses are performed on a technical object,
- the state in which a technical object waits for post-repair diagnosis,
- the state in which post-repair diagnoses are performed on a technical object,
- the state in which a service is performed on the day on which a technical object is used (so called daily service),
- the state in which a technical object waits to undertake realization of a transport task (after bringing back the task serviceability state a technical object does not perform the scheduled transport task due to the method of organizing the transport tasks, e.g. in an urban bus transport maintenance system determined by the existing transport task schedule, so called “timetable”),
- the state in which a technical object waits due to unserviceability of the environment,
- the state of a scheduled standstill of a technical object (no transport tasks e.g. in an urban bus transport maintenance system resulting from the schedule of the transport tasks, including a night transport break).

In order to illustrate the considerations, the following bus maintenance states, out of the aforementioned ones, have been analysed:

- $S_1$  - the state of a scheduled standstill of a bus,
- $S_2$  - the state in which a vehicle is used (realization of a transport task),
- $S_3$  - the state in which a bus is serviced in the system environment,
- $S_4$  - the state in which a corrective service is performed on a vehicle in the maintenance system,
- $S_5$  - the state of a corrective service performed during a scheduled standstill of a bus (at so called bus depot)

It has been assumed that the set  $T$  is a sum of intervals of the bus maintenance time. It has been assumed that the codes of the selected vehicle maintenance states correspond to the codes of the states of the analysed stochastic process  $\{X_t, t \in T\}$ . The possible transitions between the selected bus maintenance states have been determined. A matrix of the process state change intensity has been assessed for the selected maintenance states.

The random variable expressing the duration of the state  $i \in S$  of the process, when the next state is  $j \in S$  with the distribution determined by the distribution function  $F_{ij}(t)$ , is denoted with the symbol  $T_{ij}$ .

Due to the structure of the data achieved on the basis of the results of investigations of a real system, being indispensable to determine the semi-Markov process  $\{X_t, t \in T\}$ , it is convenient to define such a process by determining the following three  $(p, P, F(t))$  elements:

- $p = [p_i : i \in S]$  - stochastic vector of the initial distribution process  $\{X_t, t \in T\}$ ,
- $P = [p_{ij} : i, j \in S]$  - matrix of transition probabilities of the Markov chain embedded in the process  $\{X_t, t \in T\}$ ,
- $F(t) = [F_{ij}(t) : i, j \in S]$  - matrix of distribution functions of the conditional distributions of the random variables  $T_{ij}$ ,  $i, j \in S$  of the times remaining in the states.

To simplify further investigations it has been assumed that  $F_{ij}(t) = G_i(t)$ ,  $i, j \in S$ . The function  $G_i(t)$  is a distribution function of distribution of the duration time of the state  $i \in S$ . This assumption means that the duration of the current state does not depend on the next process state.

The state space  $S$  consists of five states  $S = \{S_1, S_2, S_3, S_4, S_5\}$  in the considered example. The possible transitions between the selected bus maintenance states, presented by the relation (15), were determined on the basis of identification of a real investigation object (a maintenance system of an urban bus transport system) and the maintenance processes performed therein.



$$P = \begin{bmatrix} 0 & p_{12} & 0 & p_{14} & p_{15} \\ p_{21} & 0 & p_{23} & p_{24} & 0 \\ p_{31} & p_{32} & 0 & p_{34} & 0 \\ p_{41} & 0 & 0 & 0 & 0 \\ p_{51} & 0 & 0 & p_{54} & 0 \end{bmatrix} \quad (15)$$

The transition matrix of the embedded Markov chain estimated on the basis of the results from the performed preliminary maintenance investigations is formulated as follows:

$$P = \begin{bmatrix} 0 & 0,9998 & 0 & 0,0001 & 0,0001 \\ 0,986 & 0 & 0,013 & 0,001 & 0 \\ 0,11 & 0,84 & 0 & 0,05 & 0 \\ 1 & 0 & 0 & 0 & 0 \\ 0,9999 & 0 & 0 & 0,0001 & 0 \end{bmatrix} \quad (16)$$

The values of the estimators of the maximum credibility, formulated as stated below, have been adopted as statistical estimations of the transition probabilities of the embedded Markov chain:

$$\hat{p}_{ij} = \frac{n_{ij}}{\sum_{j \in S} n_{ij}} \quad (17)$$

where:

$n_{ij}$  - the number of the direct chain state changes, from the state  $i$  into the state  $j$  in its finite process realization.

The determined limiting distribution of the Markov chain embedded in the considered semi-Markov process is presented in the Table 1.

Table 1. Limiting distribution of the embedded Markov chain

$g_1$	$g_2$	$g_3$	$g_4$	$g_5$
0,49362066	0,49897069	0,00648662	0,00087267	0,00004936

The expected values  $E(T_i)$ ,  $i \in S$  of the distributions determined by the empiric distribution function are the estimations  $\Pi_i$  of the expected value of the time  $T_i$  of duration of the state  $i \in S$ :

$$\Pi_i = \frac{1}{n_i} \sum_{m=1}^{n_i} (t_i^{(m)}) \quad (18)$$

where:

$$n_i = \sum_{j \in S} n_{ij},$$

$t_i^{(1)}, \dots, t_i^{(n_i)}$  - independent realizations of the random variable  $T_i$  which stands for the duration of the state  $i$ .

The expected times of duration  $\Pi_i$  of the considered maintenance states (expressed in hours) estimated on the basis of the preliminary data are presented in the Table 2.

Table 2. Expected values of times of duration of the analysed maintenance states

$\Pi_1$	$\Pi_2$	$\Pi_3$	$\Pi_4$	$\Pi_5$
6	15,7608	0,0456	2,16	0,0336

The determined limiting distribution of the semi-Markov process constituting the model of the maintenance process of a single bus is presented in the Table 3.

Table 3. Limiting distribution of the analysed process

P <sub>1</sub>	P <sub>2</sub>	P <sub>3</sub>	P <sub>4</sub>	P <sub>5</sub>
0,27352245	0,72627600	0,00002732	0,00017408	0,00000015

#### 4. Model of maintenance process of a set of vehicles

Assuming that  $n$  of homogenous vehicles with the codes  $k \in N$ , forming the set  $Z$  of vehicles, are used in the maintenance system, a simplified model of the state change process of the elements in this set has been developed.

It has been assumed that the independent semi-Markov processes  $\{X_k(t) : t \geq 0\}$ ,  $k \in N = \{1, \dots, n\}$  determined by identical kernels  $Q(t)$  described with the relation (4) are the model of the bus maintenance process. The assumption that the processes are independent is just an approximation of the real maintenance processes. In fact, some bus states may have influence over the maintenance states of other buses.

The random vector:

$$\mathbf{X}(t) = [X_1(t), X_2(t), \dots, X_n(t)] \quad (19)$$

describes the process of changes of maintenance states of the set of buses of the considered vehicle maintenance system. With such an assumption it is possible to determine the total distribution of this random vector, that is:

$$P\{X_1(t) = i_1, X_2(t) = i_2, \dots, X_n(t) = i_n\} = P_{i_1}(t) P_{i_2}(t) \dots P_{i_n}(t), \quad (20)$$

where:  $i_1, i_2, \dots, i_n \in S$ .

The random variable:

$$N_i(t) = \#\{k \in N : X_k(t) = i\}, \quad t \geq 0, \quad i \in S \quad (21)$$

stands for the number of buses in the state  $i$  at the moment  $t$ .

The random vector  $\{(N_1(t), N_2(t), \dots, N_g(t)) : t \geq 0\}$  has multinomial distribution, which means:

$$P\{N_1(t) = i_1, N_2(t) = i_2, \dots, N_5(t) = i_5\} = \frac{n!}{i_1! i_2! \dots i_5!} [P_1(t)]^{i_1} [P_2(t)]^{i_2} \dots [P_5(t)]^{i_5} \quad (22)$$

where:  $i_1 + i_2 + \dots + i_5 = n$ .

The equation [7] results from the limit theorem for the semi-Markov processes:

$$\begin{aligned} \lim_{t \rightarrow \infty} P\{N_1(t) = i_1, N_2(t) = i_2, \dots, N_5(t) = i_5\} &= \\ &= \frac{n!}{i_1! i_2! \dots i_5!} \lim_{t \rightarrow \infty} [P_1(t)]^{i_1} [P_2(t)]^{i_2} \dots [P_5(t)]^{i_5} = \frac{n!}{i_1! i_2! \dots i_5!} P_1^{i_1} P_2^{i_2} \dots P_5^{i_5} = \\ &= \frac{n! \pi_1^{i_1} m_1^{i_1} \pi_2^{i_2} m_2^{i_2} \dots \pi_5^{i_5} m_5^{i_5}}{i_1! i_2! \dots i_5! \left( \sum_{i \in S} \pi_i m_i \right)} \end{aligned} \quad (23)$$

The expected value of the considered random vector is formulated as:

$$E[(N_1(t), N_2(t), \dots, N_5(t))] = (nP_1(t), nP_2(t), \dots, nP_5(t)). \quad (24)$$

The coordinates of this vector stand for the expected number of buses in the analysed maintenance states  $i$ ,  $i = 1, 2, \dots, 5$ , at the moment  $t$ . Therefore, the value:  $E[(N_i(t)) = nP_i(t)$ ,  $i \in S$ ,  $t \geq 0$  stands for the expected number of buses in the state  $i$  at the moment  $t$ .



The variance of the random variables  $N_i$  takes the form:

$$V[(N_i(t)) = nP_i(t)(1 - P_i(t)), \quad i \in S, t \geq 0, \quad (25)$$

while the covariance is expressed with the relation:

$$\text{Cov}[(N_i(t), (N_j(t)) = -nP_i(t)(1 - P_j(t)), \quad i, j \in S, i \neq j, t \geq 0. \quad (26)$$

The expected value of the random variable  $N_i$  which stands for the number of buses in the state  $i$  in a system working for a long time may be determined using the relation:

$$E[N_i] = \lim_{t \rightarrow \infty} E[(N_i(t))] = nP_i, \quad i \in S. \quad (27)$$

The expected value of the random vector  $[N_1, N_2, \dots, N_5]$  in the considered model is:

$$E[(N_1, N_2, \dots, N_5)] = (nP_1, nP_2, \dots, nP_5). \quad (28)$$

The coordinates of this vector stand for the expected number of buses in the determined states in a system working for a long time. The statistical estimation of the elements of this vector is:

$$E(N_i) = nP_i, \quad i \in S. \quad (29)$$

The limiting variance for the state  $i \in S$  is:

$$V[N_i] = nP_i(1 - P_i), \quad i \in S, \quad (30)$$

while the limiting covariance of the state pairs is expressed with the relation:

$$\text{Cov}[(N_i(t), (N_j(t)) = -nP_i(1 - P_j), \quad i, j \in S, i \neq j. \quad (31)$$

The determined expected numbers of buses in the specified states in a system working for a long time for the investigated bus maintenance system and the adopted data and  $n = 203$  are presented in the Table 4.

Table 4. Statistical estimation of the expected number of buses in the specified states in a system working for a long time ( $n = 203$ )

$E(N_1)$	$E(N_2)$	$E(N_3)$	$E(N_4)$	$E(N_5)$
55,53	147,43	0,01	0,04	0,00

It is possible to simulate such an event that the scope of the transport service realization is reduced. Such a situation may take place when it is not profitable to realize transportation by means of specific bus lines or in case of a failure to win another tender for the transportation tasks performed before. If it is decided not to handle one of the bus lines, the number of the necessary vehicles would be reduced by 17 vehicles. For such a variant, the determined expected values of the number of buses in the specified states in a system working for a long time are presented in the Table 5. The calculation results may serve to preliminarily forecast the demand for the corrective service realization both in the system (service station) and in its environment (technical emergency service units), as well as the system operation costs and the number of vehicles necessary to provide continuous transportation.

Tab. 5. Statistical estimation of the number of buses in the specified states in a system working for a long time ( $n = 186$ )

$E(N_1)$	$E(N_2)$	$E(N_3)$	$E(N_4)$	$E(N_5)$
50,88	135,09	0,01	0,03	0,00

## 5. Summary

The purpose of the investigations presented herein was, among others, to show a possibility to use selected stochastic processes for mathematical modelling the system and the process of vehicle maintenance.

The considered example of the model of maintenance process of urban transport buses is characterised by a considerable simplification (due to the nature of the work). However, the presented way to create models of that type and analyse them indicates that they may be used to preliminarily forecast the system state, and to simulate changes of the internal and external interactions affecting the system and to support the decision makers in the decision making process concerning control of the maintenance process and the system in which it is performed.

The analysis of results of the investigations performed shows that the developed model is susceptible to a change of the input parameter values.

The mathematical models of the maintenance processes, performed in complex systems, are by their very nature a considerable simplification of the real processes. The consequence of this is a necessity to carefully formulate practical conclusions resulting from investigating those models. However, in the opinion of the author, it does not limit the purposefulness of developing and analysing models of that type. The analysis of the results of investigating those models, for the model parameter values, determined on the basis of the results of maintenance tests performed in a real transport system, makes it possible to formulate conclusions and opinions both of a qualitative and (to the limited extent) quantitative nature.

Appropriate formulation of the investigation goals, expected results and variants of simulation of behaviour of the analysed system makes it possible, due to analysing the models of that type, to perform, among other things, preliminary evaluation of influence of the considered decision variants (concerning such things as the number of vehicles required to assure effective realization of the transport tasks, frequency and scope of the technical services performed, etc.) on the course and effectiveness of the investigated maintenance process.

The presented method to build models of changes of vehicle maintenance states and the semi-Markov process used to model the maintenance process of urban transport buses may be, in a relatively simple way, applied for other maintenance systems than the considered one.

## References

- [1] Bobrowski D.: Mathematical models and methods of reliability theory in examples and exercises. WNT, Warsaw 1985.
- [2] Bobrowski, D., *Probabilistics in technical applications*. WNT, Warsaw 1986.
- [3] Buslenko, N., Kałasznikow, W., Kowalenko, I., *Theory of complex systems*. PWN, Warsaw 1979.
- [4] Koroluk, W.S., Turbin, A.F., *Połmarkowskije processy i ich priloženija*. Naukowa Dumka, Kijów 1976.
- [5] Landowski, B., *Maintenance model of a certain class of technical objects*. Scientific Journals No. 229. Mechanics 48. University Publishing House ATR, Bydgoszcz 2000.
- [6] Mine, H., Osaki, S., *Markowskije processy priniatija reszenij*. Science, Moscow 1977.
- [7] Woropay, M., Grabski, F., Landowski, B., *Semi-Markov model of the vehicle operation and maintenance processes within an urban transportation system*. Scientific Publishers PTNM, the Archives of Automotive Engineering Vol. 7, No. 3, 2004.
- [8] Woropay, M., Knopik, L., Landowski B., *Modelling the maintenance and operation processes in a transport system*. Library of Maintenance Problems. ITE, Bydgoszcz - Radom 2001.
- [9] Woropay, M., Landowski, B., Neubauer, A., *Controlling reliability in transport systems*. Library of Maintenance Problems. ITE, Radom 2004.
- [10] Woropay, M., Landowski, B., *Simulation analysis of the maintenance and operation processes in an urban transport system*. Scientific Journals No. 212. Mechanics 42. University Publishing House ATR, Bydgoszcz 1998.



## EFFECT OF SUPPLY VOLTAGE ON THE DOSAGE OF FUEL IN INJECTION SYSTEM THE COMMON RAIL TYPE

Kazimierz Lejda, Adam Ustrzycki

Rzeszow University of Technology  
Al. Powstańców Warszawy 8, 35-959 Rzeszów, Poland  
tel.: +48 17 8651597, +48 17 8651531  
fax: +48 17 8543112  
e-mail: klejda@prz.edu.pl, austrzyc@prz.edu.pl

### Summary

*Common Rail systems are most frequently used solution to the fuel supply system of Diesel engines. This is due to their high potential to shape the characteristics of fuel injection. One of the important requirements for each injection system is precision dose control and its onset, that is, as a consequence of the start of the combustion process. The most important parameters affecting the accuracy of dosing injection systems are, of course injection time, pressure of fuel in the rail and the fuel temperature. Influence on the size of the dose but also other factors, which include the supply voltage, which may be subject to significant change during the start-up of engine. The issue of start-up is becoming of interest to EURO standards, as the processes occurring in the course have a significant impact on the level of pollutants in the exhaust of internal combustion engine. Increased in this period, emissions of toxic compounds results from the unstable processes in the engine cylinder, as well as dynamic changes in the parameters of injection and in the start-up system, in particular, changes in voltage resulting from a large collection of current from the battery. Thus, the article attempted to determine the impact of voltage supply on the dosage of fuel in different operation conditions of the injection system. In particular attention was paid to the size of the dose and the actual changes at the beginning of fuel injection voltage changes. The study was conducted on a test stand, which were the main components of the test bench Bosch EPS-815 with electronic measurement of fuel dose and the visualization system AVL Visioscope. Control of the injector was performed using the self-developed controller.*

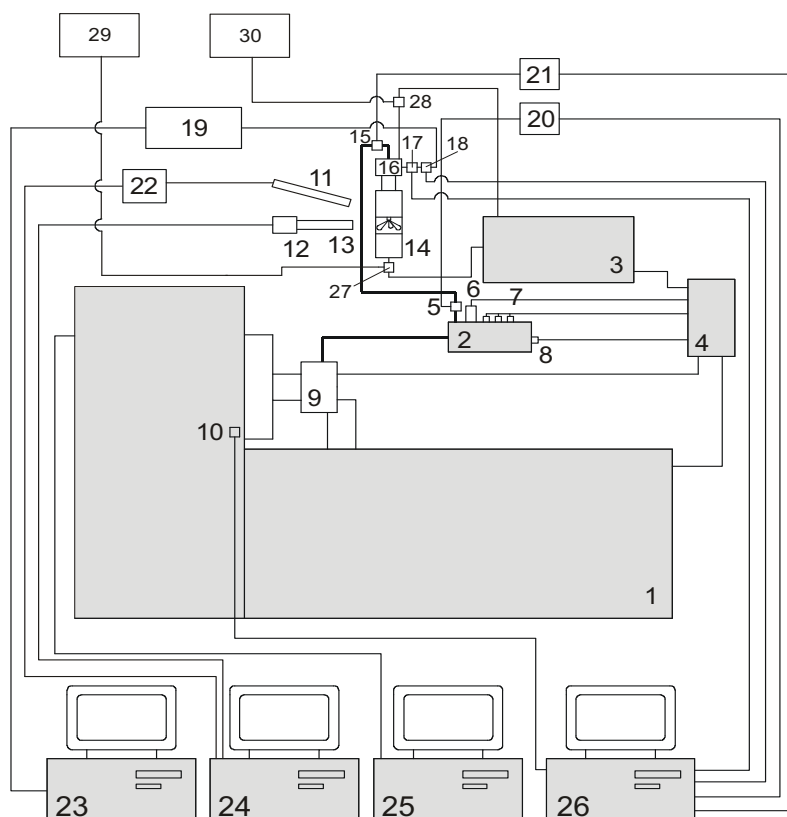
**Key words:** Common rail, fuel injection, control injection, precision dosing of fuel

### 1. Introduction

Common Rail fuel supply systems have high potential in shaping the fuel injection characteristics. For that reason, they are now widely used systems of fuel injection for diesel engines [3, 7, 8]. Diesel injection system is expected to provide a high precision metering of fuel amount injected into the cylinder, accuracy in injection start timing control and repeatability of that. Many factors contribute to above capacities including, inter alia, accurate control of injection duration and timing, which depends on the electronic control unit design and the kind of input signals that it uses, the injection pressure, the fuel parameters [4, 5, 10, 11], and the power supply voltage. On the accuracy of injected fuel amount, the factors related to the injection process progressing have also a significant impact, especially when multi-split injection is implemented. Pressure pulsations triggered by pilot injection, the amplitude of which may reach even 60 MPa, change the fuel quantity of main injection and its start angle position as well [9]. The changes in voltage, especially during the engine start-up, can be so considerable, that in effect they may cause

the changes of the injector coil current value and emerged magnetic stream. Fluctuations of this stream will affect the magnetic force lifting the injector control valve, so the entire range of injector operation.

## 2. Test stand and measurement methodology



Research in each measurement series were carried out at a fixed temperature of the injected fuel, which was measured in outlet pipe of the measuring chamber. The temperature of the fuel in the tank was stabilized at around  $40 \pm 1^\circ\text{C}$ . As the testing device the Bosch injector from the engine Fiat Multijet 1.3 (marked 445 010 083) was used. For injector operation control the electronic unit developed in Department of Automotive Vehicles and Internal Combustion Engines of Rzeszów University of Technology was used. Detailed description of the controller is presented in the work [1].

The primary purpose of the study was to determine the injected fuel amount and actual start of fuel injection depending on supplying voltage. The study was conducted for single injection strategy in order to avoid the changes in injection delivery that may arise from variations of pressure due to implementation of multi-split injection [2,6]. In order to determine precisely the actual start of injection, the progress of fuel spray was recorded by visualization system AVL Visioscope with an angular resolution of  $0.1^\circ$  of pump shaft revolution. That accuracy level was possible to obtain owing to use of pulse angle encoder AVL 365C mounted on the shaft of test bench. Pulses generated by the transmitter were also used as the input signal for the electronic injector controller. In this case, the angular resolution of 720 pulses per revolution was available, what gives a very high precision of controlling the start of fuel injection.

For recording the progress of injection process a digital VGA camera and the endoscope of AVL Visioscope system were used. Figure 2 presents the photographs of fuel sprays in the measuring chamber that were captured in the same angle position of pump shaft but for different values of supply voltage.

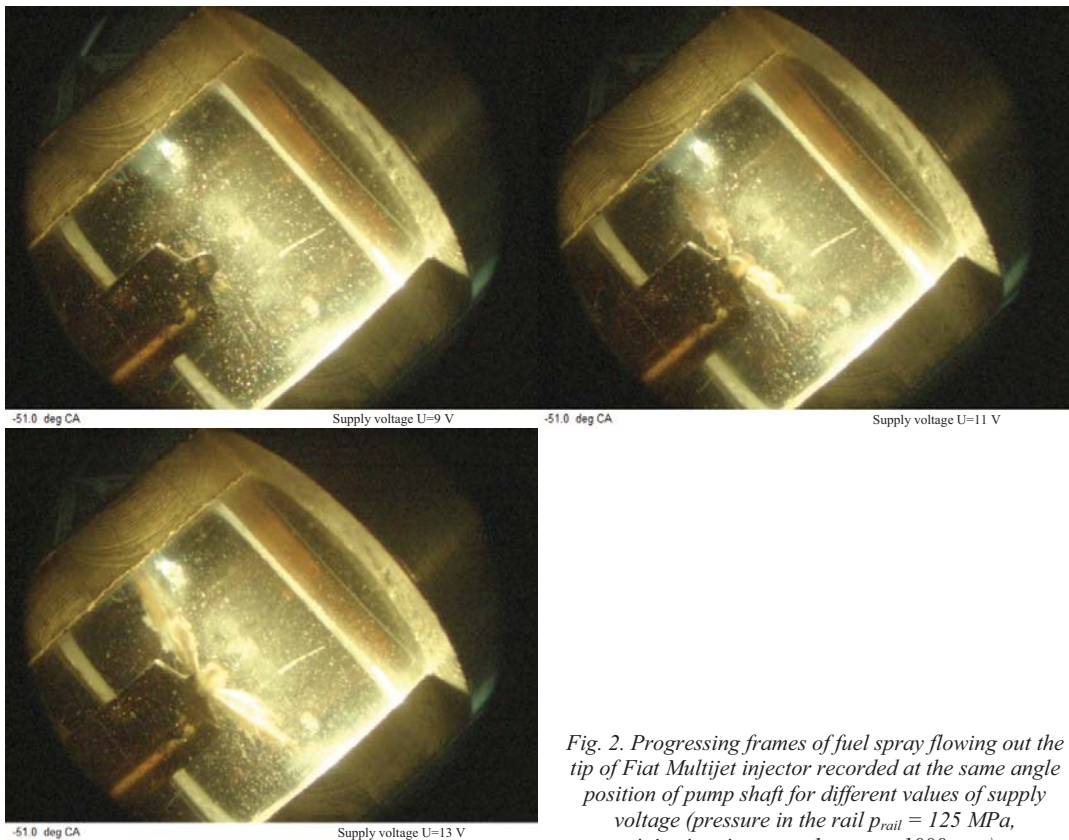


*Fig. 2. Progressing frames of fuel spray flowing out the tip of Fiat Multijet injector recorded at the same angle position of pump shaft for different values of supply voltage (pressure in the rail  $p_{rail} = 125 \text{ MPa}$ , injection time  $t_{inj} = 1 \text{ ms}$ ,  $n = 1000 \text{ rpm}$ )*

As can be noticed, at the supply voltage of 9 V the fuel sprays there are at the initial phase of their progress, while at the supply voltage of 13 V they are already in mid-expanded stage.

The injector control system was powered from a battery, which was also connected to the charger with a free and precise adjustment of supplying voltage and current feature. It allows for the voltage power supply to stay highly stable and reliable. The research were conducted for the voltage varied from 9 to 13 V, beginning from lower value. In order to perform it, the battery was partially discharged and loaded by an additional resistance increasing current consumption. Since the study was conducted at different durations of the injection, which causes the changes in the injector input current, each time after changing the injection time the supply voltage was re-adjusted. The tests were made for injection durations changed in the range of 1 to 3 ms, for three values of fuel pressure in the whole system equals 75, 100, and 125 MPa and at rotational speed of 1,000 rpm. In addition, for specific values of injection time and pressure some studies on the impact of supply voltage on the fuel injected quantity at different pump shaft speeds changed from 600 to 2000 rpm have been carried out.

### 3. Test results

Fig. 3 presents the volume of fuel injected versus the time of injection for different values of voltage  $U$  and fixed rotational speed  $n = 1000$  rpm and pressure in the rail 75 MPa. For the voltage below 11 V this relationship ceases to be linear, and further, for the voltage below 9.5 V, the amount of fuel injected becomes a random, and increasing the time of injection does not make it higher. Thus, these results are not included in the figure. Reducing supply voltage results in a delay in opening the electromagnetic valve and thereby the start of injection delays also (Fig. 4). For the change in supply voltage from 13 V to 9.5 V, the delay at this rotational speed is exceeds  $1^\circ$  of pump shaft angle.

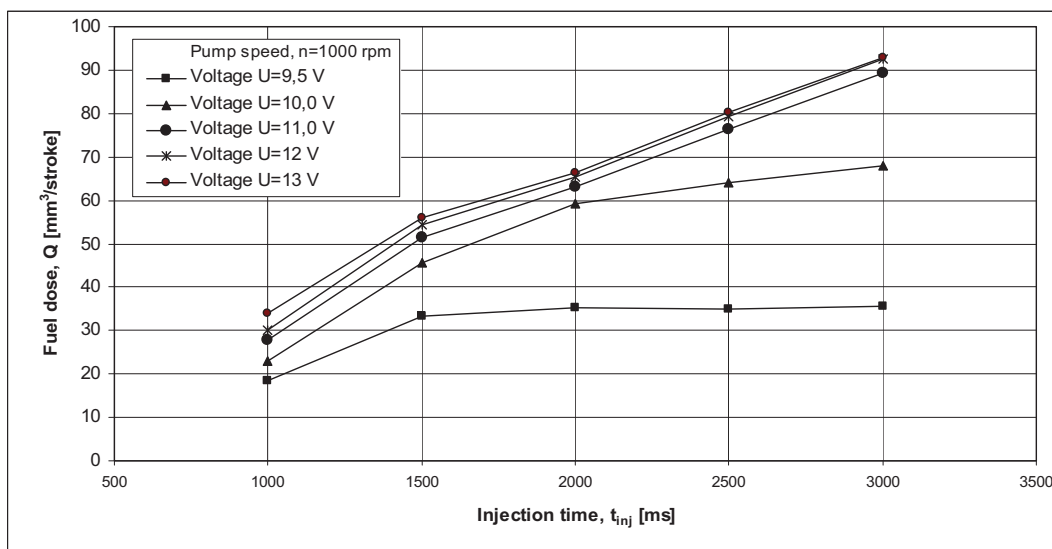


Fig. 3. The fuel dose quantity  $Q$  versus the injection time  $t_{inj}$  at different values of voltage  $U$  (the pressure in the rail  $p_{rail} = 75$  MPa,  $n = 1000$  rpm)

Fig. 5 presents the changes of the value of fuel dose quantity  $Q$  depending on the supply voltage for different values of fuel pressure in the rail and for fixed injection time of 1 ms. The temperature of the fuel flowing out the chamber was  $90^\circ\text{C}$  for the injection pressure of 100 and



125 MPa, but 75°C for the injection pressure of 75 MPa due to the fact, that attainment 90°C of fuel temperature at this value of injection pressure was not possible.

As can be seen, the variation range of injected fuel quantity is very wide; it changes about 5 mm<sup>3</sup>/stroke per each 1 V of drop, where at the voltage less than 10 V this value still increases. For longer injection time of 3 ms, these changes fit in the exponential curve; in this case a significant reduction in the injected fuel amount is already noticed at a voltage of 11 V (Fig. 6). Minor changes of fuel amount at shorter injection time can be explained by the influence of capacitor, whose stabilizing action becomes little at increasing injection time.

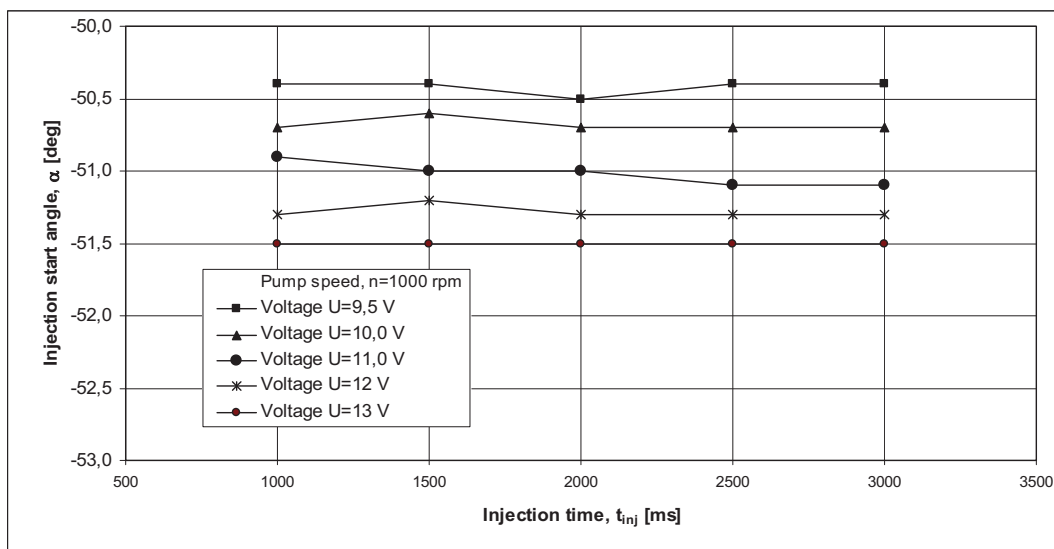


Fig. 4. Changes in the actual start of injection  $\alpha$  versus the injection time  $t_{inj}$  for different values of voltage  $U$  (the pressure in the rail  $p_{rail} = 75$  MPa,  $n = 1000$  rpm)

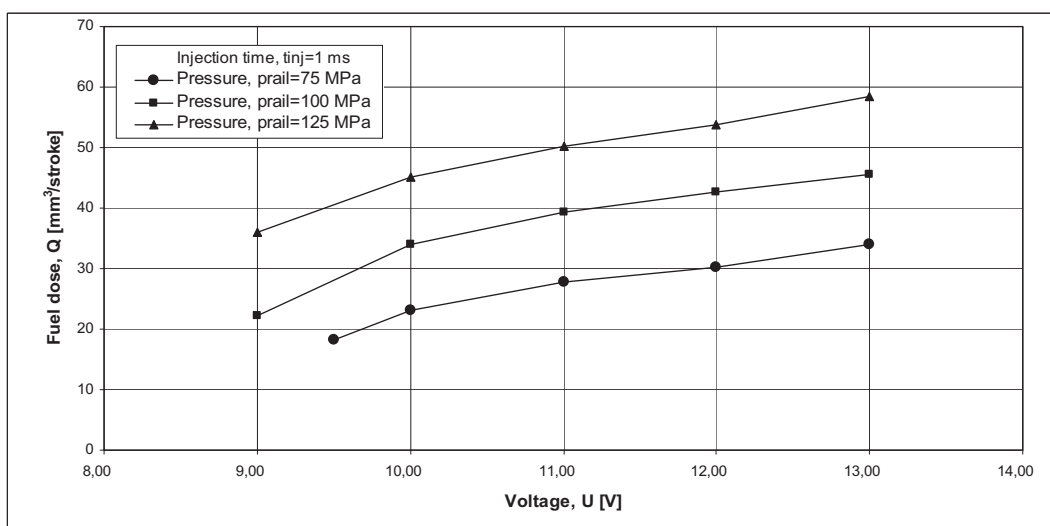


Fig. 5. Effect of supply voltage  $U$  on the fuel injected quantity  $Q$  for different values of pressure in the rail  $p_{rail}$  (injection time  $t_{inj} = 1$  ms,  $n = 1000$  rpm)

In Fig. 7 the relationship between injected fuel amount  $Q$  and pump shaft speed  $n$  for three different values of supply voltage of 9, 11, and 13 V, injection time of 3 ms and the fuel pressure of 75 MPa is presented. At 9 V, the injected fuel amount corresponds to only about 15% of the amount at higher voltage values. In principle, the injected fuel quantity does not dependent on the speed, although for larger values of supply voltage a slight increase of injected fuel volume at higher rotational speeds can be observed.

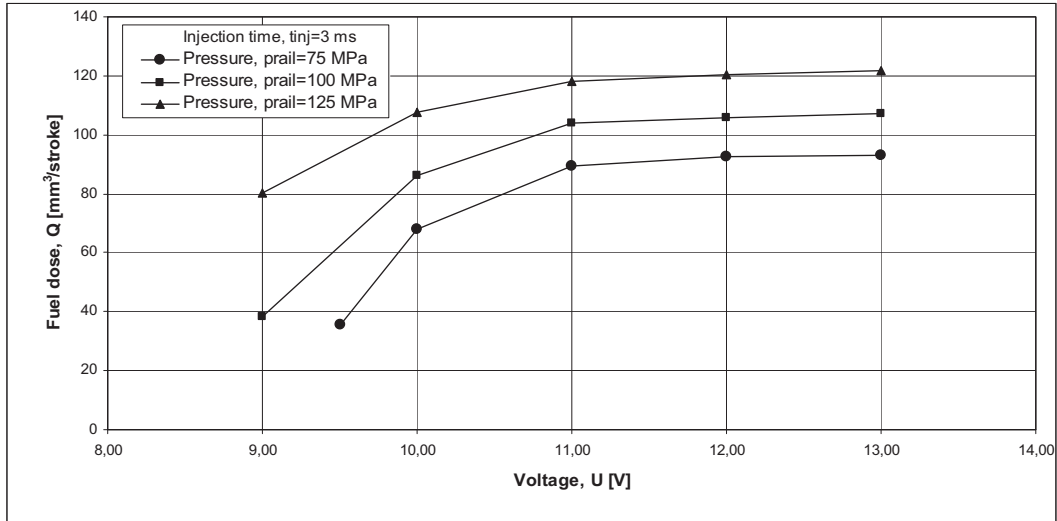


Fig. 6. Effect of supply voltage  $U$  on the injected fuel amount  $Q$  for different values of pressure in the rail  $p_{rail}$  (injection time  $t_{inj} = 3$  ms,  $n = 1000$  rpm)

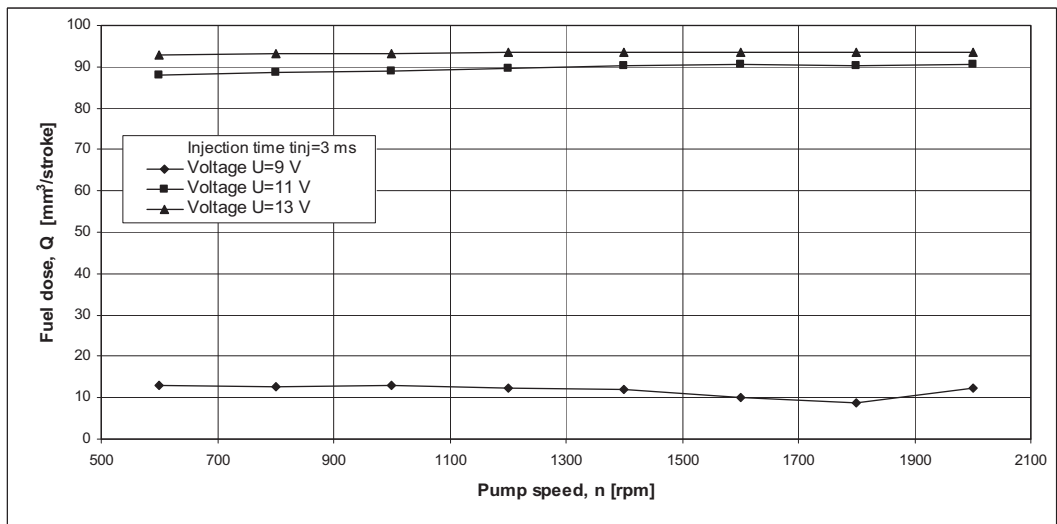


Fig. 7. The injected fuel amount  $Q$  versus the pump shaft speed  $n$  for different values of voltage  $U$  (injection time  $t_{inj} = 3.0$  ms, the pressure in the rail  $p_{rail} = 75$  MPa)

Figure 8 presents the changes in the start of injection angle position depending on the pump shaft speed. As can be seen, the time delay of needle lift associated with a reduction of voltage value is constant, what results in increasing the value of changes in injection beginning angle



position at increasing pump shaft speed. However, throughout the whole analysis range the change of voltage from 11 V to 9 V causes greater differences in the injection beginning angle position than as for the change from 13 to 11 V. In the same conditions of system operation, similar changes occur for a longer injection time.

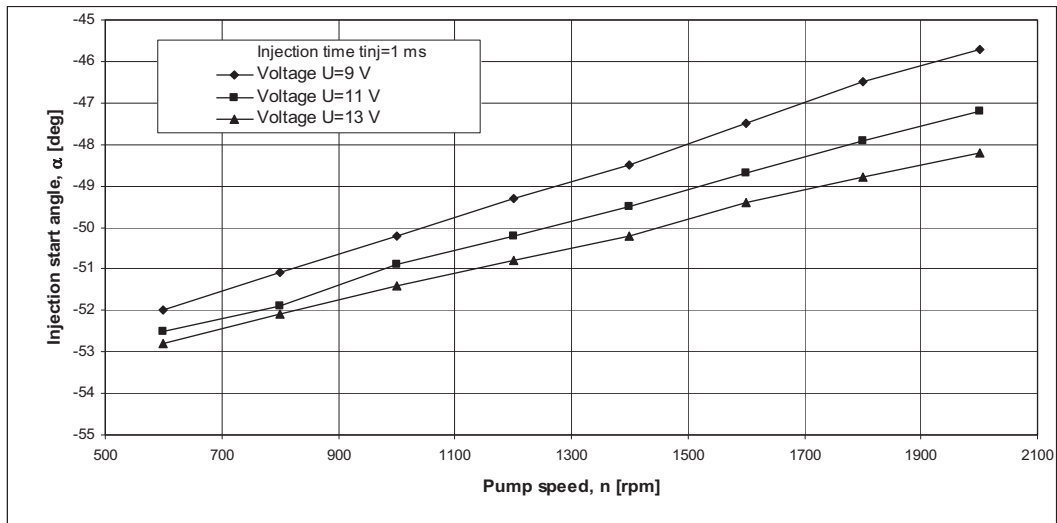


Fig. 8. Changes of the injection start angle position  $\alpha$  depending on the pump shaft speed  $n$  for different values of the voltage  $U$  (injection time  $t_{inj} = 1$  ms,  $n = 1000$  rpm)

#### 4. Conclusions

Analyzing the results obtained, it should be noted that the change in supply voltage significantly affects the injected fuel quantity. The lower injection pressure, the more significant the relative changes of that are. It may further affect the injected fuel amount, especially at low engine speeds. Changes in the angle position of the injection start for low speeds are negligible, and taking into account that at high speeds and alternator order working, the voltage fluctuations are smooth and should not be large, so their impact on this parameter can be neglected..

However, the injector may not open at all, if the voltage would be too low, especially at low fuel temperature. The injector operation principle at low values of voltage depends to a large extent on the kind of capacitor used in the controller. The boundary values of voltage, at which the injector will still work, also depend on the parameters of the injector coil, and so, also on the coil temperature, that may change due to the temperature of the fuel, as well as working time of the injector.

In conclusion, the voltage fluctuations can significantly affect the value of fuel quantity injected by the Common Rail system into the engine cylinders, which may adversely affect the emissions of pollutants in the engine exhaust. The elimination of these changes can be obtained by applying an additional electricity storage device e.g. by placing the suitably selected capacitor in the controller or by the use of a separate power source for the injectors, so that the change of the battery voltage during engine start-up and immediately after does not affect the accuracy and quality of injection control in the meaning of fuel dosing in these phases of Diesel engine work.

## References

- [1] Balawender K., *Wpływ wybranych parametrów regulacyjnych procesu wtrysku na emisję cząstek stałych w silniku wysokoprężnym typu DI*. Rozprawa doktorska. Rzeszów 2007.
- [2] Balawender K., Kuszewski H., Lejda K., Ustrzycki A., *The influence of mutual angle position of main, pilot and preinjection dose on fuel dosing in common rail system*. Journal of POLISH CIMAC - Energetic Aspects, Vol. 3, No. 1, Gdansk 2008.
- [3] Kuszewski H., Lejda K., *Wybrane metody ograniczania toksyczności spalin silnika ZS w aspekcie limitów emisyjnych*. Journal of KONES „Powertrain and Transport”, Vol. 13, No.1, Warszawa 2006.
- [4] Kuszewski H., Ustrzycki A., *Badania procesu dawkowania paliwa w zasobnikowym układzie wtryskowym*. Вісник Національного транспортного університету, No 14/2007, Київ 2007.
- [5] Kuszewski H., Ustrzycki A., *Wpływ parametrów pracy zasobnikowego układu wtryskowego na rzeczywisty początek wtrysku paliwa*. Polskie Towarzystwo Naukowe Silników Spalinowych, Silniki Spalinowe, „Mixture Formation, Ignition & Combustion”, 2007-SC2, 2007.
- [6] Kuszewski, H., Ustrzycki, A., Balawender, K., Lejda, K., *The effect of multi-phasing injection on selected parameters of high-pressure fuel system Common Rail*. Polskie Towarzystwo Naukowe Silników Spalinowych, Silniki Spalinowe, Nr 4/2008.
- [7] Lejda K., *Selected problems of fuel supply in high-speed Diesel engines*. Publishers “Meta”, Lwów 2004.
- [8] Praca zbiorowa, *Zasobnikowe układy wtryskowe Common Rail*. Informatory techniczne Bosch. WKiŁ, Warszawa 2005.
- [9] Ustrzycki A., *Wpływ zjawisk falowych na proces dawkowania paliwa w układzie wtryskowym typu Common Rail silnika wysokoprężnego*. Prace Zachodniego Centrum Akademii Transportu Ukrainy, Lwów 2009.
- [10] Ustrzycki A., Kuszewski H., *Badania początku wtrysku paliwa w układzie wtryskowym typu Common Rail*. Mat. XVII Konferencji Międzynarodowej SAKON’06 nt. „Metody Obliczeniowe i Badawcze w Rozwoju Pojazdów Samochodowych i Maszyn Roboczych Samojezdnych. Zarządzanie i Marketing w Motoryzacji”, Rzeszów 2006.
- [11] Ustrzycki A., Kuszewski H., *Wpływ temperatury wtryskiwanego paliwa na wielkość dawki w zasobnikowym układzie wtryskowym typu Common Rail*. Mat. XVIII Międzynarodowej Konferencji Naukowej SAKON’07 nt. ”Metody obliczeniowe i badawcze w rozwoju pojazdów samochodowych i maszyn roboczych samojezdnych. Zarządzanie i marketing w motoryzacji”, Rzeszów 2007.



## GAS TURBINE ENGINES – THROUGH IMPROVED MAINTAINABILITY TO IMPROVED OPERATIONAL READINESS IN NAVY HELICOPTERS

**Olgiard Wieczorek\* Jerzy Lewitowicz\*\* Andrzej Żyluk\*\***

*\*Inspectorate for Armed Forces Support*

85-915 Bydgoszcz ul. Dwernickiego 1

e-mail: [stolo@wp.pl](mailto:stolo@wp.pl)

*\*\*Air Force Institute of Technology*

01-494 Warszawa ul. Księcia Janusza 6

e-mail: [jerzy.lewitowicz@itwl.pl](mailto:jerzy.lewitowicz@itwl.pl) [andrzej.zyluk@itwl.pl](mailto:andrzej.zyluk@itwl.pl)

### *Abstract*

*Reliability needs of the military focus primarily on operational readiness, longevity, supportability, robustness. That means product performance on demand, long useful life, repair ability and satisfactory performance over environmental extremes. Availability requirements of modern systems and equipment demand that designing for maintainability must be as important as designing for other performance characteristics.*

**Keywords:** *helicopter, exploitation, gas turbine engine*

Customer needs are always very high. The challenge to the manufacturer or service provider is how to assess and define true customer expectations and then how to design, manufacture and sell the product to best meet those expectations. Military customer is specific. The air force is very specific but navy aviation is extremely specific. There are numerous differences between the needs of a typical customer and a navy aviation customer. Reliability needs of the military focus primarily on operational readiness, longevity, supportability, robustness. That means product performance on demand, long useful life, repair ability and satisfactory performance over environmental extremes [1]. A thorough understanding of the environment in which the product is intended to operate is the major consideration in determining the ability of a product to meet the operational reliability needs of the military. The environment is a critical factor in determining the suitability of the equipment for military use, especially in the navy aviation. Each product must provide operational capabilities which allow military forces to maintain technological and logistics superiority over a potential adversary even if it is just natural or induced environment which can be expected over the operational and maintenance portions of life cycle. Degradation or loss of these operational capabilities typically can result in immediate loss of human life and equipment (Fig. 1, 2) [2].



*Fig. 1*

Availability requirements of modern systems and equipment demand that designing for maintainability must be as important as designing for other performance characteristics. According to military definition, maintainability is a measure of the ability of an item to be retained in or restored to a specified condition when maintenance is performed by personnel having specified skill levels, using prescribed procedures and resources, at each prescribed level of maintenance or repair. You can find some other definitions connecting effectiveness and economy and efficiency.



*Fig.2*

There are two examples of naval helicopter engines (Fig. 3):

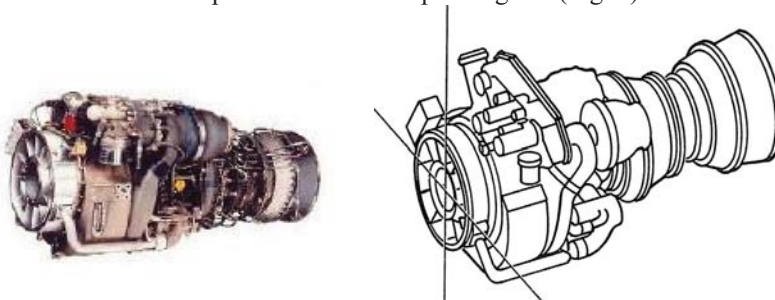


*Fig. 3*

The T700-GE-401 engine is a front drive, turbo shaft engine featuring a single spool gas generator section consisting of a five-stage axial, single stage centrifugal flow compressor, a

through-flow annular combustion chamber, a two-stage axial flow gas generator turbine, and a free or independent two-stage axial flow power turbine. The power turbine shaft, which has a rated speed of 20,900 rpm, is co-axial and extends to the front of the engine. The engine incorporates an integral inlet particle separator, a top-mounted accessory package, an engine – driven fuel boost pump, a self-contained lubrication system, condition monitoring, diagnostic provisions, a hydro mechanical control system, and an electrical control system or digital electronic control system (401C version) providing power turbine speed control, dual engine load sharing, temperature limiting, and redundant power turbine over speed protection. The T700-GE-401 engine also has a contingency power rating for use under one engine inoperative conditions.

Engine control system has all the components necessary for the proper and complete control of the engine. This system provides for fuel handling, fuel computation, compressor bleed and variable geometry control, PT over speed control protection, over temperature protection and torque matching. This system is self-contained and does not require external electrical power for any controlling functions. It also allows replacement of any weapon replaceable assembly (WRA) without calibration. The following units make up the control system:

- Hydro mechanical control unit, The HMU schedules fuel for combustion. It contains a high-pressure pump. The HMU has an actuator arm that positions the inlet guide vanes, the variable compressor vanes, and the anti-icing bleed and start valve. The HMU responds to engine inlet air temperature (T2), to compressor discharge air pressure (P3), and to a trim signal from the ECU/DEC to set fuel flow and variable vane positioning. It is designed to be adjusted at depot only. Adjustments to the HMU are safety wired to prevent adjustment at intermediate maintenance level,
- Electrical control unit (ECU) /Digital electronic control (DEC), Used for diagnostic testing of the engine electrical control system, interface with the test stand system and some sensors,
- Fuel boost pump. The fuel boost pump is an engine-mounted suction-type pump. It is not self priming.
- Fuel filter. The main parts of the fuel filter are: a disposable filter element, an impending bypass indicator button, a bypass relief valve, and an actual filter bypass sensor.
- Overspeed and drain valve which has three functions. First, it sends fuel through the main fuel manifold to the fuel injectors for starting, accelerating, and engine operation. Second, it purges the fuel injectors of fuel when the engine is shut down. It does this by allowing compressor discharge air (P3) to pass through the injectors. Third, it controls Np overspeed by cutting off engine fuel flow.
- Anti-icing bleed and start valve
- Ignition exciter. The ignition system is a noncontiguous, ac-powered, capacitor discharge type. It includes two igniter plugs, two electrical ignition leads, and an ignition exciter assembly. Power is supplied to the ignition exciter assembly by the engine's alternator during starting only.
- Np sensor: The power turbine rotor speed (Np) governing system compares the signal sent from the Np sensor with the Np selected by the operator. It varies fuel flow by actuating the torque motor in the Hydro mechanical control unit (HMU). Power turbine rotor speed is governed with  $\pm 1\%$  of required rotor speed.

There are some engine control components, test cell systems and diagnostic equipment. Turbine gas temperature (TGT) limiting system. The TGT limiting system overrides the power turbine rotor speed governing system and the load-sharing system when TGT reaches 1542°F. It limits fuel flow to hold a maximum 1542°F TGT by actuating the torque motor in the HMU. The TGT limiting system is accurate to within  $\pm 9^\circ\text{F}$ . Np over speed protection system. The Np over speed protection system (fig. 12) receives a power turbine speed signal from the torque and over



speed sensor. When  $N_p$  exceeds  $25,000 \pm 250$  rpm, output from the protection system activates a solenoid in the ODV. This shuts off fuel flow causing the engine to shut down. Load-sharing system. In twin-engine installations, the digital electronic controls (DEC) compare torque signals, for automatic load sharing. Hot Start Prevention (HSP). The HSP system prevents over temperature during engine start. The HSP system receives power turbine speed signal, gas generator speed signal, and turbine gas temperature (TGT). When  $N_p$  and  $N_g$  are below their respective hot start reference and turbine gas temperature (TGT) exceeds  $1652^\circ\text{F}$  and output from the HSP system activates a solenoid in the ODV. This shuts off fuel flow and causes the engine to shut down. Fault Indication. The DEC contains signal validation for selected input signals within the electrical control system. Signals are continuously validated when the engine is operating at flight idle and above. If a failure has occurred, the failed component or related circuit will be identified by a pre-selected fault code. It is possible to have more than one fault detected. Each code should be treated as an individual fault. It should be noted that the signal validation does not recognize aircraft instrument related failure. Fault codes will be displayed on the engine torque indicator.

Next the TW3-117M engine for the Mi-14 helicopters (Fig. 4) designed by S. Izotow team at Klimov Company. The turbine converts the potential energy of gas to mechanical work of the rotor that can be used by the consuming device. New materials have enforced some improvements to increase the gas temperature before the turbine without changing the geometry of the flow section, and the takeoff power. Further improvements are made to develop an advanced cooling system, use new materials including cermets, and reduce the weight of the turbine.



*Fig. 4*

Each type of engine has its own manual containing introductory information necessary to assure proper maintenance of the system. It includes all items having an approved mandatory component replacement interval and those items requiring Conditional inspections that shall be accomplished at the occurrence of an over limit situation. Conditional Inspection requirements include a brief description of what is to be performed and a reference to the manual or directive containing detailed requirements. Replacement items are indicated in unit hours, calendar time, cycles or event and are arranged by engine systems. All T700 engine hardware is tracked with Aeronautical Equipment Service Record. There are some cases like: salt water landing, hard landing, over-water hoisting operation, over-torque, overspeed, sudden stoppage, over temperature, oil pressure loss, engine operation limits exceeded, required conditional inspection in compliance with technical manual cards. The Chief Engineer established maintenance program for Naval Air Force which outlines the system of three levels of maintenance: organizational level (O-level), Intermediate (I-level) and depot-level (D-level) maintenance. The most interesting is the I-level maintenance. The objective of to enhance and to sustain the combat readiness and mission capability of support at the nearest location with the lowest practical resource expenditure. It consists of: maintenance on aeronautical components, calibration of designated equipment,

processing of components from non-mission capable planes, incorporation of technical directives, age exploration of a plane.

Correct and very precise diagnose and troubleshooting need technicians with years of experience on aircraft [2, 3]. Training is given with the emphasis on real-life incidents as a result of a human error and structure fatigue. The key is our ability to manage the volume and diversity of information required to keep engines running, and easy and fast access to that for those making repairs.

## References

- [1] Kustroń K., Lewitowicz J.: *Niesprawności i uszkodzenia statków powietrznych*. XXXIII Szkoła Niezawodności. Szczyrk 2005 (in Polish).
- [2] Sergiusz Szablowski: *Przegląd kontrolny ASP w systemie obsługiwanego śmigłowca pokładowego SH-2G*. AIRDIAG'05, Warszawa 2005 (in Polish).
- [3] Lewitowicz J. i inni: *Podstawy eksploatacji statków powietrznych*. T. 4. *Badanie eksploatacyjne statków powietrznych*. Wyd. ITWL, Warszawa 2007 (in Polish).







## DAMAGES TO STRUCTURAL COMPONENTS AND UNITS OF A GAS TURBINE ENGINE

Jerzy Lewitowicz\* Olgierd Wieczorek\*\* Andrzej Żyluk\*

*\*Air Force Institute of Technology*

*01-494 Warszawa ul. Księcia Janusza 6*

*e-mail: [jerzy.lewitowicz@itwl.pl](mailto:jerzy.lewitowicz@itwl.pl) [andrzej.zyluk@itwl.pl](mailto:andrzej.zyluk@itwl.pl)*

*\*\*Inspectorate for Armed Forces Support*

*85-915 Bydgoszcz ul. Dwernickiego 1*

*e-mail: [stolo@wp.pl](mailto:stolo@wp.pl)*

### **Abstract**

*Safe operational use of an technical system, depends on properties and characteristics thereof, external excitations, and the correctly performed process of operation/maintenance of this system. Unserviceability and failures/damages to the system are the most essential problems, which – if not identified on time – can result in an accident (a crash or failure). The issues of safety, unserviceability and failures/damages have been exemplified with those occurring to gas turbine engines.*

**Keywords:** *exploitation, failures, gas turbine engine*

### **1.Introduction**

Causes of damages are pretty well recognized owing to rich maintenance experience and examination of engineering objects and units thereof. They are usually deeply rooted in physical and chemical phenomena (effect of the process of the IV type, according to description in [6.13]), but can also be effected by maintenance activities that may provoke the boundary limits, e.g. of strength/resistance, wear-and-tear limits, etc. of particular components are exceeded. Causes of damages/failures are grouped into four classes: direct, indirect, primary, and secondary ones.

Effects of damages have their impact on the performance of operational tasks, reliability, safety, and economic effectiveness of operation/maintenance. The more important component of an engineering object (from the point of view of its functionality), the more serious effects brought about by a damage/failure to this component. Damages/failures may occur in the course of operational use of the object as well as the maintenance thereof. It is obvious that damages to an engine (its structural component or unit) while it is operated in the air are essentially different from those occurring on the ground.

### **2. Damages/failures to engines**

The term ‘engine damage’ comprises damages to the engine structure, units as well as particular components (structural members and parts) that the units are composed of. Damages to parts and structural members may bring about damages to the whole unit/assembly in the composition of which they enter; also, to other units/assemblies of a given object.

Any damage is defined as the loss of physical properties and/or peculiar features by the structural component, i.e. an event that results in the transition of the engineering structure from the fit-for-service condition into the unfit-for-service condition.

The most essential criterion of rating an engineering event among damages/failures is a change in a feature/a set of features or its/their deviation from those, on the grounds of which the structural component/unit is claimed to be either 'fit-for-use' or 'unfit-for-use'.

From the standpoint of the engineering-object operation, damages/failures may be either typical, i.e. well recognized and identified, described in operational/maintenance documentation, or new ones, or those taking new forms. The latter compose a new set and occur in the course of current operation/routine maintenance. These new forms of damages/failures or of the object's remaining unserviceable may prove single events or system-attributable ones. In operational and maintenance practice they are responded to with suitable preventive actions.

Damages/failures occur due to the willfully or unwittingly exceeded permissible loads (e.g. by the aircrew, operator, servicing staff), externally originated effects and disturbances, or natural physical and chemical phenomena typical of the performed tasks (workload) or time. The following events may be numbered among them: the wear-and-tear of tribological nodes, corrosion, materials ageing, etc. [1, 9, 14].

The problem with damages to structural components/parts of an engineering object is typical of the whole operational phase thereof, although different causes predominate at different operational-phase stages.

Throughout the whole operational phase of an engineering object the structural members thereof get degraded. Operating conditions (material effort, deformations, wear-and-tear, etc.), to some extent unpredictable – extreme, conditions of externally induced actions/influences that are able to change randomly all of them prove decisive in the reduction of the ultimate strength of the structure(s) of the engineering object and parts/structural components in the object's functional units/assemblies.

Damages to an engineering object, in particular while in operation, considerably affect safety, but also all rates of engineering availability that feature the operational readiness, i.e. readiness to perform tasks. Damages attributable to many and various causes can be classified as a) predictable, and b) unpredictable ones. Predictable damages develop at locations easy of access and subjected to the diagnosing (with different methods out of a variety of diagnostic techniques).

Damages to turbine engines applied in aircraft power plants comprise approximately 25% of the total number of disadvantageous events of this kind.

Damages to engineering objects (such as turbine engines), units/assemblies and structural members thereof are classified according to various criteria. From the point of view of damage identification and preventive treatment, they are classified for what follows:

- type of an object (electrical, mechanical, hydraulic, etc. system),
- physical nature of the damage,
- causes of damages,
- ways of restoring the 'fit-for-use' state.

Damages/failures to engineering objects and structural components thereof may also be divided into the following groups:

- primary (independent),
- secondary (dependant),
- natural, and
- forced damages.

Primary damages are usually effected by:

- natural ageing and wear-and-tear processes, fatigue, corrosion, etc.,
- failures after permissible regimes have been exceeded,
- structural, manufacturing, and material-inherent latent defects,
- faulty operational and/or servicing practices.

Primary damages give grounds for statistical inference on the components' life and reliability [6, 7, 8]. Secondary damages are recorded as effects of primary damages.

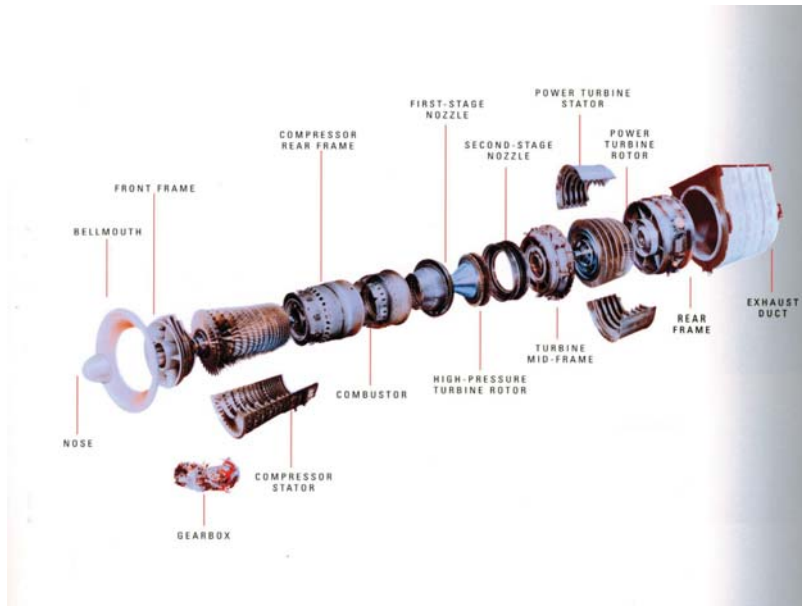


*Fig. 1. Structure of turbine engine for maritime applications*

Operational/maintenance practice proves that each and every structural member of a turbine engine (Fig. 1) is susceptible to damages/failures which occur for various reasons. The most essential causes comprise [2 - 7, 14]:

- variable aerodynamic loads,
- increase in loads (in particular, exceeding permissible values),
- impact loads,
- vibration of rotating components/parts and those exposed to cyclic changes of position, e.g. in the to-and-fro motion,
- acoustic vibration,
- heat effects,
- out-of-standard actions by aircrew members and engineering staff responsible for maintenance,
- weather effects (turbulence, corrosion) and nature-imposed ones (birds),
- effects of destructive warfare agents, foreign matter, etc.

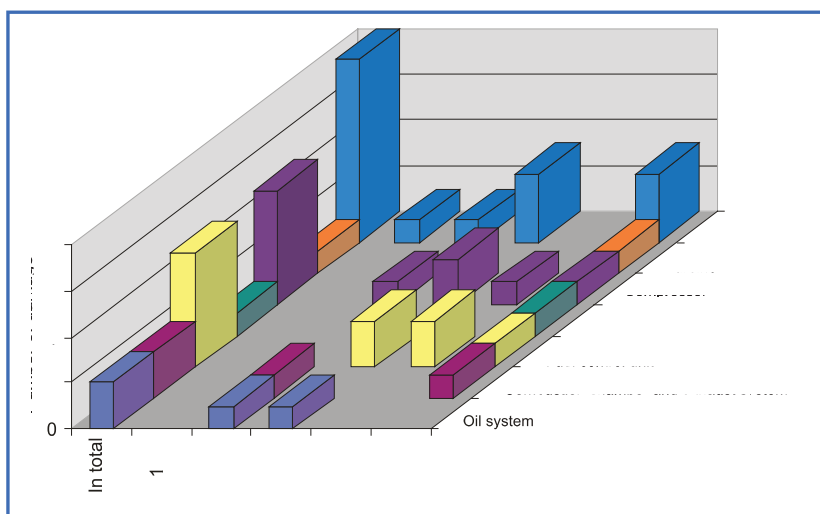


Fig. 2. Quantitative statement of damages/failures to systems and units/assemblies of turbine engines AI-25

Fig. 2 shows exemplary quantitative statements of damages to systems and units/assemblies of the AI-25 turbine engines, recorded while operating a small fleet of aircraft in the five years' period.

Damages to the engine due to the exceeding of specified values or symptoms of irregular engine operation often compels adjustments of engine units, replacement of a damaged unit, building the damaged/failed component/part or unit out of the engine. Such operations can be carried out either on the engine test bench (for engines after overhaul or withdrawal from service) or built in the object where it is operated (sea vessel or aircraft).

### 3. Mechanical damages

Damages of the mechanical type due to foreign-matter collisions contribute to the greatest extent to failures to the structures of the engine block, air inlets, and compressor, the fact being confirmed by the records. In aviation, they most often occur during the take-off and landing and are usually effected by concrete and/or soil chips, and birds. Detection of such damages during routine inspections/maintenance usually produces no difficulty, whereas any failure to detect them can generate top hazards (Figs 3 and 4) [1 - 3, 9, 11, 13].

### 4. Corrosion damages, tribological and fatigue failures

Primary causes of such damages/failures are physical and chemical phenomena, and exceeded performance parameters (service loads). These are as follows: corrosion (Fig. 4), erosion, cavitations, tribological wear, fatigue and brittle cracking. Detection of damages/failures effected by such phenomena often proves very difficult. They are usually found in the form of the unit's failure to operate, pits that weaken the structure, etc. The engineering diagnosis [1 - 4, 10 - 11, 13, 15] offers tools and techniques to detect and identify them. Figs 5 – 8 show examples of such damages/failures.



*Fig. 3. Exemplary mechanical and heat-induced damages in the form of cracks and material defects in the turbine engine structure*

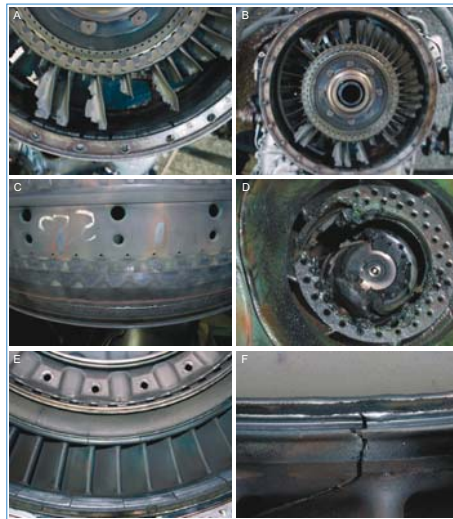


*Fig. 4. Fatigue-corrosion-attributable damages to turbine-engine structural components*

## 5. Description of the occurrence of damages/failures to a set of turbine engines

The occurrence of damages/failures to engineering systems (turbine engines included) that belong to a homogeneous set is featured with the ‘unfit-for-use’ states of structural components or units/(sub)assemblies. In the case of reparable systems (engines), any damages/failures are removed by means of the restoration process.



*Fig. 5. Types of corrosion – macroscopic image of the surface-layer cross-section*

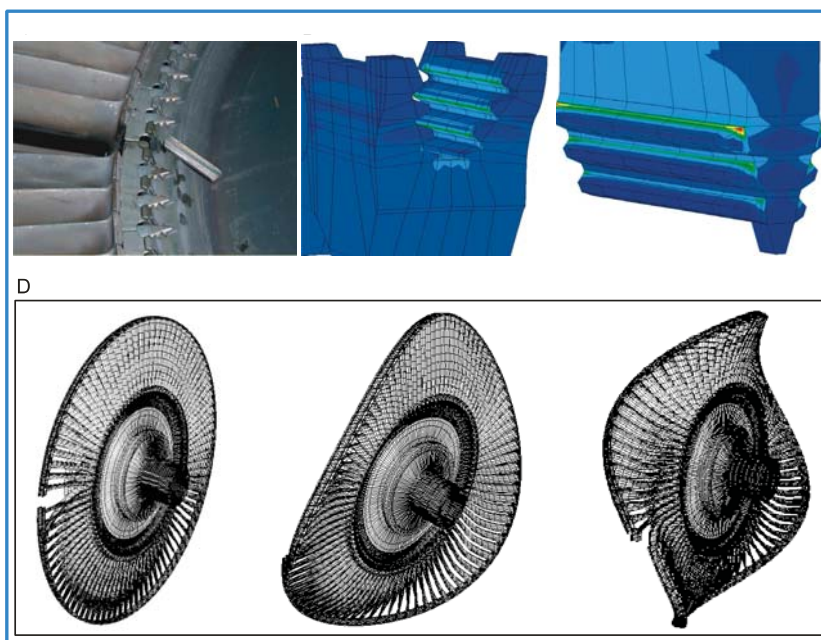


*Fig. 6. Operation-induced III<sup>o</sup> damage to the turbine of a jet engine [12]*

*A – blade ring of the turbine, one blade lacking; B – simulation of destruction of the blade locking piece;  
C- simulation of vibration destructive to the blade locking piece; D – simulation of vibration  
of turbine with one blade lacking*

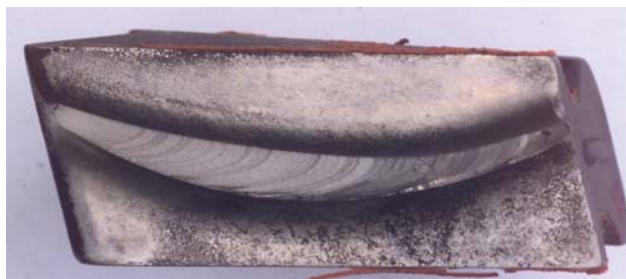


*Fig. 7. Examples of fatigue failures to turbine engine's compressor blade*





Fig. 8. A damaged bearing of the turbine engine shaft

The stochastic occurrence of damages/failures to a set of engines can be described as soon as probability distributions of emerging events (damages/failures) within a certain assumed time interval of system's operation.

Engines belong to the class of reparable engineering systems featured with that the reliability  $R(t)$  after restoration should not change. Unfortunately, there are such engines for which both the number of observed damages/failures and failure rates increase after the major repair/general overhaul. The AL aero engine is a good example. This fact can be explained in the following way: the design structure proves faulty, or incorrect general-overhaul procedures have been developed and recommended by the manufacturer. For such systems, the probability  $P_\tau$  of the random variable of the number of defects/failures  $U_\tau$  in time interval of the system's operation  $[0 \leq \tau \leq t]$  can be most often described with the following expression:

$$P_\tau(t) = \frac{(\lambda t)^n}{n!} \exp[-\lambda t] \quad (1)$$

where:  $\lambda$  - operational failure rate,  
 $n$  - the number of observed damages/failures.

The expected value of equation (1) is as follows:

$$\mathbf{E} \{U_\tau\} = \lambda t = \Lambda \quad (2)$$

For any structural component/part, engine unit/assembly ( $\kappa$ ), the probability  $P_\kappa$  of the random variable of the number of defects/failures  $U_\kappa$  in time interval of the system's operation  $[0 \leq \tau \leq t]$  can be described with the following expression:

$$P_\kappa(t) = \binom{\Lambda}{m} p_\kappa^m (1 - p_\kappa)^{\Lambda - m} \quad (3)$$

of the expected value:

$$\mathbf{E} \{U_\kappa\} = \Lambda p_\kappa \quad (4)$$

where:  $p_\kappa$  - conditional probability that a given component, assembly/unit of the  $\kappa$  type gets failed if the engine is damaged,  
 $m$  - the number of observed damages/failures.

For the  $F$  set of structural components, units/assemblies in engines in service the expected value takes the following form:

$$\mathbf{E} \{F U_{\kappa}\} = F \wedge p_{\kappa} \quad (5)$$

All the above-mentioned values of parameters and conditional probabilities are arrived at by means of suitable statistical surveys under real operating conditions.

## References

- [1] Błachnio J.: *Badanie uszkodzeń statków powietrznych powstających w procesie eksploatacji*. [w] Problemy Badań i Eksploatacji Techniki Lotniczej, R. 5. T. 2. Wydawnictwo ITWL, Warszawa 1993 (in Polish).
- [2] Korczewski Z.: *Contemporary diagnostic methods for ship engines: a report on scientific research activity of Polish Naval Academy in his field*. Polish Maritime Research, Vol. 15. 2 (56). 2008.
- [3] Korczewski Z.: *Failures' identification of cylinder liners of marine diesel engines in operation*. V International Scientific – Technical Conference EXPLO – DIESEL & GAS TURBINE'07, Gdańsk 2007.
- [4] Kustroń K., Lewitowicz J.: *Niesprawności i uszkodzenia statków powietrznych*. XXXIII Szkoła Niezawodności. Szczyrk 2005 (in Polish).
- [5] Lewitowicz J.: *Fizyczne aspekty niesprawności i uszkodzeń statków powietrznych*. Przegląd Wojsk Lotniczych i Obrony Powietrznej, Z. 2. 2002 (in Polish).
- [6] Lewitowicz J.: *Podstawy eksploatacji statków powietrznych*. T. 1. *Statek powietrzny i elementy teorii*. Wyd. ITWL, Warszawa 2001 (in Polish).
- [7] Lewitowicz J.: *Podstawy eksploatacji statków powietrznych*. T. 3. *Systemy eksploatacji statków powietrznych*. Wyd. ITWL, Warszawa 2006 (in Polish).
- [8] Lewitowicz J.: *Przyczyny uszkodzeń statków powietrznych i ich wpływ na niektóre charakterystyki eksploatacyjne*. XXIV Szkoła Niezawodności. Szczyrk 1996 (in Polish).
- [9] Lewitowicz J. i inni: *Podstawy eksploatacji statków powietrznych*. T. 4. *Badanie eksploatacyjne statków powietrznych*. Wyd. ITWL, Warszawa 2007 (in Polish).
- [10] Mironiuk W.: *Possibilities to bearings of the gas turbine engine LM 2500 on the basis of oil research*. V International Scientific – Technical Conference EXPLO – DIESEL & GAS TURBINE'07, Gdańsk 2007.
- [11] Nazarko P.: *Wykorzystanie fal sprężystych w monitorowaniu stanu konstrukcji*. Journal of Aeronautica Integra, No 1 (2). 2007 (in Polish).
- [12] Rządkowski R., Szczepanik R., Kwapisz L., Przysowa R., Drewczyński M.: *Natura frequencies of the last stage turbine bladed disco the aircraft engine*. AIRDIAG'05, Warszawa 2005.
- [13] Szczepanik R., Witoś M.: *Monitorowanie stanu technicznego turbinowych silników lotniczych*. Prace Naukowe ITWL, Z. 10, 2000 (in Polish).
- [14] Tomaszek H., Żurek J., Jasztal M.: *Prognozowanie uszkodzeń zagrażających bezpieczeństwu statków powietrznych*. Wydawnictwo ITE, Radom 2008 (in Polish).
- [15] Zboiński M., Lewitowicz J., Bieńczak K., Wolski J.: *Badanie zużycia łożysk w silnikach lotniczych w procesie eksploatacji*. II Konferencja Problemy Eksploatacji Techniki Wojskowej, Kielce 2000 (in Polish).





## DRAWING CONCLUSIONS ABOUT RELIABILITY OF POWER SYSTEMS FROM SMALL NUMBER OF STATISTICAL DATA

**Roman Liberacki**

*Gdansk University of Technology*  
*ul. Narutowicza 11/12, 80-950 Gdańsk, Poland*  
*tel.: +48 58 3471850, fax: +48 58 3472430*  
*e-mail: [romanl@pg.gda.pl](mailto:romanl@pg.gda.pl)*

### **Abstract**

*Gathering reliability data is quite difficult. Potential sources of such data are: reliability guides and handbooks, data collecting during operation of technical devices, expert judgments. Practice shows that very often the statistical sample we have to our disposal is small and non – homogenous. The goal of the author was to verify, if it is possible to draw out useful in practice conclusions about reliability of technical items from small statistical sample and how to do it. In the article two potential ways to deal with the problem of small reliability data sample have been presented. First way is based on using mathematical statistics methods, the second way uses the fuzzy sets theorem methods.*

**Key words:** power system, reliability data, statistics, fuzzy sets.

### **1. Introduction**

The key problem in making reliability analysis of power systems, is getting credible reliability data, which are the entrance data to created mathematical models. The probabilities of suitable technical elements failures are on generality these data. Problem in this place appears - where from to draw these data. The sources of reliability data for technical structures can be: reliability guides and handbooks, data collecting during operation of technical devices, reliability tests, experts' opinions. Practice shows that very often the statistical sample we have to our disposal is small and non – homogenous.

The goal of the author was to verify, if it is possible to draw out useful in practice conclusions about reliability of technical items from small statistical sample and how to do it.

At first some assumptions have been made: non repairable items have been considered, the statistical distributions of time to failure of items and parameters of those distributions have been objects of interest as well as probability of failure in given period of time.

The two potential ways to deal with the problem of small reliability data sample have been considered. First way was to use mathematical statistics methods, the second way, to solve the problem, was to use the fuzzy sets theorem methods.

### **2. Mathematical statistics methods**

Mathematical statistics methods are based on statistical hypothesis testing. We need to remember that there are two possible errors made in a statistical decision process. Error of the first

kind known as an  $\alpha$  error – which is the error of rejecting a hypothesis when it is actually true. Error of the second kind known as a  $\beta$  error – which is the error of failing to reject a hypothesis when it is in fact false.

In practical applications it is very hard to determine the probability value  $\beta$  of the error of the second kind. When the statistical sample is small and non – homogenous it is just impossible. That is why our care is focused only on the error of the first kind. In advance we impose the probability value of the error  $\alpha$ , which in reliability analysis applications is mostly equal 5 % and is called the level of significance.

First of all we have to state the relevant hypotheses to be tested. Then we carry out the test of significance to reject our hypothesis, or to say that there is no reason to reject the hypothesis. The very important thing is to remember that we cannot say the hypothesis is true, in the best case we can only establish that there is no reason to reject the hypothesis.

## 2.1. Overview of parametric statistics models

Three typical models, described in handbooks [2, 3], have been studied to answer a question: if it is possible to draw out useful in practice conclusions about reliability of technical items from small statistical sample using those models.

### Model 1

Let's make an assumption that our statistical parameter is time to failure of an item. The time to failure has the normal distribution  $N(\mu, \sigma)$  with the mean value  $\mu$  and the standard deviation  $\sigma$ . Moreover the standard deviation value is known for the population of such items.

The hypothesis about the mean value ( $H_0: \mu = \mu_0$ ) is tested against the alternative Hypothesis  $H_a (\mu \neq \mu_0)$  with the significance level of a test  $\alpha$ .

We can see at once, that such model is not useful for drawing conclusions about reliability of technical items if the standard deviation value  $\sigma$  for population is not known. At our considerations the  $\sigma$  value is not known, so the model 1 is useless.

### Model 2

Let's make an assumption that our statistical parameter is time to failure of an item. The time to failure has the normal distribution  $N(\mu, \sigma)$  with the mean value  $\mu$  and the standard deviation  $\sigma$ . Moreover both: the mean value  $\mu$  and the standard deviation value  $\sigma$  are not known for the population of such items. The hypothesis about the mean value ( $H_0: \mu = \mu_0$ ) is tested against the alternative Hypothesis  $H_a (\mu \neq \mu_0)$  with the significance level of a test  $\alpha$ .

To verify the hypothesis  $H_0$  in such case, we can use the hypothesis testing model based on the Student's t distribution. The  $\sigma$  value is estimate than from the sample we have in our disposal.

The model can be useful for us on one condition: we have to be convinced, that the time to failure of technical items has a normal distribution.

### Model 3

Let's make an assumption that our statistical parameter is time to failure of an item. The time to failure has the unfounded statistical distribution with the mean value  $\mu$  and the standard deviation  $\sigma$ . Both parameters  $\mu$  and  $\sigma$  are not known. The hypothesis about the mean value ( $H_0: \mu = \mu_0$ ) is tested against the alternative Hypothesis  $H_a (\mu \neq \mu_0)$  with the significance level of a test  $\alpha$ . To verify the hypothesis  $H_0$  in such case, we can use the hypothesis testing model based on the zero – one standardised normal distribution  $N(0,1)$ . The  $\mu$  and  $\sigma$  values are estimate from the sample we have in our disposal.

The model can be used only when we have at our disposal a large statistical sample number. The large sample number means at least 30 observations [2]. Some authors say 100 or more

observations [3]. Using this model we can estimate the mean value and standard deviation of time to failure of item but we cannot find out the time to failure distribution density function shape.

Similarly, like it was done in the above models for the mean value, we can also make statistical significance tests, using the above models, for the standard deviation values. However there are some conditions to choose the model [2]:

When we have the normal distribution  $N(\mu, \sigma)$  of time to failure,  $\mu$  and  $\sigma$  values are not known and sample number  $n \leq 50$  then we choose model 1.

When we have the normal distribution  $N(\mu, \sigma)$  of time to failure,  $\mu$  and  $\sigma$  values are not known and sample number  $n > 50$  then we choose model 2.

When we have the normal distribution  $N(\mu, \sigma)$  of time to failure,  $\mu$  and  $\sigma$  values not known and sample number  $n \leq 50$  then we choose model 3.

It's worth to notice that we can use those three models for statistical significance tests only if we are convinced, that the time to failure of the item has normal distribution.

## 2.2. Overview of nonparametric statistics models

Nonparametric hypothesis testing models are used when we do not know the random variable probability density function shape as well as parameters of the function. We have face to such situation very often in reliability analysis. However using data set, we have in our disposal, we are able to build a histogram of time to failure (which is our random variable) first, and then make density estimation based on the data to evaluate theoretical probability density function of time to failure.

Statistical hypothesis testing in this case let us only to find out how much our theoretical model (theoretical density function) is adequate to our data distribution in the sample we have. Unfortunately, we never can be sure the model will be adequate to whole population of technical items being the object of our interest.

The most popular nonparametric tests in statistics are: the Pearson's chi - square test and the Kolmogorov - Smirnov test, in that case used as a nonparametric tests of equality of one-dimensional probability distributions used to compare a sample with a reference probability distribution.

The most suitable, to solve the problem given in this article, seems to be the Kolmogorov - Smirnov test. The Pearson's chi - square test needs a large sample (at least 100 items). For the Kolmogorov - Smirnov test a much smaller sample will be enough. Of course the test is adequate for different density functions of the random variable. Moreover the Kolmogorov-Smirnov test is the only test usually used to test whether a given distribution function  $F(x)$  is the underlying probability distribution of  $F_n(x)$ , the procedure may be inverted to give confidence limits on  $F(x)$  itself. If one chooses a critical value of the test statistic  $D_\alpha$  such that  $P(D_n > D_\alpha) = \alpha$ , then a band of width  $\pm D_\alpha$  around  $F_n(x)$  will entirely contain  $F(x)$  with probability  $1 - \alpha$  [4].

The last feature is very important in reliability analysis, because if the random variable is time to failure of the item, then the density function is just the unreliability function. So we are able not only to estimate the unreliability function but also to find the confidence limits for estimated unreliability function.

If the density function of time to failure of technical items is normal, then we can replace the Kolmogorov - Smirnov test by the Lilliefors test (sample size  $n \leq 500$ ) or the Shapiro Wilk test (sample size  $n > 30$ ) or Anderson - Darling test. The last test is more powerful [4].

### 3. Methods based on fuzzy logic

At the beginning let's make an assumption, that we have no statistical data of time to failure of technical items. The only way to collect needed reliability data is to use experts judgments. It is very difficult for experts to give answers in the form of numerical values, for example: the time to failure of the item is 5000 hours or the failure probability per year is 0,003. Much easier is to ask them using linguistic values. The problem arise - how to converse the linguistic values into numerical values. The fuzzy logic can be helpful to deal with the problem.

Assume that the object of our interest is the probability of failure of technical item during one year period of time. The idea of the author is to test the truthfulness of the sentence given in such form: "The item will fail in the one year period of time". Experts give their opinions shown in Tab. 1.

*Tab. 1. An example of using expert opinions in reliability analysis of technical items*

<b>Tested sentence:</b>	<b>Possible experts opinions:</b>
The item will fail during one year period of time.	(1) Sentence is absolutely truth. (2) Sentence is very truth. (3) Sentence is truth. (4) Sentence is rather truth. (5) Sentence is truth or false. (6) Sentence is rather false. (7) Sentence is false. (8) Sentence is very false. (9) Sentence is absolutely false.

Now we can transform expert opinions into fuzzy numbers according to so called "standard degrees of truth" proposed by Baldwin in [1] with the membership functions  $\mu(v)$  given in Fig. 1.

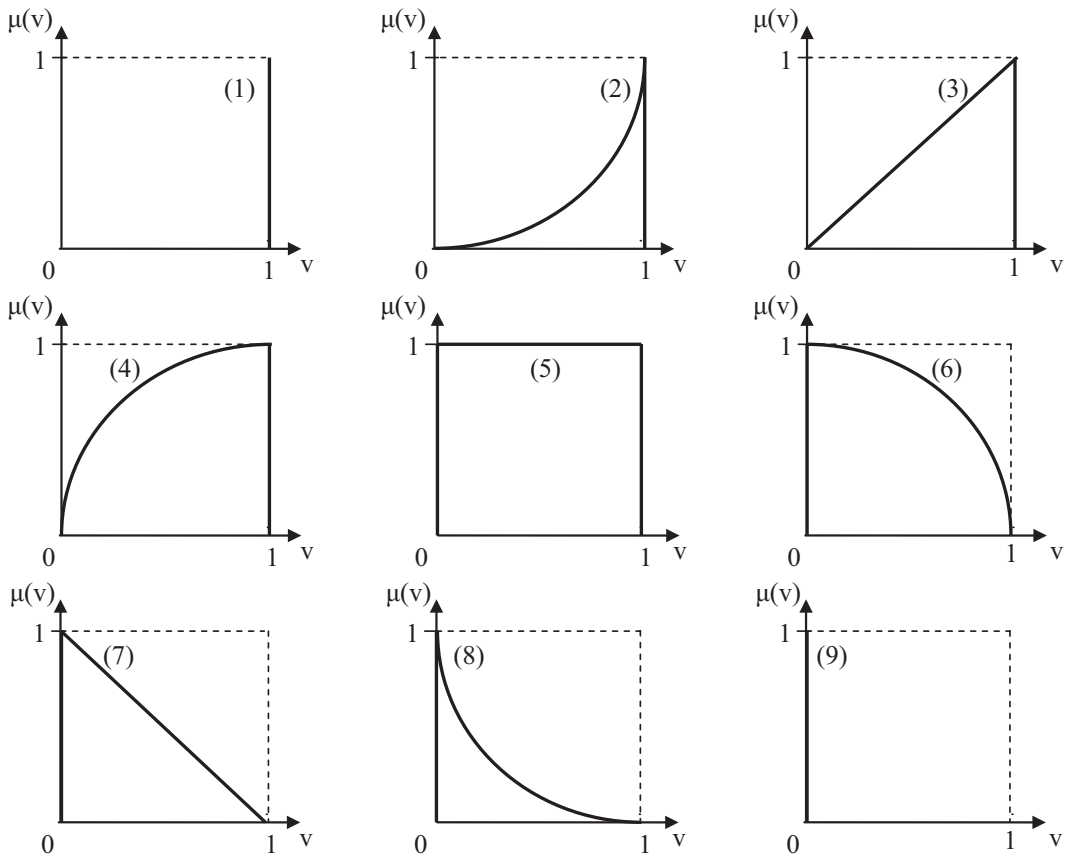


Fig. 1. Standard degrees of truth by Baldwin given as the fuzzy numbers

As the result we receive unreliability value  $F$ , for given period of time, as a fuzzy number. For instance:

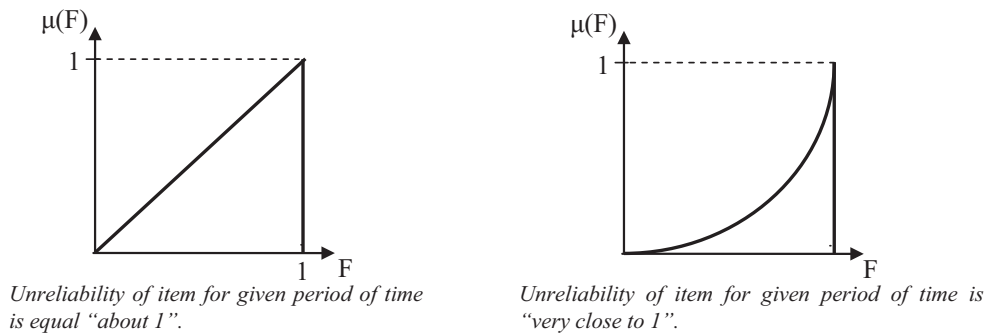


Fig. 2. Examples of unreliability values given in the form of fuzzy numbers

Fuzzy logic is a very good tool when we have in our disposal very imprecise data. In contrast with binary logic, where the truth has only two values (1 – true, 0 – false) fuzzy logic variables of truth may vary from 0 to 1. It gives us possibility to deal with reasoning that is approximate rather than precise. And such situation is very typical in reliability analysis of technical system.

Another interesting way to solve the problem of reliability data evaluation, in author's opinion, seems to be the possibility theory. The main idea of possibility theory is to replace probability measure with possibility measure and necessity measure.

If we are not able to evaluate probability value of item failure, we can try to evaluate the possibility measure and necessity measure – what is much easier. Let assume  $A$  – is event of item failure. Between probability, possibility and necessity measure there is relationship given below [1]:

$$N(A) \leq P(A) \leq \Pi(A) \quad (1)$$

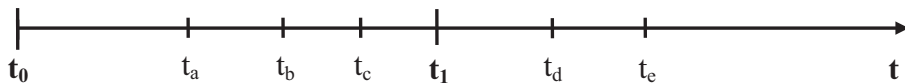
where:

$N(A)$  – necessity measure of event  $A$ ,

$P(A)$  – probability measure of event  $A$ ,

$\Pi(A)$  – possibility measure of event  $A$ .

Now let's try to illustrate usage of the possibility and necessity measure in reliability analysis on example. Given:  $A$  – event of the item failure during one year period of time and 5 statistical data in form of time to failure of five items ( $a, b, c, d, e$ ) presented in Fig. 3.



$t_0 - t_1$  – one year period of time,

$t_0 - t_a$  – time to failure of item  $a$ ,

$t_0 - t_b$  – time to failure of item  $b$ ,

$t_0 - t_c$  – time to failure of item  $c$ ,

$t_0 - t_d$  – time to failure of item  $d$ ,

$t_0 - t_e$  – time to failure of item  $e$ ,

Fig. 3. Time to failure of items

Given the above set of data we can evaluate:

Possibility measure of event  $A$ :  $\Pi(A) = 1$ ,

Necessity measure of event  $A$ :  $N(A) = 3/5 = 0,6$ .

So we can give a statement 1: Probability of item failure during one year period of time can range between (0,6 ; 1).

Imagine now that we have a new information about another ( $f$ ) item time to failure.

First situation: the time to failure of a new item is less then one year – then a new necessity measure is  $N'(A) = 4/6 = 0,67$  so we have a new statement 2: Probability of item failure during one year period of time can range between (0,67 ; 1). Conclusion: statement 2 is not contradicted to statement 1. Statement 1 is still truth.

Second situation: the time to failure of a new item is more then one year – then a new necessity measure is  $N''(A) = 3/6 = 0,5$  so we have a new statement 3: Probability of item failure during one year period of time can range between (0,5 ; 1). Conclusion: statement 3 is contradicted to statement 1. Statement 1 is not truth, but statement 1 is more pessimistic than statement 3 what is consistent with the rule of the worst case which is often used in reliability analysis. Statement 1 then is still worthy for us.

#### 4. Final remarks

In the authors opinion, it is possible to draw out useful in practice conclusions about reliability of technical items from small statistical sample, using statistical methods, fuzzy logic and possibility theory.

We should always to remember, that received results in reliability analysis are never sure. We have to deal with the problem of large uncertainty. Fuzzy logic and probability are the ways of expressing uncertainty.

With the very small data set it is very hard to talk about probability in the classical sense, even from statistical point of view. We should rather to use fuzzy numbers, fuzzy probability with the help of experts judgments or the possibility theory, as it has been shown in the article.

#### References

- [1] Dubois, D., Prade, H., *Possibility Theory. An Approach to Computerised Processing of Uncertainty*, New York 1988.
- [2] Kołowrocki, K., *Wybrane wykłady z rachunku prawdopodobieństwa i statystyki matematycznej*, Fundacja Rozwoju Wyższej Szkoły Morskiej w Gdyni, Gdynia 1994.
- [3] Krywicki, W., Bartos, J., Dyczka, W., Królikowska, K., Wasilewski, M., *Rachunek prawdopodobieństwa i statystyka matematyczna w zadaniach, część II Statystyka matematyczna*, Wydawnictwo Naukowe PWN, Warszawa 1995.
- [4] Stephens, M. A., *EDF Statistics for Goodness of Fit and Some Comparisons*". Journal of the American Statistical Association 69, 1974.







## ANALYSIS OF THE ACTUAL DAMAGES TO THE MARINE ENGINES FROM THE POINT OF VIEW OF DIAGNOSTIC SYSTEMS' CAPABILITIES

**Zbigniew Łosiewicz**

*Zachodniopomorski Uniwersytet Technologiczny w Szczecinie*

*Al. Piastów 41, Szczecin, Poland*

*Tel. +48 600 275 871*

*e-mail: [HORN.losiewicz@wp.pl](mailto:HORN.losiewicz@wp.pl)*

### **Abstract**

*In the article there are presented different operating events leading to the same consequences, i.e. permanent engine damage. The analysis has been carried out of diagnostic actions performed by the operators, of the usefulness of diagnostic systems existing on these ships as well as analysis of the operating values of the latest diagnostic systems in respect of possibility to prevent the described consequences of operating events*

**Key words:** *piston engine of the main ship drive, technical state of engine, diagnostic parameters, diagnosing system, operating events, efficient operation of ship engine*

### **1. Introduction**

Task of the diagnostic system (SDG) is to provide the diagnostic data concerning a ship engine (diagnosed system - SDN). SDG and SDN form a diagnostic system. Efficiency of SD depends on a possibility to obtain accurate and reliable diagnostic information, which enables a mechanic to make accurate and reliable operating decisions.

In the presented operating events such information was missing, what resulted in considerable damages and threat to the crew and ship safety.

In the article there are presented different operating events leading to the same consequences, i.e. permanent engine damage. The analysis has been carried out of diagnostic actions performed by the operators, of the usefulness of SD existing on these ships as well as analysis of the operating values of the latest SDs in respect of possibility to prevent the described consequences of operating events.

### **1. Examples of damage to marine engine identification**

#### **1<sup>st</sup> Example**

In the four-stroke engine if the ship propulsion plant the crack and tear off of the connecting-rod big end bottom cover took place.

After visual inspection of the engine it has been established that a cause of the failure was damage to the bottom cover of a connecting-rod big end.

► Results of the accident examining board inspection:

“Cause of a fatigue crack of the cover was repair by pad welding of discontinuity found in manufacture process after forging and machining operation.

As it results from examination of the damaged part, a cause of failure was the faulty heat treatment in manufacturing process. After pad welding no actions were performed in purpose to eliminate thermal stresses. The fact was neglected that the above element was not among the consumable elements and that it was supposed to serve through a whole period of the engine operation, but it was damaged after 4 years despite it had certificates of two recognised classification societies.

The engine elements getting out of the crankcase caused damage to the oil and fuel pipes. Before black-out occurred in result of stoppage of the engine coupled with a shaft generator, the fuel and oil had been sprinkled around the engine room in result of a pressure generated by the fuel and oil pumps driven by electric motors. It should be admitted that there was an unbelievable luck that the ignition did not occur and fire did not break out, which could have had disastrous consequences”.

“Consequences.

In result of the occurred event a crack of piston no. 4 took place, a piston and crank system was pushed outside (Fig.1), the crank bearing cracked, camshaft case was torn off the cylinder block along 3000 mm length, camshaft was bended, material was torn out in the lower part of cylinder sleeve guiding, the sleeve was planished and wedged up with a connecting rod, the crank-pin no. 4 was deeply damaged, the rotating masses of the system connecting rod were damaged, the fuel pipe cracked and heavy fuel mixed with lube oil (loss of approx. 6.5 t of oil), crankcase base fastening the fuel pumps no. 2, 3, 4 and 5 was torn out, the pistons, sleeves and connecting-rods of a system no. 4 + 5 were crushed.

Explosion did not cause any victims. Despite the fuel fumes the fire did not break out.”(Fig.2)[1]

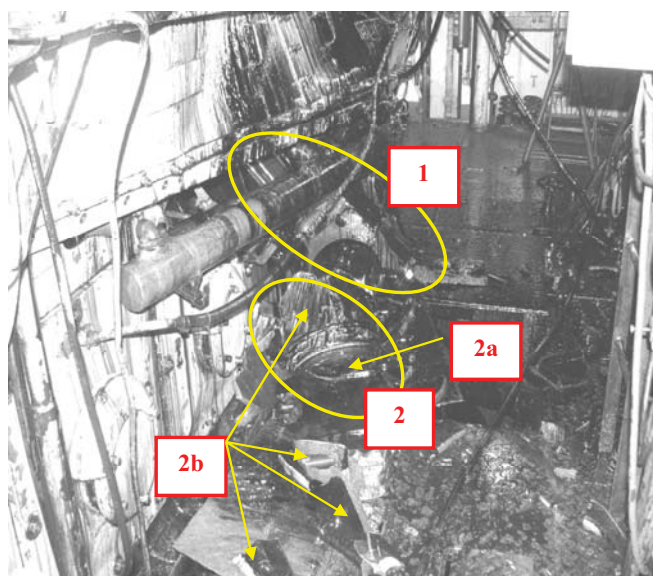


*Fig.1 Visible connecting rod – broken and pushed outside the crankcase (1) and broken piston (2): head (2a) and fragments of piston skirt (2b) [1]*

Indirect results in form of a cost of spare parts, the costs of withdrawing the ship from operation, indirect costs related to lack of propulsion.

► Applied diagnostic system has not raised a warning about exceeding of the limit values..

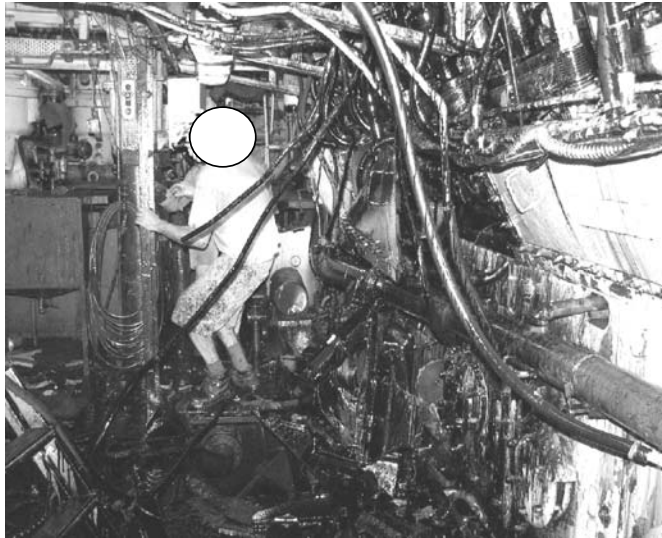


*Fig.2 Fuel spilt around the engine causes fire risk; starboard [1]*

## 2<sup>nd</sup> Example

The fuel piston ring was broken and after two days of voyage piston was seized and the connecting rod was pushed outside of the crankcase.

### ► Results of the accident examining board inspection.

Breaking up of the fuel piston ring resulted in deterioration of the process of lube oil collection from the cylinder sleeve bearing surface and damaging of the sleeve bearing surface by the damaged ring. Excess of lube oil caused origination of oil carbon deposit on the piston skirt, in the ring grooves in the piston crown and, in consequence, the piston rings were stuck with carbon deposit (Fig.3). Lockup of the broken oil ring caused spring crack, which was pushed into a space between the piston skirt and cylinder sleeve. The spring damaged a hardened sleeve surface layer and was pressed into the sleeve.

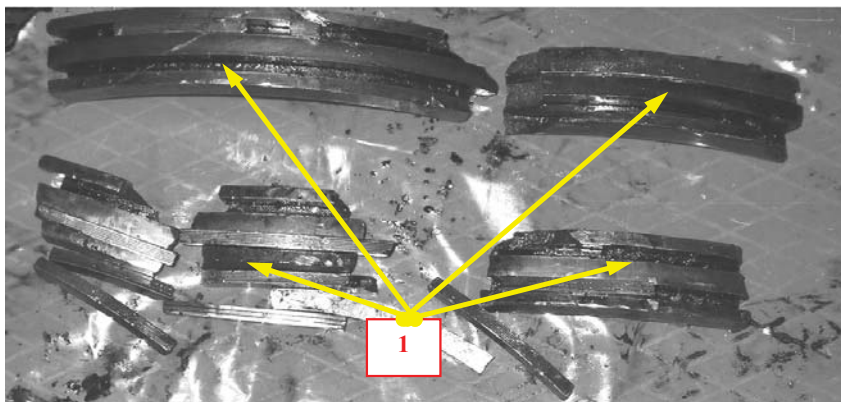


*Fig.3 Origination of oil carbon deposit on the piston skirt, in the ring grooves in the piston crown [source: Ch.Eng. Marceli Stelmaszczuk]*

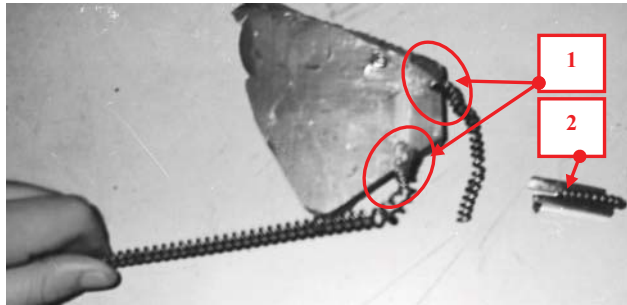


*Fig.4. The spring set in the material of cylinder sleeve (1), oil ring spring lock with a fragment of broken spring (2)*  
[source: Ch.Eng.Marceli Stelmaszczuk]

In effect of friction forces and released heat the spring material was melted into the piston material, what is shown in Fig. 4, 5. Piston seizing caused breaking off the pins fastening a bottom cover of a connecting rod big end with the connecting rod and pushing the connecting-rod outside the casing, causing the effects analogous to those caused by crack of the bottom cover of a connecting rod big end presented in the 1<sup>st</sup> Example.

In the last phase of failure a noise could be heard when the connecting-rod with a piston were being pushed outside the casing.

Pressure drop of the recycle stock and high temperature of cooling water at the outlet from seized sleeve caused the emergency engine stoppage and 'black-out' (the main engine was driving a shaft generator).



*Fig.5. Spring from the piston ring pressed into the cylinder sleeve; visible black carbon deposit originated in result of incomplete combustion of cylinder oil* [source: Ch.Eng. Marceli Stelmaszczuk]

- Applied diagnostic system has not raised a warning about exceeding of the limit values.

## **2. Diagnostic capabilities of the modern SDG**

In recent years the possibilities of engine action monitoring by the technologically advanced diagnosing systems have increased.

- Electronic analyser of combustion process, which monitors the engine action periodically, allows faster detecting of the changes in combustion process parameters
- Temperature sensors detect lower rises of combustion gases temperature at the outlet of the damaged system head,

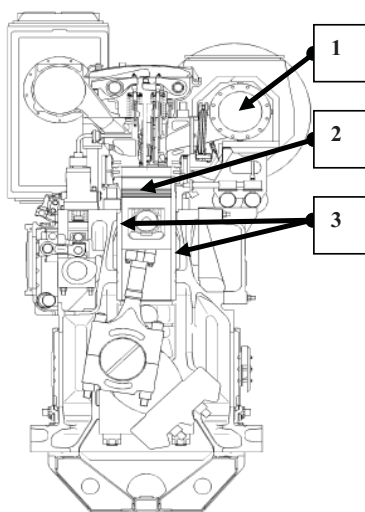


Fig.6 Four-stroke engine section with the places marked, where the sensors are mounted – 1) combustion gases temperature meter, 2) combustion process analyser, 3) detector of piston rings wear, 4) sensor of cylinder sleeve metal temperature [3]

- The systems like SIPWA-TP allow fast detection of temperature rise of the cylinder sleeves metal (Fig.7)
- Diagnosing systems like MAPEX – PR allow fact detection of piston rings wear (Fig.7)

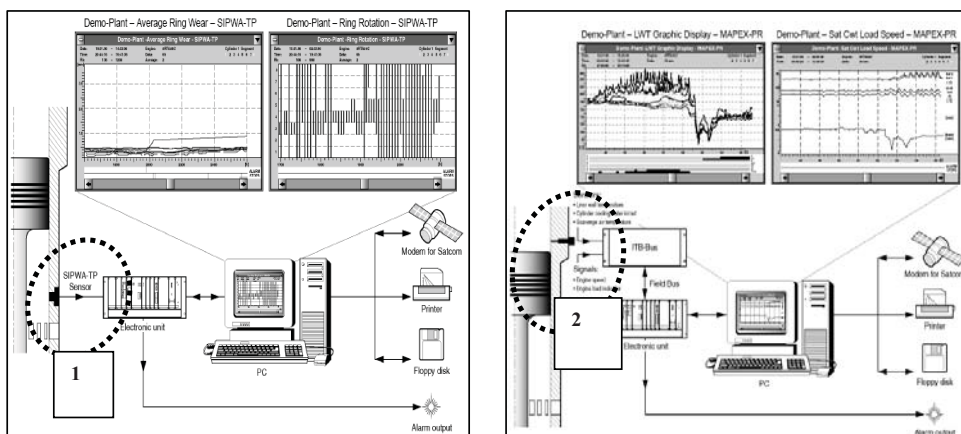


Fig.7 Monitoring of the sleeve metal temperature, a temperature sensor is marked (1), MAPEX – PR system – monitoring of the piston ring wear (2) [2]

- Use of advanced electronics to monitoring of engine action. Data are sent to a ship owner and engine manufacturer (Fig 8).

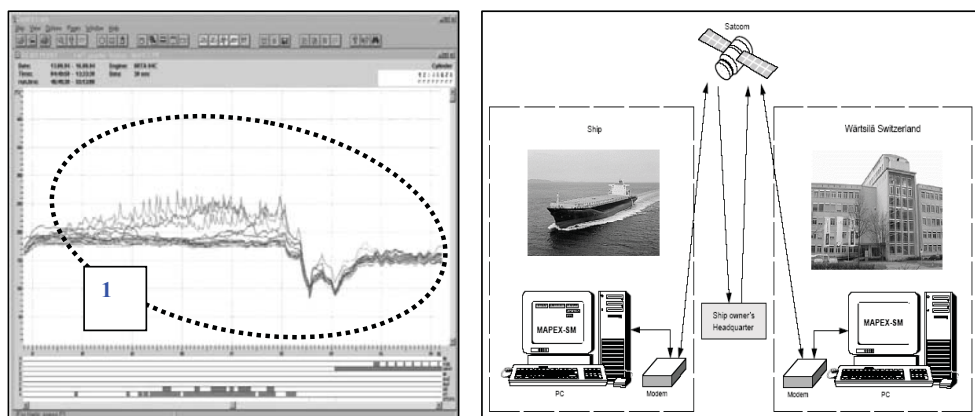


Fig.8. MAPEX – PR programme shows differences between actual measurement and the planned values, e.g. measurement of piston rings wear (1), monitoring of diagnostic parameters by the manufacturer and ship owner office (2) [2]

Increase of a number of the diagnostic data, development of a method of their analysing and processing, are leading to multicriteriality of assessment of the engine technical condition [4,5,6]. In result, probability value of the relation between the diagnostic parameters and engine technical conditions represented by them increases (Fig.9) [7]

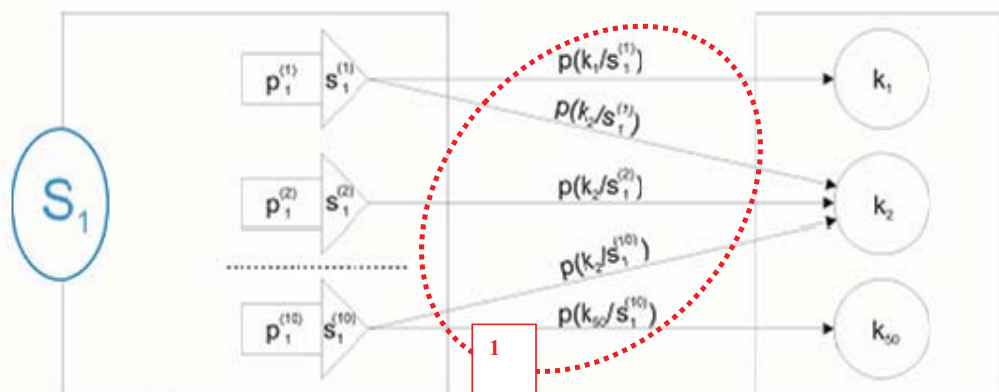


Fig.9 Probabilities of relation occurrence between the diagnostic parameters and engine technical conditions represented by them (1) [7]

## Conclusions

1. During engine operation the events occur, which can not be detected in actual time and the consequences of their occurrence can not be limited (E.1)
2. The event described as E.1 should be recognised as a human error, resulting from lack of experience and knowledge, and lack of the basic safety principles.
3. Electronic combustion process analyser allows faster detecting of the change in engine running parameters, forcing a mechanic to analyse the reasons of these changes.
4. Use of sensors of the sleeve metal temperature allows detecting the temperature rise faster than with indirect method through measurement of temperature of the sleeves cooling water



5. Application of a system determining an extent of the piston rings wear would probably allow early detection of the oil ring damage (E.2)
6. On basis of the quoted examples it is obvious how important it is to use safety procedures at every stage of engine manufacturing and operating
7. Despite the development of diagnostic systems (SD), both SDG and SDN, a very important factor in making operating decisions is an accurate and reliable diagnosis worked out by a mechanic on basis of information from SD (as good as knowledge of a design engineer and manufacturer) and resulting from his knowledge and experience
8. Development of both SDN and SDG (including application of the respective mathematical models) increases probability value of relation between the diagnostic parameters and technical engine conditions represented by them

## References

- [1] Owners Technical Documentation (cofidential).
- [2] Publications and engine documentation of Wartsila Company's.
- [3] Publications and engine documentation of MAN&BW Company's.
- [4] Girtler J., Semi-Markovian model of the process of technical state changes of technical objects. Polish Maritime Research Vol. 11, No 4(42), pp. 3-7, Gdańsk 2004.
- [5] Girtler J., *Physical aspects of application and usefulness of semi-Markovian processes for modeling the processes occurring in operational phase of technical objects*. Polish Maritime Research Vol. 11, No 3(41), pp. 25-30, Gdańsk 2004.
- [6] Pielka D., Łosiewicz Z., *Możliwości zastosowanie metod sztucznej inteligencji do diagnostyki okrętowego silnika spalinowego*, XXVI Sympozjum Siłowni Okrętowych SYMSO, Akademia Marynarki Wojennej w Gdyni, Gdynia, 2005.
- [7] Łosiewicz Z., *Probabilistyczny model diagnostyczny okrętowego silnika napędu głównego statku*, Praca doktorska, Politechnika Gdańska, Gdańsk 2008.







## ASSESSMENT OF FAILURE DISTRIBUTIONS OF MARINE POWER PLANTS FUEL OIL SYSTEMS GROUP

Zbigniew Matuszak, Grzegorz Nicewicz

Maritime Academy of Szczecin  
ul. Wały Chrobrego 1-2, 70-500 Szczecin, Poland  
tel.: +48 91 4809414, +48 91 4809442  
e-mail: [zbimat@am.szczecin.pl](mailto:zbimat@am.szczecin.pl), [niczel@wp.pl](mailto:niczel@wp.pl)

### Abstract

*For the failure moments and the time between failures of the marine power plants fuel oil systems, an attempt of defining the failure distributions has been made. The analysis was based on the observations of the failure of marine power plants fuel oil systems elements. Due to the character of the statistical data, the analysis deals only with relatively simple distributions, most frequently used in the reliability theory. Failures to the marine power plant systems of 10 ships owned by the Polish Steamship Company of Szczecin was the subject of a statistical data analysis. All the ships differed in respect to their place and time of construction as well as their technical parameters. Data on their failures refer to the fuel oil system. The data on marine power plants failures were collected in similar conditions, that is, they were supplied by an engine crew member working in the marine power plant. The data on the failures of particular marine power plant systems were obtained accordingly to the test schedule  $[N, W, T]$ , which means that  $N$  renewable objects were the subject of the test within the time  $T$ . Since the recovery time of the damaged system appeared negligibly short, when compared to the time of the test, it was assumed that consecutive recoveries overlap the failure moments. The statistical analysis dealt with moments  $t_1 \leq t_2 \leq \dots \leq t_n$  of the particular systems' consecutive failures and the length of time intervals  $\tau_n$  between the objects' consecutive failures. In order to carry out the distribution estimation, the statistical package STATISTICA was used.*

**Keywords:** marine power plant, fuel oil system, failure distributions

### 1. Introduction

There has been carried out a statistical analysis of the data concerning marine power plants systems failures on ten ships owned by the Polish Steamship Company of Szczecin. The ships were given symbols from S1 to S10. All the ships differed in respect to their place and time of construction as well as their technical parameters. The data on failures cover the following six marine power plant systems: lubricating oil system - LOS, sea water cooling system - SWCS, fresh water cooling system - FWCS, fuel oil system - FOS, compressed air system - CAS and steam system - SS [2, 3].

The data on marine power plants failures were collected in similar conditions, that is, they were supplied by an engine crew member working in the marine power plant.

The data on the failures of particular marine power plant systems were obtained accordingly to the test schedule  $[N, W, T]$ , which means that  $N$  renewable objects were the subject of the test within the time  $T$ . Since the recovery time of the damaged system appeared negligibly short, when

compared to the time of the test, it was assumed that consecutive recoveries overlap the failure moments.

The statistical analysis dealt with moments  $t_1 \leq t_2 \leq \dots \leq t_n$  of the particular systems' consecutive failures and the length of time intervals  $\tau_n$  between the objects' consecutive failures.

The following has been assumed [2, 3]:

- 1) on ships S1 - S5 time is measured from the moment of the first failure repair;
- 2) for ships S6 - S10 time intervals  $\tau_n$  between the consecutive failures do not include the time between the beginning of sea voyage and the first failure;
- 3) time between the last failure and the end of the observation, that is after 180 days, was taken into consideration.

Total numbers of failures in particular systems of ten tested ships' marine power plants have been presented in table 1.

Table 1. Total number of failures to particular marine power plant systems of all the tested ships

Name of the system	Total number of failures										
	S1	S2	S3	S4	S5	S6	S7	S8	S9	S10	Sum
Lubricating oil system - LOS	3	1	5	6	2	3	21	8	8	9	66
Sea water cooling system - SWCS	7	3	4	4	2	11	5	8	8	5	57
Fresh water cooling system - FWCS	6	2	6	3	2	7	8	9	5	7	55
Fuel oil system - FOS	8	12	5	12	6	19	23	17	7	12	121
Compressed air system - CAS	2	1	2	2	2	5	5	8	3	6	36
Steam system - SS	4	6	3	2	3	10	4	9	3	6	50
Sum	30	25	25	29	17	55	66	59	34	45	385

On the basis of the table, most failures, that is 30% of all of them, can be pointed out in the fuel oil system. It is to be noticed, that among all the tested ships, the prevailing number of failures occurred in case of three of them, that is, S6, S7 and S8.

On the basis of the obtained field data on the system failures, for particular systems, there was built a mathematical model of distribution of time to failure and time between failures.

Due to the type of the statistical data, the most favored distributions appeared relatively simple ones, most frequently applied to the reliability theory. Thus, the possibility of building a model based on the following distributions was sequentially examined:

- the exponential distribution, with probability density function

$$f(t) = \lambda e^{-\lambda t} \quad \text{dla } t \geq 0, \quad (1)$$

- the Weibull distribution, with probability density function

$$f(t) = \alpha \beta^{-\alpha} t^{\alpha-1} e^{-\left(\frac{t}{\beta}\right)^\alpha} \quad \text{dla } t > 0, \quad (2)$$

- the log-normal distribution, with probability density function

$$f(t) = \frac{1}{t\sigma\sqrt{2\pi}} e^{-\frac{(\ln t - \mu)^2}{2\sigma^2}} \quad \text{dla } t > 0, \quad (3)$$

- the gamma distribution, with probability density function

$$f(t) = \frac{\beta^\alpha t^{\alpha-1}}{\Gamma(\alpha)} e^{-\beta t} \quad \text{dla } t > 0. \quad (4)$$

The results of the Kruskal-Wallis test, aided by the program *STATISTICA 8.0*, for the statistical data of fuel oil system failure moments  $t_n$  concerning all the 10 tested ships, at the assumed significance level  $\alpha=0,05$ , turn out to come from one general population (for space reasons the analysis has not been enclosed). However, when considering the statistical data concerning the time between the fuel oil system failures ( $\tau_n$ ) of the 10 analyzed transport ships at the significance level  $\alpha=0,05$ , the hypothesis that they come from one general population needs to be rejected.

Thus, multiple comparisons of rank means (*post-hoc* tests) for the data of the time between failures ( $\tau_n$ ) in reference to each pair of the 10 ships, using the program *STATISTICA 8.0* have been performed. For each comparison, there have been computed 'z' values and 'p' values. On the basis of the obtained results it has been concluded that data from ships S3, S5 and S7 are significantly different from each other. Therefore, it was assumed that the data could belong to various populations. However, to the data from S1, S2, S4, S6, S8, S9 and S10 there was applied the Kruskal-Wallis test, whose results point out that there are no bases for rejecting the hypothesis that they come from one general population at the significance level  $\alpha=0,05$ . A broader presentation of the above analyses goes far beyond the frames of the paper and would require a separate publication, what has initially been done in [1].

On the basis of the obtained results, data on fuel oil system failures of S1, S2, S4, S6, S8, S9, S10 concerning both consecutive failure moments ( $t_n$ ) and time between failures time ( $\tau_n$ ) need to be treated as coming from one general population. Therefore, an attempt of estimation of the obtained empirical distributions by means of the relatively simple theoretical exponential, gamma, log-normal and Weibull distributions, most frequently applied to the reliability theory. In case the exponential, gamma, or log-normal distributions have been accepted as the models, the program *STATISTICA 8.0* enables adjustment and application of tests of goodness of fit. But in reference to the Weibull distribution, it only allows for the estimation of the distribution parameters by the Maximum Likelihood test. Such an analysis has been carried out by means of the statistical package *STATGRAPHICS*, enclosed in [2].

## 2. Tests of goodness of fit

Tests of goodness of fit allow for the verification of the null hypothesis that an analyzed random variable has a distribution which belongs to the appropriate distribution group. The oldest test of goodness of fit appears Pearson's chi-square test, first presented in 1900 [4]. The test can not be applied to small size samples ( $n < 50$ ) [4, 5]. In case of small size samples the Kolmogorov-Smirnov test is used.

Program *STATISTICA* [4, 5] performs the chi-square test by default on the basis of the number of the observed and expected frequencies. Categories containing expected frequencies lower than 5 are grouped to make classes of higher frequency. The number of degrees of freedom for chi-square test statistics is computed in the following way:

$df = \text{number of categories} - \text{number of parameters} - 1$ ,

where:

- *number of categories* refers to the number of classes in the frequencies table, where the expected frequencies are higher than 5;
- *number of parameters* refers to the parameters of the appropriate theoretical distribution.

If the chi-square test outcome is marked with "df adjusted", it means that to compute chi-square test statistic, the program joined the categories with expected frequencies lower than 5. In particular, the neighboring categories are joined until their frequency becomes higher than 5.

If the test demonstrates statistical significance (that is, *p*-value is lower than the assumed significance level, usually 0,05), the hypothesis, that the observed data are liable to a specific distribution, is rejected [4, 5].

The Kolmogorov-Smirnov test can be computed, or not, depending upon the settings on the chart *Options*. In case of two samples, the Kolmogorov-Smirnov test is the test of statistical significance differences between them. Just like the test for one sample, the test statistic compares cumulative distribution functions, in this case it deals with cumulative distribution functions of two samples (e.g. the observed and the simulated values). Big difference between the cumulative distribution functions shows that the data come from two different populations. The test may turn out useful when building a model for assessment whether the expected results (based on the

simulation input data) differ from the observed ones. A significant difference between the expected and observed outcomes usually reveals the model's insufficiency for demonstrating dependencies between the input and output data [4, 5].

In the *Kolmogorov-Smirnov test* group there may be set options for Kolmogorov-Smirnov test. Calculations can be done on the basis of categorized data by clicking the button *Yes (categorized)* - (computing is faster) or using raw data (the procedure is slower; button *Yes (continuous)* must be pressed to make use of this method). In the first case the program calculates the value of D-max statistic on the basis of grouped data, whereas in the second case, at every point it performs calculations of cumulative expected frequencies based on the ordered data. Kolmogorov D-max statistic is the biggest of the absolute differences between the observed and expected cumulative values of the distribution. If the Kolmogorov-Smirnov test shows statistical significance (that is, the  $p$  -value appears lower than the assumed significance level), we may reject the hypothesis assuming that the observed data are subject to the hypothetical distribution.

Using the *STATISTICA 8.0* program (chart *Distribution fitting*), the verifications of null hypothesis of fitting the distribution of the failure moments ( $t_n$ ) and the time between failures ( $\tau_n$ ) in marine power plants fuel oil systems with the following theoretical distributions: exponential, gamma and log-normal were carried out; for this purpose Kolmogorov-Smirnov (continuous) test was applied. For reasons of space the *STATISTICA 8.0* spreadsheets with the observed and expected frequencies and the outcome of the tests of goodness of fit data with theoretical distributions fit have not been included. The results of the tests of goodness of fit have been shown on histograms and cumulative histograms of marine power plants fuel oil systems failure moments ( $t_n$ ) and the time between failures ( $\tau_n$ ) with probability density functions and cumulative distribution functions of the discussed theoretical distributions.

### 3. Results of the tests of goodness of fit of the consecutive failure moments

The performance of the Kolmogorov-Smirnov test for the exponential distribution, has resulted in its following parameters: number of categories: 17; lower limit: 0; upper limit: 170; lambda: 0,0139; observed mean: 71,7130; observed variance: 1907,3664.

Histogram and cumulative histogram of the consecutive marine power plants fuel oil systems failure moments with the probability density function of the exponential distribution and the cumulative distribution function of the exponential distribution and with the Kolmogorov-Smirnov test results inserted have been shown in fig. 1.

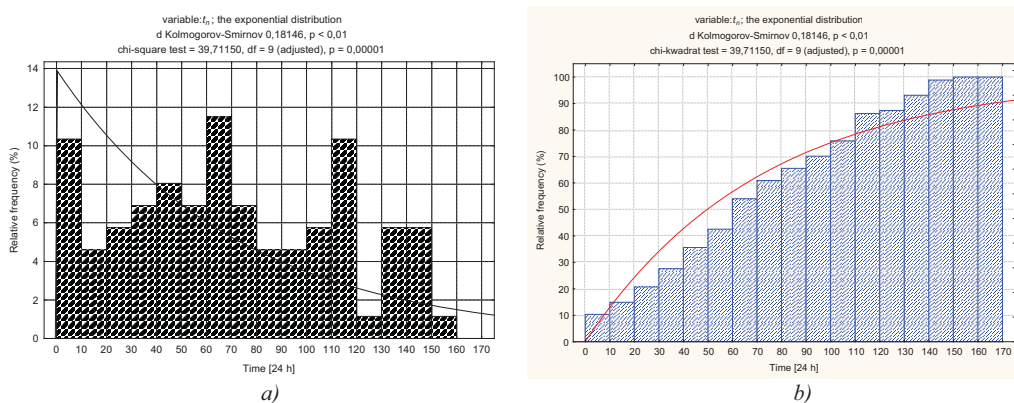


Fig. 1. Histogram (a) and cumulative histogram (b) of the consecutive failure moments of marine power plants fuel oil systems with probability density function of the exponential distribution (full line) (a) and cumulative distribution function of the exponential distribution (full line) (b) and with the results of the Kolmogorov-Smirnov test inserted

There are no bases for accepting the null hypothesis that the empirical distribution of the marine power plants fuel systems consecutive failure moments  $t_n$  complies with the exponential distribution.

The Kolmogorov-Smirnov test applied to the gamma distribution has resulted in its following parameters: number of categories: 17; lower limit: 0; upper limit: 170; scale parameter: 64,6862, shape parameter: 3,2067; observed mean: 71,7130; observed variance – 1907,3664.

Histogram and cumulative histogram of the consecutive marine power plants fuel oil systems failure moments with the probability density function of the exponential distribution and the cumulative distribution function of the exponential distribution and with the Kolmogorov-Smirnov test results, inserted, have been shown in fig. 2.

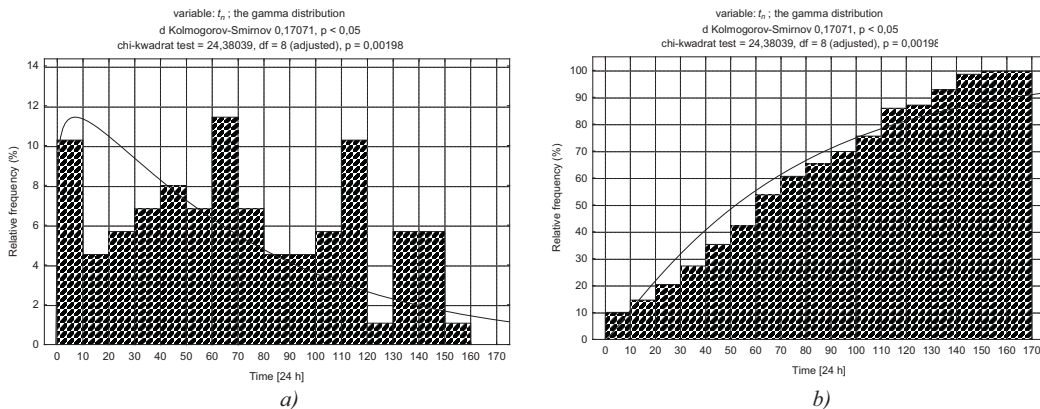


Fig. 2. Histogram (a) and cumulative histogram (b) of the consecutive failure moments of marine power plants fuel oil systems with probability density function of the gamma distribution (full line) (a) and cumulative distribution function of the gamma distribution (full line) (b) and with the results of the Kolmogorov-Smirnov test inserted

There are no bases for accepting the null hypothesis assuming that the empirical distribution of the marine power plants fuel oil systems consecutive failure moments  $t_n$  complies with the gamma distribution.

The Kolmogorov-Smirnov test applied to the log-normal distribution has resulted in its following parameters: number of categories: 17; lower limit: 0; upper limit: 170; mean (M): 3,7573; variance: 3,20669; observed mean: 71,7130, observed variance: 1907,3664.

Histogram and cumulative histogram of the consecutive marine power plants fuel oil systems failure moments with the probability density function of the log-normal distribution and the cumulative distribution function of the log-normal distribution and with the Kolmogorov-Smirnov test results, inserted, have been shown in fig. 3.

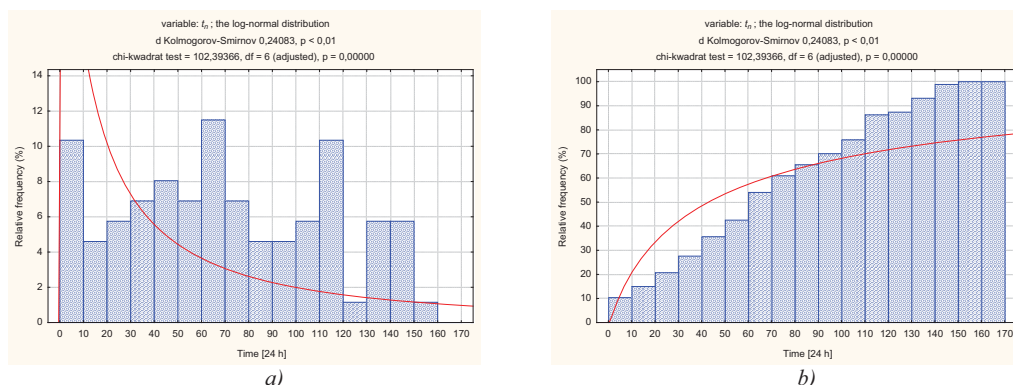


Fig. 3. Histogram (a) and cumulative histogram (b) of the consecutive failure moments of marine power plants fuel oil systems with probability density function of the log-normal distribution (full line) (a) and cumulative distribution function of the log-normal distribution (full line) (b) and with the results of the Kolmogorov-Smirnov test inserted

There are no bases for accepting the null hypothesis that the empirical distribution of the marine power plants fuel systems consecutive failure moments  $t_n$  complies with the log-normal distribution.

To define the goodness of fit of the obtained empirical distribution of the marine power plants fuel oil systems' consecutive failure moments  $t_n$  with the Weibull distribution, a graphical method (the window *Graphs 2D>Histograms 2D* of the program *STATISTICA 8.0*) have been used. Parameters of the Weibull distribution  $\alpha$ ,  $\beta$  have been estimated by the Maximum Likelihood test. The obtained parameters for the distribution are as follows: number of categories: 17; lower limit: 0; upper limit: 170;  $\alpha=1,2665$ ;  $\beta=75,5095$ .

Histogram and cumulative histogram of the consecutive marine power plants fuel oil systems failure moments with the probability density function of the Weibull distribution and the cumulative distribution function of the Weibull distribution have been shown in fig. 4.

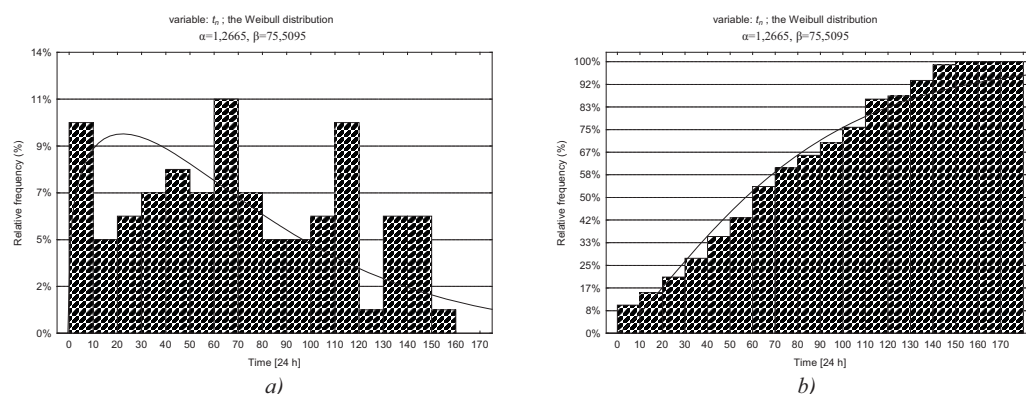


Fig. 4. Histogram (a) and cumulative histogram (b) of the consecutive failure moments of marine power plants fuel oil systems with probability density function of the Weibull distribution (full line) (a) and cumulative distribution function of the Weibull distribution (full line) (b) with the distribution parameters  $\alpha=1,2665$ ,  $\beta=75,5095$

#### 4. Results of the tests of goodness of fit of the time between failures

The Kolmogorov-Smirnov test applied to the exponential distribution has resulted in its following parameters: number of categories: 13; lower limit: 0; upper limit: 130; lambda: 0,0704; observed mean: 14,1979, observed variance: 247,5795.



Histogram and cumulative histogram of the time between the failures of marine power plants fuel oil systems with the probability density function of the exponential distribution and the cumulative distribution function of the exponential distribution and with the Kolmogorov-Smirnov test results, inserted, have been shown in fig. 5.

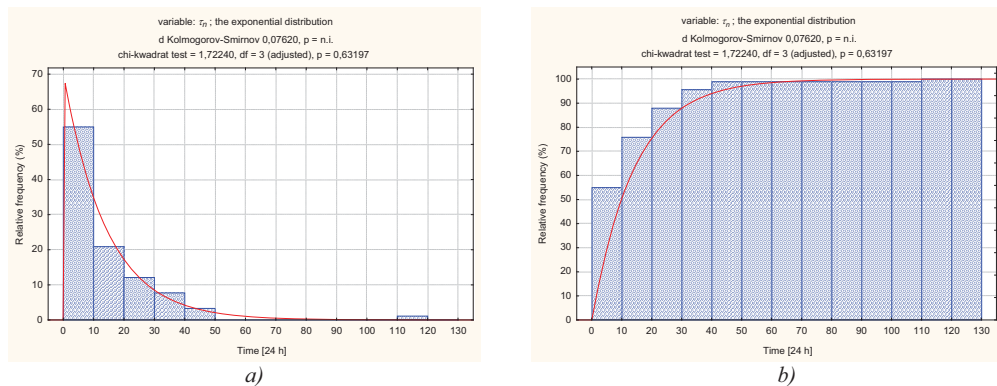


Fig. 5. Histogram (a) and cumulative histogram (b) of the time between failures of marine power plants fuel oil systems with probability density function of the exponential distribution (full line) (a) and cumulative distribution function of the exponential distribution (full line) (b) and with the results of the Kolmogorov-Smirnov test inserted

There are no bases for rejecting the null hypothesis that the empirical distribution of the time between failures  $\tau_n$  of the marine power plants fuel oil systems complies with the exponential distribution.

The Kolmogorov-Smirnov test applied to the gamma distribution has resulted in its following parameters: number of categories: 13; lower limit: 0; upper limit: 130; scale parameter: 13,8525; shape parameter: 1,6149; observed mean: 14,1979; observed variance: 247,5795.

Histogram and cumulative histogram of the time between the failures of marine power plants fuel oil systems with the probability density function of the gamma distribution and the cumulative distribution function of the gamma distribution and with the Kolmogorov-Smirnov test results, inserted, have been shown in fig. 6.

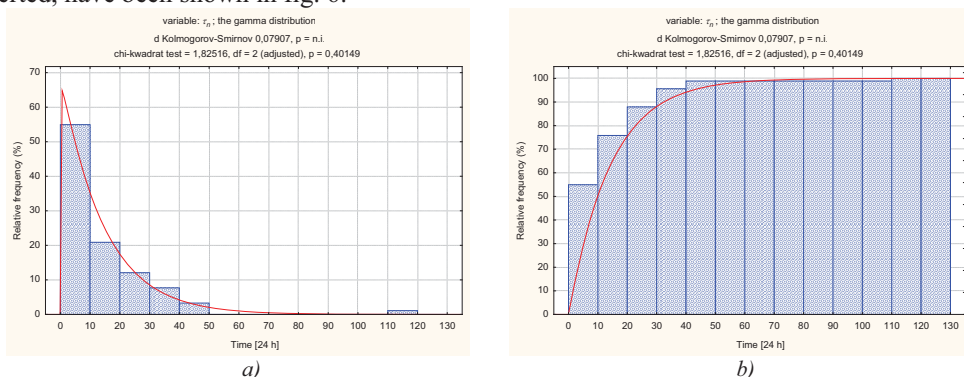


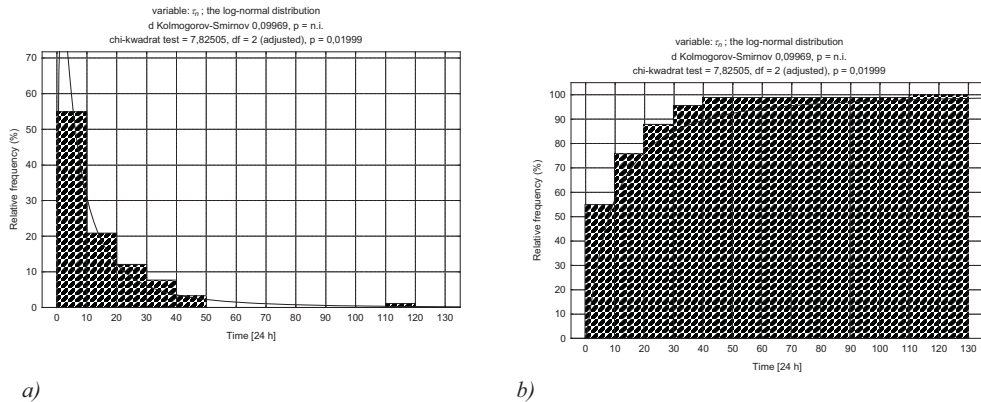
Fig. 6. Histogram (a) and cumulative histogram (b) of the time between failures of marine power plants fuel oil systems with probability density function of the gamma distribution (full line) (a) and cumulative distribution function of the gamma distribution (full line) (b) and with the results of the Kolmogorov-Smirnov test inserted

There are no bases for rejecting the null hypothesis that the empirical distribution of the time between failures  $\tau_n$  of the marine power plant fuel system complies with the gamma distribution.

The Kolmogorov-Smirnov test applied to the log-normal distribution has resulted in its following parameters: number of categories: 13; lower limit: 0; upper limit: 130; mean (M):

2,0908; variance: 1,6149; observed mean: 14,1979; observed variance: 247,5795.

Histogram and cumulative histogram of the time between the failures of marine power plants fuel oil systems with the probability density function of the log-normal distribution and the cumulative distribution function of the log-normal distribution and with the Kolmogorov-Smirnov test results, inserted, have been shown in fig. 7.



a) b)  
Fig. 7. Histogram (a) and cumulative histogram (b) of the time between failures of marine power plants fuel oil systems with probability density function of the log-normal distribution (full line) (a) and cumulative distribution function of the log-normal distribution (full line) (b) and with the results of the Kolmogorov-Smirnov test inserted

There are no bases for rejecting the null hypothesis that the empirical distribution of the time between failures ( $\tau_n$ ) of the marine power plants fuel oil systems complies with the log-normal distribution.

To define the goodness of fit of the obtained empirical distribution of the time between failures in the marine power plants fuel oil systems ( $\tau_n$ ) with the Weibull distribution, a graphical method (the window *Graphs 2D>Histograms 2D* of the program *STATISTICA 8.0*) have been used. Parameters of the Weibull distribution  $\alpha, \beta$  have been estimated by the Maximum Likelihood test. The obtained parameters for the distribution are as follows: number of categories: 13; lower limit: 0; upper limit: 130;  $\alpha=0,9928$ ;  $\beta=14,1522$ .

Histogram and cumulative histogram of the time between failures ( $\tau_n$ ) of marine power plants fuel oil systems and the probability density function of the Weibull distribution and the cumulative distribution function of the Weibull distribution have been shown in fig. 8.

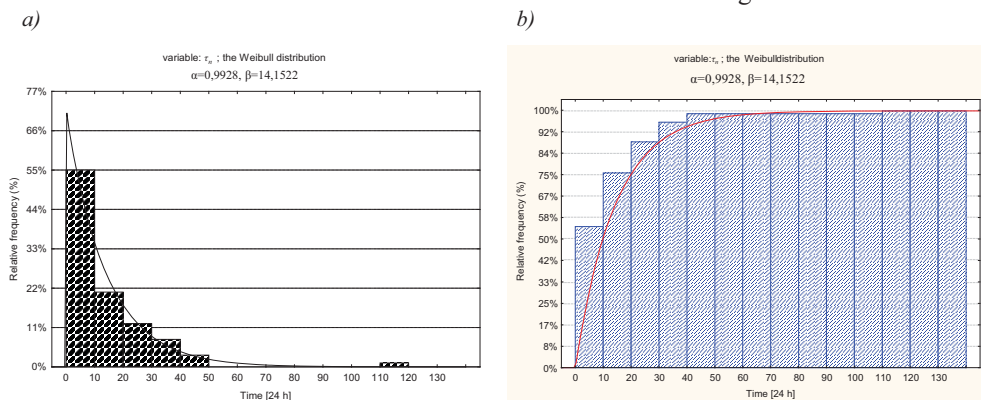


Fig. 8. Histogram (a) and cumulative histogram (b) of the time between failures of marine power plants fuel oil systems with probability density function of the Weibull distribution (full line) (a) and cumulative distribution function of the Weibull distribution (full line) (b) with the distribution parameters:  $\alpha=0,9928$ ,  $\beta=14,1522$



## 5. Final remarks

In case of the consecutive failure moments of the marine power plants fuel oil systems, non of the discussed theoretical distributions turns out a sufficiently appropriate model for the obtained empirical distribution.

However, for the time between failures of the marine power plants fuel oil systems, there are no bases for rejecting the null hypothesis assuming the obtained empirical distribution comply with each of the considered theoretical distributions, that is, the exponential, gamma, log-normal and Weibull.

Program *STATISTICA 8.0* enabled the fit of the theoretical distribution and carrying out the tests of goodness of fit in case of the assumption that exponential, gamma and log-normal distributions become the models. But in reference to the Weibull distribution, due to the Maximum Likelihood test, only the distribution parameters could be estimated. The analysis carried out by means of a statistical package *STATGRAPHICS*, presented in [2], in reference to the Weibull distribution, brought slightly different, more unique results; but it was made by a much older statistical package than *STATISTICA 8.0*, and for the space reason it was not possible to discuss in details the comparison of the test results obtained by means of both statistical packages.

## References

- [1] Chybowski L., Matuszak Z., *Porównanie kompleksowych pakietów oprogramowania do prowadzenia wieloaspektowej analizy niezawodności*. Sbornik naučných trudow meždunarodnoj baltijskoj asociacii maszynostroiteliej BALTTECHMASZ -2006, Izdatelstwo KGTU, Kaliningrad 2006, pp. 277-289.
- [2] Matuszak Z., *Modeli otkazow i prinadležnost dannyh ob otkazach k generalnoj sowokupnosti na primierie sudowych energetičeskich ustanowok*. Kaliningradskij gosudarstwiennyj techničeskij uniwersytet, Kaliningrad 2002, Monografia.
- [3] Matuszak Z., *Kompozicii raspredelenij charakteristik nadiožnosti i modeli otkazow sistem sudowych energetičeskich ustanowok*. Kaliningradskij gosudarstwiennyj techničeskij uniwersytet, Kaliningrad 2003, Monografia.
- [4] Stanisław A., *Przystępny kurs statystyki. Tom 1: Statystyki podstawowe*. StatSoft, Kraków 2006.
- [5] StatSoft – Statistica 8.0, *Podręcznik elektroniczny STATISTICA*.





## HEAVY DUTY DIESEL EMISSION ROAD TESTS

**Jerzy Merkisz, Jacek Pielecha**

*Poznań University of Technology*  
*ul. Piotrowo 3, 60-965 Poznań*  
*tel.: +48 61 6652207, fax: +48 61 6652204*  
*e-mail. jerzy.merkisz@put.poznan.pl, jacek.pielecha@put.poznan.pl*

**Wojciech Gis**

*Motor Transport Institute*  
*ul. Jagiellońska 80, 03-301 Warszawa*  
*tel.: +48 22 8113231/125*  
*e-mail: wojciech.gis@its.waw.pl*

### **Abstract**

*The paper present the results of emission tests of city buses (Euro 5 hybrid and Euro 4 conventional diesel), under real traffic conditions with the use of a portable emission testing system. The tests have been carried out in city traffic conditions on road portions of several kilometers each; The test results contain information on the vehicle emission level in operation and pertain to real road conditions.*

**Keywords:** *emissions, road tests, diesel engines, hybrid drivetrains*

## **1. Introduction**

Contemporary vehicle manufacturers focus not only on the comfort and safety of their products but also on the issues related to the fuel economy [3, 18] and the emission level [1]. Owing to a high commitment of the vehicle manufacturers recent years saw a reduction of vehicle emission level from Euro 1 to Euro 4, which reduces the pollution by more than 90% [1].

European emission regulations for heavy duty vehicles set forth in Directive 1999/96/WE are commonly known as Euro 1...5 standards. Since October 2005 all newly homologated vehicles and since October 2006 all newly registered commercial vehicles (*Heavy Duty Diesel*, including buses) have had to comply with the Euro 4 standard. More stringent standard - Euro 5 will come into force in October 2008 (homologation) and October 2009 (registration) respectively. Additionally, the Directive 2005/55/WE adopted in 2005 introduced the EEV standard (*Enhanced Environmentally Friendly Vehicle*) for vehicles of particularly low emission level. The purpose of this directive is to replace the previous directives 88/77/EEG, 96/1/WE, 1999/96/WE and 2001/27/WE through a unification and consolidation of the regulations in a single act. Directive 2001/27/WE came into force on 9.11.2006. As the Euro 4 standard was introduced, the manufacturers of all powertrains of heavy duty vehicles including city buses had to fit them with OBD (*On-Board Diagnostic*) emission monitoring system [2, 4, 10, 14]. The implementation of the Euro 4 and Euro 5 standards

forced the manufacturers to come up with new solutions such as EGR (exhaust gas recirculation) or SCR (selective catalytic reduction), the latter requiring an on-board supply of a solution of carbamide (AdBlue).

Currently, more attention is drawn to the measurement of the emissions under variable operating conditions, particularly regarding heavy duty vehicles. Emission testing in road conditions is in higher demand than stationary driving cycles. On-road emission testing became possible owing to a rapid advancement of the measuring techniques that came in recent years [5, 6, 8, 13, 17]. The said advancement also aimed at the measurement of extremely small pollutant concentration in the exhaust gas [7, 9, 15]. The Institute of Combustion Engines and Transport with a portable emission testing system carried out a series of on-road emission tests of two city buses with two different powertrains: hybrid and conventional diesel.

## 2. Emission testing methodology

The on-road emission tests were carried out in city traffic in Poznań (Fig. 1). The tests were performed on the city main streets in the afternoon, when the traffic was moderate. Such conditions were selected in order to ensure the highest possible use of the engine work field (regular bus operation was simulated including 10 second stops at the bus stops). The object of the tests were two buses manufactured by Solaris: one unit was fitted with a hybrid engine (Hybrid H18) and the other one – with a conventional diesel engine (U18 Aarhus) – characteristics – Tab. 1. The buses were selected based on the similarity of service routes (number of passengers) and at the same time in such a way that there was a possibility of comparing their functionality and ecology under real conditions.

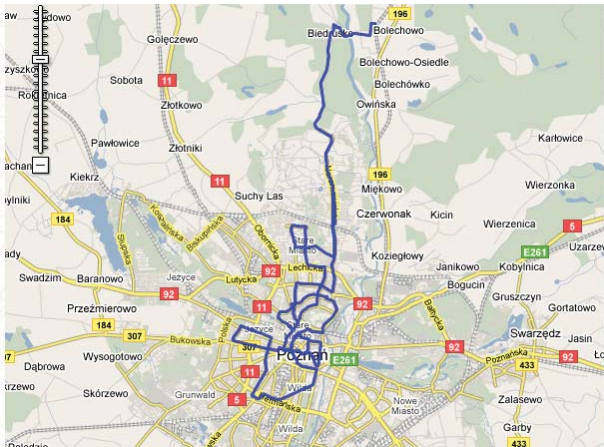


Fig. 1. A road portion (routes marked) used for the measurement of the buses emission level

Tab. 1. Technical data of the tested buses

Parameter	Conventional diesel bus	Hybrid Bus (diesel + electric)
1	2	3
Engine type	DAF PR 265	Cummins ISB 250
Displacement [cm <sup>3</sup> ]	9200	6700
Emission standard	Euro 4	Euro 5
Transmission	VOITH DIWA 86 4.5	ALLISON Ep50
Vehicle weight [kg]	16,700	17,800
Vehicle weight full load [kg]	21,200	22,000

For the measurement of the exhaust emissions the authors used a portable SEMTECH DS analyzer [9, 16] by SENSORS LTD (Fig. 2). The analyzer measured the fuel consumption and the exhaust emissions (Tab. 2) at the same time recording the exhaust mass flow. The exhaust gases entering the analyzer through a sensor maintaining the temperature of 191°C (Fig. 3) were filtered for particulate matter (diesel) and then the concentration of hydrocarbons was measured in a FID (flame ionization detector). Next, the exhaust gases were cooled down to a temperature of 4°C and the measurement of the concentration of NO<sub>x</sub> took place (non-dispersive method with the use of ultraviolet radiation that enabled the measurement of both nitrogen oxide and nitrogen dioxide), carbon monoxide, carbon dioxide (non-dispersive method with the use of infrared radiation) and oxygen (electrochemical analyzer). The data could be directly transferred to the analyzer central unit from the vehicle diagnostic system and the GPS.



Fig. 2. View of the testing device (Semtech DS for exhaust emissions tests) fitted in the bus

Tab. 2. Characteristics of the portable exhaust gas analyzer SEMTECH DS

Parameter	Method of measurement	Accuracy
1	2	3
1. Concentration of		
CO	NDIR – non-dispersive (infrared), range 0–10%	±3%
HC	FID – flame ionization, range 0–10,000 ppm	±2.5%
NO <sub>x</sub> = (NO + NO <sub>2</sub> )	NDUV – non-dispersive (ultraviolet), range 0–3000 ppm	±3%
CO <sub>2</sub>	NDIR – non-dispersive (infrared), range 0–20%	±3%
O <sub>2</sub>	electrochemical, range 0–20%	±1%
Sampling frequency	1–4 Hz	
2. Exhaust gas flow	Mass flow intensity T <sub>max</sub> up to 700°C	±2.5% ±1% of the range
3. Pre-heating time	15 min	
4. Response time	T <sub>90</sub> < 1 s	
5. Supported diagnostic systems	SAE J1850/SAE J1979 (LDV) SAE J1708/SAE J1587 (HDV) CAN SAE J1939/J2284 (HDV)	



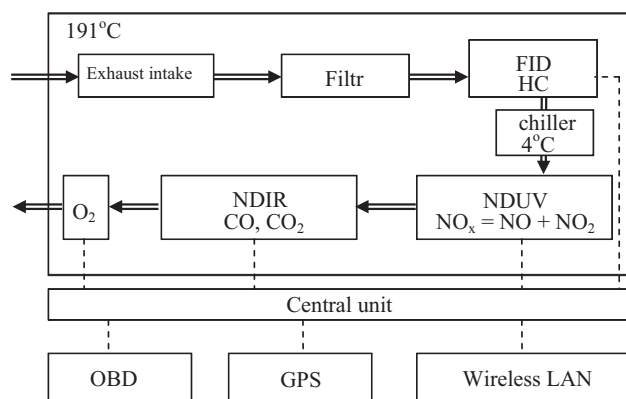


Fig. 3. Schematics of the portable analyzer SEMTECH DS – exhaust gas flow (==) and electrical connections (- - -) shown

### 3. Tests results and analysis

With the use of the portable system the emissions of CO, HC, NO<sub>x</sub>, CO<sub>2</sub> with 1 second interval were measured as well as the changes in the engine speed and torque– the parameters taken from the vehicle OBD (CAN SAE J1939) and used to calculate the emissions related to the unit energy of the engine. Example data recorded during the cruise are shown in Fig. 4. The ECU of the hybrid vehicle limited the torque of the diesel engine when the vehicle began to move – while accelerating up to the speed of 5 km/h the electric motor was used and the diesel engine remained idle (lower toxic emissions).

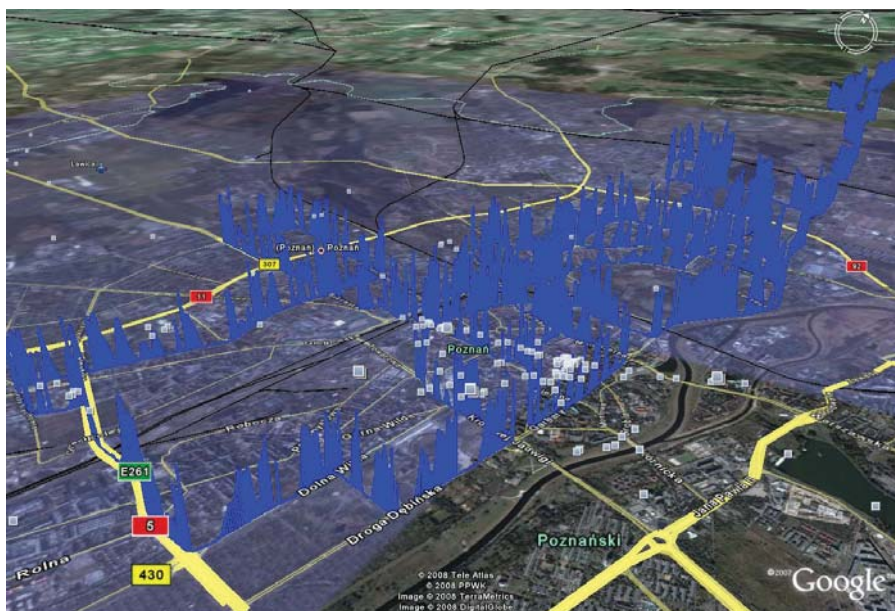


Fig. 4. Example measurement recording (CO<sub>2</sub> emission overlaid on the vehicle route during the emission tests)

The calculations of the time density characteristics for the engine parameters in the urban traffic revealed certain dependencies that characterize the share of given parameters of engine opera-

tion in the total cruise time (Fig. 5). For the hybrid bus a large share of the operating time falls within the engine operation range of 700–900 rpm and engine load of approximately 10%. For the bus with the conventional powertrain, over 2000 s (approx. 20% of the engine operating time, total engine operating time amounts to 10,200 s) of the engine operating time was 600 rpm and the engine load approximately 10%. The ranges of engine parameters used in the city traffic were: idle speed (for both of the tested buses) and the external characteristics operating range (maximum load for a given engine speed). At the same time, for the hybrid bus a higher share of part loads is more visible.

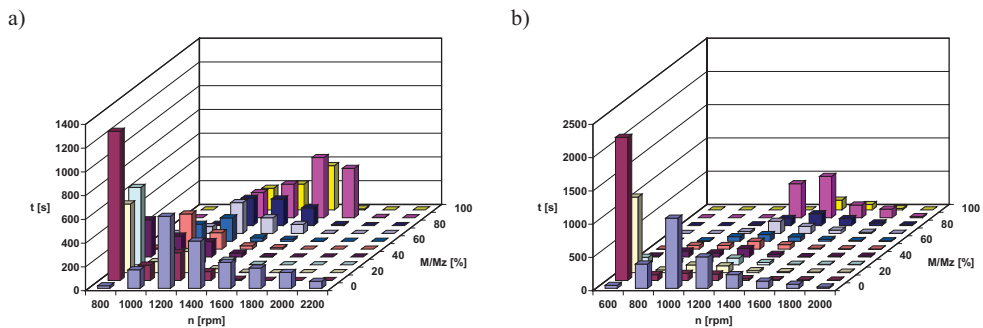


Fig. 5. Characteristics of the operating time density: a) hybrid, b) conventional diesel

The highest intensity of the CO<sub>2</sub> emission in the tested city traffic conditions we can observe for medium engine speeds and for the maximum engine torque (hybrid vehicle, Fig. 6a) and for the conventional diesel engine the CO<sub>2</sub> emission (fuel consumption) increases proportionally to the engine speed and engine load (Fig. 6b). The CO<sub>2</sub> emissions for the hybrid vehicle are approximately 20–30% lower than the analogical values for a conventional diesel vehicle. This could indicate a lower fuel consumption; the total fuel consumption is calculated with the use of this data as well as the share of the engine operation in given engine speed ranges and loads.

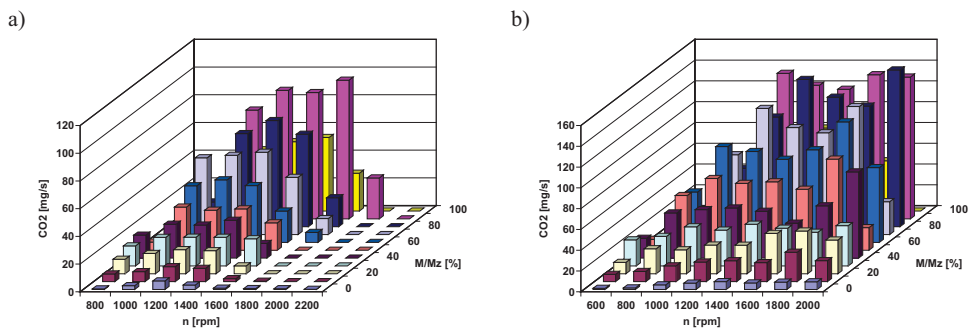


Fig. 6. Time density characteristics of the CO<sub>2</sub> emission: a) hybrid, b) conventional diesel

The maximum intensity of CO emission, given in milligrams per second, falls within the range of maximum engine loads and medium engine speeds (hybrid vehicle, Fig. 7a) and for the conventional vehicle this range is approximately 4–5 times wider (maximum for high loads and medium engine speeds, Fig. 7b). This mainly results from the differences in the engine capacity and the fact that for the hybrid vehicle medium loads are more frequently the case as compared to the conventional diesel engine, which operates at high loads for most of the time.

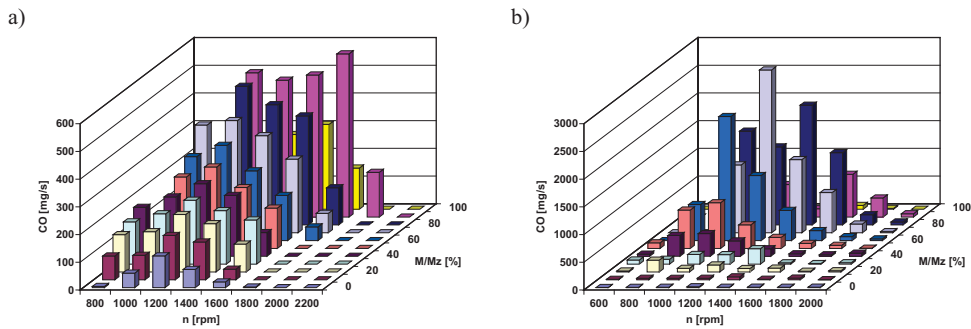


Fig. 7. Time density characteristics of the CO emission: a) hybrid, b) conventional diesel

The maximum values of the emission of hydrocarbons for both of the powertrains is similar (approximately 25–35 mg/s), yet, for the hybrid vehicle only the maximum values reach 25 mg/s (Fig. 8a); in the range of medium engine speeds and engine loads the values do not exceed 20 mg/s (Fig. 8b). For the conventional diesel vehicle there is a nearly linear dependence between the HC emission and the engine speed and load (the maximum is observed for the maximum values of the engine speed and load).

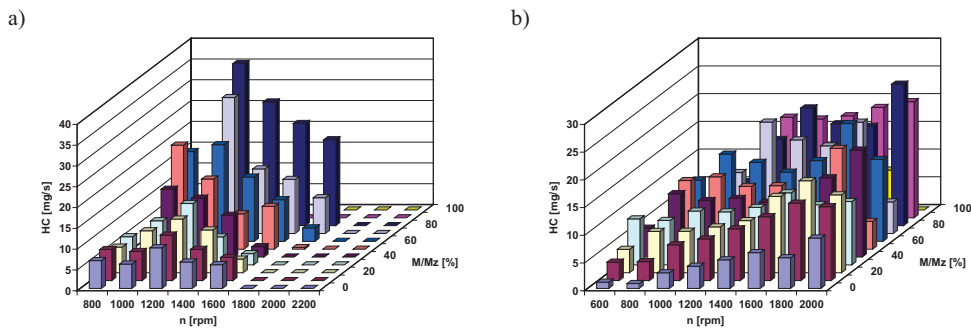


Fig. 8. Time density characteristics of the hydrocarbons emission: a) hybrid, b) conventional diesel

The area of elevated NO<sub>x</sub> emission in a hybrid vehicle (Fig. 9a) falls within the range of low engine speeds in the whole range of engine loads and the maximum engine speed and high engine load. This could be the effect of the application of selective catalytic reduction in this vehicle, where, at high exhaust gas temperatures the reduction of NO<sub>x</sub> occurs. For the vehicle with the conventional powertrain (no SCR) a linear growth of NO<sub>x</sub> emission is observed as the engine speed and engine load increase (Fig. 9b).

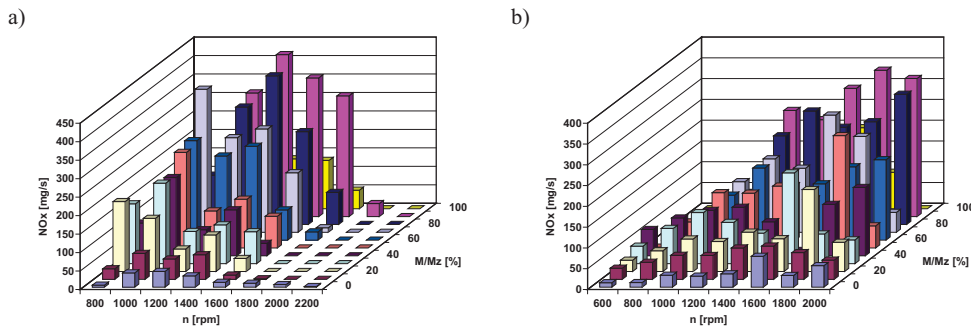


Fig. 9. Time density characteristics of the NO<sub>x</sub> emission: a) hybrid, b) conventional diesel



#### 4. Comparison of the emission level of the tested engines

The emission intensity under real conditions was calculated with the help of the time density characteristics of the engine operation ( $u_{n,M/M_z}$ ) and the characteristics of the emission intensity for a  $j$  toxic compound  $e_j(n, M/M_z)$ :

$$E_{real,j} = \sum_n \sum_{M/M_z} \{u_{n,M/M_z} \cdot e_j(n, M/M_z)\}, \quad (1)$$

where:

$E_{real,j}$  – emission of a  $j$  toxic compound under real conditions,

$n$  – engine speed,

$M/M_z$  – relative engine load.

Knowing the effective power in each range (determined by the engine speed and load), the unit emissions of the toxic compounds were compared, related to the engine power during the whole test cycle. The following values were obtained for the hybrid bus: HC – 0.193 g/(kW·h), CO – 3.981 g/(kW·h), NO<sub>x</sub> – 2.711 g/(kW·h) and CO<sub>2</sub> – 570.2 g/(kW·h). For the conventional diesel bus: HC – 0.282 g/(kW·h), CO – 9.130 g/(kW·h), NO<sub>x</sub> – 3.128 g/(kW·h) and CO<sub>2</sub> – 763.3 g/(kW·h). The above, when compared, discloses lower values for the hybrid vehicle: CO by 56.4%, HC by 31.8%, NO<sub>x</sub> by 13.3% and CO<sub>2</sub> by 25.3% as compared to the conventional power-train (Fig. 10).

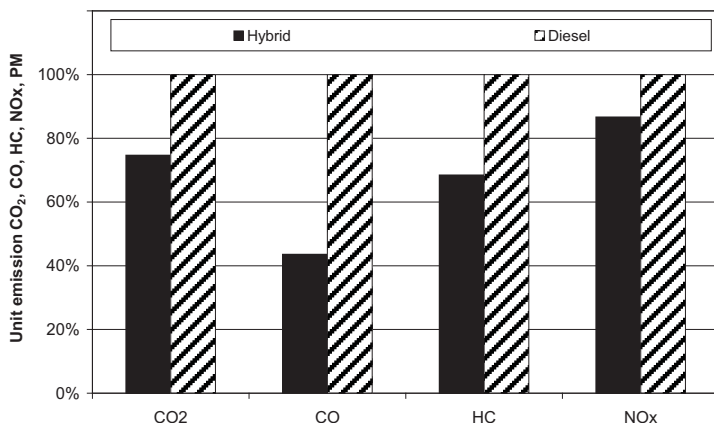


Fig. 10. Relative values of the unit emissions of toxic compounds during the on-road tests (hybrid and conventional diesel)

#### 5. Engine emission level indexes

From the information presented in the paper such as the characteristics of the share of engine operation at given engine speeds and loads as well as the characteristics of emission intensity we can obtain the factor of multiplication of the increase (decrease) of the emissions under real traffic conditions as opposed to the values obtained during the homologation test. The emission index (for a given toxic compound) has been defined as follows [12]:

$$k_j = \frac{E_{real,j}}{E_{cycle(norm),j}}, \quad (2)$$

where:

$j$  – toxic compound for which the emission index has been determined,

$E_{real,j}$  – emission intensity obtained under real conditions ([g/(kW·h)]),

$E_{cycle(norm),j}$  – emission intensity obtained in the ESC or ETC test ([g/(kW·h)]) or the boundary values adopted as permissible for a given emission standard.

The knowledge of the actual emission and the test emission (or the one compliant with the standard) may serve to determine the emission indexes of the toxic compounds of a given vehicle. If there is no information on the engine toxic emissions in the ESC or ETC test, we can adopt the permissible values according to the Euro emission standard which is binding for a given vehicle.

From the data included in Tab. 3 the emission indexes were obtained for each vehicle as they complied with different emission standards, hence the actual emission of a hybrid bus was compared with the emission values set out in Euro 5 (ETC test as the vehicle was fitted with an after-treatment system) and the actual emission of the conventional diesel bus was compared with the emission values set out in Euro 4 and the ESC test as the engine was not fitted with aftertreatment systems other than Oxicat. Because the standard does not provide for the CO<sub>2</sub> emission level the unit CO<sub>2</sub> emission was converted into unit fuel consumption and then the mean overall efficiency of the engine was estimated in the whole road test ( $\eta_{o \text{ Hybrid}} = 0.48$ ,  $\eta_{o \text{ Diesel}} = 0.36$ ).

Tab. 3. Emission level under real traffic conditions and emission indexes obtained in the tests for the hybrid and conventional vehicle

Parameter	CO	HC	NOx	CO <sub>2</sub>
1	2	3	4	5
Actual emission (hybrid) [g/(kW·h)]	<b>3.981</b>	<b>0.193</b>	<b>2.711</b>	<b>570.2</b>
Actual emission (conventional) [g/(kW·h)]	9.130	0.282	3.128	763.3
ESC test emission				
Euro 4 [g/(kW·h)]	1.5	0.46	3.5	–
Euro 5 [g/(kW·h)]	<b>1.5</b>	<b>0.46</b>	<b>2.0</b>	–
ETC test emission				
Euro 4 [g/(kW·h)]	4.0	0.55	2.0	–
Euro 5 [g/(kW·h)]	<b>4.0</b>	<b>0.55</b>	<b>2.0</b>	–
Emission index [–]	Hybrid bus			
ESC included	2.645	0.419	1.350	–
ETC included	<b>0.993</b>	<b>0.351</b>	<b>1.350</b>	–
Emission index [–]	Conventional bus (Diesel)			
ESC included	<b>6.086</b>	<b>0.613</b>	<b>0.894</b>	–
ETC included	2.282	0.513	1.564	–

The analysis of the emission indexes obtained for the two different buses (Fig. 11) shows that the hybrid bus has advantages in terms of both – fuel economy such as lower CO<sub>2</sub> emission and ecology such as lower emission indexes for CO and HC (lower than 1). This means that during its operation the bus releases fewer toxic compounds to the atmosphere than in the dynamic ETC test (in reference to a unit of energy). The emission index obtained for NOx amounts to 1.35 – this means that the emission of this compound during the road tests is 35% higher than in the ETC test. The emission indexes obtained for the conventional bus show that the emission of CO has been exceeded (more than 6 times) in the road test. The emission of the other toxic compounds does not

exceed the boundary values set out in the Euro 4 standard. It should be noted that for the conventional bus the emission indexes were obtained through the data related to the Euro 4 standard and the ESC test.

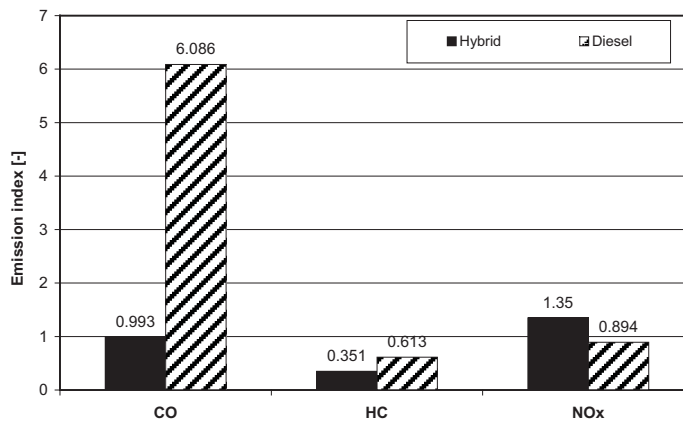


Fig. 11. Comparison of the emission index of the two buses in terms of real road emissions as opposed to the limits set out in the emission standards

## 6. Conclusions

A hybrid bus is more environment friendly because of a lower emission of CO<sub>2</sub> (fuel consumption) by 25% and a lower emission of other toxic compounds such as CO by 60%, HC by 30%, NOx by 15% as opposed to a conventional bus.

The analysis of the emission indexes shows that the emission values in the homologation test (ESC or ETC for a Euro 4 or Euro 5 vehicle) and the values in the real operation vary. For a conventional bus the differences of certain toxic compounds (as opposed to the emission set out in Euro 4 in the ESC test) are high and amount to: CO 6 times higher, HC 1.5 times lower and NOx emission similar. For the hybrid bus (opposed to the emission set out in Euro 5 in the ETC test) the following emission values were obtained under real traffic conditions: NO<sub>x</sub> emission 35% higher, HC emission 65% lower and CO emission similar. The elevated NO<sub>x</sub> emission during the tests can result from an inappropriate selection of the engine for this particular vehicle (an engine of higher capacity and power would be required so that it could more frequently operate on part loads).

The defined emission indexes could come in handy in the classification of vehicle fleets in terms of toxic emissions according to their year of manufacture, emission limit compliance, mileage or conditions of operation.

## Literature

- [1] AVL, *Current and Future Exhaust Emission Legislation*, AVL List GmbH, Graz 2007.
- [2] Gao, Y., Checkel, M. D., *Emission Factors Analysis for Multiple Vehicles Using an On-Board, In-Use Emissions Measurement System*, SAE Technical Paper Series 2007-01-1327.
- [3] Gao, Y., Checkel, M. D., *Experimental Measurement of On-Road CO<sub>2</sub> Emission and Fuel Consumption Functions*, SAE Technical Paper Series 2007-01-1610.
- [4] Greening, P., *European Light-Duty & Heavy Duty OBD – Legislative Update*, On-Board Diagnostic Symposium: Light and Heavy Duty, Lyon-Villeurbanne 2007.

- [5] Jehlik, H., *Challenge X 2008 – Hybrid Powered Vehicle On-Road Emissions Findings and Optimization Techniques: A 4 Year Summary*, Sensors 5th Annual SUN (SEMTECH User Network) Conference, 25-26.09.2008.
- [6] Johnson, K., Durbin, T., Cocker, D., Miller, J., Agama, R., Moynahan, N., Nayak, G., *On-Road Evaluation of a PEMS for Measuring Gaseous In-Use Emissions from a Heavy-Duty Diesel Vehicle*, SAE Technical Paper Series 2008-01-1300.
- [7] Khair, M., Khalek, I., Guy, J., *Portable Emissions Measurement for Retrofit Applications – The Beijing Bus Retrofit Experience*, SAE Technical Paper Series 2008-01-1825.
- [8] Khalek, I., *Status Update on the PM-PEMS Measurement Allowance Project*, Sensors 5th Annual SUN (SEMTECH User Network) Conference, 25-26.09.2008.
- [9] Korniski, T., Gierczak, C., Wallington, T., *Laboratory Evaluation of the 2.5 Inch Diameter SEMTECH® Exhaust Flow Meter with Gasoline Fueled Vehicles*, Sensors 4th Annual SUN (SEMTECH User Network) Conference, 22.10.2007.
- [10] McCarthy, M., *Update on Light Duty OBD II*, On-Board Diagnostic Symposium: Light and Heavy Duty, Lyon-Villeurbanne 2007.
- [11] Merkisz, J., Pielecha, J., Gis, W., *Comparison of Vehicle Emission Factors in NEDC Cycle and Road Test*, APISCEU 2008, Beijing 2-6.11.2008.
- [12] Merkisz, J., Pielecha, J., Gis, W., *Possibilities of Evaluation of Vehicle Emissivity with the use of OBD II System in Road Tests*, Better Air Quality (BAQ) 2008, Bangkok 12-14.11.2008.
- [13] Quan, H., *ARB's Stockton Heavy-Duty Vehicle Laboratory and Portable Emission Monitoring System (PEMS) Activities*, Sensors 5th Annual SUN (SEMTECH User Network) Conference, 25-26.09.2008.
- [14] Palocz-Andresen, M., *Completion of the OBD- with the OBM-(On-Board- Measurement)-Technology*, Predelli O.: Onboard-Diagnose II, Expert Verlag, Renningen 2007.
- [15] Rapone, M., Ragione, L., Meccariello, G., *Characterization of Real-World Bus Driving Behavior for Emission Evaluation*, SAE Technical Paper Series 2007-24-0112.
- [16] Shahinian, V. D., *SENSOR tech-ct Update Application Software for SEMTECH Mobile Emission Analyzers*, Sensors 4th Annual SUN (SEMTECH User Network) Conference, 22.10.2007.
- [17] Sharp, C. A., Feist, M., *Results of the HDIUT Gaseous PEMS Measurement Allowance Program and Update on PM Program Status*, Sensors 4th Annual SUN (SEMTECH User Network) Conference, 22.10.2007.
- [18] Zhao, F. F., *Technologies for Near-Zero-Emission Gasoline-Powered Vehicles*, SAE International, Warrendale 2007.



## **HISMAR - UNDERWATER HULL INSPECTION AND CLEANING SYSTEM AS A TOOL FOR SHIP PROPULSION SYSTEM PERFORMANCE INCREASE**

**Marek Narewski**

*Polski Rejestr Statków SA  
80-416 Gdańsk, Al. gen. J. Hallera 126,  
tel.: 058 361 700, fax +48 58 346 03 92  
e-mail: [m.narewski@prs.pl](mailto:m.narewski@prs.pl)*

### **Abstract**

*The cost of ship operation is dominated by the cost of fuel. The efficiency of ship propulsion depends on number of parameters. After selection of the most important we can further analyze them for taking relevant action to increase the ship propulsion efficiency. Biofouling of underwater part of ship's hull has direct influence on vessel resistance and engines power required to maintain the speed or keep optimal fuel consumption. HISMAR is a name of the project directed on development of robotic system that can be used to introduce new approach to keep ship hull clean and almost free of bio-fouling. Frequent cleaning using HISMAR robotic system could be a new tool to increase ship performance as well as conduct specific types of ship hull surveys underwater. New approach for inspection and cleaning needs field research to validate the financial and technical benefits. The HISMAR Project no 012585 was founded by EU-FP6 Framework Program.*

**Keywords :** *underwater cleaning, robotic system, underwater inspection, ship propulsion, efficiency*

### **1. Introduction**

We observe continuous growth both the global and EU shipping fleet. When speaking about the measures that can be taken to improve the shipping efficiency one of major issues is hull performance increase by the reduction of the wave and frictional resistance and increase of propulsion system efficiency. Whilst shipping is one of the cleanest forms of transportation, the fouling of ships reduces efficiency, increases fuel consumption and in extreme cases - corrosion. To minimize wave drag, special attention is given the smooth ship hull design and construction quality. The numerous efforts focus on frictional drag reduction using not only computational techniques. Modern anti-fouling paints and special low friction coatings are another large area of investment into research and achieved spectacular performance. When speaking about the increasing efficiency of the propulsor system there is a number of another opportunities like new highly efficient diesel engines, advanced propeller designs as well as promoted by some companies propeller coating techniques that prevent biofouling. Some guidelines and draft data regarding potential savings due to lowering of fuel consumption can be found in technical

literature. An example taken from data collected by Wartsila is presented in Table 1. The important comment to that table is that, there is very limited amount of data available that could be referenced as being confirmed by measurements at real sea conditions. Bearing that in mind, when using such data for calculation of potential savings we have to treat that figures as guidance. More detailed data can be collected during research on ship performance using real object data gathered during ship operation. This is quite complex task and will need certain financial resources and positive approach from ship operators to collect and validate the data with assistance of ship crew.

**Table 1. Estimated savings due to selected measures applied to various types of ships**

Ship Type	Tanker	Container	Ro-Ro	Ferry
<b>Efficiency measures</b>				
Hull clearing	< 3%	< 2%	< 2%	< 2%
Propeller clearing and polishing	<10%	<10%	<10%	<10%
Modern hull coatings	< 9%	< 9%	< 5%	< 3%
Propeller efficiency measurement	< 2%	< 2%	< 2%	< 2%
Constant versus variable speed operation	< 5%	< 5%	< 5%	< 5%

Source: Wartsila [1]

It is obvious, that machinery that operates for longer time and at higher power and loading is more susceptible to failures. Lower engine loading in general means lower wearing of certain components of ship drive system that could lead to longer operational life of the ship propulsion. Furthermore, it results in better reliability of the main propulsion and resulting ship safety improvement - particularly important for tankers, bulkcarriers, ro-ro and passenger ships. Monitoring of the ship hull condition for estimation of fouling or coating roughness measurements when coupled with means for cost effective ship hull cleaning (an example could be HISMAR system), could be valuable operational tool that could be used for ships in operation. Such procedure could be a part of more complex propulsion efficiency audits being a part of modern ship hull survey procedures.

## 2. Environmental and legal aspects

There is ongoing discussion at International Marine Organisation (IMO) with regard to Marpol Annex V (Regulations for the Prevention of Pollution by Garbage from Ships). IMO has already defined the residue from hull scrubbing as ships waste and it is therefore covered by the convention. As a consequence of this, it is likely that restrictions will be introduced as to where and how ship hulls may be scrubbed. The scrubbing of hulls by divers is forbidden within many European harbours. Fouling on a hull increases a ship's drag through the water, thus increasing the amount of power required to maintain the same speed or reducing the speed of the vessel for a given power. Fundamental data on that subject can be found in reference [2]. It is estimated that serious fouling can increase the drag on a ship by up to 40%, reducing the speed by up to 2 knots and increasing the fuel consumption by 10÷20% [3]. For the shipping industry, this means increased costs and time delays. The extra fuel consumption also increases greenhouse gas emissions, being composed of NO<sub>x</sub>, SO<sub>x</sub> and CO<sub>2</sub> from ships by up to 20 million tonnes per annum. Although shipping produces the least amount of greenhouse gases annually when compared to other modes of transportation, under the Kyoto agreement the EU is committed to a 5% reduction in emissions by 2012.

### **3. Underwater ship hull cleaning -- advantages and tools**

For over 130 years people have thought about machines or robots for cleaning ship hulls. Various devices and technology has been developed and tested. Only few developments have found wider application, an example could be hydraulic brush system operated by diver (BrushCart). In recent years, we are observing growing interest in robotic system that are developed to cope with the bigger ships and eliminate diver's presence underwater. Important issue is stress on marine ecology requirements. Robots are able to cope with that case using suitable tools. However, the investment in robotic system may be substantially high, such system will be able to work continuously underwater and possibly above the water where divers do not have access. Plug in sensor modules could allow to conduct detailed inspection of the almost whole hull during the same mission.

#### **3.1 Brush technology**

Brushes are used in cleaning carts, handheld polishers and some robotic systems and are able to cope with almost all types of fouling. Most systems consist of one or more rotating brushes pneumatically, or hydraulically driven. This requires the minimum of equipment beyond the cleaning device itself thus reducing the cost of the system. Before the ban on tributyltin (TBT) came in, brush technology was preferred to underwater jetting systems, as it was easier and more economical to use. However, the increase in use of environmentally friendly low friction coatings can cause a problem, as these coatings are less durable and more easily damaged by the abrasive action of the brushes. Research has shown that bristle density, angle and gauge have a greater effect on shear and normal forces produced by brushes, while the brush speed and stand-off distance has little or no effect. The main point demonstrated by the research was the selection of the brush cleaning system and forces involved is dependant on a number of factors and their relationship is very complex. The major problems in cleaning using heavy duty brushes could have place when dealing with calcerous forms of fouling.

#### **3.2 Water jetting technology**

The use of high pressure water jets has become an accepted alternative to brush cleaning systems. Unlike the brush-based systems, water jets can be easily controlled by reducing or increasing the pressure from the pump. A water jet's effectiveness is dependant on the surface, pressure of water, jetting angle and distance from the cleaning surface. Jet nozzles, such as CaviJet or SwirlJet have been developed to enable effective cleaning of the hull underwater. Tests using cavitating water jet nozzles showed that the cleaning process can remove various types of fouling from hull coatings, while at the same time, minimizing the damage to the coating. Although jet washing provides increased control of the cleaning process, the perceived increase in the cost of the equipment is still thought to be prohibitive. In hase of the HISMAR system low pressure jetting will be sufficient to remove effectively and safely the layer of slime from the hull surface.

### **4. Cleaning problems**

Diver(s) presence enhances the risk of diving accidents at work. Some data revealed by HSE show that probability of diver accidents during professional diving operation is higher than in farming or civil engineering. The number of accidents in offshore and inshore diving is in a range 20-40 for 100000 dives while fatal accidents occur in number of 6-7 for 100000 dives. Additionally to the risky job, diver has limited time to be able to work underwater so a team of divers is required to perform cleaning task. An open issue is the cost of diver safety measures



and environment protection requirements that must be taken into consideration discussing the cost benefits. Remotely controlled machines are not able to clean the whole wetted ship surface due to some hull features that restrict the robot operation. Ship bow and stern, due to hull shape are very difficult for automatic cleaning and that area will probably be cleaned by divers. Generally it is assumed that cleaning of 80% of the ship underwater area from slimes could provide suitable effect of drag reduction.

## **5. HISMAR idea**

The abbreviation HISMAR stands for **Hull Identification System for Maritime Autonomous Robotics**. HISMAR is intended to be a multifunctional robotic platform which will be able to perform specific inspection or maintenance tasks such as structural integrity monitoring of the ship's hull or cleaning operations. Apart from Project leader - Newcastle University, the other partners in the project were Graal Tech of Genoa; the UK's Shipbuilders and Shiprepairers Association; TecnoVeritas of Portugal; Polski Rejestr Statków; Robosoft of France; Carnival; Moscow State Technological University; Royal Thai Navy and TEPAC Technology & Patent Consulting of Germany.

Robotic platform is to be deployed for the board of the ship, harbour service craft or from the pier using simple crane or special launching and retrieval device. The control over the vehicle is provided via the special umbilical with power, control lines and hoses used for removal of cleaning wastes to the surface. Intervention with the use of HISMAR robot needs some preparation before the vehicle is placed on the surface of the ship hull. The desired situation is the case when digital data of the ship hull construction are provided to the robot control computer. On the other hand, at start of the job a map of the hull is automatically charted, recording the location of every weld, thickness change, rivet and indentation on the ship's surface. Adjustable jets of pressurised sea water blast the marine growth off the surface of the ship which is then sucked up into the main chamber. Here, ca 150 litres of water a minute is filtered and the bio-fouling removed and rendered harmless to the local environment. In this way, the ship's robotic 'vacuum' can continuously roam the ship's hull, preventing the build up the layer of slime.

Hull surveying is an important part of any vessel's life span and a number of periodic inspections of the hull are required during the vessel's life. Currently, the minimum requirement is for a visual inspection of the hull and with some thickness measurements being taken in specific areas of the hull, or where a probable defect might have occurred. These are usually performed using an ultrasonic sensory system that is placed on the plate's surface. Due to the size of the detection head and the skill required to operate the equipment, only a small proportion of a vessel's hull can be accurately measured. A full hull inspection is required to be performed in dry dock every five years, but up to 20% of the hull may not be inspected due to the vessel's dock supports. Between these class renewal inspections, intermediate hull inspections are required. These are general visual underwater inspections performed by divers. However, in recent years a number of robots have been developed to improve the accuracy, coverage and reliability, while reducing the time and cost of the inspection. The current robotic systems available are limited to visual inspection and ultrasonic plate thickness measurements.

## **6. The critical components of the HISMAR Robotic Platform**

The HISMAR robot design is presented in Fig 1 and 2. The key systems of the robot include:

### *Drive Systems & Central Robotic Platform*

Key to the HISMAR robotic platform is the versatile central drive module. This incorporates the robot's drive systems, navigational sensor systems and control electronics. Robot is linked with



the surface by a mean of specialised umbilical that contain power and data conductors and possibly hydraulic hoses for removal of cleaning debris.

#### *Cleaning & Debris Extraction Systems*

The cleaning system will utilize a water jetting to clean the hull. The jet spray system is intended to provide the customer with sufficient control for their cleaning needs while preventing damage to the hull coatings. A complete extraction and waste handling system is to be developed to comply with current and future marine environmental legislation.

#### *Mapping & Navigation Systems*

HISMAR's unique mapping and navigation system will allow for full autonomy of the robot after the initial process of mapping the hull. This will allow for complete or partial cleaning of a ship's hull, the latter being complete at the crew's convenience with no loss of operating time. The map will be a permanent record of the condition of the ship's hull, being updated by the navigational system whenever a cleaning operation is performed.

### **7. HISMAR robotic system advantages**

Marine growth on ships is a huge environmental and financial problem for the marine industry and HISMAR offers a unique solution to both of these — and more. Created is a system that works totally independently — in or out of the water — and not only keeps the ship clean but also feeds back vital information about the hull's condition. Because the map it follows is so detailed, if there is a change to its path caused by corrosion or a crack in the steel then it feeds this information back. This means it can be used as an additional check the condition of ship's hull and provide important reference data for classification society surveyors. All other developed cleaning or inspection systems currently available are remotely controlled during their operation, requiring highly skilled and experienced operators to effectively clean the hull, while the ship is out of operation and usually in dry dock. The advantage of the HISMAR robot is that it is an autonomous system so it can continue cleaning with the ship remaining in service.

The platform can be launched whenever the vessel is in port or at anchor. The device will be able to complete its tasks partially whilst in one port and be re-launched at successive points to complete the task. The generic platform will offer the option of using targeted plug-in modules to perform specific inspection or maintenance tasks such as structural integrity monitoring of the ships hull or carrying out cleaning and waste recovery operations. This project offers a means to effectively and efficiently undertake hull inspection and maintenance thereby extending the safe working life of the vessel. Cleaning of the hull ensures the vessel maintains the lowest possible hydrodynamic resistance and consequently reduces amount of fuel oil consumed. Therefore ensuring a clean and smooth vessel underwater hull surface reduces vessel emissions and reduces operating costs.

### **8. Validation of fuel consumption data and effectiveness of cleaning**

There is noticeable amount of published data providing general information about cleaning benefits but only few data available that provide reliable figures of possible savings due to periodical cleaning of the ship hulls. A very optimistic diagram that presents possible advantages from cleaning ship hull is given in Fig. 3. Some companies are offering advisory optimization services of vessel performance and in some cases also hull cleaning underwater using hydraulic tools. Up to our knowledge, only one company is using specialized ROV system and no reliable commercial or scientific data regarding its performance are available.

Taking decision about cleaning requires certain data to be analyzed. US Navy underwater husbandry practice requires the decision to be taken after underwater inspection and precise estimation of the area covered by fouling after comparison with reference data. Other commercial practice requires analysis of periodically collected voyage data as well as basic data about the prime mover operation like – rpm, specific heating value of fuel oil, fuel oil consumption, power measured by special device or torsionmeter, turbocharger revolutions, exhaust gas temperature – just as example. In that case, the collected data are subject of evaluation using dedicated software by commercial company on a subscription basis. In case of some ships and sea routes potential savings are big enough to pay for kind of ship services..

## **9. Conclusions**

The use of remotely controlled technology for underwater cleaning is subject of numerous R&D activities. Commercially available devices are not cheap and the cleaning in dry dock is much more popular and usually coupled with class surveys. Prime target for robotic tool is to achieve performance and cost of operation at the competitive level. Hull cleaning by cost-effective robotic devices that are able to cope with slime will limit fouling and lower the fuel consumption. The use of intelligent crawling underwater robots will expand as there will be more comparable data available describing ship propulsion performance increase as a result of more frequent robotic cleaning. Collection of reliable data about the financial and technical benefits of the robotic cleaning technology will be important for independent assessment of ship propulsion system performance. Plate thickness measurements and other data describing ship hull condition that will be collected by robot during cleaning missions could be further used by classification societies for class renewal surveys. The hull surveying using innovative robotic technology is in development phase and needs additional funds to be recognized as mature technique recommended for wider use.

## **References**

- [1] Boosting Energy Efficiency, Energy Efficiency Catalogue, Ship Power R&D, Wartsila Presentation, 19 Sept. 2008, Source: Internet.
- [2] R.L.Townsin, The ship hull fouling penalty, pp 9-15, Biofouling 2003 Vol. 19 (Supplement).
- [3] CASPER: The leading edge in vessel performance – Propulsion Dynamics, 2008.
- [4] HISMAR News Report No 1/2007 and 2/2007.

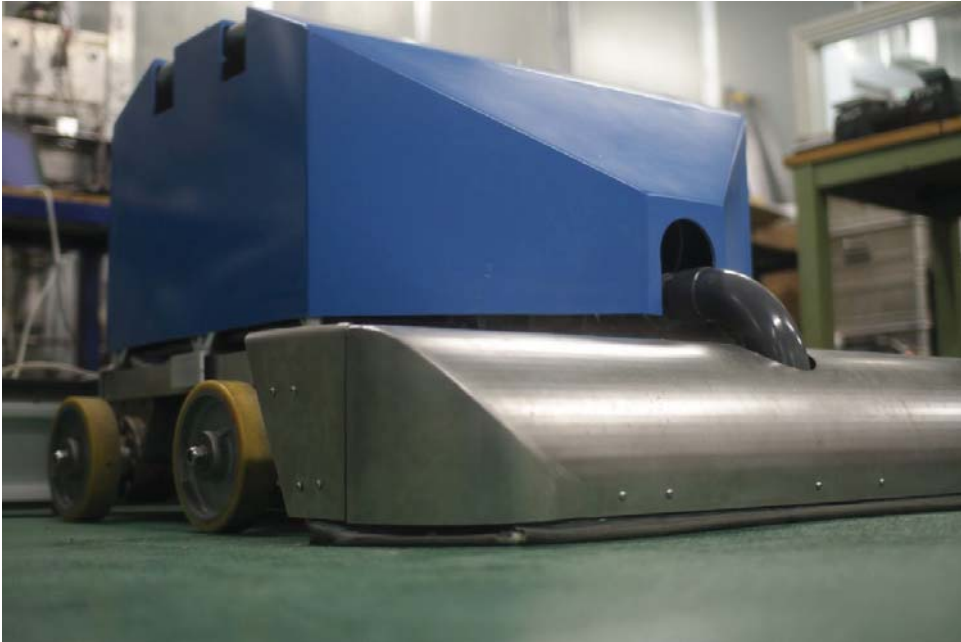


*Fig. 1 General view of HISMAR robot prototype*

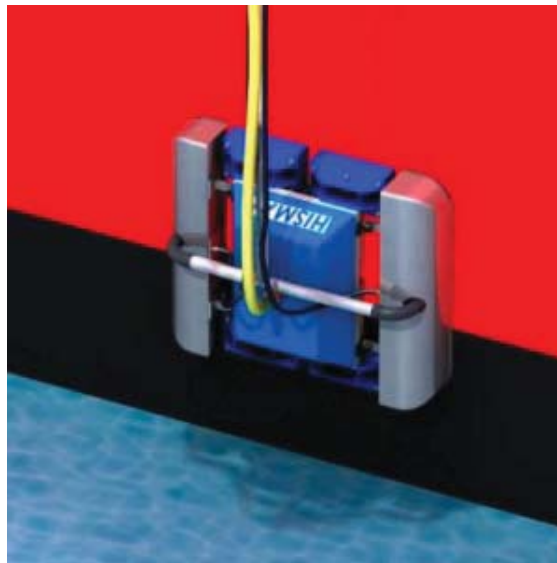


*Fig. 2 General view of HISMAR robotic platform*

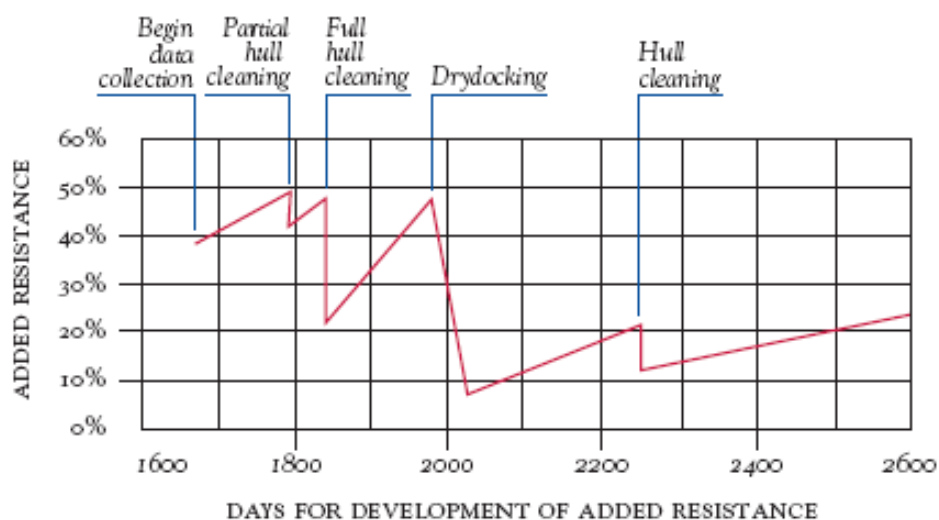


Fig. 3 Long term development of hull and propeller resistance [2]

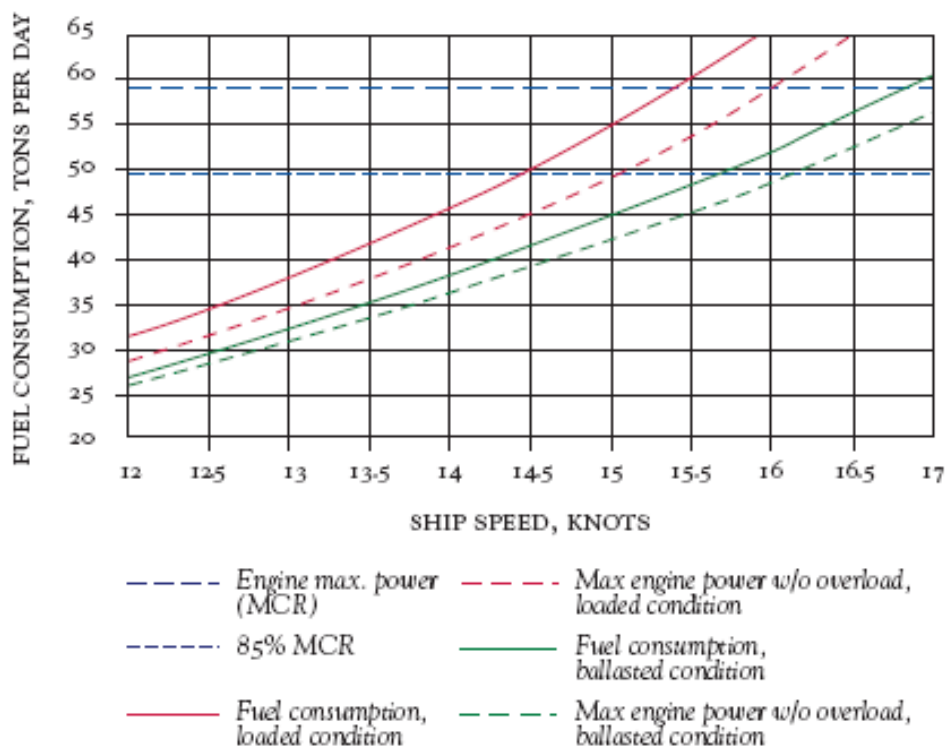


Fig. 4. Vessel performance in comparison to sea trials [2]



## A MODEL OF MARINE VESSELS MOVEMENT TO ESTIMATE HARMFUL COMPOUNDS IN THE VESSELS EXHAUSTS

**Małgorzata Pawlak**  
**Leszek Piaseczny**

*Polish Naval Academy in Gdynia*  
69, Smidowicza Str., 81-103 Gdynia, Poland  
tel.: +48 58 626 26 03, fax: +48 58 626 25 03  
e-mail: malgopawlak@tlen.pl, piaseczny@ptnss.pl

### **Abstract**

*Marine transport development and related to it, an increase in emission of harmful compounds forming when burning marine fuels, enforces conducting research on that emission in sea regions located in the vicinity of agglomeration areas. The basis for formulating the models of emission of harmful compounds in marine engines exhausts is formulation and study of the vessels movement models. The models ought to take into consideration the specificity of the processes taking place while a vessel is moving, which influence the formation of harmful compounds and their emission intensity. Emission models can be later used in formulating models of pollutants dispersion and their immission in the areas distant from the source of pollution, e.g. in city agglomeration regions. The paper indicates the possibility of using the Automatic Identification System as a source of statistical data, which can be used to define parameters and characteristics of the vessels movement. Identification of such a model was illustrated by the examples of the Gdansk Bay region.*

**Key words:** movement models, emission, toxic compounds in exhausts, marine engines

### **1. Introduction**

Emission of harmful compounds in engines of different applications constitutes a significant ecological problem of the 21<sup>st</sup> century. For a few decades there have been made many attempts to describe emission and its intensity with some specialised mathematical models [1-5]. When mobile sources of emissions are considered, majority of such models are formulated to conduct research on emission of motorization origin [1-3], both for road vehicles and off-road vehicles (mainly construction equipment and agricultural machinery). There exist also models of emission for aircraft vehicles (planes, helicopters). However, relatively few attempts are made to perform spatial modelling of pollutants emission distribution for the area where the source of these pollutants is the vessels movement. The problem of emission of pollutants in marine engines exhausts is all the more essential, as contrary to observed global land-based emissions decrease, it is projected that international shipping emissions will continuously be growing [6]. Such a situation results from dynamic development of marine transport – it is assumed that over 90 % of the world's total trade is carried by sea [7].

Movement models to estimate emission of pollutants from engines of motorization and aircraft origins, which have been formulated for many years, constitute a significant input into the development of modelling the pollutants emission from combustion engines. However, due to

significant differences in topographic, hydrometeorological conditions and the specificity of vessels maintenance, they cannot be directly applied in estimation of emission of these pollutants in marine engines exhausts.

Existing inventories of distribution of a mean number of vessels in a given sea area in given period of time, although they give a general idea on the vessel traffic intensity in a given area, they are often too general and imprecise, especially in the cases when the research do not aim at determining the mean number of vessels in a given sea region, but aim at describing the trajectory of individual vessels operating in a given sea area at given time interval. Modelling should also take into consideration technical parameters of an individual vessel (type, load, power etc.), which would be helpful in modelling the emission and dispersion of toxic compounds in the vessel exhausts.

## 2. Deterministic model of the marine vessels movement

The length of the segment joining any two points  $P_{i-1}, P_i$ ,  $i = 1, \dots, N$ , of coordinates  $(x_i, y_i)$ , between which a vessel moves:

$$|P_{i-1}P_i| = \sqrt{[x(t_i) - x(t_{i-1})]^2 + [y(t_i) - y(t_{i-1})]^2}, \quad (1)$$

and after transformations (applying the Lagrange's theorem about average value):

$$|P_{i-1}P_i| = \sqrt{[x'(\theta_i)]^2 + [y'(\vartheta_i)]^2} \Delta t_i, \quad (2)$$

where  $\theta_i$ ,  $\vartheta_i$  are points from interval  $[t_{i-1}, t_i)$ , and  $\Delta t_i = t_i - t_{i-1}$ .

Analysis of emission and its intensity of the compounds in exhausts, should begin with determination of the randomly changing vessel speed at a given time  $t$ , since the emission intensity depends on this value. Vector stochastic process  $\{\mathbf{V}(t) = (V_x(t), V_y(t)) : t \in T\}$  describes the randomly changing vessel speed. At a given time  $t$ , this value is a two-dimensional random variable indicating a momentary speed vector. It should be noticed that between the random processes of vessel trajectory:  $\{\mathbf{S}(t) = (X(t), Y(t)) : t \geq 0\}$  and speed  $\{\mathbf{V}(t) = (V_x(t), V_y(t)) : t \geq 0\}$  there exist the obvious relations:

$$\frac{d\mathbf{S}(t)}{dt} = \mathbf{V}(t), \quad t \geq 0, \quad \mathbf{S}(t) = \int_0^t \mathbf{V}(x) dx, \quad t \geq 0 \quad (3)$$

From equation (3) there come the following formulas:

$$V_x(t) = \frac{dX(t)}{dt}, \quad V_y(t) = \frac{dY(t)}{dt} \quad (4)$$

Realisation of the process  $V(t)$  can be thus described by the following formulas:

$$v_x(t) = \frac{dx(t)}{dt}, \quad v_y(t) = \frac{dy(t)}{dt} \quad (5)$$

After transformations, the length of the speed vector is determined:

$$|\mathbf{v}(t)| = \sqrt{[v_x(t)]^2 + [v_y(t)]^2} \quad (6)$$

In modelling the marine vessels movement, there can be assumed that in time intervals  $[t_{i-1}, t_i)$ ,  $i = 1, \dots, N$  the vessel speed is constant:  $|\mathbf{v}(t)| = v_i$ ,  $i = 1, \dots, N$ , and therefore the intensity of their exhausts emission will be constant:  $f(x(t), y(t)) = \lambda_i$ ,  $t \in [t_{i-1}, t_i)$ ,  $i = 1, \dots, N$ .

In reality, due to the yawing, the vessel route from point  $P_{i-1}$  to point  $P_i$  along a given trajectory, differs from the trajectory determined theoretically by drawing a line from point  $P_{i-1}$  to point  $P_i$ . The yawing can be written as:

$$\frac{\Delta S}{S} = \pi^2 \left( \frac{\psi_{om}}{v \cdot \tau} \right)^2$$

where:  $\psi_{om}$  – yawing amplitude;  $v$  – vessel speed;  $\tau$  – period of dominant harmonic of yawing.

Therefore, due to yawing, the vessel route from point  $P_{i-1}$  to point  $P_i$  is longer than  $\Delta s_i = v_i \Delta t_i$  by a random value  $D_i$ ,  $i = 1, \dots, N$ , and therefore the mass of exhausts emitted at this route interval will increase by a random value  $\Delta m_i = \lambda_i D_i$ ,  $i = 1, \dots, N$ . There can be accepted a preliminary hypothesis that the random variables  $D_i$ ,  $i = 1, \dots, N$  are mutually independent and have Gaussian distributions  $N(d_i, \sigma_i)$ ,  $i = 1, \dots, N$ , where  $d_i = \varepsilon \Delta s_i$ ,  $\sigma_i = \rho \Delta s_i$ ,  $i = 1, \dots, N$ . Factors  $\varepsilon$ ,  $\rho$  are the coefficients of the average route elongation and of the standard error of route elongation.

### 3. Stochastic model of vessels movement

Number of vessels operating in a given sea area varies in time, which constitutes therefore a stochastic process. Such a process is determined with a symbol  $\{X(t): t \in T\}$ . The value of this process at time instant  $t$  means the number of vessels operating in a given sea area at instant  $t$ . Realisations of this process are the functions of constant intervals. Any change of states appears at a moment of entering or leaving an analysed sea area by a vessel. The first approximated model of this process can be assumed the **non-homogenous Markov process** of discrete set of states  $S = \{0, 1, 2, \dots\}$ .

Stochastic process  $\{X(t): t \in T\}$  of finite or denumerable set of states is called the *Markov process*, if for any  $t_0, t_1, \dots, t_n, t_{n+1} \in T$  such as  $t_0 < t_1 < \dots < t_n < t_{n+1}$  and any  $i, j, i_0, i_1, \dots, i_{n-1} \in S$ ,

$$P\{X(t_{n+1}) = j | X(t_n) = i, X(t_{n-1}) = i_{n-1}, \dots, X(t_0) = i_0\} = P\{X(t_{n+1}) = j | X(t_n) = i\} \quad (7)$$

If  $t_0, t_1, \dots, t_{n-1}$  are interpreted as the past instants,  $t_n$  as the present instant, and  $t_{n+1}$  as the incoming instants (future), then the equation defining the Markov process means that conditional distribution of ‘future’ states does not depend on the ‘past’ if the present state of the process is known.

If  $T = N_0 = \{0, 1, 2, \dots\}$ , then the Markov process is called the *Markov chain*, and if  $T = R_+ = [0, \infty)$ , then it is the Markov process with ‘continuous time’.

Conditional probabilities

$$P_{ij}(t_n, t_{n+1}) = P\{X(t_{n+1}) = j | X(t_n) = i\}, i, j \in S \quad (8)$$

are called the probabilities of passing from state  $i$  at instant  $t_n$  to state  $j$  at instant  $t_{n+1}$ . Let  $t_n = s, t_{n+1} = t$ , where  $0 \leq s < t$ . From the definition of Markov process there result the following corollaries:

- 1)  $P_{ij}(s, t) \geq 0$  for all  $i, j \in S$  and  $s, t \in T$ ,  $s < t$ .
- 2)  $\sum_{j \in S} P_{ij}(s, t) = 1$  for all  $i \in S$  and  $s, t \in T$ ,  $s < t$ .
- 3)  $P_{ij}(s, t) = \sum_{k \in S} P_{ik}(s, u) P_{kj}(u, t)$  for all  $i, j \in S$  and  $s, u, t \in T$ ,  $s < u < t$ , (Chapman-

Kolmogorov equation).

Markov process is called **homogenous**, if probabilities of passing depend only on the difference of instants  $(t-s)$ :  $P_{ij}(s, t) = P_{ij}(t-s)$ . For  $s = 0$ ,  $P_{ij}(0, t) = P_{ij}(t)$ .



Let  $\{X(t): t \in [0, \infty)\}$  be Markov process of discrete set of states  $S$ . Functional matrix, whose elements are the probabilities of transition:

$$P_{ij}(s, t) = P\{X(t) = j \mid X(s) = i\}, i, j \in S, \quad 0 \leq s < t \quad (9)$$

will be designated as:

$$\mathbf{P}(s, t) = [P_{ij}(s, t) : i, j \in S]. \quad (10)$$

The Chapman-Kolmogorov equation in matrix notation will be as follows:

$$\mathbf{P}(s, t) = \mathbf{P}(s, u)\mathbf{P}(u, t) \quad (11)$$

It can be assumed that there exist uniform  $t$ -relative limits

$$\lambda_i(t) = \lim_{h \rightarrow 0} \frac{1 - P_{ii}(t, t+h)}{h}, \quad i \in S, \quad (12)$$

$$\lambda_{ij}(t) = \lim_{h \rightarrow 0} \frac{P_{ij}(t, t+h)}{h}, \quad i, j \in S \quad (13)$$

and they are continuous functions of parameter  $t$ .

For homogenous Markov process, the intensities of transitions are constant  $\lambda_{ij}(t) = \lambda_{ij}$ .

The Chapman-Kolmogorov equation can be written in the form of:

$$P_{ij}(s, t+h) = \sum_{k \in S} P_{ik}(s, t)P_{kj}(t, t+h), \text{ where } i, j \in S \text{ and } 0 \leq s < t < t+h. \quad (14)$$

Subtracting from both sides of the equation  $P_{ij}(s, t)$  and dividing by  $h$ , there is obtained:

$$\frac{P_{ij}(s, t+h) - P_{ij}(s, t)}{h} = \sum_{k \in S} P_{ik}(s, t) \frac{P_{kj}(t, t+h)}{h} + P_{ij}(s, t) \frac{P_{jj}(t, t+h) - 1}{h}. \quad (15)$$

Passing to the limit at  $h \rightarrow 0$ , assuming that in case of Markov process of countable set of states, the convergence defining the intensities  $\lambda_{kj}(t)$ ,  $k, j \in S$  at every determined  $j$  is uniform in relation to  $k$ , the following system of differential equations is obtained:

$$\frac{\partial P_{ij}(s, t)}{\partial t} = \sum_{k \in S} P_{ik}(s, t) \lambda_{kj}(t), \quad i, j \in S \quad (16)$$

The initial condition constitutes the natural equality:

$$P_{ij}(s, s) = \delta_{ij} = \begin{cases} 1 & \text{dla } j = i \\ 0 & \text{dla } j \neq i \end{cases} \quad (17)$$

In a similar way, the can be derived some differential equations allowing to calculate one-dimensional distribution of the process:

$$P_j(t) = P\{X(t) = j\}, \quad j \in S.$$

From the formula for total probability, it is obtained:

$$P_j(t+h) = \sum_{i \in S} P_i(t)P_{ij}(t, t+h), \quad j \in S \quad (18)$$

Subtracting from both sides  $P_j(t)$ , dividing by  $h$  and passing to the limit at  $h \rightarrow 0$ , the following system of equations is obtained:

$$P'_j(t) = \sum_{i \in S} P_i(t) \lambda_{ij}(t), \quad j \in S \quad (19)$$

The initial condition in this case constitutes the initial distribution of the process  $P_i(0) = p_i^0$ ,  $i \in S$ .

For homogenous Markov process, Kolmogorov system of equations (18) is brought to the system of linear differential equations of constant coefficients:

$$P'_j(t) = \sum_{i \in S} P_i(t) \lambda_{ij}, \quad j \in S \quad (20)$$

Such a system of differential equations is the most often solved using operators, applying Laplace's transformation:

$$L[P_i(t)] = \tilde{P}_i(s) = \int_0^{\infty} P_i(t) e^{-st} dt. \quad (21)$$

Making use of the property:  $L[P_i'(t)] = s\tilde{P}_i(s) - P_i(0)$ , the Laplace system of differential equations undergoes transformation. As a result, there is obtained the following system of linear equations, where unknown are the Laplace transforms:  $\tilde{P}_i(s)$ ,  $i \in S$ :  $s\tilde{P}_j(s) - p_j^0 = \sum_{i \in S} \tilde{P}_i(s)\lambda_{ij}$ ,  $j \in S$  [8].

One of limiting theorems for homogenous Markov processes with 'continuous time' at time  $t \rightarrow \infty$  goes as follows:

Let  $\{X(t): t \in [0, \infty)\}$  be a homogenous Markov process of finite set of states  $S$  and of the intensity matrix  $\Lambda = [\lambda_{ij} : i, j \in S]$ . If there is such a real positive number  $t_0$ , that at least one column of the matrix  $\Pi = [p_{ij}(t_0) : i, j \in S]$  contains one column consisting of all the positive elements, then there exist limiting probabilities:

$$\lim_{t \rightarrow \infty} P_j(t) = \lim_{t \rightarrow \infty} P_{ij}(t) = P_j, \quad j \in S \quad (22)$$

and they meet the system of linear equations

$$\sum_{i \in S} P_i \lambda_{ij} = 0, \quad j \in S, \quad \sum_{j \in S} P_j = 1. \quad (23)$$

Therefore, the limiting distribution is determined by solving the system of linear equations, whose coefficients depend only on constants of the transition intensity.

Using **non-homogenous Markov process** as a model of the movement of objects navigating in a given sea area is possible if there is assumed that the Markov process  $\{X(t): t \in T\}$ , the value of which at instant  $t$  constitutes the number of vessels operating in a given sea area at instant  $t$ , is a single process, which means that in a short time interval the state can change by one. The matrix of the intensity of transitions [8]:

$$\Lambda(t) = [\lambda_{ij}(t) : i, j \in S = \{0, 1, 2, \dots\}] \quad (24)$$

of this Markov process is as follows [8]:

$$\Lambda(t) = \begin{bmatrix} -\alpha_0(t) & \alpha_0(t) & 0 & 0 & 0 & \dots & 0 \\ \alpha_1(t) & -(\alpha_1(t) + \beta_1(t)) & \beta_1(t) & 0 & 0 & \dots & 0 \\ 0 & \alpha_2(t) & -(\alpha_2(t) + \beta_2(t)) & \beta_2(t) & 0 & \dots & 0 \\ 0 & 0 & \alpha_3(t) & -(\alpha_3(t) + \beta_3(t)) & \beta_3(t) & \dots & 0 \\ \dots & \dots & \dots & \dots & \dots & \dots & \dots \\ \dots & \dots & \dots & \dots & \dots & \dots & \dots \\ \dots & \dots & \dots & \dots & \dots & \dots & \dots \end{bmatrix} \quad (25)$$

Analytical solution of the system of the linear heterogeneous differential equations (18) in general form is practically impossible. However, it is possible to find an approximated solution, assuming that the elements of the matrix of the intensity of passages are constant in given time intervals and that the set of states of the process is finite  $S = \{0, 1, 2, \dots, n\}$ . Asymptotic distribution is received when solving the system of equations (23), in which given coefficients  $\lambda_{ij}$  are the elements of the matrix of the intensity of transition:

$$\Lambda(t) = \begin{bmatrix} -\alpha_0 & \alpha_0 & 0 & 0 & 0 & \dots & 0 \\ \alpha_1 & -(\alpha_1 + \beta_1) & \beta_1 & 0 & 0 & \dots & 0 \\ 0 & \alpha_2 & -(\alpha_2 + \beta_2) & \beta_2 & 0 & \dots & 0 \\ 0 & 0 & \alpha_3 & -(\alpha_3 + \beta_3) & \beta_3 & \dots & 0 \\ \dots & \dots & \dots & \dots & \dots & \dots & \dots \\ \dots & \dots & \dots & \dots & \alpha_{n-1} & -(\alpha_{n-1} + \beta_{n-1}) & \beta_{n-1} \\ \dots & \dots & \dots & \dots & \dots & \beta_n & -\beta_n \end{bmatrix} \quad (26)$$

The solution of this system of equations, having replaced the constants with the functional coefficients is of the following form [8]:

$$p_0(t) = \frac{1}{1 + \sum_{k=1}^n \frac{\alpha_0(t)\alpha_1(t)\dots\alpha_{k-1}(t)}{\beta_1(t)\beta_2(t)\dots\beta_k(t)}} \quad (27)$$

$$p_k(t) = \frac{\alpha_0(t)\alpha_1(t)\dots\alpha_{k-1}(t)}{\beta_1(t)\beta_2(t)\dots\beta_k(t)} p_0, \quad k=1,2,\dots,n$$

The number  $n$  is the maximal number of vessels in the sea area.

If in a given time interval  $[\alpha, \beta]$ , the distribution of the number of vessels in the sea area is constant, then the number  $K$  can constitute the integer part of the expected value:

$$E[X(t)] = \sum_{k=0}^n k p_k \quad (28)$$

In order to realize the described above stochastic model of movement of the vessels operating in Gdansk Bay region, it is necessary to know the number of vessels operating in the analysed area, their distributions in relation to the vessels types, their size, speed, power and kind of main engines etc.

### 3. Estimation of some parameters of a model of emission of harmful compounds in marine vessels exhausts

Estimation of the intensity of movement of the vessels operating in a given sea area at particular time interval, and on its basis – determination of emission of harmful compounds in exhausts of the vessels engines, is possible with the use of data transmitted in the *Automatic Identification System* (AIS), registered by the shore installation, which traces the vessels movement in a given sea area. For the marine vessels passing through certain test segments (fig. 1), situated perpendicularly to shipping lanes approaching the ports of Gdynia and Gdansk, as well as the shipping lane splitting into those two shipping lanes (in the proximity of Hel port), there were analysed the movement parameters of the vessels operating in a given sea area at given time interval.

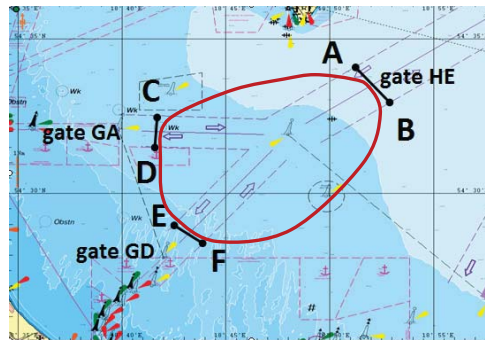


Fig. 1. Map of Gdansk Bay area where there are marked the test intervals [9] of geographic coordinates:  
 $\overline{AB} = (54,58325^{\circ}\text{N}; 18,85362^{\circ}\text{E}) (54,45917^{\circ}\text{N}; 18,88191^{\circ}\text{E})$  – gate GD;  $\overline{CD} = (54,54200^{\circ}\text{N}; 18,69511^{\circ}\text{E})$   
 $(54,52508^{\circ}\text{N}; 18,69326^{\circ}\text{E})$  – gate GA;  $\overline{EF} = (54,48666^{\circ}\text{N}; 18,70878^{\circ}\text{E}) (54,47326^{\circ}\text{N}; 18,73178^{\circ}\text{E})$  – gate HE.

There were examined the vessels passing in the period of one month (from 1<sup>st</sup> to 30<sup>th</sup> June 2006) through the test intervals (called later: ‘gates’) shown in fig.1. In the analysed Gdansk Bay region (fig.1), the total number of vessels operating in June 2006 amounted to 627 (fig.2). On average, during 24 hours, to the analysed area through the gates there were entering from 3 to 8 vessels (in case of vessels entering the analysed area through the GD gate and GA gate), and from 9 to 14 vessels (in case of vessels entering the analysed area through the HE gate) (rys.3). Majority of these vessels were entering the analysed area in the afternoon (through gates GD and GA) and at time interval 00.00-12.00 (through gate HE) (fig.4).

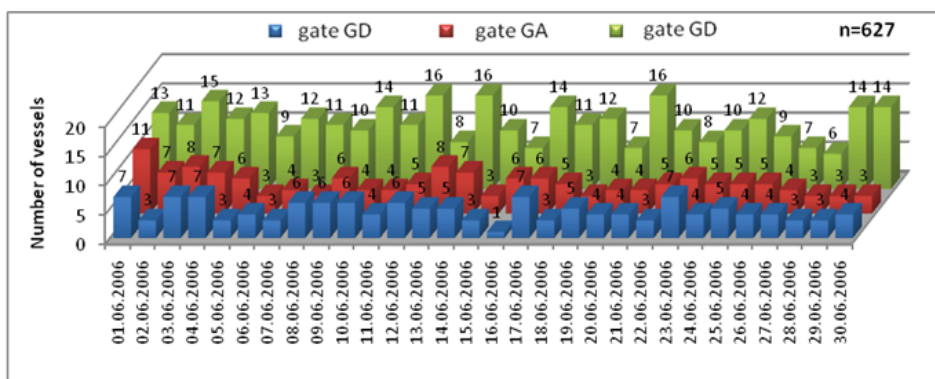


Fig. 2. A 24-hour distribution of the number of vessels: a) outward bound passing through ‘gate GD’; b) outward bound passing through ‘gate GA’; and c) passing through ‘gate HE’ and going towards of Gdansk port or Gdynia port (in the period of 01-30.06.2006)

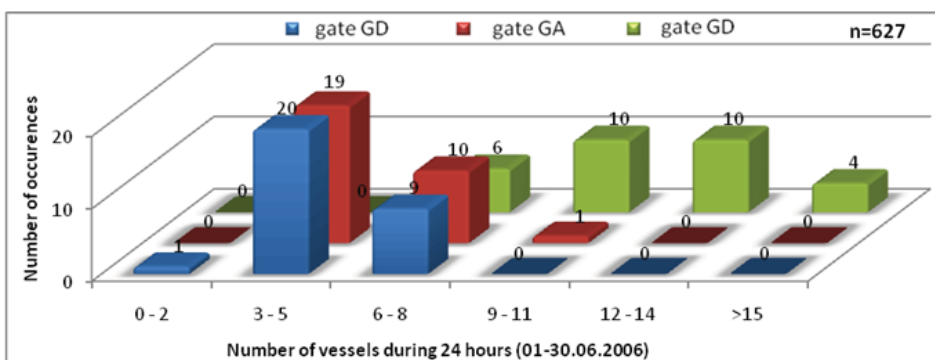


Fig. 3. A 24-hour distribution of the number of vessels: a) outward bound passing through ‘gate GD’; b) outward bound passing through ‘gate GA’; and c) passing through ‘gate HE’ and going towards of Gdansk port or Gdynia port (in the period of 01-30.06.2006)

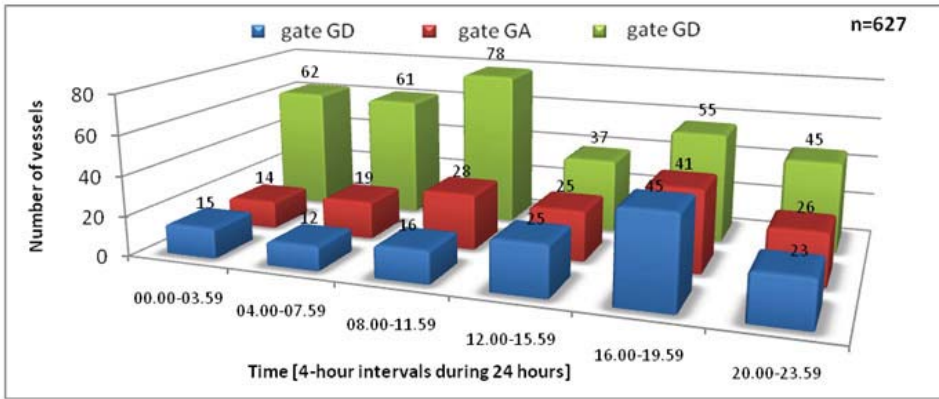


Fig. 4. Distribution of the number of vessels: a) outward bound passing through 'gate GD'; b) outward bound passing through 'gate GA'; and c) passing through 'gate HE' and going towards of Gdansk port or Gdynia port, depending on time intervals during 24 hours (in the period of 01-30.06.2006)

Analysis of the available statistical data allowed to determine values of momentary speed  $v^*$  of the vessels entering the analysed area in analysed period of time. As it can be noticed, the most frequent speed of the vessels entering the area through individual gates, was from 8 to 18 knots (fig.5).

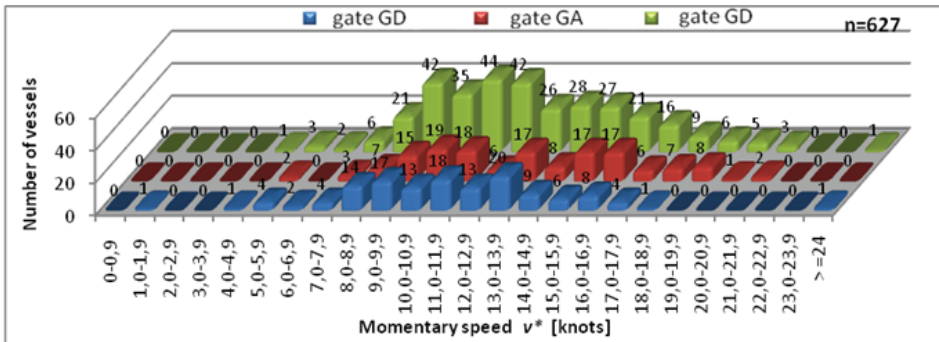


Fig. 5. Distribution of the momentary speed  $v^*$  (velocity over ground) [in knots] for vessels a) outward bound passing through 'gate GD'; b) outward bound passing through 'gate GA'; and c) passing through 'gate HE' and going towards of Gdansk port or Gdynia port (in the period of 01-30.06.2006)

The volume of the underwater part of a hull  $V$  was calculated for the analysed group of vessels on the basis of assumed simplified shape of a hull [10]. On the basis of the obtained results, it can be stated that most of the analysed vessels were the ones relatively small – of underwater hull volume up to 25000 m<sup>3</sup> (fig. 6).

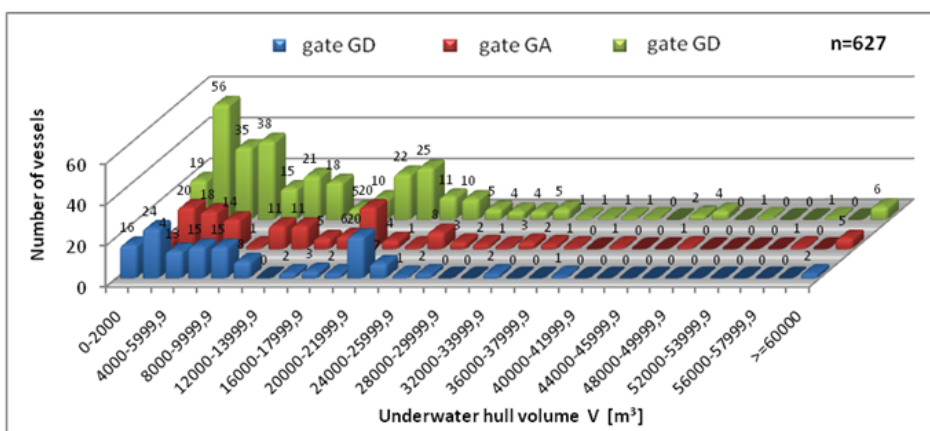


Fig. 6. Distribution of the underwater hull volume of the vessels a) outward bound passing through 'gate GD'; b) outward bound passing through 'gate GA'; and c) passing through 'gate HE' and going towards of Gdansk port or Gdynia port (in the period of 01-30.06.2006)

From the analysed group of vessels there were chosen the ones, which in the period of 01-30.06.2006 were passing through gates GD and GA and going towards gate HE (in total there were 289 vessels). On the basis of analysed change in momentary speed  $v^*$  of individual vessels, read when they were passing consecutive two gates, there was calculated the probability of the occurrence of the speed change. There were taken into account the changes of the range of 0.1 knots. In figures 7 and 8, it is shown the probability of occurrence of an increase and decrease in speed (by  $x$ -knots) on the route between individual gates. Function  $y$ , described by a 4<sup>th</sup> order polynomial, means that probability, and  $R^2$  means the adjustment coefficient.

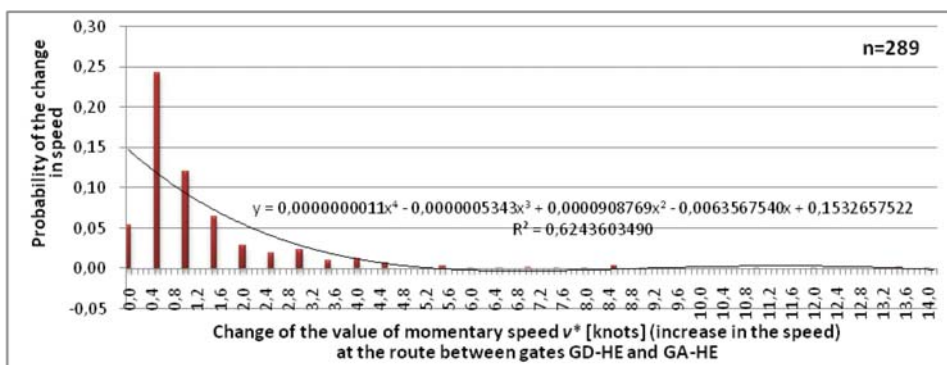


Fig. 7. Probability of occurrence of an increase in momentary speed (by  $x$ -knots) for the analysed group of vessels operating at the route between gates GD-HE and GA-HE (in the period of 01-30.06.2006)

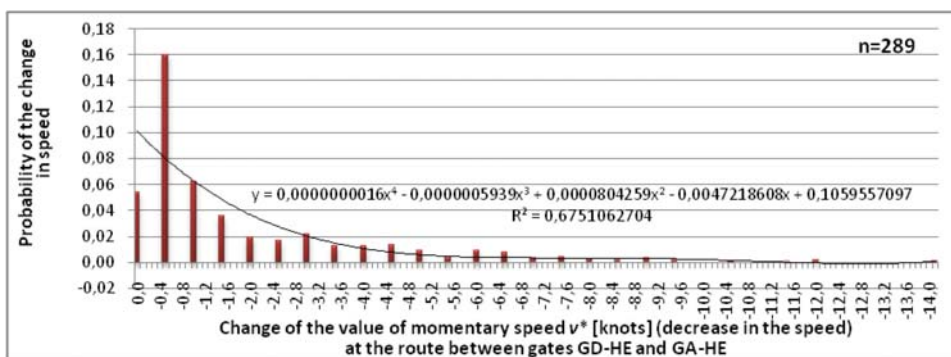


Fig. 7. Probability of occurrence of a decrease in momentary speed (by x-knots) for the analysed group of vessels operating at the route between gates GD-HE and GA-HE (in the period of 01-30.06.2006)

From the analysis of the charts shown in fig. 7 and fig. 8, it results that the changes in the vessels speed on the route from gate GD to gate HE and from gate GA to gate HE are slight, and the probability of occurrence of the changes in speed by more than one knot is very low (below 0.12).

#### 4. Conclusion

In the paper, there were presented formulation and estimation of parameters of models of movement of the vessels operating in the Gdansk Bay region in a particular time period. The analysis was possible with the use of statistical data obtained via *Automatic Identification System* (AIS), which appeared to be a tool that can be effectively used in such purposes. The proposed method is possible to be applied in the process of determination of an approximated level of the toxic compounds emission in marine engines exhausts in given se region at particular time.

#### References

- [1] *COPERT II - Computer Programme to Calculate Emissions from Road Transport - Methodology and Emission Factors*. European Environment Agency. European Topic Center on Air Emission, 1997.
- [2] Chłopek Z., *Modelowanie procesów emisji spalin w warunkach eksploatacji trakcyjnej silników spalinowych*. Prace Naukowe. Seria „Mechanika” z. 173. Oficyna Wydawnicza Politechniki Warszawskiej. Warszawa 1999.
- [3] Drag Ł., *Modelowanie emisji i rozprzestrzeniania się zanieczyszczeń ze środków transportu drogowego*, Archiwum Motoryzacji, Wyd. Naukowe Polskie Towarzystwo Naukowe Motoryzacji, Nr 1/2007, 2007.
- [4] Cooper, D.A., *Exhaust emissions from ships at berth*. Atmospheric Environment 37, 2003.
- [5] Cooper D.A., Gustafsson T., *Methodology for calculating emissions from ships - 1. Update of emission factors*, 2004.
- [6] European Commission Directorate General Environment Service Contract on Ship Emissions, *Assignment, Abatement and Market-based Instruments, Task 1 - Preliminary Assignment of Ship Emissions to European Countries*, Final Report, ENTEC UK Limited, 2005.
- [7] IMO Marine Environment Protection Committee (MEPC), 53<sup>rd</sup> Session, Agenda Item #4. *Prevention from Air Pollution from Ships*. London, 2005.
- [8] Grabski F., *Stochastyczne modele ruchu jednostek pływających*. Sprawozdanie z realizacji projektu badawczego Nr 502 009 31/1187 pod kier. L. Piasecznego. AMW w Gdyni, Gdynia, 2008.
- [9] Naus K., *Opracowanie statystyczne strumieni obsługi jednostek morskich na wytypowanym torze wodnym*, Akademia Marynarki Wojennej, Instytut Nawigacji i Hydrografii Morskiej, Gdynia, 2008.
- [10] Pawlak M., Piaseczny L., *Mathematical models of the vessels movement for determination of toxic compounds emission*. Materiały konferencyjne IV Międzynarodowej Konferencji Naukowo-Technicznej p.t. Obsługiwanie Maszyn i Urządzeń „OMiU 2008”. Akademia Morska w Szczecinie, 2008.





## MODELLING EXHAUST EMISSION FROM VESSELS IN THE GULF OF GDAŃSK AREA

**Tomasz Kniaziewicz, Leszek Piaseczny**

*Polish Naval Academy*

*Smidowicza Street 69, 81-103 Gdynia, Poland*

*tel.: +48 58 6262851, 6262603*

*e-mail: tkniaziewicz@wp.pl, piaseczny@ptnss.pl*

### **Abstract**

*The area of the Gulf of Gdańsk, just like port towns and coastal regions, is vulnerable to pollution contained in the exhaust gases of industrial plants, power plants, vehicles and harmful compounds contained in exhausts of vessels. In order to determine the share of vessels in polluting atmospheric air and to counteract the harmful effects of toxic compounds in marine engine exhausts it is necessary to know the values of those compounds' emission from particular vessels, which is possible by knowing the movement parameters of vessels, the values of concentrations of particular compounds for these parameters and the atmospheric conditions in the region of their occurrence.*

*The object of balancing emission of pollution contained in the exhausts from engines propelling vessels are the processes of global emission, averaged in a sufficiently long time period, which is determined first of all by the efficiency of averaging the variable conditions of the objects' operation. Due to the impossibility of making emission measurements on vessels in the region of research, it is necessary to work out suitable models of estimating emission of toxic compounds, based on proper measurement tests simulating navigational conditions in the Gulf of Gdańsk as well as mathematical models.*

*The work presents conditions related to modelling the emission of exhaust compounds from vessels engines in the region of the Gulf of Gdańsk, with particular consideration to estimating the values of toxic compounds concentration.*

**Keywords:** *emission, dispersion, modelling, marine engines, exhausts*

### **1. Introduction**

The problem of air pollution in ports and approaches to ports is important inasmuch as the ports are usually close to or on the territories of large cities, and their restricted area causes large concentration of vessels in a small area. Widely conceived operational conditions are not insignificant either, among them being the way of engine operation, the frequency of occurrence and character of non-stationary states, transitory processes characterised by considerably larger emission of toxic compounds than during sailing in open areas with constant engine load. The way of operation is also affected by external conditions, that is the effect of marine environment on the engine's work. Certainly the kinds of fuel and lubricating oil affect exhaust toxicity in no smaller degree.

The research currently carried out concerning atmosphere pollution caused by the emission of harmful compounds from traction engines (airplane and car engines) [1-3] provides very large contribution to the development of modelling of imission of harmful compounds emitted from diesel engines, but due to the difference in both topographic and hydrometeorologic conditions and the specificity of vessel operation, they cannot be applied for estimating imission in coastal areas [4].

Modelling emission of particular exhaust components from exhaust systems of marine engines during movement in a particular area constitutes one of the key problems of balancing and making input data for dispersion models.

The object of balancing emission of pollution contained in the exhausts from engines propelling vessels are the processes of global emission, averaged in a sufficiently long time period, which is determined first of all by the efficiency of averaging the variable conditions of the objects' operation.

The factors determining global emission of substances contained in marine engines exhausts have been classified and described in [4,5].

The process of modelling emission and dispersion of toxic compounds (ZT) in marine engine exhausts (which are the elements of modelling the imission of these compounds), is very complex and requires the knowledge of five basic parameter groups [5,6]:

- vessel parameters: length, breadth, draft, technical condition of propulsion system, kind of propulsion (including kind and number of engines), kind and number of propellers, etc.;
- vessel movement parameters: speed and course;
- external conditions: wind direction and force, air and water temperature, atmospheric pressure, air humidity, state of the sea;
- number of vessels, with consideration to category;
- topographic parameters of the area: terrain kind and profile (water, land).

Models of emission from land means of transport created in Europe, like HBEFA, COPERT, DVG and DRIVE-MODEM [7,8] endeavour first of all to take into account the largest possible number of parameters affecting emission, yet with such a large number of factors and the complex description of phenomena determining the emission process, simplifying assumptions cannot altogether be avoided.

## 2. Modelling emission of exhausts from marine engines

In work [9] there has been considered the trajectory of vessel movement as the realisation of a two-dimensional stochastic process  $\{S(t) = (X(t), Y(t)) : t \geq 0\}$ , assuming that the process is of multidimensional distribution of continuous type and continuous realisations. The realisation of such a process is a two-dimensional trajectory dependent on time  $\{s(t) = (x(t), y(t)) : t \in T\}$ .

The equation describing the mass of exhausts emitted can be presented as follows:

$$M = \int_{\alpha}^{\beta} f(s(t)) |v(t)| dt, \quad (1)$$

where:

$v(t)$  length of vessel velocity vector.

Assuming that in the time intervals  $[t_{i-1}, t_i]$ ,  $i = 1, \dots, N$  the speed of the vessel is constant

$$|v(t)| = v_i, \quad i = 1, \dots, N, \quad (2)$$

and the intensity of exhaust emission is constant

$$f(x(t), y(t)) = \gamma_i, \quad t \in [t_{i-1}, t_i], \quad i = 1, \dots, N, \quad (3)$$

the lower estimation of emitted exhaust mass is obtained

$$M = \sum_{i=1}^N M_i, \quad (4)$$

where:

$$M_i = \gamma_i v_i \Delta t_i, \quad i = 1, 2, \dots, N.$$

The mass of emitted exhausts in particular area  $\mathcal{A}$  in time interval  $[t_{i-1}, t_i]$  is the sum of masses emitted by all vessels in this time interval in the area. If  $W^{(k)}$ ,  $k = 1, \dots, K$  denotes the mass of exhausts emitted by the  $k$ -th vessel, then the total mass of exhausts emitted in area  $\mathcal{A}$  in time interval  $[t_{i-1}, t_i]$  is a random variable

$$W_K = \sum_{k=1}^K W^{(k)}, \quad (5)$$

Random variable  $W_K$  as the sum of independent random variables with normal distribution has normal distribution with expected value

$$E(W_K) = \sum_{k=1}^K W^{(k)} = \sum_{k=1}^K [E(\Delta M^{(k)}) + M^{(k)}] = \sum_{k=1}^K [M^{(k)} + \varepsilon^{(k)} \sum_{i=1}^N \gamma_i^{(k)} \Delta s_i^{(k)}], \quad (6)$$

Standard deviation of these random variables is equal to

$$\sigma(W_K) = \sqrt{\sum_{k=1}^K V[\Delta M^{(k)}]} = \sqrt{\sum_{k=1}^K \rho^{(k)} \sum_{i=1}^N [\gamma_i^{(k)} \Delta s_i^{(k)}]^2}, \quad (7)$$

In this model the number of vessels  $K$  has been assumed to be constant. In reality the number of vessels varies randomly in time, so it is a stochastic process [10].

Work [11,12] presents a method of approximate identification of vessel movement model, and for estimating the parameters and characteristics of exhaust emission from vessels sailing in the Gulf of Gdańsk region it is necessary to know the number of vessels navigating in the region analysed, their distribution with regard to kind, size, speed, power and kind of main propulsion engines etc.

### 3. Modelling load of vessel main propulsion engines in order to estimate the value of toxic compounds emission in the exhausts

The amount of emitted harmful compounds in marine diesel engines depends on values describing the state of engine work like torque  $M_o$ , engine speed  $n$ , thermal state of the engine  $J$ , technical state of the engine  $Z$  (parameters of load exchange system, state of TPC system, technical state and proper regulation of injection apparatus), condition of environment  $G$  (e.g. ambient temperature, pressure, air humidity) and variable sailing resistance of vessel  $O$  (vessel resistance in shallow water, vessel resistance while moving in a canal, air resistance and waving effect). It can thus be written down that the emission of the  $n$ -th harmful compound in exhausts  $e_n$  will have the form:

$$e_n = f(M_o, n, J, Z, G, O),$$

To calculate the vessel's momentary power  $P^*$  there have been used methods of calculating the power necessary to sail with speed  $v_s$  based on calculations of resistance of sea-going vessels. There are a number of methods of calculating resistance of sea-going commercial vessels, among the most widespread being: Papiel's, Ayre's, Lap's, Taylor's and Kabaczyński's. The first two permit the determination of total (towing power) resistance, the three other only residual resistance.

All methods (excluding Papiel's and Ayre's) have vessel resistance comparable to resistance determined from model experiments, therefore additions have to be applied for them similar to those for resistance determined from model experiments. Only Papiel's method, which in the range of smaller speeds gives results considerably higher than those obtained by other methods, supposedly takes account of those additions.

In connection with the amount of information available concerning the vessels' dimensions and momentary speed  $v^*$  obtained from AIS system [13,14], two methods were accepted for calculating the value of momentary power  $P^*$ : Papiel's and the Admiralty's.

In Papiel's method the power necessary for the vessel's sailing with speed  $v_s$  may be presented by means of the equation:

$$P_o = \frac{V}{L} \frac{x}{\lambda} \sqrt{\psi} \frac{v_s^3}{C_p} = f\left(\frac{v_s^3}{C_p}\right), \quad (8)$$

where:

$V$  – volume of the vessel's underwater part [ $m^3$ ],

$L$  – vessel's length on the waterline [ $m$ ],

$v_s$  – vessel's speed [ $k$ ],

$x$  – coefficient dependent on the number of shafts, taking account of protruding parts,

$\lambda$  – length allowance coefficient calculated from the formula  $\lambda = 0.7 + 0.3 L/100$ ,

$\psi$  – hull fineness coefficient.

In the case of Admiralty's method the equation describing the power necessary for the vessel to sail with speed  $v_s$  is significantly simplified and has the following form:

$$P_o = \frac{v_s^3 D^{2/3}}{C_0}, \quad (9)$$

where:

$P_o$  – power required (towing power bound with hull resistance),

$C_0$  – Admiralty's coefficient for towed power,

$v_s$  – vessel speed [ $k$ ],

$D$  – vessel's displacement [ $m^3$ ].

On the basis of formulae (8) and (9) there were calculated the values of momentary power  $P^*$ , whose distributions have been presented in Figs 1 and 2.

On the basis of results analysed it can be stated that the differences in calculated values of momentary power determined by Papiel's and Admiralty's methods are significant. Therefore, particular attention should be paid to the means of determining momentary power, as successively the value of toxic emission for particular vessels is calculated on its basis, which entails further simplifications and errors.

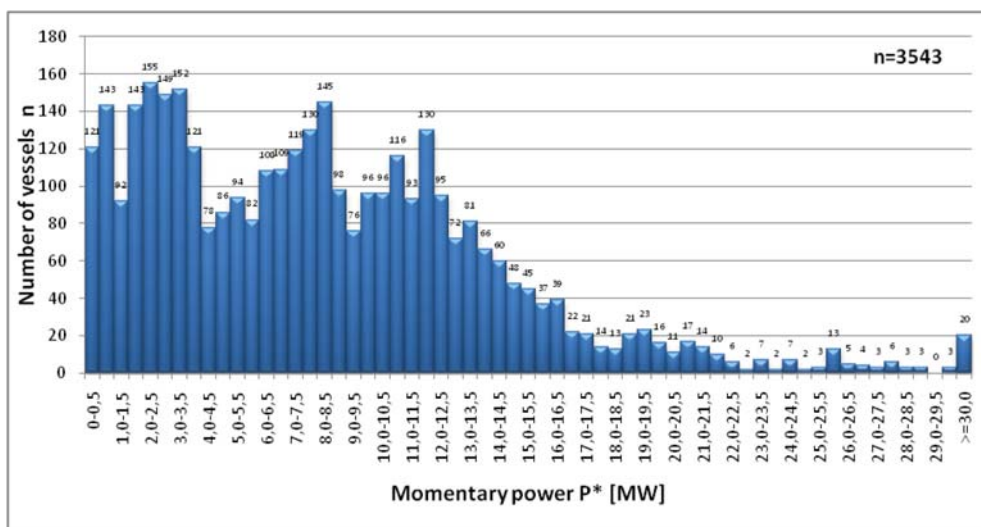


Fig. 1 Distribution of momentary power  $P^*$  [MW] calculated by Papiel's method for vessel group tested [9]

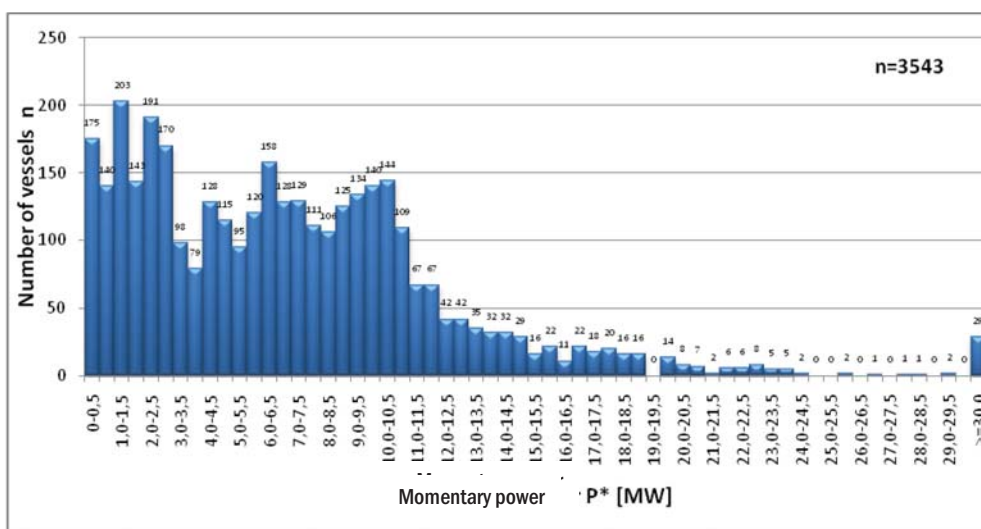


Fig. 2. Distribution of momentary power  $P^*$  [MW] calculated by Admiralty's method for vessel group tested [9]

For a more accurate assessment of the emission value of particular toxic compounds there were worked out tests for examining the concentration of toxic compounds in the exhausts of main engines of vessels sailing in the Gulf of Gdańsk. For this purpose, out of the group of vessels sailing in the examined area in a period embracing 11 months 63 vessels were picked out with the highest incidence index, which gave 3543 observations [15].

On the basis of momentary power values of vessels tested  $P^* = P_c/P_n$  4 and 10-phase tests of exhaust toxicity were prepared. Seeing that most of the considered vessels sail according to typical propeller characteristic, modified test E3 acc. to ISO 8170 part 4 was accepted as initial test. The modification consisted in altering the values of weight coefficients, which in the original test characterise the whole range of the engine's operation, and in the case considered are to pre-

sent conditions of engine work on the Gulf of Gdańsk fairways. Particular values of four-phase tests have been presented in Table 1[16].

In Fig. 3 there have been compared the emission values of nitrogen oxide calculated by means of E3 test according to ISO 8170-4 and prepared 4-phase test A (required power  $P_0$  determined by Admiralty method) and 4-phase test P (required power  $P_0$  determined by Papiel method).

The difference between results of  $\text{NO}_x$  emission results obtained on the basis of E3 tests according to ISO8178-4 and 4-phase tests A and P seem to be insignificant (from 0.1 to 0.47 g/(kW·h)). Yet if the typical powers of vessels sailing in the Gulf of Gdańsk are taken into consideration, e.g. ferry “Stena Nornica” sailing from Gdynia (114 observations within 1 year, engines power 39600kW), then such slight differences in tests give  $\text{NO}_x$  emission intensity respectively from 3.96 to 18,61 kg/h. In relation to  $\text{NO}_x$  emission values from vehicles these are significant values and should not be ignored.

Tab.1. Proposition of 4-phase exhaust toxicity tests of vessels sailing in the Gulf of Gdańsk acc. to propeller characteristic taking consideration of the method of engine power determination

Engine speed [% $n_n$ ]	100	91	80	63
Load [% $P_n$ ]	100	75	50	25
Weight coefficient $P^{1)}$	0.20	0.38	0.40	0.02
Weight coefficient $A^{2)}$	0.22	0.20	0.41	0.17
Weight coefficient of E3 test acc. to ISO 8178-4	0.20	0.50	0.15	0.15

<sup>1)</sup> weight coefficient P - required power  $P_0$  determined by Papiel’s method,

<sup>2)</sup> weight coefficient A - required power  $P_0$  determined by Admiralty’s method.

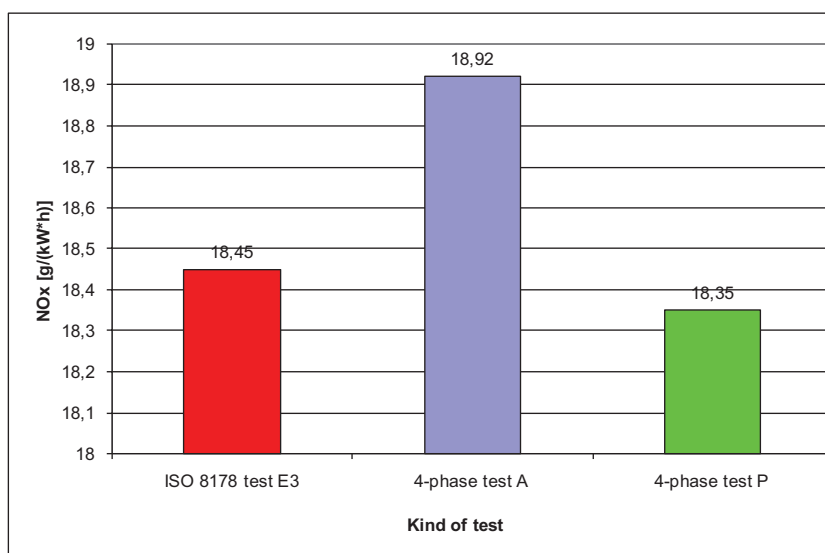


Fig.3. Comparison of  $\text{NO}_x$  emission values [g/(kW·h)] calculated by E3 test acc. to ISO 8170-4, 4-phase test A (required power  $P_0$  determined by Admiralty’s method) and 4-phase test P (required power  $P_0$  determined by Papiel’s method)

## Recapitulation

The modelling of emission of harmful compounds is a very important problem and a complex one at the same time. The scientific research work conducted at present devoted to pollution spreading concerns pollution in atmospheric air of stationary origin (power and industrial plants), motorisation and recently also airplanes. Current studies which concern first of all motorisation, because of, among other things, the size of marine engines, cannot find application for modelling emission of toxic compounds from marine engines, as the model structure depends not only on its destination but largely also on the amount and quality of input data.

The possibility of obtaining data from AIS system like ship's name, length, breadth and type, universal time bound with the vessel's passing through the „gate”, course and velocity over the ground (COG, VTG) and the ship's draft permit the creation of innovative models describing vessel traffic in the area researched and the emission of harmful compounds in exhausts both for one vessel and the whole researched area.

The method of calculating power required for vessel propulsion has significant influence on the final results of determining values of toxic compounds emission in the exhausts of vessels. During analysis of data obtained from AIS system and simulated loads of main engines it was found that vessels mostly sail in the Gulf of Gdańsk with a load of  $0.4 \div 0.6 P_n$  and  $0.9 \div 1.0 P_n$ . Yet due to the lack of hull resistance characteristics of vessels considered it seems pointless to make tests in the function of vessel velocity.

It should be added here that apart from problems that motorisation experts are coping with when modelling the emission of toxic compounds, in the case of vessels among the parameters disturbing the accurate determination of emission of particular compounds (due to lack of information or its variability) there should be additionally counted the engine's technical condition, fuel apparatus in particular, and atmospheric conditions (particularly wind direction and force).

## References

- [1] Chłopek, Z., *Modelowanie procesów emisji spalin w warunkach eksploatacji trakcyjnych silników spalinowych*, PN Politechniki Warszawskiej, Mechanika, z.173, Warszawa 1999.
- [2] Brzozowska, L., Brzozowski, K., *Komputerowe modelowanie emisji i rozprzestrzeniania się zanieczyszczeń samochodowych*, Wydawnictwo Naukowe „Śląsk”, Katowice – Warszawa 2003.
- [3] Kotlarz, W., *Turbinowe zespoły napędowe źródłem skażeń powietrza na lotniskach wojskowych*, Wyższa Szkoła Oficerska Sił Powietrznych, Katedra Płatowca i Silnika, Dęblin 2003.
- [4] Kniaziewicz, T., *Problemy modelowania emisji szkodliwych składników spalin z silników okrętowych w rejonach miejskich aglomeracji nadmorskich*, Zeszyty Naukowe Politechniki Częstochowskiej 162, MECHANIKA 26, Częstochowa 2006.
- [5] Kniaziewicz, T., Piaseczny, L., *Model of NO<sub>x</sub> Emission by Sea-going Vessels Navigating in the Gulf of Gdansk Region*, Silniki Spalinowe PTNSS – 2007-SC3, Poznań 2007.
- [6] Kniaziewicz, T., *Problems of Modeling NO<sub>x</sub> Emission from Marine Diesel Engines*, Journal of KONES Powertrain and Transport, vol.15, No.4, p. 227-234, Warszawa, 2008.
- [7] Drag, Ł., *Modelowanie emisji i rozprzestrzeniania się zanieczyszczeń ze środków transportu drogowego*, Archiwum Motoryzacji nr 1/2007.
- [8] Jourard, R., *Methods of Estimation of Atmospheric Emission from Transport: European Scientific State of the Art*, Action COST319 final report, LTE 9901 report, 1999.
- [9] Pawlak, M., Piaseczny, L., *Modelowanie ruchu jednostek morskich dla określania emisji związków toksycznych spalin*, Czasopismo Techniczne „Mechanika” z. 7-M/2008, str. 319-334, Kraków, 2008.



- [10] Kniaziewicz, T., Piaseczny, L., Merksiz, J., *Stochastic Models of Emission of Toxic Compounds in Marine Engines Exhaust*, Journal of POLISH CIMAC. Vol. 3, No. 1, p. 129-138, Gdańsk, 2008.
- [11] Pawlak M., Piaseczny L., *Model ruchu jednostek morskich dla określenia emisji związków szkodliwych spalin*. Materiały Konferencji Explo-Diesel & Gas Turbine, Międzyzdroje, kwiecień 2009.
- [12] Grabski, F., *Stochastyczne modele ruchu jednostek pływających*, Fragment sprawozdania z realizacji projektu badawczego Nr 502 009 31/1187. AMW Gdynia 2008.
- [13] Felski, A., Piaseczny, L., *Monitoring of the movement of the objects on the Gdansk bay in order to recognize the characteristics of their main propulsion systems*, Combustion Engines, No. 2007-SC1, p. 377 – 382. Poznań 2007.
- [14] Kniaziewicz, T., Piaseczny, L., *Możliwość wykorzystania informacji z systemu AIS w modelowaniu emisji składników spalin z silników statków w rejonie Zatoki Gdańskiej*, Zeszyty Naukowe AMW Nr 4, Gdynia 2008.
- [15] Kniaziewicz, T., Piaseczny, L., *Modelling the Emission of Toxic Compounds in Marine Engine Exhaust Gas*, Czasopismo Techniczne „Mechanika” z. 7-M/2008, str. 239-249, Kraków, 2008.
- [16] Pawlak, M., *Testy badania stężenia związków toksycznych w spalinach silników głównych statków pływających po obszarze Zatoki Gdańskiej*, Fragment sprawozdania z realizacji projektu badawczego Nr 502 009 31/1187. AMW Gdynia 2008.



## APPLICATION OF ARTIFICIAL INTELLIGENCE METHODS IN DIAGNOSTIC OF A SHIP COMBUSTION ENGINE – MAPS OF DIAGNOSTIC PARAMETERS

Dariusz Pielka  
Zbigniew Łosiewicz

*The West Pomeranian University of Technology*  
Al. Piastów 41, Szczecin, Poland  
Tel. +48 600 275 871  
e-mail: [dpielka@adnet.com.pl](mailto:dpielka@adnet.com.pl)  
e-mail: [HORN.losiewicz@wp.pl](mailto:HORN.losiewicz@wp.pl)

### Summary

*In the real ship's conditions, the methodology of taking an operational decision is based on the analysis of simple diagnostic data. The quality of a correct multi-criteria analysis of such data is the more dependant on the SDG diagnostic system the lower the professional competences of the engine operator. The complexity of the problem requires application of quick methods that analyse the information in a multifaceted way. The description of the current states of the engine operation can be presented in the form of a topographic map showing the current values of the operation parameters of the system, as scaled and correlated points on a plane. A change in the values of the operation parameters is imaged as a change in reciprocal location of points on the plane. On the basis of a topographic description, a classification of the engine operation state can be carried out by means of a neural classifier. Such a method of the engine operation classification will allow for obtaining a very high capability of the diagnostic system for adaptation and analysis of untypical states of the object and an easily construed visualisation of results.*

**Key words:** artificial intelligence, diagnostic of a ship Diesel engine, map of diagnosis parameters, diagnostic system.

### 1. Introduction

Different breakdowns of rates of a piston combustion engine operation can be encountered in the literature.

In the operational practice, a marine engineer operates an engine that can be diagnosed with the methods available on a ship. The diagnostic system (SD) existing on the ship consists of the diagnosed system – the engine (SDN) adapted in a specified way for fitting of a diagnostic system (SDG) to it, consisting of sensors. The accuracy and reliability of the diagnosis depends on many factors, including the accuracy of selection of measurement points, the type of measured parameters, the measurement accuracy, the correct analysis of diagnostic data and the quality of the drawn conclusions – as good as the knowledge and the experience of the engine operator and the knowledge of an engineer who designs a diagnostic system.

An essential problem is the multi-criteria analysis of the measurement data and imaging of results of such analysis. The competences of operators are very different and they are often not able to correctly read and use the results prepared and given by the SDG, which influences the level of rationalism of their operational decisions. In the real ship's conditions, the methodology of taking an operational decision is based on the analysis of simple diagnostic data that can include parameters of power media (most often the values of temperature and pressure) or accessible process parameters, e.g. the charge compression process in the cylinder or the combustion process. The quality of a correct, multi-criteria analysis of such data is the more dependant on the SDG diagnostic system the lower the professional competences of the engine operator.

The complexity of the problem requires application of quick methods that analyse the information in a multifaceted way. Identification in the shortest time of processes taking place in the engine is very essential. Therefore the description of current states of the engine operation can be presented in the form of a topographic map of states that images the current values of the operation parameters of the system as scaled and correlated points on a plane. On the basis of the topographic description, a classification of the engine operation condition can be carried out by means of a neural classifier. Such a method of the engine operation classification will allow for obtaining a very high capability of the diagnostic system for adaptation and for analysis of untypical states of the object and an easily construed visualisation of results.

## 2. Criteria structures taken for identification of the engine state

Example criteria structures that can be taken for identification of the engine state include:

- **construction structure** (different materials of specific physical and chemical properties, adequately fitted tribological systems, etc.),
- **organisational structure** (co-operating subassemblies and assemblies of devices and the engine, operating within a precisely specified time, adjusted and controlled),
- **process structure** (combustion process, cooling process, heating process, wear process (friction, oxidation, ageing, etc.).

There is a set of couplings between the structures that can be determined in an experimental way but they cannot be predicted in a computational way with too many non-measurable unknowns and the necessity to apply many simplifications.

Changes in the structures, in their serial dependences differ between themselves with their characters.

Changes taking place in the structure of interdependencies of mechanical parts are visible and immediately detectable and identifiable (vibrations, noise, pressure loss of media, tightness of systems, e.g. hydraulic, compression pressure systems, etc.).

Changes in the process structure are often detected with a long delay, are detectable but hardly identifiable, often with wrongly determined genesis and predictions (e.g. high temperature of exhaust gases – it may mean too low injection pressure, too large openings of an injector – but the reason can be different than the injector, e.g. too low fuel viscosity (too low temperature for a particular sort of fuel), wrong injection time, wrong ignition time, wrong time of valve opening, wrong process of head and cylinder liner cooling, leaky piston and cylinder system.

The parameters of the engine operation determining the technical condition of the engine, closely attributed to the adequate structure and the area of the engine can be topologically imaged on the “map of parameters” with anomalies, possibly explicitly geometrically or colouristically deformed

and clearly suggesting the operational decision to the operator as an alternative to any graphs and fields of operation non-identifiable and non-comprehensible to the operator (with different levels of technical knowledge).

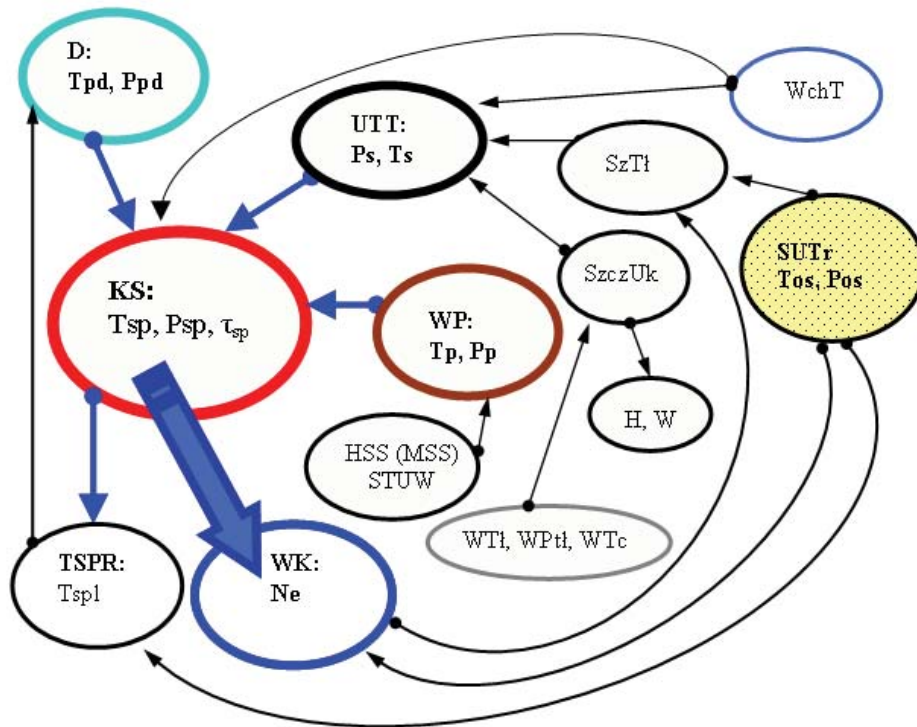


Fig.1 Dependence of the combustion process on the criteria structures of the engine:

**KS – combustion chamber:**  $T_{sp}$  – combustion temperature,  $P_{sp}$  – combustion pressure,  $\tau_{sp}$  – combustion time  
**D – supercharging:**  $T_{pd}$  – supercharging air temperature,  $P_{pd}$  – supercharging air pressure, **TSPr** – turbocharger,  
**UTT – liner-piston system:**  $P_s$  – compression pressure,  $T_s$  – compression temperature,  $T_{spl}$  – temperature of exhaust gases,  $SzTl$  – piston speed,  $SzcUk$  – system tightness,  $WPtl$  – dimension of piston rings,  $WTl$  – dimension of piston grooves,  $WTe$  – dimension of cylinder liner,  $WchT$  – cooling water for liner, **WP – fuel injection:**  $T_p$  – fuel temperature,  $P_p$  – fuel pressure, **HSS (MSS) STUW** – hydraulic controlling system, **MSS** – mechanical controlling system, **STUW** – technical condition of injection system, **WK – crankshaft:**  $N_e$  – shaft power, **SUTr – lubrication of tribological systems:**  $T_{os}$  – temperature of lubricating oil,  $P_{os}$  – pressure of lubricating oil

### 3. Maps of diagnostic parameters of an engine

The Fig. 2 shows the idea of creating maps of diagnostic parameters of an engine. A circle is the simplest geometric figure, on the basis of which the initial model has been based. It is possible to create a 'set of maps' divided into 'packages of maps', the quantity of which is limited only by the capacities of electronic equipment. Due to editorial limitations, the idea has been presented on a single map.

The 'map' should, in a simple way, signal the trends of changes in particular structures. Centric circles set the rings (three outer ones separated from the inner ones by a dotted line) defining the values of parameters: the white ring means normal state, the broken ring (outside the white one)

means excess of parameters above the upper limit of normal values, the dotted ring (inside the white one) means excess of parameters below the lower limit of normal values. In order to facilitate understanding of the idea, the image area (image on the screen) has been divided into four zones.

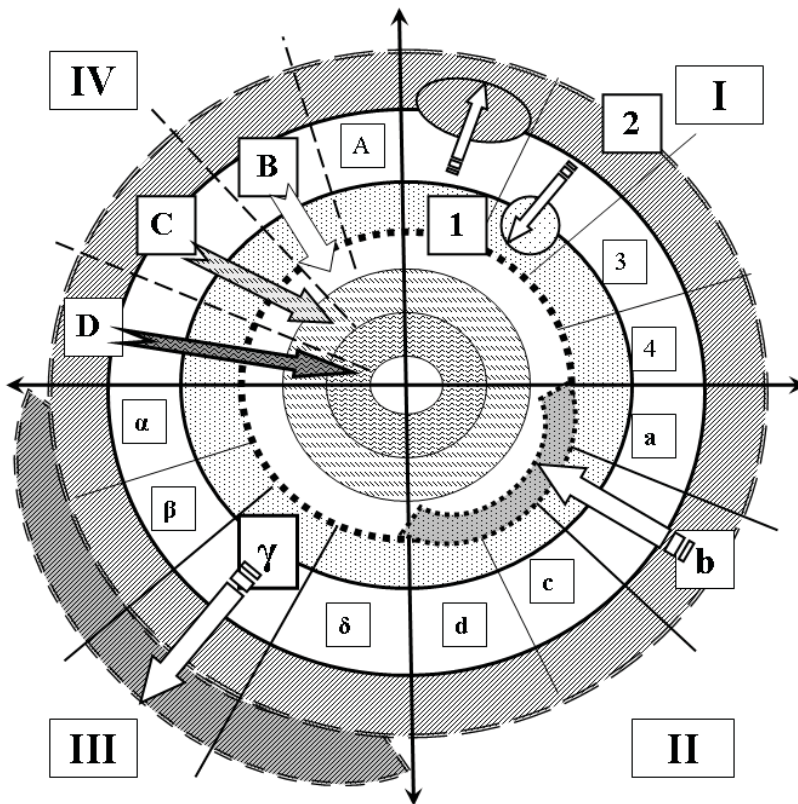


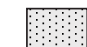


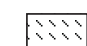



Fig. 2. Idea of creating of a map of diagnostic parameters of an engine:

-  - field "I-1" excess of the upper limit of the normal parameter relating to the dimension or the operation of an engine element or subassembly
-  - field "I-2" excess of the lower limit of the normal parameter relating to the dimension or the operation of an engine element or subassembly
-  - field "II-b" excess of the lower limit of the normal parameter relating to the dimension or the operation of a device or the engine system
-  - field "III-γ" excess of the upper limit of the normal parameter relating to the dimension or the operation of a device or the engine system
-  - field "IV-B" - a field determining the state of full efficiency of an engine
-  - field "IV-C" - a field determining the state of partial efficiency of an engine
-  - field "IV-D" - a field determining the state of inefficiency of an engine



- "outer circles" - a field determining normal values of parameters (green colour)



- "outer circles" - a field determining excess of the lower value of the normal parameter (yellow colour)



- "outer circles" - a field determining excess of the upper value of the normal parameter (red colour)

► In the zone marked with "I", excess of limits of parameters concerning particular systems or devices has been shown (depending on the class of the map detailing):

- in the field "1" visualisation of excess of the upper limit of the normal parameter has been shown,
- in the field "2" visualisation of excess of the lower limit of the normal parameter has been shown,

► In the zone marked with "II" and "III", excess of limits of parameters concerning subassemblies or the whole engine has been shown

After processing by the logic system, the influence of the parameter change on a subassembly or the whole engine can be shown:

- in the field "II" visualisation of excess of the lower limit of the normal parameter of the engine operation resulting from change in one or in several parameters of the engine elements operation has been shown (e.g. damage to the injection system in one system),
- in the field "III" visualisation of excess of the upper limit of the normal parameter of the engine operation has been shown,

► In the zone marked with "IV" visualisation of the condition of the whole engine has been shown ("inner" rings limited from outside with a dotted line):

- in the field "B", the white arrow shows the field (white) of normal operation of the whole engine marked with green colour,
- in the field "C", the grey arrow shows the field (marked with a thin wavy line) of limited operation marked with yellow colour,
- in the field "D", the dark grey arrow shows the field (marked with a dense wavy line) of unsuitability for operation marked with red colour,

In practice, such approach to the analysis of states of the engine operation can be accomplished with use of artificial neural networks. The advantages of such implementation methods are their high flexibility, versatility and possibility to use them for analysis of the object without the necessity of having the mathematical description of the object. The neural networks have got the ability for parallel processing of information and recognition of topographic maps reflecting the current state of an object under diagnosis.

For recognition of the object's condition one can use two types of networks: learning networks and self-learning networks.

The learning networks are most often used for well defined problems where we have got the knowledge what the network's response will be. For the learning networks it is possible to create a neural classifier of states (double-state or triple-state). However, the structure of such classifier is complex and the learning process is quite laborious. Input of new elements into the tested system requires changing of the neural network architecture and its re-teaching.

An alternative solution is the application of the Kohonen's neural network. Such networks have got the feature of topographic imaging of complex shapes, thanks to which they learn any imaging.



Another feature of such network is the process of self-learning consisting in competition between neurons. The neural network responds to the input signals. Obtaining of the final order of the system of neurons corresponds to the diagnostic maps of an object under testing. Input of new elements into the system does not require significant changes, and the neural network adapts itself to new tasks. A detector of the hybrid diagnostic system of a ship engine can make the neural classifier of the object's conditions. The neural networks analyse signals coming from the diagnosed object. On the basis of the base, the expert's system takes decisions by making use of the information about the current map of the object's state gained through the neural network.

#### 4. Summary

Modern ship engines need rational operation aiming at both increasing their reliability and their efficiency. Therefore development of diagnosing systems that make use of the most modern technological achievements enabling processing of data is evident. Depending on the type of diagnostic information and the expected results of operation of a diagnosing system, different mutually supplementing methods of data processing are used.

Therefore, application of neural networks as a supplement of statistical and probabilistic methods used at different stages of the engine control and diagnostic processes allows for shortening the time for assessment of technical condition of elements, subassemblies as well as the whole engine. The idea of maps of diagnostic parameters presented in the paper is another trial of visualisation of the results of the SDG operation that allows a mechanic for determination of the condition of the engine in a short time as well as for monitoring the trends in changes of diagnostic parameters. At the same time, it may contribute to selection of an unambiguous operational decision of high degree of reliability worked out by the SDG to the mechanic.

#### References

- [1] Duch W., Korbicz J., Rutkowski L., Tadeusiewicz R., *Sieci neuronowe*, Wydawnictwo Naukowo - Techniczne, Warszawa, 2000.
- [2] Girtler J., Kuszmider S., Plewiński L.: *Wybrane zagadnienia eksploatacji statków morskich w aspekcie bezpieczeństwa żeglugi*. WSM w Szczecinie, Szczecin 2003.
- [3] Korbicz J., Koscielny J., Kowalczyk Z., Cholewa W., *Diagnostyka procesów*, WNT, Warszawa 2002.
- [4] Łosiewicz Z Pielka D., *Założenia ekspertowego systemu monitoringu i sterowania wybranych procesów eksploatacyjnych tłokowego silnika spalinowego*, Zeszyty Naukowe nr 71, Akademia Morska w Szczecinie, Szczecin, 2003.
- [5]. Pielka D Łosiewicz Z., *Możliwości zastosowania metod sztucznej inteligencji do diagnostyki okrętowego silnika spalinowego*, Zeszyty Naukowe nr 162 K/2, AMW w Gdyni, s. 261-266, AMW w Gdyni, Gdynia 2005.





## MODEL TESTS OF PISTON RING-CYLINDER LINER COLLABORATION ON HIGH POWER ENGINES

**Wojciech Serdecki**

*Institute of Combustion Engines and Transport  
Poznań University of Technology  
3, Piotrowo St., 60-965 Poznań  
tel. +48 665 2243, fax: +48 6652204  
e-mail: wojciech.serdecki@put.poznan.pl*

**Piotr Krzymień**

*Institute of Combustion Engines and Transport  
Poznań University of Technology  
3, Piotrowo St., 60-965 Poznań  
tel. +48665 2239, fax: +48 6652204  
e-mail: piotr.krzymien@put.poznan.pl*

### **Abstract**

*Proper selection of materials for cylinder liner and piston rings, correct design of collaborating surfaces as well as the use of lubricating oils of better and better properties assure long and reliable operation of piston rings in small and medium size engines. In the case of high power engines, especially marine ones failures caused by incorrect collaboration of rings and liner still happen. Supply and correct distribution of lubricating oil over cylinder surface could be one of the causes of this phenomenon.*

*Regulations introduced by classification societies make impossible research on piston ring – cylinder liner set of running engines. Mathematical models or simulation test benches are the possible way of carrying out such tests.*

*This paper presents some test rigs and analytical models revealing their advantages and shortcomings.*

**Keywords:** *combustion engine, friction losses, measuring methods*

### **1. Introduction**

Full information on phenomena accompanying the collaboration of engine kinematic pairs is available from tests carried out on running engines but such tests very often are impossible. For example, tests on collaboration of marine engine kinematic pairs such as piston rings and cylinder liner require an installation of certain type of sensors (pressure, temperature or distance, for instance) that means a need for changes in construction of collaborating parts. Such modifications on marine engines are forbidden by the classification societies because they can considerably affect the ship's safety.

Tests on material models of piston–cylinder assembly parts could be a substitution for an investigation on phenomena accompanying the collaboration of these elements conducted on a real engine. Such models allow to reconstruct the operational conditions of frictional associations , geometry of mating parts contact, kinematics and dynamics of their loading as well as phenomena occurring by the process of lubrication. An additional advantage of such tests is a relatively low cost, short time needed for carrying out the investigation and no chance for engine failure.

Another way to evaluate the phenomena present on engine subassemblies is a construction and running the mathematical models of these subassemblies. It is noteworthy that a mathematical model is merely an approximation and should be validated in a course of tests carried out on a real engine or at least on its material model. Successive chapters of this paper will present selected constructions of test benches where investigation on piston ring – cylinder liner collaboration could be performed and the most significant information about mathematical models will be provided.

## 2. Model test benches for tests on piston ring – cylinder liner collaboration

Tests benches where investigation on collaboration of piston cylinder group elements could be carried out can be classified into those entirely designed and constructed for this purpose and other ones constructed on the basis of a typical engine where certain parts and subassemblies have been modified.

The model test benches of the first type offer wider possibilities for investigation, because the constructional details such as the range of operational parameters adjustment, location of sensors, selection of measurement devices could be foreseen at the very beginning stage of design. On the other hand, they are much more expensive than those using parts of a typical combustion engine.

Taking into consideration methods employed for investigation one can distinguish test stands using optical and electrical methods.

Test stands presented in Figs 1 and 2 are the examples for the use of optical methods in tests on evaluation of ring–liner collaboration quality.

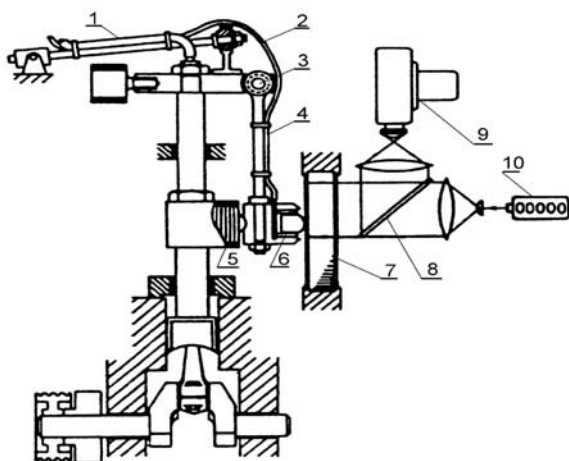


Fig. 1. Model tests stand for optical measurement of oil film parameters: 1 – high pressure pipe supplying air to the actuator, 2 – lubricating oil supply pipe, 3 – joint, 4 – slider leading beam, 5 – air actuator, 6 – slider, 7 – glass plate, 8 – semitransparent plate, 9 – camera, 10 – coherent light source (laser) [2]

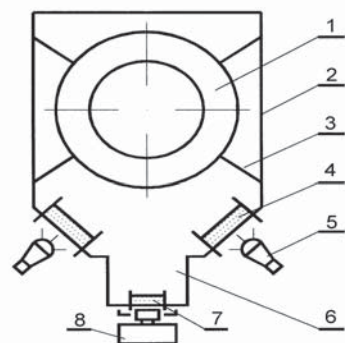


Fig. 2. Schematic of the piston-cylinder assembly model, projector and observer (camera) positions for reflection method: 1 – glass cylinder, 2 – dark chamber, 3 – diaphragm, 4 – primary filter, 5 – impulse xenon lamp, 6 – camera box, 7 – secondary filter, 8 – camera [2]

The test stand presented in Fig. 1 has been constructed on the basis of a typical IC engine equipped with systems for research on oil film formed between models of ring (6) and cylinder (7). The model of ring fixed to a piston moves reciprocally relative to a steady glass plate lubricated with oil and ring pressure against the plate is exerted by a pneumatic servomotor (5). Through a semitransparent plate(8) and transparent one (7) a laser beam (10) comes to the oil layer (oil film) which makes that as a result of interaction between reflected and falling waves an arrangement of interference strips characteristic for a momentary oil layer thickness is being recorded by the camera (9). There is a possibility to reproduce the changes in oil film thickness throughout the entire cycle of engine operation thanks to the further analysis of recorded images.

The test stand presented in Fig. 2 offers a quite different method of oil film evaluation. Cylinder liner made of cast iron has been substituted by a glass model (1). The cylinder surface is being lubricated with oil mist outflowing from slide bearings and additionally with oil sprayed to precisely specified regions of liner by a set of special jets (omitted in Fig. 2) which allows for a continuous adjustment of oil dose. Thanks to strong xenon lamps it is possible to observe and record (camera 8) the oil layer over the cylinder surface and to estimate certain oil parameters including oil layer thickness and oil film extent, in particular.

Design of the stand presented in Fig. 3 is quite different from a typical model of engine piston-cylinder assembly. A flat slat (5) representing a piston ring slides over a plate (1) covered with lubricating oil. Differently than in real engine the oil layer is not renewable, i.e. fresh oil does not come to the plate in consecutive strokes. The slat is fixed in a groove cut in a flat model of piston (clamp 7) hanged on transducer (8). It is pressed on against the moving plate with a flat spring or hydraulic actuator controlled by a special circuit. It is possible to fix in the clamp a series of slats of profiles corresponding to the face profile of a real piston ring.

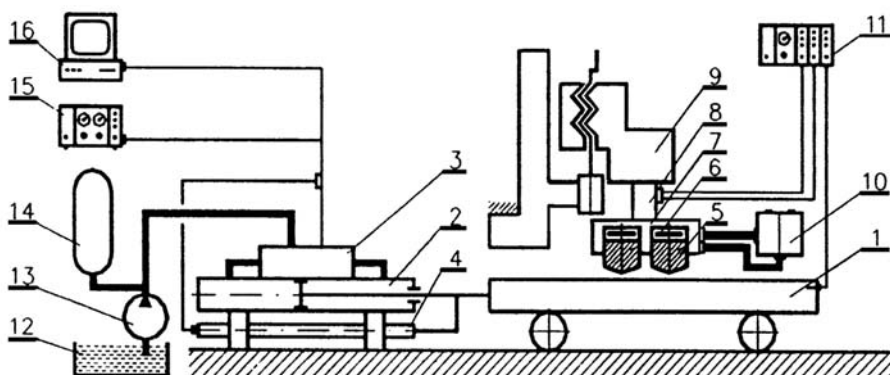


Fig. 3. Schematic of test stand: 1 – plate, 2 – actuator, 3 – control valve, 4 – position resistor, 5 – slat, 6 – flat spring, 7 – piston model, 8 – force transducer, 9 – support, 10 – slat pressure system, 11 – measuring&control system, 12 – hydraulic oil reservoir, 13 – oil pump, 14 – pressure accumulator, 15 – analogue control system, 16 – digital control system [5]

The hydraulic oil from oil reservoir (14) is being pumped to the control valve (3) by the oil pump (13). According to the position of control valve the oil is being pumped to the left or right side of the actuator plunger (2) which results in the movement of cart with the plate simulating cylinder liner surface.

Either an analogue (15) or digital (16) control system can be used. The first one allows for a reciprocating movement according to gradually selected parameters of speed and amplitude.

When applying the digital control system it is possible to use a computer program which allows to realize an arbitrary motion of the plate including a reciprocating movement, typical for combustion engines.

Due to a sophisticated measuring system (11) which is a part of the simulation stand it is possible to determine oil film essential parameters like thickness, pressure and friction forces connected with the motion of ring model. Also other sensors monitoring plate motion and recording its position, speed and acceleration are installed on the test stand.

Taking into consideration features of the stand including possibility of tests on rings of big size and different profile geometry it can be assumed provisionally that this test stand allow to conduct tests on oil film parameters of the engine of high power. Next chapter will validate this assumption.

### 3. Is it possible to test a ring-liner collaboration on a test stand?

Both marine and generator engines belong to the group of high power engines (power higher than 100 kW/cyl) as well as the bigger railway engines which have the power indices close to the border value [3]. Among those mentioned the biggest are two stroke low speed marine engines. Their popularity results from the highest efficiency (nowadays beyond 50%) and possibility of consumption so called heavy fuel of relatively low price.

The stroke to cylinder diameter ratio is the characteristic parameter for contemporary marine diesels of high power where it reaches the value of 4 (this secures continuity of oil film over cylinder surface thanks to the high value of the piston mean speed at low rotational speed). For engines of higher rotational speed the value of this parameter is far lower (see Table 1).

*Tab.1. Vital technical data of exemplary engines of high power [1, 3, 4]*

Engine Technical data	locomotive		generator		marine	
	12LDA28	214D40	L23	L21	L35MC	K80MC-
D cylinder diameter [mm]	280	230	230	210	350	800
S piston stroke [mm]	360	300	300	310	1050	2592
k ratio (S/D)	1.28	1.30	1.30	1.47	3.0	4.00
Rotational speed [rpm]	750	750	720	900	210-178	93-70
Power per cylinder [kW/cyl]	94.7	77.2	130	190	650	3640
$\lambda$ ratio	0.25	0.26	0.25	0.23	0.42	0.44
Piston mean speed [m/s]	9.0	7.5	7.2	9.3	7.35	8.10

Full reconstruction of engine kinematics on the model stand would mean the same piston displacement with similar speed. It means that it is impossible to fulfill conditions listed in Table 1 on the presented test stand [5,6]. Boundary value of speed that could be performed on test stand is about 12 rad/s which corresponds to the piston mean speed of about 3.8 m/s (when maximum is 4 m/s), i.e. the value several times lower than that on real marine engine (see Fig. 4).

Course of speed vs. crank angle presented in Fig. 4 show only the maximum value of speed and its position expressed as corresponding angle. Presentation of speed fluctuations at selected points of its displacement seems to be a better form of such illustration (see Fig. 5).

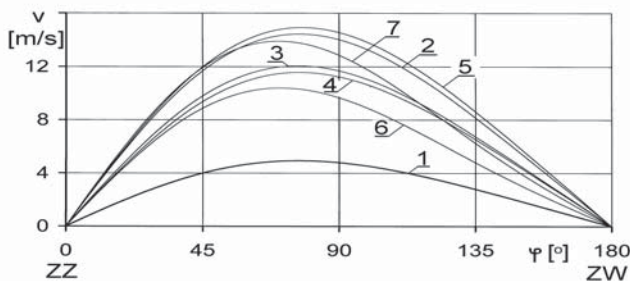


Fig. 4. Courses of speed vs. crank angle for: 1 – model test stand 2 – the LDA28 engine, 3 – the D40 engine, 4 – the L23 engine, 5 – the L21 engine, 6 – the L35MC engine 7 – the K80MC engine

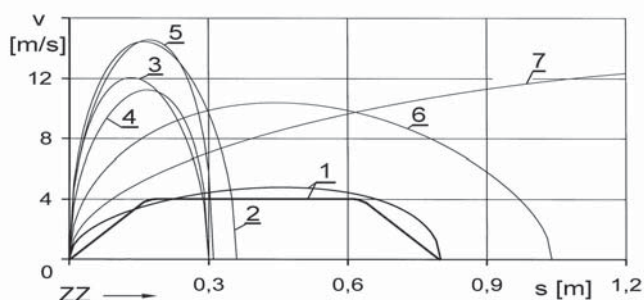


Fig. 5. Courses of speed vs. displacement for: 1 – model test stand 2 – the LDA28 engine, 3 – the D40 engine, 4 – the L23 engine, 5 – the L21 engine, 6 – the L35MC engine 7 – the K80MC engine

According to the test stand technical data the range of plate stroke is several centimeters to less than one meter (0.8 m) which allows for reproduction of ring displacement of most of locomotive and generator engines but could not represent the long stroke marine engine (of far longer stroke).

Digital control of plate movement makes possible any kind of displacement between both dead center with a constant speed of 4 m/s (horizontal line no 1 in Fig. 5). Though the ring movement with constant speed differs from that on a real engine it can be employed for tests because it facilitate the evaluation of the effect of ring selected design parameters on the formation of oil film.

As it comes from the above considerations full reproduction of piston and rings movement (taking into account speed and range) would not be possible on the presented test stand, which does not mean that it is completely aimless. For the engines of stroke longer than the plate range another kind of tests could be performed, namely over the sections shorter than the stroke. On the other hand, for engines of shorter stroke tests could concern speeds lower than the nominal one. Thanks to the fact that both the oil layer thickness and the friction force are approximately proportional to the speed of ring movement, the value of these parameters can be estimated this way for a real engine.

A large number of input values for which tests could be performed makes that investigation could be time consuming and expensive and the results obtained could be of low value. The reasonable solution could be development of stand mathematical model (as a computer program). Such creation and further application (after validation) could improve the effectiveness of research and carry them out within a range possible to be performed on the test stand.

#### 4. Mathematical model of test stand

Description of the test stand presented in chapter 2 shows that this solution does not allow for a full reproduction of phenomena encountered on the engines of high power (listed in Table 1). Beside differences resulting from different kinematics of the stand following shortcomings should be noted: omitting the effect of ambient pressure, low operational temperature (ambient temperature), ring sliding over unreconstructed oil layer, constant value of ring pressure against the plate.

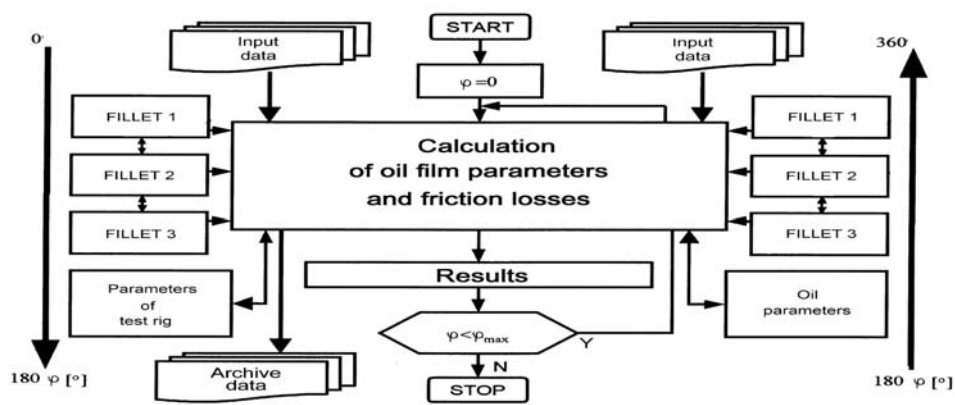


Fig. 6 Block schematic diagram of test stand mathematical model [5]

Fig. 6 shows the most important modules and mutual connections of the model. Within initial 180 grades of crank angle the slat encounters the fresh layer of oil on the plate which secures fully flooded contact with plate (at the inlet). Along with the increase in plate speed the pressure in oil film increases which eventually causes the rise in oil layer thickness. After the maximum oil layer thickness came along in the region of maximum speed, a slow decrease appears. Thanks to so called squeeze effect this pressure drop does not reach the value of zero at both dead centers. At consecutive strokes (180 to 360 degrees and beyond) the slat slides over the oil layer left after previous stroke. The layer thickness slowly decreases because the oil surplus is being swept towards the plate turning points. As a result the slat face area covered with oil also decreases.

Computations carried out according to the described model give courses of oil layer thickness (in front, behind and under the slat), pressure distribution in oil film as well as courses of friction force. Results can be presented in tables or graphs and can be further processed.

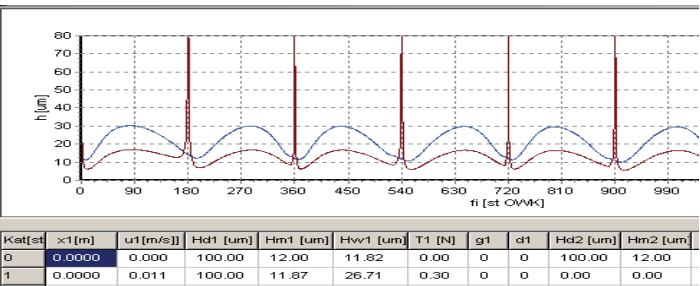


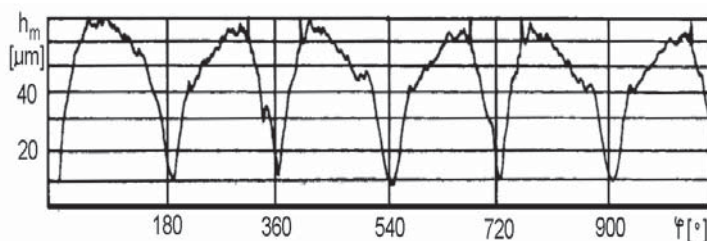
Fig. 7. A view of computer program chart – noticeable fragments of oil film parameter computations performed on the test stand



Exemplary picture of simulation program chart with courses of minimum oil film thickness and the thickness of oil layer left behind the slat is presented in Fig. 7.

Fig. 8 shows a comparison of minimal oil film thickness measurement results recorded on test stand (a) with results of model computations (b) carried out for input data corresponding to the stand operational parameters. As it can be seen maximum and minimum values of oil film thickness are the same, also the drop in thickness along the consecutive strokes is very similar. There are numerous discontinuities and waves on the course of recorded film thickness which result from plate shape imperfections not taken into consideration in the computational program.

a)



b)

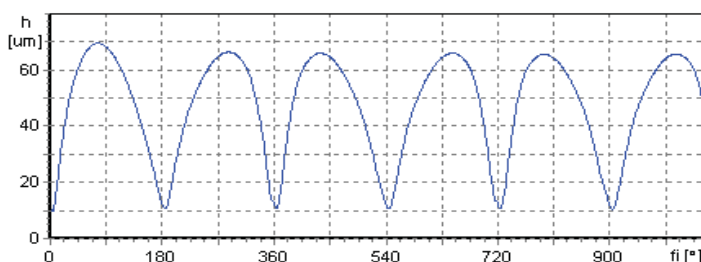


Fig. 8. Courses of oil film minimum thickness recorded on model stand (a) and for mathematical model (b)

## 5. Summary and conclusions

Summarizing analyses presented in the previous part of this paper one can note that the presented test stand allows:

- to evaluate phenomena accompanying the collaboration of piston ring and cylinder liner in a presence of lubricating oil, including oil film thickness and friction force, for a single ring (slat) or the complete set of rings,
- to reconstruct partially the piston movement for long stroke marine engines
- to reconstruct phenomena accompanying the piston movement for locomotive and generator engines, however at speeds lower than nominal ones.

On the other hand, use of computational program allows to execute tests within the range unreachable for the test stand.

At present efforts on development of the model stand are being carried out towards possibility of refreshing the oil layer over cylinder surface in a way similar to that applied on marine engines and perform the test at higher temperature of operation.



## Literatura

- [1] Gronowicz J., Kasprzak B., *Lokomotywy spalinowe*. WKiŁ, Warszawa 1989
- [2] Iskra A., *Studium konstrukcji i funkcjonalności pierścieni w grupie tłokowo-cylindrowej*. Wydawnictwo Politechniki Poznańskiej, Poznań 1996.
- [3] Kopczyński M., Mańczak W., *Rozwój konstrukcji dwusuwowych silników okrętowych na tle osiągnięć firmy H. Cegielski-Poznań S. A.* Silniki Spalinowe nr 3, 2006.
- [4] Marine Engine Programme – MAN B&W, informator, 2007.
- [5] Serdecki W., *Badania współpracy elementów układu tłokowo-cylindrowego silnika spalinowego*. Wydawnictwo Politechniki Poznańskiej, Poznań 2002.
- [6] Serdecki W., Krzymień P., *Assessment of possibilities of testing the high power engine piston ring-cylinder collaboration on a model test standing*. Journal of KONES Powertrain and Transport. European Science Society of Powertrain and Transport Public, vol.15 No. 2, Warsaw 2008



## SELECTED PROBLEMS TO LOSS AND MAINTAIN THE PROPRIETES OF TECHNICAL OBJECTS.

**Zbigniew Smalko**

*Air Force Institute of Technology*  
ul. Księcia Bolesława 6, 01-494 Warszawa 46, Polska  
tel.: +48 22 6852282

### **Abstract**

*Durability is one of the most important features of components (elements and subsystems) and technical technical objects as a whole. By durability we understand the capability of an item to maintain its useful properties under given circumstances of work and maintenance until a limit state is achieved. Borderstates are understood as states when an object for technical reasons, economic reasons or functional reasons (innovative) and/or for other essential reasons is no longer fit for use. The measure of durability of technical objects is a period of use after which a objects loses its serviceability according to its design. The moment a technical object loses its required properties is called the top border of durability. However, it is worth noting, that the moment starting from which an item is no longer fit for use is not always a distinct one. Therefore, a multi-aspect selection of criteria determinating the upper limit of operation time is the crucial issue.*

**Keywords:** *durability, usability, maintainability*

### **KINDS OF DURABILITY**

A loss of required usable properties characteristics can result inter alia from technical reasons, economic reasons or perished innovativeness as it is present hereinafter.

*The economic durability* is identified with retention usable properties until the moment when further maintaining of requested technical availability is found to be uneconomic. This is dependent on both economic and technical factors. An important measure of durability in light of the economic aspect is the unit price of maintaining an objects availability and the profitability of its use.

*The innovative durability* is identified with the preservation of usable features until a new generation of competitive and non-compatible technical objectss appears, when at the same time a possible modernisation of an item is uneconomic. An important feature in terms of innovativeness is a prospective rise in profits due to the employment of a new generation technical objects. The necessity to terminate the use of a technical objects can be result from its incompatibility with the technospheric environment.

*The safety durability* is identified with retention already existing usable properties until hazards occur. A need to terminate the operation of an object can result from non-fulfilment of objects safety requirements in the human- object-environment system .

It is obvious that the technical durability -the physical durability to be exact - is what constitutes a reference base for all considerations on a lost worthiness of a given technical objects.

*The technical durability* is identified with retaining a required value of usable features until the possibility to maintain usable features to ensure a required level of the operational availability by means of repairs and technical services is irretrievably lost.

The technical durability expires due to the depletion of technical expendability since there is no technical possibility of upgradeability of an object.

*The measure of life (durability)* of a technical objects is the service life after the termination of which a technical objects loses its capability of use according to its designed application.

For human- object -environment systems one uses the term of liveliness, which applies to a multiple renovation (including a biological renovation) and sustaining of functions (including life functions) over a defined period of use under determined conditions. For the above systems also the notion of survival under sudden overloads (e.g. during an attack, sudden weather changes, hurricanes, tsunami, volcanic erosions) etc. is used. Due to this, an object loses irrevocably its capability of further functioning.

## LOSS OF USABLE PROPERTIES

The technical durability is considered usually at the macroscopic level and the physical durability at the microscopic level.

In case of the macroscopic level (considering constraints between objects elements and subassemblies which create the structure of a technical objects in the energetic meaning). On a microscopic level one considers interatomic constraints, which occur in material structures. The material of design elements is considered a system with a structure of constraints, superimposed onto microscopic material particles.

Considering the durability of a design material one takes into account the laws of *the physics of failure*. Therefore the *physical durability* is expressed as a limit period resulting from the loss of the hardness of its components against the effect of enforcing factors, in particular of working factors.

The art of engineering consists, inter alia, in finding the relations between defects in the substance of a design material and the failure of the technical objects as a whole.

Three destructive phenomena play the basic role: fatigue, metal corrosion and wear due to friction. The first process results in fractures and breaks of shaped pieces. The result of the two other phenomena, is a loss of the surface material layer, called wear. The results of these phenomena decide, inter alia, whether the usefulness of an objects can be technically restored.

Exceeding the permissible values of usable features (states of characteristics) related to a correct functioning of an object, causes a variety of unwanted phenomena and events.

Such damages may leave an object in an unwanted technical state, in which this item does not fulfill its required usable functions; loses the capability of repairing it and/or it does not satisfy safety requirements..

According to a thorough analysis the durability is defined with two notions - *strength and resistance (hardness)*

**The strength** is a property define the capability of a design material subjected to allowable loads to maintain required usable properties. It is understood as a capability of maintaining - maintainability - of the internal cohesiveness of a material until permissible working loads are exceeded.

One distinguishes an immediate strength and fatigue strength, i.e. a capability of a repeated taking on of usable loads. In the latter case, a destructive process, called a fatigue occurs and results in brittle ruptures, slip ruptures and split ruptures as well as in plastic and elastic deformations.

The probability of occurrence of this kind of damage is a basis to determine the upper limit of the use-time of design elements.

The strength is a property, therefore a physical value, expressed in units of measure, which consequently can have particular numerical values.

**The resistance** is a feature which defines the capability of a structural material and associations of technical objects elements to maintain the required element characteristics and associations when subject to impact of external and internal forcing factors..

The requisite cohesiveness of a system is maintained thanks to the internal energy of cohesion binding material parts of a system.

There are three basic factors, which contribute to maintaining the system's resistance; these are: proper strength of an item, properly selected load acting on an item and a controlled speed of deterioration of objects characteristics.

The resistance can be regarded as a non-measurable feature (a behaviour manifestation). E.g. technical objects can have a resistance or not. This resistance can be described only approximately as very low, low, high or very high etc

## **PRESERVATION OF OBJECTS USABILITY**

Considering technical technical objects as consisting of assemblies, association of kinetic and static elements, one considers them as macro systems of a structure of constraints superimposed on cooperating design elements.

As a result of destructive processes within systems of associated design elements *natural and imparted usable constraints disappear* as well as *parasite constraints develop*. This is the reason why components lose their worthiness and consequently rendering useless of the objects as a whole. One distinguishes two extreme states of technical objects.

The first extreme state being the one in which an item loses its capability of processing and transferring energy (due to evolved additional parasitic constraints and/or disappearance of useful constraints).

The second extreme technical state is a state when an item loses its capability of performing working moves and obtainment of a required speed of relocation – movement (due to a change of purposeful constraints to restricted constraints and due to an elastic deformation of constraints and kinematical pairs under the impact of forces and temperature).

According to a thorough analysis the durability is described with a set of two notions *maintainability and supportability*.

**The maintainability** – a feature of a machine and technical equipment, defines its capability of performing maintenance as well as service and repair steps within a given time.

These steps are: repairs to restore a requisite condition (state), a technical service to maintain a required condition and a technical inspection to determine the technical condition of a technical object.

*The tractability of maintenance* consists in features, which enable easy services and repair of a technical objects as well as keeping a technical objects in a required condition by way of an appropriate strategy of maintenance.

*The strategy of maintaining* of a demanded technical operational stand-by is a rational time schedule of inspections of the technical objects condition and preventing steps or upgrading steps. This strategy consists in a determination of such work periods of technical objects, which satisfy to the best advantage technical, organisational and cost limitations.

The measure of the maintainability can be e.g. such a 'physical value' like performed technical steps or a property (a behaviour manifestation), e.g. a technical objects shows the capability of maintenance or repair or it does not. It can be also definite - not clearly - as a very low, low, high or very high etc. capability.

**The supportability** – a feature expressing a *serviceability* and usefulness of technical equipment and means to maintain a machine in a required technical state.

As a result of very advanced technical progress, the use of machines is more and more dependent on professional maintenance. Performing maintenance and technical checks calls for modern inspection and measuring devices, availability of service with spare parts and appropriate consumables. Logistic service guarantees safe and effective use of technical objects.

A measure of the *supportability* can be e.g. such a physical quantity as a required diagnosing time, spare parts delivery time etc. or e.g. a feature of behaviour like accessibility or non-accessibility of services [0,1]. It can also be described approximately as a very low, low, high or very high professionalism of maintenance.

## CONCLUSIONS

Therefore in order to estimate durability the following aspects have to be determined:

- a technical aspect: *lack of technical means of restoring a required technical condition* due to an overly dispersed energy of internal structural cohesiveness of an object
- an economic aspect: *non-profitability of further use* due to an excessive rise in unit operating costs
- aspects of innovation: innovative manufacture of technical objects of *an increased output*,
- *new properties and better compatibility* as a result of new requirements for use, which are a consequence of a new generation of solutions.

## BIBLIOGRAPHY

- [1] Arendarski J., *Trwałość i niezawodność budynków mieszkalnych*, Arkady, Warszawa, 1987.
- [2] Grzesiak K. Kołodziejcki I., Netzel Z., *Badania trwałościowe obiektów technicznych*. WNT, Warszawa, 1968.
- [3] Haviland R.P., *Niezawodność urządzeń technicznych*, PWN, 1968.
- [4] Mazur M., *Terminologia techniczna*, WNT, Warszawa 1961,
- [5] Norma "Wybór wskaźników niezawodności", PN-77/N-04010, PKNMiJ, Warszawa, 1977.
- [6] Radkowski S., *Podstawy bezpiecznej techniki*, OFPW, Warszawa, 2003.
- [7] Smalko Z., *Charakterystyki spolegliwości układu-człowiek maszyna*, Materiały Szkoły Niezawodności PAN, Szczyrk 2007,
- [8] Smalko Z., *Selected problems of description and estimation of durability*, Journal of KONBiN, No 2(4) 2008, Warsaw.
- [9] Warszyński M., *Niezawodność w obliczeniach konstrukcyjnych*, PWN, 1988.



## RANDOMNESS OF ROLLING BEARINGS' ELEMENTS GEOMETRY AS PROBABILISTIC FACTOR OF BEARINGS FATIGUE LIFE

**Michał Styp-Rekowski**

*University of Technology and Life Sciences  
al. Prof. S.Kaliskiego 7, 85-789 Bydgoszcz, Poland  
tel.: +48 52 3408623, fax: +48 52 3408245  
e-mail: [msr@utp.edu.pl](mailto:msr@utp.edu.pl)*

### **Abstract**

*The great number of factors generate situations that real dimensions of each machine elements are different from nominal ones. In the case of rolling bearings elements mentioned disagreements are small – their values are rank of micrometers. However, such small differences can generate significant changes of operational features of bearings. The analysis of influence of ball dimensional deviation on load distribution in ball bearings is presented in this paper. The probability of occurrence of ball diameters of the range of acceptable values is statistically determined. Random distribution of this important dimensions results in other than nominal level of internal stresses (in the contact area of balls and raceways) and therefore true values of some operational features of bearings are other – the most often smaller – than calculated ones. In presented analysis sequence of occurrence of different ball diameters is also taken into account.*

**Key words:** ball bearing, dimensional deviation, operational features of bearing, random character of balls diameter

### **1. Preface**

A lot of factors which determine each manufacturing process cause situation which has random character. In this connection real dimensions of every machine elements, including rolling bearings, are encumbered with machining dimensional deviations. Therefore, real dimension can differ from nominal in some value, however, not greater than boundary value for specific accuracy class of machining. Consequently, in case of rolling bearings the essential factor is dimensional selection of their elements because it determines inner load distribution in contact area of rolling elements and raceways. The more uniform distribution - the achievement of calculated durability of bearings close to the true value is more probable.

The statistical analysis of probability of existence in the bearings the balls' diameters of specified values is presented below. The results of analysis are necessary for exact analytical designation of fatigue life of the rolling bearings, e.g. Applied in combustion engines.

For standard rolling bearings analytical procedures are well-known and experimentally verified, instead for special bearings – this kind is analyzed in this paper – appears necessity of description new ones.

### **2. Load distribution inside bearing**

The rolling bearings contain rolling elements (e.g.: balls, rollers, needles) of different diameters

(of course in the range of acceptable deviations for specific bearings' accuracy class), just for that reason real load distribution, and thus also contact pressure between rolling elements and raceways, will be distorted in comparison to analytical – Fig. 1.

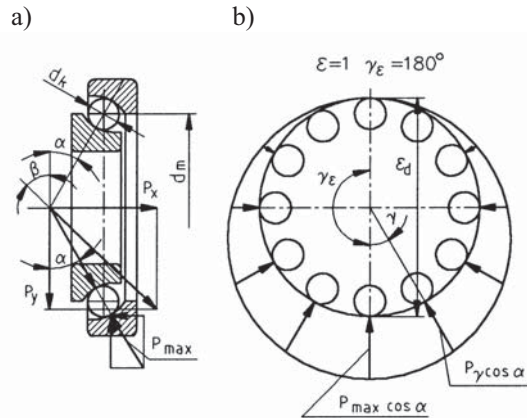


Fig. 1. Theoretical load distribution in angular ball bearing: a) distribution of forces in contact area of balls and raceways, b) distribution of internal load of bearing circuit for determined load conditions

The values of internal load existing in the rolling bearings and stresses in the contact area of balls and raceways one can calculate by well-known relationships, e.g. [2, 5]. For inner forces  $P_\gamma$  it is the following equation:

$$P_\gamma = P_{\max} \left[ 1 - \frac{1}{2\varepsilon} (1 - \cos \gamma) \right]^{\frac{3}{2}}, \quad (1)$$

in which:

$$P_{\max} = \frac{P_y}{J_y(\varepsilon)z \sin \alpha}, \quad (2a)$$

or

$$P_{\max} = \frac{P_x}{J_x(\varepsilon)z \sin \alpha}, \quad (2b)$$

where:

- $P_{\max}$  - maximum internal force,
- $\varepsilon$  - load distribution factor,
- $\gamma$  - position angle,
- $P_{x,y}$  - load components, respectively: axial or radial,
- $J_{x,y}$  - load integrals, respectively: axial or radial,
- $z$  - number of the balls,
- $\alpha$  - contact angle.

For calculation of the maximum contact stress value  $\sigma_{\max}$  the following relationship is used [5]:

$$\sigma_{\max} = \frac{858}{a^* \cdot b^*} \left[ P_{\max} (\sum \rho)^2 \right]^{\frac{1}{3}}, \quad (3)$$

where:

- $a^*, b^*$  - dimensionless axis of contact ellipse, respectively: semimajor or semiminor,



$\Sigma\rho$  - curvature sum.

In consideration of the fact that loads values are function among others of rolling bearings dimensions (especially contact area geometric features), calculated values of inner loads existing in the bearing, assigned to specific angles, one should admit as approximate values.

As a result of changed distribution, attitude towards nominal load distribution, and thereby other values of contact pressure, bearings' fatigue life can be different (most often smaller) because amplitude values of stresses in contact area of rolling elements and bearings' rings also are different (usually greater than nominal).

In order to settle quantitative determination of that influence, below the analysis is carried out. To this aim theory of probability is applied [1]. Analysis is conducted on the example of angular ball bearing applied in the front wheel hub of a bicycle.

### 3. Analysis of balls dimensions

The accuracy of rolling bearings is determined conjointly by geometrical constructional features of following bearings' elements:

- rolling elements (balls, rollers, needle rollers, barrels, cones).
- inner ring,
- outer ring,

In manufacturing consideration, conveniently is to assume that bearing element diameter (in analyzed example – ball) is redundant dimension. Its value is assorted to specific, measured values of raceways diameters of rolling bearings – on the outer and inner rings. Thanks to it, the proper value of clearance is obtained in the bearing.

In the all manufacturing processes surface geometric structure (SGS), with random and determined components, is generated on machined elements [7]. Therefore, true dimension is stochastic quantity – different from nominal dimension assumed by designer. For the aim of balls selection, in order to limit range of these differences, in standard [6] are created nine accuracy classes. In each class, values of boundary deviations of: diameter, geometrical tolerance and surfaces' roughness are determined. On account of diameters' spread in the inspection lot, in quoted standard the division of individual accuracy classes to dimensional groups and subgroups is suggested.

The rolling bearings are composed of finite, strictly determined number of rolling elements (balls)  $z$ . Therefore, the probability of existing of balls with determined diameters should be limited and refer to the lot number  $z$ . The distribution of diameter deviations in the lot of balls is presented in Fig. 2.

Individual quantities in the mentioned figure are defined in standard [6]. The way of their values delimitation is also described in this reference. In below presented considerations the most fundamental of them is  $V_{D_{wL}}$  – scatter of diameters in the lot. It is the difference between the greatest  $D_{wL \max}$  and the smallest  $D_{wL \min}$  average balls' diameter in the lot.

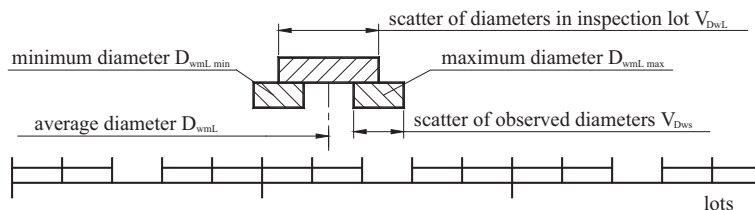


Fig. 2. The distribution of bearings' balls dimensional deviations in inspection lot

Particular attention should be paid to the fact that average ball diameter  $D_{wm}$  is arithmetic average of the greatest and the smallest individual balls' diameters.

#### 4. Randomness of balls' diameters - statistical distribution

Factor  $X$ , refers to true ball diameter, have Gaussian distribution with average value  $m$  and standard deviation  $s$ . This fact may be written as follows:

$$X \sim N(m, s), \quad (4)$$

In the bearing exist the balls with the diameters in specific accuracy class, therefore new random variable  $\tilde{X}$  is introduced. Its features limit the set above mentioned what can be note as follows:

$$\tilde{X} = \begin{cases} X & \text{for } |X - m| \leq a \\ 0 & \text{for } |X - m| > a \end{cases}, \quad (5)$$

This variables set has Gaussian distribution, with two-sided section, limited by assumed deviations values  $a$  of average balls diameters. This type of distribution is shown in Fig. 3.

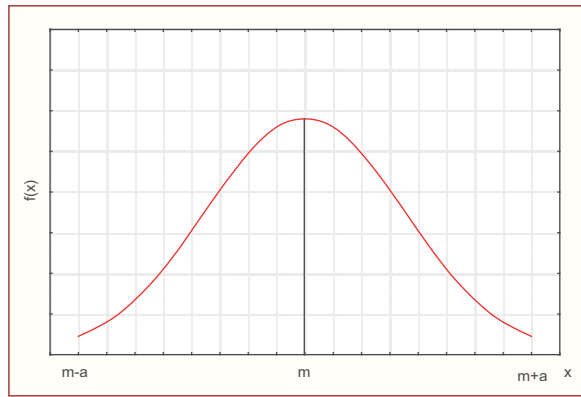


Fig. 3. The graph of probability density function of random variable  $\tilde{X}$

The probability density function of analyzed factor  $\tilde{X}$  has alternate form:

$$f_{\tilde{X}}(x) = \begin{cases} \frac{1}{cs\sqrt{2\pi}} e^{-\frac{(x-m)^2}{2s^2}} & \text{for } |x-m| \leq a \\ 0 & \text{for } |x-m| > a \end{cases}, \quad (6)$$

where:

$c$  – constant, calculate from equation:

$$c = 2 \left[ 1 - \phi\left(\frac{a}{s}\right) \right], \quad (7)$$

in which

$\phi(x)$ , for  $x = a/s$  – distribution function of standard Gaussian distribution,

which can be described by relationship:

$$\phi(x) = \frac{1}{\sqrt{2\pi}} \int_{-\infty}^x e^{-\frac{u^2}{2}} du, \quad (8)$$

and

$u$  – working variable.

The distribution function of random variable  $\tilde{X}$ , in individual function intervals, assumes values in accordance with dependences mentioned below:

$$F(x) = \begin{cases} 0 & \text{if } x \leq m-a \\ \frac{1}{c} \left\{ \phi\left(\frac{x-m}{s}\right) - \phi\left(-\frac{a}{s}\right) \right\} & \text{if } m-a < x \leq m+a, \\ 1 & \text{if } x > m+a \end{cases} \quad (9)$$

Let  $X_{1,n}, X_{2,n}, \dots, X_{n,n}$  are ordinal statistics from random test  $(X_1, X_2, \dots, X_n)$  arising from distribution with distribution function  $F(x)$ . The value of average  $r$ -th ordinal statistics  $X_{r,n}$  one can assign from relationship:

$$EX_{r,n} = n \binom{n-1}{r-1} \int_{m-a}^{m+a} x f(x) [F(x)]^{r-1} [1-F(x)]^{n-r} dx, \quad (10)$$

In the case of analyzed real rolling bearing, parameters' values in equation (10) are following:

- $n = z = 9$ ,
- $r = 1, 2, \dots, 9$ .

The statistic assumed in presented analysis:

$$W_n = X_{n,n} - X_{1,n} \quad (11)$$

is called the range of the sample and it is difference between maximum and minimum average diameter in the sample – see Fig. 2. For example, in 40<sup>th</sup> accuracy class of the bearings, value of this quantity, according to standard [6], is equal  $\pm 16 \mu\text{m}$ . Average value of the range of the sample, for  $n$  elements in the sample, can be calculated from relationship:

$$EW_n = \int_{-\infty}^{\infty} \{1 - F^n(x) - [1 - F(x)]^n\} dx, \quad (12)$$

Analytical solution of considered problem makes possible to illustrate the dependence of  $EW_n$  on standard deviation  $s$ . This way can be determined which part of the range  $\langle m-a, m+a \rangle$  is covered by ordinal statistics  $X_{1,9}, X_{2,9}, \dots, X_{9,9}$ .

In this aim dependence of average value of range of sample  $EW_n$  on standard deviation is evaluated for the whole lot. For better interpretation of computation's results, values of ratio  $EW_n/2a$  are given on the  $Y$ -axis – Fig 4.

With the help of above described procedure, values of balls diameters are calculated, in assumption that machined balls are subjected to Gaussian distribution with two-sided section. In the calculations the true constructional features of tested bearings are taken as input data.

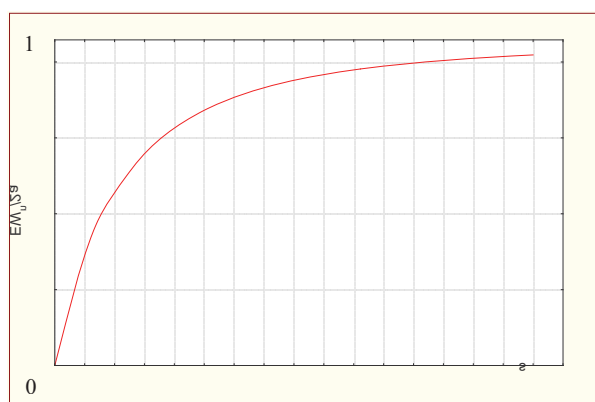


Fig. 4. Dependence of  $EW_n$  versus standard deviations (value and unit of  $s$  – adequate to basic size)

As results of calculation the following values of balls diameters  $d_k$  were obtained: 4.754, 4.757, 4.760, 4.762, 4.762, 4.762, 4.764, 4.767, 4.770 mm. They composed input set of quantities in bearings' fatigue life calculations.

## 5. Probabilistic analysis of bearings fatigue life

As earlier was found, differences between nominal and true diameters of balls in the bearings, which are contained inside the range of particular sample (in considered example the lot of analyzed size is  $z = 9$  and it is equivalent to balls number in the bearing), cause that inner loads distribution, shown in Fig. 1, is only theoretical. The true value of amplitude, as the result of such changing load, will be also other than theoretical. Thus, there are good reasons to state that analytical fatigue life will be different from determined on experimental way.

The sequence of the balls of differentiated diameters occurring in the bearing is also random factor. Differences of balls' diameters cause differentiation of contact stress - see equations (2) and (3), therefore, order of balls sequence – Fig. 5, generates changes of stress amplitude – quantity which decides about fatigue life of bearings.

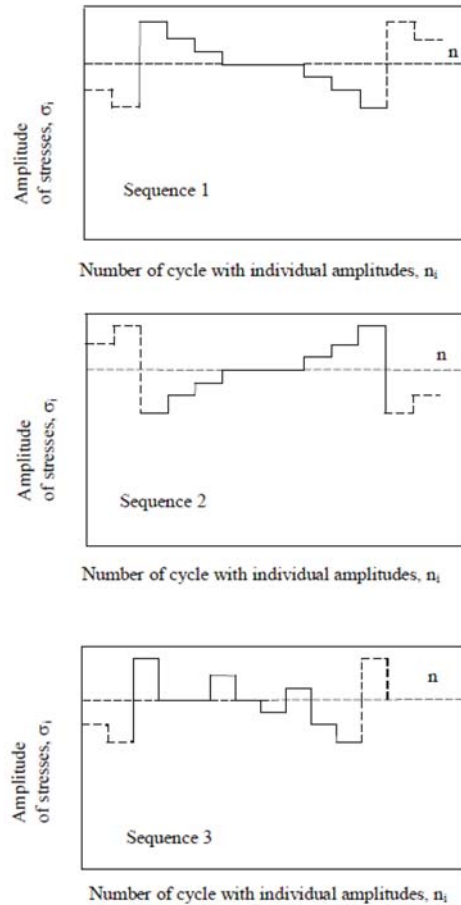


Fig. 5. The examples of possible cycles of load in the contact ball-raceway caused by nominal dimension deviations of ball diameters: seq.1) decreasing sequence, seq.2) ascending sequence, seq.3) mixed sequence;  $n$  – nominal level of stresses' amplitude

The above figures show that balls' sequence existing in the bearing directly determines run of load cycle, therefore, it can have significant meaning for fatigue life of analyzed rolling bearings [8, 9].

## 6. Closure

In the operational processes of all machines one observed that durability of correctly serviced bearings' pairs is different (usually greater) than determined on computational way. This is caused by analytical methods imperfection. That is why evolution of computational methods is observed, e.g. [3, 4, 10]. It appears in including increasing number of the factors, which determine durability of bearings.

Application of the above presented analysis in constructional practice should increase calculations accuracy and thereby, to induce better closing of analytical and practical results. This way the mathematical models, describing observed changes will be more correlated (congruent) to real run of researched phenomena.

## References

- [1] Draper N.R., Smith H., *Applied Regression Analysis*, John Wiley & Sons Inc., New York – London - Sydney 1973.
- [2] Harris T.A., *Rolling Bearing Analysis*, 3<sup>rd</sup> edition, John Wiley & Sons Inc., New York 1991.
- [3] Ioannides E., *Life Prediction in Rolling Element Bearings*, in: *New Direction in Tribology*. Proceedings of I<sup>st</sup> World Tribology Congress, pp. 281÷290, London 1997.
- [4] Krzemiński Freda H., *Modern Methods of Calculation of Rolling Bearings Fatigue Life*, Tribologia No. 2, pp. 223÷232, 1993 (in Polish).
- [5] Krzemiński Freda H., *Rolling Bearings*, PWN, Warsaw 1985 (in Polish).
- [6] Oczóś K.E., Lubimov V., *Geometrical Structure of Surfaces*, Rzeszów Technical University Publishers, Rzeszów 2003 (in Polish).
- [7] Polish standard PN-83/M-86452 – *Rolling Bearings. Balls*.
- [8] Styp-Rekowski M., *Significance of Constructional Features for Angular Ball Bearings Life*, Scientific Number of Technical and Agricultural University, series Dissertations, No. 103, Bydgoszcz 2001 (in Polish).
- [9] Szala J., *Assessment of Machines Elements Fatigue Life in Random and Programmable Load*, Scientific Number of Technical and Agricultural University, series Mechanics, No. 22, Bydgoszcz 1980 (in Polish).
- [10] Warda B., *New Computational Model of Rolling Bearings Fatigue Life*, Proceedings of XVII<sup>th</sup> Symposium on Fundamentals of Machine Design, pp. 265÷268, Lublin 1995 (in Polish).



## APPLICATION OF MARINE ENGINE ROOM SIMULATORS WITH 3D VISUALIZATION FOR EMERGENCY OPERATING PROCEDURES TRAINING

**Leonard Tomczak**

Gdynia Maritime University  
ul. Morska 81-87, 81-225 Gdynia, Poland  
tel.: +48 58 6901331, fax: +48 58 6901399

### Abstract

*It is well established that one of the major factors of accident prevention on board is the perfect theoretical and practical knowledge possessed by engine room officers while operating engines and auxiliary equipment.*

*This paper describes the latest developments in 3D computer simulation applications, designated for the familiarization with marine machinery, specially taking into account the emergency operating procedures training.*

*The experiences in 3D computer simulation application, the benefits and advantages of use of computer simulation in educational process of engine room officers in the Gdynia Maritime University are equally presented in this paper.*

*This paper describes an example of application of new 3D simulation techniques in engine room simulator based on modern - computer controlled engine room with low speed main engine MAN Diesel LMC type, applied on a container ship, where trainees have possibilities to develop operational skills, update their know-how and refresh emergency procedures.*

*This installation plays a vital role in the safety on board. Thus, it is of extreme importance that trainees acquire the capacity to react in a prompt and effective manner to emergency situations. This new 3D simulation technique specially emphasizes the relation between simulation and realism of machinery operation. The simulator described in the paper provides for a new approach to navigation through the different system's elements, allowing for an easy and quick access to basic engine room operation (valve opening/closing, setting position of switches, push-buttons etc.). This has been possible due the application of state-of-the art 3D visualisation with zoom techniques.*

*The basic tasks for computer simulation in maritime education are equally described, taking into consideration the new methods and emergency procedures training.*

*This papers' conclusion is that the use of 3D computer simulation in maritime education results in increased emergency preparedness and in consequence, leads to hazard mitigation and reduces the risk of human error in the operation and maintenance of marine equipment.*

**Keywords:** 3D computer simulation, marine engine room simulators.

## 1 Introduction

Marine engine simulators allow for operation of emergency situations that are not permissible under normal exploitation conditions due to safety limitations. Simulator's software includes also assessment features that enable objective review of trainees acquired capacities. During simulator



exercise the instructor is able to apply various exercise set-ups (initial conditions) and scenarios that include different fault finding tasks.

For this reason, engine room simulators are more and more used in maritime academies as a valuable asset for educational process [1]. The application of engine room simulators is also recommended by STCW 95 IMO Convention [2].

It is worthwhile mentioning that marine engine room simulators have also some basic disadvantages. Namely, they include lots of simplifications, abbreviations and schematic presentation of machinery systems as a result of the fact that they are presented only in 2D visualization. Hence, the trainee with perfect knowledge of simulator operation can experience serious problems with real ship power plant operation, because the graphical presentation and operating procedures of the simulator are distinct from the reality.

For this reason, manufacturers of engine room simulators begin to apply 3D graphical system's layout presentation in order to provide a machinery configuration as close as possible to reality.

The main problem in creation of 3D simulators is to provide for proper navigation through the system's elements [4,5,6]. Engine room is a complex, multi level and complicated set of sub-systems, equipment and machinery and this is a new challenge for entities creating such kind of simulators.

It is also necessary to allow for an easy and quick access to basic engine room operation (valve opening/closing, setting position of switches, push-buttons etc.). It is possible to achieve this feature by applying zoom techniques for selected elements of the system. Users of 3D simulators should also be able to observe the system's elements from pre-select specific parts of the engine room.

Based on the author's experiences with the application of different types of simulators, a better solution consists in navigation by mouse cursor and zooming facilities.

The application of new 3D simulation techniques in marine engineering education shall be analysed on the examples of full mission, hardware type engine room simulator with low speed main engine.

A new technique of navigation through the system's elements has been applied in this virtual reality simulator, providing for a solution of the main problem in creation of 3D visualisation. The latest development includes also a combination of 3D and 2D diagram presentation, which enables to follow how a certain device really functions and gives a complete picture of its structure. The presented solutions have improved considerably the level of simulator fidelity in relation to real machinery. In consequence, it was possible to eliminate the disadvantages of the engine room simulator with typical 2D presentation consisting in a schematic and simplified presentation of machinery systems.

The application of virtual simulation in teaching the operation of complex marine machinery leads to a better understanding of the functioning principles of both the equipment and the systems in comparison with traditional educational methods. As a result, trainees are far better prepared to deal with real life operation of machinery, thus increasing in a considerable manner the standards of safety of ship operation.

On the other hand, software, due to its features enables the trainee to repeat in an unlimited number of times the required operations, thus to achieve the necessary preparedness level.

The engine room simulator based on the medium speed engine room simulator is one of the first simulators which use hardware type of consoles combined with 3D visualization.

This simulator specially enhances the operational procedures related to emergency situations, like electrical black-down, emergency manual operation of the main engine with propulsion system as well as auxiliary machinery in case of remote control failure. As it has been said before, these procedures may not be trained in real life conditions due to safety constraints. From didactic point of view the best solution is to combine hardware version of engine room simulator with 3D visualization. Such combination improves in a considerable manner the safe operation of marine

engine room, as the crew members have previously been trained in relation to various fault scenarios.

## 2 LER3D Low speed engine room simulator's description

The application of new 3D simulation techniques in marine engineering education shall be analyzed on the examples of software type engine room simulator with low speed main engine. The LER3D virtual reality simulator provides for a new approach to navigation through the different system's elements, allowing for an easy and quick access to basic engine room operation (valve opening/closing, setting position of switches, push-buttons etc.). This has been possible due the application of state-of-the art 3D visualisation with zoom techniques. The latest development includes also a combination of 3D and 2D diagram presentation, which enables to follow how a certain device really functions and gives a complete picture of its structure. The presented solutions have improved considerably the level of simulator fidelity in relation to real machinery. In consequence, it was possible to eliminate the disadvantages of the engine room simulator with typical 2D presentation consisting in a schematic and simplified presentation of machinery systems.

This simulator is designated for training students of maritime academies as well as for different types of marine vocational training centres. The simulator has universal features and may be used both for training merchant and navy fleet crew.

The main purpose of the LER3D simulator is the practical preparation of the trainee for engine room operation, and more particularly:

- familiarization with the basic engine room installation (compressed air system, fresh and sea water cooling system, lubricating, fuel oil system etc.), specially taking into account training on the base of modern, computer controlled engine room;
- acknowledgment with main engine and auxiliary equipment exploitation procedures;
- propulsion system maneuvering ;

The software also generates the main engine room's sound.

The simulator has been developed in compliance with:

- STCW Code: Section A-1/12 and Section B-1/12.
- ISM Code: Section 6 and Section 8.

A general view of the LER3D simulator engine room (main engine ) has been presented on fig.1.

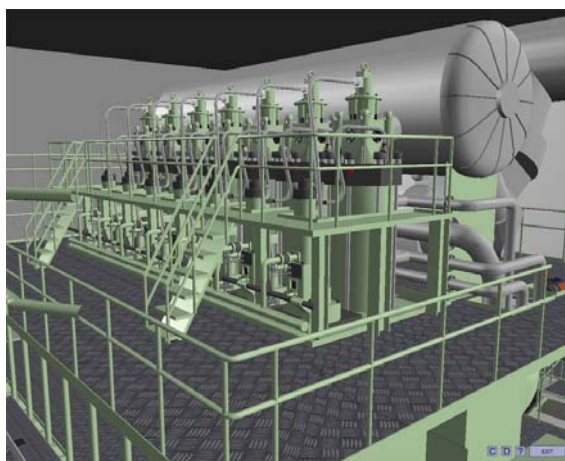


*Fig. 1 Low Speed Engine Room Simulator LER3D – General view of main engine*

It is well known that one of the major factors of accident prevention on board is the perfect theoretical and practical knowledge possessed by engine room officers while operating engines and auxiliary equipment. The basic role of Low Speed Engine Room Simulator LER3D is the familiarization with different operational modes, required for achieving a high level of emergency preparedness [6].

The basic role of this simulator is the familiarization with different operational modes.

This simulator allows not only for training under normal operation conditions but also for emergency operation procedure training. The more familiar the trainee is with the equipment the faster and more effective are his reactions to a state of emergency [3].

On fig. 2 main engine's emergency control local station is presented.



*Fig. 2 Low Speed Engine Room Simulator LER3D - Main engine emergency local control station*

One of the important elements for training emergency operating procedure in LER3D simulator is the emergency power plant. The basic role of the Emergency Power Plant is to supply electric current, in case of failure of main diesel generators.

General view of 3D Emergency Power Plant simulator is shown on fig.3.



*Fig.3 Emergency Power Plant – 3D simulator's general view*

Emergency Power Plant diesel engine view with control panel zoom selection is presented on fig. 4.



*Fig.4 Emergency Power Plant simulator - Diesel engine with control panel*

Diesel engine starting procedure can be effectuated in two ways:

- from control panel with application of electrical starter (24 V available)
- by emergency hydraulic starter (24 V not available) – fig. 5

In case of diesel engine emergency operation, the trainee ought to create proper pressure in hydraulic bottle and by manual lever start the engine. Emergency hydraulic engine's starter is shown of fig. 5.

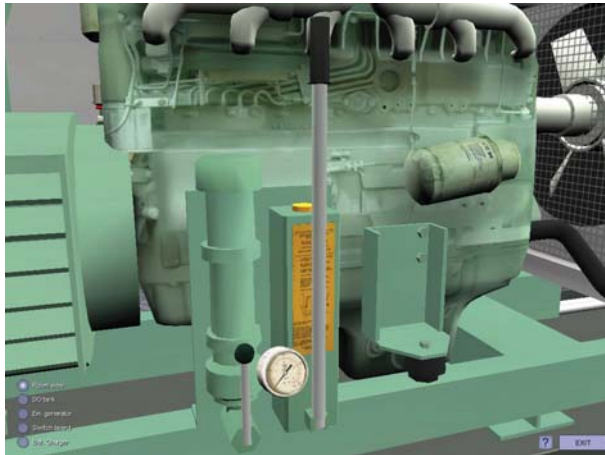


*Fig.5 Emergency hydraulic starter*

One of possibilities to improve realism and fidelity of operation procedures training is application of touch screen. On fig. 6 use of touch screen is presented for hydraulic starter emergency operation.



*Fig. 6 LER3D Engine Room Simulator – Application of touch screen for hydraulic starter emergency operation*

Emergency operation procedures are emphasizes in hydraulic systems operation.

On fig. 7 steering gear installation (rotary vane type) is presented. Trainee, by pressing push-buttons on solenoid control valve can change rudder position in emergency ( manual) way.



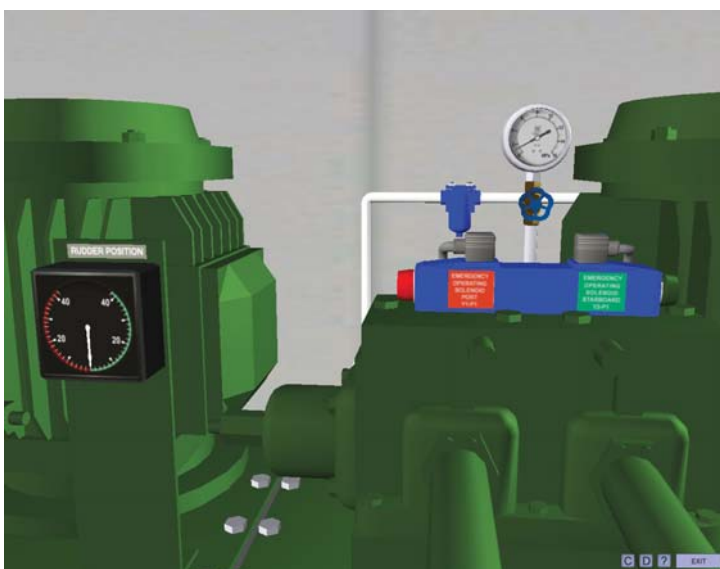


*Fig.7 Steering gear installation - Solenoid control valve with emergency push-buttons*

Another example of engine room installation where it is possible to train emergency situation is fire fighting system. An example of S-type fuel oil separator fire simulation is shown on fig. 8

LER3D Low Speed Engine Room Simulator in relation to fire fighting system consist of:

- CO<sub>2</sub> system
- Water mist system (fig. 9 – 10)

Described engine room simulator allows for very detailed operating procedure training like CO<sub>2</sub> or water mist system activation.



*Fig. 8 S-type fuel oil separator fire simulation*



*Fig. 9 Water mist system – activation panel on engine control room*



*Fig. 10 Water mist activation in Diesel generators section*

LER3D virtual reality engine room simulator can support and facilitate preparation of trainee for use of full mission, hardware type of engine room simulator.

This software type simulator is first of all intended for individual students' training (one student – on PC). Typical configuration of PC classroom is 8 till 12 stations + instructor station. Examples of PC classroom with two screen solution on each station and PC projector is shown on fig. 11.





*Fig.11 LER3D Engine Room Simulator – PC classroom*

### 3. Conclusion

The application of engine room simulators with 3D visualization, in maritime education leads to a better understanding of the marine machinery and results also in increased emergency preparedness and in consequence, leads to hazard mitigation and reduces the risk of human error in the operation and maintenance of marine equipment.

The application of simulator gives the operator of equipment the opportunity to get acquainted with the system's operation, before starting real life usage. For this reason, more and more often, manufacturers of marine equipment supply their products accompanied with software type of simulators.

As it results from the above, the latest developments in simulation techniques, including 3D presentation enhances the above mentioned benefits, as it brings the engine room simulators closer to reality. In consequence, the gap between operating marine machinery in simulation conditions and in real life is decreased.

As it has been mentioned above, proper navigation through the 3D simulator's elements is the key point in order to achieve the didactic purposes. The new concepts of view selection, zooming features of elements and operation by cursor and mouse clicking, as applied in LER3D low speed engine room simulator, described in this paper, appears to be very effective and easily adaptable by trainees in practice.

Due to the specificity of operating marine equipment in real life conditions, the didactic goals in marine education are directly linked with achieving preparedness for emergency situations. Such preparedness may only be achieved if the trainee is familiar with both the equipment and its operating modes, including emergency situations.

In the near future, this type of 3D solutions should be applied more and more often in engine room simulators design. The presented simulators are related to marine machinery, but the concept of composition and navigation through the system's elements can be easily applied for the purposes of any type of technical equipment and shall contribute in a similar manner to hazard prevention.

To summarize, the application of engine room simulators with 3D visualization is a valuable hazard prevention tool as it reduces the level of human error in the operation and maintenance of marine equipment.

## References

- [1] R.Cwilewicz, L.Tomczak, Z.J. Pudlowski, Effective application of engine room simulators in marine engineering education, *Proc. 3<sup>rd</sup> Global Conference on Engineering Education*, Glasgow, Scotland, United Kingdom, 2002,
- [2] STCW - Standards of Training, Certification and Watchkeeping for Seafarers 78/95 Convention International Maritime Organization, London, United Kingdom, 1996
- [3] H. Chen , The latest developments in engine room simulator WMS-1004 for marine training needs, *Proc. ICERS6 International Conference on Engine Room Simulators*, Wuhan, China, 2004,
- [4] R..Cwilewicz, L.Tomczak., The latest developments in the application of 3D graphical presentation in computer based training – interactive programs for marine mechanical engineering students, *Proc.. 8<sup>th</sup> UICEE Annual Conference on Engineering Education*, Kingston, Jamaica, 2005,
- [5] S.J.Cross S., Enhancing competence based training and assessment for marine engineers through the realism of virtual presentation, *Proc.ICERS7 International Conference on Engine Room Simulators*, Portoroz, Slovenia 2005,
- [6] R. Cwilewicz, L. Tomczak, The role of computer simulation programs for marine engineers in hazard prevention by reducing the risk of human error in the operation of marine machinery, *Proc 4<sup>th</sup> International Conference on Computer Simulation In Risk Analysis and Hazard Mitigation - Risk Analysis IV*, 2004,
- [7] F. Donders F., The pedagogical issues related to the use of virtual engine room environment, *Proc.ICERS7 International Conference on Engine Room Simulators*, Portoroz, Slovenia 2005,
- [8] L. Tomczak, Practical aspects of 3D graphical applications in marine Engineering Education, *Global Journal of Engineering Education*, 9(2), 2005,
- [9] L. Tomczak, Application of 3D visualization in marine engine room simulators, *Proc. 7<sup>th</sup> International Conference on Engine Room Simulators (ICERS7)* , Portoroz, Slovenia, 2005,
- [10] R. Cwilewicz, L.Tomczak, Application of 3D computer simulation for marine engineers as a hazard prevention tool, *Proc 5<sup>th</sup> International Conference on Computer Simulation In Risk Analysis and Hazard Mitigation - Risk Analysis V*, WIT PRESS Southampton, Boston, 2006,
- [11] R. Cwilewicz, L.Tomczak, The application of virtual engine room simulators in maritime engineering education, *Proc. 9<sup>th</sup> UICEE Annual Conference on Engineering Education*, Muscat, Oman, 2006,
- [12] L.Tomczak, The latest developments of 3D visualization in marine engine room simulators, *Proc. International Conference on Engine Room Simulators (ICERS8)*, Manila, Philippines, 2007
- [13] R. Cwilewicz, L.Tomczak, , Improvement of ship operations' safety as a result of the application of virtual reality engine room simulators *Proc. 6<sup>th</sup> International Conference on Computer Simulation In Risk Analysis and Hazard Mitigation - Risk Analysis VI*, WIT PRESS Southampton, Boston, 2008,
- [14] L.Tomczak, The new generation of engine room simulators with application of 3D visualization, *Journal of Polish CIMAC*, Gdańsk, Poland Vol.3 No. 2, 2008



## THE RULES OF INFERENCE IN MACHINE STATE RECOGNITION

Henryk Tylicki

*University of Technology and Life Science  
ul. S. Kaliskiego 7, 85-789 Bydgoszcz, Poland  
tel.: +48 52 340828, fax.: +48 52 308283  
e-mail: tylicki@utp.edu.p*

### Abstract

*The results of investigations connected with the implementation of the procedures of monitoring the technical condition of machine engines and their investigation for the chosen arrangements of mechanical vehicles were introduced. The examples of the rule of inference of diagnostic were passed for the gathering of diagnostic parameters and the opinion of the state.*

**Keywords:** machine state recognition, procedure algorithmization, conclusion rules

### 1. Introduction

The usage in exploitation process of machines technical state evaluation methods, being the basis of the automation of state recognition, requires the determination of diagnostic parameters set, diagnostic tests assignment and method optimization of diagnosis, genesis, forecasting. The realization of these tasks depends on many factors related to the level of machine complexity, the quality of exploitation process and the course of wear process. For this purpose it is necessary to identify the methods of machine state recognition, create procedures possible to use in the machine state recognition process, as well as determine the rules of concluding being an element of the on-board software of machine state recognition system [2, 3, 5, 6, 10, 11].

Machine state recognition is a process which ought to enable:

- a) real-time estimation of the machine's technical state on the basis of diagnostic researches results, through the control of state and the location of damages in case of the machine's disability;
- b) anticipation of the machine's state in the future on the basis of incomplete history of diagnostic researches results, which enables time estimation of the machine's flawless operation or the value of work done by the machine in the future;
- c) anticipation of the machine's state in the past on the basis of incomplete history of diagnostic researches results, which enables the estimation of the machine's state or the value of work done by the machine in the past.

### 2. Problem characteristics

The problem of state evaluation, prognosis and genesis of the machine's state is equally important at the stage of construction preparation, production and exploitation, and the main

problems appearing during the solution of the machines' state recognition task are [4, 6, 7, 8, 10]:

- a) formalizing the aim of diagnosis, forecasting and genesis of the machine's state;
- b) the description of the machine's state changes in the exploitation time;
- c) building a diagnostic model – the relation between state characteristics and diagnostic parameters;
- d) the solution of state diagnosis task;
- e) the solution of state forecasting task;
- f) the solution of state genesis task.

The machine's state  $W(\Theta_n)$  at the moment in time  $\Theta_n$  can be characterized with the use of the parameter values set  $\{y_j(\Theta); j=1,...,m\}$ . The machine at the moment  $\Theta_b$  (machine's state diagnosis task) is in the state of aptitude  $S^0$ , when satisfied is the condition:

$$W(\Theta_n) = W^0 \Leftrightarrow \forall (j=1,...,m) \quad [\{y_{j,d}\} \leq \{y_j(\Theta_b)\} \leq \{y_{j,g}\}], \quad (1)$$

where:  $\{y_{j,d}\}$ ,  $\{y_{j,g}\}$  – sets of upper and bottom boundary values of diagnostic parameters.

Respectively, it is possible to formulate the condition of aptitude at the moment  $\Theta_{n+\tau}$  (forecasting task) [9,10,14]:

$$W(\Theta_{n+\tau}) = W^0 \Leftrightarrow \forall (j=1,...,m) \quad [\{y_{j,d}\} \leq \{y_j(\Theta_{b+\tau})\} \leq \{y_{j,g}\}], \quad (2)$$

whilst the elements of the set  $\{y_j(\Theta_{b+\tau})\}$  are unknown, hence the necessity of foreseeing them in the assumed time range  $\tau_1$ . The element  $\tau_1$  means the time range for which the forecasting process is realized (the element  $\tau_1$  is also called advance or “prognosis time horizon”). In this aspect, the time evaluation of machine's passage from the aptitude state into the inaptitude state is determined by the results of diagnostic parameters prognoses  $\{y_j(\Theta_{b+\tau})\}$  signaling the exceeding of boundary values.

Similarly we can formulate the condition of aptitude at the moment  $\Theta_{b-\tau_2}$  (machine's state genesis task):

$$W(\Theta_{b-\tau_2}) = W^0 \Leftrightarrow \forall (j=1,...,m) \quad [\{y_{j,d}\} \leq \{y_j(\Theta_{b-\tau_2})\} \leq \{y_{j,g}\}], \quad (3)$$

Whilst some elements of the set  $\{y_j(\Theta_{b-\tau_2})\}$  are unknown, hence the necessity of foreseeing them in the assumed time range  $\tau_2$ . The element  $\tau_2$  means the time range for which the genesis process is realized (the element  $\tau_2$  is also called advance or “genesis time horizon”). In this aspect, the estimation of the machine's state or the value of work done by it in the past are determined by the results of diagnostic parameters values genesis  $\{y_j(\Theta_{b-\tau_2})\}$ .

The main problems appearing at the solution of such defined tasks are: the selection of “the best” diagnostic parameters describing the actual state and their change in exploitation time, diagnostic test determination, the determination of forecasted value of diagnostic parameter for prognosis horizon  $\tau_1$ ,  $y_{jp}(\Theta_{b+\tau_1})$  with the help of “the best” prognosis method, and the determination of the next diagnosis or operation  $\Theta_d$ , the determination of genesis value of diagnostic parameter for genesis horizon  $\tau_2$ ,  $y_{jp}(\Theta_{b-\tau_2})$  with the help of “the best” Genesis method, and the estimation of the machine's state, work done by it in the past, and the determination of the cause of an existing damage.

The above used notion “the best” is connected with the acceptance of appropriate criteria and considering these problems in the categories of optimal solution search, whilst taking into consideration many estimation criteria, it is necessary to consider these problems in the categories of polioptimal solution [1, 10].

### 3. The algorithm of machine state recognition

The scheme of determining procedures for machine state recognition is shown in the Fig.1, whilst the algorithm of the use of the appointed optimal diagnostic parameters set, optimal diagnostic test, optimal genesis method and optimal method is shown in the Fig.2.

Summing up the considered in this chapter problems concerning theoretical bases of the state recognition process methodology, it is necessary to state that:

1. The process of machine state recognition includes the following kinds of diagnostic research: state evaluation, genesis and prognosis.

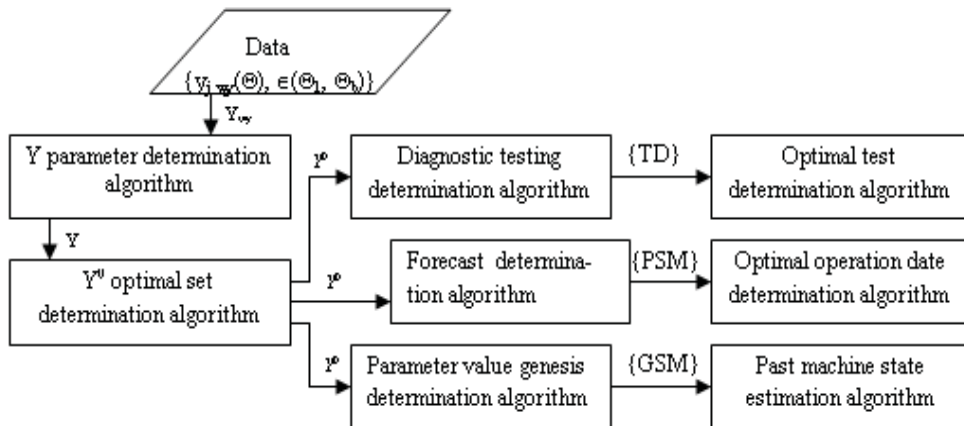


Fig. 1. Scheme of determining procedures for machine state recognition

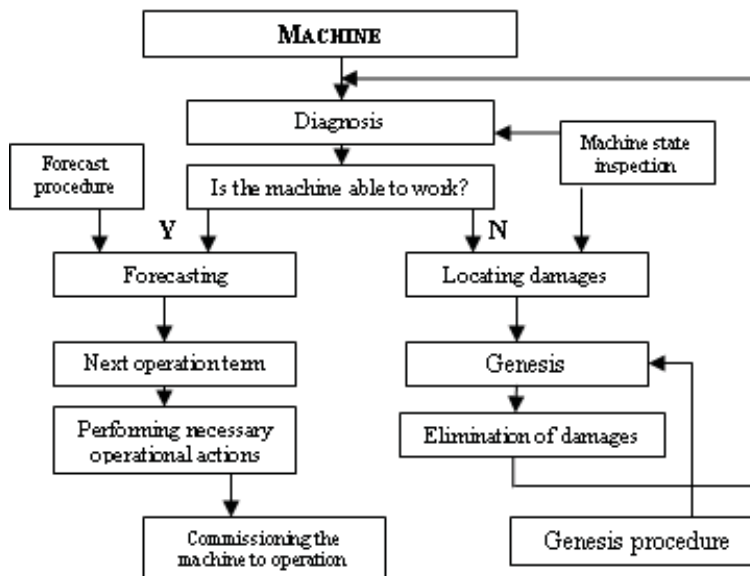


Fig.2. Scheme of machine state recognition realization

2. In the process of machine state recognition, an important element is the determination of the diagnostic parameters set:
  - a) for the evaluation of the machine's state considering the criterion of machine states differentiation;
  - b) in the process of prognosis and genesis with the use of criteria of: correlation between the diagnostic parameter value and the state and machine's exploitation time, and the information capacity of the diagnostic parameter.
3. In the procedure of machine state evaluation, analyzed was the possibility to use the following methods for examining the relations between diagnostic parameters and the machine's states:
  - a) mean test examination;
  - b) examining the distance of trust ranges of the diagnostic parameter mean value;
  - c) examining the changeability of the diagnostic parameter value.
4. The presented estimations allow to state that it is possible to create appropriate algorithms of the machines' technical state recognition, and appropriate concluding rules vital for creating the software of the on-board machine technical state recognition system.

#### **4. On-board state recognition system**

Created rules of diagnostic models identification, established procedures of acquisition and processing of information on state changes of examined models, their implementation in information technology, as well as proposed state recognition procedures (diagnosis, genesis, prognosis) are the basis of on-board diagnostic systems construction. In this chapter we presented the assumptions for the construction of the on-board machine state recognition system, the rules for its design, and the procedure of the diagnostic system construction [10, 11].

The idea of the on-board state recognition system ought to be included in the organizational range of the new machine's design, including the problems determining:

- a) functional features;
- b) construction features;
- c) exploitation and operation conditions;
- d) operational resource base potential;
- e) economic calculation.

Taking into consideration the above assumptions, the creation rules of the on-board machine state recognition system should include:

1. The project analysis – concerns the analysis of needs and possible problem solutions, the analysis of economic calculation concerning the construction of the system, as well as the analysis of functional, technical and economic requirements including the relation of manufacture and exploitation costs of the system to the acquired benefits in result of its use;
2. System design – concerns the determination of the architecture of microprocessor, modules, interfaces and other components, as well as software in the aspect of the system useful features fulfillment, including:
  - a) logical project – concerns logical aspects of system, processes and information flow organization,
  - b) functional project – concerns the function description of system elements and their co-operation,
  - c) construction project – concerns the structure description of system elements (e.g. processor, memory, communication, input and output, clock, power supply);
3. The construction of system work simulator (computer) – its purpose is to ensure the initial evaluation of system work with simulated machine states;
4. System implementation – the aim is to create and build a physical model performing the assumed functions of the system;

5. System quality assurance – concerns testing the programs and exploitation research;
6. System documentation preparation – including the construction, requirements and limitations, functioning and operational procedures.

The object of the machine state recognition system working involves:

1. In the area of State Evaluation:
  - b) concluding on the machine state based on the relations between the measured values of diagnostic parameters set and their nominal values on the basis of the created state control test;
  - c) concluding on the machine state location based on the relations between the measured values of diagnostic parameters set and their nominal values on the basis of the created damage location test.

In the module State Evaluation we experience:

- a) diagnostic matrix creation on the basis of input data;
- b) the possibility to edit the diagnostic matrix;
- c) saving to a text file.
2. In the field State Genesis based on the concluding on a possible cause of the located disability state of the machine according to the algorithm:
  - a) optimal diagnostic parameter (maximum weight value);
  - b) optimal genesis method (minimum genesis mistake value);
  - c) minimum value of the distance between the diagnostic parameter value with the range of genesis mistake and the boundary value of the diagnostic parameter  $d_{\min}$ ;
  - d) correlation of the minimum distance value  $d_{\min}$  with the machine's disability states  $s_i$ , with the simultaneous testing of circumstances and exploitation conditions of their occurrence, as the potential cause of the located machine's disability state.

In the module State Genesis we experience:

- a) the determination of genesis value of diagnostic parameter and genesis mistake;
- b) the determination of the minimum distance between the genesis value of the parameter and its boundary value;
- c) testing the influence of exploitation factors (number of parameters, row size) over the state genesis;
- d) the visualization and record of approximation or interpolation function for chosen parameters of a chosen object in the form of a graph and a report (Fig. 3).



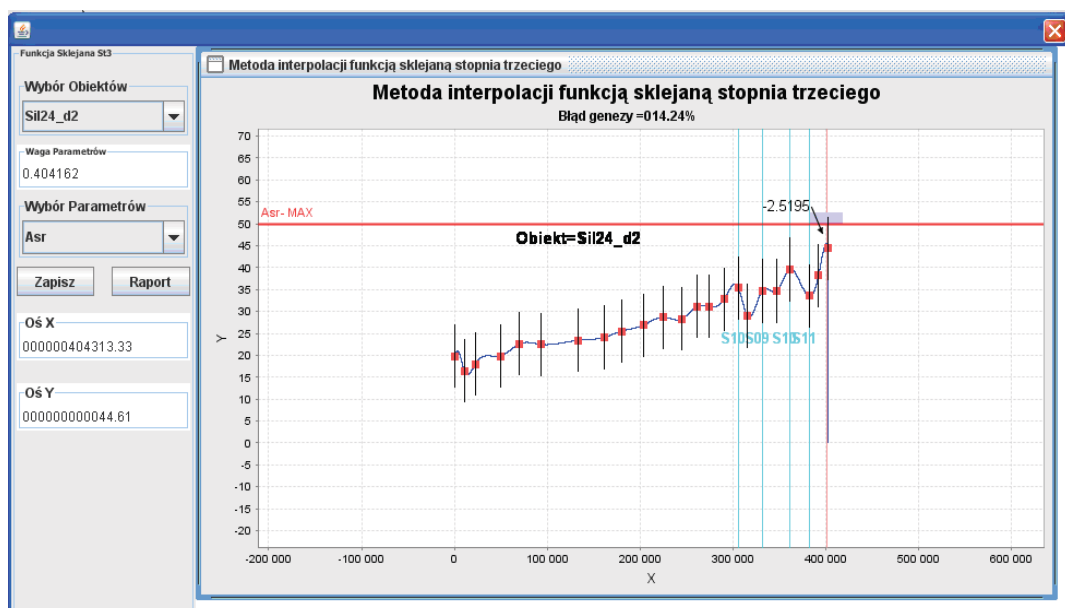


Fig. 3. Interpolation method with the third-degree compound function from the State Genesis module (estimating the genesis value of the parameter  $\text{NO}_2$  (weight  $w_1=0,9229$ ) for the interpolation with the combined function, type 3)

3. In the area State Prognosis on the estimation of the date of the next machine operation  $\Theta_d$  (accepting the minimum date value  $\Theta_{d1}$ ,  $\Theta_{d2}$ ) on the basis of the analysis of values of dates generated by two prognosis methods for the next operation date  $\Theta_{d1}$  and  $\Theta_{d2}$  according to the algorithm:
  - a) optimal diagnostic parameter (maximum weight value);
  - b) optimal prognosis method (minimum prognosis mistake value);
  - c) minimum value of the next operation date  $\Theta_d$ .

In the module State Prognosis we experience:

- a) the determination of the prognosis value of the diagnostic parameter and prognosis mistake,
- b) the determination of the diagnosis and operation date of the machine;
- c) testing the influence of exploitation factors (number of parameters, time row size, prognosis horizon value) over the state prognosis;
- d) the visualization and record of analyzed prognosis models for chosen parameters of the chosen object (Fig. 4).

For the realization of the above system functions it is necessary to use the object programming procedures. Then the basic module of the machine state recognition system is the knowledge base <OBJECT, ATTRIBUTE (state characteristic) – VALUE>. The object defined in the state recognition system are the systems and units of the machine.

The information on the machine state have hierarchical structure, where general information take the highest level, e.g. for the State Evaluation (machine state control), and lower levels are predestined for more detailed information (system damage location).

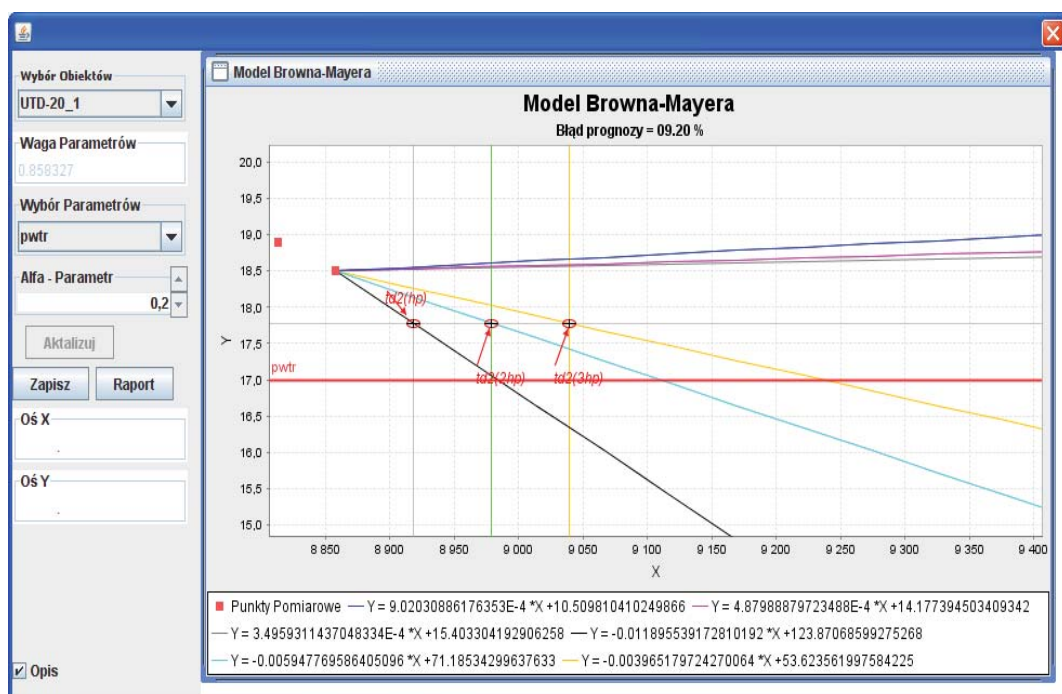


Fig. 4. Brown-Mayer model from the State Forecast module (Estimating the prognoses value of the parameter  $p_{wtr}$  (weight  $w_1=0,858$ ) and date  $\Theta_d(\tau=\Delta\Theta, \tau=2\Delta\Theta, \tau=3\Delta\Theta)$  for Brown-Mayer model, type 1 ( $\alpha=0,2$ ))

An ideal state recognition system is an on-board diagnostic system performing state control, damage location, state genesis and state prognosis functions. In this case the cost of the machine rises, however the machine's exploitation effectiveness grows as all the state recognition functions are performed. Such solution of the state recognition system can be appropriate for critical machines or other special machines.

A less costly solution is an on-board state recognition system which performs only state control functions. In this case the external state recognition system can forecast the state or locate the damages of the object and perform the genesis of the disability state. It can be a universal system used for diagnostic researches of different machines.

## 5. Dedicated conclusion rules

The analysis of research results (for example) of machine state prognosis methodology allows to formulate dedicated conclusion rules of type "IF – THEN" or "IF – THEN – ELSE" in the area of:

- diagnostic parameters optimization;
- state prognosis.

In case of the combustion engine UTD-20, the generated rules have form:

- for diagnostic parameters set  $Y^0$ :
  - if  $w_{ij} \geq 0,05$  then  $y_j \in Y^0$ ,
  - or if  $w_{ij} = w_{ijmax}$  then  $y_j \in Y^0$ ;
- for state prognosis:

- if  $w_{1j} = w_{1jmax}$  and if  $w_{1j} \geq 0,9$  then  $y_j \in Y^o$  and the set  $Y^o$  is a single-element set,  $Y^o = Y^{o1}$ ,
- if  $w_{1j} = w_{1jmax}$  and if  $w_{1j} < 0,9$  then  $y_j \in Y^o$  and the set  $Y^o$  is not a single-element set,  $Y^o = Y^{oo}$ ,
- if the prognosis mistake of Holt method (with appropriate values of the parameters  $\alpha, \beta$ ) for the set  $Y^{o1} <$  prognosis mistake of the Brown–Mayer method (with an appropriate value of the parameter  $\alpha$ ) for the set  $Y^{o1}$ , then the method of value prognosis of the set  $Y^{o1}$  is the Holt method (with appropriate values of the parameters  $\alpha, \beta$ ), otherwise the prognosis method of the value  $Y^{o1}$  is the Brown–Mayer method (with an appropriate value of the parameter  $\alpha$ ),
- if the value of the next examination date of the engine UTD-20  $\Theta_{d1} (Y^{o1}) \leq$  value of the next examination date of the engine  $\Theta_{d2} (Y^{o1})$ , then the method to estimate the next examination date of the engine is the method of levelling the prognosis mistake value, otherwise it is the prognosis method of diagnostic parameter boundary value,
- if the prognosis mistakes for methods: Holt (with appropriate values of the parameters  $\alpha, \beta$ ) or Brown–Mayer (with an appropriate value of the parameter  $\alpha$ ) for diagnostic parameters of the set  $Y^{oo}$  take minimum values, then prognosis methods of values of appropriate diagnostic parameters of the set  $Y^{oo}$  are the above methods,
- if the value of the next examination date of the engine UTD-20  $\Theta_{d1} (Y^{oo}) \leq$  value of the next examination date of the engine  $\Theta_{d2} (Y^{oo})$  then the method to estimate the next examination date of the engine (for the considered diagnostic parameter) is the method of levelling the prognosis mistake value, otherwise it is the prognosis method of diagnostic parameter boundary value,
- if the value of the next examination date of the engine UTD-20  $\Theta_d$  is determined for  $Y^{oo}$ , then this values is the weighed value of the value  $\Theta_{dw}$ .

The presented conclusion rules in range of machine state prognosis, after performing appropriate verification researches, could be the basis for dedicated software of a machine state recognition system in an on–line mode (for an on-board system) and off–line (for a stationary system).

## 6. Conclusion

From the analysis of action requirements, and the configuration of the on-board machine state recognition system, it results that the architecture of the system should assure:

- a) the system configuration in the range of beforehand determined needs, including inserting the appropriate number of diagnostic parameters, their boundary values, and nominal values of diagnostic parameters, machine state, machine operational time;
- b) measuring and recording diagnostic signals measured values according to determined conditions (the beginning and end of the measurement, which values, and when they are recorded);
- c) diagnostic concluding on the basis of relation analysis between the standard values and the measured values on the basis of diagnostic conclusion rules analysis;
- d) machine state visualization, including exploitation decisions generation (able, unable, damage location, other).

From the above it results that it becomes necessary to create a data base in which, apart from boundary and nominal values sets, and the set of diagnostic parameters values recorded during exploitation, there are diagnostic conclusion rules.

The presented conclusion rules can be the base for programming the machine state recognition system in an online mode (for an on-board system) and offline mode (for a stationary system).

The presented algorithm of conclusion rules generation unambiguously identifies the machine's set, system or the machine, in the aspect of their state recognition, which should enable the creation of a dedicated software (for machines' sets and systems) of the state recognition system.

## References

- [1] Ameljańczyk, A., *Multiple optimization* (in Polish), WAT, Warszawa 1986.
- [2] Batko, W., *Synthesis methods of prediction diagnoses in technical diagnostics* (in Polish), Mechanika, z. 4. Zeszyty Naukowe AGH, Kraków 1984.
- [3] Bowerman, B., L., O'Connel, R., T., *Forecasting and Time Series*, Doxbury Press (USA), 1979.
- [4] Box, G., Jenkins, G., *Time series analysis, forecasting and control*, London 1970.
- [5] Brown, R., G., *Statistical Forecasting for Inventory Control*, Mc Graw-Hill, New York 1959.
- [6] Cempel, C., *Evolutionary symptom models in machine diagnostics* (in Polish), Materiały I Kongresu Diagnostyki Technicznej, Gdańsk 1996.
- [7] Inman, D., J., Farrar, C., J., Lopes, V., Valder, S., *Damage prognosis for aerospace, civil and mechanical systems*, John Wiley & Sons, Ltd. New York 2005.
- [8] Staszewski W.,J., Boller C., Tomlinson G.,R.: *Health Monitoring of Aerospace Structures*. John Wiley & Sons, Ltd. Munich, Germany 2004.
- [9] Theil, H., *Applied economic forecasting*, North-Holland, Amsterdam 1971.
- [10] Tylicki, H., *Optimization of the prognosis method of mechanical vehicles technical state* (in Polish), Wydawnictwa uczelniane ATR, Bydgoszcz 1998.
- [11] Żółtowski, B., *Diagnostic system for the metro train*, ICME, Science Press, pp.337-344, Chengdu, China 2006.





## SELECTED ISSUES OF MODELING THE ACCUMULATOR INJECTION SYSTEMS IN NAVAL COMBUSTION ENGINES

Mirosław Walkowski

*The Polish Naval Academy  
Chair of Marine Power Plants  
ul. Śmidowicza 69, 81-103 Gdynia, Poland  
tel.: +48 58 6262653  
e-mail: mwal@interia.eu*

### **Abstract**

*In the paper has been made an attempt to replace the conventional system of fuel dose control and injection passing angle with electronic control system, which has been realized this manner, that selected hydraulic accumulator, injector C-R type and fuel dose controller has been attached the marine engine.*

*It has been assumed, that by controlling the current impulse of controller it is possible to model whichever size of fuel dose, injected to the combustion chamber and to control the injection lasting time.*

*Fuel which feeds the engine must flow through differently formed/shaped channels of particular component elements of fuel system. In relation to this, there has been made an attempt of presenting the method of modelling fuel flow through the chosen sections of fuel system with different shapes of cross-section.*

**Keywords:** *damping by the parallel surfaces, flow through the apertures, energetic loss*

### **1. Introduction**

In the construction of model describing the course of complex phenomena occurring in the process of fuel injection in bunker systems it is essential to consider many specific problems connected with the flow of this liquid through channels with complex shapes.

In this paper there has been made an attempt of describing the fuel flow through the apertures, pipes with section different from the circular, also the manner of calculating the hydraulic resistance of two flat surfaces has been presented.

The significant problem at estimating the operation of hydraulic appliances, which are parts of gear feeding the vessel engines by fuel under high pressure, is the proper estimation of tightness of moving connections of parts cooperating with each other.

In the mobile joints between two cooperative parts (e.g. between piston and cylinder in the piston pump, between rotor and housing in the gear pump, between needle and atomizer cylinder) the narrow apertures always arise what is conditioned by defined constructional backlash. As far as the basic criterion for flows in the pipes is obtaining the lowest resistances, the aim is to obtain the highest resistance in the flows through apertures that guarantees possibly lowest flow delivery.

### **2. Flows through the apertures between needle and atomizer cylinder**

Considering the very low size of one of cross dimensions of aperture, flow through the aperture

is usually a laminar motion [1,2,3]. It was experimentally affirmed that Reynolds' critical ordinal for apertures (related to the minimal size of aperture), when the transition from laminar flow to turbulent flow occurs, ranges

$$Re = \frac{v_{\text{ur}} \cdot s}{\nu} \approx 600 \div 1000,$$

where:

$v_{\text{sr}}$  – mean velocity in the aperture,

$s$  – minimal size of aperture,

$\nu$  – kinematic viscosity coefficient.

## 2.1. Frictional flow in the flat aperture at zero pressure gradient

Let us take under consideration the flow in aperture between two parallel flat plates with infinite span and one of them moves to other that is immobile at constant velocity  $v_0$  on the thin layer of liquid with thickness  $s$  (Fig.2.1.).

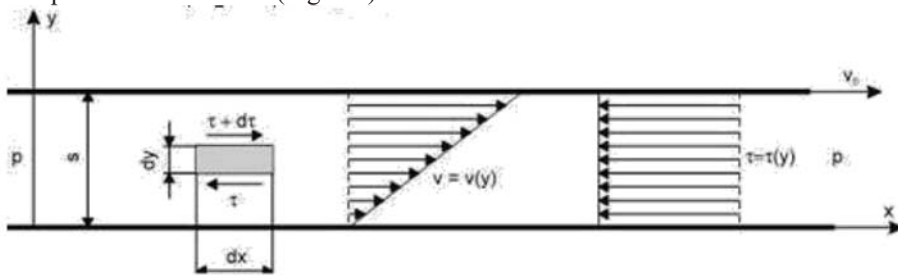


Fig.1. Flow in the flat aperture caused by the motion of upperplate

Pressure in the inlet section of such formed aperture is the same as in the outlet section ( $dp/dx = 0$ ). Because of adhesion forces, the elements of liquid directly adjoining to plates remain in the release condition toward them. Whereas the indirect thin layers of liquid will translocate to each other, velocity gradient will be different from zero ( $dv/dy \neq 0$ ) in normal direction to the pan motion. Assumption of infinite span of plates allows considering the flow in aperture as a flat flow. On the assumption that temperature in the layer of liquid is constant also its viscosity has not changed.

The infinitesimal element of prism form with section  $dx \cdot dy$  and unit spam  $dz = 1$  is taken under consideration in this layer of liquid. From the condition of force equilibrium on the direction of axis  $x$  we obtain:

$$p \cdot dy \cdot 1 - p \cdot dy \cdot 1 + (\tau + d\tau) \cdot dx \cdot 1 - \tau \cdot dx \cdot 1 = 0,$$

and further  $d\tau = 0 \rightarrow \tau = C$  where  $C$  means constant.

Distribution of shear stress in considered flow in the aperture is homogenous.

Introducing Newton's formula of the dependence of shear stress on velocity gradient in normal direction we obtain

$$\tau = \mu \cdot \frac{dv}{dy} = C, \quad \text{and after merger} \quad v = \frac{C}{\mu} \cdot y = C_1,$$

Constant  $C$  i  $C_1$  are defined on the basis of marginal conditions. For the approved system connected with the immobile plate is

$$\text{for } y=0 \rightarrow v=0 \quad y=s \rightarrow v=v_0 \quad \text{so } C_1=0 \quad \text{and } C=\mu \frac{v_0}{s}$$

Substituting defined values to (2.1) we obtain the relation on velocity distribution



$v = v_0 \cdot \frac{y}{s}$ , so the velocity distribution in the aperture is linear distribution. Flow delivery

through the section  $F=s \cdot b$  is equal to  $Q = \int_0^s v \cdot b \cdot dy = \frac{v_0}{2} \cdot s \cdot b$

It is obvious that mean flow velocity in the aperture  $v_{av} = \frac{v_0}{2}$

Previously introduced relations allow calculating the speed of shaft rotating at constant angular velocity around the axle which overlaps with the pan axle at presence of very small aperture in comparison to diameter of (Fig. 2.2)  $s/D \ll 1$ , where:  $D$  – diameter of shaft;  $s$  – size of radial aperture.

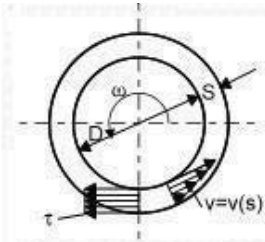


Fig. 2.2. Laminar flow in the ring aperture caused by the speed of shaft

At low relative aperture, the curvature of layer of liquid could be omitted and treated as flow in the flat aperture with linear distribution of velocity and homogenous distribution of shear stress. Defining the shaft length as  $l$ , moment of friction would be

$$M = \tau \cdot \pi \cdot D \cdot l \cdot \frac{D}{2} = \mu \cdot \frac{v_0}{s} \cdot \pi \cdot l \cdot \frac{D^2}{2},$$

where:  $v_0 = \omega \cdot D/2$  – speed of shaft, so:

$$M = \mu \cdot \omega \cdot \pi \cdot l \cdot \frac{D^3}{4},$$

It should be emphasized that the laminar flow in aperture between

the shaft and co-axial pan occurs for the Reynolds' critical ordinal  $Re \leq 30 \cdot \sqrt{\frac{D}{s}}$ .

## 2.2. Flow in the flat aperture under the influence of pressure differences

The second flat flow in the aperture, which has broad practical application, is the flow between parallel immobile plates under the influence of pressure difference. Such flows occur in the flat and cylindrical distributor, in the piston pump and hydraulic engines in piston–cylindrical opening and in the valves and other hydraulic sets. Considering very small nominal dimensions of apertures, flow velocities in the apertures have not reached such high values, to cause the turbulent flow in them. In principle, they will be the laminar flows.

The laminar stationary liquid flow in the flat aperture between two parallel plates is considered, omitting the phenomena, which occur on the edges of aperture and thermal processes.

Receiving reference standard (axis  $x$  agrees with the flow direction and places/situates in the longitudinal centre of aperture, axis  $y$  in perpendicular direction to the walls of aperture) was isolated the elementary prism with  $2y \times l \times l$  dimensions (Fig. 2.3) [1,2].

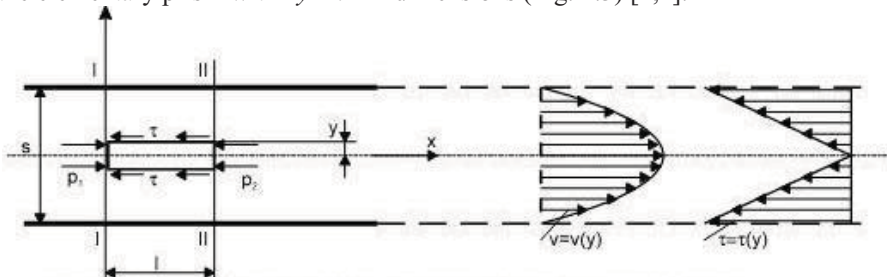


Fig. 2.3. Scheme of flow in the flat aperture caused by the pressure difference

From the condition of force equilibrium influencing on this elementary prism we obtain

$$p_1 \cdot 2 \cdot y \cdot l - p_2 \cdot 2 \cdot y \cdot l - 2 \cdot \tau \cdot l \cdot l = 0$$

where:

$p_1$  and  $p_2$  – pressure in sections I – I and II – II,

$\tau$  – shear stress on the lower and upper wall (considering flat flow the stress on the side walls gives resultant equal to zero).

$$\tau = -\mu \cdot \frac{dv}{dy} \rightarrow \frac{dv}{dy} < 0,$$

After substitution and reduction we obtain

$$(p_1 - p_2) \cdot y = -\mu \cdot \frac{dv}{dy} \cdot l,$$

defining

$$\frac{p_1 - p_2}{l} = \frac{\Delta p}{l}, \quad dv = -\frac{\Delta p}{2 \cdot \mu \cdot l} \cdot y \cdot dy,$$

Integral of this equation

$$v = -\frac{\Delta p}{2 \cdot \mu \cdot l} \cdot y^2 + C,$$

From the marginal conditions

$$y = \pm \frac{s}{2}, \quad v = 0,$$

was determined constant  $C$  of above equation

$$C = \frac{\Delta p}{2 \cdot \mu \cdot l} \cdot \frac{s^2}{4},$$

The formula for velocity distribution in the aperture will take the final form

$$v = \frac{\Delta p}{2 \cdot \mu \cdot l} \cdot \left[ \frac{s^2}{4} - y^2 \right],$$

Velocity distribution in the aperture is parabolic.

Velocity reaches the maximal value in the longitudinal centre of aperture

$$v_{\max} = \frac{\Delta p}{8 \cdot \mu \cdot l} \cdot s^2,$$

Mean velocity of the aperture

$$v_{\text{ar}} = \frac{2}{3} \cdot v_{\max} = \frac{\Delta p}{12 \cdot \mu \cdot l} \cdot s^2,$$

Flow delivery through the aperture with unit breadth

$$Q = \frac{\Delta p}{12 \cdot \mu \cdot l} \cdot s^3,$$

and for the aperture with breadth,  $b \gg s$

$$Q = \frac{\Delta p}{12 \cdot \mu \cdot l} \cdot b \cdot s^3,$$

Pressure decrease at velocity  $v_{\text{ar}}$

$$\Delta p = \frac{12 \cdot \mu \cdot l \cdot Q}{b s^3} = \frac{12 \cdot \nu \cdot l \cdot \gamma \cdot v_{\text{ar}}}{g \cdot s^2},$$

Flow loss through the flat aperture amounts to

$$h_l = \frac{12 \cdot \nu \cdot l \cdot v_{\text{ar}}}{g \cdot s^2},$$

or in analogous form to the formula for flow loss in the pipelines

$$h_l = \lambda \cdot \frac{l}{D_h} \cdot \frac{v_{\text{ar}}^2}{2 \cdot g},$$

where:

$D_h = 2 \cdot s$  – hydraulic diameter,

$\lambda = 96/Re$  – flow loss coefficient for the aperture,

$Re = (v_{sr} \cdot D_h)/\nu$  – Reynolds' critical ordinal.

Power lost at the flow through aperture is equal to work which is necessary to translocate the liquid through aperture at pressure difference equal to pressure loss

$$N_p = Q \cdot \Delta p = \frac{s^3}{12 \cdot \mu} \cdot \frac{(\Delta p)^2}{l} \cdot b,$$

Above considerations and introduced formulas are correct on the assumption of constant viscosity in aperture. In reality/as a matter of fact the viscosity of liquid depends on temperature and pressure, which change along the aperture. For practical equations with sufficient accuracy is accepting the mean arithmetical value of kinematic viscosity coefficient

$$\nu_{ar} = \frac{\nu_1 + \nu_2}{2},$$

where:  $\nu_1$  and  $\nu_2$  define values of kinematic viscosity coefficient which matches temperature in the inlet/outlet of aperture.

The most common flow in the hydraulic appliances is the flow occurring between two parallel walls, which is caused by the pressure difference at simultaneous parallel translocation of walls.

The examples could be: the flow between rotating toothed-wheel rim and gear casing and the flow between cylinder and atomizer needle at their mutual relative motion in the engine atomizers.

If it is considered the laminar flow between two flat parallel walls and one of them moves with constant velocity  $v_0$  at pressure gradient different from zero ( $dp/dx = (\Delta p/l) \neq 0$ ), it could be regarded as total of two flows: fractionous flow with linear velocity distribution and flow caused by the pressure difference with parabolic velocity distribution.

When wall moves according to the direction of flow presented in Fig 2.4., velocity distribution of flow in the aperture to the co-ordinate system in the longitudinal centre plate is analytically defined by the formula:

$$v = v(y) = v_0 \cdot \left[ \frac{y}{s} + \frac{l}{2} \right] + \frac{\Delta p \cdot s^2}{8 \cdot \mu \cdot l} \cdot \left[ 1 - \frac{4 \cdot y^2}{s^2} \right],$$

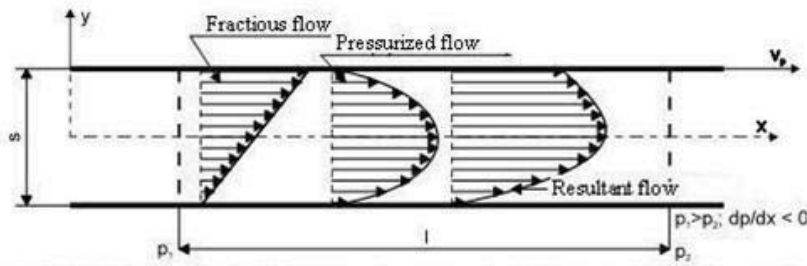


Fig. 2.4. Velocity distribution in the flat aperture at pressure difference and upper plate moving according to the direction of pressurized flow

If the wall moves in the opposite direction to the flow caused by the differential pressure, velocity in the cross-section of aperture will be

$$v = v(y) = -v_0 \cdot \left[ \frac{y}{s} + \frac{l}{2} \right] + \frac{\Delta p \cdot s^2}{8 \cdot \mu \cdot l} \cdot \left[ 1 - \frac{4 \cdot y^2}{s^2} \right],$$

Velocity distribution in this case presents Fig. 2.5.

Knowing the velocity distribution, the value of mean velocity and the flow delivery is easy to define

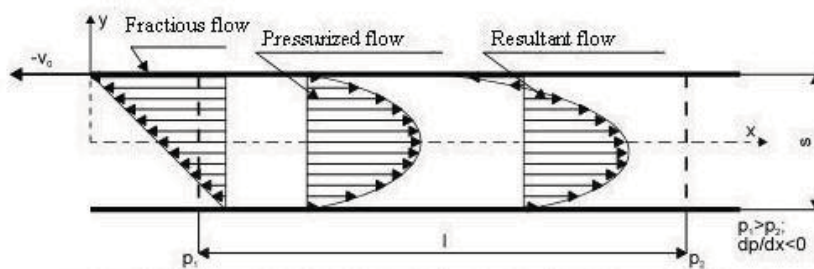


Fig.2,5. Velocity distribution in the total pressurized flow in the aperture at motion of upper plate opposite to the direction of pressurized flow

$$v_{ir} = \frac{\Delta p \cdot s^2}{12 \cdot \mu \cdot l} \pm \frac{v_0}{2},$$

sign „ + ” – when plate moves in direction of lower pressure,

sign „ - ” – when the direction of plate is opposite.

The relation defines flow delivery through the aperture with span b

$$Q = \left[ \frac{\Delta p \cdot s^3}{12 \cdot \mu \cdot l} \pm \frac{v_0}{2} \cdot s \right] \cdot b,$$

(sign „ ± ” like at defining mean velocity).

### 2.3. Hydraulic loss in the pipes with section different from circular. Hydraulic radius

The loss in the rectiaxial pipes with circular cross has been previously considered [1,2,3].

There should be put a question to what degree the presented considerations and formulas could be correct in solving the practical tasks in case of pipes with section different from the circular and pipes with circular section.

At calculating the hydraulic loss, the significant source of energy loss is shear stress appeared on the pipe walls, which was caused by liquid viscosity. Loss caused by the liquid friction will be the higher, the higher is circumference of washed by the liquid in relation to pipe section. At the same delivery and the same section, the flow resistance in the pipe with rectangular section will be higher than flow resistance and it in turn will be higher than the resistance in pipes with circular section. It is because circle has the lowest relation of circumference to section among all plane figures. Pipes with circular sections are the most beneficial taking under friction loss. So it is not difficult to draw to conclusion that measure, which is characteristic of values of loss occurring in pipes with different sections, is the relation of liquid section  $F_s$  to wetted circumference  $l_{zw}$ , i.e. to the circumference where liquid meets with walls.

This relation is called the hydraulic diameter  $r_h = \frac{F_s}{l_{zw}}$

Fig. 2.6 presents examples of hydraulic diameters for cases, which are most common in practice.

For the flat apertures, where the width of aperture  $a$ , is significantly higher in comparison to high  $s$ , the values of hydraulic radius  $r_h = \frac{s}{2}$ .

Although there can not be the dynamic similarity of flows in the pipes with circular and non-circular-section, still on the basis of experiments it could be assumed that the character of variation of coefficient  $\lambda$  in pipes with different sections will be analogous at the same Reynolds' critical ordinals.

$$r_h = \frac{\frac{1}{4} \cdot \pi \cdot d^2}{\pi \cdot d} = \frac{d}{4} \quad r_h = \frac{F_s}{l_{zw}} \quad r_h = \frac{a^2}{4 \cdot a} = \frac{a}{4} \quad r_h = \frac{a \cdot b}{2 \cdot (a + b)},$$

Especially at lack of experimental data for not very accurate calculations of flow loss in the pipes with sections different from the circular could be used formulas given for circular flow without fear of making glaring mistakes.

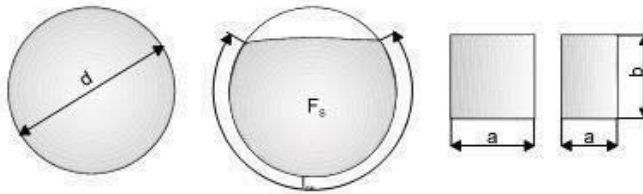


Fig. 2.6. The examples of hydraulic radii for the most common pipe sections

Because hydraulic diameter for the circle-section  $r_h = d/4$ , formula on calculating the hydraulic loss for pipes with any section will have following form 
$$h_l = \lambda \cdot \frac{l}{4 r_h} \cdot \frac{v_{ur}^2}{2 \cdot g}$$

where loss coefficient  $\lambda$  is defined for the particular zones on the basis of formulas for sections with circular-section, where Reynolds' critical ordinal is following

$$Re = \frac{4 \cdot r_h \cdot v_{ur}}{\nu},$$

## 2.4. Hydraulic resistance of two parallel round surfaces immerse in liquid and approaching

In the present point the motion of two parallel plates immersed in liquid and approaching to each other will be considered, what concerns the sections of motion of atomizer needle in extreme positions [4].

Two parallel flat round plates with diameter  $R$  are located one above other in low distance from each other; space between them is filled with liquid. By pushing out the liquid the plates approach to each other at constant velocity  $u$ . Task lies in calculating the resistance, which plates meet. [4].

To calculate above task the installed set of parallel round plates was oriented to cylindrical coordinates with the beginning of set in the middle of bottom plate (which is assumed as immobile). The motion of liquid is axially symmetrical and because the liquid layer is very thin, in fact it is the motion along the radius ( $v_z \ll v_r$ ), where  $\frac{\partial v_r}{\partial r} \ll \frac{\partial v_r}{\partial z}$ .

So the motion equation has form:

$$\eta \cdot \frac{\partial^2 v_r}{\partial z^2} = \frac{\partial p}{\partial r}, \quad \frac{\partial p}{\partial z} = 0 \quad (a) \quad \frac{1}{r} \cdot \frac{\partial(r \cdot v_r)}{\partial r} + \frac{\partial v_z}{\partial z} = 0 \quad (b)$$

with following marginal conditions:

$$v_r = v_z = 0, \text{ when } z = 0; \quad v_r = 0, \quad v_z = -u, \text{ when } z = h; \quad p = p_0, \text{ when } r = R$$

where  $\eta$  – dynamic viscosity,  $h$  is the distance between plates and pressure  $p_0$  is the exterior pressure. From the equations (a) we obtain:

$$v_r = \frac{1}{2 \cdot \eta} \cdot \frac{dp}{dr} \cdot z \cdot (z - h),$$

Merging equation (b) after  $dz$  we obtain 
$$u = \frac{1}{r} \cdot \frac{d}{dr} \cdot \int_0^h r \cdot v_r \cdot dz = -\frac{h^3}{12 \cdot \eta \cdot r} \cdot \frac{d}{dr} \cdot \left( r \cdot \frac{dp}{dr} \right),$$

from which 
$$p = p_0 + \frac{3 \cdot \eta \cdot u}{h^3} \cdot (R^2 - r^2),$$

Total resistance force influencing on the plate is equal to 
$$F = \frac{3 \cdot \pi \cdot \eta \cdot u \cdot R^d}{2 \cdot h^3}.$$

#### 4. Conclusions

Simulation calculations for the chosen sections of feeding system has been presented on the basis of theoretical and empiric relations without verification and tests on the real feeding installation in fuel system C – R. type.

As it results from the initial observations of measure results on the stand, the above-proposed relations are the output basis for detailed analysis of phenomena, which occur in the selected sections of fuel gear.

To verify the approved model, the experimental tests should be conducted on the test stand, which is replica of feeding system 1SB and the obtained result should be used to adjust the approved calculation model.

#### References

- [1] Baszta, T., *Urządzenia hydrauliczne. Konstrukcja i obliczenia (in Polish)*. WNT, Warszawa 1961.
- [2] Gałęska, M., Kaczmarczyk, J., Maruszkiewicz, J., *Hydromechanika stosowana*. Wojskowa Akademia Techniczna im. J. Dąbrowskiego. Warszawa 1972.
- [3] Guillon, M., *Teoria i obliczanie układów hydraulicznych*. WNT. Warszawa.
- [4] Landau, L.D., Lifszyc, E.M., *Hydrodynamika*. Wydawnictwo Naukowe PWN. Warszawa 1994
- [5] Ochocki, W., *Numerycznie sterowane systemy wtrysku paliwa silników wysokoprężnych*. Wydawnictwo Poznańskiego Towarzystwa Przyjaciół Nauk. Poznań 1994.
- [6] Sobieszczański, M., *Modelowanie procesów zasilania w silnikach spalinowych. Zagadnienia wybrane*. WKŁ, Warszawa 2000.
- [7] Walkowski, M., *Modelowanie działania zaworu sterującego dawką paliwa w układzie wtrysku typu common rail*. VII Międzynarodowa Konferencja Naukowa SILNIKI GAZOWE 2006. Zeszyty Naukowe Politechniki Częstochowskiej 162. MECHANIKA 26. Wydział Inżynierii Mechanicznej i Informatyki. Częstochowa 2006.
- [8] Walkowski, M., *Selected problems of modelling the working of container injection systems of common rail type*. Journal of POLISH CIMAC, EXPLO – DIESEL & GAS TURBINE '07. VINTERNATIONAL SCIENTIFIC – TECHNICAL CONFERENCE. Gdańsk – Stockholm – Tumba POLAND – SWEDEN 11 – 15 May 2007. GDAŃSK UNIVERSITY OF TECHNOLOGY, Faculty of Ocean Engineering and Ship Technology, Department of Ship Power Plants.
- [9] Walkowski, M., *Determining the characteristics of control valve in a common rail injection system of a combustion engine*. SILNIKI SPALINOWE. Czasopismo naukowe Nr 2007 – SC2, Wydawca: Polskie Towarzystwo Naukowe Silników Spalinowych.



## INFLUENCE OF AXIAL COMPRESSOR FLOW PASSAGE GEOMETRY CHANGES ON GAS TURBINE ENGINE WORK PARAMETERS

Paweł Wirkowski

*The Polish Naval Academy*  
ul. Śmiedowicza 69, 81-103 Gdynia, Poland  
tel.: +48 58 6262756, fax: +48 58 6262963  
e-mail: [pawir@o2.pl](mailto:pawir@o2.pl), [p.wirkowski@amw.gdynia.pl](mailto:p.wirkowski@amw.gdynia.pl)

### Abstract

*The paper deals with the problem of influence of changes variable stator vanes axial compressor settings of gas turbine engine on work parameters of compressor and engine. Incorrect operation of change setting system of variable vanes could make unstable work of compressor and engine. This paper presents theoretical analysis of situation described above and results of own research done on real engine. On the base of results of experiment there were determined mathematical equations determining relationships of changes of particular engine work parameters in function of variable inlet guide stator vanes setting angle. There are presented results of the solution of mathematical equations, which describe the changes of engine work parameters values too.*

**Keywords:** gas turbine, axial compressor, variable stator vanes, modelling

### Parameters, abbreviations and subscripts

$\alpha_1$	- air stream outlet angle with stator vanes,
$\alpha_{KW}$	- setting angle of variable stator vanes,
$\beta_1, \beta_2$	- air stream inlet and outlet angles in rotor vanes,
$c_{1a}$	- axial component of air stream absolute speed on rotor blades inlet,
$c_{1u}, c_{2u}$	- circumferential components of air stream absolute velocity on the inlet and outlet rotor blades,
CO	- combustor,
HPC	- high pressure compressor,
HPT	- high pressure turbine,
$\eta_s^*$	- compressor efficiency,
$i$	- air stream inlet angle on rotor blades,
LPC	- low pressure compressor,
LPT	- low pressure turbine,
LK	- variable stator vane,
$\dot{m}$	- air mass flow,
$n$	- compressor rotor speed,
$\omega$	- angular velocity,
$p_{fuel}$	- fuel pressure,
$P_{nom}$	- nominal engine power,
PT	- power turbine,
$\pi_s^*$	- compression ratio,
$u$	- circumferential speed,



$w_1, w_2$  - air stream relative speed on inlet and outlet rotor blades,  
 $VIGV$  - variable inlet guide vanes,  
 $\Delta c_u, \Delta w_u$  - air stream whirl in the rotor,  
 $VIGV$  - variable inlet guide vanes,  
 $z$  - number of inlet guide stator vanes,

## 1. Introduction and purpose of research

When in the compressor construction is assembled system of setting change of variable stator vanes its task is to make optimal cooperation engine units during the permanent improvement of compressor characteristic. Perturbations in the operation of this system could cause changes in work of compressor and engine similarly as in the case of changes caused by changes of rotational speed or polluted interblades ducts of compressor.

Compressor stage unitary work on radius is defined on the base of equation of angular momentum and it has form

$$l_{st} = \omega \cdot r \cdot (c_{2u} - c_{1u}) = u \cdot \Delta c_u = u \cdot \Delta w_u \quad (1)$$

where:

$\omega$  – angular velocity,  $u$  – tangential velocity,  $r$  – rotor radius,  
 $c_{1u}, c_{2u}$  – circumferential components of air stream absolute velocity on the inlet and outlet rotor blades on radius  $r$ ,  
 $\Delta c_u, \Delta w_u$  – air stream whirl in the rotor.

That work is constant on whole depth of rotor blade. The sum of works is the unitary work of stage [2]. Involved change of variable stator vanes angle setting at a constant level rotational velocity (constant  $u$ ) caused change of air stream inlet angle in rotor vane  $\beta_l$  (Fig. 1). It caused change of axial component of air stream absolute velocity on inlet  $c_{1a}$  what is equivalent with the change of air mass flow  $\dot{m}$  and change of air stream whirl  $\Delta w_u$  in rotor. It influences on efficiency and work of stage.

The purpose of investigations, which was carried out on real engine was determination of influence of incorrect operation of axial compressor inlet guide variable stator vanes control system of gas turbine engine on compressor and engine work parameters.

Compressor characteristic is a relationship between compression ratio  $\pi_s^*$ , compressor efficiency  $\eta_s^*$  and air flow mass  $\dot{m}$  and compressor rotational velocity  $n$ . It makes possible to determine the best condition of compressor and another engine units mating. The characteristic is used to select optimal conditions of air flow regulation and assessment of operational factors on compressor parameters.

Therefore compressor should be so controlled in operational range of rotational velocity that the compressor and engine mating line has a stock of stable work. The main rule of compressor control during the change of their rotational velocity or flow intensity is to keep up the stream inlet angles  $i$  value near zero. One of the most popular ways of axial compressor control is changing their flow duct geometry by application of inlet guide stator vanes or variable stator vanes of several first compressor stages [2].

This solution makes it possible to change of air stream inlet angle on rotor blades of compressor stages by change of stator vanes setting angles during the change of compressor rotational velocity. Fig. 1 illustrates the rule of regulation of variable stator vanes.

For average values of operational range of compressor rotor speed is situation in Fig. 1b – speed values and directions with subscript number 1. In this situation is intermediate angle setting of stator vanes. Air stream inlet angle on rotor blades do not cause disturbance of stream flow by interblades ducts. For lower values of compressor rotor speed and in consequence lower values of absolute axial component velocity  $c_{1a}'$ , it is necessary to reduce the stream outlet angle

of variable stator vanes  $\alpha_l$  (Fig. 1a). The angle reduction range should allow keeping the same value of stream inlet angle on rotor blades. Analogical situation takes place during the work of compressor with higher rotational speed. For higher rotational speed absolute axial component speed  $c_{1a}''$  increases. In this situation for keeping stable work of compressor and in consequence constant value of stream inlet angle on rotor blades, it is necessary to increase the stream outlet angle of variable stator vanes – Fig. 1c. Application in gas turbine engine construction of control system of flow ducts geometry has a bearing on a run of unstable processes.

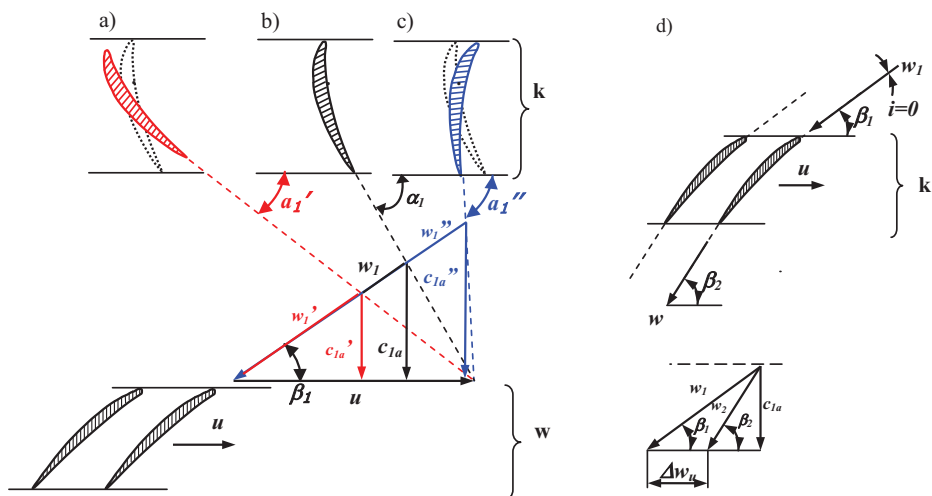


Fig. 1. Essence of control of compressor's axial stage by changing the setting angle of stator vanes ring at changeable air flow velocity; a) decreased axial velocity, b) analytical axial velocity, c) increased axial velocity, d) schema of flow round of axial compressor rotor blades during constant rotor speed and constant air stream inlet angles; k – variable stator vanes ring, w – rotor vanes ring

## 2. Object of research

The object of research is type DR 77 marine gas turbine engine, which is a part of power transmission system of a warship. It is three-shaft engine with can-ring-type combustor chamber and reversible power turbine (Fig. 2).

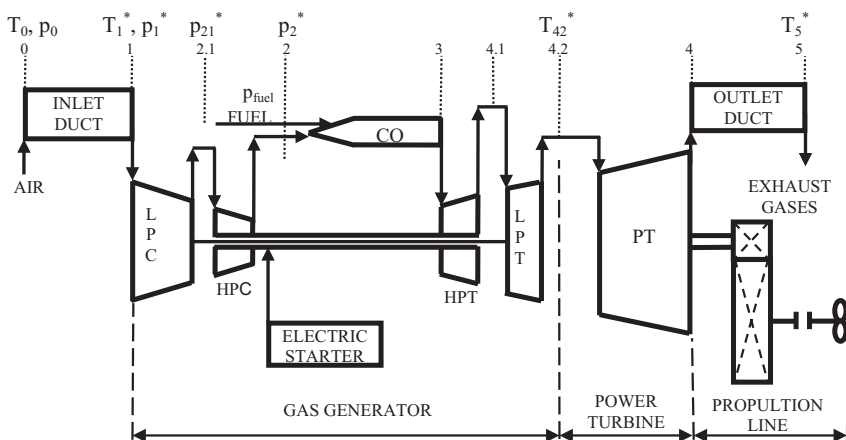


Fig. 2. Block diagram of DR77 gas turbine engine

In compressor construction configuration of this engine there are used inlet guide stator vanes which make possibilities to change the setting angle incidence (change of compressor flow duct geometry) in dependance on engine load. This process is operated by control system which working medium is compressed air received from last stage of high pressure compressor. On Fig. 3 is presented block diagram of flow control signal of variable stator vanes system.

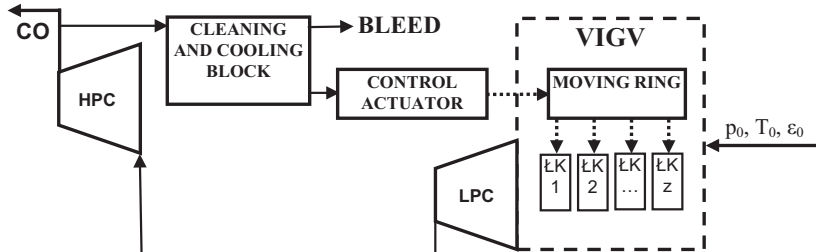


Fig. 3. Block diagram of stator vanes change setting mechanism

Compressed air from the last stage of high pressure compressor is supplied to working space of control actuator by cleaning and cooling block. Compressed air exerts pressure on control actuator elements. It causes moving of control piston which is connected with moving ring. This ring moves on circumference of compressor body. Ring is connected with stator vanes by levers. When the ring is moving stator vanes realize rotational motion changing the air stream outlet angle  $\alpha_l$  (Fig. 1). In cleaning and cooling block are made holes. During research air stream was bled by the holes and less air was supplied to the actuator. It caused change of setting angle  $\alpha_{KW}$  of variable stator vanes. In consequence of that change flow duct geometry was changed.

The experiment was carried out on an engine load  $0,5P_{nom}$  with taking into consideration atmospheric conditions. For this load setting angle of variable vanes has value  $\alpha_{KW} = -4^\circ$ . During change engine load in the whole range from idle to full load setting angle  $\alpha_{KW}$  of variable vanes changes in range from  $-18^\circ$  to  $+18^\circ$ . During experiment a few parameters of engine work was measured and registered. It was made for three different setting angle  $\alpha_{KW}$  of variable vanes: A-  $\alpha_{KW} = -4^\circ$ , B-  $\alpha_{KW} = -11^\circ$ , C-  $\alpha_{KW} = -18^\circ$ . Tab. 1 presents measured and registered parameters.

Tab. 1. Parameters of engine DR77 work measured during research

Parameter	Measurement range	Unit	Parameter name
$n_{LPC}$	0 – 20000	$[\text{min}^{-1}]$	low pressure rotor speed
$n_{HPC}$	0 – 22000	$[\text{min}^{-1}]$	high pressure rotor speed
$n_{PT}$	0 – 10000	$[\text{min}^{-1}]$	power turbine rotor speed
$p_1$	-0,04 – 0	$[\text{MPa}]$	subatmospheric pressure on compressor inlet
$p_{21}$	0 - 0,6	$[\text{MPa}]$	air pressure on low pressure compressor outlet
$p_2$	0 - 1,6	$[\text{MPa}]$	air pressure on high pressure compressor outlet
$p_b$	0 - 10,0	$[\text{MPa}]$	fuel pressure before injectors
$T_1$	-203 - 453	$[\text{K}]$	air temperature on compressor inlet
$T_{42}$	273 - 1273	$[\text{K}]$	exhaust gases temperature on inlet power turbine

### 3. Results of research

Change angle vanes setting from position A to position C caused the increase of air flow resistance by stator vanes. In consequence of that subatmospheric pressure on the compressor inlet  $p_1$  decreases. It causes pressure decrease in next parts of compressor and engine flow duct. In this way reduced air density flowing by compressor, for stable quantity of stream fule suppllied to combustor, causes increase of compressors rotor speed. The most noticeable is increase of low pressure compressor rotor speed caused by directly influence on this compressor incorrectly

setting variable stator vanes. Gasodynamical connection between the low pressure compressor and the high pressure compressor absorbs disturbances work of low pressure compressor which are transferred on high pressure compressor. Therefore range of change high pressure compressor rotor speed is lower than low pressure compressor. In this experiment it is below 1% and it is in measuring error of sensor range.

Change of subatmospheric pressure is above 5% undisturbed value of this parameter. Changes of low and high pressure compressor outlet pressure are adequately above 1,3% and above 2,4% undisturbed value of angle setting  $\alpha_{KW} = -4^\circ$ .

Changes of pressure and air mass flow intensity values accompanied disturbed work of compressor, during constant fuel mass flow intensity in combustor, caused enrichment of fuel mixture. As a result of that, temperature combustor outlet gases increases. In experiment was confirmed the tendency changes of gases temperature values even though the range of those changes is in measuring error of sensor range.

On the base of results of experiment there were determined the mathematical equations modelling the changes of particular engine work parameters in the function of variable inlet guide stator vanes setting angle  $\alpha_{KW}$  :

$$n_{SNC} = 0,7449\alpha_{KW}^2 + 2,602\alpha_{KW} + 9234,5 \quad (2)$$

$$n_{SWC} = 0,0204\alpha_{KW}^2 - 1,1224\alpha_{KW} + 12598 \quad (3)$$

$$p_1 = -10^{-6}\alpha_{KW}^2 - 10^{-6}\alpha_{KW} + 0,0077 \quad (4)$$

$$p_{21} = 10^{-16}\alpha_{KW}^2 + 0,0029\alpha_{KW} + 2,9814 \quad (5)$$

$$p_2 = 2 \cdot 10^{-16}\alpha_{KW}^2 + 0,0143\alpha_{KW} + 8,1771 \quad (6)$$

$$T_{42} = 0,0204\alpha_{KW}^2 + 0,1633\alpha_{KW} + 526,33 \quad (7)$$

Fig. 4 presents results of mathematical modelling of engine work parameters. Modelling was carry out an state engine load what was equivalent unchangable fuel mass flow. In this case range of change of variable inlet guide stator vanes setting angle  $\alpha_{KW}$  was widen from  $-18^\circ$  to  $+18^\circ$ . Researches in range  $\alpha_{KW}$  from  $-4^\circ$  to  $+18^\circ$  were not possilble to realize on real engine. It is caused by technical restrictions on the engine.

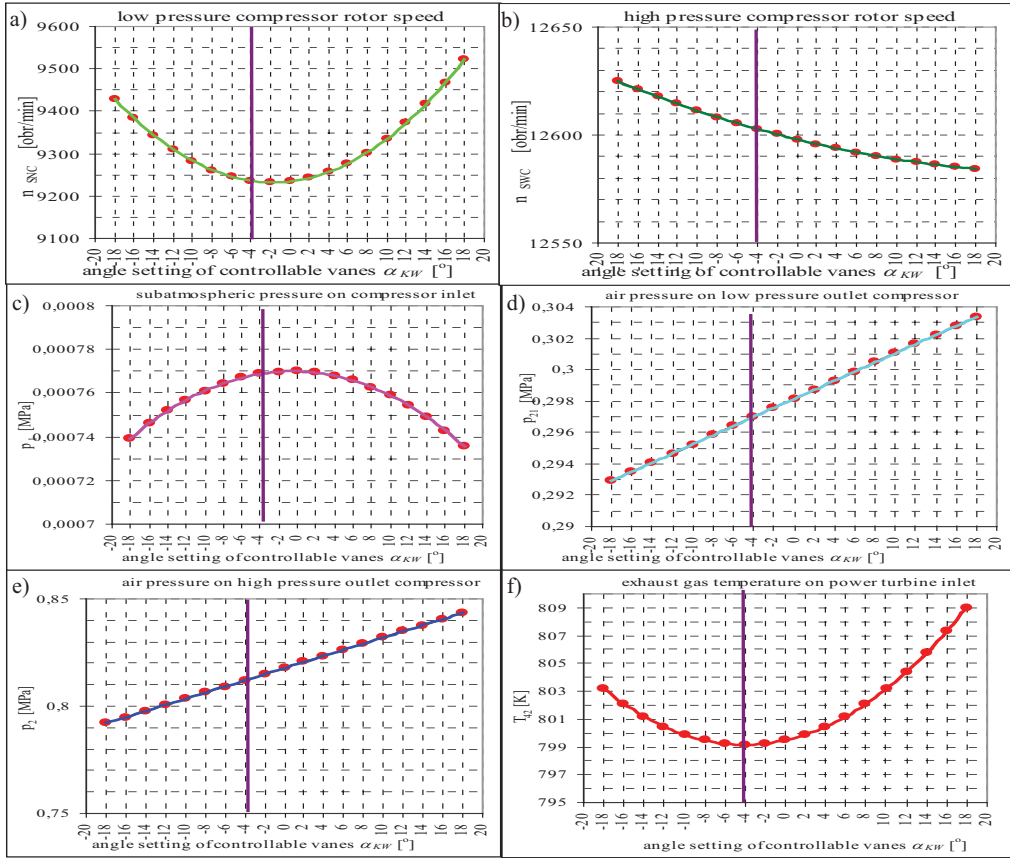


Fig. 4. Change of values of engine work parameters in function of variable inlet guide stator vanes setting angle gotten during mathematical simulation

#### 4. Conclusions

Change of values of variable inlet guide stator vanes setting angle  $\alpha_{KW}$  from  $-4^\circ$  to  $+18^\circ$  caused the increase of stream outlet angle of variable stator guide vanes  $\alpha_1$  (Fig. 1). It decreases air flow drag on low pressure compressor inlet that caused decrease of subatmospheric pressure. During keeping the constant engine load (constant fuel mass flow) absolute axial component velocity  $c_{1a}$  increases. It exerts an influence on air mass flow  $\dot{m}$  increase. Simultaneously the absolute axial component velocity  $c_{1a}$  increase caused decrease of air stream whirl in rotor  $\Delta w_u$ . In consequence of that low pressure compressor rotor speed increases (Fig. 4a). In connection with decrease of subatmospheric pressure the increase of air pressure on low pressure outlet compressor is caused (Fig. 4d). In spite of the slight decrease of high pressure compressor rotor speed the increase of air pressure on low pressure outlet compressor involves the increases of air pressure on high pressure outlet compressor (Fig. 4e). This slight decrease of high pressure compressor rotor speed caused increase of gases flow drag in the next gas turbine engine units for the combustor. The effect of above is a slight increase of exhaust gas temperature on power turbine inlet.

Multi-shaft construction of gas turbine engine reduces effects of incorrectly setting of variable vanes. Therefore compressors of three-shaft gas turbine engine do not require variable stators vanes as many stages as compressor of two-shaft engine with the same achievements.

Preliminary research confirms the necessity of inspection the correct operation of variable stator vanes system control. It makes possibility of elimination this factor from group of factors informing about technical state of engine which are identified during the diagnostic inspections.

## References

- [1] Charchalis A.: *Diagnostics of marine gas turbine engines* (in Polish). Published by Polish Naval Academy, Gdynia, 1991.
- [2] Dzygadło Z. et al.: *Rotor units of gas turbine engines* (in Polish). Transport and Telecommunication Publishing House (WKiŁ), Warszawa, 1982.
- [3] Korczewski Z.: Wirkowski, P., *Modelling gasodynamic processes within turbine engines' compressors equipped with variable geometry of flow duct*, IV International Scientifically-Technical Conference "Explo-Diesel & Gas Turbine '05", Gdańsk-Międzyzdroje-Kopenhaga, Wyd. Politechnika Gdańska, Gdańsk 2005, 227-236.
- [4] Marschal D.J., Muir D.E., Saravanamuttoo H.I.H.: *Health Monitoring of Variable Geometry Gas Turbines for the Canadian Navy*, The American Society of Mechanical Engineers 345 E, 47 St., New York, N.Y.10017.
- [5] Wirkowski, P., *Influence of changes of axial compressor variable stator vanes setting on gas turbine engine work*, V International Scientifically-Technical Conference POLISH CIMAC "Explo-Diesel & Gas Turbine '07", Gdańsk-Stockholm-Tumba, Published by Gdańsk University of Technology, Gdańsk 2007, 511-518.
- [6] Wirkowski P.: *Modelling the characteristics of axial compressor of variable flow passage geometry, working in the gas turbine engine system*, Polish Maritime Research, No 3/2007, Published by Gdańsk University of Technology, Gdańsk 2007, 27-32.
- [7] Wirkowski P.: *Simulation of changes of gas turbine engine work parameters equipped with variable inlet stator vanes axial compressor*, 12<sup>TH</sup> International Conference „Computer systems aided science, industry and transport”- TRANSCOMP 2008, Zakopane 1-4 December 2008, Published by Radom University of Technology, Radom 2008, 591-596.







## THE MULTI-EQUATIONAL MODELS IN THE ANALYSIS OF RESULTS OF MARINE DIESEL ENGINES RESEARCH

Ryszard Zadrag

Naval University of Gdynia  
Ul. Śmidowicza 69, 81-103 Gdynia, Poland  
tel.: +48 58 6262829  
e-mail: [zadra\\_g@wp.pl](mailto:zadra_g@wp.pl)

### Abstract

*Contemporary empirical researches on the object, which is combustion engine, are proceeded basing on the theory of experiment. Available software applications to analyze the experimental data commonly use the multiple regression model, which enables studying effects and interactions between input values of the model and single output variable. Using multi-equational models gives free hand at analyzing measurement results because it enables analysis of effects and interaction of many output variables. In this paper author presents advantages of using the multidimensional regression model on example of researches conducted on engine test stand.*

**Keywords:** marine diesel engine, theory of experiment, toxic compounds, emission

### 1. Introduction

Contemporary empirical researches on the object, which is combustion engine, are conducted basing on the theory of experiment. Basic purpose of such proceeded scientific researches is to prove the relation between the input signals (introduced by researcher) and output signals (observed by him). The final purpose of statistic analysis of the results of measurements is to determinate functions of the test object and the empirical model of functional engine. Related to this task very wide equations using calculus of probability, theory of stochastic processes and differential calculus are very time-consuming and without computer technique and specialist software are practically impossible. In the process of solving problems concerning interrelationships and complementary approximation issues, statistic correlations, relevancy assessment and inaccuracy of measurements and also adequacy of functions of test object with mathematical issues and graphic defining special points are used available computer programs, among all package STATISTICA PL. Mentioned programs are based on the analysis of variation and they assure:

- defining coefficients of function regression in the test object;
- assessing principal effects and interactions;
- defining correlations of input and output values;
- assessing adequacy of function in the test object (empirical functional model);
- defining mathematical dependences assumed by the operator, which results from the elaborated functional model.

It should be emphasized that the statistic computer analysis could relate to various models which do not concern interactions at various stages of complication, which are accepted in the description of model of input values. Simultaneously there is possibility of rejecting (disregarding) in the statistic analysis both at choice selected input values describing the object and various types of interactions. It means that choice of the appropriate (most adequate) model depends on the operator and his knowledge about the specialist theoretical basis of the researched issue.

At assumed lower accuracy of projecting reality and in practice in case of defining the character of changes (trend) of output values there is possibility of significant simplification of approximating polynomials by concerning only input values and only these of interactions which are statistically significant. Also the stage of approximating polynomials decides about the stage of model complexity and complication of basic values. So it is justifiable pursuing to creating models with the possibly simple form and the most profitable linear models. It is supposed that with regard for making some mistakes it is better to describe researched issue with non-linear character in small linear sections than in single complex non-linear complete section.

Commonly used software securing the experiment planning and its further analysis do not give free hand in analyzing collected material but they use prepared above presented schemes of analysis. So interfering in the program (program package) is impossible. Noticeable in the recent period development of social, medical and economic sciences caused rapid progress in using statistic methods which secure planning the experiment [3,9,10]. Especially econometria has great achievements in this field and new approach to the statistic analysis could be successfully used in technical researches [2]. Among all using the multi-equational models gives possibilities to study the correlations between input and output values and additionally concern feedbacks between output variables and gives possibility of their direct analysis. Such assumption in contrary to commonly used multiple regression is closer to real conditions even if considering the Diesel dilemma i.e. dependence between CO, HC and NO<sub>x</sub> concentration.

Below are presented results of researches on the fuel feeding system of the engine (injection system) using the double-value fractious plan and multi-equational model.

## 2. Researches on the fuel feeding system of the engine using double-value fractious plan

The object of research was fuel feeding system in the single-cylinder test engine 1SB installed in the Exploitation Laboratory of Shipping Power Stations in the Naval Academy [11].

To identify the influence of technical condition of engine on the energetic parameters of engine, there were defined sets of the input values (given parameters) and output values (observed parameters).

### 1. Set of the input values X:

- $x_1$  – rotational engine speed  $n$  [rev/min];
- $x_2$  – engine torque  $T_{iq}$  [N·m];
- $x_3$  – leak of the cylinder-injection pump piston set  $S_{pw}$  [ $\mu\text{m}^2$ ];
- $x_4$  – leak of the discharge valve of pulverizer needle  $S_{zt}$  [ $\mu\text{m}^2$ ];
- $x_5$  – leak of the skirt of pulverizer needle  $S_i$  [ $\mu\text{m}^2$ ];
- $x_6$  – leak of the needle cone in the pulverizer setting  $S_r$  [ $\mu\text{m}^2$ ];
- $x_7$  – erosive wear of the pulverizer nozzle  $S_e$  [ $\mu\text{m}^2$ ];
- $x_8$  – coking of the pulverizer nozzle  $S_k$  [ $\mu\text{m}^2$ ];
- $x_9$  – strain injector spring  $\Delta P$  [MPa].

### 2. Set of the output values Y:

- $y_1$  – fuel injection advance angle  $\alpha_{ww}$  [°OWK];
- $y_2$  – fuel injection angle  $\alpha_w$  [°OWK];

- $y_3$  – injector opening pressure  $p_{owtr}$  [MPa];
- $y_4$  – maximal fuel injection (forcing) pressure  $p_{wtr(max)}$  [MPa];
- $y_5$  – speed of pressure accumulation in the cylinder  $(\Delta p/\Delta \alpha)_s$  [MPa $^\circ$  OWK];
- $y_6$  – speed of pressure accumulation in the injection conduit  $(\Delta p/\Delta \alpha)$  [MPa $^\circ$  OWK];
- $y_7$  – fuel consumption per hour  $B$  [g/h];
- $y_8$  – outlet exhaust temperature from the cylinder  $T_{g1}$  [K];
- $y_9$  – mean indicated pressure  $p_{mi}$  [MPa];
- $y_{10}$  – compression pressure during the fuel injection  $p_c$  [MPa];
- $y_{11}$  – highest compression pressure  $p_{c(max)}$  [MPa];
- $y_{12}$  – maximal combustion pressure  $p_{max}$  [MPa];
- $y_{13}$  – angle at the moment of maximal combustion pressure  $\alpha_{pmax}$  [° OWK];
- $y_{14}$  – carbon monoxide concentration in the outlet exhaust manifold  $C_{CO(k)}$  [ppm];
- $y_{15}$  – carbon monoxide concentration in the crankcase  $C_{CO(s)}$  [ppm];
- $y_{16}$  – hydrocarbon concentration in the outlet exhaust manifold  $C_{HC(k)}$  [ppm];
- $y_{17}$  – hydrocarbon concentration in the crankcase  $C_{HC(s)}$  [ppm];
- $y_{18}$  – nitric oxide concentration in the outlet exhaust manifold  $C_{NOx(k)}$  [ppm];
- $y_{19}$  – nitric oxide concentration in the crankcase  $C_{NOx(s)}$  [ppm];
- $y_{20}$  – oxygen concentration in the exhausts  $C_{O_2}$  [%];
- $y_{21}$  – air-excess coefficient  $\lambda$ .

For this present paper analysis of the input values were limited to seven values ( $y_{14}$ ,  $y_{15}$ ,  $y_{16}$ ,  $y_{17}$ ,  $y_{18}$ ,  $y_{20}$ ,  $y_{21}$ ).

As a result of conducted analysis there double-value fractional plan with possibly highest resolution ( $R = III$ ) and maximal incomplication of interaction of values describing the functional empirical model of fuel feeding system of engine was worked out to realize laboratory artificial tests. Presented in the beginning remarks of general nature and results of analyzed own researches justified linear model [7,11] assumed in the tests of fuel feeding system of engine. Therefore statistic analysis is limited to justification of chosen model, defining approximating polynomials and also characteristic and estimation using possible statistic measures.

As a result of conducted analysis was accepted model considering double-factor interactions, in which the highest values of determination coefficient  $R^2 = 1$  and total of rest  $MS = 0$  characterize all polynomials approximating output values. Values of these measures indicate that the model is according to the theory of experiment the accepted model is most adequate. Considerably lower values of determination coefficient and significant total of rest are characteristic of the model without interactions, and what is more these differences are depend on defined output values.

Graphic confirmation of rightness of decision can be also exceptional diagrams in Fig. 1.

Determined approximating polynomials allow to define any dependences between individual variables and also to calculate and estimate the influence of introduced (simulated) failures (wear) of the elements in fuel injection equipment on the work and toxicity indicators of engine [3,8]. It is assumed that it is possible to define relations (correlations) between the parameters of structure and exhaust toxicity indicators directly or indirectly using the engine operating indicators. It is assumed that this way it would be possible to select diagnostic parameters of defined elements or sets of engine fuel equipment among the exhaust compounds.

### 3. Researches on the fuel feeding system of engine using the multi-equation models

As it was mentioned above, commonly available models which were used to test analysis and based on an analysis of the multiple regression have not given possibility of research in the model of input variable (1) connections [2]. Fundamental feature of the models with correlative equations

is the fact that they allow the existence of feedback between the input variables, which is certainly a real issue.

Below will be presented theoretic basis of the multi-equational models and its practical use on example of the presented in advance plan of experiment.

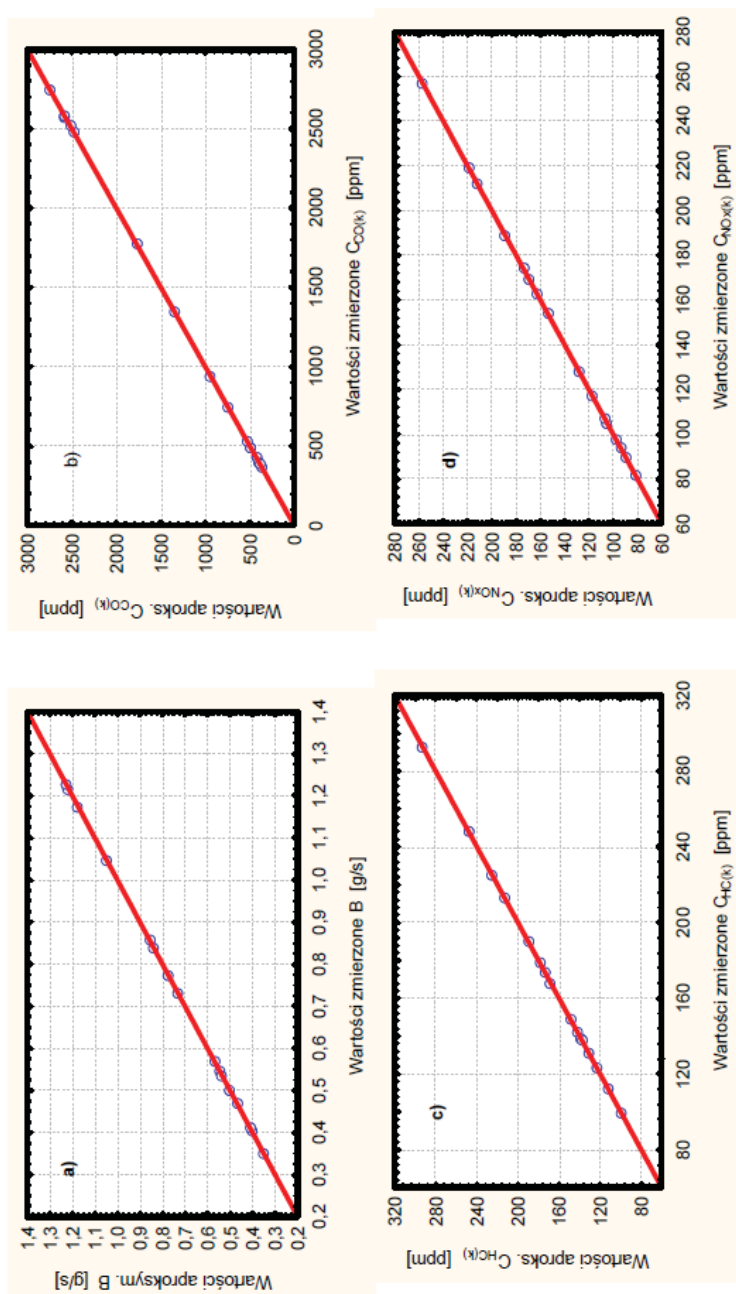


Fig. 1. Dependences between approximated and measured values in the model with interactions fuel consumption, b) concentration of carbon oxides; c) concentration of hydrocarbons; d) concentration of nitric oxides in the outlet exhaust manifold



$x_9$ —power loss of strain of the pulverizer spring  $\Delta p$ .

$$\tilde{\mathbf{Y}} = \begin{bmatrix} \tilde{Y}_{11} & \tilde{Y}_{21} & \cdots & \tilde{Y}_{M1} \\ \tilde{Y}_{12} & \tilde{Y}_{22} & \cdots & \tilde{Y}_{M2} \\ \vdots & \vdots & \vdots & \vdots \\ \tilde{Y}_{1K} & \tilde{Y}_{2K} & \cdots & \tilde{Y}_{MK} \end{bmatrix},$$
 $y_7$  – oxygen concentration in the outlet manifold  $C_{O2k}$ .
$$B^{-1}BY = (B^{-1}AX) + B^{-1}\xi,$$
$$Y = B^{-1}AX + B^{-1}\xi.$$
$$\Pi := B^{-1}A, \quad \eta := B^{-1}\xi \quad (3)$$
$$\mathbf{Y} = \mathbf{I}\mathbf{X} + \boldsymbol{\eta} \quad (4)$$
$$\mathbf{\Pi} = \begin{bmatrix} \pi_{10} & \pi_{11} & \cdots & \pi_{1N} \\ \pi_{20} & \pi_{21} & \cdots & \pi_{2N} \\ \vdots & \vdots & \ddots & \vdots \\ \pi_{M0} & \pi_{M1} & \cdots & \pi_{MN} \end{bmatrix}, \quad \mathbf{\eta} = \begin{bmatrix} \eta_1 \\ \eta_2 \\ \vdots \\ \eta_M \end{bmatrix}.$$
[illegible]
$$J_i(\pi_{i0}, \pi_{i1}, \dots, \pi_{iN}) = \sqrt{\sum_{v=1}^k (\pi_{i0} + \pi_{i1}\tilde{x}_{1v} + \pi_{i2}\tilde{x}_{2v} + \dots + \pi_{iN}\tilde{x}_{Nv} - \tilde{y}_{iv})^2}, \quad i = 1, 2, \dots, M \quad (6)$$
$$\pi_{ji}^0, \quad i=1,2,\dots,M, \quad j=0,1,\dots,N$$

reduced form of model (5) can be defined from the identity

$$\hat{\Pi}^T = (\tilde{X}^T \tilde{X})^{-1} \tilde{X}^T \tilde{Y} \quad (7)$$

where matrix of coefficients is following:

$$\hat{\Pi}^T = \begin{bmatrix} \pi_{10}^0 & \pi_{20}^0 & \cdots & \pi_{M0}^0 \\ \pi_{11}^0 & \pi_{21}^0 & \cdots & \pi_{2M}^0 \\ \vdots & \vdots & \ddots & \vdots \\ \pi_{1N}^0 & \pi_{2N}^0 & \cdots & \pi_{MN}^0 \end{bmatrix},$$

The next step of analysis is defining the matrix of variation and co-variation of estimator  $\Pi$ , examining the confidence range for individual coefficient of multiple regression  $\pi_{ij}$ , which is a coefficient of matrix  $\Pi$ , defining the coefficient of multiply correlation  $R$  [1,5,6].

All of those variables which possibly could have influence on the forming variable value  $Y$  should be considered while constructing the regression model. Not every of these variables are significant in the model. To verify which of input variables have not significant influence on the output variables  $Y$  the relevancy test should be use to every of obtained coefficients of model at individual variables. This test allows to verify the hypothesis that value of regression coefficient is zero. Only after rejecting such hypothesis we can claim that specific variable is significant in the linear regression model. Variables, at which regression coefficients are not significantly different from zero, should be removed from the model and construct model with lower amount of explanatory variables [2].

Final multi-equational model in which all coefficient are significant and it can be used in practice e.g. for diagnostic purposes we obtain only at the second or third stage, what is more at every stage coefficients of multi-equational regression of individual model are estimated, their statistic relevance and removes variables with regression coefficients insignificant from zero [2].

In considered case statistic  $t$  has arrangement  $t - \text{Student}$  at  $K-N-1=20-9-1=10$  freedom stages and relevance indicator  $\alpha = 0,1$ , and read off the schedule table  $t - \text{Student's}$  crucial value  $t_\alpha = 3,169$  [1]. After conducting the series of test it is seems that the criteria are too severe. It was experimentally certify that lower values  $t_\alpha$  significantly approach the model.

After verifying the relevancy of its parameters and rejecting insignificant values as a result, it comes to the considerable simplification of models. The result of analysis is that following dependences occur [11]:

$$\begin{aligned} y_1 &= f(x_1, x_2) \\ y_2 &= f(x_2, x_7) \\ y_3 &= f(x_2, x_8) \\ y_4 &= f(x_2, x_4, x_5, x_6) \\ y_5 &= f(x_2, x_3, x_4, x_5, x_6, x_7) \\ y_6 &= f(x_4, x_5, x_6, x_7) \\ y_7 &= f(x_1, x_2, x_6) \end{aligned}$$

In accordance with (1) an equation  $y_1$  describing change of air-excess  $\lambda$  has form:

$$y_1 = b_{12}y_2 + b_{13}y_3 + b_{14}y_4 + b_{15}y_5 + b_{16}y_6 + b_{17}y_7 + a_{10} + a_{11}x_1 + a_{12}x_2.$$

After reducing (considering relevance of coefficients) the equation was accepted

$$y_1 = b_{12}y_2 + b_{17}y_7 + a_{10} + a_{12}x_2.$$

Differences between the measured parameters and parameters obtained from the multi-equational model  $\tilde{y}_\nu - \hat{y}_\nu$ ,  $\nu \in \overline{1,20}$  are insignificant. It is confirmed by the courses of dispersion compared in the Fig. 2. The result of their analysis is that adjusting obtained model to values obtained in the experiment are significant.

In case of other models the equations of output variable are following:



$$y_2 = b_{21}y_1 + b_{23}y_3 + b_{24}y_4 + b_{25}y_5 + b_{26}y_6 + b_{27}y_7 + a_{20} + a_{21}x_1 + a_{22}x_2$$

$$y_3 = b_{32}y_2 + b_{35}y_5 + b_{37}y_7 + a_{38}x_8$$

$$y_4 = b_{41}y_1 + b_{45}y_5 + b_{47}y_7 + a_{40} + a_{44}x_4 + a_{45}x_5 + a_{46}x_6$$

$$y_5 = b_{52}y_2 + b_{53}y_3 + b_{54}y_4 + b_{57}y_7 + a_{50}$$

$$y_6 = b_{61}y_1 + b_{67}y_7 + a_{60} + a_{64}x_4 + a_{65}x_5 + a_{67}x_7$$

$$y_7 = b_{71}y_1 + b_{72}y_2 + a_{70} + a_{72}x_2$$

Analyzing equations obtained as a result of model equation researches it should be state that:

- in case of first equation i.e. dependence describing changes of air-excess coefficient  $\lambda$ , it depends on the changes of load of torque  $T_{lq}$  and along with them appear changes of carbon oxide concentration in the outlet manifold and changes of nitric oxide concentration. Relation between changes of CO and NO<sub>x</sub> is accurate, because in both case amount of oxygen decides about emission of these compound. In case unsupercharged engine of Increase of load also causes the decrease of amount of fresh load in the cylinder.
- in case of carbon oxide concentration in the outlet manifold  $C_{COk}$  ( $y_2$ ) the equation combines dependence between carbon oxide concentration in the crankcase  $C_{COs}$ , hydrocarbon concentration in the outlet manifold  $C_{HCk}$  and in the crankcase  $C_{HCs}$ , nitric oxide concentration  $C_{NOxk}$ , oxygen concentration  $C_{O2}$  and two input parameters i.e. rotational engine speed  $n$  i and load  $T_{lq}$ . Analyzing values of the coefficients the most significant are coefficient which are responsible for the amount of oxygen in the combustion chamber. The most insignificant is coefficient which forms value of NO<sub>x</sub>.
- carbon oxide concentration in the crankcase  $C_{Cos}$  ( $y_3$ ) is described by the changes of carbon oxide concentration in the outlet manifold  $C_{COk}$ , nitric oxide concentration  $C_{NOxk}$  and input value i.e.: coking pulverizer nozzle  $S_k$ . The greatest influence has variable  $C_{NOxk}$ , and it results from the previous researches, because the linear dependence between emission of  $C_{Cos}$  and  $C_{NOxk}$  is noticeable.
- in case of concentration of hydrocarbons in the outlet manifold  $C_{HCk}$  ( $y_4$ ) the equation combines dependence between air-excess coefficient  $\lambda$ , concentration of hydrocarbon in the crankcase  $C_{HCs}$ , concentration of nitric oxides  $C_{NOxk}$  and input values, i.e. loss of leakproofness in the pumping valve  $S_{zt}$ , wear of the skirt of pulverizer needle  $S_i$  and wear of taper sealing part of pulverizer needle in the injector setting  $S_r$ . The most significant is air-excess coefficient  $\lambda$ . Also significant is variable  $C_{NOxk}$  though it has opposite direction to  $\lambda$ . At the similar level of impact remains input variable  $S_i$ , i.e. wear of the skirt of pulverizer needle.
- concentration of hydrocarbons in the crankcase  $C_{HCs}$  ( $y_5$ ) is described by the output variables, first of all concentration of hydrocarbons in the outlet manifold  $C_{HCk}$ , which as it was known from the previous researches changes in proportion to concentration of  $C_{HCs}$ , at similar level of impact remain  $C_{COk}$  and  $C_{NOxk}$ , although they are inversely proportional to  $C_{NOxk}$ .
- changes of concentration of nitric oxides  $C_{NOxk}$  ( $y_6$ ) describes first of all the dependence of air-excess coefficient  $\lambda$ , i.e. factor which is directly responsible for forming the nitric oxides. At the lower level is variable  $C_{O2}$ . Changes of concentration of nitric oxides  $C_{NOxk}$  are also described by input variable  $S_i$ , i.e. wear of the skirt of pulverizer needle.
- changes of oxygen concentration in the outlet manifold  $C_{O2}$  ( $y_7$ ) are described, similarly to the changes of  $\lambda$  from the first equation, first of all air-excess coefficient, from the first equation first of all air-excess coefficient, oppositely correlated nitric oxide concentration in the outlet manifold  $C_{COk}$ . Similarly correlated is also input variable which comes from engine load by torque  $T_{lq}$ .

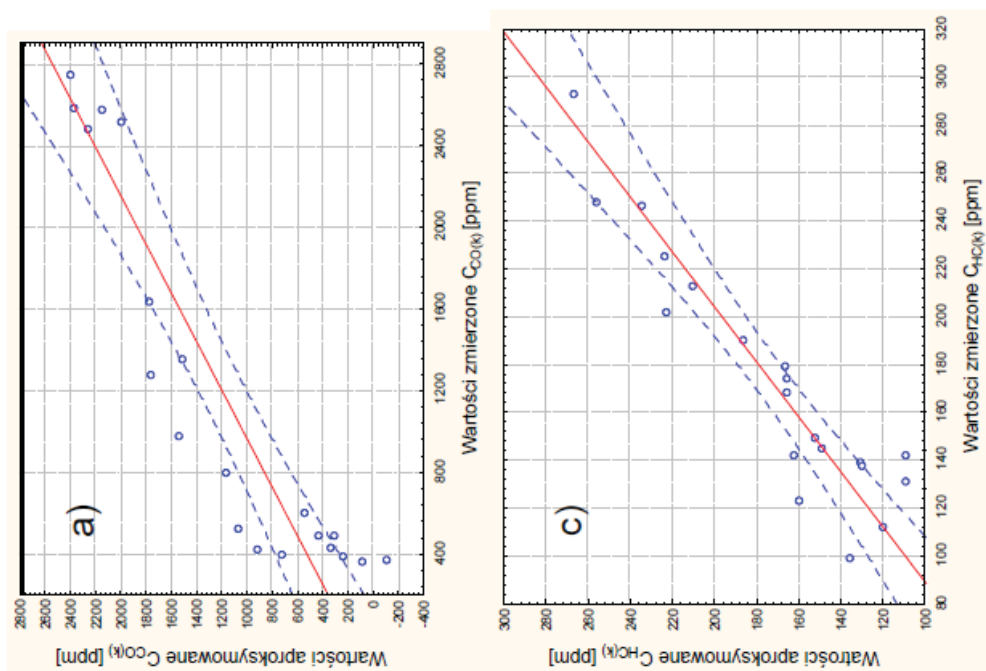


Fig. 2. Dependences between the approximated and measured values in the multi-equational model  
a) concentration of carbon monoxide in the manifold; b) concentration of carbon monoxide in the crankcase; c)  
concentration of hydrocarbons in the manifold; d) concentration of hydrocarbon in the crankcase

#### 4. Conclusions

Presented description of the active experiment space by the multidimensional models gives great possibilities in analysis of measurement data and scientific conclusions. Furthermore, assuming that coefficients' matrix  $\Pi^T$  is orthogonal, there is a possibility of fulfilling reverse task, that is assessing, with complex relevance at known input variables, which describe work point i.e. engine rotational speed  $n$  and torque load  $T_{iq}$ , the other input values. In the nearest future authors will work on this issue.

#### References

- [1] Koško M., Osińska M., Stępińska J., *Ekometria współczesna*, TONiK, Toruń 2007.
- [2] Kukiłka L., *Podstawy badań inżynierskich*, Wydawnictwo Naukowe PWN, Warszawa 2002.
- [3] Moore D.S., *Analiza statystyczna danych doświadczalnych*, Wydawnictwa Naukowo-Techniczne, Warszawa 1983.
- [4] Osiński Z., Wróbel J., *Teoria konstrukcji maszyn*, PWN, Warszawa 1982.
- [5] Pająk E., Wieczorowski K., *Podstawy optymalizacji operacji technologicznych w przykładach*, PWN, Warszawa – Poznań 1982.
- [6] Piaseczny L. i inni, *Metody ograniczenia emisji związków toksycznych tłokowych silników spalinowych eksploatowanych w silowniach okrętowych*, Sprawozdanie z projektu badawczego nr T12D 006 13, AMW, Gdynia 2000.
- [7] Polański Z., *Planowanie doświadczeń w technice*, PWN, Warszawa 1984.
- [8] Robertson J., Robertson S., *Pełna analiza systemowa*, Wydawnictwa Naukowo-Techniczne, Warszawa 1999.
- [9] Sienkiewicz P., *Analiza systemowa – podstawy i zastosowania*, Wydawnictwo Bellona 1994.
- [10] Zadrąg R. i inni, *Modele identyfikacji stanu technicznego silnika na podstawie oceny emisji składników spalin*, Sprawozdanie z projektu badawczego nr 4T12D 055 29, AMW, Gdynia 2008.



## CONSTITUTION OF USEFUL PROPERTY OF COMPOSITE MATERIALS

Joachim Zimniak

*University of Technology and Agriculture  
Faculty of Mechanical Engineering  
tel.: +48 52 340 87 21, fax.: +48 52 340 82 45  
ul. Prof. S. Kaliskiego 7, 85 – 763 Bydgoszcz, Poland  
e-mail: zimniak@utp.edu.pl*

### **Abstract**

*In the thesis some problems concerning fabrication of composites based on present knowledge and author's own experience have been revealed. The methods of fabrication of the composites take into consideration following operations like size-reduction, agglomeration and compounding (mixing components) in solid (grainy) state to obtain the composite of determined properties assigned for processing operations like injection moulding, extrusion or press moulding.*

**Keywords:** grainy materials, rubber powder, mixing, composites

### **1. Introduction**

Production of materials from polymer about required properties joins mostly with selection of suitable polymer materials (more and more often of composite materials – obtained from waste material “thermoplastic materials” and waste material “rubber”) also selection of proper methods of processing [1-5]. Processing of composite materials will demand complex interlocking in technological process of each composition process [4-6]. The principle problem from scientific point of view and utilitarian are prospecting of conditions connected with constitution required proprieties of composite materials also qualification of conditions processing these composites in aspect their uses in practice [7-9].

### **2. Aim of this paper**

Aim of this work is present idea permitting on qualification of conditions constitution of composite materials in technological process, aim of receipt of products from materials about given properties and definite qualities. One accepted argument, that exists one profitable harvest of composition process constituting properties needs will be this injection, extrusion or pressing) of composite materials (produced from waste material “foil” and rubbers) and that are special manners of their realization (for example characteristic conditions of process agglomerating-plant of foil, of crumbling for rubbers and mixing) which proper selection will be decide about qualities

of products received from these materials. Basing on the literature study, preliminary research in industry [10,11] and a long-term international co-operation [6,12-14] and especially with the Technical University of Chemnitz/Germany, composition processes were developed (see Table 1). These are:

- Process of crumbling of input – materials (connected from them such problems how obtainment reproducible of fraction, estimation of size and of shape and of external surface of elementary grains),
- Process of mixing of input – materials (in solid state constants - about figure of grains) and of additional components (often also about grainy figure) and estimation of degree level of mixed composite materials with methods direct or indirect,
- Process of processing principle obtained of composite materials (in dependences from needs will be this injection, extrusion or pressing).

In Table 1 (column 1) one seized in synthetic manner these composition process, which in essential manner can influence on proprieties of useful composite materials. From table results, that condition rational elaborations in wanted solutions is nearer recognition replaced of composition process, which qualitatively would qualify influence select factors constructional-technological (appointed in column 3 embracing for example kind, dimensions of material crumbled and mixed), described by functions of object of researches, on physical sizes qualifying effectivity suitable composition process (appointed in table 1 in column 2, as measure). Will demand this so uses and leadership proper researches methods.

*Tab.1. Summary composition of composition process constituting properties of composite materials [4,6,7,9,13,14]*

Name of composition process		Measure qualifying effectivity of composition process	Technological-constructional factors essential for composition process
1		2	3
A Agglomerating-plant	OB I	torque $M_o$ , force of cut: $F_c$	$M_o, F_c = f(a_1, a_2, \dots, a_n)$
B Crumbling	OB II	torque $M_o$ , force of cut: $F_c$	$M_o, F_c = f(a_1, a, \dots, a_n)$
C Mixing	OB III	power $N$ , time $t_m$ , level of mixed $M_m$	$N, t_m, M_m = f(b_1, b_2, \dots, b_n)$
D Process of processing (pressing, injection, extrusion)	OB IV	pressure $p_p$ , time $t_p$ of pressing	$p_p, t_p = f(c_1, c_2, \dots, c_n)$
E Verification of researches	OB V	Tensile strength $R_m$ , level of mixed. $M_m$	$R_m, M_m = f(V_1, \varphi V_n, \dots, \varphi_n)$
F Other	OB N	.....	$\Psi, \Phi = f(x_1, x_2, \dots, x_n)$

### 3. Experimental part

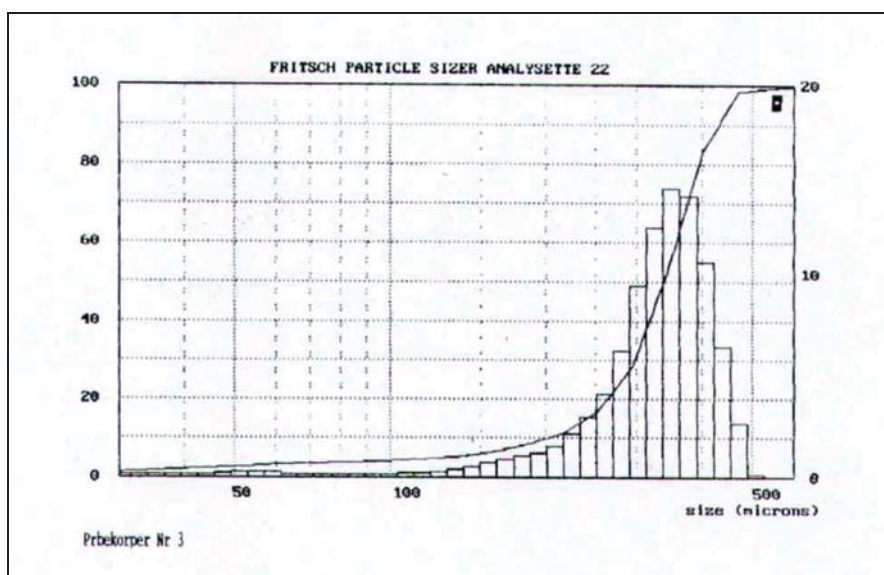
To reach founded aim of work one passed research laboratory basing on program of researches, using following materials

- from recycling (agglomerate) polythene (PE-LD) about grain class equal 1.0 mm:

- crumbled waste material rubber (about nearing proprieties to practical Tyres of vehicles of rubber type SBR) about grain classes given below.

On suitable position research [12, 14], one crumbled waste material of rubber, with aim of obtainment of suitable grain classes. In result passed strainer analyses in (accordance to PN-71/C-04501) one obtained rubber powder about following grain classes: 0.2; 0.4; 0.6 and 0.8 mm. On Fig. 1 one showed of for example distribution curve grain for different classes grain rubbers. btained fractions of rubber powder one added (in masses) according to material from recycling in following quantities: 5, 10, 15, 20 and 25%.

a)



b)

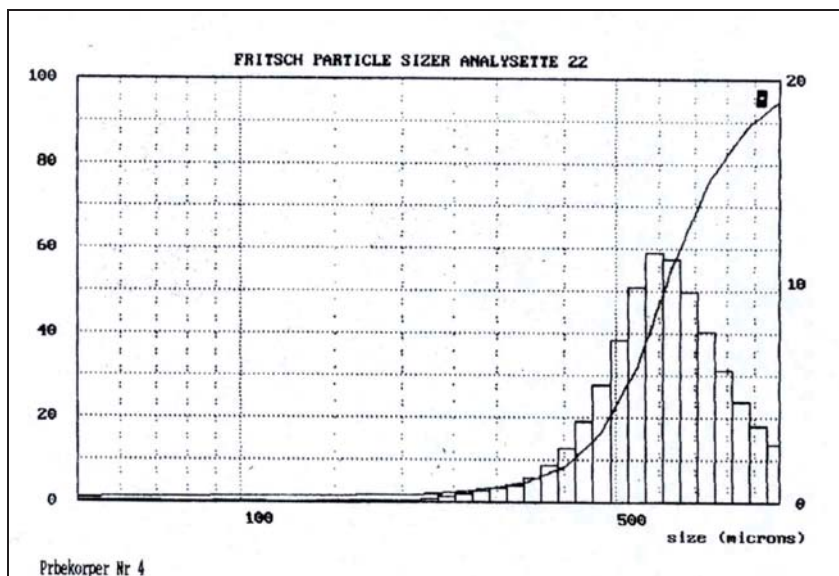


Fig. 1. Example- distribution curve for grain classes 0.4 (and) and 0.6 mm( b)



Process mixings of components in state solid and estimation of quality of process mixing one realized according to provided for procedures in description of position research [13, 14], with utilization of computer programmer COREL PHOTO-PAINT. Received samples at random according to literature [9], one subjected to estimation of degree confusions( with immediate method) showed proprieties of mixture nearing two component to homogeneous [10,11]. From replaced received at random samples composite one executed with method of injection and of pressing pressure – according to C (tab. 1) samples about standardized shapes and dimensions to researches strength with aim of verification of mechanical propriety according to D (tab. 1). Results of researches of influence suitable grain classes (0.2; 0.4; 0.6; 0.8) and contents of rubber powder V[%] in recycling PE-LD on endurance on extension one represented graphically on Fig. 2 and 3.

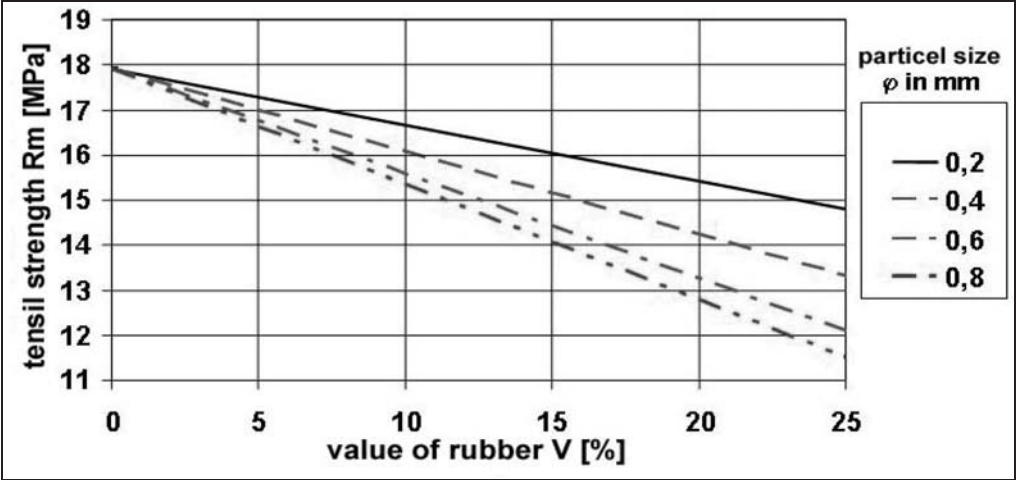


Fig. 2. Influence contents of rubber powder V[%] and sizes of grains(  $\phi = 0.2$ ; 0.4; 0.6 and 0.8 mm) on endurance on extension  $R_m$  [MPa] – for pressing

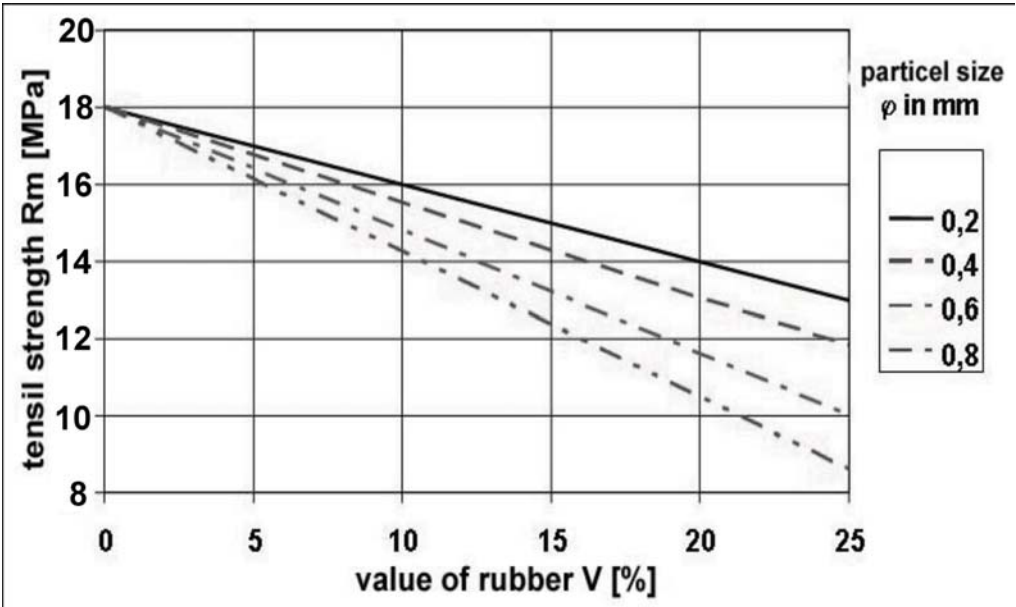
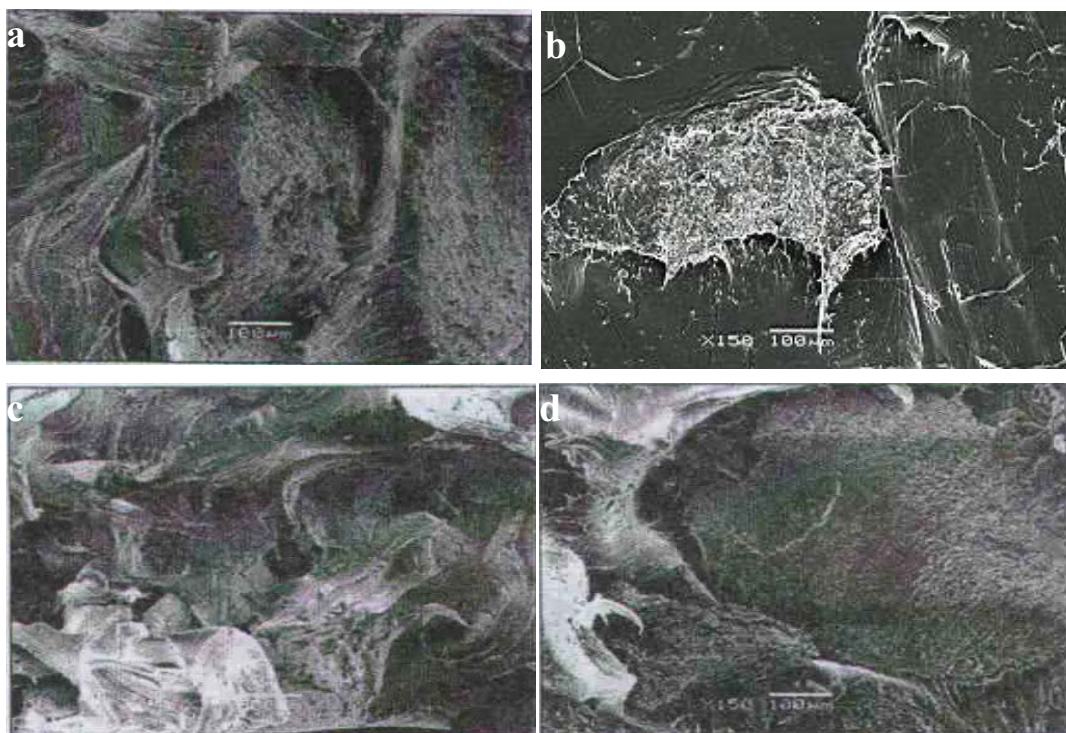


Fig. 3. Influence contents of rubber powder V[%] and sizes of grains( $\phi = 0.2$ ; 0.4; 0.6 and 0.8 mm) on endurance on extension  $R_m$  [MPa] – for injections



Analysing nearer courses of each function one can notice, that essential influence on research feature in section from 0 to 25% has manner of preparation of samples, of melting's of crumbling and content of powder in recycling. prepared Samples by pressing show considerably higher values than injected. However fall of strength is not similar- identical for all of grain classes. Interesting is that least fall one can notice for composite in all section of content powder rubber for grain classes equal 0.2 mm.

This will create possibility of minimalizing fall of strength by using of rubber powder about dimensions below 0.1 mm. Use in future researches and uses of rubber powder on level sub-micro( $10^{-6}$ ) or most profitably on level nana( $10^{-9}$ ) will permit probably to obtain composite about unparalleled to this times proprieties chemical-physics [2,6-10]. As goes for fall of tensile strength for remaining grain classes (composite with participation of powder about dimensions 0.4; 0.6 and 0.8 mm) this is more considerable to greater in content. On all observed microstructure, in this also for example shown on Fig. 4 one can notice comparatively little adhesion among warp (PE-LD) and with interpolations (grains of rubber) - refers this especially microstructure shown on fig. 4c and of fig. 4d.



*Fig. 4. Microstructure turns of samples about different contents and to class grain rubber powder: And – 10% of rubber powder about class 0.4 mm, b- 20% and 0.4 mm, c – 10% and 0.8, d – 20% and 0.8 mm*

This observation will demand of however further researches especially in range of measurement of adhesion on border: polymer material – grain of powder. Research should be so realized with regard of wider section of classes grain and greater contents of rubber powder

#### 4. Conclusions

There were no procedures to analyze the fabrication of composites made of thermoplastic film wastes and rubber wastes in connection with properties of components in solid (grainy) state

before compounding and press moulding by now. Because of specific basic operations the tests were carried out on special test stands using phenomenological methods. The results have enabled determination of the most advantageous directions for designing technological lines within the range of utilization of selected plastics and rubber wastes. The results might also be used for designing other constructional-technological solutions which would concern fabrication of composites based on other secondary polymeric materials.

## References

- [1] Sikora, R., *Przetwórstwo tworzyw wielkocząsteczkowych*. Wydawnictwo Edukacyjne, Warszawa, 1997.
- [2] Błędzki, A., *Recykling materiałów polimerowych*. WNT, Warszawa 1997.
- [3] Brandrup, J., *The economic and Ecological aspects of Reprocessing of Plastics Wastes*. Polimery 1997, 42, nr 11-12. pp. 645-650.
- [4] Brandrup, J., Bittner, M., Michaeli, W., Menges, G., *Die Wiederverwertung von Kunststoffen*. Carl Hanser Verlag, München Wien 1995, pp. 22-26, and pp. 363-373.
- [5] Feller, W.: *An introduction to probability theory and its applications*. Vol. I, second edition. New York, London 1961.
- [6] Gawęł, I., Ślusarski, L., *Reutilisation of spent tyre scrap Rubber for modification of Asphalt*. Polimery 43, nr 5 1998, pp. 280-285.
- [7] Mennig, G., Michael, H., Rzymiski W., Scholz H.: *Polimery* 1997, **38**, pp. 234 – 236.
- [8] Michael, H., Scholz H., Mennig, G.: *Kautschuk Gummi Kunststoffe*, 1999, **28**, pp. 510-513
- [9] Pahl, M.H., Sommer K.: *Mischen von Kunststoffen und Kautschukprodukte*. VDI, Düsseldorf 1993.
- [10] Jurkowska, B., Jurkowski, B., *Sporządzanie kompozycji polimerowych. Elementy teorii i praktyki*. WNT, Warszawa 1997.
- [11] Boss, J., *Moc, czas mieszania materiałów ziarnistych*. Wyd. WSI Opole, 1991 *Studia i Monografie*, **z. 39**.
- [12] Flizikowski, J., *Rozdrabnianie tworzyw sztucznych*. Wydawnictwa ATR, Bydgoszcz 1998.
- [13] Zimniak, J., Michael, H. *Zeszyty Naukowe* nr 233, Wyd. ATR w Bydgoszczy, *Mechanika* **z. 50**, Bydgoszcz 2001. pp. 329 – 337.
- [14] Zimniak, J.: *Analyse von Grundprozessen der Aufbereitung von Kompositwerkstoffen aus ausgewählten Kunststoff- und Gummiabfällen*. Habilitationsarbeit, Technische Universität Chemnitz'04. <http://archiv.tu-chemnitz.de/pub/2004/0177>.



## METHODS OF ESTIMATING THE AVAILABILITY OF VEHICLES

Jarosław Ziółkowski

Wojskowa Akademia Techniczna  
ul. Kaliskiego, 00-908 Warszawa, Poland  
tel.: +48 22 6837109, fax: +48 22 6837382  
e-mail: jziolkowski@wat.edu.pl

### Abstract

The article presents methods of estimating the availability of vehicles supported by numerical examples. All the cases concern the vehicles used in air base logistic system. Markov chains and processes have been used to work out the mathematical model of their usage.

**Key words:** availability, usage, service

### 1. Introduction

The mathematical model has been built on the basis of analyzing states collection for vehicles used in air base logistic system. Each of the technical objects can be at certain time  $t$  in one of extinguished states, which make numerable (finite) set of states. The usage is understood as the movement of the vehicle on the extinguished states collection.

The model of vehicle usage as a random process  $X(t)$  with finite set of states.  $X(t) = S_i$  means that in time  $t$  the analyzed vehicle is in a state  $S_i$ . The realization of the process is meant as a sequence of extinguished states and their durations. The sequence, their durations and frequency are dependent first of all on work organization, the types of vehicles, the structure of subsystems collaborating in usage process [7].

### 2. The description of usage states for vehicles

Used vehicles can be in different states whose number is limited. Three models of emergency vehicles in air bases A, B and C of different states collection have been analyzed. Model A (Fig.1) does not include the system of vehicle restoration meant as the replacement of used vehicle with the new one (in working order).

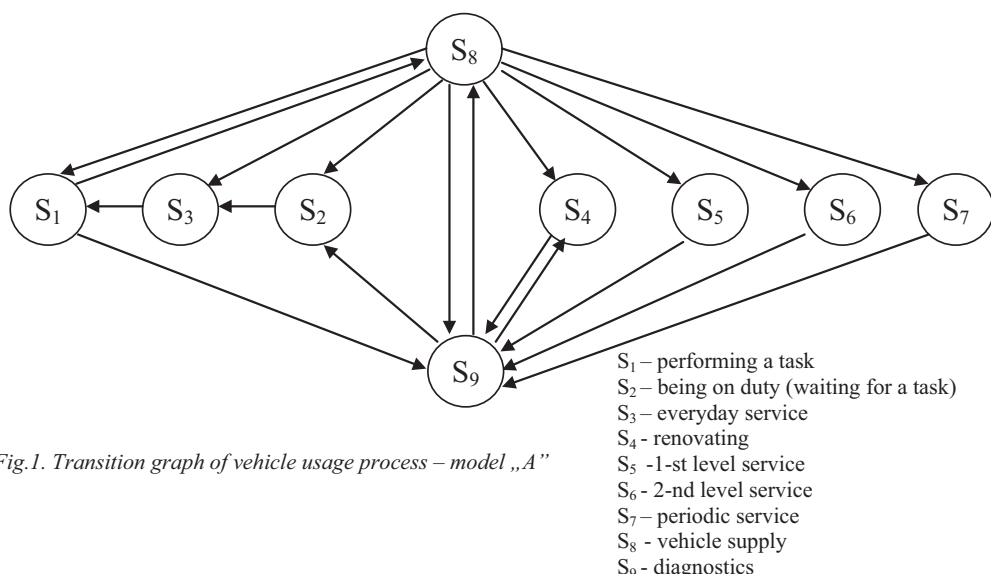


Fig.1. Transition graph of vehicle usage process – model „A”

Unknown theoretical probabilities of transition are estimated by empirical probabilities in a year time – transition frequencies for a vehicles as:

$$\omega_{ij} = n_{ij} / n_i \quad (1)$$

where:

$n_i = \sum_j n_{ij}$  - the number of transitions from  $S_i$  state;

$n_{ij}$  – the numbers of transitions from state  $i$  to  $j$  in a period of time.

Stochastic process  $X(t)$  in a continuous time is ergodic, if at least one positive boundary probability of finding a vehicle in state  $S_j$  for  $t \rightarrow \infty$  exist, which is called ergodic probability  $p_j$ :

$$p_j = \lim_{t \rightarrow \infty} P(X(t \in <t, t + \Delta t>) = S_j); \quad p_j \geq 0; \quad \sum_j p_j = 1 \quad (2)$$

where:

$p_j$  – boundary probabilities;

$P(X(t \in <t, t + \Delta t>) = S_j)$  - the probability of being in state  $j$  in time interval  $<t, t + \Delta t>$  for a vehicle.

Boundary (ergodic) probabilities fulfil standardizing conditions which means that at least one of them is positive. In relation to Markov processes it was proved [1, 2, 3] that if boundary probabilities exist, they can be calculated from boundary matrix in  $n$  steps  $M_n = M_1^n$ . In other words the linear equation or equivalent matrix equation must be solved, i.e. coming from continuous time  $t$  to discrete time  $n$  being of number of further experiment of observing the vehicle in time  $\Delta t$ :

$$\bigwedge_j p_j = \lim_{n \rightarrow \infty} p_{ij}(n) = \sum_i p_i p_{ij} \Leftrightarrow M_1^T [p_j] = [p_j], \text{ przy } \sum_j p_j = 1 \quad (3)$$

where:

$M_1^T$  - transposed transition matrix  $M_1$ ;

$[p_i]$  – vector of ergodic probabilities;

$p_{ij}$  – probability of transition from state  $i$  to state  $j$ .

Giving consideration to a condition:  $M^T \cdot [p_j] = [p_j]$ , and  $\sum_j p_j = 1$ , for A model

boundary probabilities must be calculated by doing the following systems of equations shown in this matrix form:

$$\begin{bmatrix} 0 & 0 & p_{31} & 0 & 0 & 0 & 0 & p_{81} & 0 \\ 0 & 0 & 0 & 0 & 0 & 0 & 0 & p_{82} & p_{92} \\ 0 & p_{23} & 0 & 0 & 0 & 0 & 0 & p_{83} & 0 \\ 0 & 0 & 0 & 0 & 0 & 0 & 0 & p_{84} & p_{94} \\ 0 & 0 & 0 & 0 & 0 & 0 & 0 & p_{85} & 0 \\ 0 & 0 & 0 & 0 & 0 & 0 & 0 & p_{86} & 0 \\ 0 & 0 & 0 & 0 & 0 & 0 & 0 & p_{87} & p_{79} \\ p_{18} & 0 & 0 & 0 & 0 & 0 & 0 & 0 & p_{98} \\ p_{19} & 0 & 0 & p_{49} & p_{59} & p_{69} & p_{79} & p_{89} & 0 \end{bmatrix} \cdot \begin{bmatrix} p_1 \\ p_2 \\ p_3 \\ p_4 \\ p_5 \\ p_6 \\ p_7 \\ p_8 \\ p_9 \end{bmatrix} = \begin{bmatrix} p_1 \\ p_2 \\ p_3 \\ p_4 \\ p_5 \\ p_6 \\ p_7 \\ p_8 \\ p_9 \end{bmatrix} \quad (4)$$

$$\sum_{j=1}^9 p_j = 1 \quad (5)$$

Model B of a vehicle maintenance description additionally takes into account the replacement state  $S_{10}$  (Fig.2), which is the reflection state with the same probability transitions  $S_{10}$  ( $p_{910} = p_{109}$ ) and zero  $p_{1010}=0$ .

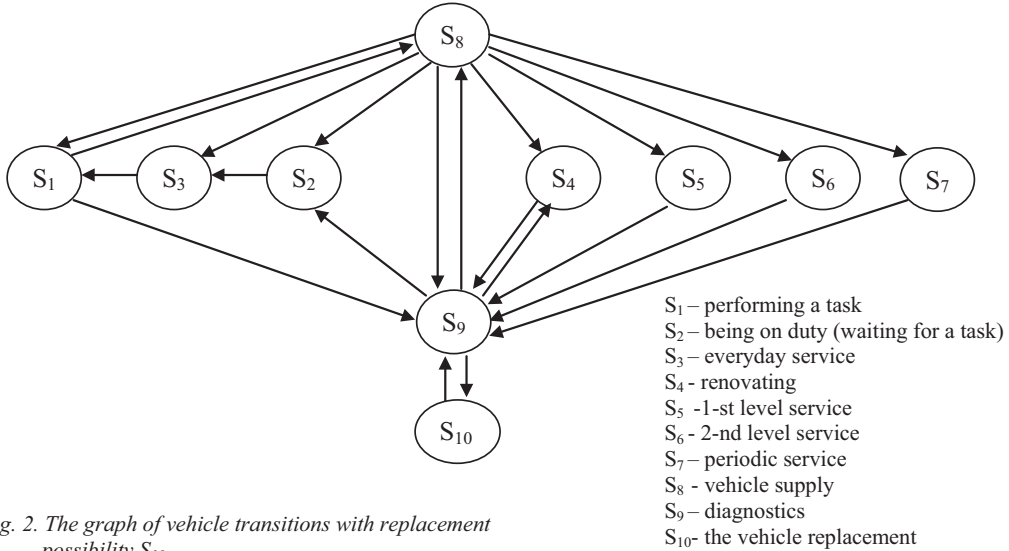


Fig. 2. The graph of vehicle transitions with replacement possibility  $S_{10}$

Also for B model the following systems of equations for ergodic probabilities  $p_j$  have been estimated:

$$\begin{bmatrix}
 0 & 0 & 0 & 0 & 0 & 0 & 0 & p_{18} & p_{19} & 0 \\
 0 & 0 & p_{23} & 0 & 0 & 0 & 0 & 0 & 0 & 0 \\
 p_{31} & 0 & 0 & 0 & 0 & 0 & 0 & 0 & 0 & 0 \\
 0 & 0 & 0 & 0 & 0 & 0 & 0 & 0 & p_{49} & 0 \\
 0 & 0 & 0 & 0 & 0 & 0 & 0 & 0 & p_{59} & 0 \\
 0 & 0 & 0 & 0 & 0 & 0 & 0 & 0 & p_{69} & 0 \\
 0 & 0 & 0 & 0 & 0 & 0 & 0 & 0 & p_{79} & 0 \\
 p_{81} & p_{82} & p_{83} & p_{84} & p_{85} & p_{86} & p_{87} & 0 & p_{89} & 0 \\
 0 & p_{92} & 0 & p_{94} & 0 & 0 & 0 & p_{98} & 0 & p_{910} \\
 0 & 0 & 0 & 0 & 0 & 0 & 0 & 0 & p_{109} & 0
 \end{bmatrix}
 \begin{bmatrix}
 p_1 \\ p_2 \\ p_3 \\ p_4 \\ p_5 \\ p_6 \\ p_7 \\ p_8 \\ p_9 \\ p_{10}
 \end{bmatrix}
 =
 \begin{bmatrix}
 p_1 \\ p_2 \\ p_3 \\ p_4 \\ p_5 \\ p_6 \\ p_7 \\ p_8 \\ p_9 \\ p_{10}
 \end{bmatrix} \quad (6)$$

$$\sum_{j=1}^{10} p_j = 1 \quad (7)$$

In model C undetermined (universal) state  $S_{11}$ , (Fig. 3) has been taken into account. It separates the states from  $S_1$  to  $S_{10}$  and has zero probability of return ( $p_{11,11}=0$ ;  $p_{11,j} \geq 0$ ;  $p_{i,11} \geq 0$  for  $i, j \neq 11$ ).  $S_{11}$  state is meant as time losses of a vehicle being of each of the remaining states resulting from organizational reasons (technical etc.). in a real time  $S_{11}$  is parallel, but in the graph it has a terraced character.

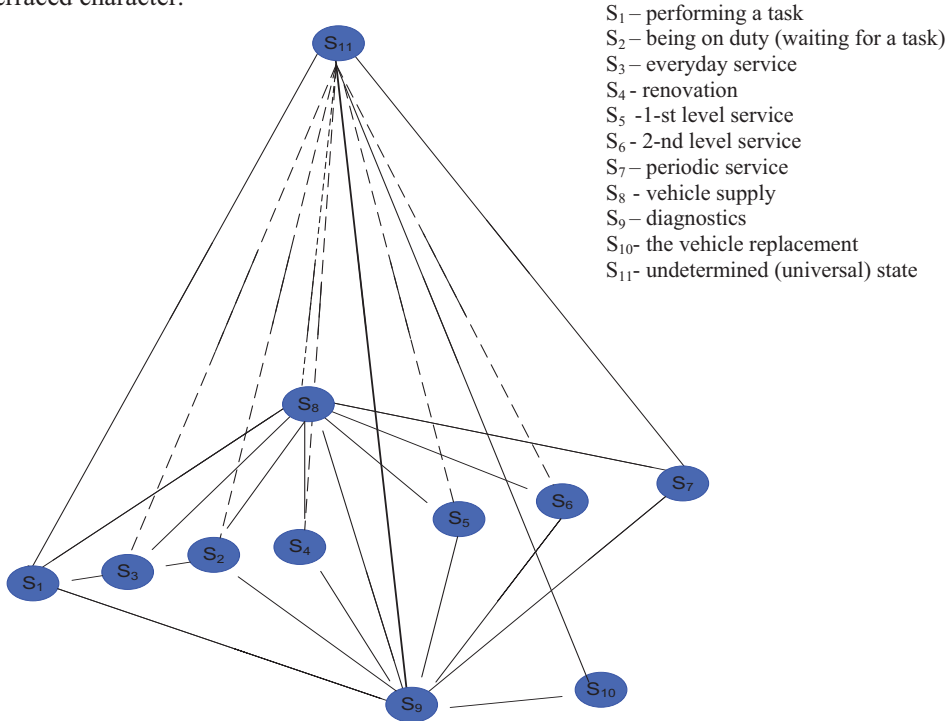


Fig.3. The graph of vehicle transitions. The vehicle renovation and replacement SA well as finite times of transition between states are covered

Ergodic probabilities  $p_j$  can be calculated in accordance with (3). Suitable systems of equations for C model have been written in matrix form:

$$\begin{bmatrix}
0 & 0 & 0 & 0 & 0 & 0 & 0 & p_{18} & p_{19} & 0 & p_{1,11} \\
0 & 0 & p_{23} & 0 & 0 & 0 & 0 & 0 & 0 & 0 & p_{2,11} \\
p_{31} & 0 & 0 & 0 & 0 & 0 & 0 & 0 & 0 & 0 & p_{3,11} \\
0 & 0 & 0 & 0 & 0 & 0 & 0 & 0 & p_{49} & 0 & p_{4,11} \\
0 & 0 & 0 & 0 & 0 & 0 & 0 & 0 & p_{59} & 0 & p_{5,11} \\
0 & 0 & 0 & 0 & 0 & 0 & 0 & 0 & p_{69} & 0 & p_{6,11} \\
0 & 0 & 0 & 0 & 0 & 0 & 0 & 0 & p_{79} & 0 & p_{7,11} \\
p_{81} & p_{82} & p_{83} & p_{84} & p_{85} & p_{86} & p_{87} & 0 & p_{89} & 0 & p_{8,11} \\
0 & p_{92} & 0 & p_{94} & 0 & 0 & 0 & p_{98} & 0 & p_{9,10} & p_{9,11} \\
0 & 0 & 0 & 0 & 0 & 0 & 0 & 0 & p_{10,9} & 0 & p_{10,11} \\
p_{11,1} & p_{11,2} & p_{11,3} & p_{11,4} & p_{11,5} & p_{11,6} & p_{11,7} & p_{11,8} & p_{11,9} & p_{11,10} & 0
\end{bmatrix} \cdot \begin{bmatrix} p_1 \\ p_2 \\ p_3 \\ p_4 \\ p_5 \\ p_6 \\ p_7 \\ p_8 \\ p_9 \\ p_{10} \\ p_{11} \end{bmatrix} = 0 \quad (8)$$

$$\sum_{j=1}^{11} p_j = 1 \quad (9)$$

After having solved the system of equations (8) i (9), taking into account the empiric probabilities for presented models A, B and C in discrete time the following results have been achieved (Fig. 4):

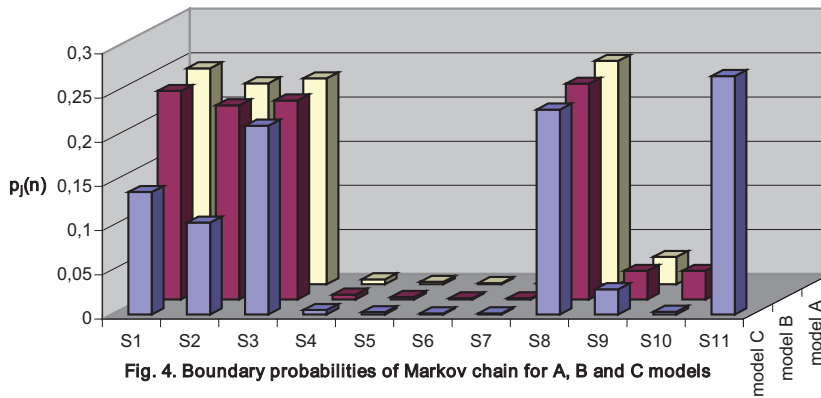


Fig. 4. Boundary probabilities of Markov chain for A, B and C models

Ergodic probabilities  $p_j(t=n)$  for  $S_j$  state estimated from Markovs chains are the probabilities of input for each state. For example probability of duty  $p_3=0,23$  means that the limit of duty state number is 23% of all vehicles states number in a considered period of time. It does not mean that the vehicle was on duty in 23% in average in  $T_o$ . However probabilities  $p_j(n)$  for Markov chains are ergodic and applicable to state collection process but not a physical time. Therefore they cannot be interpreted in a real time. Only after the standardizing of the transition



matrix, which means taking into account the duration time for each states (transitions from discrete times to real one by means of transition intensity  $\lambda_{ij}$  ) achieved results will show the real situation of vehicle usage.

### 3. A method to determine functional availability of vehicles

To estimate ergodic probabilities for continuous time in compliance of Markov processes matrix equations are fulfilled [2]:

$$(\Lambda^T)[p_j] = 0 \quad (10)$$

and

$$\sum_j p_j = 1 \quad (11)$$

where:

$\Lambda=[\lambda_{ij}]$  – intensity matrix with diagonal elements  $-\lambda_{ii}$  and  $\lambda_{ij}$ .

For A model the ergodic probabilities satisfy the equation system with its standardization condition (12):

$$\begin{bmatrix} -\lambda_{11} & 0 & \lambda_{31} & 0 & 0 & 0 & 0 & \lambda_{81} & 0 \\ 0 & -\lambda_{22} & 0 & 0 & 0 & 0 & 0 & \lambda_{82} & \lambda_{92} \\ 0 & \lambda_{23} & -\lambda_{33} & 0 & 0 & 0 & 0 & \lambda_{83} & 0 \\ 0 & 0 & 0 & -\lambda_{44} & 0 & 0 & 0 & \lambda_{84} & \lambda_{94} \\ 0 & 0 & 0 & 0 & -\lambda_{55} & 0 & 0 & \lambda_{85} & 0 \\ 0 & 0 & 0 & 0 & 0 & -\lambda_{66} & 0 & \lambda_{86} & 0 \\ 0 & 0 & 0 & 0 & 0 & 0 & -\lambda_{77} & \lambda_{87} & 0 \\ \lambda_{18} & 0 & 0 & 0 & 0 & 0 & 0 & -\lambda_{88} & \lambda_{98} \\ \lambda_{19} & 0 & 0 & \lambda_{49} & \lambda_{59} & \lambda_{69} & \lambda_{79} & \lambda_{89} & -\lambda_{99} \end{bmatrix} \cdot \begin{bmatrix} p_1 \\ p_2 \\ p_3 \\ p_4 \\ p_5 \\ p_6 \\ p_7 \\ p_8 \\ p_9 \end{bmatrix} = 0$$

$$\sum_{j=1}^9 p_j = 1 \quad (12)$$

For B model the ergodic probabilities satisfy the equation system with its standardization condition (13):

$$\begin{bmatrix}
-\lambda_{11} & 0 & \lambda_{31} & 0 & 0 & 0 & 0 & \lambda_{81} & 0 & 0 \\
0 & -\lambda_{22} & 0 & 0 & 0 & 0 & 0 & \lambda_{82} & \lambda_{92} & 0 \\
0 & \lambda_{23} & -\lambda_{33} & 0 & 0 & 0 & 0 & \lambda_{83} & 0 & 0 \\
0 & 0 & 0 & -\lambda_{44} & 0 & 0 & 0 & \lambda_{84} & \lambda_{94} & 0 \\
0 & 0 & 0 & 0 & -\lambda_{55} & 0 & 0 & \lambda_{85} & 0 & 0 \\
0 & 0 & 0 & 0 & 0 & -\lambda_{66} & 0 & \lambda_{86} & 0 & 0 \\
0 & 0 & 0 & 0 & 0 & 0 & -\lambda_{77} & \lambda_{87} & 0 & 0 \\
\lambda_{18} & 0 & 0 & 0 & 0 & 0 & 0 & -\lambda_{88} & \lambda_{98} & 0 \\
\lambda_{19} & 0 & 0 & \lambda_{49} & \lambda_{59} & \lambda_{69} & \lambda_{79} & \lambda_{89} & -\lambda_{99} & \lambda_{109} \\
0 & 0 & 0 & 0 & 0 & 0 & 0 & 0 & \lambda_{910} & -\lambda_{1010}
\end{bmatrix}
\begin{bmatrix}
p_1 \\ p_2 \\ p_3 \\ p_4 \\ p_5 \\ p_6 \\ p_7 \\ p_8 \\ p_9 \\ p_{10}
\end{bmatrix} = 0$$

$$\sum_{j=1}^{10} p_j = 1 \quad (13)$$

Also for C model equation systems in matrix form with standardized condition are fulfilled (14):

$$\begin{bmatrix}
-\lambda_{11} & 0 & \lambda_{31} & 0 & 0 & 0 & 0 & \lambda_{81} & 0 & 0 & \lambda_{1,11} \\
0 & -\lambda_{22} & 0 & 0 & 0 & 0 & 0 & \lambda_{82} & \lambda_{92} & 0 & 0 \\
0 & \lambda_{23} & -\lambda_{33} & 0 & 0 & 0 & 0 & \lambda_{83} & 0 & 0 & \lambda_{3,11} \\
0 & 0 & 0 & -\lambda_{44} & 0 & 0 & 0 & \lambda_{84} & \lambda_{94} & 0 & \lambda_{4,11} \\
0 & 0 & 0 & 0 & -\lambda_{55} & 0 & 0 & \lambda_{85} & 0 & 0 & \lambda_{5,11} \\
0 & 0 & 0 & 0 & 0 & -\lambda_{66} & 0 & \lambda_{86} & 0 & 0 & \lambda_{6,11} \\
0 & 0 & 0 & 0 & 0 & 0 & -\lambda_{77} & \lambda_{87} & 0 & 0 & \lambda_{7,11} \\
\lambda_{18} & 0 & 0 & 0 & 0 & 0 & 0 & -\lambda_{88} & \lambda_{98} & 0 & \lambda_{8,11} \\
\lambda_{19} & 0 & 0 & \lambda_{49} & \lambda_{59} & \lambda_{69} & \lambda_{79} & \lambda_{89} & -\lambda_{99} & \lambda_{10,9} & \lambda_{9,11} \\
0 & 0 & 0 & 0 & 0 & 0 & 0 & 0 & \lambda_{9,10} & -\lambda_{10,10} & \lambda_{10,11} \\
\lambda_{11,1} & 0 & \lambda_{11,3} & \lambda_{11,4} & \lambda_{11,5} & \lambda_{11,6} & \lambda_{11,7} & \lambda_{11,8} & \lambda_{11,9} & \lambda_{11,10} & -\lambda_{11,11}
\end{bmatrix}
\begin{bmatrix}
p_1 \\ p_2 \\ p_3 \\ p_4 \\ p_5 \\ p_6 \\ p_7 \\ p_8 \\ p_9 \\ p_{10} \\ p_{11}
\end{bmatrix} = 0$$

$$\sum_{j=1}^{11} p_j = 1 \quad (14)$$

After having solved the above-mentioned system of equations the boundary probabilities of the Markov process are obtained  $p_j(t)$  for a vehicle (if they exist). If we put the transitions intensities to a system of equations (14) and are not able to solve it that means that the whole process is non-ergodic (not periodic, not regular). One thing we can do is simulation, which shows the irregularity of the process. Moreover it allows to estimate the level of non-ergodicity. Another way [4,5,7] is to calculate the availability according to the relationships (15):

$$K = \frac{\sum_{i=1}^n \bar{T}_G}{\sum_{i=1}^n \bar{T}_G + \sum_{i=1}^n \bar{T}_N} \quad (15)$$

where:

$\sum_{i=1}^n \bar{T}_G$  – total sum of medium times of staying a vehicle in availability;

$\sum_{i=1}^n \bar{T}_N$  – total sum of medium times of staying a vehicle in unavailability .

The medium time of staying a vehicle in a considered state collection could be estimated by taking into consideration historical events[6]. Empirical results for the vehicles used in logistic air base system have been presented in tables 1-3.

Tab. 1. Collection of data about medium number of entrance, medium transition probabilities, medium time of staying (hrs) and intensities of (1/year)  $S_1$ - $S_{11}$  states for a vehicle – C model

State	$S_1$	$S_2$	$S_3$	$S_4$	$S_5$	$S_6$	$S_7$	$S_8$	$S_9$	$S_{10}$	$S_{11}$
$\bar{n}_i$	214	161	330	8	4	2	2	358	45,656	2	416
$p_i(n)$	0,138	0,104	0,213	0,005	0,002	0,001	0,001	0,232	0,029	0,001	0,269
$\bar{t}_i$	869,3	5656,3	13,75	252	22	16	240	0,2265	11	240	1439,43
$\hat{\lambda}_i$	10,077	1,5487	637,09	34,762	398,18	547,50	36,50	38675,5	796,4	36,5	6,086

Tab. 2. Collection of data about medium number of entrance, medium transition probabilities, medium time of staying (hrs) and intensities of (1/year)  $S_1$ - $S_{10}$  states for a vehicle – B model

State	$S_1$	$S_2$	$S_3$	$S_4$	$S_5$	$S_6$	$S_7$	$S_8$	$S_9$	$S_{10}$
$\bar{n}_i$	173	161	165	4	2	1	1	179	23,65	1
$p_i(n)$	0,243	0,226	0,232	0,005	0,002	0,001	0,001	0,251	0,033	0,001
$\bar{t}_i$	1159,3	5656,3	22	504	144	288	240	4,376	22	720
$\hat{\lambda}_i$	7,556	1,548	398,2	17,38	60,83	30,42	36,50	2001,8	398,2	12,2

Tab. 3. Collection of data about medium number of entrance, medium transition probabilities, medium time of staying (hrs) and intensities of (1/year)  $S_1$ - $S_9$  states for a vehicle – A model

State	$S_1$	$S_2$	$S_3$	$S_4$	$S_5$	$S_6$	$S_7$	$S_8$	$S_9$
$\bar{n}_i$	173	161	165	4	2	1	1	179	22
$p_i(n)$	0,244	0,227	0,233	0,005	0,002	0,001	0,001	0,252	0,031
$\bar{t}_i$	1159,33	6376,3	22	504	144	288	240	4,376	22
$\hat{\lambda}_i$	7,5561	1,3738	398,18	17,38	60,83	30,42	36,50	2001,83	398,18

Where:

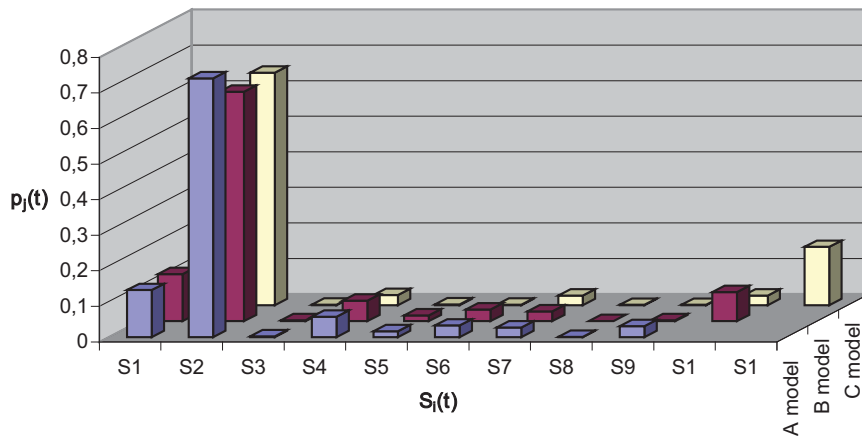
$\bar{n}_i$  – the average transition number from  $S_i$  in  $T_0$  period;

$\bar{\omega}_i$  – frequency  $S_i$  state in a considered collection state  $l - s$  ( $s = 9; 10$  or  $11$ );

$\bar{t}_i$  – the average duration time for  $S_i$  state before entrance to all  $S_j$  states in  $T_0$  period;

$\hat{\lambda}_i$  - intensity of  $S_i$  state;

Mathematical dependencies for parameters mentioned above have been presented in [5] thesis.



**Rys. 5. Probabilities  $p_j(t)$  of staying in availability for vehicles**

Fig. 5 describes probabilities staying in availability  $p_j(t)$  for vehicles in a considered  $S_i$  states, which are calculated as:

$p_i = \frac{\bar{t}_i}{\bar{T}_0}$ , while availability has been calculated according to (15) relationship;

where:

$$\bar{T}_G = \bar{t}_1 + \bar{t}_2$$

$$\bar{T}_N = \sum_{i=3}^S \bar{t}_i \text{ for } S=1-9 \text{ for A model, } S=1-10 \text{ for B model, } S=1-11 \text{ for C model.}$$

#### 4. Conclusions

Estimated annual average sum of tenses  $\bar{t}_1 + \bar{t}_2$  for vehicles population in availability is from 6526 hrs (realistic C model) to 7535,63 hrs (optimistic A model – table 3), it means that the availability is from 0,745 to 0,86 in  $T_0$  period.

The availability of vehicle population is high, but there is also time margin in a year  $t_{11} = 1439,43$  hrs (model C), resulting mainly from time losses during replacement  $S_{10}$  and renovating  $S_4$  of the vehicles (tab.1-3). It enables to improve the availability up to 16%. Therefore model C with  $S_{11}$  state is justify and realistic. Withdrawal from usage decrease the number of vehicle population on average 7% in a year, but the replacement time is usually longer than one month.  $S_{10}$  state cannot be omitted because it significantly changes the duration time balance for all states of the

vehicles. Models B i C with  $S_{10}$  state reflect the simulation of renovating and replacement of the population in long periods of time.

All presented models are stable and their non-ergodicity in real time is only according the simulation 0,2-1% for availability state after 3 years. The reason for their non-ergodicity can be vast (broad) spectrum of duration times for considered states collection.

However Markov chains for A, B and C models are ergodic, but boundary probabilities  $p_j$  concern collection states of the process and they cannot be interpreted in real (physical) time.

It has been illustrated by the proportion of the estimated real time of refuelling max.  $p_8(t) = 4,376$  hr (tables 2 and 3) to misinterpreted ergodic time  $p_8 * 1 \text{ year} \approx 2200$  hours for discrete time estimated from  $p_8(n)$ .

## References

- [1] Bobrowski D., *Modele i metody matematyczne teorii niezawodności*, WNT, Warszawa 1985.
- [2] Fisz M., *Rachunek prawdopodobieństwa i statystyka matematyczna*, PWN, 1967.
- [3] Gniedenko B.W., Bielajew J. K., Sołowiew A.D., *Metody matematyczne w teorii niezawodności*, WNT, Warszawa 1968.
- [4] Hebda M., Mazur T., *Podstawy eksploatacji pojazdów samochodowych*, WKiŁ, Warszawa 1984.
- [5] Migdalski J., *Poradnik niezawodności - podstawy matematyczne*, Wydawnictwo Przemysłu Maszynowego WEMA, Warszawa 1982.
- [6] Ziółkowski J., *Analiza systemu logistycznego bazy lotniczej w aspekcie gotowości*, rozprawa doktorska, ITWL, Warszawa 2004.
- [7] Żurek J., *Problemy gotowości techniki lotniczej, Praca zbiorowa: Problemy badań i eksploatacji techniki lotniczej*, t.2, ITWL, Warszawa 1993.



## DIAGNOSTIC SYSTEM OF MACHINE EXPLOITATION

**Bogdan ŻÓŁTOWSKI**

*Uniwersytet Technologiczno – Przyrodniczy*  
*ul. S. Kaliskiego 7, 85-763 Bydgoszcz*  
[bogzol@utp.edu.pl](mailto:bogzol@utp.edu.pl)

### **Abstract**

*This work presents the main descriptors of the diagnostic system of machine exploitation. This problem contains: the measurements of technical state symptoms, the determination of their boundary values, and the frequency of diagnostics. This problem and the tasks in the system of machine exploitation supported with computer techniques constitutes about the rank of the discussed problem.*

**Keywords:** *machine diagnostics, symptoms of the state, boundary value, frequency of diagnostics*

### **1. Introduction**

The knowledge of the machine's technical state results from the need of making rational decisions about the "quality", and further treatment of the machine. It can be a decision on further use, on undertaking appropriate preventive interventions, or on the introduction of construction, technology or exploitation changes.

Discussed in this work are chosen problems of machine state diagnosis, emphasizing the problems of the new strategy of machine exploitation, including state symptoms, determination of the boundary value of measured symptoms, and determining deadlines of consecutive terms of diagnosis.

The introduction of diagnostic systems makes it possible to improve the organization and management of machine usage in industrial institutions with the help of computer technology.

### **2. Main problems in machine diagnostics**

The growing level of complexity of machines and criticality of their function within safety and economics, force constructors and users of these objects to know their current technical state, and to use them considering prognosis. This is possible, if at construction stage equipment and diagnostic procedures are integrated with the object.

### **Generation of vibration signals in the description of machine condition changes.**

Evaluation of the machine dynamic state with the use of generated by them physical processes requires the association of functional parameters of the evaluated object with the set of measures and the opinions of output processes.

While functioning of the machines, in the consequence of the existence of a number of external factors (environmental forcing, from different machines) and internal (aging, wastes, co-operation of

elements), there are disorders of balance state in the machine, which spread in a springy medium – the material of which the machine is built.

The disorder has dynamic character and sustain the conditions of balance between the state of among the condition inertia, elasticity, the suppression and extortion.

The disorder spreads from the source in the form of waves in the way dependent from physical properties, and the configuration borders, dimensions and shape of the machine. This in result causes wave energy scattering, their bending, reflection and mutual superposition. The existence of sources and spreading of disorders causes the occurrence of vibrations of machine elements and the surrounding environment. These processes are the basis of building a model of signal generation determining the manner of constructing, functioning and state changes of the object.

The sequence of assumptions leading to the signal generation model can be presented with the use of a cybernetic model, as in the Fig. 1.

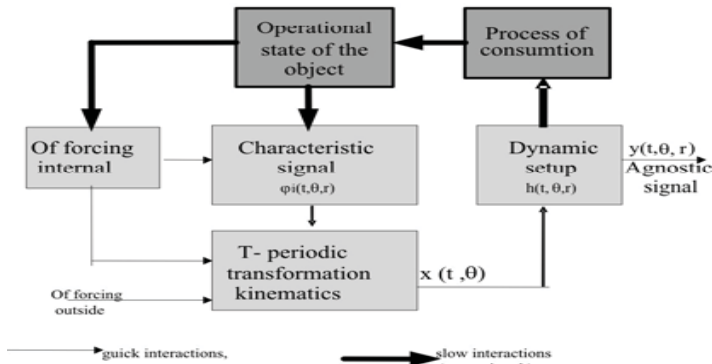


Fig.1 Model of diagnostic signal generation of a machine

The presented way of interpreting the signal  $y(\theta, r)$  is, in a general case of machines of periodic working, true, but not always as simple as in the Fig. 2.

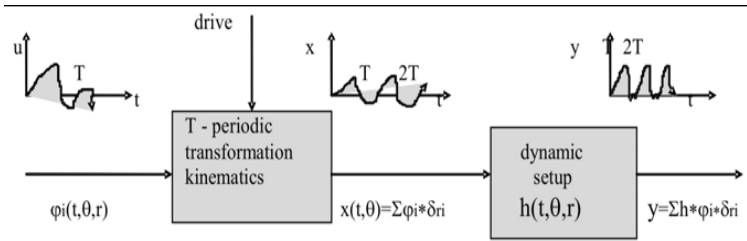


Fig.2. Transformation of the characteristic signal  $\phi_i$  into the output signal  $y$  as the model of signal generation in machines [2]

The example of such formulation of the problem is the main transmission of the bridge of a vehicle whose generation model is presented in the Fig. 3.

The received output signal in any place of the transmission casing is a weighed sum of answers to all elementary events  $Un(t, r)$ , occurring always in the same sequence in separate dynamic partial systems of impulse function of transition  $hn(t, \theta, r)$ . These effects, after going through certain



dynamic systems, sum up and undergo an additional deformation on the transmission corpse, whilst the change of place of receiving the “r” signal is also connected with the transmittance change.

The notion  $n(t, \theta)$  describes a random effect occurring because of the existence of dynamic micro-phenomena, such as friction, roughness, etc. The output signal of any receiving point can be approximately expressed with the equation:

$$y_k(\theta, r) = \sum a(k) h_i(t, \theta, r) * [u_i(t, \theta, r) + n(t, \theta, r)] \quad (1)$$

where: the impulse transition function  $h(*)$  corrupts also the properties of the corpse,  $a(k)$  gives different weights of summing connected with the receiving point “r”.

Main problems of machine diagnostics include:

- acquiring and processing diagnostic information;
- building of models and diagnostic reports;

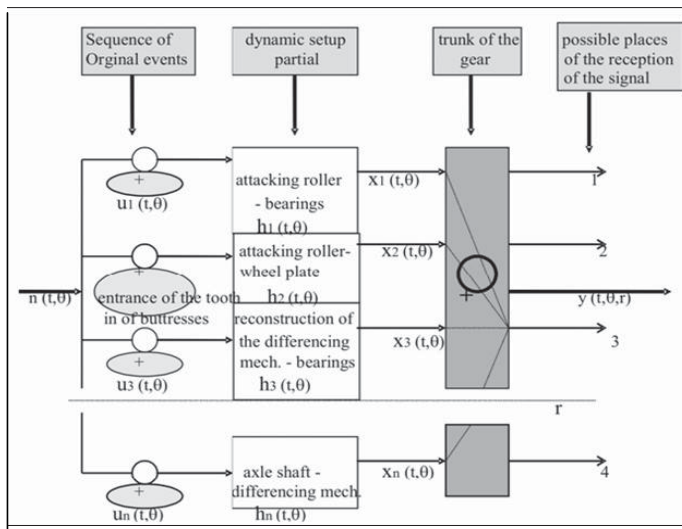


Fig.3. Model of the diagnostic signal generation of the toothed transmission

- the diagnostic inference and boundary value;
- the classification of machine state;
- the expected time of next diagnosis;
- presenting the decision information.

Measuring system for the aims of the modern diagnostics of machines consists of two basic elements:

- the equipment in which distinguished are the modules: conditioning subsystem and processing of signals, the subsystem of processing signals of the phase gauge, the subsystem of the industrial computer, the subsystem of power supply,
- the software, consisting of the modules: operating system (VxWorks), the software of the modules of signal processing and analysis, software assuring communication between the layers of the system, software for storage and archivization of measuring data, software managing the work of the system (configuration of the system, testing the system, the initialization of measuring sessions).

The introduced structure of the measuring system uses the newest solutions, both in hardware and software. The applied solutions easy extension of the system and including it for any diagnostic system.

The problems troubling the practice of applying methods of diagnosis (Fig. 4):

1. The time of forming the diagnostic symptom.

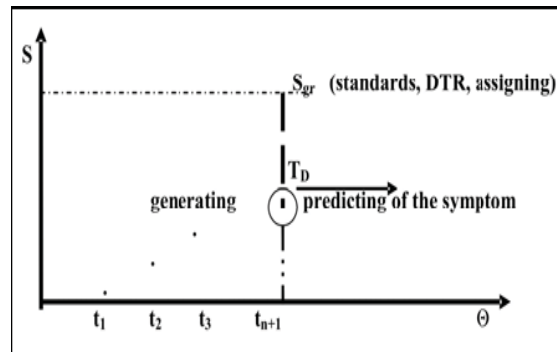


Fig.4. System diagnostic actions

2. The change the boundary symptom - preventive system.
3. Complex state evaluation: the measurements of symptoms, reference to the boundary value, prognosis of the state, estimation of next diagnosing, the genesis of the cause of the measured symptom changes.

### 3. Diagnostic system of machine exploitation

Contemporary machines determined by such features as: functionality, reliability, availability, safety, mobility and flexibility of operation. Formation and maintenance of these features is possible with methods of technical diagnostics which enables:

- diagnostic construction and production of new machines and maintenance of machines in the condition of functional ability.

The use of the machines is characterized by:

- sets of randomly changing times of the correct work;
- randomly changing moments of the beginning and changing lengths of times of task duration;
- intensive work of people and machines in randomly changing period of exploitation time;
- the influence of randomly changing conditions of exploitation;
- various kinds of tasks executed in short periods of time.

The needs and conditions of market economy justify the necessity to introduce modern authorized strategy of the machine production and exploitation. In the proposition of this strategy, we do not lose the so-far accomplishments of the newest strategy of exploitation according to the state, but it is creatively modernized. The proposed strategy of exploitation – ASEM – indicates the creator and responsible for the product by name. The manufacturer interested in the quality and later the sale is responsible for the product from the very idea, through construction, production and exploitation, until utilization after the liquidation of the object.

The same manufacturer constructs and produces their products based on the newest achievements of technical thought, they protect their product with their own service during exploitation, and also they provide objects with diagnostic (preferably automatic) means.

The effectiveness of solutions in applying this strategy requires the improvement of: machine diagnostic models, the methods of diagnosing and prognosis of the machine state, economic, exact and reliable diagnostic equipment, the principles of the diagnostic vulnerability formation, the algorithms of conducting the maintenance of the machines in the ability state, methods of evaluating the efficiency of diagnosis and machine exploitation system. The specified questions embrace the whole problem and unambiguously establish the directions of the development of machine technical diagnostics.

The users of machines are interested particularly in their task ability, for determining which the following are necessary:

- determining the symptoms of ability state;
- determining the boundary values of ability state symptoms,
- determining the class of object ability,
- determining diagnosis periodicity.

The distinguished diagnostic tasks will be selectively discussed below, whilst their detailed description can be found in the author's works [6,7].

#### 4. Boundary values of state symptoms

Task ability in the symptom notion is unambiguously described by the boundary value of the measured state symptoms.

Exceeding the boundary value means that the machine enters the state of accelerated wear characterized by high probability of a sudden breakdown.

Realized most often in the industrial practice passive and passive-active diagnostic experiments give state symptoms which are compared during concluding with boundary values available in many national, foreign, trade norms, or with data from own experience. When, however, there are no such norms for the examined machine, helpful can be the statistic description of a random exploitation process with the use of decay thickness or the frequency of the observed symptom occurrence.

Estimating the symptom boundary value for a safe shutdown of a machine before failure can be realized with the use of statistical methods.

The formula for determining  $S_{gr}$  minimizing the probability of failure, with the set, acceptable probability of redundant repair  $A$  can be written down in the form [1]:

$$P_g \cdot \int_{S_{gr}}^{\infty} \left( \frac{S}{X_g} \right) dS = A \quad (2)$$

where:  $P_g$  - the ability probability.

According to Birger [1]:  $A = k (1 - P_g)$ , where:  $k$  - the coefficient of the store ( $k = 1-3$  for usual damages,  $k = 3-10$  for dangerous damages),  $P_g$  - availability the machines determined from the dependence:  $P_g = N_z / N_z + N_n$ , where:  $N_z$  - the number of fit machines,  $N_n$  - number of unfit machines.

The row of simple transformations leads in the effect to the dependence:

$$S_{gr} = \bar{s} \pm \sigma_s \sqrt{\frac{P_g}{2A}} \quad (3)$$

The received estimation of symptom boundary value based on the mean value, dispersion and repair politics, gives good basis for simple determination of boundary values of examined state measures in the industrial practice.

## 5. Diagnosis periodicity

The growth of intensity of the occurrence of damages along with wearing away the exploitation potential of the machine forces the need to optimize diagnosis periodicity. From the course damage intensity of the machine, it is concluded that that in the period of intensity growth it is necessary to increase the frequency of diagnosing.

This helps to reduce expenditures on the exploitation of the machine (the decrease: wear intensiveness, waste of the fuel, spare parts, material use), and at the same time the costs and time consumption, and the machine turn-off time grow.

The optimization of diagnostic periodicity comes down to two basic questions: how often to perform diagnosis?, in what range to perform the next diagnosis?.

There are several possibilities to determine diagnosing periodicity (the method of symptom boundary values, the methods of the smallest sum of exploitation costs), whilst for their realization indispensable are numerous statistical data, often troublesome (in the sense of amount and reliability) to obtain.

In this work, the question of diagnostic periodicity has been considered symptom notion, using a known symptom boundary value. Performing  $n$ -measurements of a chosen in a separate procedure signal measure (symptom), and determining on their basis a boundary value according to the dependence (2), there is a need to determine the date of the next diagnosing  $t_d$ . The essence of the method presented in the works [6,7] show that the date of next diagnosing is estimated from the dependence (Fig. 5):

$$t_d = \frac{(1 - P_r)(S_{gr} - S_m)}{S_m} \theta_m \quad (4)$$

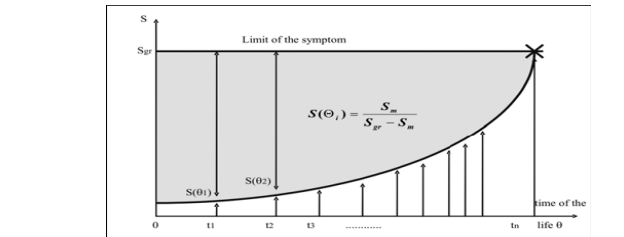


Fig.5. Periodicity of diagnosing in the symptom notion

## 6. Management of exploitation system

All of economic organizations have a certain system of management which fulfills its requirements within the realization of an accepted strategy. This is particularly essential for those which have a considerable influence on the course of production process (logistics, exploitation, tools and equipment), or control its fixed assets of considerable, from the point of view of the company, values (movement maintenance, repairs, check-ups) [4].

Subsystem functions:

- it conducts the classification and record of all fixed assets,
- it proposes basic technical-economic indexes,
- it supervises the exploitation of fixed assets,
- it analyses data from monitoring and makes decisions,
- it infers the liquidation of fixed assets,

- it plans, supervises and realizes all kinds of examination, maintenance and repairs,
- it establishes basic norms, records and accounts for performed works,
- it plans the supply of spare parts and necessary materials for repairs,
- it offers and motivates leasing, offers and motivates outsourcing,
- it organizes storage of spare parts, their distribution and accounting for,
- it plans investment tasks, organizes and realizes the purchase of machines and equipment,
- it organizes the receipt of fixed assets,
- it prepares the technologies of repairs.

Analyzing the range of functions attributed to the system for realization, it is possible to determine what groups of data ought to enter it, as well as what data it generates.

The model of exploitation system management was built on the basis analysis of two basic criteria, i.e. the flow and type of data, and functions realized by individual modules. The structure of exploitation system management, together with the flow of data, is shown in the fig. 6.

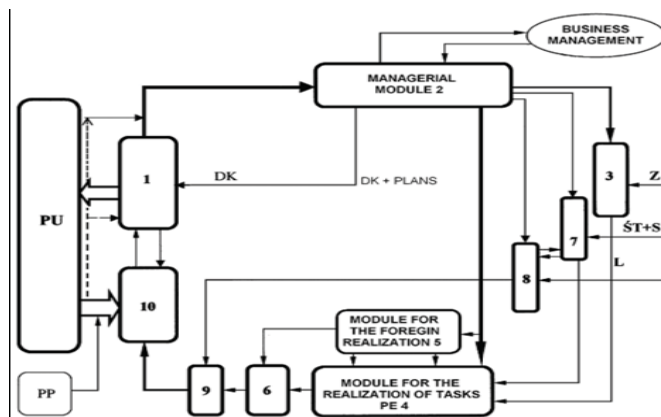


Fig.6. Model of exploitation system management

Separate modules creating the structure of the system realize the following functions:

1. The module of data processing is responsible for processing data sent to the system. Carriers and media of the transmission can be considerably diverse.
2. The managerial module, to which data of various degrees of aggregation enter from the module of data processing. It can be stated that about 80% of the data is processed according to the assigned algorithms, creating a basic set for the need of SE management.
3. The logistic module, which delivers indispensable materials, equipment, components and standardized machine elements for the needs of realized repairs; manages stock and analyses the level of stores, runs the record of distributed supplies, analyses their waste for individual orders, organizes and supervises transport of purchased technological equipment, co-operates with company's logistics in the range of the economy of scrap-iron.
4. The task realization module which realizes or supervises the realization of examinations and a bigger part of repairs.
5. The module of the strange realization, registering the range of repair works ordered to a third party.
6. The control module, checking the quality and range of realized works, outside and own.
7. The module of technical base renovation, purchase of machines, renovation and repairs.

8. The personnel training module, motivation and training of workers.
  9. The accounting module, creates abstract summaries, as well as controls the needs for the realization of certain operations.
  10. The technical module realizing the functions: planning, constructional, technological, technical state evaluations of the possessed equipment, record and updating, the emission of records.
- PU* - the exploitation subsystem which exploits machines and equipment.
- PP* - Remaining subsystems. Relations of these subsystems with the exploitation management system are defined to a smaller degree.

The construction of the model of the exploitation management system allows to identify the basic elements of its surroundings, as well as of the modules creating the subsystem itself.

## 7. Summary

The accomplishment of diagnostics in recent years using the achievements of many fields of science, allow treat it as a tool of formation and evaluation of machines, at all stages of their existence.

Looking at present trends of machine development it should be recognized that currently the growth of their quality is contained mainly in the sphere of automation. Automatic acquisition of measurable features is becoming the only objective way of evaluating and forming the quality of machines.

The range of investigations in the field of methodology of diagnostics includes such questions as: the source of diagnostic information, signals and diagnostic symptoms, the principles of detailed methods of diagnostics, modeling in diagnostics, diagnostic experiments, supporting diagnostics with modern computer technologies, diagnosing in systems of human engineering and social engineering, and the organizational and economic aspects of applying diagnostics. These question respectively apply to: source of information from the physical side and from the informative side, further bases of methods and investigative techniques, simulation and experimenting in diagnostics, and modern inference and visualization of worked out diagnostic-exploitation decisions.

## References

- [1] Birger I.A., *Technical diagnostics*. Science, Moscow, 1978, (p. 32, in Russian).
- [2] Cempel C., *Basis vibroacoustics of diagnostic machines*. WNT, Warsaw, 1982.
- [3] Grudzewski I., Pietrowski H., *The module organization of the enterprise*. ZN, IOPM, 1989.
- [4] Jaskulski Z., *The influence of chosen internal factors on efficiency of management of production companies*. Conference materials of Diagnostics '99, Bydgoszcz 1999.
- [5] Pietrowski H., *Module system of the organization of the enterprise*. PWE, Warsaw 1981.
- [6] Zoltowski B., *Basis of the diagnostics of machines*. ATR, Bydgoszcz, 1996.
- [7] Zoltowski B., Cempel C., *Engineering of diagnostics machines*. ITE, Radom 2005.



## PROCEDURE OF CONSTRUCTING AND EVALUATING LINEAR DIAGNOSTIC MODELS OF COMPLEX OBJECTS

**Bogdan ŻÓŁTOWSKI**

*Uniwersytet Technologiczno – Przyrodniczy*  
*ul. S.Kaliskiego 7, 85-763 Bydgoszcz*  
*e-mail: [bogzol@utp.edu.pl](mailto:bogzol@utp.edu.pl)*

### Abstract

*In this work presented are chosen problems of machines' technical state diagnosis with the use of identification and technical diagnostics methods. Relations between methods of dynamic state evaluation and methods of technical state evaluation were indicated. Example modal analysis results illustrate the complexity of projecting dynamic state researches into diagnostic researches of machine state evaluation.*

**Key words:** *technical diagnostics, identification, modeling, modal analysis.*

## 1. INTRODUCTION

Destruction processes of technical systems force the need to supervise changes of their technical state. It is possible with the use of technical diagnostics methods.

Methods and means of modern technical diagnostics are a tool of machine state diagnosis, which is the basis of decisions made at each stage of their existence.

Many previous works of the author [1,2,3,4,5] clearly indicate connections between machine dynamics and technical diagnostics, especially vibration diagnostics. The bases of identification, modeling and concluding fully convince towards the dominating role of vibrations in machine state identification [6,7,8,9].

Properly planned and realized experiment is the base to obtain diagnostically sensitive signals which processed will determine state diagnosis procedures. The processing includes: creation of numerous signal measures in time domain, frequencies and amplitudes, selection and reduction of the number of signal measures, creation and analysis of effectiveness of cause-and-effect models, as well as evaluation of the righteousness of made diagnostic decisions.

The realization of these tasks is possible only through broad support from information technology, which in this work is presented in the form of SIBI programs.

Practical applications of the presented ideas has been verified in researches on complex objects exploited in difficult climate conditions.

## 2. DYNAMICS AND DIAGNOSTICS

Into quality measures of machine's technical state, i.e. its dynamics, included is the level of vibration amplitudes, as well of the machines as the lot, and also of relative vibrations of separate elements and parts. Overall vibrations of the machine can be perceived as an external symptom



while they are responsible for the level of interferences emitted into the environment. Relative vibrations of separate elements, however, influence mainly the state of internal forces in the machine, i.e. at its level of dynamic stress amplitudes.

Identification can concern both the construction of models and the reconstruction of the examined model state, which leads straight to the problem of technical diagnostics.

The process of diagnostic identification includes:

- \* modeling (symptom or structural),
- \* identification experiment (simulation and/or real),
- \* estimation of diagnostic parameters (state features or symptoms),
- \* diagnostic concluding.

The specificity of diagnostic identification tasks is different from general identification in the way that it includes a number of additional elements enhancing this process. These are:

- constructing models of diagnostic signals generation,
- choosing features of object structure state and diagnostic symptoms,
- modeling cause-and-effect relations,
- evaluating the accuracy of choosing variables for the model,
- determining boundary values of the symptoms,
- classifying the states and determining diagnosis periodicity.

Methods of identification can be divided concerning: the kind of identified model, the kind of experiment, identification criterion applied, as well as estimation procedure applied. In general these are: methods of analysis, time, frequency, correlation, regression, factor analysis, as well as iteration methods described in works of many authors [2,4,6,5,8].

For simple objects, a good tool to evaluate their changeable dynamic state are methods of simple identification which use amplitude-frequency spectrum. Searching rezonans frequency and amplitude value in this frequency with the use of tests (impulse, harmonic and random) are relatively well mastered in research techniques of our enterprises [2,5].

Another way of describing and analyzing the dynamic state of machines is a modal analysis used as a theoretical, experimental and exploitation method. It uses frequencies of own vibrations, values of suppression and forms of vibrations to describe the changing machine state, and it is used to improve the finished elements method. The presented procedures are based on the knowledge of the system model, and the conclusions drawn from the actions on the models depend on their quality. Depending on the aim of the performed dynamic analysis of the object, different requirements are set for the constructed models, and their evaluation is conducted with different experimental methods.

### 3. DESCRIPTION OF OBJECT STATE CHANGES

The dynamic state of the object can be, in the easiest case, described with a model of 1 degree of freedom – Fig.1. A conventional description of this model are known relations (1-4) indicating that vibrations well reflect the state of the machine. A description of this model can be achieved within  $m$ ,  $k$ ,  $c$  categories, or through  $a$ ,  $v$ ,  $x$  researches.

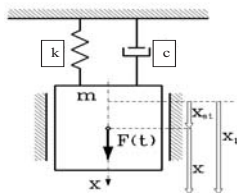


Fig.1. Model of a system of 1 degree of freedom.  $m$ ,  $k$ ,  $c$  = vibration process ( $a$ ,  $v$ ,  $x$ )

$$m \ddot{x} + c \dot{x} + kx = F(t) \quad (1)$$

$$x = A \sin(\varpi \cdot t + \phi) \quad (2)$$

$$v = \frac{dx}{dt} = A\omega \cos(\omega t + \varphi) \quad (3)$$

$$a = \frac{d^2 x}{dt^2} = \frac{dV}{dt} = -A\varpi^2 \sin(\varpi t + \varphi) \quad (4)$$

Identification of his model (1) from the experimental side is the  $a$ ,  $v$ ,  $x$  measurements for different time moments, which reflects the changes of the object state and is widely applied in vibration diagnostics. The solution of the task in the  $m$ ,  $k$ ,  $c$ , categories, however, requires a number of solution conversion of the equation (1) for determining:

$$\begin{aligned} c_{kr} &= 2m\varpi & c_{kr} &= 4\Pi mf \\ k &= m \cdot \varpi^2 & k &= 4\Pi^2 mf^2 \end{aligned} \quad (5)$$

Determining the value (5) requires realizing identification experiment from which the frequency  $f$  or frequency  $\omega$  can be determined. Here is useful the simple identification or modal analysis directly giving the values of own frequencies  $\omega$  from the stabilization diagram – Fig.2.

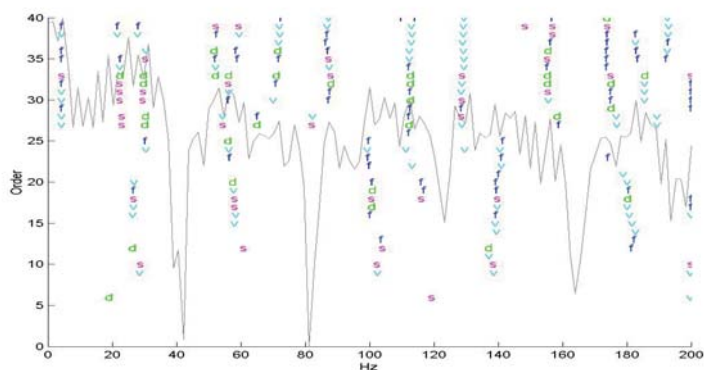


Fig.2. Stabilization diagram for  $\omega$  determination

The problem becomes more complicated for models of many degrees of freedom (more than 3). Here also the problem of object state identification can be solved from the measurement side (a, v, x), while from the side of determining m, k, c own problem needs to be solved.

$$(K - \omega^2 M) \cdot q_0 = 0 \quad (6)$$

Equation (6) presents a linear system of homogeneous algebraic equations:

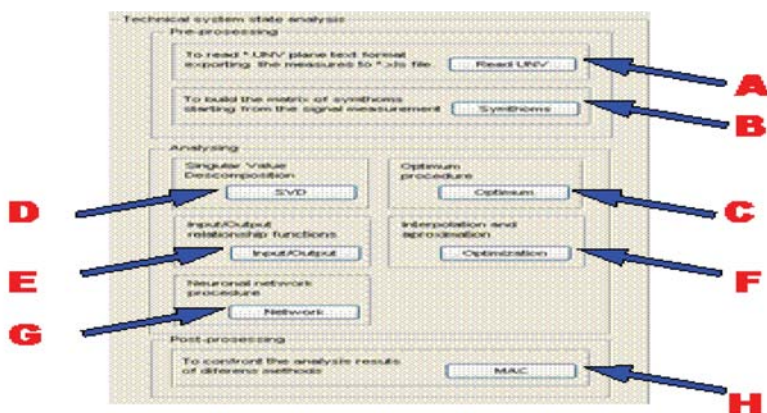
$$\begin{aligned} & (k_{11} - \omega^2 m_{11})q_1 + (k_{12} - \omega^2 m_{12})q_2 + \cdots + (k_{1n} - \omega^2 m_{1n})q_n = 0 \\ & (k_{21} - \omega^2 m_{21})q_1 + (k_{22} - \omega^2 m_{22})q_2 + \cdots + (k_{2n} - \omega^2 m_{2n})q_n = 0 \\ & \begin{matrix} \cdots & \cdots & \cdots & \cdots & \cdots \\ (k_{41} - \omega^2 m_{41})q_1 & + & (k_{42} - \omega^2 m_{42})q_2 & + & \cdots + & (k_{nn} - \omega^2 m_{nn})q_n = 0 \end{matrix} \end{aligned} \quad (7)$$

A solution for  $q \neq 0$  exists when the main matrix determinant  $(K - \omega^2 M) = 0$ , i.e.  $\det(K - \omega^2 M) = 0$ . Solving the system of equations (7) own values can be determined, and from them the frequencies of own vibrations, indispensable for the object identification ( $\lambda = \omega^2 = \frac{k}{m}$ ).

#### 4. IDENTIFICATION RESEARCHES SOFTWARE (SIBI)

More and more frequently conducted identification researches of machine dynamic state, used for the evaluation of the state changes, fault development and location of the occurred state causes, were the basis for creating a specialized software system. It allows acquiring and processing measurement data, creating many measures of diagnostic signals, examining their diagnostic sensitivity, statistic processing and diagnostic concluding. The program was named Information System of Identification Researches (System Informatyczny Badań Identyfikacyjnych – SIBI).

The structure of the program is a module construction which includes the following modules (Fig.3.):



Rys. 4.1. Główne okno dialogowe programu SIBI

Fig.3. Main dialog box of SIBI program

- A.** **READ UNV** module which allows processing data from **UNV** format into **XLS** format.
  - B.** **SYMPTOMS** module which allows defining, determining and creating matrix of many measures of vibration processes.
- Modules A and B are part of software responsible for acquiring and processing vibration processes in order to acquire observation matrix of vibration estimators.
- C.** **OPTIMUM** module uses the method of ideal point for individual evaluation of the sensitivity of measured symptoms of vibration processes.
  - D.** **SVD** module used for determining generalized damage measures, and for the evaluation of damage development. Using the SVD method allows a multidimensional description of the state of the examined object.
  - E.** **INPUT/OUTPUT** module used for the analysis of similarities between vibration processes, and for determining different exploitation measures of the examined object.
  - F.** **OPTIMIZATION** module used for creating models and data in genesis (with approximation and interpolation methods), diagnosis and prognosis of object states.
  - G.** **NETWORK** module using neuron nets for state classification on the basis of obtained results in the form of time rows.
- C, D, E, F, G modules are elements of 2 parts of the software allowing the performance of statistic concluding and cause-and-effect relations, as well as visualization of the obtained results.

## 5. CAUSE-AND-EFFECT MODELING

Many state measures acquired in experiments requires the reduction of over measurement, which is possible with the use of OPTIMUM procedure (statistic evaluation of separate measures) or SVD (for the multidimensional approach). Optimized set of symptoms is the basis of constructing cause-and-effect, most often regressive, multidimensional models (Fig.4).

$$y = -2,68061w1 - 0,54083 \text{ row1} - 0,49318 x1 + 2,01273 w2 + 0,35480 \text{ row2} + 2,26940 x2 - 0,02717 H(f) + 0,06833 H(f)L + 0,01696 g2xy - 92,00391 \text{ ARMS}(t) + 12,99146 \text{ bkurt} + 239,69713 Cs - 200,58670 I - 44,37385$$

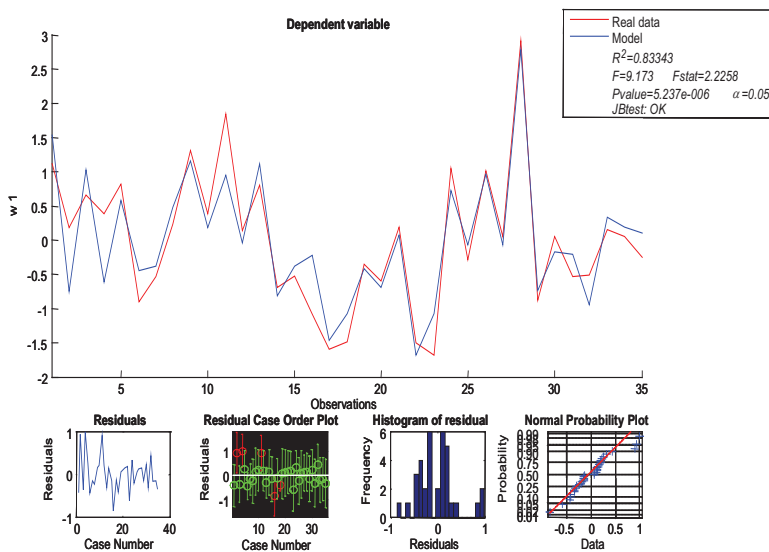


Fig.4. Regressive model determination

The wellness of the model is evaluated with the help of the determination coefficient  $R^2$ , and the number of component symptoms determines its accuracy – Fig.5.

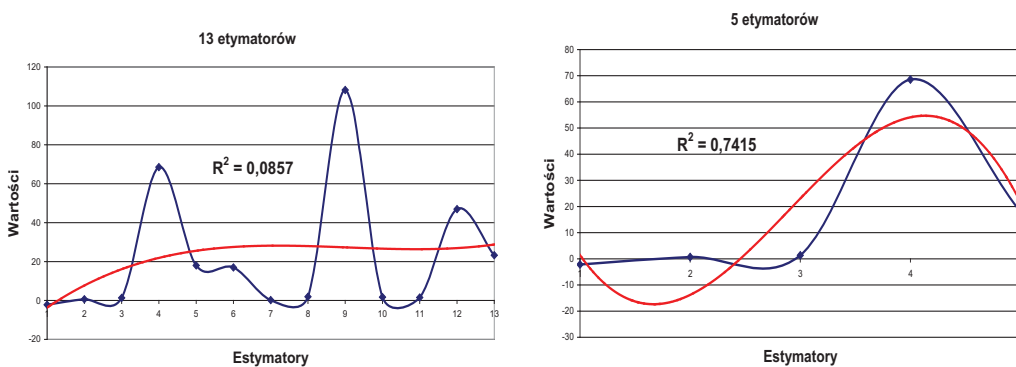


Fig.5. Number of measures v. accuracy of the model

## 6. CONCLUSIONS

Presented in this work considerations concern the modeling of object dynamic state with the use of description and researches within the range of identification, distinguishing modal analysis and ideas directly supporting different methods of forming machine dynamics.

The knowledge of the dynamic state and structure of the system allows to describe its behavior, and allows creating prognosis models of the system behavior in the function of dynamic evolution time, based on the model of the technical state symptoms growth. Most often, however, there are no known equations describing behaviors of the system in the function of dynamic evolution time, which accounts for the need to apply new tools to examine the dynamic state. There is, therefore, the requirement to experimentally verify analytical technical models as the proper one is a model which is verified in practice. An experiment is, therefore, often only an inspiration for further researches leading to the optimization of the construction.

## LITERATURE

1. Bendat J.S., Piersol A.G., *Methods of analysis and measurement of random signals*, [in Polish] PWN, Warszawa, 1996.
2. Broch J.T., *Mechanical Vibration and Shock Measurements*, Brüel & Kjaer, 1980.
3. Cempel C., *Vibroacoustical Condition Monitoring*, Ellis Hor. Ltd., Chichester, New York, 1991.
4. Cholewa W., Kiciński J., *Technical diagnostics. Reverse diagnostic models*, [in Polish] Wydawnictwo Politechniki Śląskiej, Gliwice 1997.
5. Eykhoff P., *Identification In dynamic systems*, [in Polish] BNInż. Warszawa.1980.
6. Giergiel J., Uhl T., *Identification of mechanical systems*, [in Polish] PWN, Warszawa, 1990.
7. Kaźmierczak H., Kromulski J., *Methods of parametric identification in application into construction diagnostics, Exploitation problems*, [in Polish] 6/93 MCNEMT Radom 1993.
8. Morrison F., *Art of dynamic systems modeling*, [in Polish] WNT, Warszawa, 1996.
9. Tylicki H., *Optimization of the process of vehicle mechanical state prognosis*, [in Polish] Rehabilitation thesis, No 86, ATR Bydgoszcz, 1999.
10. Uhl T., *Computer-enhanced identification of mechanical construction models*, [in Polish] WNT, Warszawa 1997.
11. Żółtowski B., *Diagnostic identification of technical objects. Problems of machines exploitation*, [in Polish] Z.1 (105), PAN, 1996.
12. Żółtowski B., *Computer enhancement of identification*, [in Polish] ZN P.Św. nr.49, 1996 (s.55-71).
13. Żółtowski B., *Machine diagnostics basics*, [in Polish] Wyd. ATR, Bydgoszcz, 1996.
14. Żółtowski B., *Multidimensional monitoring of the track-vehicle interface of a railway system*, Besanson, 2007.
15. Zoltowski B., Castañeda L., *Monitoreo Multidimensional de la Interfase Vía-Vehículo de un Sistema Ferroviario* Congreso Internacional de Mantenimiento – ACIEM – Marzo 2007, Bogotá, Colombia.